14th INTERNATIONAL WORKSHOP ON MEASUREMENT & COMPUTATION OF TURBULENT FLAMES

TNF 2018

DUBLIN

JULY

27-28

IRELAND

blank

TNF 2018

DUBLIN IRELAND JULY 27-28

14th INTERNATIONAL WORKSHOP ON MEASUREMENT & COMPUTATION OF TURBULENT FLAMES

SPONSORS

ANSYS®

Continuum®
The High Energy Laser Company™

edgewave

LaVision
We count on Photons

Sirah
Lasertechnik

Princeton Instruments

ERCOFTAC

TECHNISCHE UNIVERSITÄT DARMSTADT

SFB/Transregio 150
Turbulente, chemisch reagierende Mehrphasenströmungen in Wandnäh

TNF14 Workshop Proceedings – Table of Contents

TNF14 Workshop Proceedings – Table of Contents

SUMMARY

Fourteenth Workshop on Measurement and Computation of Turbulent Flames (TNF14)

July 27-28, Dublin, Ireland

Christoph Arndt, Rob Barlow, Bassam Dally, Andreas Dreizler, Benoît Fiorina, Rob Gordon, Peter Hamlington, Evatt Hawkes, Matthias Ihme, Johannes Janicka, Andreas Kempf, Wolfgang Meier, Michael Mueller, Adam Steinberg, Jeff Sutton, Luc Vervisch

INTRODUCTION

The objective of the TNF Workshop series is to provide a framework for collaborative experimental and computational research on fundamental aspects of turbulent combustion. The emphasis has been on measurement, DNS, and modeling of turbulence-chemistry interactions in flames that are relatively simple in terms of both chemistry and flow geometry. The workshop series was initiated in 1996 to address validation of RANS based models for turbulent nonpremixed jet flames. Although the TNF acronym has been retained, the word *nonpremixed* has been dropped from the title, and our scope has expanded over the past decade to address three challenges:

- Development and evaluation of modeling approaches that are accurate over a broad range of combustion modes and regimes (nonpremixed, partially-premixed, stratified, and fully premixed).
- Extension to more complex fuels (beyond CH_4) and fuel mixtures that are of practical interest.
- Establishment of a more complete framework for verification and validation of combustion LES, including quality assessment of calculations, as well as development of approaches for quantitative comparisons of multidimensional and time-resolved data from experiments and simulations.

Additionally, there has been increasing activity in the areas of flame-wall interaction (FWI) and combustion at elevated pressure. Our overall goal is to accelerate the development of advanced combustion models that are soundly based in fundamental science, rigorously tested against experiments and DNS, and capable of predicting flame behavior over a wide range of conditions.

One of the most useful functions of this workshop series has been to provide a framework for collaborative comparisons of measured and modeled results. Such comparisons are most informative when multiple modeling approaches are represented and when there has been early communication and cooperation regarding how the calculations should be carried out, particularly in the treatment of boundary conditions, and what results should be compared. Experience has shown that comparisons on new target flames can generate significant new insights, but also many new questions. These questions motivate further research, both computational and experimental, and subsequent rounds of model comparisons. Another important function of the workshop series is to provide overviews of new work on established target cases, as well as new burner configurations and emerging topics that are relevant to our overall goals and have potential to attract a critical mass of people interested in collaboratively investigating the new burner or topic.

Previous workshops were held in Naples, Italy (1996), Heppenheim, Germany (1997), Boulder, Colorado (1998), Darmstadt, Germany (1999), Delft, The Netherlands (2000), Sapporo, Japan (2002), Chicago, Illinois (2004), Heidelberg, Germany (2006), Montreal, Canada (2008), Beijing, China (2010), Darmstadt, Germany (2012), Pleasanton, California (2014), and Seoul, Korea (2016). Proceedings and summaries of all the workshops are available at tnfworkshop.org.

TNF14 engaged 98 registered participants from 16 countries. Additionally, with help from local organizers in Dublin, five satellite workshops of the International Symposium on Combustion were held at the Trinity College Conference Center. This allowed for combined sessions with the Premixed Turbulent Flames (PTF) Workshop and with the International Sooting Flames (ISF) Workshop on topics of mutual interest. Coordination among the organizers allowed researchers to participate in multiple workshops with minimal inconvenience.

The main TNF14 sessions addressed:

- Sydney Compositionally Inhomogeneous Flames
- Update on Cambridge Swirl Flames
- Modeling of CO in Turbulent Flames
- Highly Turbulent Premixed Flames (Joint PTF/TNF Session)
- Progress of Turbulent Sooting Flames (Joint ISF/TNF Session)
- Enclosed Flames and Flames at Elevated Pressure
- Flame-Wall Interaction
- Multi-mode Combustion

The complete TNF14 Proceedings are available for download in pdf format from tnfworkshop.org. The pdf file includes the list of participants, workshop agenda, summary abstracts of the technical sessions, presentation slides, and two-page abstracts of 30 contributed posters.

The move to this new web site follows termination of support for turbulent combustion research at Sandia by the U.S. Department of Energy, Office of Basic Energy Sciences. Most of the content from the old site has been moved, and we look forward to an easier process of adding content in the future.

TNF14 ORGANIZING COMMITTEE

Robert Barlow, Andreas Dreizler, Benoît Fiorina, Christian Hasse, Matthias Ihme, Andreas Kempf, Peter Lindstedt, Assaad Masri, Joe Oefelein, Heinz Pitsch, Steve Pope, Dirk Roekaerts, Luc Vervisch

ACKNOWLEDGMENTS

The work of all the session coordinators and contributors is gratefully acknowledged. Sponsorship funds were provided by ANSYS, Continuum Lasers, Edgewave, ERCOFTAC, La Vision, Princeton Instruments, Sirah Lasers, and TU Darmstadt through the SFB/Transregio 150 Project. These contributions allowed reduction of registration fees for university faculty, postdocs, and students.

PLANNING

The 2020 TNF Workshop will be held in Adelaide, Australia prior to the 38th Combustion Symposium. It is likely that the schedules of the TNF, ISF, and PTF Workshops will again overlap on the Friday and Saturday before the Symposium, and it is expected that organizers will coordinate to make the combined event as informative and productive as possible.

HIGHLIGHTS OF PRESENTATIONS AND DISCUSSIONS

The sections that follow were condensed from session summaries in the full proceedings. Comments and conclusions given here are based on the perspectives of the authors and do not necessarily represent consensus opinions of the workshop participants. This summary does not attempt to address all topics discussed at the workshop or to define all the terms, acronyms, or references. Readers are encouraged to consult the complete TNF14 Proceedings and also the Proceedings of previous TNF Workshops, because each workshop builds upon what has been done before.

Sydney Compositionally Inhomogeneous Flames

Coordinators: Benoît Fiorina and Michael Mueller

The objective of this session was to compare recent simulations of the Sydney compositionally inhomogeneous piloted flames and survey progress since the last Workshop. Some key points are as follows: 1) An update on the experimental measurements was presented, including a comparison of previous datasets as well as new measurements at the University of Sydney for non-reacting flows made to directly address a number of modeling issues identified at the last Workshop associated with predictions of the mixture fraction field. 2) Analysis by the Princeton group revealed that the behavior of the pilot-coflow shear layer is very different for "cold" and "hot" configurations. All LES contributions underpredicted the breakdown of this shear layer in the reacting configuration. The influence of the predicted stability of the pilot-coflow shear layer on the variance between the computations and discrepancies with the experimental measurements for the mixture fraction remains an open question. 3) Analysis of the flame structure computed by all groups reveals difficulty in predicting the temperature field, especially downstream of the pilot-coflow shear layer. Identification of the cause of the discrepancies through a standard comparison between computed and measured scalar radial profiles is difficult. Post processing to compute the Wasserstein metric showed consistency among simulation results, and this approach should be further explored. 4) Some convergence among simulations compared to TNF13 is apparent, but difference between simulations and experiments remain. The next effort on this configuration should focus on analyzing existing results with the objective of writing a joint paper.

Update on Cambridge Swirl Flames

Coordinators: Benoît Fiorina, Andreas Kempf and Eray Inanc

The main objective of this session was to present new simulation results for the stratified swirl flames investigated at Cambridge and Sandia, with particular attention to CO modeling. New simulation results on the non-stratified, non-swirled SwB1 case were also compared with recently published flame-resolve simulations. For the swirled cases, five international groups contributed results based on their own established techniques. The results showed that the CO predictions in the swirled case are problematic close to the burner, unlike for the non-swirled variant. The Duisburg group demonstrated that the almost laminar flow in the large recirculation zone (RZ) in the swirl cases required a larger computational domain and longer run-time than for the non-swirled case. All groups applied adiabatic combustion models. While there is an effect of heat loss close to the bluff body surface, as demonstrated at TNF13 by the Paris group, the contributing groups showed that the main thermochemical properties of the fluid after three inner tube diameters were in good agreement when using an adiabatic solver. Generally, the computed Reynolds-averaged mean major quantities, such as momentum, equivalence ratio, temperature and mass fractions of CH_4, O_2, and CO_2, agreed well with the measurements slightly further downstream, whereas the spread angle of the swirled jet was under-predicted. Most of the deviations, however, occurred close to the bluff-body. Contributors came to the conclusion that the resolution and the settlement time of the RZ could cause these deviations. CO and H_2 mass fractions were over-estimated close to the burner. The closest agreement was obtained by a Monte-Carlo FDF method. The Duisburg-group also presented results using an ATF/FGM model with the same boundary conditions and computational grid, but the computationally more expensive Monte-Carlo technique provided a better agreement

for most quantities. Larger deviations were observed for the stratified cases SwB7 and SwB11. However, results suggest that stratification can be predicted acceptably well by using FGM.

Modeling of CO in Turbulent Flames

Coordinators: Andreas Kempf and Benoit Fiorina

This session focused on issues related to prediction of CO in LES of turbulent flames. By comparison with the temperature or major species mass fractions, the CO prediction is more sensitive to the modeling of detailed combustion chemistry and subgrid scale flame wrinkling, due to the wide range of time scales in CO chemistry. CO formation/consumption is sensitive to three physical phenomena: i) the flame enthalpy (or heat losses); ii) the flame regimes (premixed, non-premixed, stratified, etc.); and iii) the subgrid scale flame wrinkling. Three target cases were selected to establish the state-of-the-art: Preccinsta combustion chamber (stable, $\phi = 0.83$); Cambridge swirl flame (SwB3); and Sydney inhomogeneous flames (Lr75-57 and Lr75-80). After a brief review of experimental issues, modeling challenges to CO prediction in turbulent flames were discussed, and then results from the target cases were presented and analyzed.

Comparison between numerical and experimental data for the Preccinsta combustor showed that temperature is well captured by non-adiabatic simulations, unlike adiabatic computations that over predict temperature in the near wall region. Heat losses have a strong impact on the CO formation, such that adiabatic simulations strongly overestimate measured profiles. A strong effect of the mesh refinement is also observed. This behavior is attributed to the lack of modeling of the impact of subgrid scale flame wrinkling on the CO mass fraction.

Simulations of the Cambridge SwB3 flame show significant variation in the mean CO profiles. In particular, the overestimation of the CO production by the Thickened Flame model for LES is evident. Simulations conducted using a filtered wrinkled flamelet table show that accounting for the impact of subgrid scale flame wrinkling on filtered species improves the CO prediction.

Discussion on the Sydney piloted inhomogeneous jet flames highlighted difficulties in predicting the mixing and temperature fields, especially downstream of the pilot-coflow shear layer. It is therefore difficult to draw clear conclusions on the origins of the CO deviation. However, the results appear sensitive to the flame regime assumption made to tabulate the chemistry. In particular, premixed flamelet based models tends to overestimate the CO profiles, whereas tabulation based on non-premixed flame archetype are more adapted to this jet flame configuration.

Highly Turbulent Premixed Flames (Joint PTF/TNF Session)

Coordinators: Adam Steinberg, Peter Hamlington, Luc Vervisch, Matthias Ihme, Evatt Hawkes, Jeff Sutton

This joint session was presented in three parts. The first provided an overview of recent observations made through experiments and DNS regarding the structure and dynamics of highly turbulent premixed flames. The second covered methods and issues in modeling of such flames. The third dealt with needs for further improvements in simulations and experiments to address knowledge gaps.

Observations on structure and dynamics (Steinberg, Hamlington):

Experiments in high Karlovitz number flames have primarily involved multi-dimensional imaging (PLIF, Rayleigh, PIV). The most prevalent configurations have been atmospheric-pressure methane/air jet- or Bunsen-flames issuing into a large coflow of combustion products. Imaging experiments consistently show broadened preheat zones (CH_2O), but results on the transition to broadened reaction zones has not been fully consistent. Discrepancies may be due to different definitions of Karlovitz number, the influence of geometry, or effects of mixing between main

reactants and the hot coflow. Both DNS and experiments have shown significant stratification at the reaction zone in high-Ka flames having large differences in jet and coflow equivalence ratio.

The influence of combustion on turbulence has been a key area of interest, which has primarily been studied through DNS of isotropically forced turbulence. The flame influences the structure of the turbulence by suppressing small scales through increased temperature/viscosity, and by enhancing large scales through pressure-dilatation effects. The flame also induces anisotropy in the direction of the flame normal and changes the alignment of vorticity and strain rate. Both of these effects diminish with increasing Karlovitz number. Backscatter – viz. net up-scale transfer of kinetic energy – has been observed in DNS through analyses in physical space, Fourier space, and wavelet space. This process can lead to energization of large scale turbulent motions in some DNS.

Perspectives on modeling
(Vervisch) In the practice of real burners, it was discussed how high Karlovitz combustion actually goes with a drastic reduction of the Damköhler number. Two routes were examined to support the existence of low Damköhler combustion. First, the discrepancy between the enhancement in overall burning rate and the enhancement in flame surface area measured for high-intensity turbulence has been reported in the context of scaling laws for diffusivity enhancement from eddies smaller than the flamelet thickness. The factor quantifying this discrepancy is formalized as a closed-form function of the Karlovitz number. Second, basic scaling laws were presented which suggest that the overall decrease of the burning rate due to very fast mixing can be compensated by the energy brought to the reaction zone by burnt gases. The results confirm the possibility of reaching, with the help of a vitiated mixture, very high Karlovitz combustion before quenching occurs.

(Ihme) Three aspects were considered. First, a Lagrangian flamelet analysis was performed on three canonical DNS cases to identify whether these high-Ka flames retain an inherent flamelet character. This analysis showed the presence of an intact but weakened inner core flamelet structure that is well represented by 1D elongated flame-elements. Entrainment of hot combustion products by turbulent transport leads to mixing of the unburned reactants that can be well represented by a partially premixed reactor. Since the flame-structure and burning intensity is controlled by the upstream reactant mixture, it is unlikely that unstrained premixed flamelet methods are able to describe such flame regimes without taking into account the reactant mixing at the subgrid. Second, LES modeling efforts on vitiated flames were reviewed. It was concluded that current combustion models capture the main features of turbulent flame-structure at moderate Ka-regimes; in general, models were found to over predict the reactivity at higher Ka; and extensions of flamelet models show promise but lack key-physical aspects. Third, potential merits of combustion model adaptation and data assimilation techniques were discussed to improve predictions and take advantage of extensive measurements that are generated from high-speed, multi-dimensional measurements.

Needs for further improvement
(Hawkes) It was argued that the development of practical combustion models should be the primary objective of DNS work going forward. New opportunities were identified in conducting partial *a posteriori* tests, where some model inputs are taken directly from DNS, in order to focus attention of the performance of specific sub-models. Based on insights from very high-Re experiments, is was suggested that higher Re needs (somehow) to be accessed by DNS. The need to increase effort on cases with complex geometries (e.g., having recirculation zones, mean shear, etc.) was highlighted; these cases should have parametric sets and also preferably involve flows that can be computed straightforwardly with LES at resolutions where the models are actually doing some work.

(Sutton) Experimental needs were discussed in the context of current knowledge gaps, which include the understanding of configuration effects (i.e., geometry, pressure, turbulence generation, fuel type, etc.), characterization of the internal structure of turbulent flames, and the effects of turbulence-induced stratification. It was argued that specific measurement needs include

quantitative multi-scalar measurements, high-resolution velocity measurements, simultaneous velocity/scalar measurements, heat release rate measurements, and the coordination of new burner designs with modeling efforts. Mach number and compressibility effects were discussed; new measurements in turbulent, compressible flames have shown that turbulence is not attenuated through the flame, but rather flame-generated turbulence is observed. Finally, emerging capabilities to derive chemical mode and heat release rate from scalar measurements and to achieve high-spatial resolution in velocity measurements were highlighted.

Progress of Turbulent Sooting Flames (Joint ISF/TNF Session)

Coordinators: Bassam Dally and Michael Mueller

The objective of the session was to bring together the TNF and ISF turbulent flames communities to discuss common problems and strategies for addressing experimental and computational challenges in turbulent sooting flames. Overviews were presented on current experimental capabilities for turbulent sooting flames (time resolved LII, CARS, two-line atomic fluorescence for temperature, and krypton PLIF for mixture fraction) as well as target flames and computational comparisons. The two types of targets accentuate different aspects of soot-turbulence-chemistry interactions, with jet flames stressing small-scale interactions including slow PAH chemistry, and recirculating flows stressing large-scale interactions, notably the residence time at different mixture fractions where different growth mechanisms dominate. For comparisons with experimental measurements, progress between consecutive ISF Workshops has been rapid with decreasing variance between models with detailed model improvements being made based on insights from limited experimental measurements and DNS data. However, the fundamental challenge in understanding the underlying physics and uncovering the source of discrepancies is a lack of data, particularly (simultaneous) data on flame structure, combining temperature and speciation with soot measurements. These overviews were followed by comments from three panelists: Simone Hochgreb discussed experimental configurations, measurement techniques, and experimental challenges; William L Roberts highlighted recent progress at KAUST in making high-pressure measurements in turbulent sooting flames; Venkat Raman discussed the differences in the modeling challenges between jet flames and recirculating flows with respect to small-scale and large-scale intermittency. The importance of history in soot evolution was also discussed and the need to identify canonical configurations that match the history of soot evolution in technical combustion systems. Fundamental differences between detailed, PAH-based soot models and semi-empirical, acetylene-based soot models were also highlighted with a suggestion to design experiments to stress each class of models.

Enclosed Flames and Elevated Pressure

Coordinators: Christoph Arndt and Wolfgang Meier

Recent experiments and simulations of enclosed flames and flames at elevated pressure, as well as associated experimental and computational challenges, were discussed. In the first part of the session, contributions on experiments and simulations of swirl combustors at atmospheric and elevated pressure as well as a test case of a jet flame at elevated pressure were presented, including: “Experimental study on dynamics of lean premixed swirl flames” from Shanghai Jiao Tong University; “Experimental and numerical investigation of the response of a swirled flame to flow modulations in a non-adiabatic combustor” from Centrale Supélec; “SFB 606 Gas Turbine Model Combustor” from DLR Stuttgart; “LES studies on enclosed swirl flames in laboratory combustors” from the University of Cambridge; “High-pressure syngas jet flames (CHN)” from KAUST; and “LES studies on enclosed swirl flames in industrial combustors” from the University of Cambridge. The second part of the session focused on FLOX® and MILD combustion with contributions on: “Flameless combustion in a lab-scale furnace” from TU Delft; “Confined and pressurized jet in hot and vitiated coflow burner” from Adelaide and Sydney; “High-pressure enclosed jet flames” from DLR Stuttgart; and “Investigation of a high pressure jet flame with heat losses using tabulated and finite rate chemistry” from University Duisburg-Essen.

Flame Wall Interaction

Coordinators: Andreas Dreizler and Johannes Janicka

Flame-wall interaction (FWI) was introduced as a TNF topic in 2014, and a first target case of side-wall quenching (SWQ) was introduced at TNF13. FWI leads to flame quenching related to heat losses and incomplete combustion causing primary pollutant formation such as carbon monoxide (CO) and unburnt hydrocarbons (UHC). A deeper understanding of turbulent flames in the vicinity of walls is needed to improve combustion modelling for practical systems.

The experimental portion of this session introduced a Forced Laminar Axisymmetric Quenching (FLAQ) burner developed by the University of Melbourne to study FWI and the interaction of cooling jets with flames. An overview of experimental progress by TU Darmstadt to significantly enlarge the data base of the SWQ target flames was presented. Discussion focused on selected issues with the following conclusions: 1) Quenching distance is decreased for increasing wall temperatures causing an enhanced heat transfer rate within the FWI zone. 2) For a fixed wall temperature CO/T scatter plots for stoichiometric methane/air flames show an impact on CO-formation for wall distances below 0.2 mm whereas CO-oxidation at high temperatures (T > 1500 K) is influenced already for wall distances up to ~1 mm. These effects were attributed to differences in chemical time scales in relation to time scales for heat transfer. 3) Correlations of normalized heat release and curvature of premixed flames in the near-wall region indicate an influence of Lewis-number.

Compared to TNF13 a large group contributed FWI simulations, including both DNS and modelling studies of various configurations. Only a few of the many results and conclusions documented in the proceedings are mentioned here. The quenching distance for turbulent conditions decreases and the magnitude of the maximum wall heat flux increases in comparison to the corresponding laminar HOQ values for cases with Le<1. All the modelling assumptions associated with high Damköhler number ($Da \gg 1$) and presumed bi-modal PDF of c are rendered invalid close to the wall. Both conventional flame surface density (FSD) and scalar dissipation rate (SDR) closures for mean reaction rate break down in the near-wall region. Flame velocity seems to be the governing parameter in the turbulence-chemistry interaction more than flame thickness vs. turbulence length scales. Based on DNS studies, a modified FSD-based closure for mean reaction rate in terms of flame-wall interaction has been proposed. LES of the SWQ target case using detailed chemistry and FGM-based tabulated chemistry showed similar wall-normal temperature profiles but strongly different CO profiles due to large diffusion effects close to the wall that are not reflected in the FGM tabulation.

Multi-mode Combustion

Coordinator: Rob Gordon

This session follows from discussions in TNF13 on combustion regime indicators and reaction progress markers. Key information from TNF13 was briefly reviewed, then highlights were presented on recent progress in four areas: 1) Extention of chemical explosive mode analysis (CEMA) to include diffusion as well as local chemistry, allowing greater refinement in the identification of local combustion modes, including assisted ignition, auto-ignition, and local extinction in DNS of a high-Ka jet flame. 2) New applications of the gradient free regime identification (GFRI) method to derive chemical mode and heat release rate from experimental data. 3) An approach for selecting the most approprate models for local conditions within a simulation, based on a Combustion Model Compliance Indicator. 4) Development of a modeling approach based on Generalized Multi-Modal Manifolds.

Last Experiments at Sandia

Coordinator: Rob Barlow

This brief session outlined a series of visiting experiments conducted from March to July 2018 to take maximum advantage of the unique diagnostic capabilities of the Turbulent Combustion Laboratory before termination of DOE funding for experimental research on turbulent combustion at Sandia.

KEY CHALLENGES AND PRIORITIES

Multi-mode combustion continues to be a challenging area for fundamental understanding and for model development. There has been some convergence in simulations of the Sydney inhomogeneous flames. However, the sensitivity of these piloted flames to boundary conditions in experiments as well as simulations, particularly with respect to stability of the pilot-coflow shear layer, has complicated detailed comparison of measured and modeled results. Organizers have proposed a joint publication on the current state of understanding, and they have encouraged further analysis based on the Wasserstein metric to help quantify and interpret comparisons. One future goal in the context of multi-mode combustion might be to apply one modeling framework across regimes, which could be a single burner or multiple burners. A new multi-mode or Multi-Regime Burner (MRB), with well-controlled and characterized boundary conditions, has been developed by TU Darmstadt, and a first set of Raman/Rayleigh measurements has been conducted at Sandia (see posters by Butz et al. and Hartl et al.). Meanwhile, PIV/PLIF of the same configurations have been performed at Darmstadt. This burner could be a target case for TNF15.

Simulations of the Cambridge stratified swirl flames focused mainly on SwB3 (highest swirl number, 0.75 equivalence number in both streams). The high swirl cases exhibit a large, open recirculation zone that transports diluted products from far downstream all the way to the bluff body surface. This leads to a requirement for long run times to initialize the flow and scalar fields. Results for SwB11, (highest swirl, highest stratification) were inconclusive, due to the need for longer initialization. The highest stratification cases have and inner flow equivalence ratio of 1.125, and there appears to be some influence of Lewis number going to these cases. Further work to address these issues could be done. The new Darmstadt MRB cases also include stratified reaction zones that cross lean and rich mixture fraction values, so those flames may allow for investigation of these same issues without the complication of a very large recirculation zone.

Accurate modeling of CO remains a challenge, such that comparisons on three different target flames showed significant variation in CO predictions.

The joint PTF/TNF session on highly turbulent premixed flames provided an excellent overview of the current state of knowledge. One key point, taken from recent DNS of the Lund flames and recent experiments on the HiPilot burner, is that the highest Ka cases, which are generated at laboratory scale by surrounding a very lean reactant flow by combustion products of a more robust mixture, actually burn as stratified flames. That is, significant mixing between jet and coflow occurs before heat release, such that heat release occurs at intermediate values of mixture fraction and in the presence of a mixture fraction gradient. Creating a truly premixed flame, with uniform equivalence ratio across the flame brush, at laboratory scale remains a significant challenge. Further work is will be needed to explore the high-Ka regime of uniformly premixed flames. That said, the high-Ka stratified flames are very interesting in themselves and could be a good topic for further collaborative research. Emerging diagnostics for very-high-resolution velocity measurements and simultaneous velocity-scalar measurements show significant potential to provide new insights and valuable data on highly turbulent flames.

For turbulent sooting flames, the fundamental challenge in understanding the underlying physics and uncovering the source of discrepancies is a lack of data, particularly simultaneous data on flame structure, combining temperature and speciation with soot measurements. Filtered Rayleigh scattering combined with PIV and LII might be fruitful diagnostic direction. Raman scattering is challenging even in blue, upstream regions of sooting flames, so it is not obvious that detailed multi-scalar comparable to those acquired in TNF flames can ever become available for sooting flames. However, benefit can be gained by using the same burner geometries with non-sooting and sooting flames, that have as many parameters in common as possible.

The side-wall-quench (SWQ) flame is proposed as a future TNF target configuration. Priorities for experimental work are to measure more scalars, measure wall temperature and heat transfer, and conduct parametric variation of such things as wall temperature, surface coatings, fuel, and effusion cooling.

Important progress has been made in developing regime indicators for both simulation (CEMA including both chemistry and diffusion effects) and experiments (application GFRI methods to lifted flames and to DNS of premixed and mildly stratified flames). These and similar regime identification tools can provide insights on variations in local reaction zone structure and might be included as metrics in future comparisons between experiments and simulations.

Consideration of more complex fuels, specifically DME, took a pause for TNF14, although there work on these flames was presented at the Symposium. Repeating comments from TNF13: It is important to continue working with fuels more complex than methane. Goals should comprise computations of the entire piloted DME jet flame series (Sandia DME D-G') with focus on the accurate prediction of the degree of localized extinction. We should also seek clarification of the predictions' dependencies on the chemical mechanisms. This may include the need for a quantitative comparison of formaldehyde, as this is the measured species with the most pronounced differences for all flame and flow conditions. Quantitative LIF of formaldehyde remains a challenge. Direct measurements of intermediate species by Raman scattering have proven difficult, and no further work in this area will be possible at Sandia.

In addition to new measurements in the Darmstadt multi-regime burner (MRB), experiments have been conducted on a new version of the Sydney hot-coflow burner, which includes thermal insulation around the central jet to minimize heat transfer to the jet fluid upstream of the exit. Two types of flames have been measured: 1) Lean premixed CH_4/air jet flames into hot H_2/air products with temperature matching the adiabatic equilibrium temperature of the jet; 2) Rich CH_4/air jets, producing lifted partially-premixed flames. The first cases are analogous to the Sydney PPJB flames (Dunn et al.) but with only two streams rather than three. The lifted flame conditions were selected to emphasize either flame propagation or auto-ignition as the primary stabilization mechanism. These data sets may be available before the next workshop.

blank

TNF 2018 Participant List

	Last Name	First Name	Title	Affiliation
1	Akaotsu	Shota	Mr.	Tohoku University
2	Arndt	Christoph	Dr.	German Aerospace Center (DLR)
3	Baik	Seung Jin	Dr.	University of Duisburg-Essen
4	Barlow	Robert	Dr.	Sandia National Laboratories
5	Bénard	Pierre	Dr.	CORIA
6	Boehm	Benjamin	Dr.	Technical University of Darmstadt
7	Borukhovich	Efim	Dr.	University of Duisburg-Essen
8	Boxx	Issac	Dr.	German Aerospace Center (DLR)
9	Casey	Tiernan	Dr.	Sandia National Laboratories
10	Chen	Zhi	Dr.	Cambridge University
11	Cifuentes-Rubio	Luis-Hernando	Dr.	University of Duisburg-Essen
12	D'Ausilio	Alessandro	Mr.	Ghent University
13	De	Santanu	Prof.	IIT Kanpur
14	Dibble	Robert	Prof.	KAUST
15	Domingo	Pascale	Dr.	CNRS-CORIA
16	Dreizler	Andreas	Prof.	Technical University of Darmstadt
17	Dunn	Matthew	Dr.	The University of Sydney
18	Evans	Michael	Dr.	University of Adelaide
19	Ferraro	Federica	Dr.	German Aerospace Center (DLR)
20	Fiorina	Benoît	Prof.	Centrale Supélec, EM2C Laboratory, CNRS
21	Fuest	Frederik	Dr.	La Vision
22	Galeazzo	Flavio	Dr.	University of São Paulo
23	Geyer	Dirk	Prof.	Darmstadt University of Applied Sciences
24	Gomzikov	Leonid	Mr.	UEC-Aviadvigatel JSC
25	Gordon	Robert	Prof.	The University of Melbourne
26	Groevdal	Fredrik	Mr.	NTNU
27	Gruber	Andrea	Dr.	SINTEF Energy Research
28	Gruhlke	Pascal	Ms.	University of Duisburg-Essen
29	Guiberti	Thibault	Dr.	KAUST
30	Hampp	Fabian	Dr.	Imperial College
31	Han	Wang	Dr.	Technical University of Darmstadt
32	Han	Xiao	Mr.	Beihang University/Imperial College
33	Hartl	Sandra	Dr.	Technical University of Darmstadt
34	Hassanaly	Malik	Mr.	University of Michigan
35	Hasse	Christian	Prof.	Technical University of Darmstadt

36	Hawkes	Evatt	Prof.	University of New South Wales
37	Hernandez Perez	Francisco	Dr.	KAUST
38	Hochgreb	Simone	Prof.	Cambridge University
39	Ihme	Matthias	Prof.	Stanford
40	Im	Hong	Prof.	KAUST
41	Inanc	Eray	Mr.	University of Duisburg-Essen
42	Janicka	Johannes	Prof.	Technical University of Darmstadt
43	Ji	Weiqi	Mr.	Tsinghua University
44	Jiang	Bin	Mr.	The University of Melbourne
45	Jones	Bill	Prof.	Imperial College
46	Kempf	Andreas	Prof.	University of Duisburg-Essen
47	Kim	Namsu	Mr.	Korea Institute of Energy Research
48	Kim	Yongmo	Prof.	Hanyang University
49	Klimenko	Alex	Dr.	The University of Queensland
50	Kruljevic	Boris	Mr.	Ghent University
51	Langella	Ivan	Dr.	University of Loughborough
52	Lee	Bok Jik	Prof.	Gwangju Institute of Science and Technology
53	Li	Lei	Dr.	Shanghai Jiao Tong University
54	Li	Zhiyi	Ms.	Université libre de Bruxelles
55	Li	Zisen	Mr.	University of new South Wales
56	Lindstedt	R. Peter	Prof.	Imperial College
57	Liu	Xunchen	Dr.	Shanghai Jiao Tong University
58	Lu	Hao	Prof.	Huazhong University of Science & Technology
59	Luo	Kai	Prof.	University College London
60	Luo	Kun	Prof.	Zhejiang University
61	Magnotti	Gaetano	Prof.	KAUST
62	Maio	Giampaolo	Mr.	Centrale Supélec, EM2C Laboratory, CNRS
63	Masri	Assaad	Prof.	The University of Sydney
64	Meeks	Ellen	Dr.	ANSYS - Reaction Design
65	Meier	Wolfgang	Dr.	German Aerospace Center (DLR)
66	Menser	Jan	Mr.	University of Duisburg-Essen
67	Meraner	Christoph	Mr.	NTNU
68	Mohri	Khadijeh	Dr.	University of Duisburg-Essen
69	Moureau	Vincent	Dr.	CORIA - CNRS
70	Mueller	Michael	Prof.	Princeton University
71	Navarro-Martinez	Salvador	Dr.	Imperial College London
72	Neuber	Gregor	Mr.	ITV, University of Stuttgart
73	Perry	Bruce	Mr.	Princeton University

74	Peterson	David	Dr.	Air Force Research Laboratory
75	Pope	Steve	Prof.	Cornell University
76	Raman	Venkat	Prof.	University of Michigan
77	Rankin	Brent	Dr.	Air Force Research Laboratory
78	Ren	Zhuyin	Prof.	Tsinghua University
79	Rieth	Martin	Dr.	Sandia National Laboratories
80	Rivera	Jacob	Mr.	The University of Melbourne
81	Roekaerts	Dirk	Prof.	Delft University of Technology
82	Scholtissek	Arne	Mr.	Technical University of Darmstadt
83	Sinha	Harish	Mr.	Princeton Instruments
84	Sorrentino	Giancarlo	Prof.	University Federico II of Naples
85	Stein	Oliver	Dr.	ITV, University of Stuttgart
86	Steinberg	Adam	Prof.	Georgia Tech
87	Sutton	Jeff	Prof.	Ohio State University
88	Unterberger	Andreas	Mr.	University of Duisburg-Essen
89	van Oijen	Jeroen	Dr.	Eindhoven University of Technology
90	Vervisch	Luc	Prof.	INSA - CORIA - CNRS
91	Wang	Bosen	Mr.	ITV, University of Stuttgart
92	Wehrfritz	Armin	Dr.	University of New South Wales
93	Yang	Yue	Prof.	Peking University
94	Yi	Tongxun	Dr.	Spectral Energies
95	You	Jiaping	Mr.	Peking University
96	Zhao	Xinyu	Prof.	University of Connecticut
97	Zhou	Bo	Dr.	Sandia National Laboratories
98	Zhou	Hua	Dr.	Tsinghua University

blank

TNF2018 Workshop – Agenda

27 – 28 July 2018
Trinity College Conference Centre
Dublin, Ireland

Friday, July 27:	**Morning (Davis Theatre)**
8:00 – 8:45	Arrival and Badge Pick-up Hang posters in designated locations
8:45 – 9:00	Introduction and Announcements (Rob Barlow)
9:00 – 10:30	Sydney Compositionally Inhomogeneous Flame Comparisons (Coordinators: Benoît Fiorina, Michael Mueller)
10:30 – 11:00	*Coffee Break (Poster Session)*
11:00 – 12:00	Cambridge Stratified Swirl Flame Comparisons (Coordinators: Andreas Kempf, Benoît Fiorina, Eray Inanc)
12:00 – 13:00	Modeling of CO (Coordinators: Benoît Fiorina, Andreas Kempf)
13:00 – 14:00	*Buffet Lunch (Dining Hall)*
Friday, July 27:	**Afternoon (Davis Theatre) Joint Session of the TNF and PTF Workshops on Highly Turbulent Premixed Flames**
14:00 – 15:00	Structure and dynamics of highly turbulent flames (Coordinators: Peter Hamlington, Adam Steinberg)
15:00 – 16:00	Modeling of highly turbulent flames (Coordinators: Matthias Ihme, Luc Vervisch)
16:00 – 16:30	*Coffee Break (Poster Session)*
16:30 – 17:30	Needs for further improvements (Coordinators: Evatt Hawkes, Jeff Sutton)
18:00 –22:00	*Poster Session and Reception (Dining Hall)*
18:45–	*Fork Supper (Dining Hall)*

TNF2018 Workshop – Agenda

27 – 28 July 2018
Trinity College Conference Centre
Dublin, Ireland

Saturday, July 28:	**Burke Theatre for the 1st Session**
8:30 – 10:00	Joint Session with ISF: Linkages between sooting and soot-free turbulent flames (Coordinators: Bassam Dally, Michael Mueller)
10:00 – 10:30	*Coffee Break (Poster Session)*
	Davis Theatre
10:30 – 11:45	Enclosed Flames and Elevated Pressure 1: Model GT Combustors and Diagnostics for High Pressure (Coordinators: Wolfgang Meier, Christoph Arndt)
11:45 – 13:00	Enclosed Flames and Elevated Pressure 2: FLOX and MILD Combustion (Coordinators: Wolfgang Meier, Christoph Arndt)
13:00 – 14:00	*Buffet Lunch (Dinning Hall)*
14:00 – 15:30	Flame-Wall Interactions (Coordinators: Andreas Dreizler, Johannes Janicka)
15:30 – 16:00	*Coffee Break (Poster Session)*
16:00 – 17:00	Multi-mode combustion: Combustion Mode analysis, measurement and modelling (Coordinator: Rob Gordon)
17:00 – 17:30	Final Discussion, Action Items, and Planning (Coordinators: Rob Barlow, Andreas Dreizler)
17:30	*Adjourn*
18:45	Dinner Meeting of the TNF Organizing Committee and Session Coordinators at The Church, Junction of Mary St & Jervis St, Dublin.

Sydney Compositionally Inhomogeneous Flames

Coordinators: Benoît Fiorina, Michael E Mueller

The objective of this session was to compare recent simulations of the Sydney compositionally inhomogeneous piloted flames and survey progress since the last Workshop. The burner geometry consists of two concentric tubes surrounded by a pilot annulus and a co-flowing air stream. In the configuration considered in the Workshop, the central tube is fed with fuel and the concentric annulus fed with air. A single central tube recess distance of 75 mm was considered with two bulk jet velocities of 59 m/s and 80 m/s with varying degrees of local extinction (FJ200-5GP-Lr75-57 and FJ200-5GP-Lr75-80). At this recess distance, the fuel-air mixture exiting the burner has high degrees of composition inhomogeneity resulting in premixed combustion near the nozzle exit in the vicinity of the pilot transition to nonpremixed combustion downstream. Such mixed mode combustion processes are very much representative of practical combustion systems and pose a significant challenge for combustion model validation, particularly model that prescribe *a priori* the asymptotic mode of combustion.

The session consisted of four major parts. First, a brief overview of the burner was presented. Second, an update on the experimental measurements was presented including a comparison of previous datasets as well as new measurements at the University of Sydney for non-reacting flows made to directly address a number of modeling issues identified at the last Workshop associated with predictions of the mixture fraction field. Third, comparisons of mixing in both the non-reacting flow and reacting flows were presented and remaining modeling challenges identified. Finally, detailed flame structure comparisons were made.

At the previous Workshop, significant variance was observed in computational predictions of the mixture fraction field, even with the use of a common inflow boundary condition provided by Princeton for all cases. To aid in understanding this variance, the University of Sydney conducted an expansive experimental campaign for non-reacting flows. Two non-reacting configurations were considered: a “cold” fuel/air configuration with an unlit fuel/air pilot and a “hot” air/air configuration with a lit fuel/air pilot. Multiple recess distances and jet velocities were made available. For both the “cold” and “hot” non-reacting configurations, computational results were able to reproduce the mean and fluctuating streamwise velocity profiles, and the variance in the predictions of the mean profiles were significantly smaller between the groups for the non-reacting cases than for the reacting cases, even when using the exact same boundary conditions. Subsequent analysis by the Princeton group revealed that the pilot-coflow mixing was very different between the three configurations. In the “cold” non-reacting configuration, the coflow rapidly mixes with the low momentum-flux pilot. In the “hot” non-reacting configuration, the coflow mixes significantly slower with the high momentum-flux pilot, but the Princeton LES revealed that the pilot-coflow shear layer remained laminar in the near-field. Conversely, in the reacting configuration, the pilot-coflow shear layer becomes unstable, qualitatively consistent with the experimental measurements (e.g., RMS temperature and mixture fraction) but not quantitatively correct in any LES contribution, with all LES contributions tending to underpredict the breakdown of this shear layer. The experimental results indicate high sensitivity of blow-off to pilot conditions, which is perhaps related to the pilot-coflow shear layer stability. The influence of the predicted stability of the pilot-coflow shear layer on the

variance between the computations and discrepancy with the experimental measurements for the mixture fraction remains an open question. A number of suggestions for follow-up sensitivity analyses was discussed including turbulence models and grid resolution.

Analysis of the flame structure computed by all groups reveals difficulty in predicting the temperature field, especially downstream of the pilot-coflow shear layer. Generally, the expansion of the jet is overpredicted, judging from flow profiles. The reacting layer position is very sensitive to both fuel-air mixing and turbulent combustion, so identification of the cause of the discrepancies through a standard comparison between computed and measured scalar radial profiles is difficult at this point. To address this challenge, simulation results have been post-processed to compute the Wasserstein metric, which enables a more quantitative comparison of simulation results. Preliminary results and analysis show consistency between simulation results, but the Wasserstein analysis should be further explored to assess the ability of the simulations to predict multiple combustion regimes.

Compared to the joint study conducted two years ago at the previous Workshop, a convergence between the simulations is observed. Indeed, there is less dispersion between the computational results, but the difference between the simulations and the experimental data seems to have reached an asymptote. The modeling exercise is indeed difficult because of the number of physical challenges to overcome in this particular configuration: multiple combustion regimes, multiple streams, shear layer instabilities, turbulence, etc. It has been concluded that the next effort on this configuration should focus on analyzing existing results with the objective of writing a joint paper with contributors who are interested. It has been also suggested to add for the next TNF a new configuration in this session which eliminates some phenomena that we do not wish to focus on so we can further investigate multi-mode combustion issues. An interesting candidate could be the Multi Regime Burner currently being investigated by TU Darmstadt.

Sydney Compositionally Inhomogeneous Flame

Benoît Fiorina
EM2C Laboratory
CentraleSupélec

Michael E. Mueller
Department of Mechanical and Aerospace Engineering
Princeton University

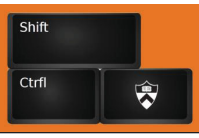

International Workshop on Measurement and Computation of Turbulent Flames
Dublin, Ireland
July 27, 2018

Outline

- Outline of Session
  - Overview of Burner (Mueller)
  - Target Cases (Mueller)
  - New Experimental Data (Mueller)
  - Computational Challenges with Mixing (Mueller)
  - Computational Contributions (Fiorina)
  - Computational Comparisons (Fiorina)
  - Computational Comparisons: Wasserstein (Ihme)
  - Summary and Conclusions (Fiorina)
  - Discussion (Fiorina/Mueller)

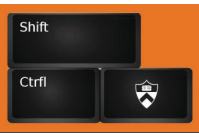

Compositionally Inhomogeneous

- Overview of Burner[1,2,3]
  - Geometrically similar to previous Sydney piloted burners
    - Fuel: CH_4
    - Pilot (5GP): C_2H_2, H_2, CO_2, N_2, air to match the C/H ratio and equilibrium temperature of methane

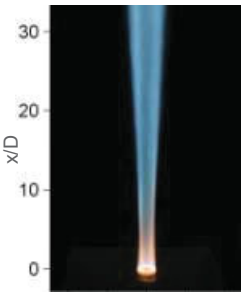

  - Rather than homogeneous fuel air mixture in the central jet, air and fuel and injected through an inner jet and annulus within the burner nozzle
    - Emphasis on the fuel injected in the inner jet and air injected in the annulus (FJ)
    - Measurements also available with air injected in inner jet and fuel injected in the annulus (FA)

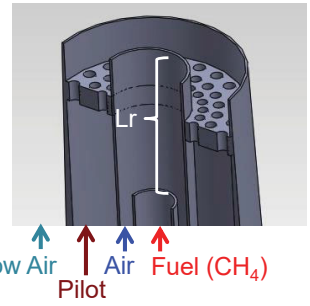

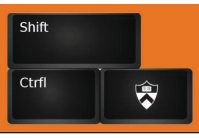

[1]S. Meares, V.N. Prasad, G. Magnotti, R.S. Barlow, A.R. Masri, Proc. Combust. Inst. 35 (2014) 1477-1484
[2]R.S. Barlow, S. Meares, G. Magnotti, H. Cutcher, A.R. Masri, Combust. Flame 192 (2015) 3516-3540
[3]H.C Cutcher, R.S. Barlow, G. Magnotti, A.R. Masri, Proc. Combust. Inst. 36 (2017) 1737-1745

Compositionally Inhomogeneous

- Overview of Burner
  - Recess distance of inner pipe can be varied to range from no premixing to inhomogeneous premixing to homogeneous premixing
    - Emphasis on inhomogeneous premixing

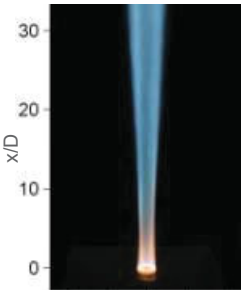

Fuel/Air Mixture at Nozzle Exit

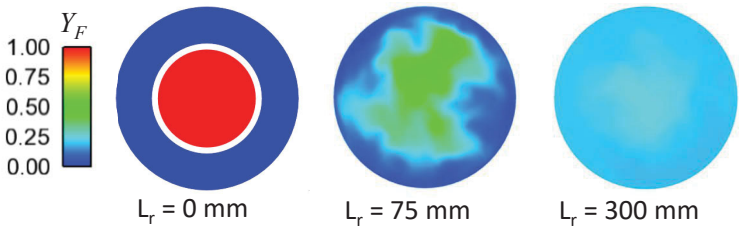

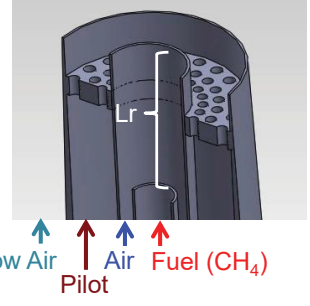

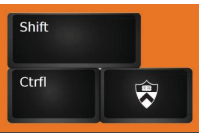

Compositionally Inhomogeneous

- Overview of Burner
  - Enhancement of Blow-Off Velocity

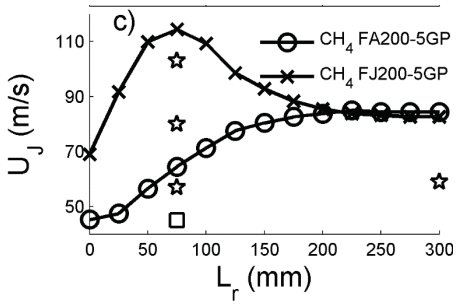

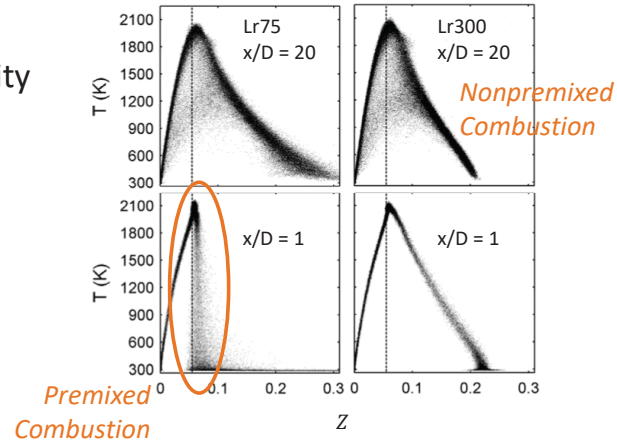

- Maximum stability at intermediate recess distance with inhomogeneity but only in FJ configuration
- Attributed to stoichiometric mixtures and subsequent premixed combustion adjacent to the pilot

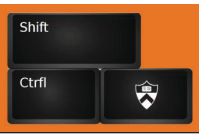

Compositionally Inhomogeneous

- Nomenclature

FJ200-5GP-Lr75-57

Configuration
FJ=Fuel in Central Jet
FA=Air in Central Jet

Central Air-Fuel Volume Flow Rate Ratio

Pilot
3GP=Three-Gas
5GP=Five-Gas

Recess Distance (mm)

Jet Bulk Velocity (m/s)

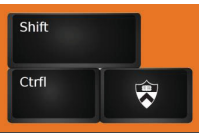

Updates on the Sydney Piloted Inhomogeneous Burner

H. Cutcher[1], R.S. Barlow[2], A.R. Masri[1]

[1]School of Aerospace, Mechanical and Mechatronic Engineering, The University of Sydney, NSW 2006, Australia

[2]Sandia National Laboratories, Livermore CA, USA

2018 International Workshop on Measurements and Computations of Turbulent Flames (TNF-14)

Dublin, Ireland, July 27–28, 2018

Raman-Rayleigh-LIF Dataset Summary

Three datasets now available:

- I2013-3GP
- I2013-5GP
- I2015-5GP

Datasets I2013-3GP and I2013-5GP have previously been available separately and provided temperature and major species mass fraction collected using a 100 μm data spacing at 7 axial locations (x/D = 1, 5, 10, 12, 15, 20 and 30).

Dataset I2015-5GP consists on new measurements on the same five flames as seen in I2013-5GP but using a 20 μm data spacing with measurements at three additional axial locations (x/D = 1, **2**, **3**, 5, **7**, 10 ,12, 15, 20 and 30) and includes measurements of three dimensional scalar dissipation rates in addition to temperature and composition.

Raman-Rayleigh-LIF Dataset Summary

Three dataset details:

I2013-3GP	Lr (mm)	U_j (m/s)	U_j/U_{bo}	Re	Res (µm)	x/D
FA200-3GP-Lr100-82	100	82	0.94	38300	100	1, 5, 10, 12, 15, 20, 30
FJ200-3GP-Lr300-82	300	82	0.78	38300	100	1, 5, 10, 12, 15, 20, 30
FJ200-3GP-Lr100-82	100	82	0.57	38300	100	1, 5, 10, 12, 15, 20, 30
FJ200-3GP-Lr100-115	100	115	0.80	53600	100	1, 5, 10, 12, 15, 20, 30
FJ200-3GP-Lr100-139	100	139	0.97	65000	100	1, 5, 10, 12, 15, 20, 30
I2013-5GP						
FA200-5GP-Lr75-45	75	45	0.70	21200	100	1, 5, 10, 12, 15, 20, 30
FJ200-5GP-Lr300-59	300	59	0.70	27600	100	1, 5, 10, 12, 15, 20, 30
FJ200-5GP-Lr75-57	75	57	0.50	26800	100	1, 5, 10, 12, 15, 20, 30
FJ200-5GP-Lr75-80	75	80	0.70	37500	100	1, 5, 10, 12, 15, 20, 30
FJ200-5GP-Lr75-103	75	103	0.90	48300	100	1, 5, 10, 12, 15, 20, 30
I2015-5GP						
FA200-5GP-Lr75-45	75	45	0.70	21200	20	1, **2**, **3**, 5, **7**, 10, 12, 15, 20, 30
FJ200-5GP-Lr300-59	300	59	0.70	27600	20	1, **2**, **3**, 5, **7**, 10, 12, 15, 20, 30
FJ200-5GP-Lr75-57	75	57	0.50	26800	20	1, **2**, **3**, 5, **7**, 10, 12, 15, 20, 30
FJ200-5GP-Lr75-80	75	80	0.70	37500	20	1, **2**, **3**, 5, **7**, 10, 12, 15, 20, 30
FJ200-5GP-Lr75-103	75	103	0.90	48300	20	1, **2**, **3**, 5, **7**, 10, 12, 15, 20, 30

9

I2013-5GP and I2015-5GP Comparison

- Initially temperature profiles are similar while there is some variation in mixture fraction profiles.
- As axial distance increases significant differences in the temperature profiles appear with the 2013 flames experiencing greater levels of local extinction.
- Differences are believed to the result of changes to mixing upstream of the burner exit, flowrate metering, and potential co-flow variations.

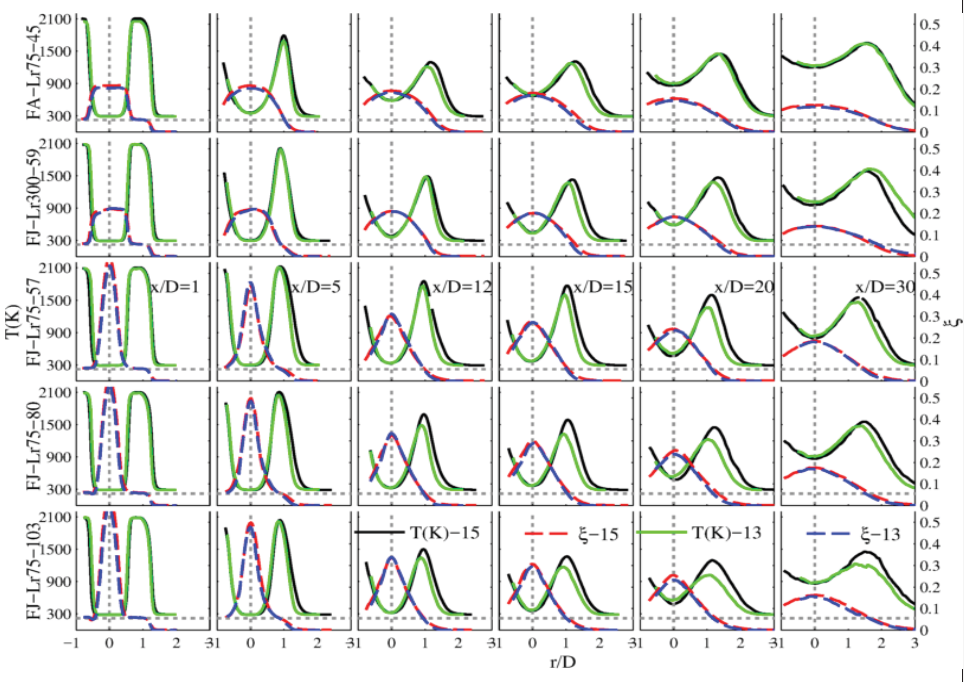

10

New LDV Measurements

Two new sets of flow field measurements from two component LDV are now available:

› Jet measurements in selected 5GP flames:

Case	Reacting	Pilot	U_p (m/s)	Lr (m)	U_j (m/s)	Jet Comp.	Locations (x/D)
FJ200-5GP-Lr300-59	Yes	5GP	3.72	300	59	Air/CNG	0.133, 1, 5, 10, 20, 30
	No						
FJ200-5GP-Lr75-57	Yes			75	57	Air/CNG	0.133, 1, 5, 10, 20, 30
	No						
FJ200-5GP-Lr75-80	Yes			75	80	Air/CNG	0.133, 1, 5, 10, 20, 30
	No						

› Boundary condition measurements of the pilots and co-flow:

Case	Reacting	Pilot	U_p (m/s)	Lr (m)	U_j (m/s)	Jet Comp.	Locations (x/D)
3 Gas Pilot	Yes	3GP	3	300	37.73	Air	0.133, 1.33
5 Gas Pilot	Yes	5GP	3.72	300	37.73	Air	0.133, 1.33
Co-flow	No	-	-	-	-	-	0.133

Non-reacting Jet Measurements

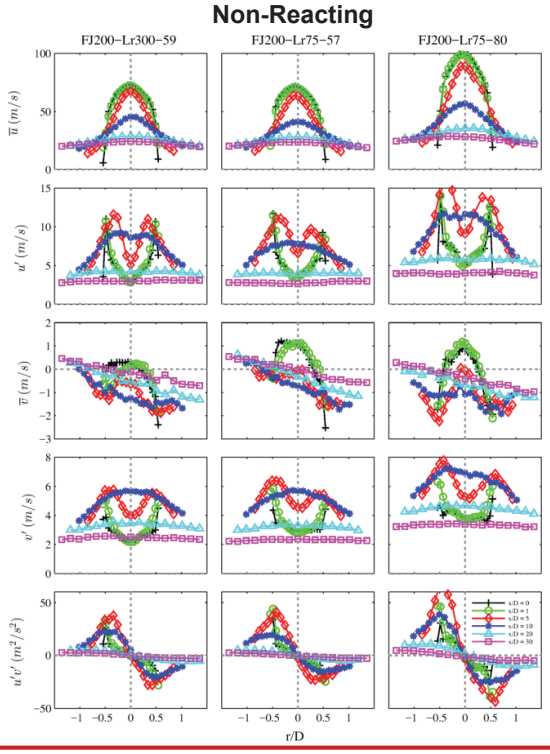

- Centreline axial velocities are approximately 1.25 the bulk jet velocity at x/D =0.13.
- Axial velocity profiles of FJ-Lr300-59 and FJ-Lr75-57 are similar despite differences in mixing profile.
- Mean radial velocities are approximately two orders of magnitude lower than the axial component.
- Reynold's stress peaks at x/D = 5.

Reacting Jet Measurements

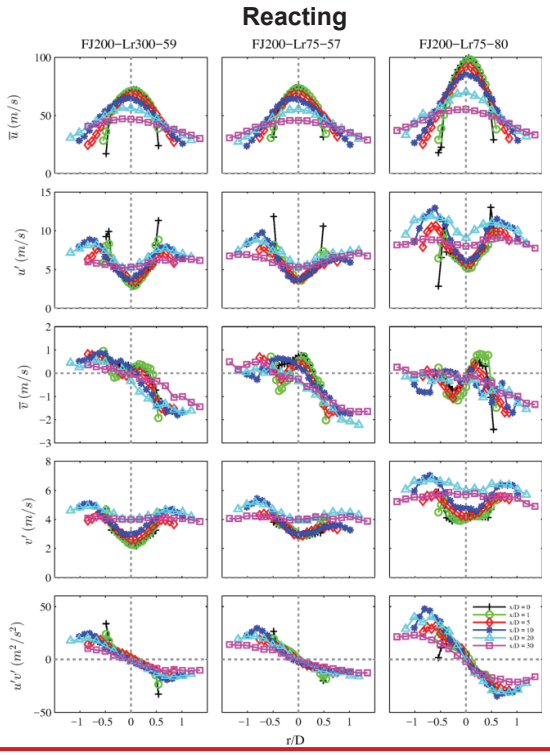

- Velocity profiles at x/D =0.13 are similar to their non-reacting counterparts
- Decay of mean axial velocity is approximately linear with axial distance.
- Reynold's stress peaks at around x/D=10 which corresponds to the peak in local extinction (x/D≈12).

Pilot and Co-flow Measurements

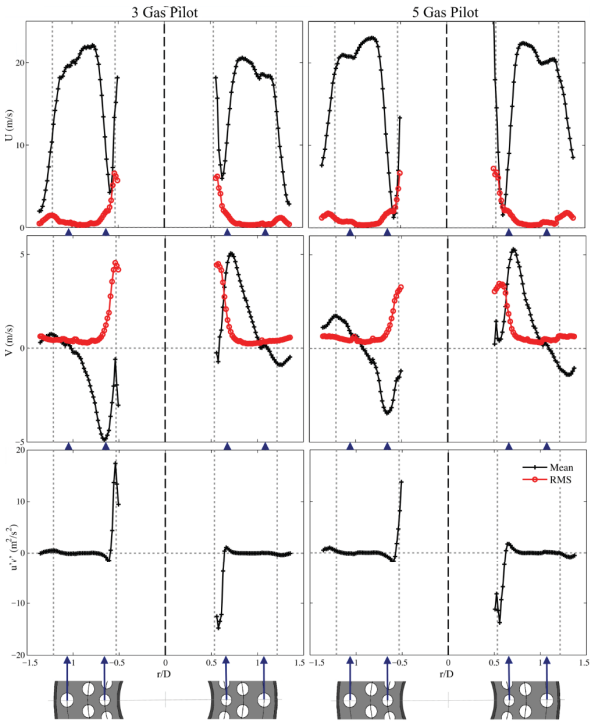

- Pilot axial velocity profiles show peaks which correspond with the location of pilot holes
- Shear layer with the jet (as indicated by Reynold's stress) extends 0.4-0.5mm into the pilot.
- Co-flow boundary layer is approximately 3.5-4mm wide.

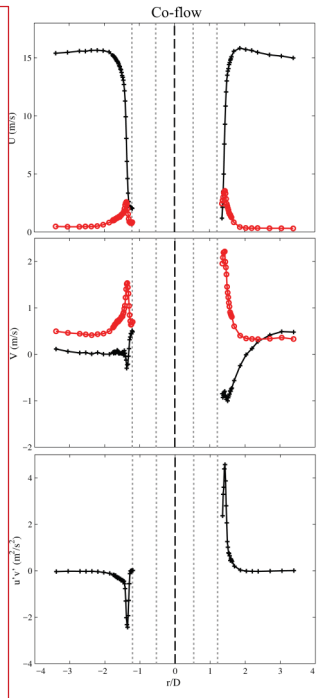

Compositionally Inhomogeneous

- Cases of Interest

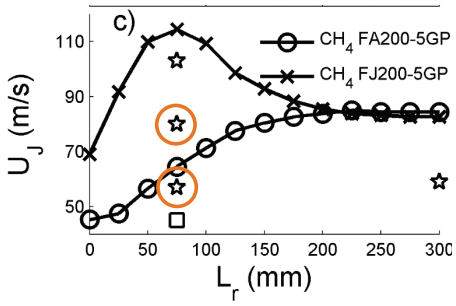

  - Focus on two cases: FJ200-5GP-Lr75-59 and FJ200-5GP-Lr75-80
    - Varying degrees of local extinction
  - Mixed mode combustion challenging to the models in the near-field but “relaxes” to nonpremixed combustion downstream

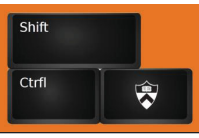

Compositionally Inhomogeneous

- Some Initial Computational Results

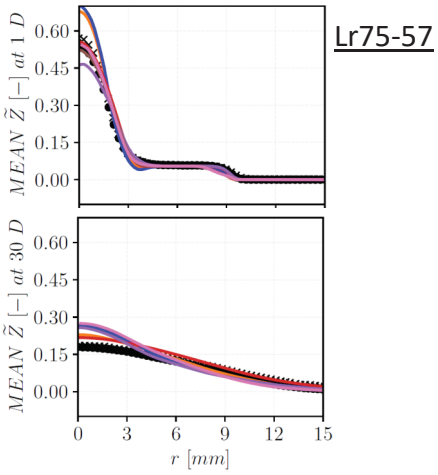

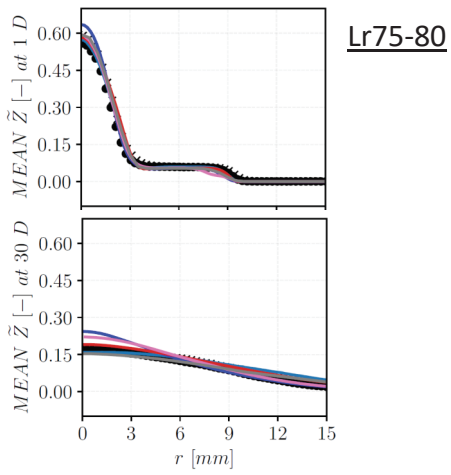

  - Observation: Even if a simulation used the correct boundary condition, mixing tended to be underpredicted downstream

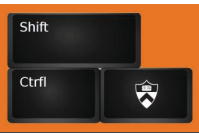

Compositionally Inhomogeneous

- Some Initial Computational Results

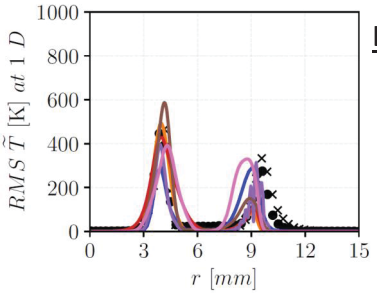

Lr75-57

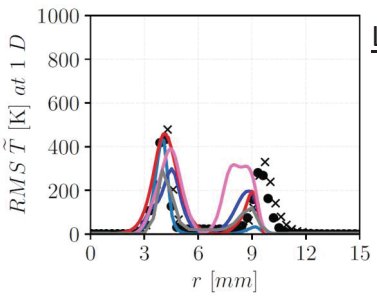

Lr75-80

  - Observation: The fluctuations in temperature (mixture fraction) are correctly predicted in the shear layer between the jet and the pilot but not between the pilot and the coflow
    - Shift in maximum toward the pilot (insensitive to everything)
    - Generally smaller magnitude (sensitive to everything)
  - What is going wrong with the mixing?

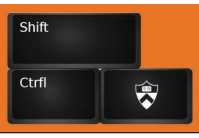

Compositionally Inhomogeneous

- Two New Non-Reacting Data Sets
  - Cold Pilot
    - Velocity (LDV)
    - FJ200-5GP-Lr300-59
    - FJ200-5GP-Lr75-57
    - FJ200-5GP-Lr75-80
  - Hot Pilot
    - Velocity (LDV)
    - FJ200-5GP-Lr300-59
    - FJ200-5GP-Lr75-80
  - Big thanks to Assaad Masri in true TNF spirit!

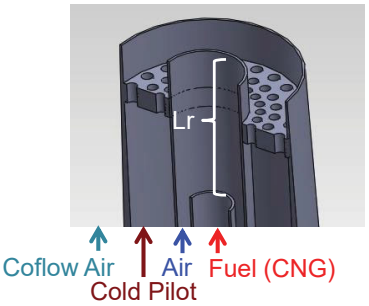

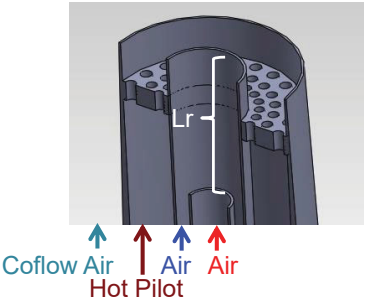

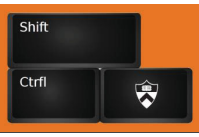

Compositionally Inhomogeneous

- Some More Computational Results
  - Cold Pilot: Lr75-57

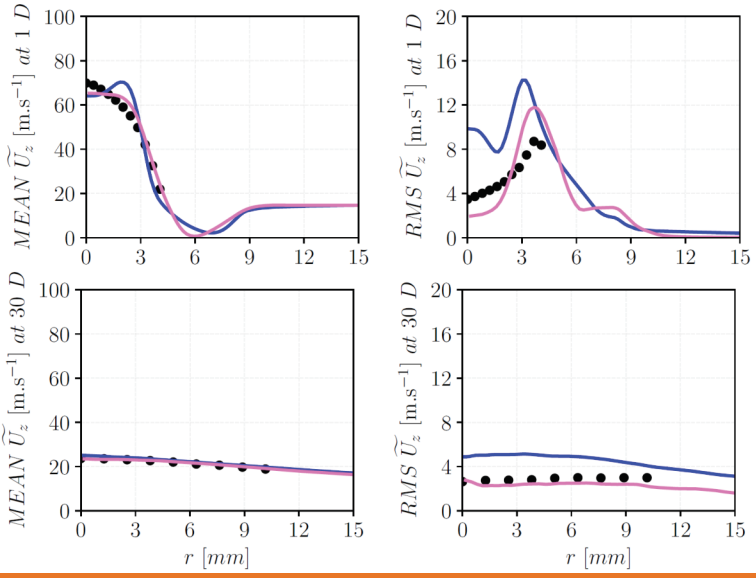

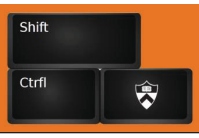

Compositionally Inhomogeneous

- Some More Computational Results
  - Cold Pilot: Lr75-80

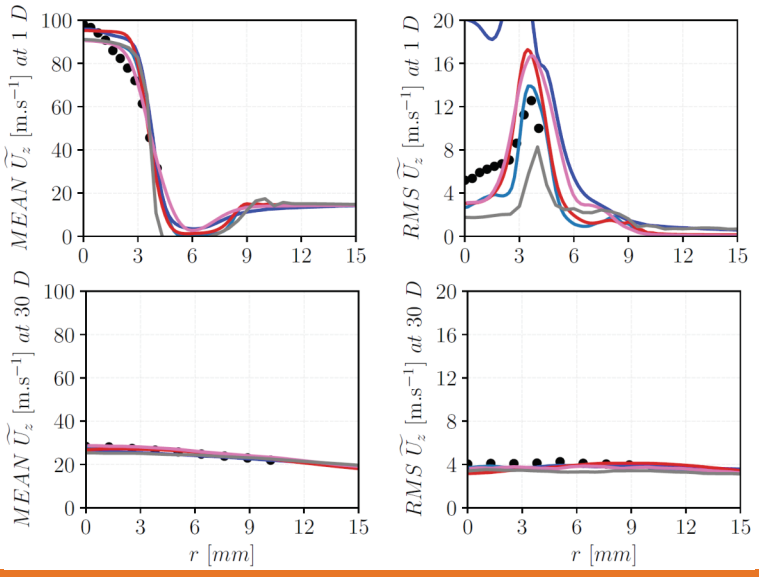

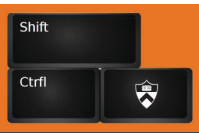

Compositionally Inhomogeneous

- Some More Computational Results
  - Hot Pilot: Lr75-80

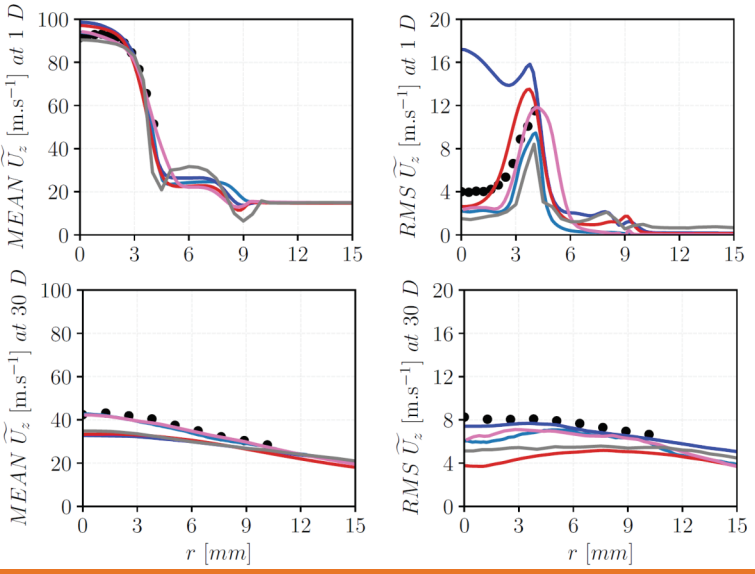

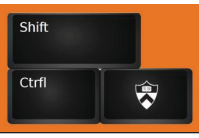

Compositionally Inhomogeneous

- Some More Computational Results

  - Conclusion: For the most part, all of the models are able to capture the velocity fields in the non-reacting flows whether the pilot is hot or cold (some details notwithstanding).
  - Why?
    - The answer may be in the stability of the pilot-coflow shear layer and its response to the heat release in the main jet.
    - The nature of this shear layer is different for each of the non-reacting cold pilot, non-reacting hot pilot, and reacting.
    - The models can capture the differences between the cold and hot pilots but of course struggle with the reacting case…

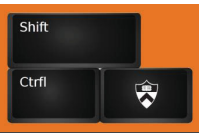

Compositionally Inhomogeneous

- Pilot-Coflow Mixing
  - LES Images of Velocity Magnitude (Perry/Mueller)

Non-Reacting (Cold Pilot)

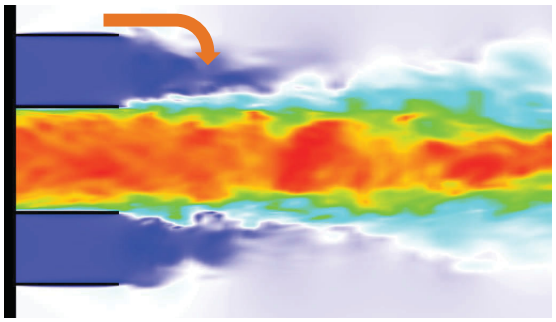

Non-Reacting (Hot Pilot)

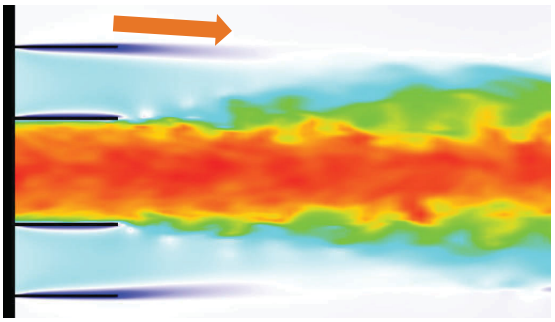

- For the cold pilot, the lower momentum flux does not allow the pilot to penetrate the coflow, so the shear layer is destroyed.
- For the hot pilot, the high momentum flux establishes a stable shear layer.

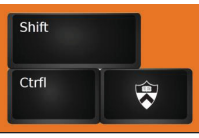

Compositionally Inhomogeneous

- Pilot-Coflow Mixing
  - LES Images of Velocity Magnitude (Perry/Mueller)

Non-Reacting (Hot Pilot)

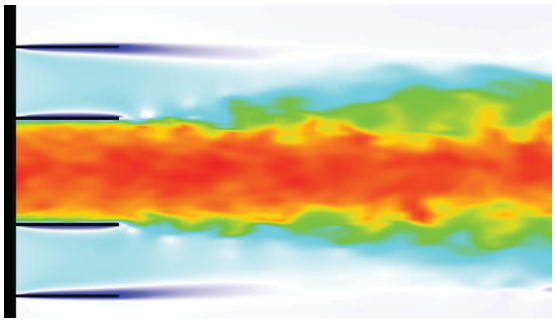

Reacting

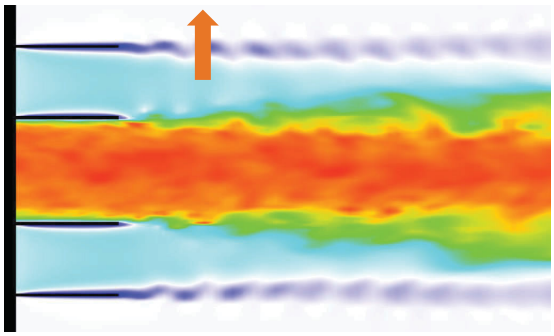

- With reactions, the thermal expansion from the heat release pushes the shear layer out, and it becomes unstable.
  - However, since mixing is underpredicted, this is not unstable enough…

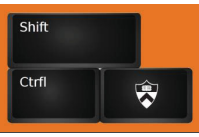

Compositionally Inhomogeneous

- Pilot-Coflow Mixing
  - LES Images of Velocity Magnitude (Perry/Mueller)

Reacting (Bulk Coflow)

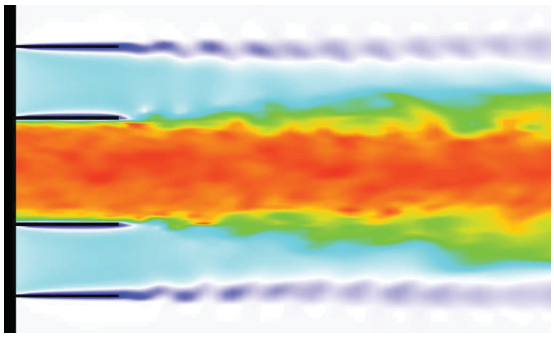

Reacting (Boundary Layer)

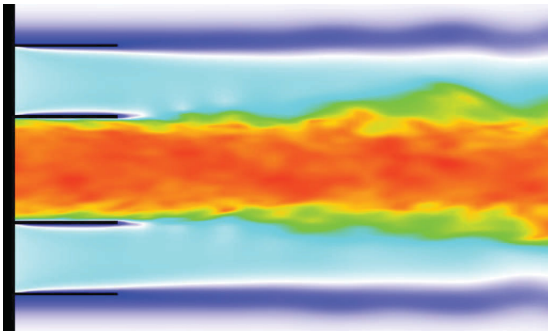

- We tried a number of different tests and have not been able to make the shear layer break down faster.
  - For example, a boundary layer profile in the coflow actually stabilizes the shear layer.

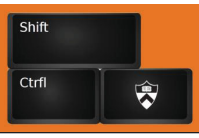

Compositionally Inhomogeneous

- Pilot-Coflow Mixing
  - Experimental study to assess sensitivity of blow-off to pilot conditions[1]

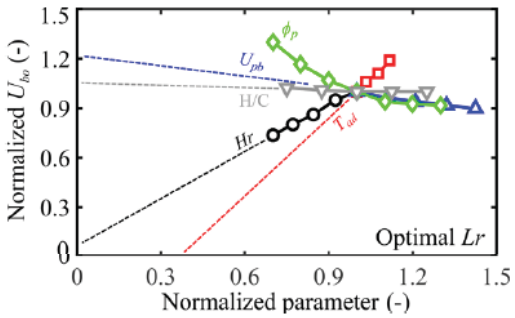

  - Similar sensitivity of the stability of the pilot-coflow shear layer?
  - What needs to be changed in the boundary conditions or the model to capture the correct instability characteristics?
    - Sensitivity to the pilot composition?

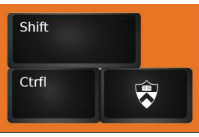

[1]T.F. Guiberti, H. Cutcher, W.L. Roberts, A.R. Masri, Energy Fuels 31 (2017) 2128-2137

Compositionally Inhomogeneous

- Availability of Computed Boundary Conditions
  - Computation of these flames actually requires three LES calculations:

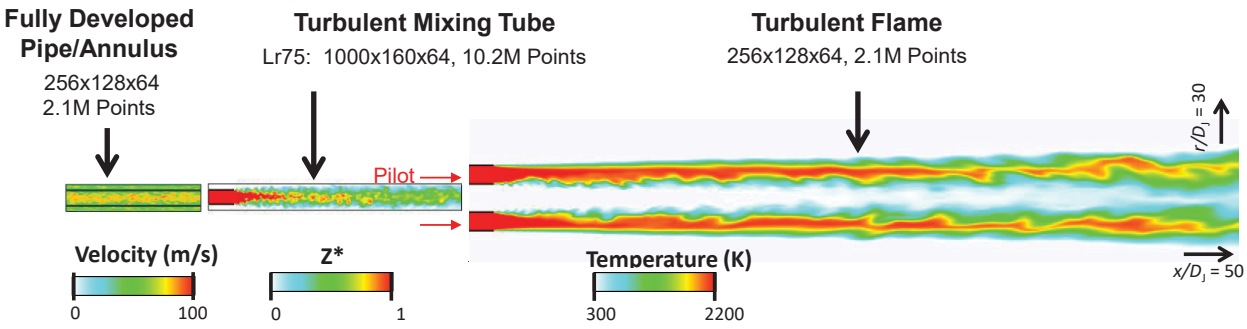

    - We have stored the unsteady boundary conditions at the end of the "mixing tube" (velocity and mixture fraction) for a number of cases, and these are freely available to save you the trouble.
      - 10,000 time steps with 0.25 μs spacing (2.5 ms total)

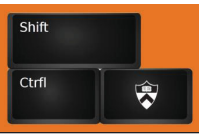

Compositionally Inhomogeneous

- Availability of Computed Boundary Conditions
  - Download link: https://drive.google.com/drive/folders/1iO_XoRUk84eiOHXFz4-MooIIsvNMSFoi?usp=sharing
  - Cases available (fuel-air and air-air)
    - FJ200-5GP-Lr75-57
    - FJ200-5GP-Lr75-80
    - FJ200-5GP-Lr300-59 (note: air-air for this case is corrupted but can be regenerated if anyone is interested)
  - Usage
    - C codes available for reading the data and testing
    - Otherwise, no restrictions (just cite our papers)
  - Contact myself and Mr. Bruce Perry with any questions

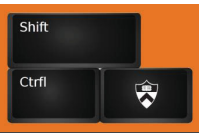

Piloted turbulent jet flame with inhomogeneous inlets

Model comparisons

Giampaolo Maio, Constantin Nguyen Van, Benoît Fiorina

EM2C - CNRS
CentraleSupélec
University of Paris Saclay

Michael Mueller
Princeton University

Matthias Ihme
Stanford University

TNF 2018
DUBLIN IRELAND JULY 27-28

8 groups for TNF14

H. Bockhorn, T. Zirwes and F. Zhang

Qing wang and Matthias Ihme

Ping Wang

Maximilian Hansinger and Michael Pfitzner

Bruce Perry, Michael Mueller

Ivan Langella, Zhi Chen

Giampaolo Maio and Benoît Fiorina

Martin Rieth and Andreas Kempf.

2

Inlet BC's

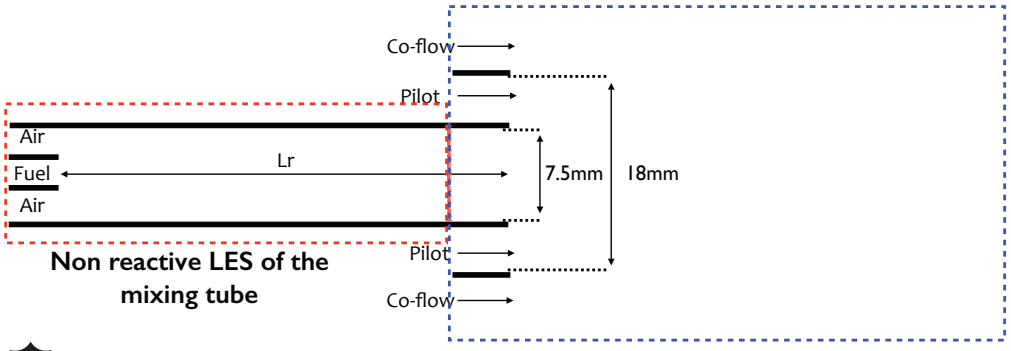

Non reactive LES of the mixing tube

Reactive LES of the combustion chamber

Bruce A. Perry, Michael E. Mueller

2016 TNF Workshop

COLD case A

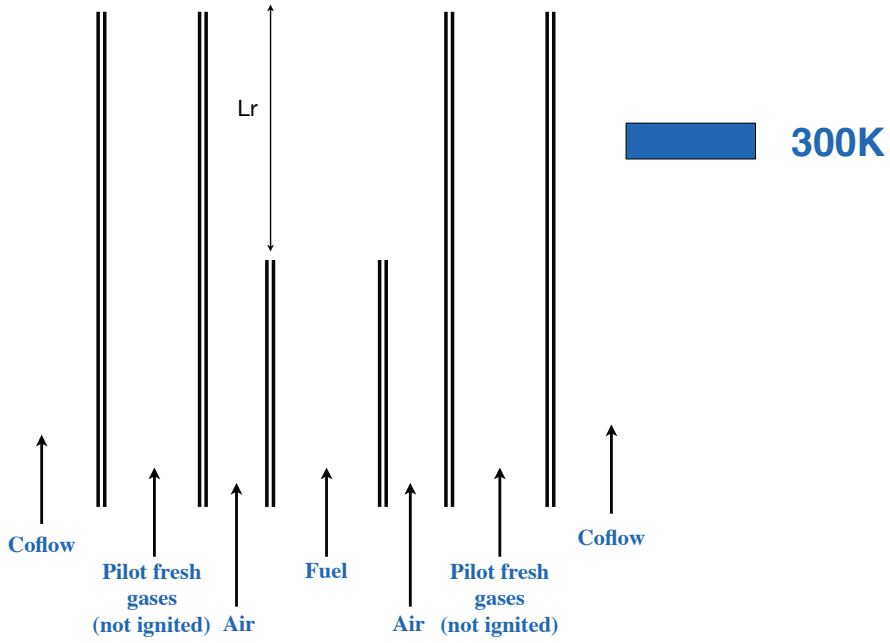

INERT HOT case B

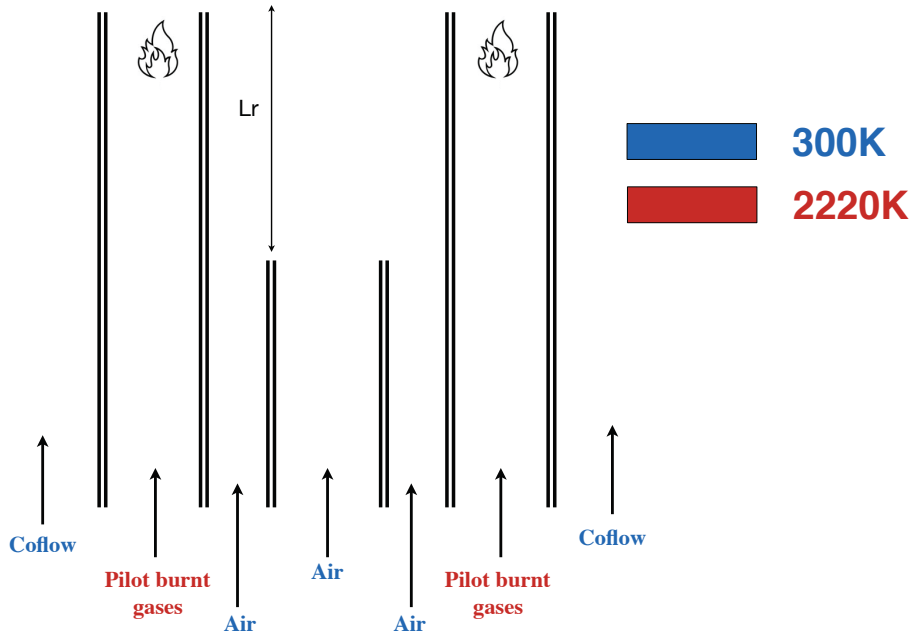

REACTIVE case C

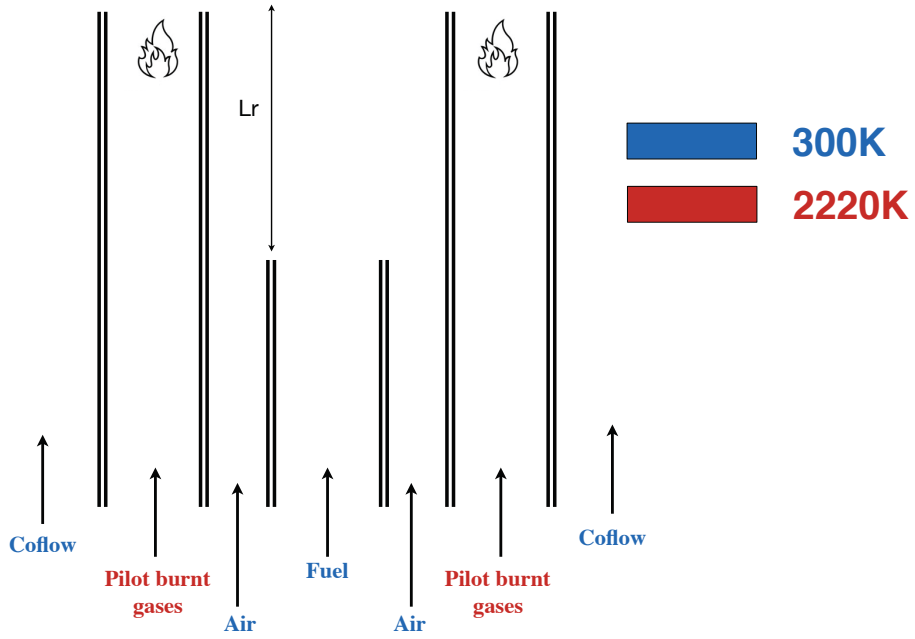

Codes

Group	Code type	Grid	Spatial scheme	temporal scheme	Turbulence	Nb of Cells
JIA	LESOCC2C Low Mach	Multibloc Structured	2nd	2nd	Dyn. Samg.	5.25M
KIT	Open Foam Compressible	Unstructured	4th	2nd order implicit	No	150M
PRI	Low Mach	Structured (cylindrical)	2nd order (momentum), 3rd order WENO (scalars)	2nd order semi-implicit	Dyn. Samg.	2.9M
EM2C	YALES2 Low Mach	Unstructured	4th	4th order explicit	Wale	53M
STA	3DA Low Mach	structured	2nd	2nd	Dyn. Samg.	1M
UBM	Open Foam Compressible	Unstructured	2nd	2nd order implicit	Wale / Keqn	4.5M
CAM	Open Foam Compressible	Unstructured	2nd order CD (momentum) 2nd order TVD (scalars)	2nd order implicit	Wale / Keqn	3.2M
DUE	PsiPhi Low Mach	Structured	2nd order CDS (mom.) 2nd order TVD (scalars)	3rd order explicit	Dyn. Samg.	18M

7

Models

Group	Turbulent Combustion Model	Chemistry
JIA	Presumed FDF	Tab. Chem. (hybrid flamelets - REDIM)
KIT	None	Skeletal (19 species)
PRI	FPV 2 mixt. Pres. FDF	Tab. Chem. (hybrid premixed)
EM2C	TFLES Ξ anal. model	Tab. Chem. (premixed)

Group	Turbulent Combustion Model	Chemistry
STA	FPV	Tab. Chem. (non-premixed)
UBM	Eulerian Stochastic field	Skeletal (19 species)
CAM	Presumed FDF	Tab. Chem. (hybrid flamelets)
DUE	Transport & presumed FDF	skeletal &Tab. Chem. (premixed)

8

Main jet BC's

Group	Main jet
JIA	Own mixing tube simulation
KIT	Own mixing tube simulation
PRI	Princeton data !
EM2C	Princeton data
STA	Own mixing tube simulation
UBM	Own mixing tube simulation
CAM	Own mixing tube simulation
DUE	Princeton data

9

Flame configurations

Group	Lr75-57			Lr75-80		
	COLD	INERT HOT	REACTIVE	COLD	INERT HOT	REACTIVE
EXPERIMENTS	U	-	U, Z, T, species	U	U	U, Z, T, species
JIA			x			
KIT			x			
PRI	x	x	x	x	x	x
EM2C				x	x	x
STA			x			
UBM	x	x	x	x	x	x
CAM	x	x	x	x	x	x
DUE	x	x	x	x	x	x

10

Experimental data
Radial profiles

Raman/Rayleigh measurements

Temperature (T)
Mixture fraction (Z)
Y_{O2} - Y_{CH4} - Y_{CO2} - Y_{H2O} - Y_{N2} - Y_{CO}

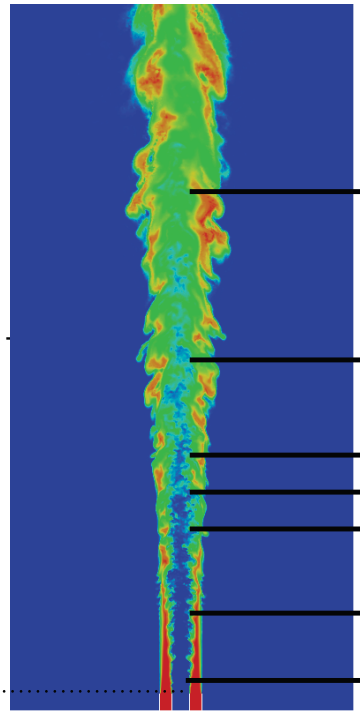

X/D = 30
X/D = 20
X/D = 15
X/D = 12
X/D = 10
X/D = 5
X/D = 1
X/D = 0

11

Mean and RMS radial profiles

12

FJ-5GP-Lr75-80

COLD

13

Lr75-80, COLD, mean axial velocity

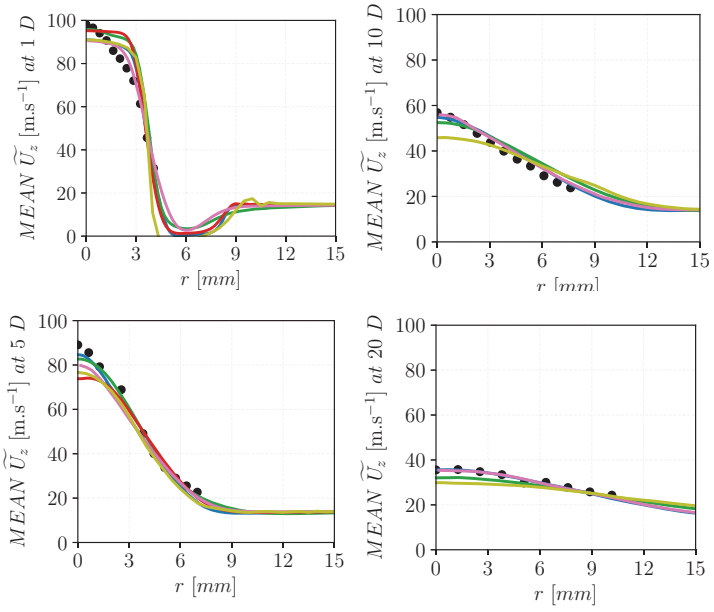

NEW !

Experiments
CAM
EM2C
PRIN
UBM
UDE

- **Fair agreement**
- **Inlet velocity mean profile not retrieved ?**

14

Lr75-80, COLD, RMS axial velocity

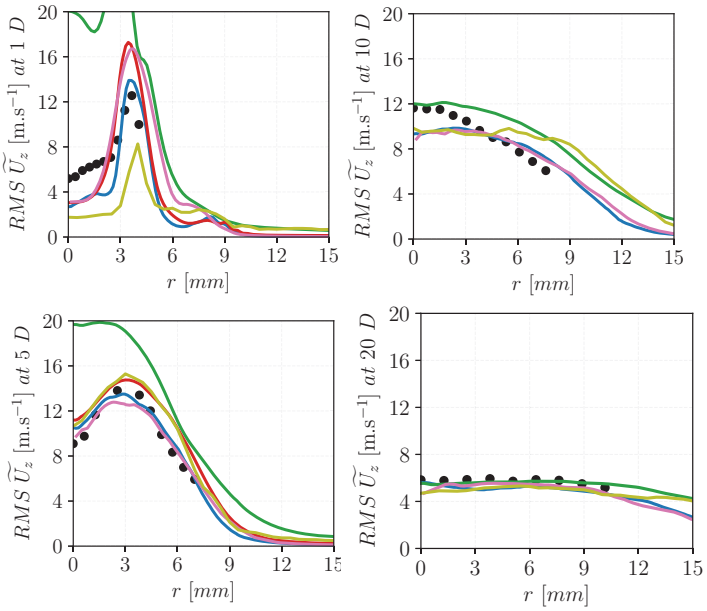

NEW !

Experiments
CAM
EM2C
PRIN
UBM
UDE

- **Turbulence quite well reproduced at the inlet**

15

Lr75-80, COLD, mean mixture fraction

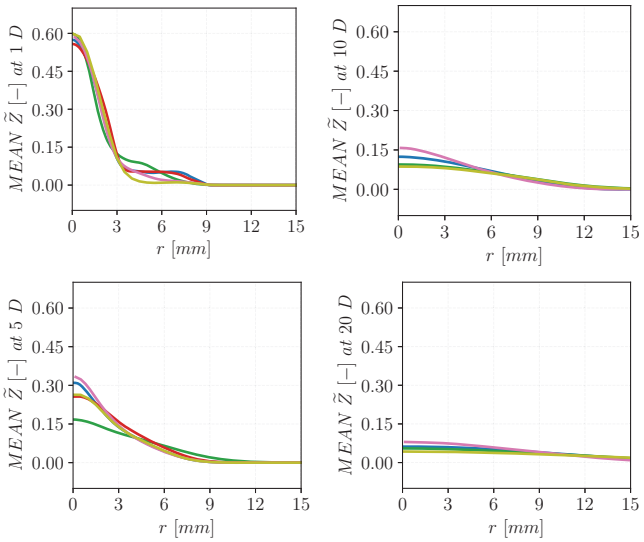

CAM
EM2C
PRIN
UBM
UDE

- **Deviation in the mixing prediction**

16

Lr75-80, COLD, RMS mixture fraction

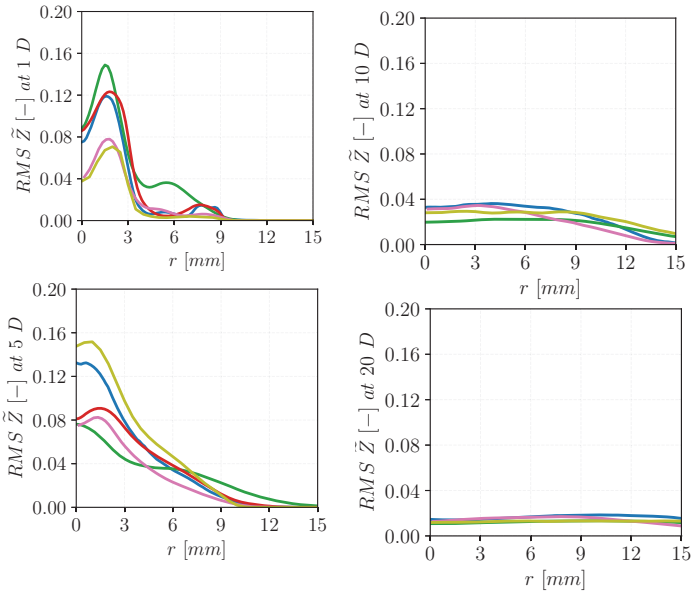

- **Large dispersion of the RMS, especially at X/D=1 and 5**

17

FJ-5GP-Lr75-80

INERT HOT

18

Lr75-80, INERT HOT, mean axial velocity

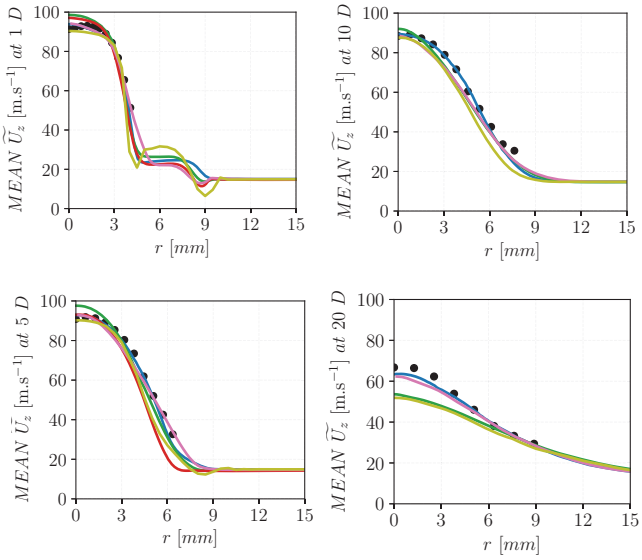

NEW !

Experiments
CAM
EM2C
PRIN
UBM
UDE

- **Better consistency between experiments and simulation observed at X/D=1**

19

Lr75-80, INERT HOT, RMS axial velocity

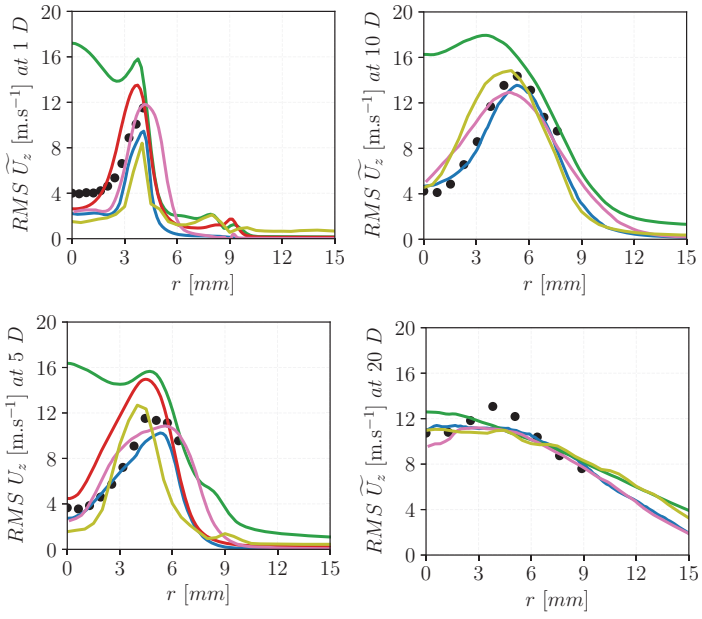

NEW !

Experiments
CAM
EM2C
PRIN
UBM
UDE

20

Lr75-80, INERT HOT, mean mixture fraction

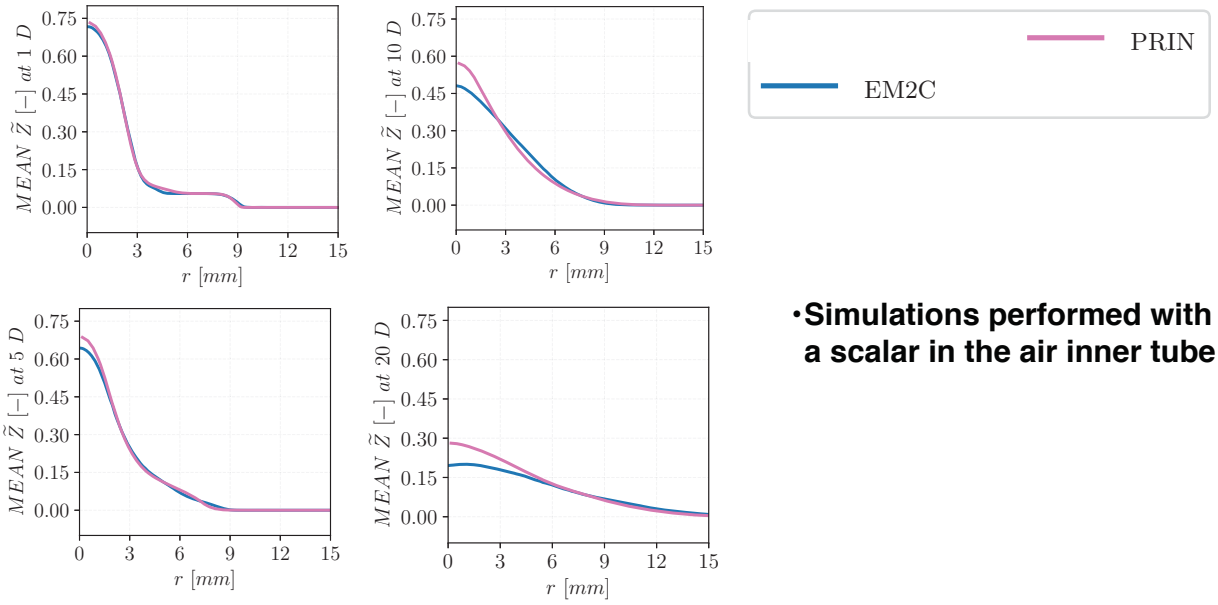

- **Simulations performed with a scalar in the air inner tube**

COLD
VS
HOT INERT

22

Mean velocity

COLD

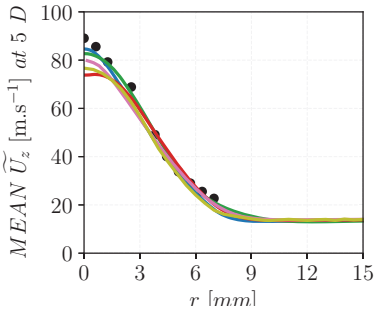

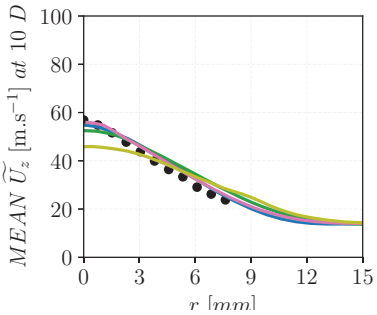

HOT INERT

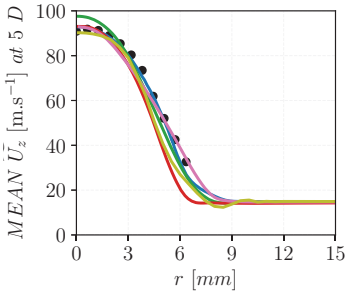

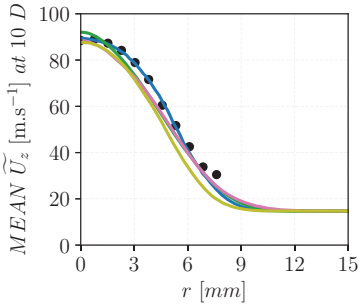

23

Mean velocity

COLD

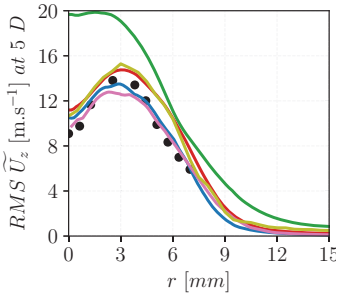

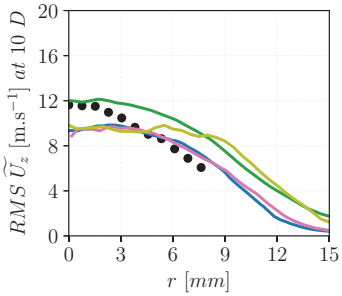

HOT INERT

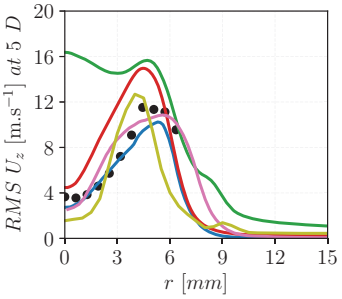

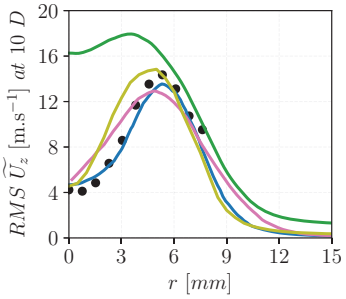

24

Mean mixture fraction

COLD

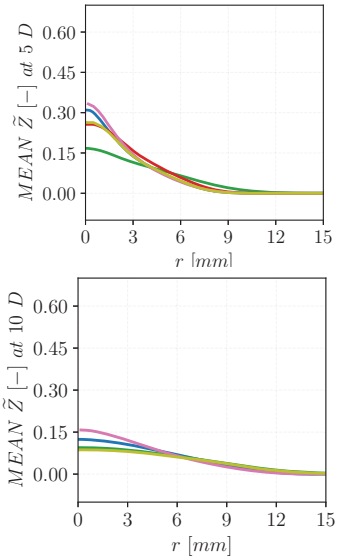

Very strong influence of the pilot on the mixing process

HOT INERT

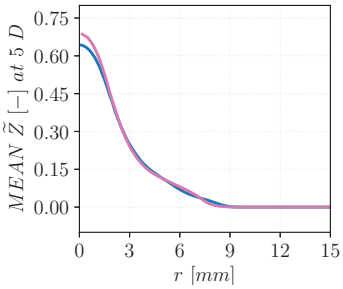

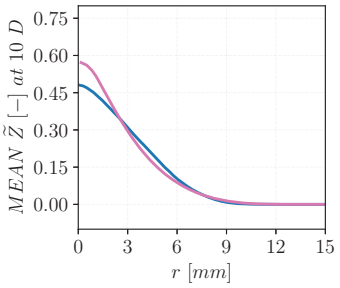

25

FJ-5GP-Lr75-57

REACTING

26

Lr75-57, REACT, mean axial velocity

NEW !

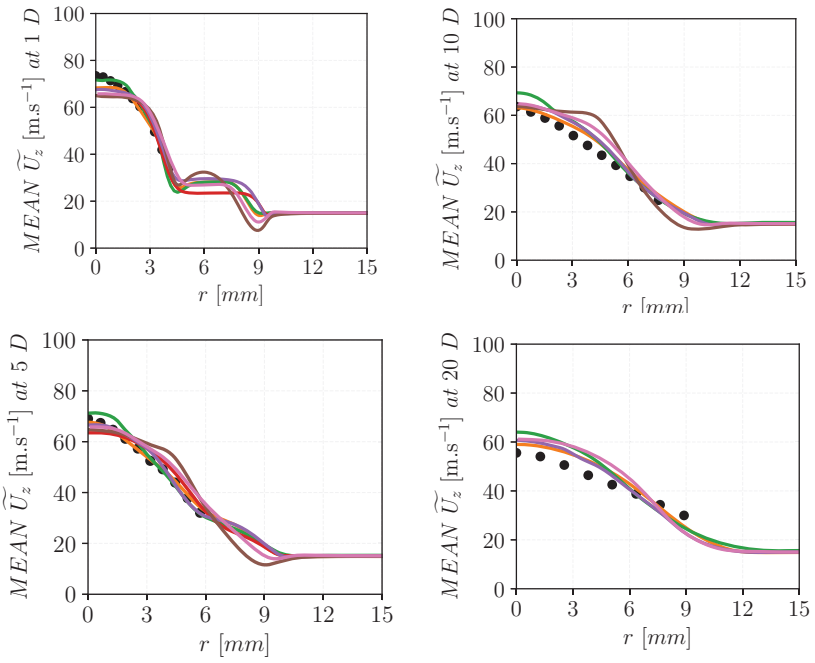

Lr75-57, REACT, mean mixture fraction

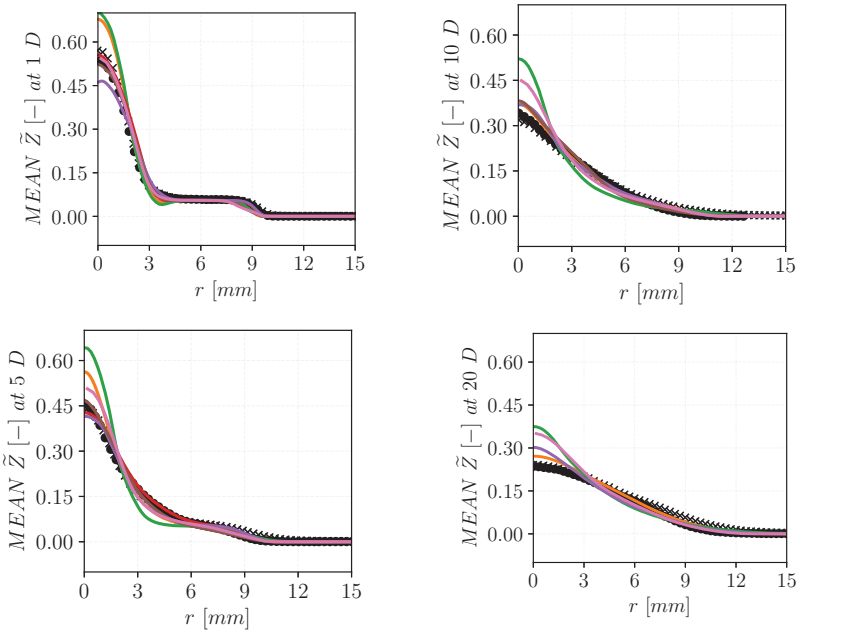

Lr75-57, REACT, RMS mixture fraction

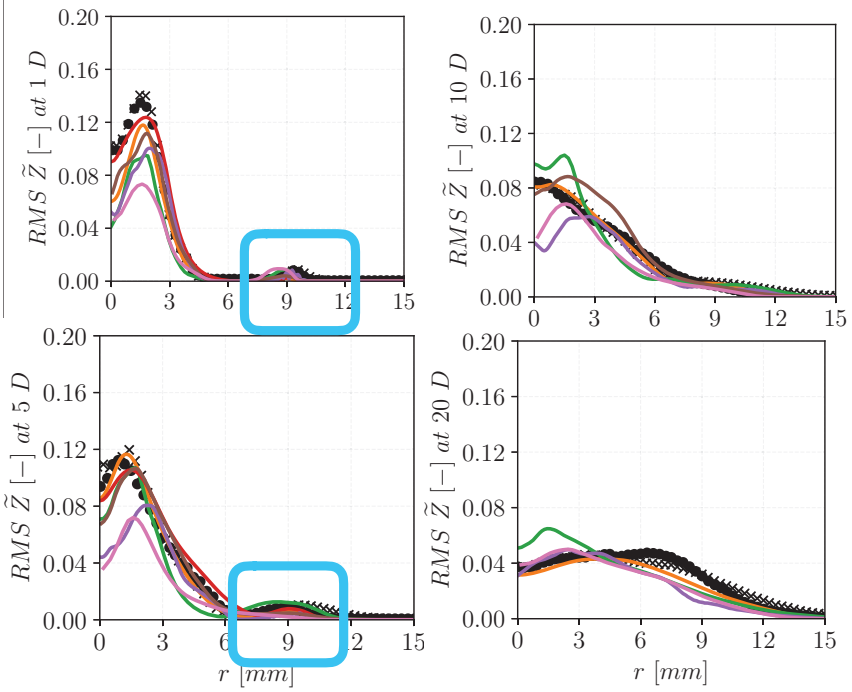

Second peak of mixture fraction RMS produced in the pilot/coflow shear layer

Lr75-57, REACT, mean temperature

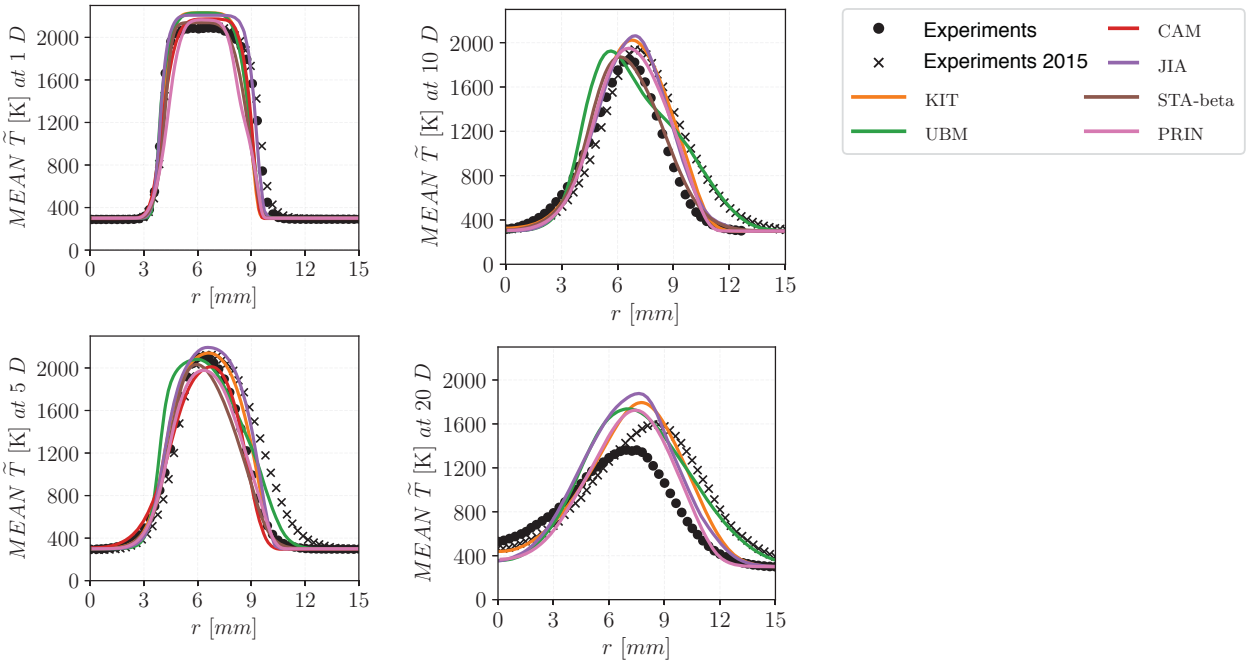

Lr75-57, REACT, RMS temperature

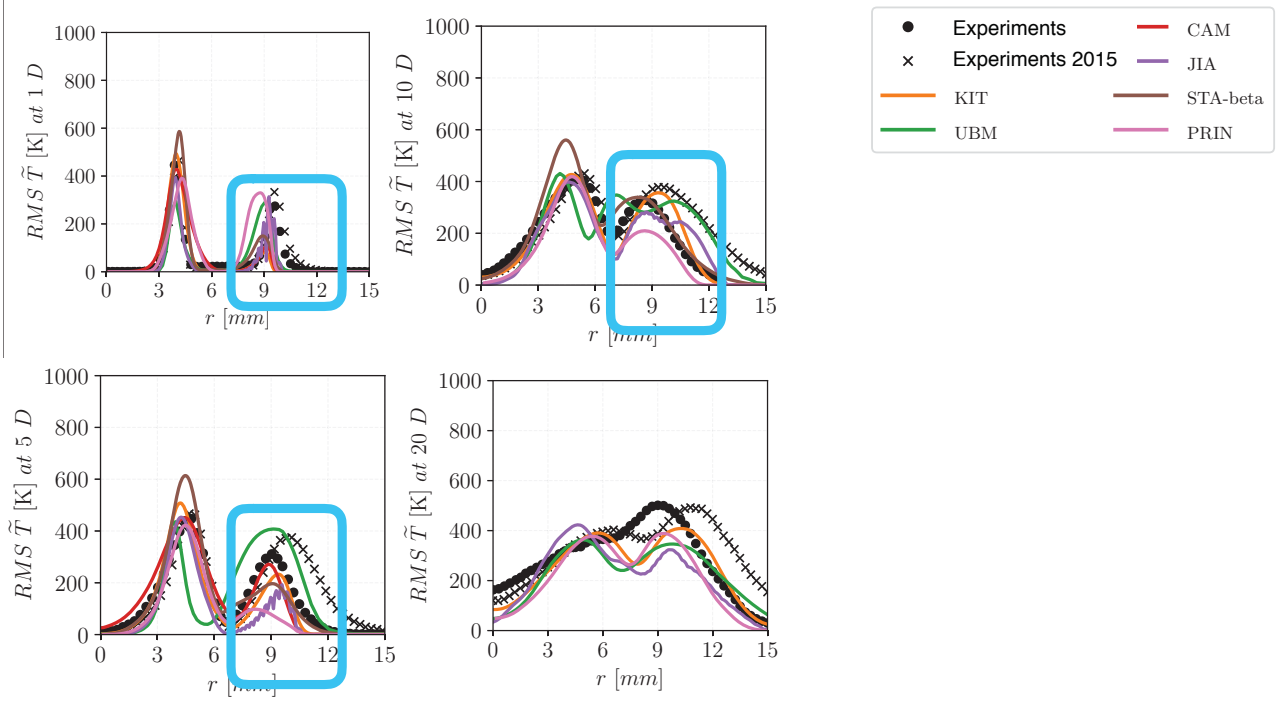

BULK Velocity
57 m/s VS 80 m/s

mean axial velocity

U_{bulk} = 57 m/s

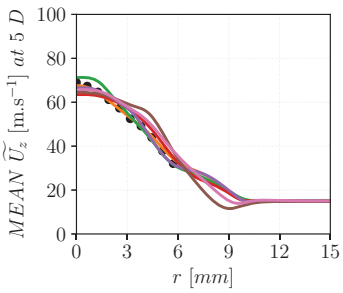

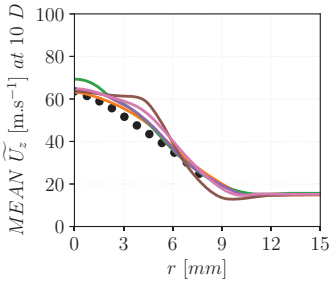

U_{bulk} = 80 m/s

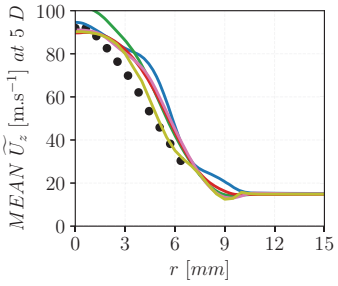

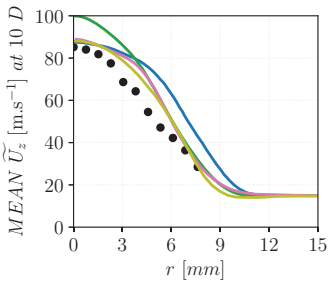

Overestimation of heat expansion

mean mixture fraction

U_{bulk} = 57 m/s

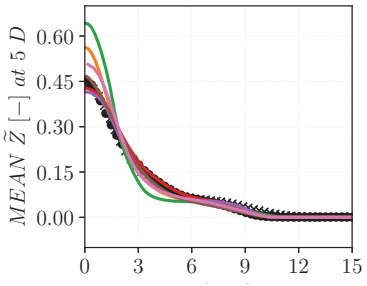

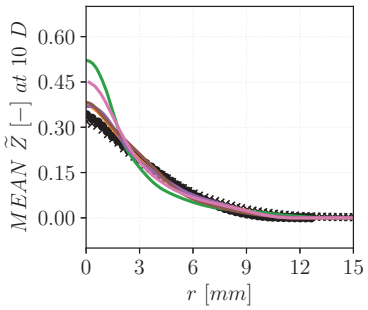

U_{bulk} = 80 m/s

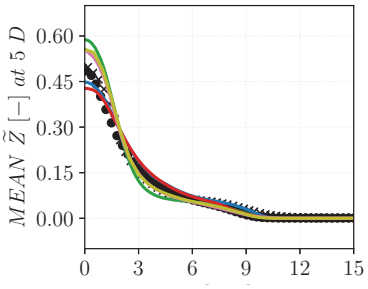

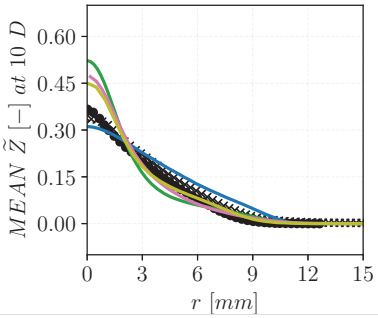

Does not capture the jet mixing

RMS mixture fraction

U_{bulk} = 57 m/s

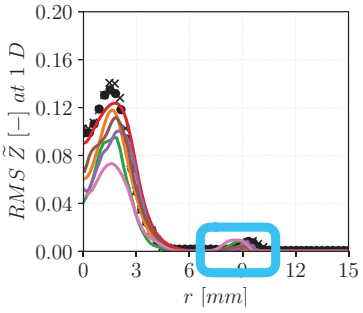

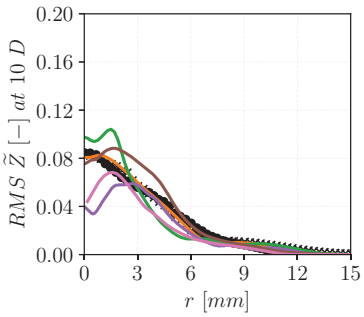

U_{bulk} = 80 m/s

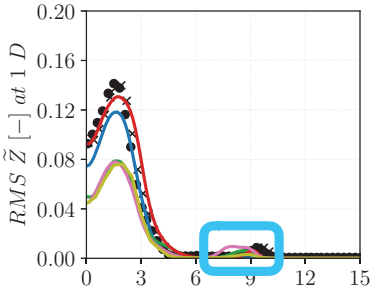

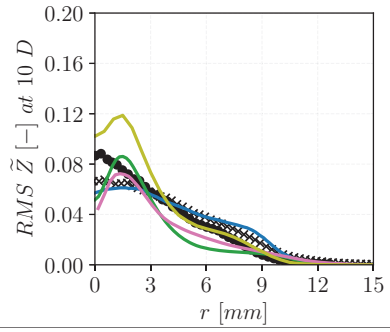

mean temperature

U_{bulk} = 57 m/s

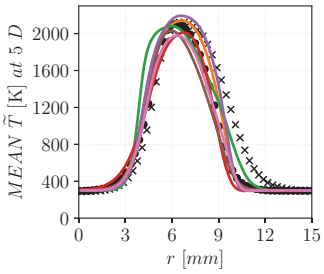

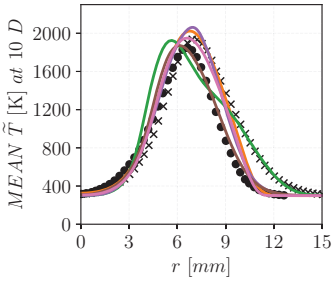

U_{bulk} = 80 m/s

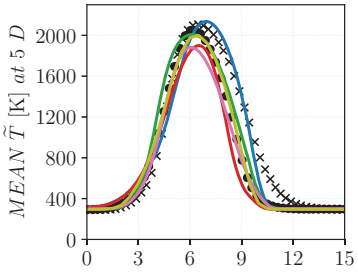

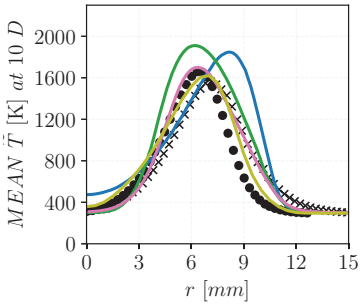

RMS temperature

U_{bulk} = 57 m/s

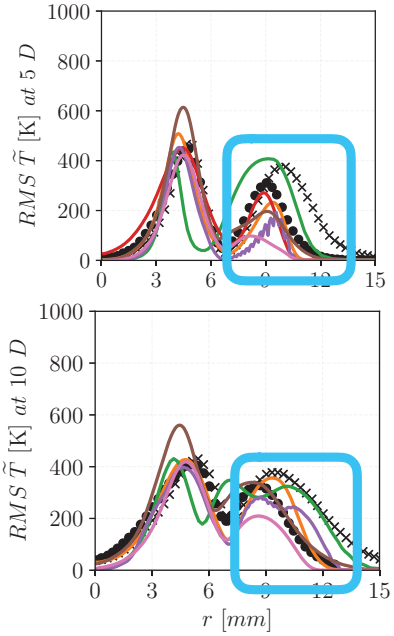

U_{bulk} = 80 m/s

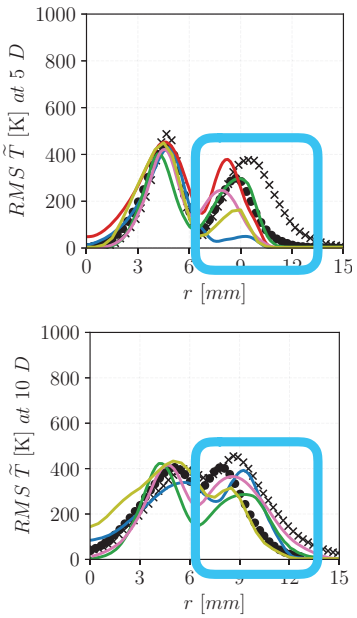

Misprediction of:
- turbulent combustion?
- mixing ?
- both ?

Scatter plot

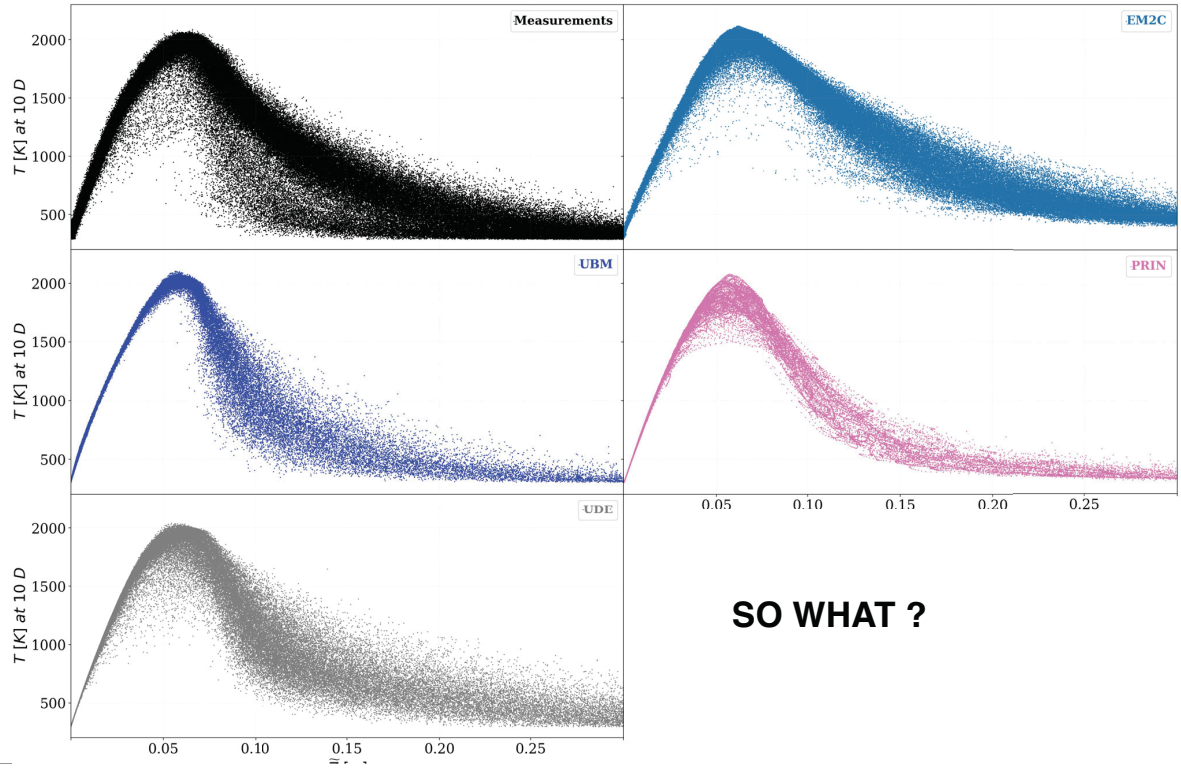

SO WHAT ?

Wasserstein metric

40

TNF convergence study

41

Lr75-80, REACT, mean mixture fraction

TNF 2016

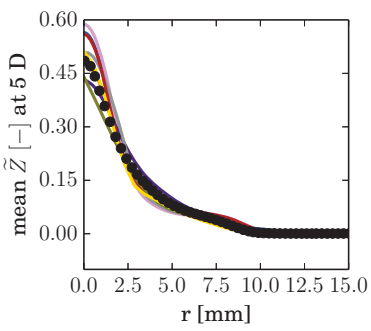

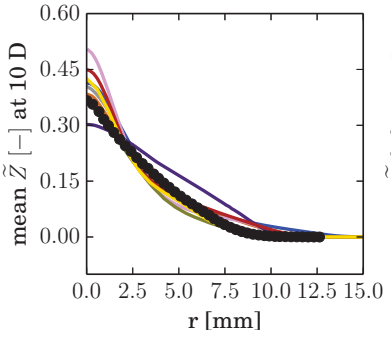

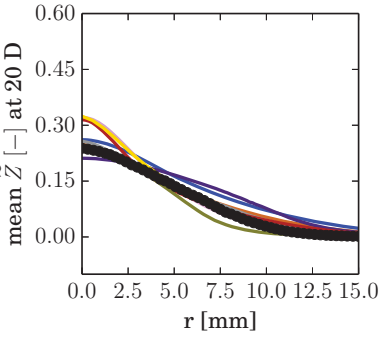

TNF 2018

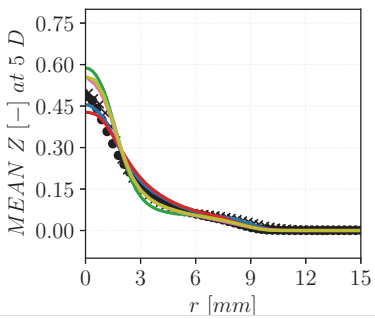

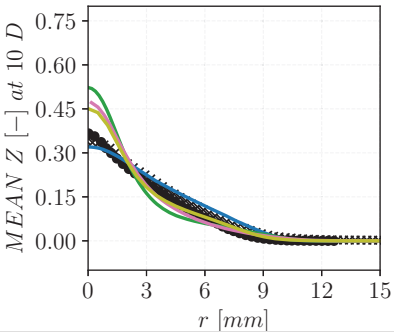

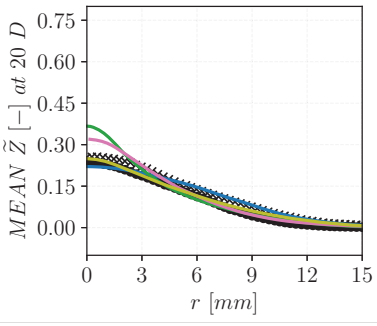

Lr75-80, REACT, mean temperature

TNF 2016

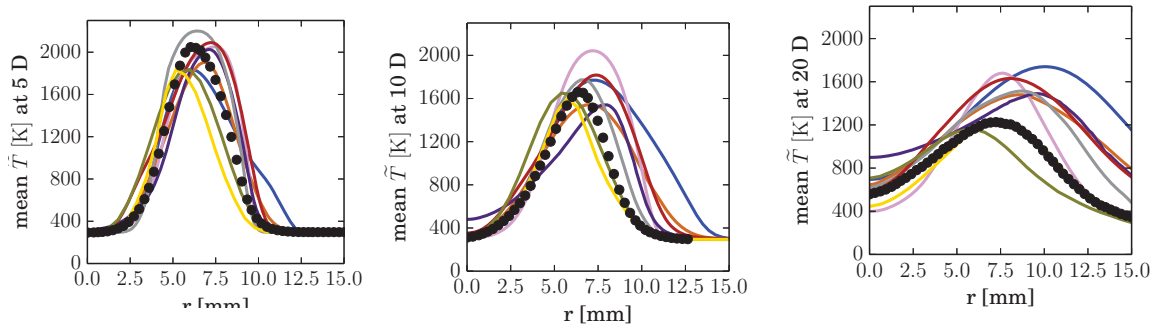

TNF 2018

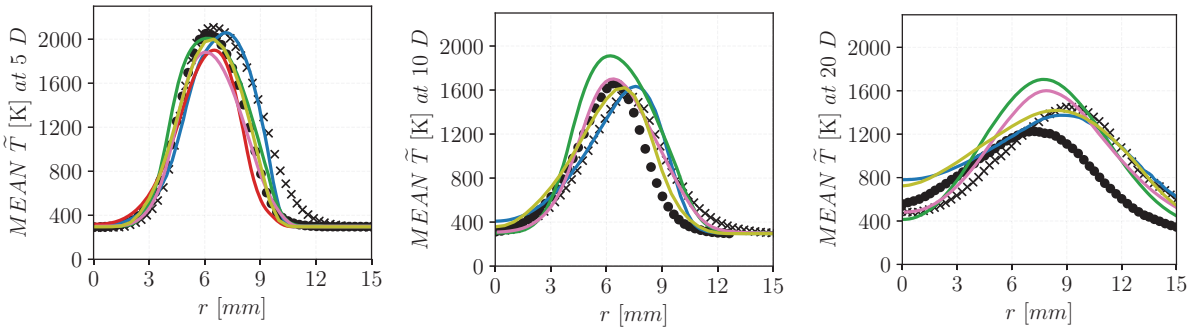

Lr75-80, REACT, mean CO

TNF 2016

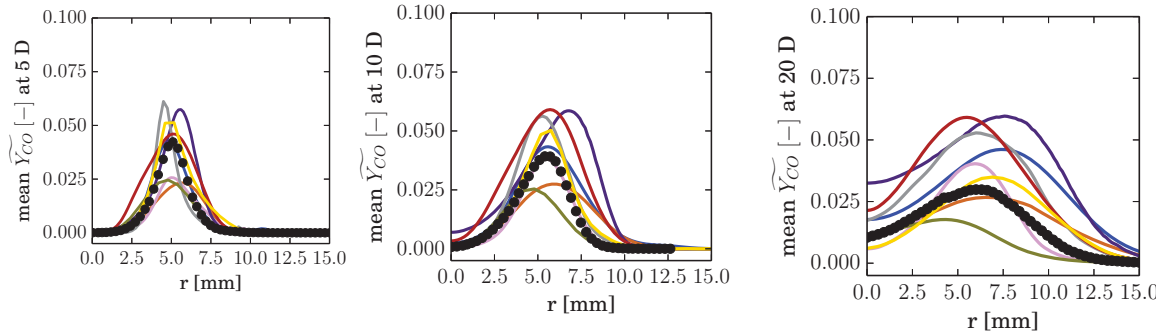

TNF 2018

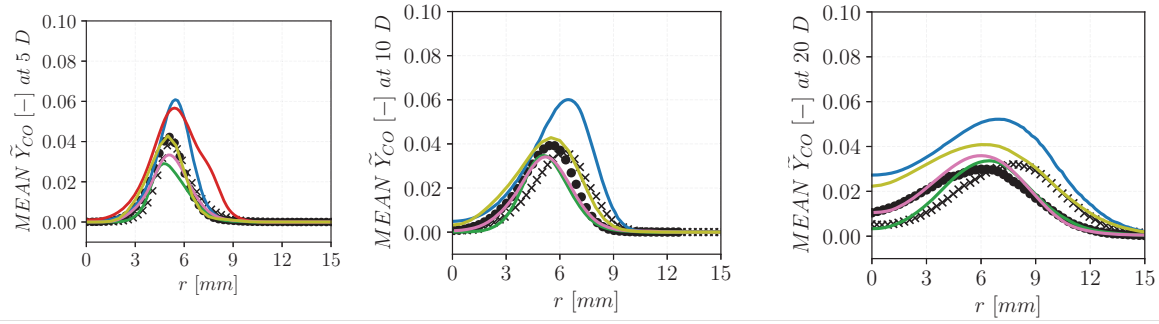

Conclusions

- Simulations have been consolidated since the last TNF: start to observe a convergence of the simulations:
  - less dispersion between numerical curves
  - but the difference between simulations and experiments seems to reach an asymptote

45

Conclusions

- Objective of such exercice:
  - Is not to match experiments or to compare models together
  - but to give a state of the art of the turbulent combustion modeling community
- State of the start is here somehow biased by
  - the number of physical challenge to overcome (combustion regime, multiple streams problem, shear layer instabilities, turbulence, etc.)
  - strong uncertainties and sensitivities (geometrical, BC's, mesh, numerics, pilot composition)
- Should try to eliminate the physical phenomena that we do not want to focus on -> firstly virtually and then see how it could be addressed experimentally

46

Thanks to the guys behind the plots !

Giampaolo Maio

Constantin Nguyen Van

47

Wasserstein metric: Quantitative Analysis of LES Modeling Results

CONTRIBTIONS: PING WANG (JIANGSU UNIVERSITY),
ZHI X. CHEN, IVAN LANGELLA (CAMBRIDGE U.)
THORSTEN ZIRWES, FEICHI ZHANG, HENNING BOCKHORN (KIT),
MAXIMILIAN HANSINGER, JULIAN ZIPS,
MICHAEL PFITZNER (BW U. MUNICH),
BRUCE PERRY, MICHAEL MUELLER (PRINCETON),
QING WANG, EMERIC BOIGNE, MATTHIAS IHME (STANFORD)

Quantitative Evaluations of Combustion Simulations

Challenge

- Quantitative evaluation of combustion model
  - Quantities: velocity, mixture fraction, temperature, species, heat-flux, emissions, …
  - Measurement: probes, line-of-sight, planar, volumetric, …
  - Data analysis: scatter, conditional, statistical, PDF, …

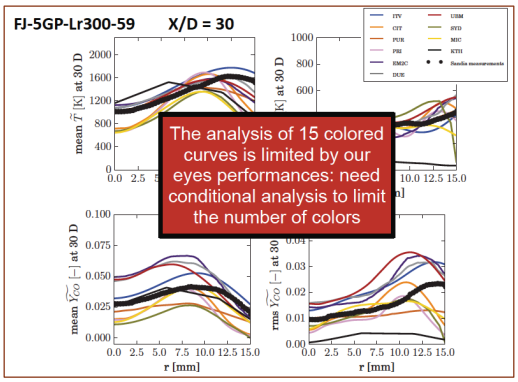

TNF13, TNF10

Quantitative Evaluations of Combustion Simulations

Challenge

- Quantitative evaluation of combustion model
  - Quantities: velocity, mixture fraction, temperature, species, heat-flux, emissions, …
  - Measurement: probes, line-of-sight, planar, volumetric, …
  - Data analysis: scatter, conditional, statistical, PDF, …

Requirements on quantitative validation metric

- Provide a single metric for quantitative model evaluation
- Combine single and multiple scalar quantities
- Incorporate differ data: scatter, simultaneous, high-speed, statistics
- Consider dependencies between measurement quantities
- Ensure conditions on non-negativity, identity, symmetry, and triangular inequality

Stanford University

Quantitative Evaluations of Combustion Simulations

- Wasserstein Metrix (aka Earth Mover Distance, EMD) as quantitative measure for assessing combustion simulations
  - Based on comprehensive representation of turbulent flame data (beyond mean and variance profiles)
  - Utilization of the rich data from experiments and transient simulations
  - Condensation of complex information to a single metric

- Metric: "Distance" between distributions
  - Consider PDF as generic representation of turbulent flame data
  - Condensation of rich information for quantitative comparison
    - "Distance" between distributions
  - Applicable to multivariate joint-PDF
  - Natural extension from Euclidean distance for deterministic data

Johnson, R., Wu, H., and Ihme, M. (2017). A general probabilistic approach for the quantitative assessment of LES combustion models. Combustion and Flame, 183, 88-101
Analysis tool available at: https://github.com/IhmeGroup/WassersteinMetricSample

Stanford University

5

Quantitative Evaluations of Combustion Simulations Wasserstein Metric (Earth Mover Distance, EMD)

Optimal transport

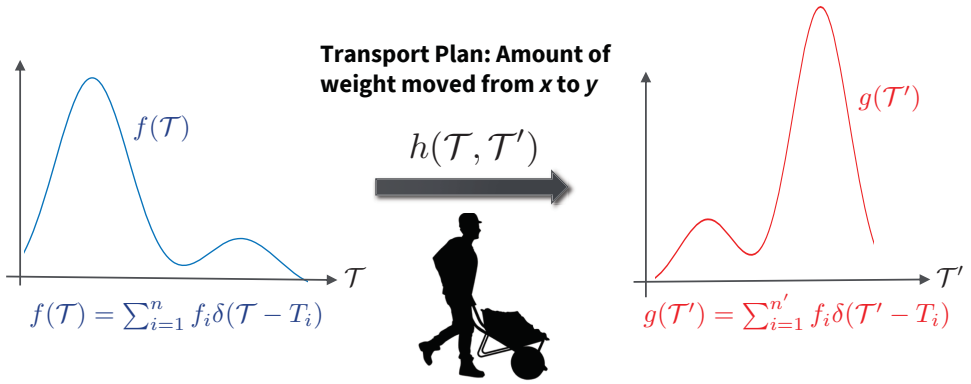

Minimal work needed to transform *f* to *g*

$$W_2(f,g) = \left(\inf_{h \in G(f,g)} \int_{\mathbf{R}^d} \int_{\mathbf{R}^d} d(\mathcal{T},\mathcal{T}')^2 h(\mathcal{T},\mathcal{T}') d\mathcal{T} d\mathcal{T}' \right)$$

Stanford University

6

Quantitative Evaluations of Combustion Simulations Wasserstein Metric

Optimal transport

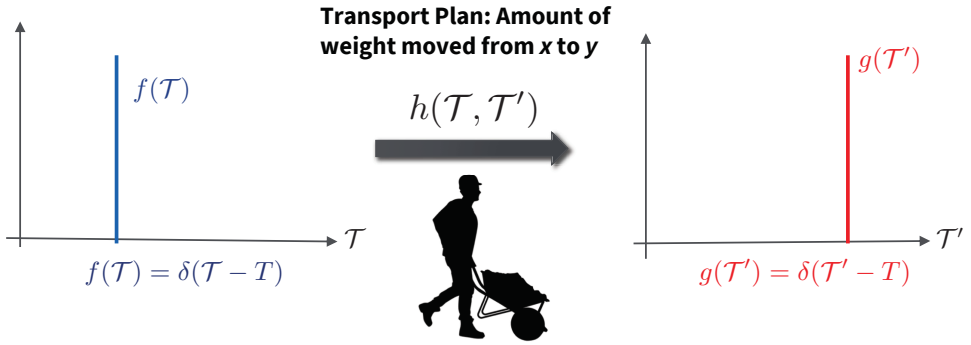

Minimal work needed to transform *f* to *g*

➔ Reduced to Euclidean distance for deterministic data

$$W_2(f,g) = |\mathcal{T} - \mathcal{T}'|$$

Stanford University

Quantitative Evaluations of Combustion Simulations Wasserstein Metric

Optimal transport

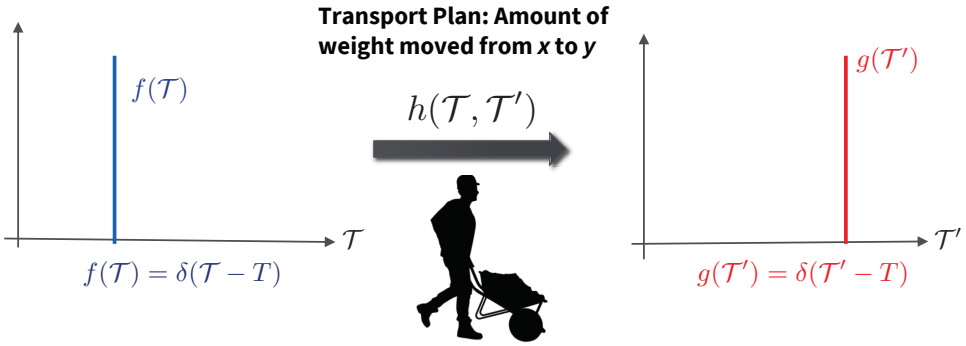

Interpretation: Metric is normalized by STDEV(T) so that $W_2(f,g) = 1$ is equivalent to "one standard deviation of quantity T "

Stanford University

Quantitative Evaluations of Combustion Simulations Wasserstein Metric

Convergence and cost

- Robust convergence of W_2 with 1000 sample points
- Cost: O(min)

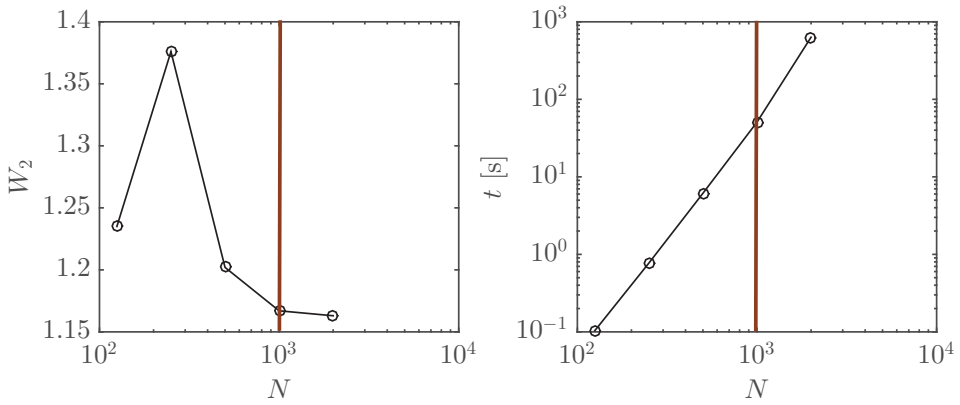

Stanford University

Application:
FJ-5GP-Lr75-57

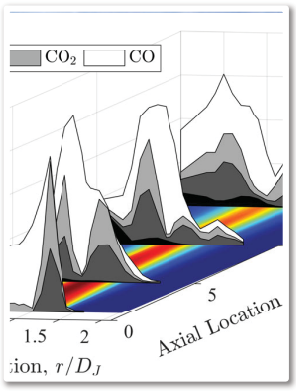

Stanford University

Presentation of the experimental dataset

Sandia/Sydney flame FJ200-5GP-Lr75-57

Quantities of interest:

- Mixture fraction
- Temperature
- Mass fraction of CO2
- Mass fraction of CO

$$f_{\mathrm{LES}}(Z, T, Y_{\mathrm{CO_2}}, Y_{\mathrm{CO}})$$
$$g_{\mathrm{Exp}}(Z, T, Y_{\mathrm{CO_2}}, Y_{\mathrm{CO}})$$

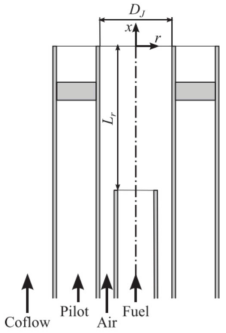

Data available:

- 1 set of experimental data, 6 contributions
- 4 variables: T, Z, CO2 and CO mass fractions
- 4 axial positions: x/D = 1, 5, 10, 15
- 16 bins of radial positions: r/D = 0:0.125:2
- 1,000 data points per radial bin

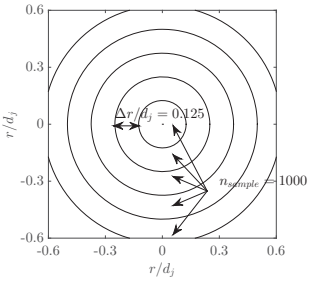

[1] R. S. Barlow, S. Meares, G. Magnotti, H. Cutcher, and A. R. Masri, "Local extinction and near-field structure in piloted turbulent CH4/air jet flames with inhomogeneous inlets," *Combust. Flame*, vol. 162, no. 10, pp. 3516–3540, 2015.
[2] S. Meares and A. R. Masri, "A modified piloted burner for stabilizing turbulent flames of inhomogeneous mixtures," *Combust. Flame*, vol. 161, no. 2, pp. 484–495, 2014.
[3] S. Meares, V. N. Prasad, G. Magnotti, R. S. Barlow, and A. R. Masri, "Stabilization of piloted turbulent flames with inhomogeneous inlets," *Proc. Combust. Inst.*, vol. 35, no. 2, pp. 1477–1484, 2015.

Stanford University

Estimation of the Wasserstein metric – Procedure

Estimation of Wasserstein metric

- For each variable, and at each axial location, the standard deviation is estimated from the experimental data (16,000 data points)
- The experimental and simulated data are normalized by the standard deviation of each quantity
- Two different computations of the Wasserstein metric for each simulation and at each axial position:
  - Radial profiles: At each radial position, 1,000 data points available at each radial bin are used to estimate W2
  - Cumulative radial profiles: 1,000 data points are randomly sampled from the experimental data and simulation to estimate W2

Stanford University

Details of the 6 simulations

Institution	KIT	BW U Munich	Stanford	Cambridge	UJS	Princeton
Number	1	2	3	4	5	6
Code used	OpenFOAM & Cantera	OpenFOAM & Cantera	3DA (low-Mach variable den.)	OpenFOAM	LESOCC2C	NGA (low-mach compressible)
Mesh type, and millions of cells	150m hex, unstructured	4.5m hex	0.2m, structured	3.2m hex, unstructured	5.25m, structured	2.9m, structured
Domain size & Min. resolution [radial / axial]	67D x 13D x 2π Tube inlet: -1D 10 / 75 microns	67D x 13D x 2π Tube inlet: -1D 30 / - Microns	20D x 20D x 2π Tube inlet: -1D 210 / - microns	50D x 15D x 15D Tube inlet: -13.3D 60 / 130 microns	76D x 33.3D x 33.3D Tube inlet: -14.7D 150 / 400 microns	50D x 32D x 2π Tube inlet: -1D 50 / - microns
Combustion mechanism	19 species, 15 reactions (reduced GRI 3.0 [1])	19 species, 15 reactions (reduced GRI 3.0 [1])	GRI 3.0	GRI 3.0	GRI 3.0 2D REDIM chemistry table [Y_CO2, Y_N2]	GRI 3.0
Turbulence and combustion models	FRC DNS	Two simulations 1 / LES: WALE (turbulence SGS), Transported PDF (ESF MC) 2/ RANS: k-eps, FPV [not used]	LES with dynamic Smagorinsky, beta PDF and FPV	Les with flamelet model, presumed PDF SGS: dynamic model [2]	LES with dynamic Smagorinsky and presumed PDF (CO2: clipped-Gaussian, N2: Top-hat)	LES with dynamic Smagorisnky (-like) model, beta PDF and FPV
Central jet inlet conditions	2 Separate LES & DNS to prescribe inlet at x/D = -1	Use data from KIT and prescribe inlet at x/D = -1	Use separate simulation to prescribe inlet at x/D = -1	Synthetic eddy method based on RANS prescribes inlet at x/D = -13.3	Periodic computation in -14.7<x/D<-10.6	Use separate simulation to prescribe inlet at x/D = -1

[1] T.Lu, C. Law, Combust. Flame 154 (2008)

[2] Z. Chen, S. Ruan, and N. Swaminathan, "Large Eddy Simulation of flame edge evolution in a spark-ignited methane-air jet," *Proc. Combust. Inst.*, vol. 36, no. 2, pp. 1645–1652, 2017.

Stanford University

13

Details of the 6 simulations

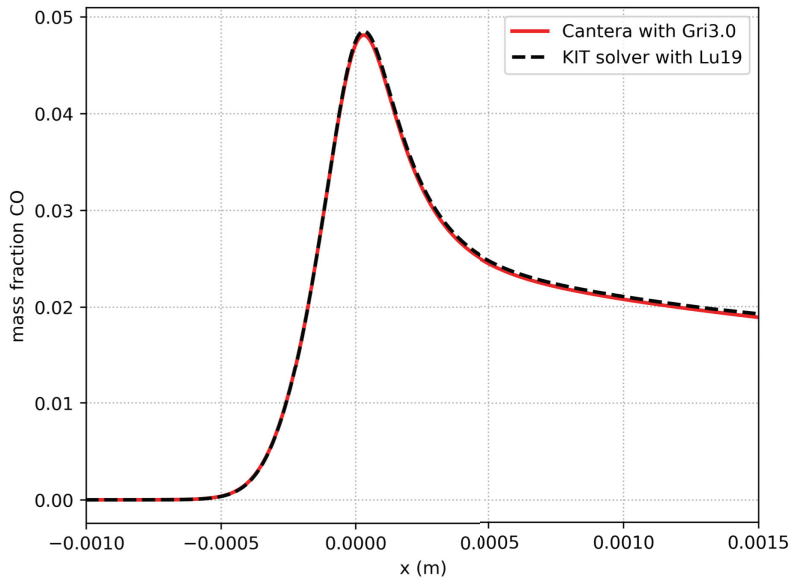

Curtesy: Thorsten Zirwes

[1] T.Lu, C. Law, Combust. Flame 154 (2008)

[2] Z. Chen, S. Ruan, and N. Swaminathan, "Large Eddy Simulation of flame edge evolution in a spark-ignited methane-air jet," *Proc. Combust. Inst.*, vol. 36, no. 2, pp. 1645–1652, 2017.

Stanford University

14

Radial profiles of Z, T, CO2 and CO – x/D = 1

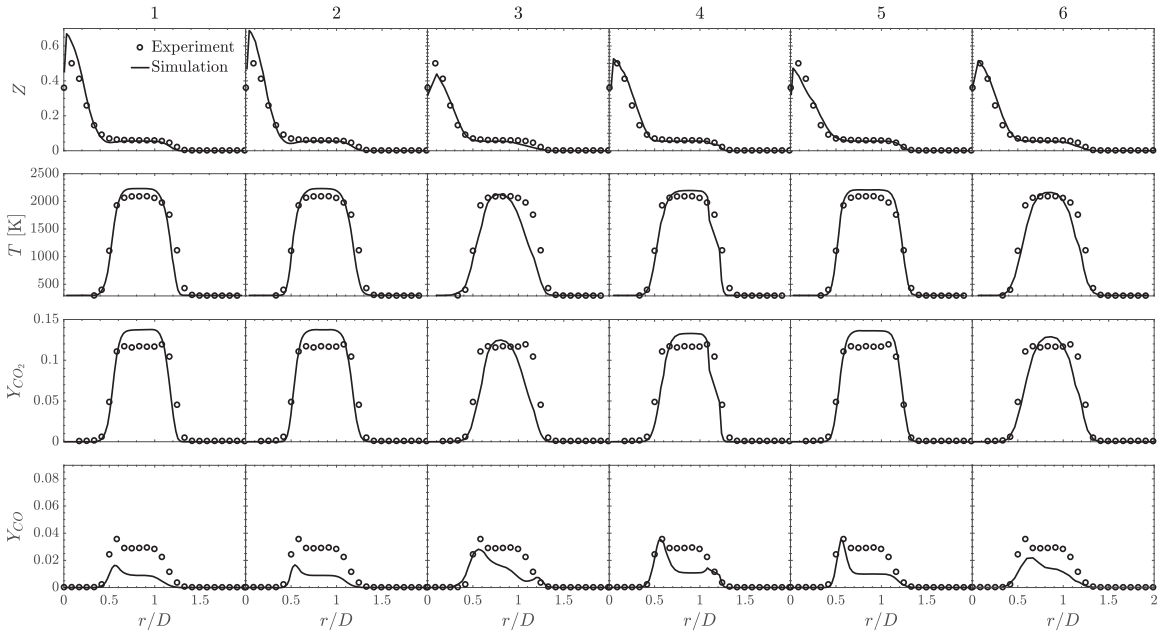

Stanford University

15

Radial profiles of Z, T, CO2 and CO – x/D = 5

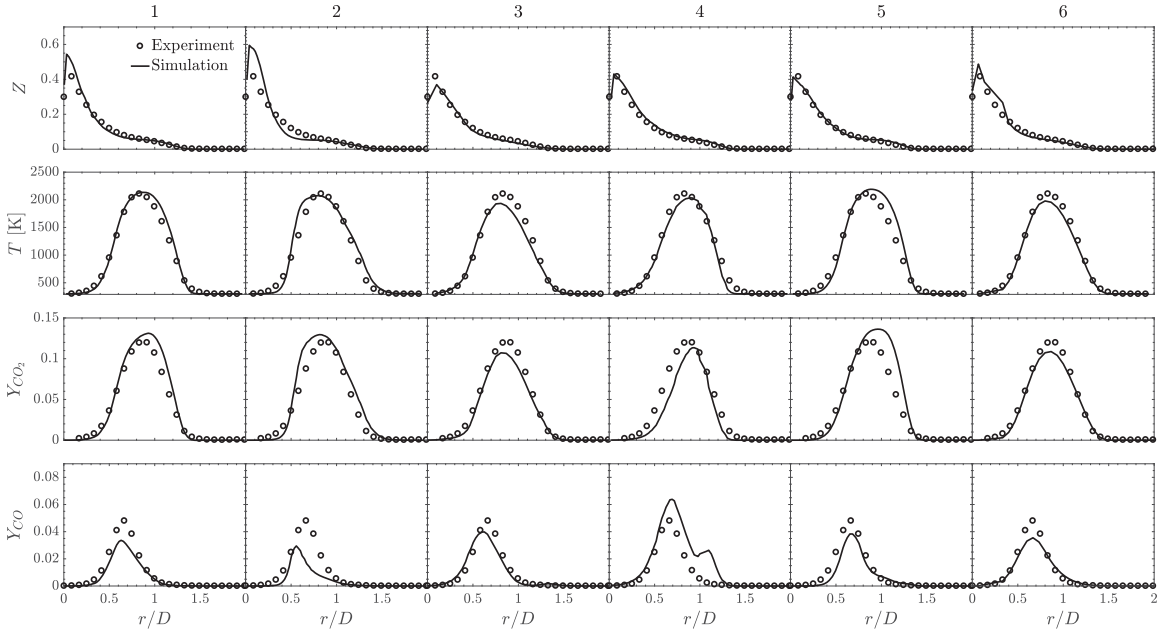

Stanford University

16

Radial profiles of Z, T, CO2 and CO – x/D = 10

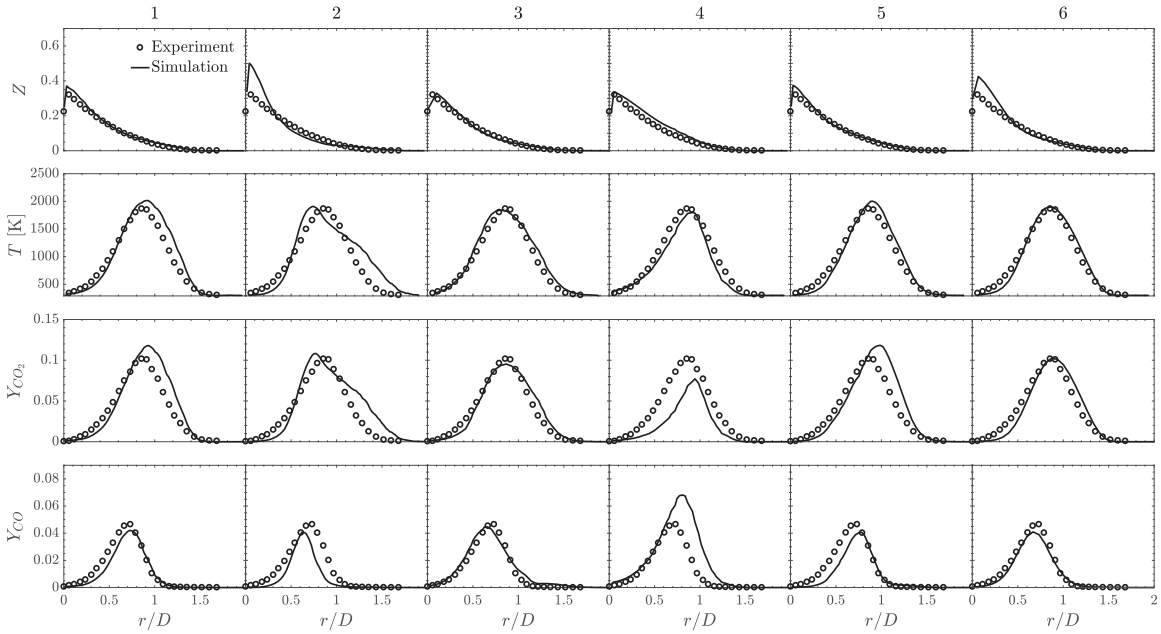

Stanford University

17

Radial profiles of Z, T, CO2 and CO – x/D = 15

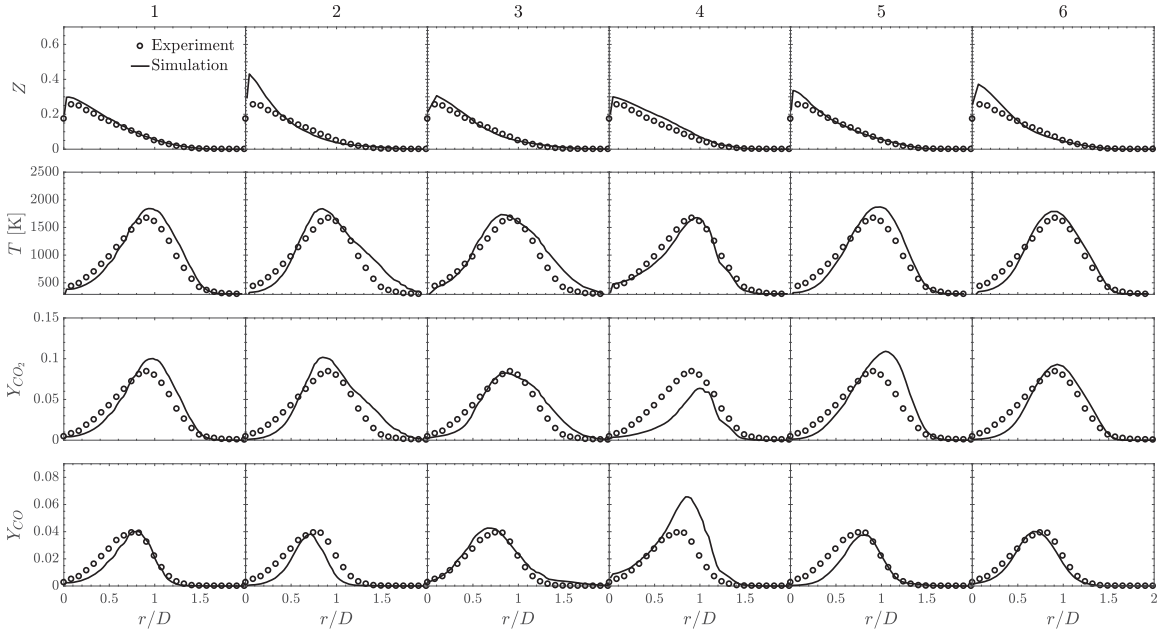

Stanford University

18

Profiles of T, CO2 and CO over Z – x/D = 1

Mixture-fraction conditioned profiles

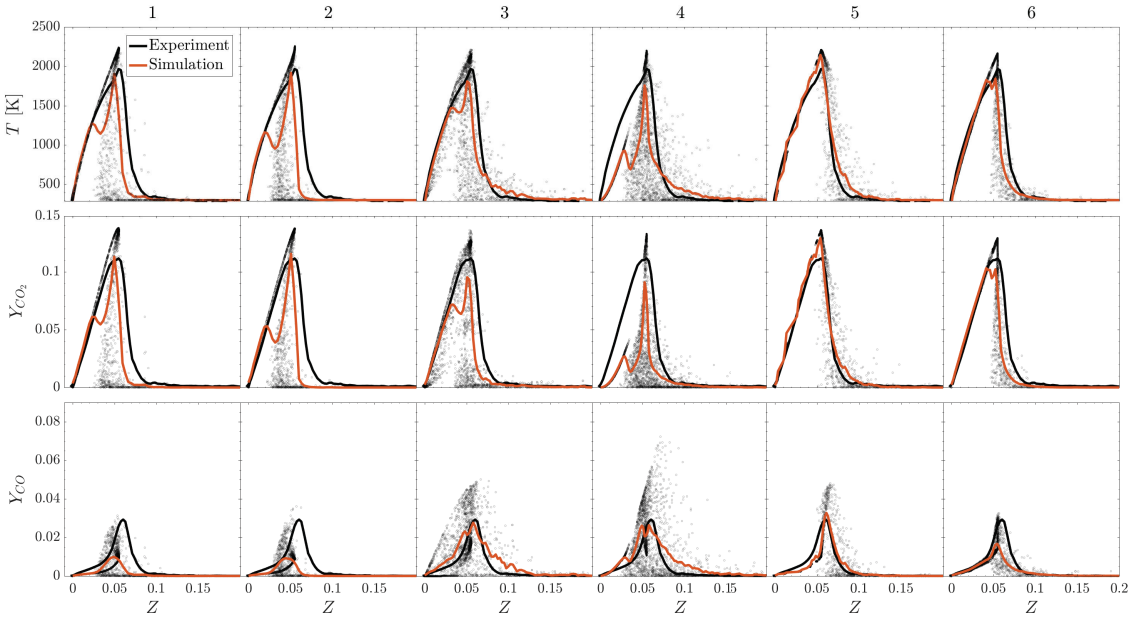

Stanford University

19

Profiles of T, CO2 and CO over Z – x/D = 5

Mixture-fraction conditioned profiles

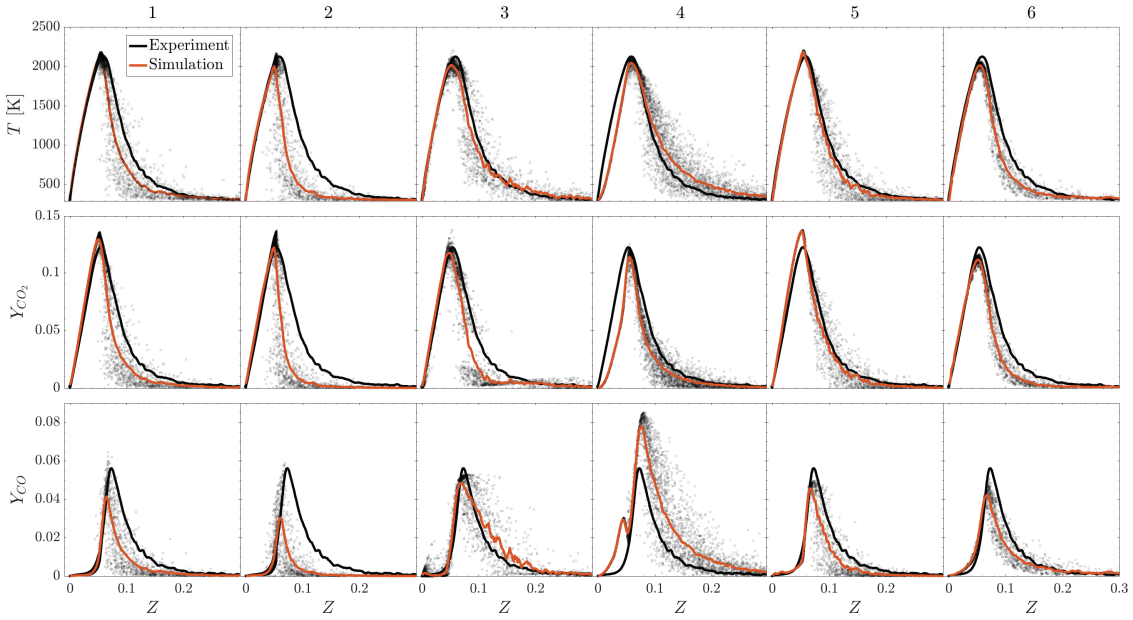

Stanford University

20

Profiles of T, CO2 and CO over Z – x/D = 10

Mixture-fraction conditioned profiles

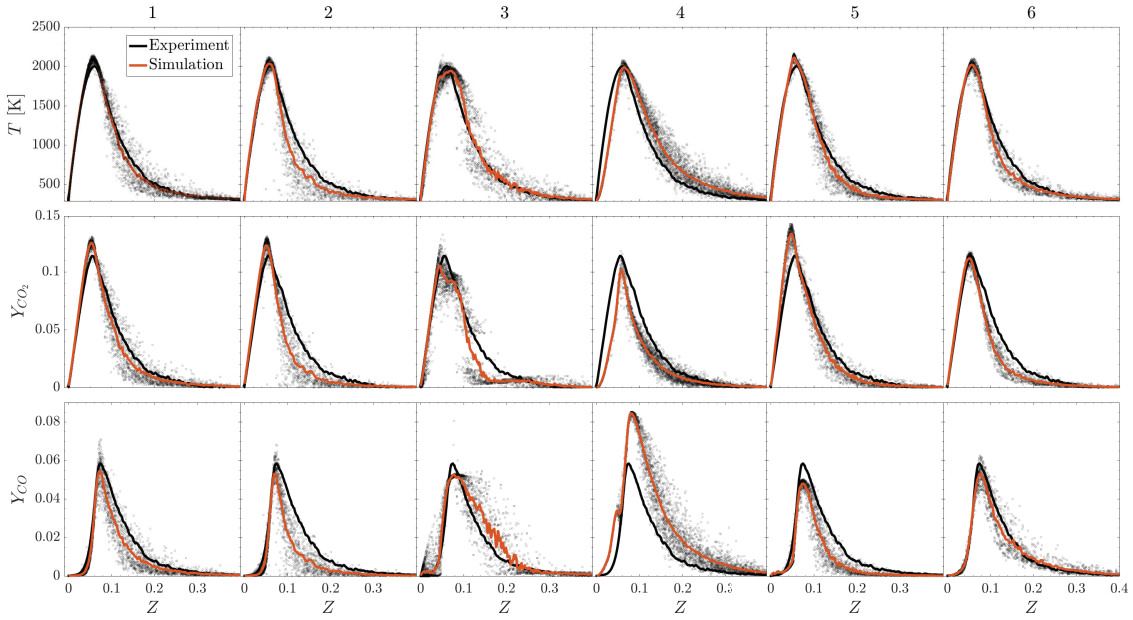

Stanford University

Profiles of T, CO2 and CO over Z – x/D = 15

Mixture-fraction conditioned profiles

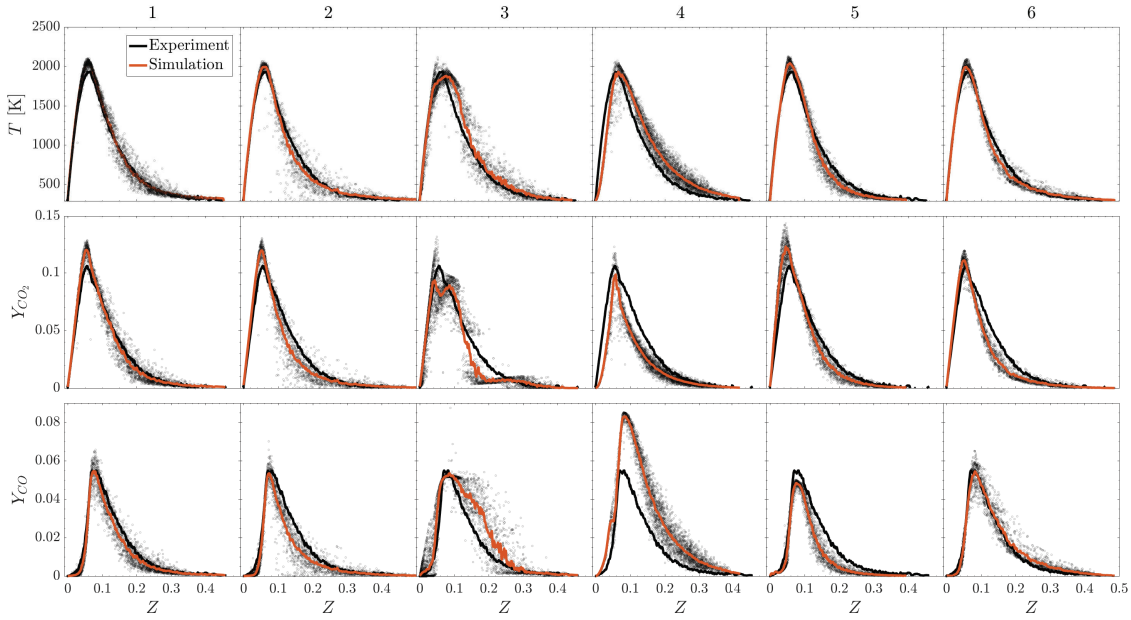

Stanford University

Overall estimate of Wasserstein metric

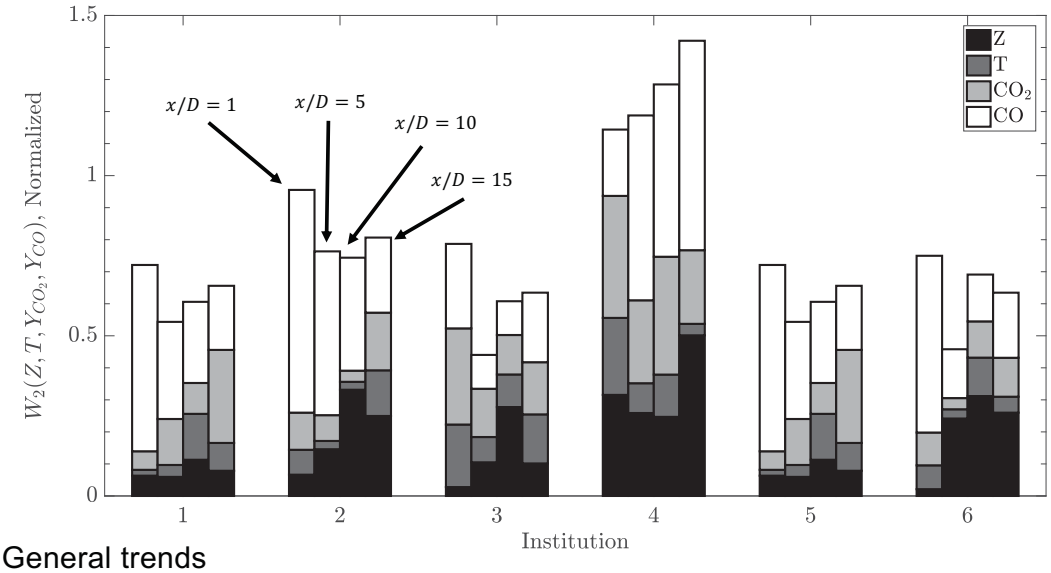

General trends

- Inflow conditions for mixture-fraction well captured by all institutions
- Comparable cumulative deviation between 0.5 and 1.5
- Expected trend of axially evolution in W2

Stanford University

Overall estimate of Wasserstein metric

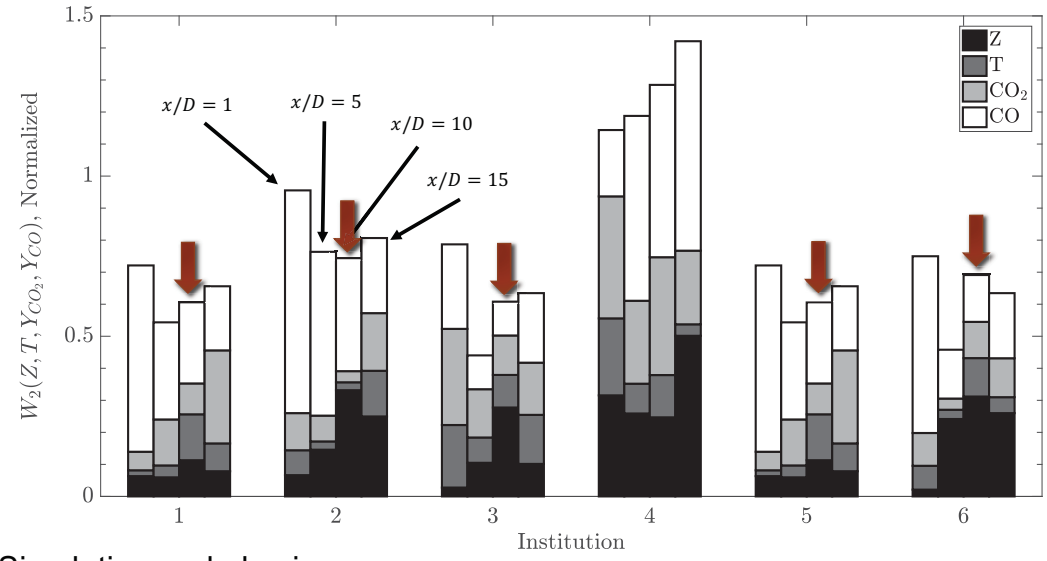

Simulation and physics

- Consistent increase in deviation at x/D = 10 → Entrainment of air into jet, suggests need for further measurements to understand deviation

Stanford University

Overall estimate of Wasserstein metric

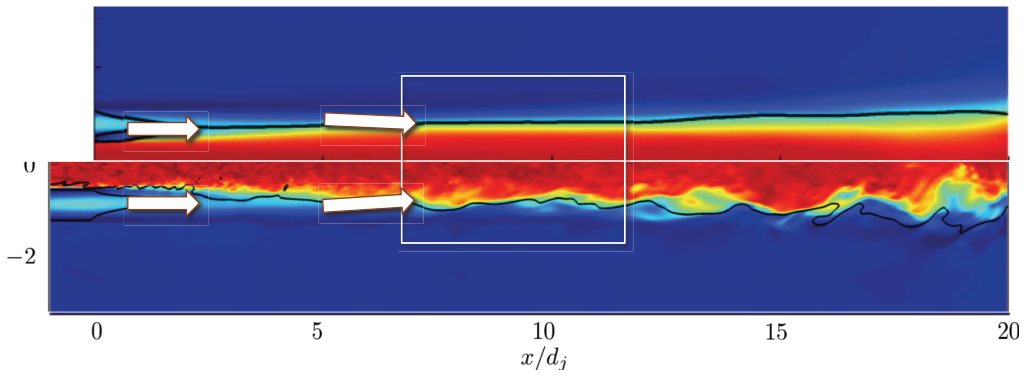

Simulation and physics

- Consistent increase in deviation at x/D = 10 → Entrainment of air into jet, suggests need for further measurements to understand deviation

Stanford University

Overall estimate of Wasserstein metric

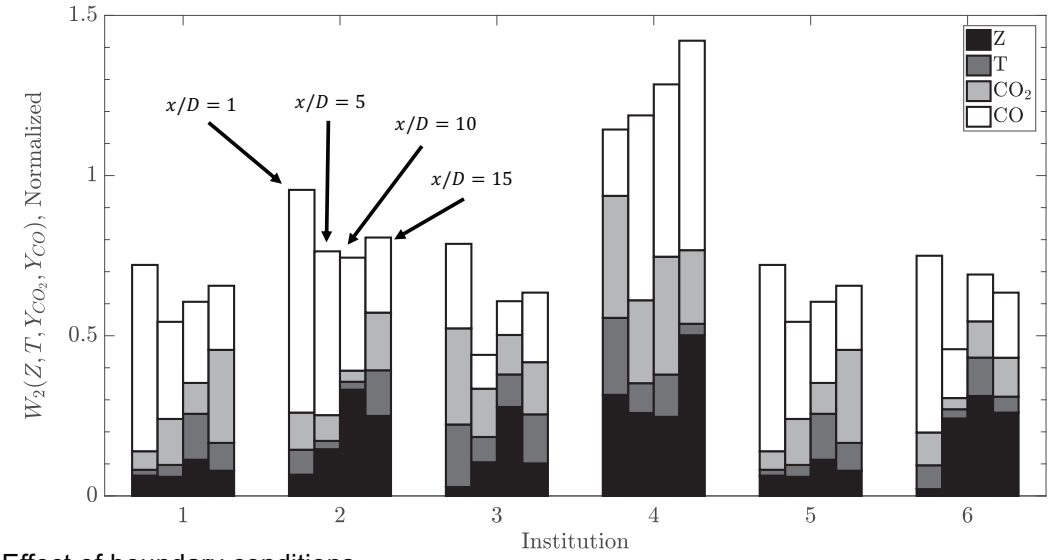

Effect of boundary conditions

- I1/I2: same boundary conditions → comparable results at x/d=1
- I1/I2/I3/I5/I6: LES, turbulent inflow: sequential pipe or upstream inflow condition ➔ seems to be necessary; no indication for need for common inflow profile

Stanford University

Overall estimate of Wasserstein metric

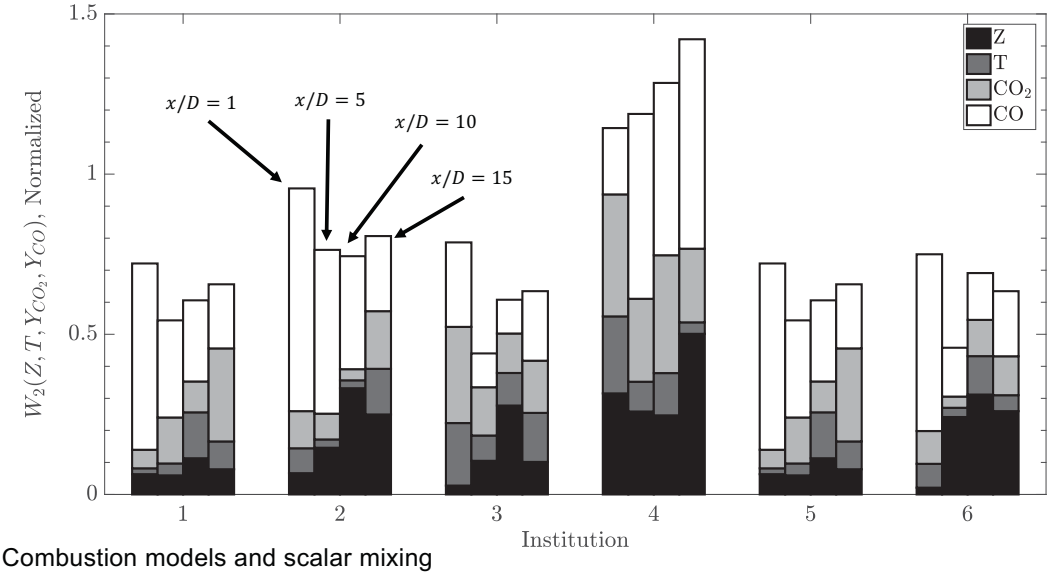

Combustion models and scalar mixing

- I1/I2/I5/I6: CO main contribution to observed deficiency ➔ specification of pilot composition ➔ need for further measurements
- I3: comparable contributions by T, CO2, CO
- I4: CO2/T difference indicates effect of inflow conditions
- I3: equal contribution from T, CO2, CO → flamelet model
- I3/I6: no appreciable difference between flamelet-type combustion models

Stanford University

Overall estimate of Wasserstein metric

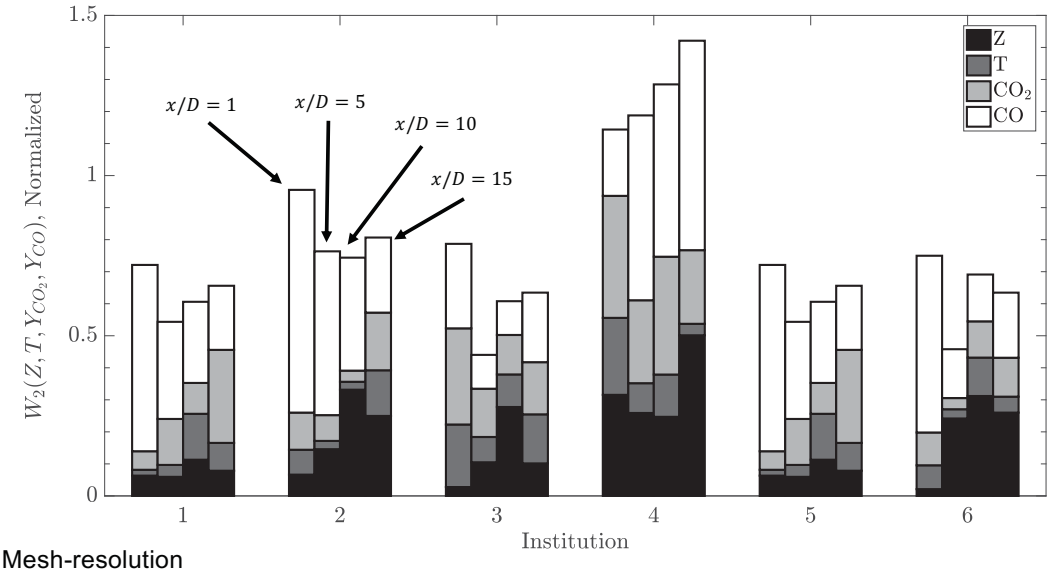

Mesh-resolution

- Mesh-refinement only has modest impact on W2 convergence
- All simulations within ½ (or less) STDEV accuracy
- I2/I4/I6: Increase in W2(Z|*x*) contribution with downstream distance ➔ mesh resolution, mixing models definciencies

Stanford University

Radial profiles of 4-variable Wasserstein metric

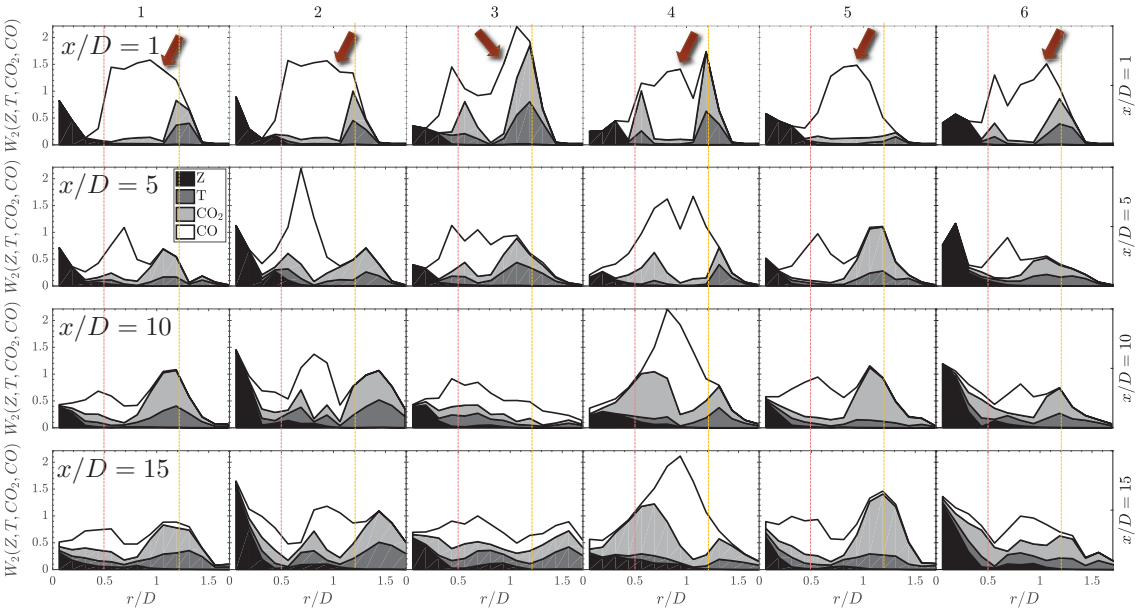

Sources of deficiency – x/D = 1;

- Jet and core-region: mixture fraction (no appreciable reactivity)
- Pilot-stream: temperature/CO2 well captured, CO is main source of deficiency ➔ characterization of CO-emission in pilot!

Stanford University

Radial profiles of 4-variable Wasserstein metric

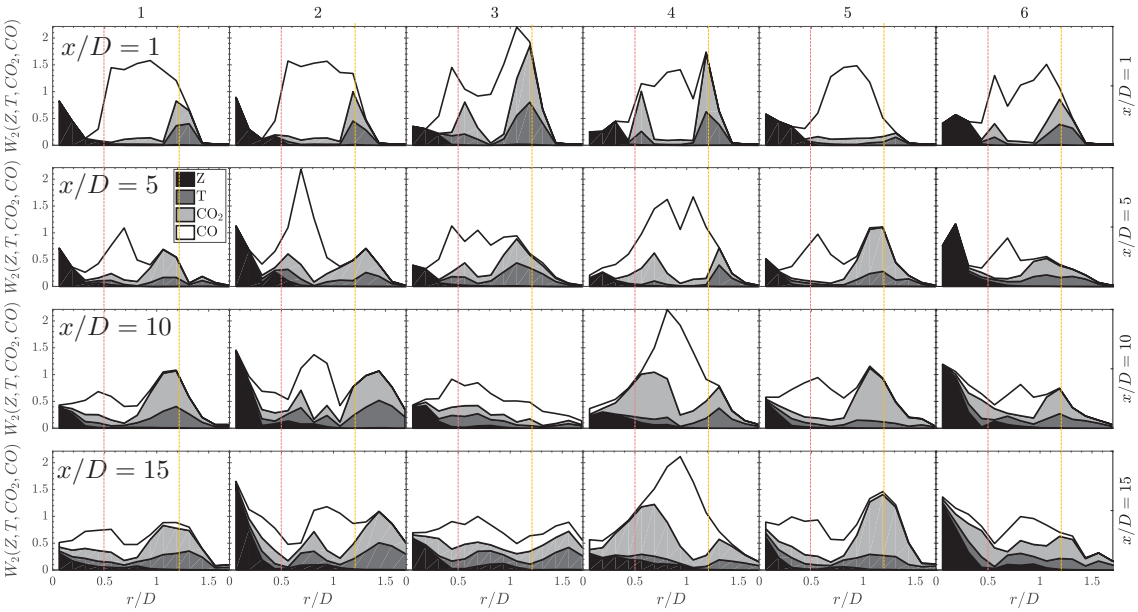

Consideration of radially correlated dependencies

- Impact of jet/pilot and pilot/coflow shear-layer
- Reduction in W2-magnitude with downstream distance
- Boundary conditions vs. Combustion model

Stanford University

Conclusion

Wasserstein metric (Earth Mover Distance) for quantitative evaluation of combustion simulations

- Consider generalization of distance in distribution space
- Applicable to statistical and instantaneous data
- Generalization of mean/rms comparisons to multiscale probabilistic data
- Considers multi-scalar correlations and scalar dependencies

- Multilevel-representation of data
  - Compounded axial profiles
  - Radial profiles

- Enable metric assessment of
  - Model performance
  - Boundary conditions
  - Physical discovery
  - Mesh-convergence

- Introduces notion of
  - Quantities of interest
  - Achievable/required accuracy

Stanford University

Piloted turbulent jet flame with inhomogeneous inlets

Conclusions & perspectives

Michael Mueller

Princeton University

Benoît Fiorina

EM2C - CNRS
CentraleSupélec
University of Paris Saclay

Matthias Ihme

Stanford University

TNF 2018
DUBLIN IRELAND JULY 27-28

Progress made since last TNF

- Very welcome update of flow measurement in non-reactive conditions
- Experimental and numerical characterization of the flow and mixing in cold and hot-inert conditions
  - ▸Shows a strong influence of the pilot stream
  - ▸Sensitivity analysis highlight the difficulties to numerically predict the mixing
- Simulations have been consolidated
  - ▸ numerical results look consistent
  - ▸ less dispersion between predictions
  - ▸ the difference between simulations and experiments reach an asymptote:
    - ▸ physical phenomena not related to combustion are not addressed
    - ▸ strong sensibility to the boundary condition uncertainties, shear layer resolution,

2

Outcome of this joined experimental-numerical study

- Data post-processed for four configurations:
  - ▸Velocity, mixture fraction, temperature and CO
    - Mean and RMS radial profiles
    - Scatter plot
    - Wasserstein metric
- Give a first state of the art quite representative
  - ▸tabulated-skeletal chemistry
  - ▸structured - unstructured solver
  - ▸presumed - transported PDF
  - ▸etc.

3

What's next ?

1. Should have a conclusion on this configuration before the next TNF
   - ▸consolidate the analysis by quantifying as much as possible the ability of the simulations to retrieve multiple combustion regime (with the Wasserstein metric ?)
   - ▸so we can illustrate the state of the art,
   - ▸write a joined paper with contributors who are interested

2. Suggest to add for the next TNF a new configuration in this session which:
   - ▸ eliminates some phenomena that we wish not want to focus on (or we don't know how to address)
   - ▸ so we can further investigate multi mode combustion issues

4

Multi-Regime Burner (MRB)

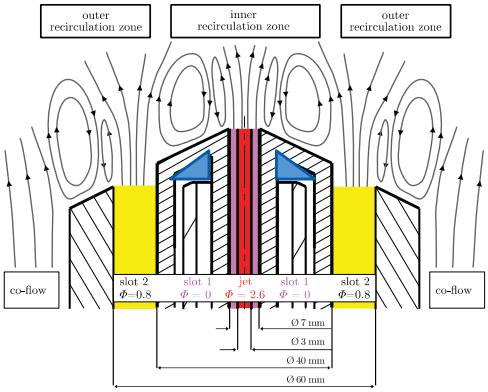

	Jet		Slot 1			Slot 2	
	ϕ	u [m/s]	ϕ	u [m/s] a	u [m/s] b	ϕ	u [m/s]
MRB 14	1.4	105	0	7.5	15	0.8	20
MRB 18	1.8						
MRB 22	2.2						
MRB 26	2.6						

- STFS/HDA/RSM/Sandia joint project, experimental/numerical methods
- Stabilize flames in confined region → premixed/part. premixed/non-premixed → multi-regime combustion model
- Burner geometry
  - Mixing of two fuel(methane)/air streams directly at nozzle exit by large shear
    - central jet (rich → NP)
    - slot 1 (rich → NP)
  - Stabilization by recirculation zone of a lean third flow on a bluff body (slot 2)
  - Slot 2: Movable block: addition of swirl
  - Defined boundary conditions (temp-cntrl)
  - Optical access for laser diagnostics

5

Darmstadt MRB – Raman/Rayleigh/LIF & GFRI

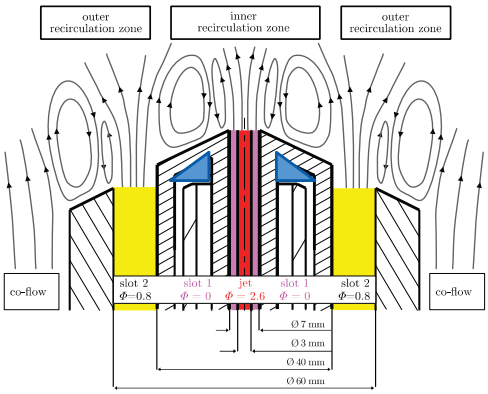

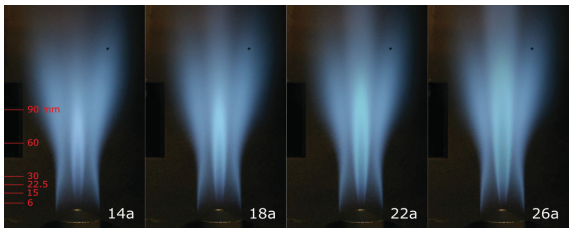

	Jet		Slot 1			Slot 2	
	ϕ	u [m/s]	ϕ	u [m/s] a	u [m/s] b	ϕ	u [m/s]
MRB 14	1.4	105	0	7.5	15	0.8	20
MRB 18	1.8						
MRB 22	2.2						
MRB 26	2.6						

6

Darmstadt MRB – Raman / Rayleigh / LIF & GFRI

MRB26,
equivalence ratios

2.6 / 0.0 / 0.8
Jet /Slot 1 / Slot 2

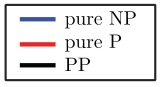

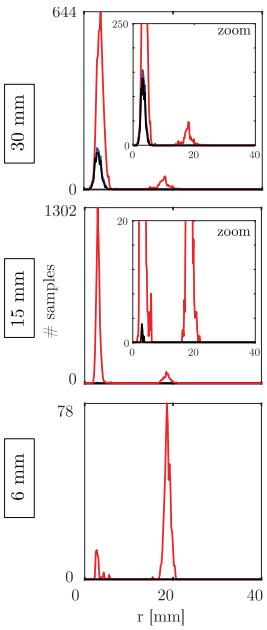

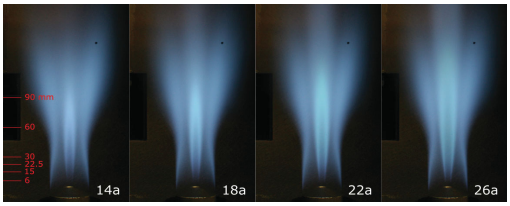

- Sandia (Rob Barlow) Raman/Rayleigh/LIF & X-PLIF
- Future: PIV/PLIF, more cases Raman/Rayleigh/1D-OHLIF (DA)
- Combustion regime identification → GFRI (S. Hartl)
  - applying CEMA, heat-release, Z,…
  - 1D Raman/Rayleigh, samples along 6mm
  - No pure premixed (PP), none-premixed and partially premixed(PP) samples

7

blank

Update on Cambridge swirled flames

Coordinators: Benoit Fiorina, Andreas Kempf and Eray Inanc

There were two objectives of this session, i.) presenting new simulation results for the stratified swirled burners investigated at Cambridge and Sandia and ii.) analyzing current CO models and developing them further.

The swirl burner SwB [Sweeney et al. C&F 159:9, 2012] includes three concentric tubes in a laminar co-flow, where the center of the tube is sealed with a ceramic cap (bluff-body) that minimizes heat-losses. The non-swirled configuration of this burner has been considered at TNF since 2012, however, the swirled configuration is now considered for the first time. Similar to the non-swirled variant, the swirled flame is stabilized by the recirculation of combustion products downstream of the central bluff-body. The strong swirl increases the strength of recirculation.

Recently, Proch et al. [C&F 180, 2017] published first flame-resolved simulations of the non-stratified and non-swirled case SwB1. The Connecticut and Duisburg groups presented their updated results on this case. These results were in agreement with the Proch data and the other groups' results. The transported FDF model used by the Connecticut group included (partially implemented) differential diffusion effects, whereas the Duisburg group applied a Monte-Carlo FDF method without differential diffusion effects. Results from these advanced models showed no improvement over the classical ATF/FGM approach.

For the swirled cases, five international groups contributed their own established techniques, i.) the group of Zhao at the University of Connecticut, ii.) the group of van Oijen at Eindhoven, iii.) the group of Parente at Bruxelles, iv.) the group of Fiorina at EM2C in Paris, and v.) the group of Kempf at Duisburg-Essen. The results presented showed that the CO predictions in the swirled case are problematic close to the burner, unlike for the non-swirled variant.

As demonstrated by the Duisburg group, the slow, almost laminar flow in the vast recirculation zone (RZ) required a larger computational domain (due to the size of the RZ) and longer run-time (due to the larger integral scales of the RZ) than for the non-swirled case. The group estimated that the domain should be at least 175 mm wide and that the flame stabilized just after one and a half flow through times of the slow co-flow. (It should be noted that these values depend on the initialization strategy.)

The heat loss effects in this configuration were claimed to be low by the experimentalists. However, it was expected that the enhanced RZ yielded more heat losses to the bluff-body in the swirled variant than in the non-swirled case. Hence, predicting correct flame propagation speeds could be difficult with adiabatic combustion models. Nevertheless, the contributed groups showed that the main thermochemical properties of the fluid after three inner tube diameters were in good agreement when using an adiabatic solver. AT TNF 14, the Paris group had demonstrated that there was an effect of heat loss in the region next to the bluff-body. Considering this finding, a non-adiabatic model could possibly improve results very close to the burner, but this hypothesis was not confirmed since no group used a non-adiabatic model.

It was apparent that some of the contributed results suffered from small computational domains or early sampling. Generally, the computed Reynolds-averaged mean major quantities, such as momentum, equivalence ratio, temperature and mass fractions of CH4, O2, and CO2, agreed well with the measurements slightly further downstream, whereas the spread angle of the swirled jet was under-predicted. The same trend was observed for the root-mean square (RMS) values. Most of the deviations, however, occurred close to the bluff-body. Contributors came to the conclusion that the resolution and the settlement time of the RZ could cause these deviations.

As for the CO and H_2 mass fractions, they were over-estimated close to the burner. The closest agreement was obtained by a Monte-Carlo FDF method. The Duisburg-group also presented results using an ATF/FGM model with the same boundary conditions and computational grid, but the computationally more expensive Monte-Carlo technique provided a better agreement for most quantities.

The Connecticut group presented the results of a transported FDF method that (partially) includes differential diffusion effects. Where the results were quite impressive, a clear advantage over simulations (from the same group) without differential diffusion was not observed. The Bruxelles group showed two sets of simulation results, using a cylindrical and a Cartesian coordinate system and grid. The radial system improved the results, however, corresponded grid size on the simulation with Cartesian coordinates were too large to expect otherwise.

Larger deviations were observed for the stratified cases SwB7 and SwB11. The Duisburg group, as the sole contributor, showed that the stratification can be predicted acceptably well by using FGM. The stratified flames were also affected by the recirculated products, which yielded strong deviations of the temperature fields near the bluff-body. Surprisingly, the predictions tended to get better at downstream locations. It was observed that the locations close to the burner featured high H_2O, CO_2 and CO concentrations, which could either be recirculated from downstream or diffused from the thin flame brush.

Cambridge Swirl Flame and Modelling of CO

TNF Workshop, 27-28 July 2018, Dublin

UDE: Alvin I. Surjana, Pascal Gruhlke, Seung J. Baik, Eray Inanc, Andreas M. Kempf*
EM2C: Constantin Nguyen-Van, Benoît Fiorina
UCONN: Hasret Turkeri, Xinyu Zhao
TUE: Suleyman Karaca, Jeroen A. v. Oijen
ULB: Zhiyi Li, Alessandro Parente

Cambridge/Sandia: Mark Sweeney, Simone Hochgreb, Matt Dunn, Rob Barlow

*andreas.kempf.uni-due.de

Configuration

Photograph and snapshot from SwB1
(Proch et al. C&F 2017)

Cases	SwB1	SwB3	SwB7	SwB11
Stratification Ratio (SR)	**1**	**1**	**2**	**3**
Φ_i	**0.75**	**0.75**	**1.0**	**1.125**
Φ_o	**0.75**	**0.75**	**0.5**	**3.75**
U_i / ms^{-1}	8.31			
U_o / ms^{-1}	18.7			
U_{co} / ms^{-1}	0.4			
Swirl Flow Ratio (SNR)	0	0.33		
Swirl Number (S)	0	0.79		
Fuel	CH_4 / air			
Co-flow	Air			

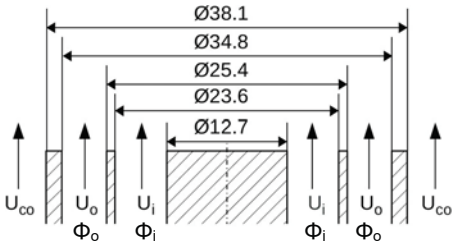

Overview SwB1

„Quasi"-DNS by Proch et al. [C&F 2017], Δ = 0.1 mm

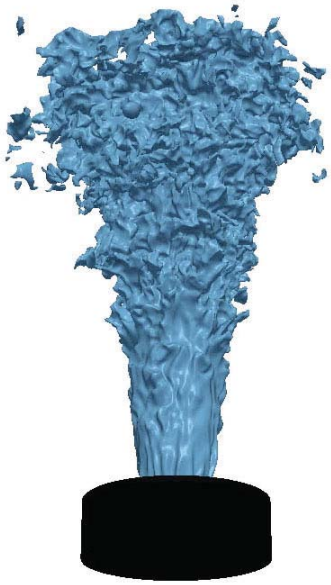

Flame Brush

Post-processed by L.Cifuentes (UDE)

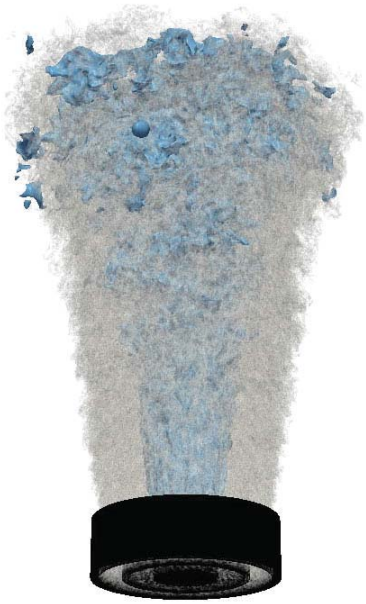

Turbulent Eddies

3

Publications

since 2012

Experimental

- M.S. Sweeney, S. Hochgreb, M.J. Dunn, R.S. Barlow, C&F 159 (2012) P. i. 2896–2911 and P. ii. 2912–2929
- M. Euler, R. Zhou, S. Hochgreb, A. Dreizler, C&F 161 (2014) 2842-2848
- G. Magnotti, R. S. Barlow Combustion and Flame (2014) 100-114
- M. M. Kamal, R. S. Barlow, S. Hochgreb, C&F 162 (2015) 3896-3913 - Also numerical
- M. M. Kamal, R. S. Barlow, S. Hochgreb, C&F 166 (2016) 76-79
- J. Apeloig, P. Gautier, E. Salaün, B. Barviau, G. Godard, S. Hochgreb, F. Grisch 18th Int. Symp. App. Laser & Imaging Techniq. Fluid Mech. (2016)

Numerical

- S. Nambully, P. Domingo, V. Moureau, L. Vervisch, C&F 161 (2014) P. i. 1756-1774 and P. ii. 1775-1791
- F. Proch, A. M. Kempf, C&F 161 (2014) 2627-2646.
- R. Mercier, T. Schmitt, D. Veynante, B. Fiorina, Proc. Comb. Inst. (2014)
- *Swirl:* T. Brauner, W. P. Jones, A. J. Marquis. *Flow, Turb. and Comb.* 96 (2016) 965-985.
- H. Zhang, Z. Yu, M. Cheng, M. Zhao, App. Math. Modelling 62 (2018) 476-498
- F. Proch P. Domingo, L. Vervisch, A. M. Kempf C&F 180 (2017) P. i. 321-339 and P. ii. 340-350

4

New Experiments, Instantaneous 3D reconstructions using Computed Tomography of Chemiluminescence (CTC)

Experimental setup

- 30 CCD cameras, mounted on an aluminium plate with equiangular spacing of 6°
- Sensor: ½ inch Sony ICX414, 659 by 494 pixels of size 9.9 µm
- Objective: Kowa C-mount lens with a focal length of 12 mm
- Schott BG40 filters used to suppress the emission from thermally excited H_2O
- Simultaneous image capturing, with camera exposure time t_{exp} = 500 µs
- Several cases, both swirled and non-swirled, have been reconstructed

The CTC

- Chemiluminescence images obtained from different angles around the flame
- The algorithm [1,2], that is based on the Algebraic Reconstrcution Technique (ART) [3], reconstructs the chemiluminescence field directly in 3D (field discretised into voxels)
- The technique was previously tested using several phantoms (exactly known fields) and real flame experiments [1,2,4]
- Depth of field and perspective distortion are accounted for

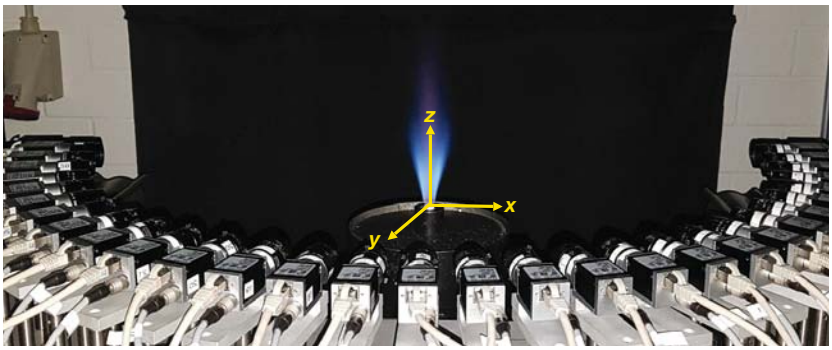

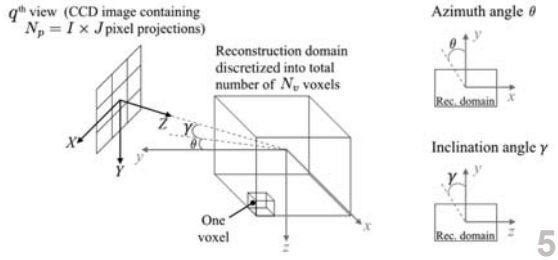

[1] J. Floyd, P. Geipel, A. Kempf, Combust. Flame 158, 2012
[2] J. Floyd, A. Kempf, Proc. Combust. Inst. 33, 2011
[3] R. Gordon, IEEE T. Nucl. Sci. 21, 1974
[4] K. Mohri, S. Görs, J. Schöler, A. Rittler, T. Dreier, C. Schulz, A. Kempf, Appl. Optics 56, 2017

5

New Experiments, Instantaneous 3D reconstructions using Computed Tomography of Chemiluminescence (CTC)

Previous phantom: LES of a turbulent premixed CH_4 / air swirl stabilised flame (TECFLAM [4])

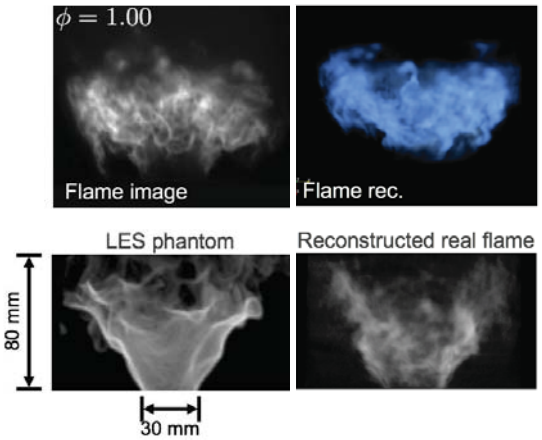

Cambridge stratified SwB1 flame reconstruction

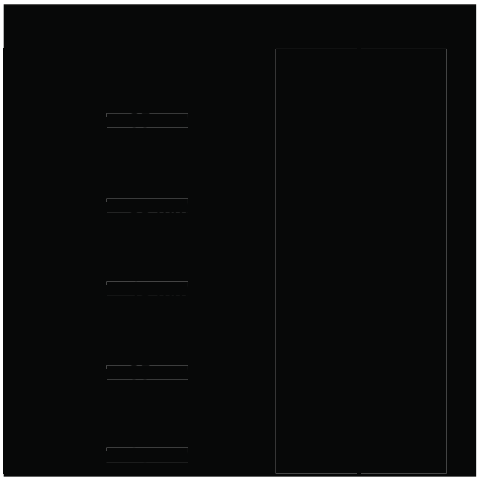

[4] K. Mohri, S. Görs, J. Schöler, A. Rittler, T. Dreier, C. Schulz, A. Kempf, Appl. Optics 56 (2017)
[5] F. Proch, A. Kempf, Combust. Flame 180 (2017))

6

CTC reconstructions of the SwB3 flame

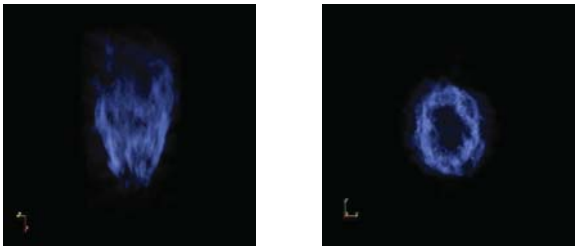

Vertical slice

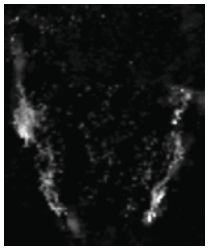

Horizontal slices

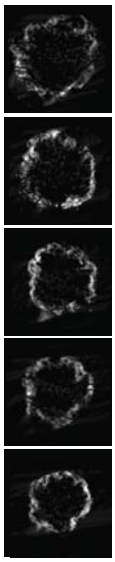

Isosurfaces

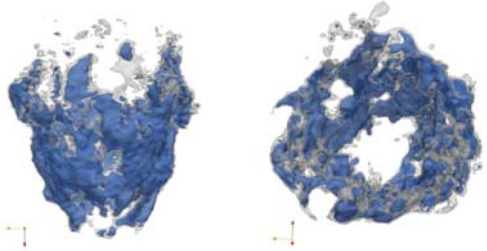

Volume rendered

7

Model comparison

TNF Spirit: Results are provided to trigger discussion and to show the state of the art. This means that „preliminary results“ are provided - contributions are welcome, even if they are not yet „journal quality“.

UDE: Alvin I. Surjana, Pascal Gruhlke, Seung-Jin Baik, Eray Inanc, Andreas M. Kempf
EM2C: Constantin Nguyen-Van, Benoît Fiorina
UCONN: Hasret Turkeri, Xinyu Zhao
TUE: Suleyman Karaca, Jeroen A. v. Oijen
ULB: Zhiyi Li, Alessandro Parente

Cambridge/Sandia: Mark Sweeney, Simone Hochgreb, Matt Dunn, Rob Barlow

Contributions for simulations

Contributor	**EM2C** **Nguyen**, Fiorina	**UDE** **Inanc**, Kempf	**UDE** **Baik**, Kempf	**UDE** **Gruhlke**, Kempf	**TUE** **Karaca**, Oijen	**UCONN** **Türkeri,** Zhao	**ULB** **Li,** Parente
Cases	SwB3	SwB3/7/11	SwB1/3/7/11	SwB1/3	SwB3	SwB1/3	SwB3
Turbulence model	Sigma (Nicoud et al.) C_m = 1.5	Sigma (Nicoud et al.) C_m = 1.5	Sigma (Nicoud et al.) C_m = 1.5	Transported K (C_e = 1.048, C_k = 0.094)	K-Equation	One-Equation	One-Equation
Combustion model/SGS Distribution	Virtual chemistry, filtered wrinkled flamelet	ATF-PFGM / Assumed PDF	Hybrid FDF-Flamelet, Monte-Carlo Particle	ATF-FGM / none	FGM / none	Transported PDF-IEM-ARM1 Mech. (nS =16)	Partially Stirred Reactor
Code	YALES2	PsiPhi	PsiPhi	OpenFOAM	OpenFOAM	OpenFOAM	OpenFOAM
Schemes: Space/Time	4th-Order TVD / RK4	2nd-Order CDS (rU) 1.5th-Order TVD (rP) / RK3	2nd-Order CDS (rU) 1.5th-Order TVD (rP) / RK3	1.5th-Order TVD / CN Blended (0.3 Exp./0.7 Imp.)	2nd-Order TVD / RK2	2nd-Order CDS (rU) 1.5th-Order TVD (rP) / RK2	2nd-Order CDS (rU) 1.5th-Order TVD (rP) / RK2
Computational Domain*	**800/100 M** hex. cells, cylinder, l=1.1m, D = 1 m (Δ = 0.25 mm)	**46.6 M** cubic cells, 180x180x180 mm^3 (Δ = 0.5 mm)	**38 M** cubic cells, 168x168x168 mm^3 (Δ = 0.5 mm)	**16.6 M** hexahedral cells, box, 180x180x180 mm^3 (Δ = 0.5 mm)**	**1.7 M** hexahedral cells, cylinder, i = 110 mm/D = 110 mm **(Δ = 0.1 mm)****	**2.4 M** hexahedral cells, cylinder, i = 200 mm/D = 400 mm (Δ = 0.25 mm)**	**6.4 M** hexahedral cells, box 180x180x180 mm^3 / (2.4 M hexahedral cells, cylinder, i = 150 mm/D = 60 mm) (Δ = 1 mm)**
Real Time*	**0.45 s**	**2 s**	**0.5 s**	**0.6 s**	**0.3 s**	**0.24 s**	**0.1 s**
Cost* and HPC	570,000 CPUh	83,000 CPUh / MagnitUDE	315,000 CPUh / MagnitUDE	91,000 CPUh / MagnitUDE	12,000 CPUh	25,000 CPUh	115,000 (20,000)*** CPUh
Cost* to sim. 1 seconds	1,260,000 CPUh	41,500 CPUh	630,000 CPUh	150,000 CPUh	40,000 CPUh	100,000 CPUh	1,150,000 (200K)*** CPUh
Cost* for 1s, 1M cells	12,600 CPUh	890 CPUh	16,600 CPUh	9,040 CPUh	23,530 CPUh	41,700 CPUh	180,000 CPUh

*Information is given for the Swirled Simulations, **Near the flame-brush, *** Second mesh data

9

SwB1

Overview SwB1

non-Swirled - no stratification

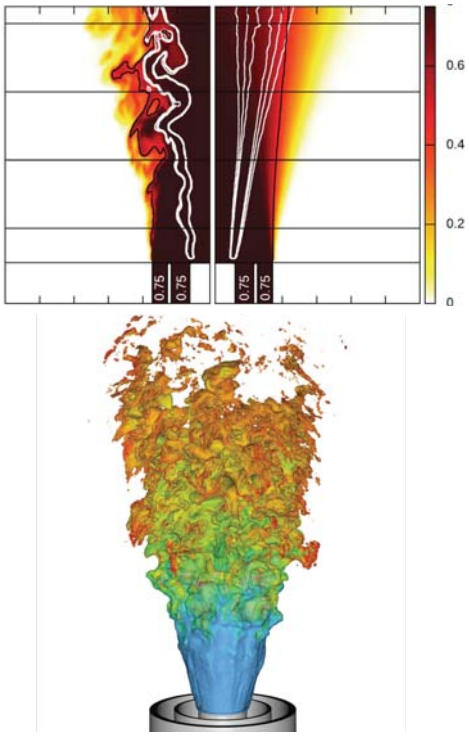

Contributions and their labels:

Experiments Sweeney et al. C&F 2012

„Quasi"-DNS Proch et al., C&F 2017

LES Proch et al., C&F 2017

- UDE - OF, Gruhlke et al., OpenFOAM
- UDE - SB, Baik et al., Hybrid FDF/Flamelet
- UCONN - ED, Türkeri et al., Trans. PDF - no Diff. Diffusion
- UCONN - DD, Türkeri et al., Trans. PDF - Diff. Diffusion

11

Overview SwB1

DNS by Proch et al. [C&F 2017], Δ = 0.1 mm

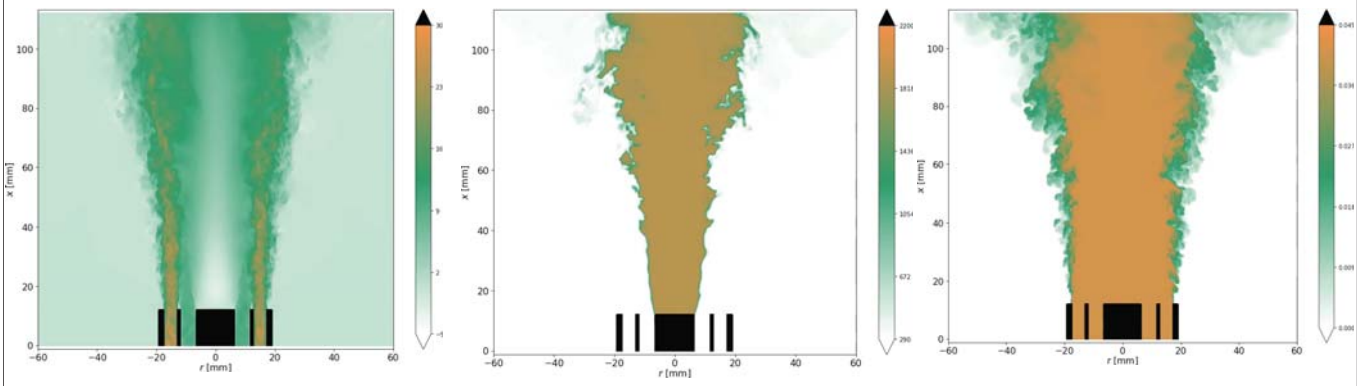

Axial Velocity | Temperature | Mixture fraction

12

Overview SwB1

DNS by Proch et al. [C&F 2017], Δ = 0.1 mm

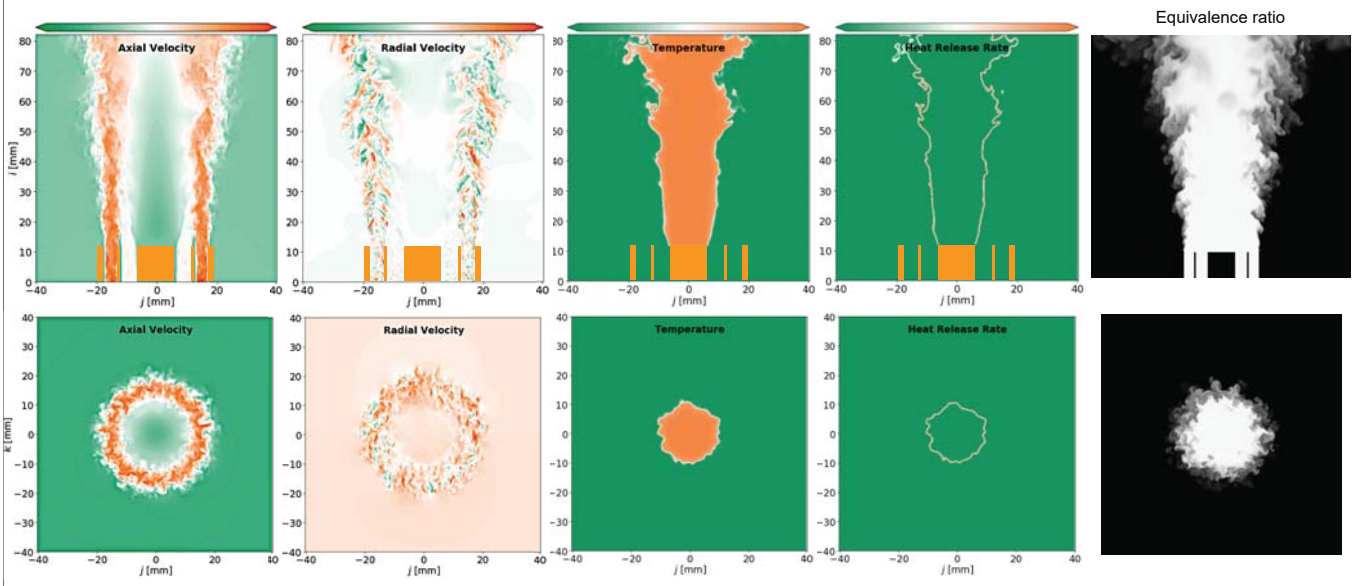

SwB1 - Axial Velocity

Mean

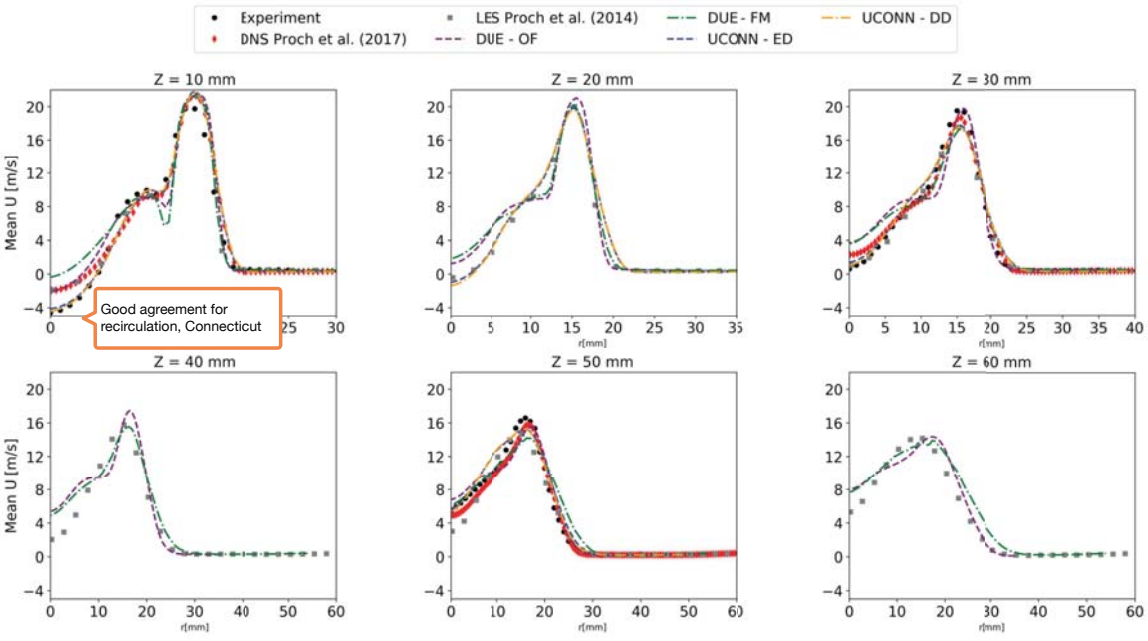

SwB1 - Axial Velocity

RMS

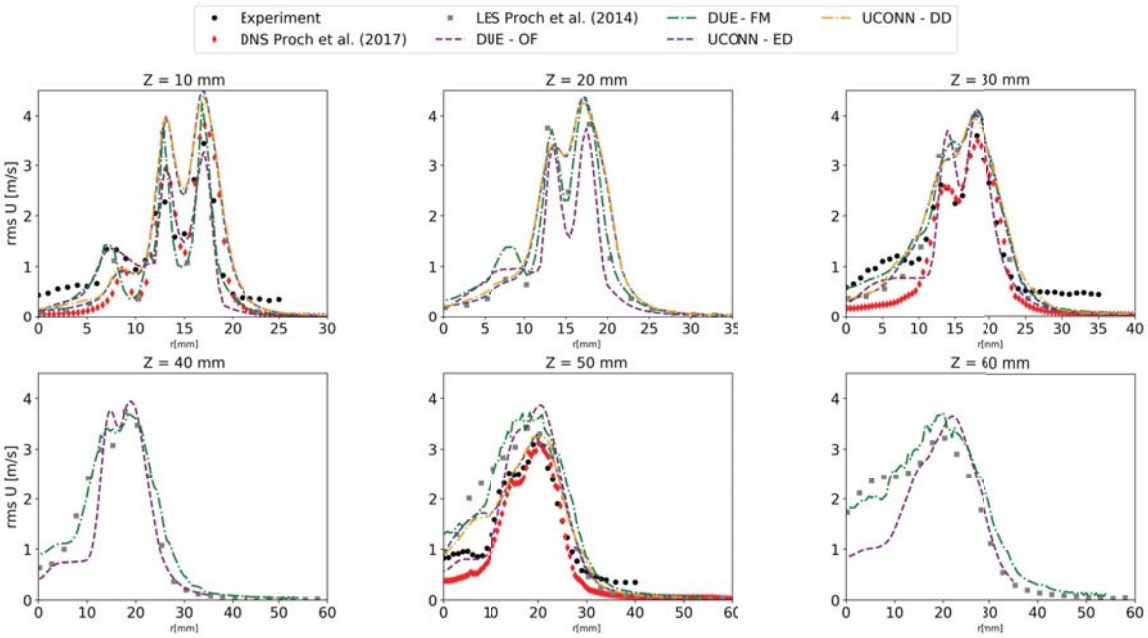

15

SwB1 - Equivalence Ratio

Mean

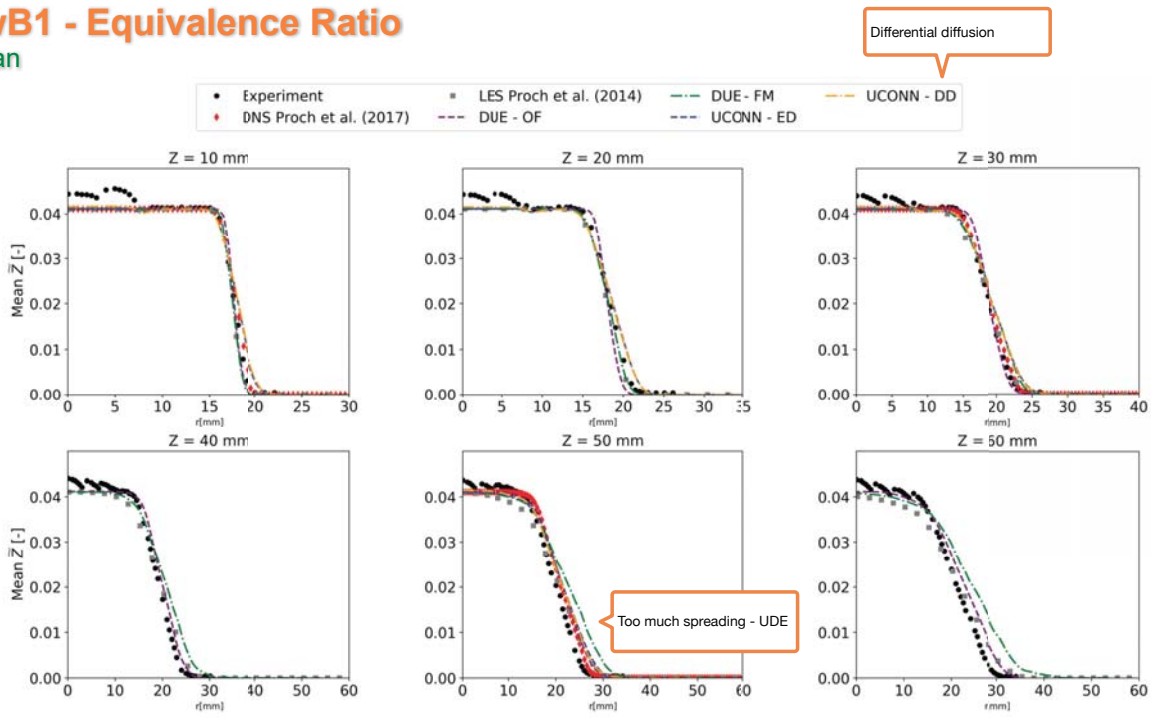

16

SwB1 - Equivalence Ratio

RMS

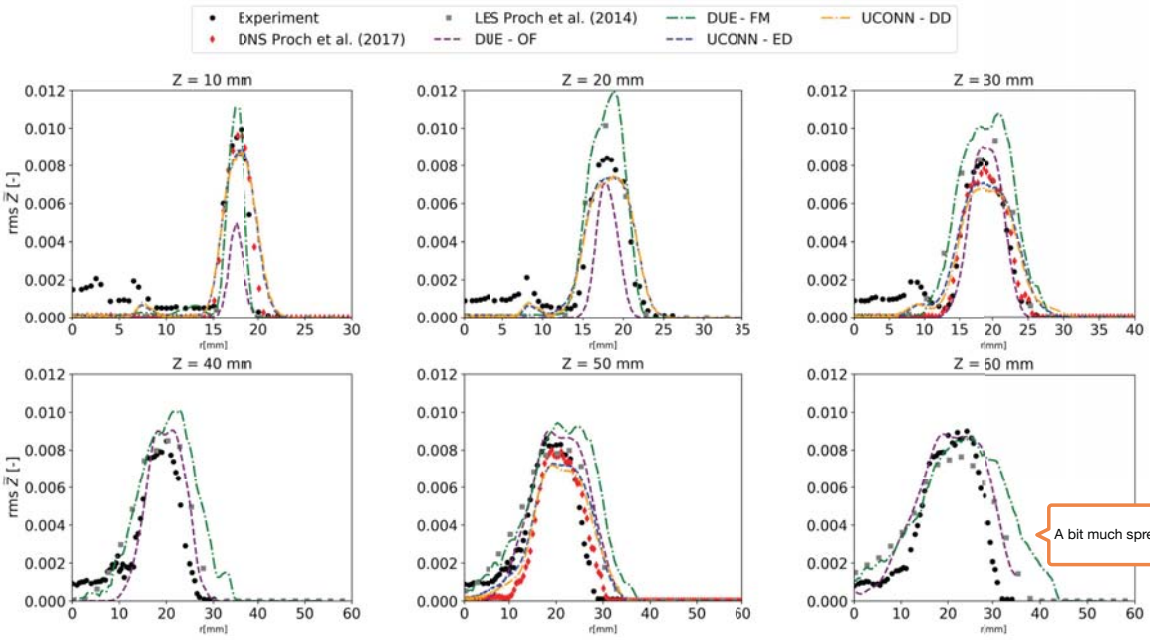

17

SwB1 - Temperature

Mean

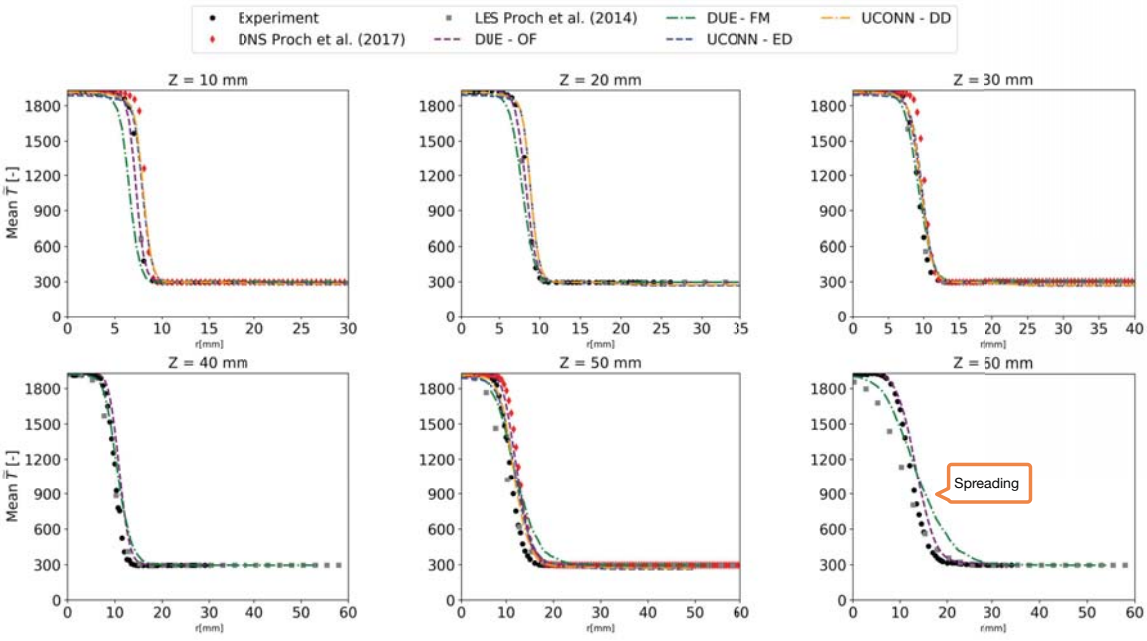

18

SwB1 - Temperature

RMS

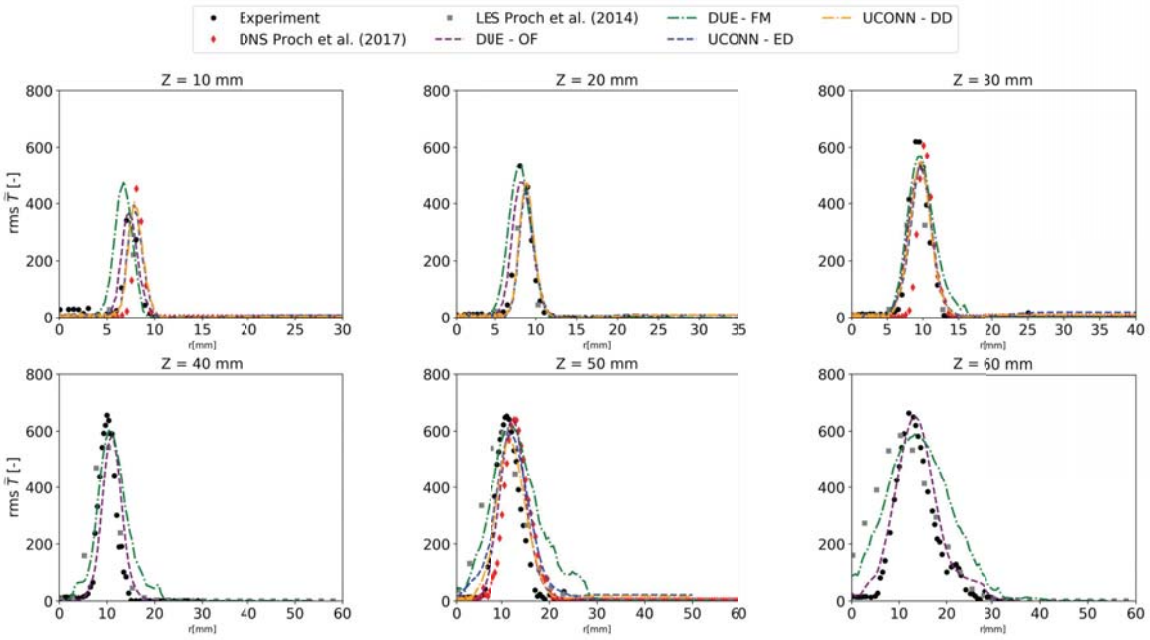

19

SwB1 - CO Mass Fraction

Mean

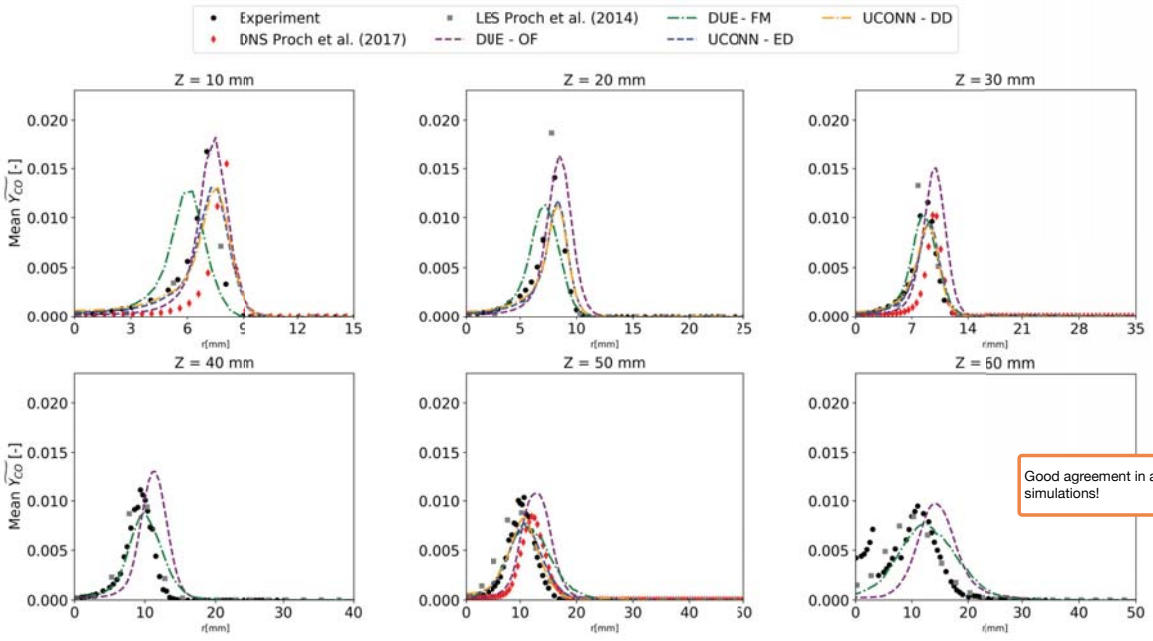

Good agreement in all simulations!

20

SwB1 - CO Mass Fraction

RMS

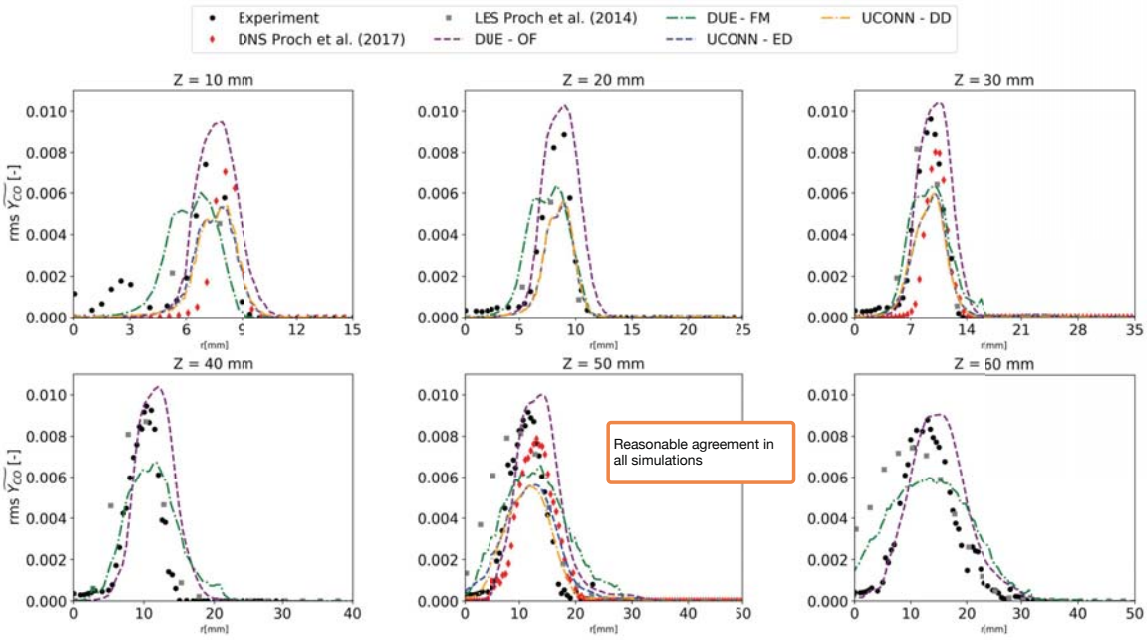

21

SwB1 - SwB5

Cross effects of heat losses and preferential diffusion on the Inner Recirculation Zone (IRZ) temperature

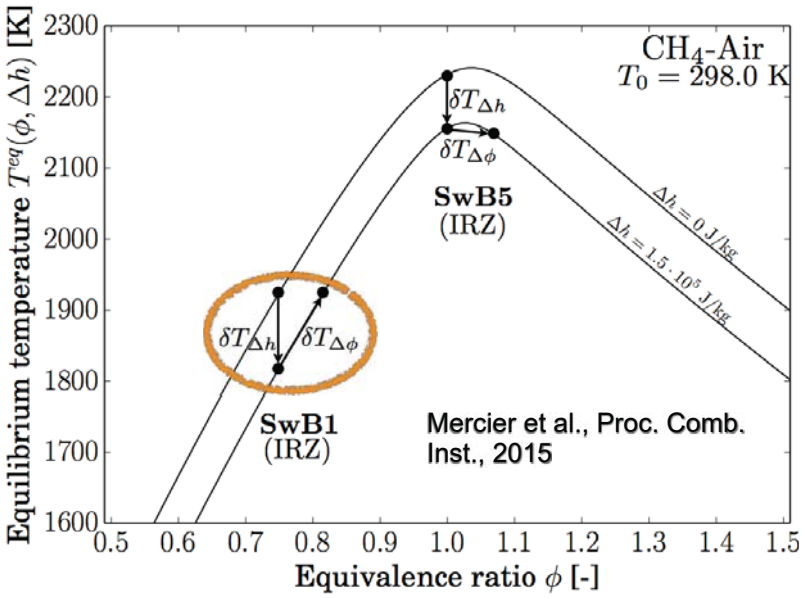

22

SwB1 - Conclusions

- SwB1 is well captured by all groups
- There is no real CO issue, even at upstream locations
- Equivalence ratios at the centreline is even under predicted where differential diffusion was included (Conneticut)
- SwB1 can be modeled and predicted well, but questions remain:
  - What happens further downstream? (Mixing of air, reactants and products)
  - What happens in stratified cases (downstream of) stratification zone?

SwB3

This swirl flame is costly to simulate:
Large recirculation zone - big domain
Slow recirculation - long initialisation to statistically converged results

As a result, most predictions look far worse than for SwB1

Overview of Cases with largest Swirl Number

LES by E. Inanc, Δ = 0.5 mm

Equivalence Ratios over 25 ms

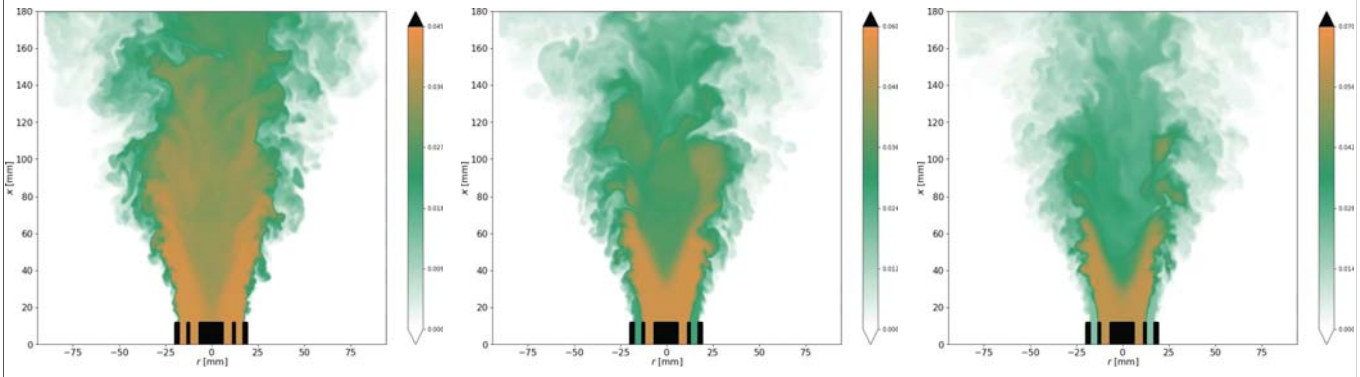

SwB3
no-stratification

SwB7
weak-stratification

SwB11
high-stratification

Overview of Cases with largest Swirl Number

LES by E. Inanc, Δ = 0.5 mm

Temperature over 25 ms

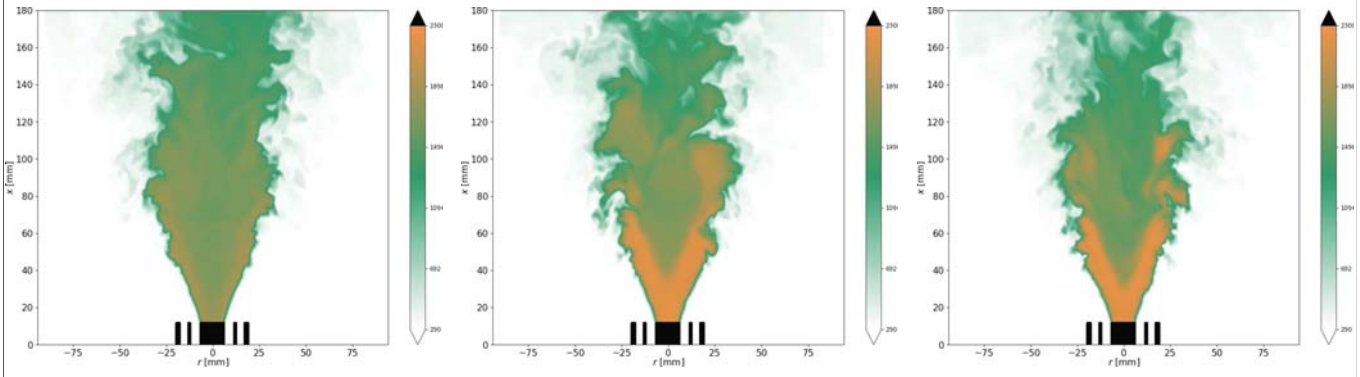

SwB3
no-stratification

SwB7
weak-stratification

SwB11
high-stratification

Overview of Cases with largest Swirl Number

LES by E. Inanc, Δ = 0.5 mm

Isosurface Flame Front

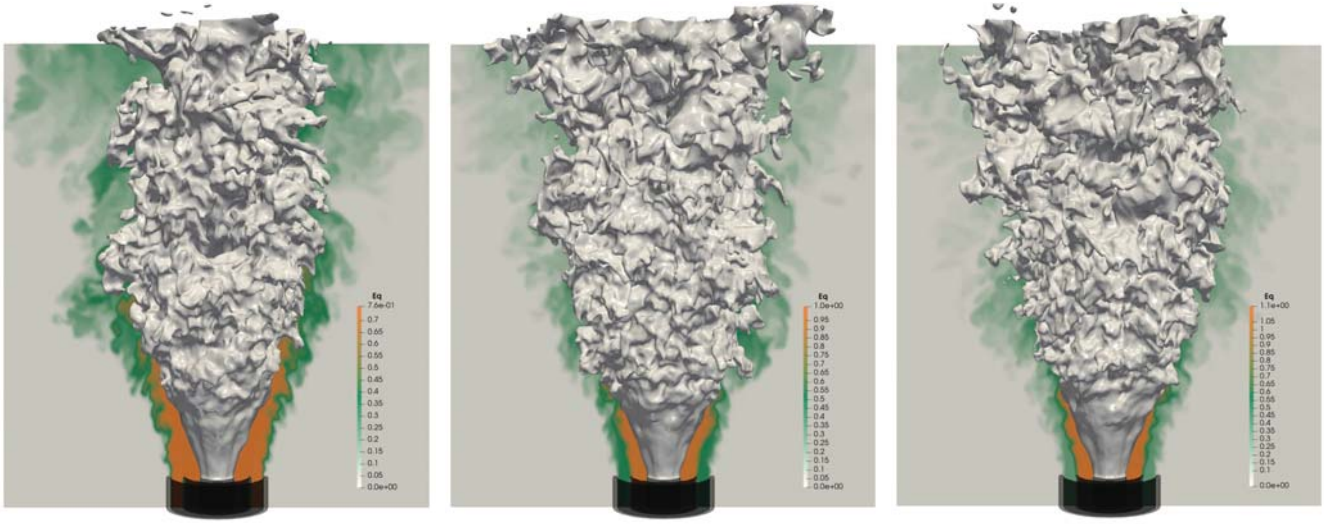

SwB3
no-stratification

SwB7
weak-stratification

SwB11
high-stratification

27

Overview SwB3

Swirled - no stratification

Contributions and their legends:

Experiments Sweeney et al. C&F 2012

- UDE AF, Inanc et al., ATF/PFGM
- UDE OF, Gruhlke et al., OpenFOAM
- UDE SB, Baik et al., Hybrid FDF/Flamelet
- TUE, Karaca et al., FGM
- TUE - CO, Karaca et al., FGM/Transported CO
- UCONN - ED, Türkeri et al., Trans. PDF
- UCONN - DD, Türkeri et al., Trans. PDF/Diff. Diffusion
- EM2C - FWF, Nguyen et al., Tabulated Chem.
- EM2C - FOC, Nguyen et al., Filtered Optimised Chem.
- ULB - CY, Li et al., PSR - Cylindrical Mesh
- ULB - CB, Li et al., PSR - Cubic Mesh

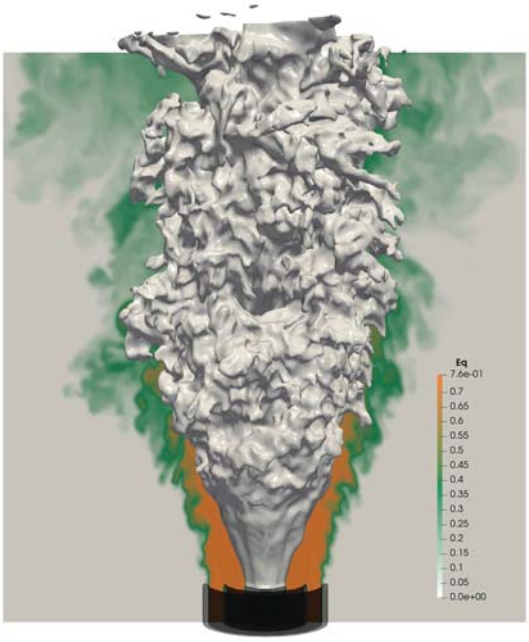

Isosurface of reaction rate. Slice colored by fresh gas equivalence ratio for the SwB3 case.

28

Overview SwB3

LES by E. Inanc, Δ = 0.5 mm

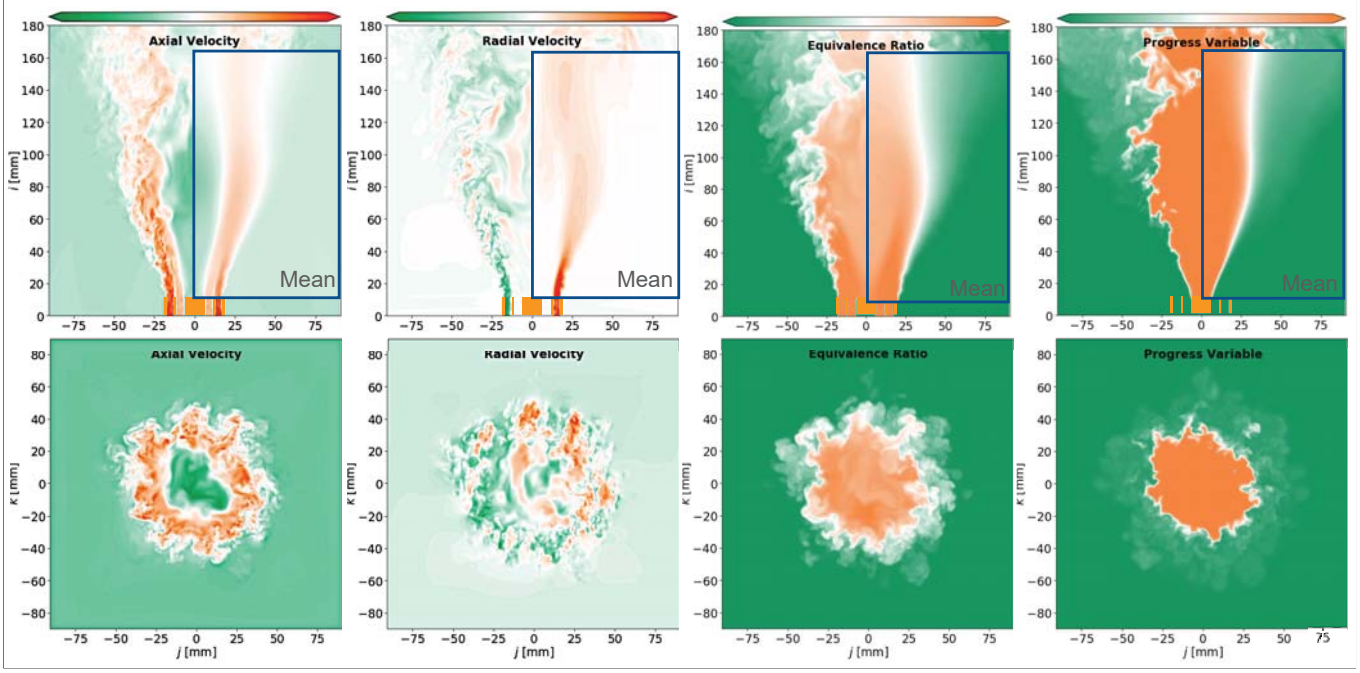

SwB3 - Axial Velocity

Mean

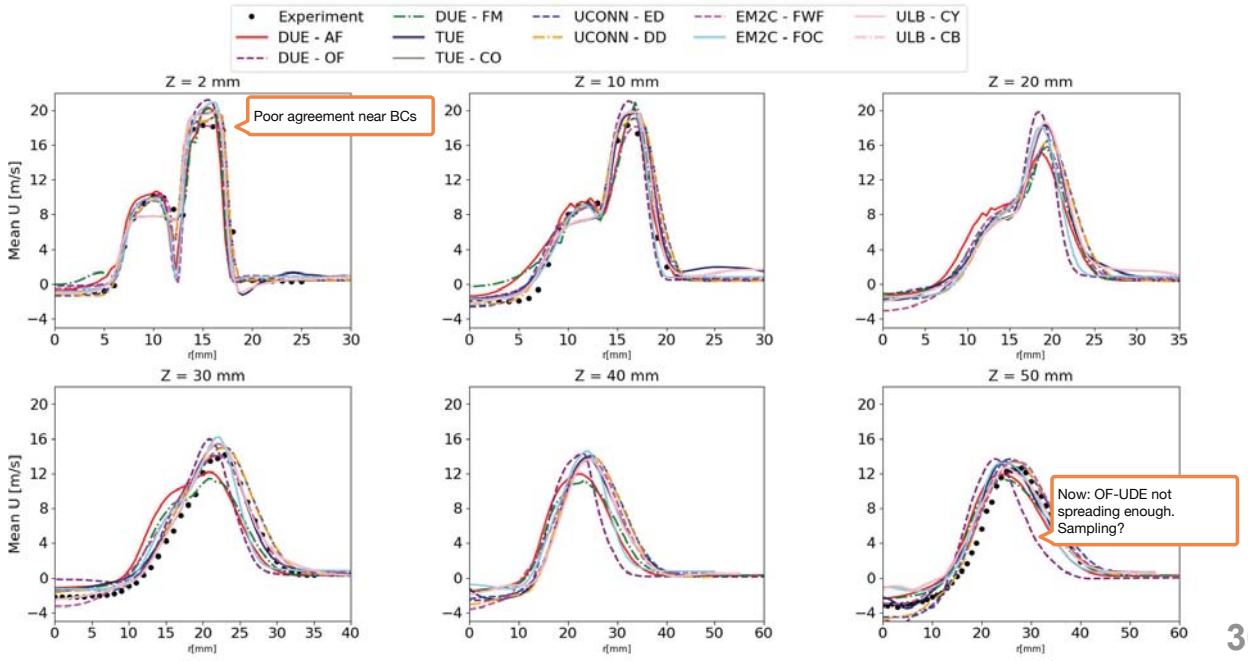

30

SwB3 - Axial Velocity

RMS

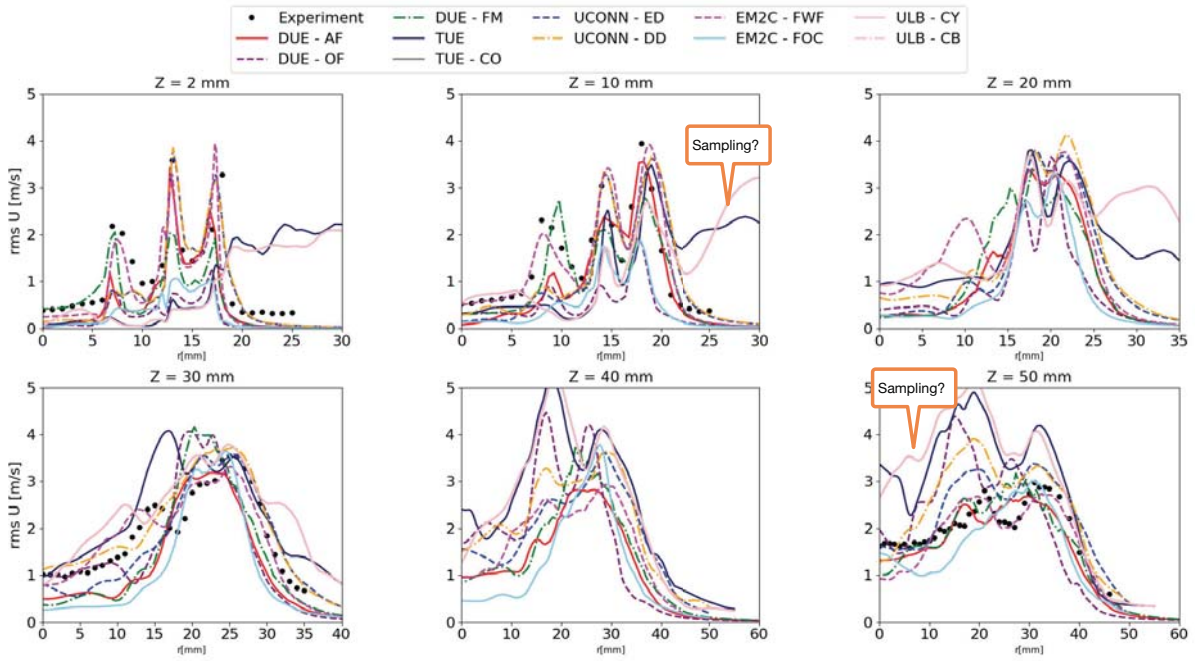

31

SwB3 - Radial Velocity

Mean

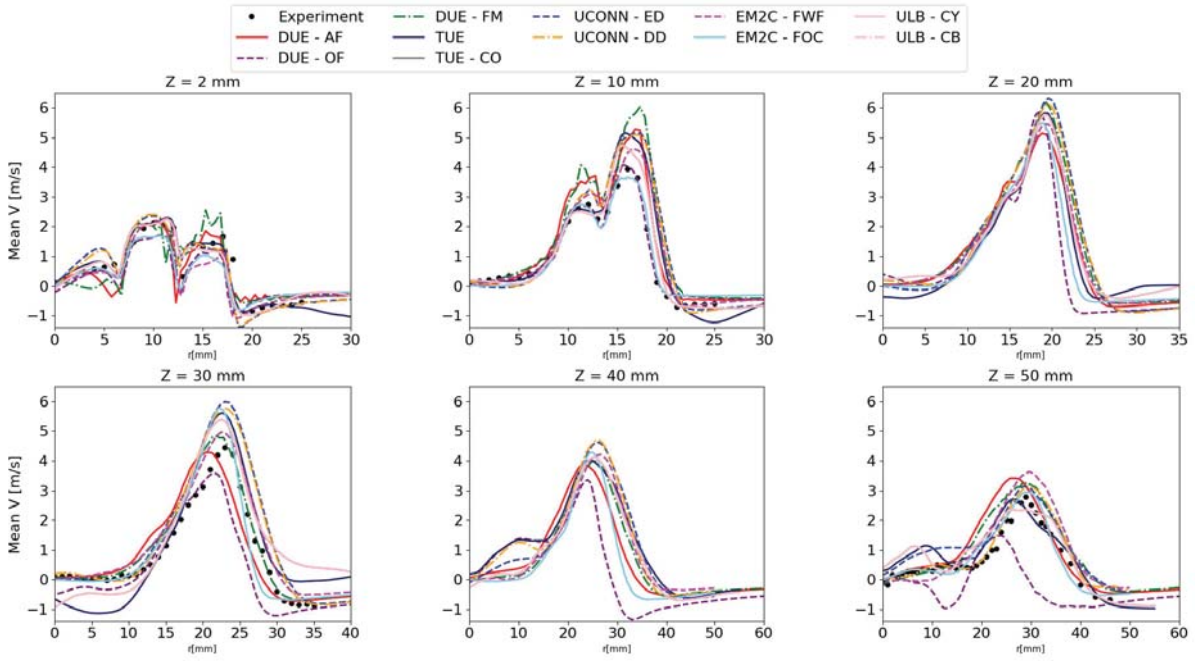

32

SwB3 - Radial Velocity

RMS

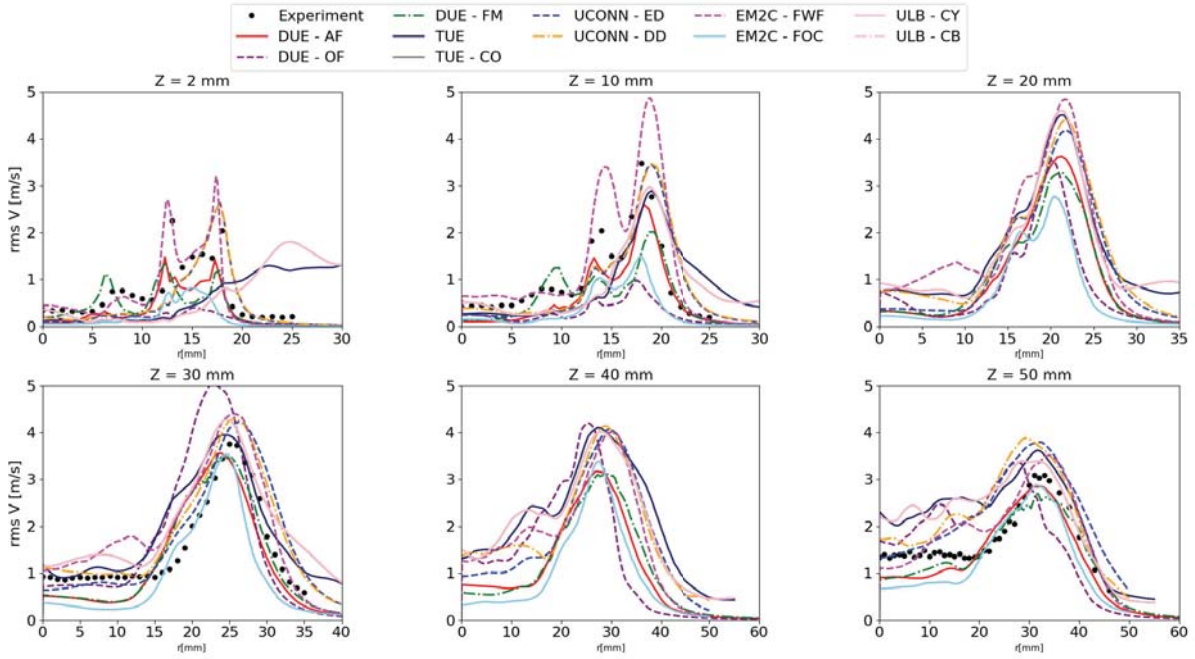

33

SwB3 - Tangential Velocity

Mean

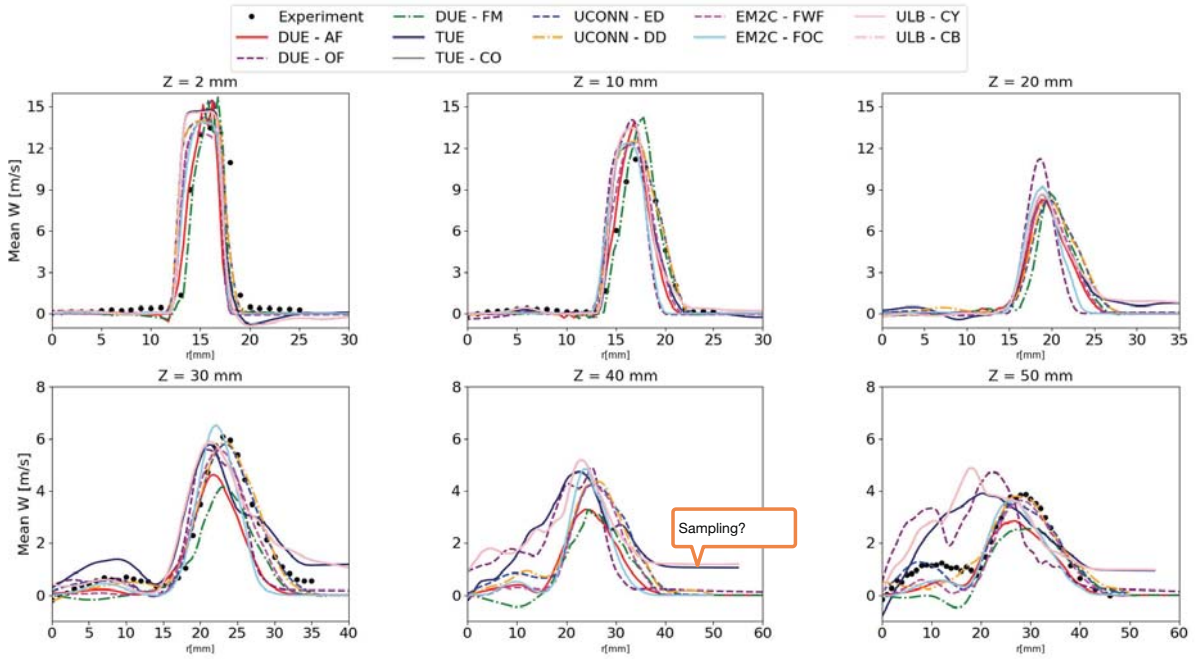

34

SwB3 - Tangential Velocity

RMS

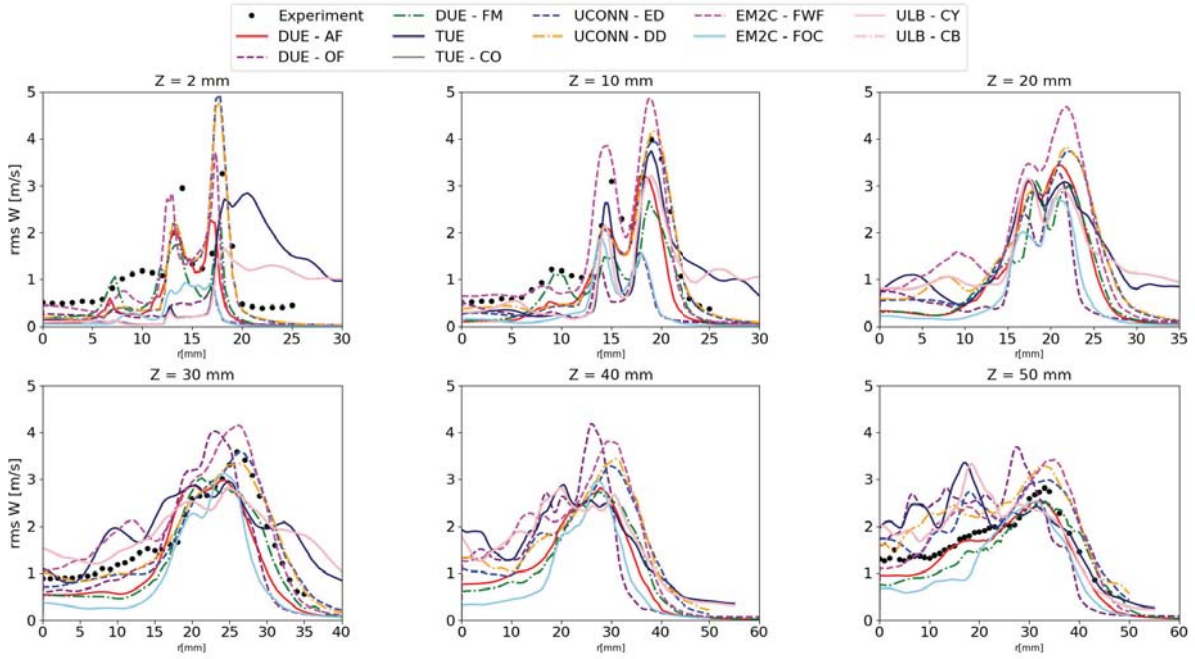

35

SwB3 - Equivalence Ratio

Mean

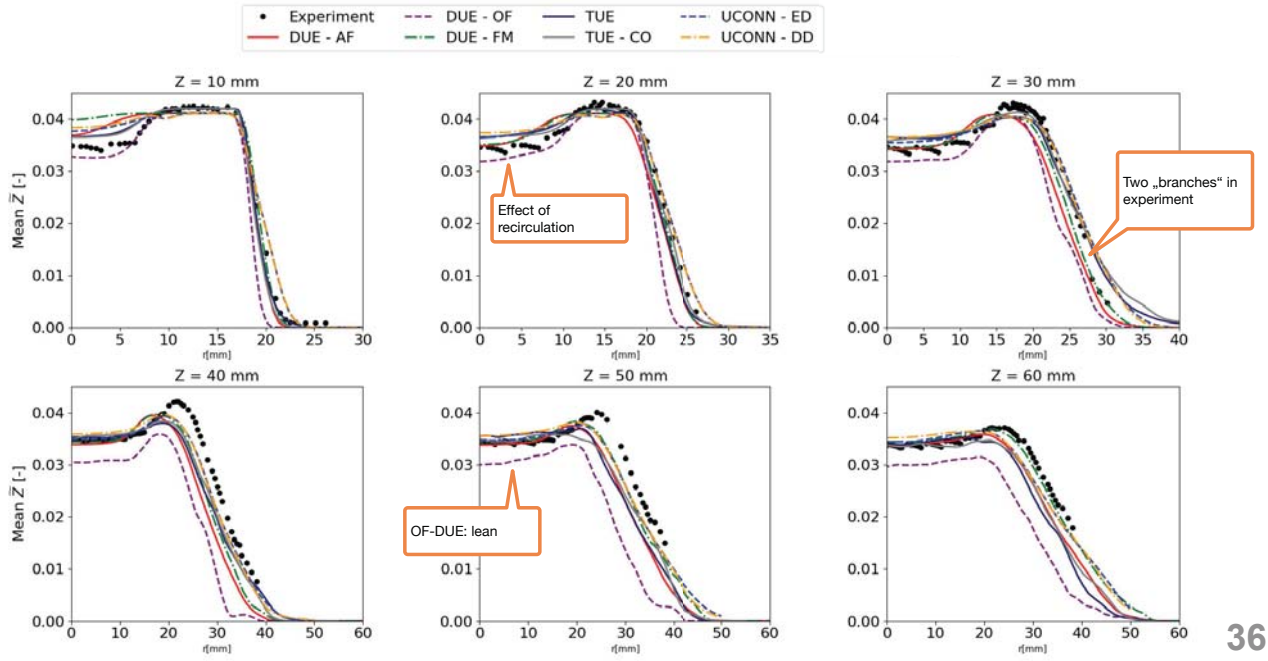

36

SwB3 - Equivalence Ratio

RMS

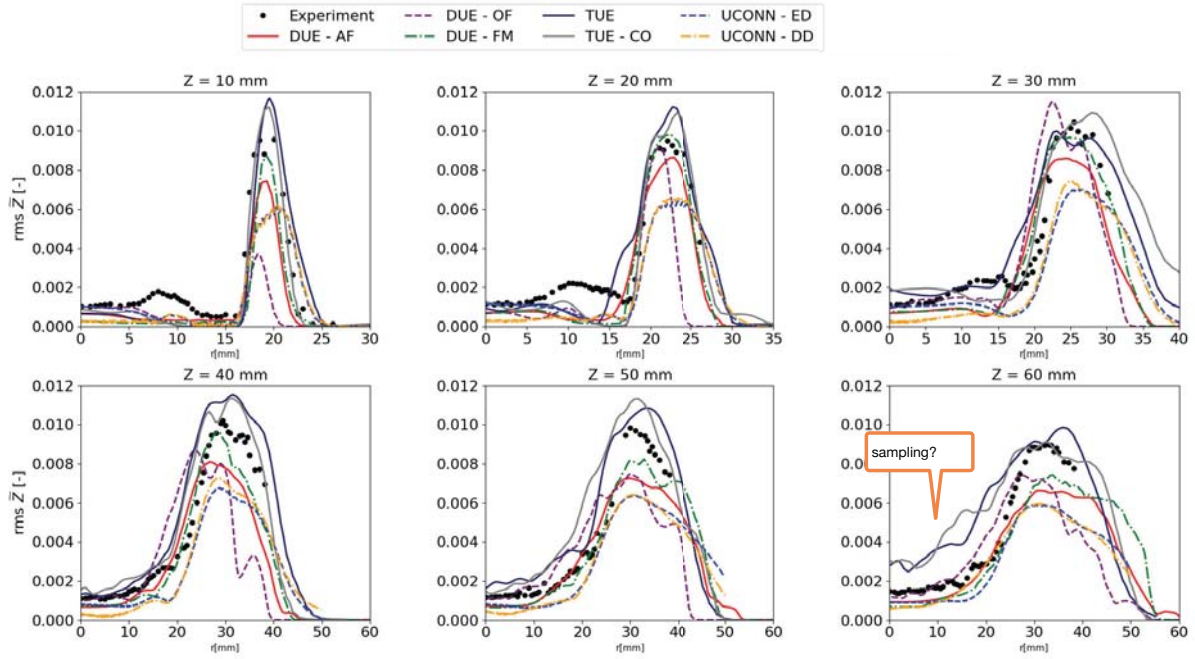

37

SwB3 - Temperature

Mean

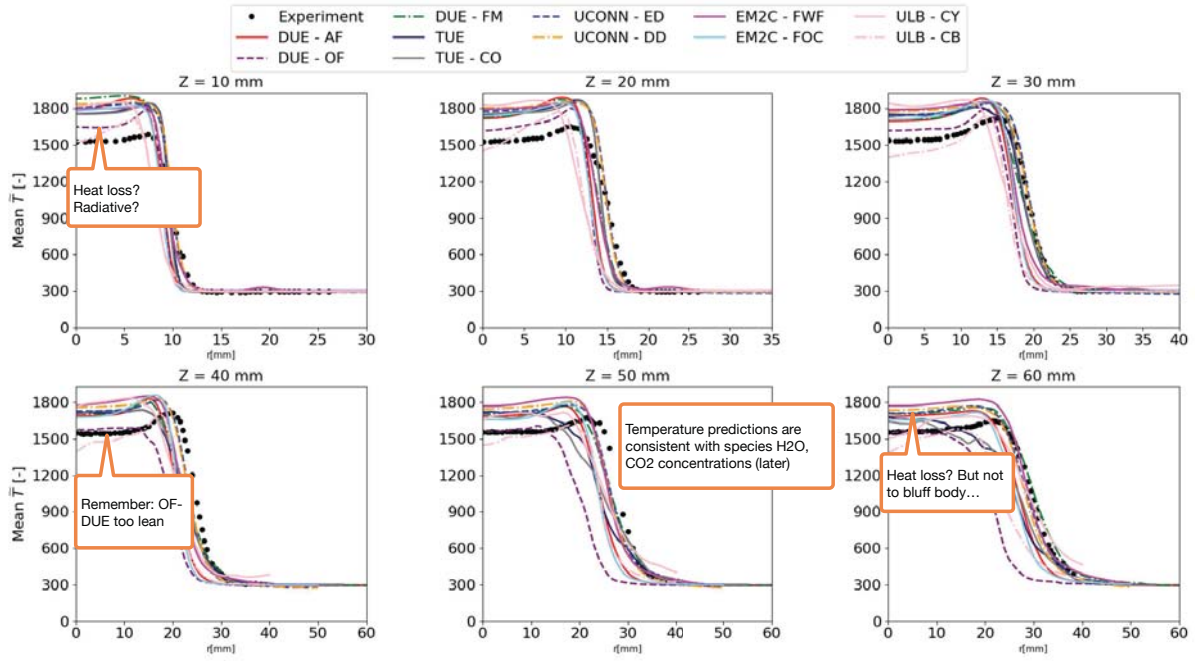

38

SwB3 - Temperature

RMS

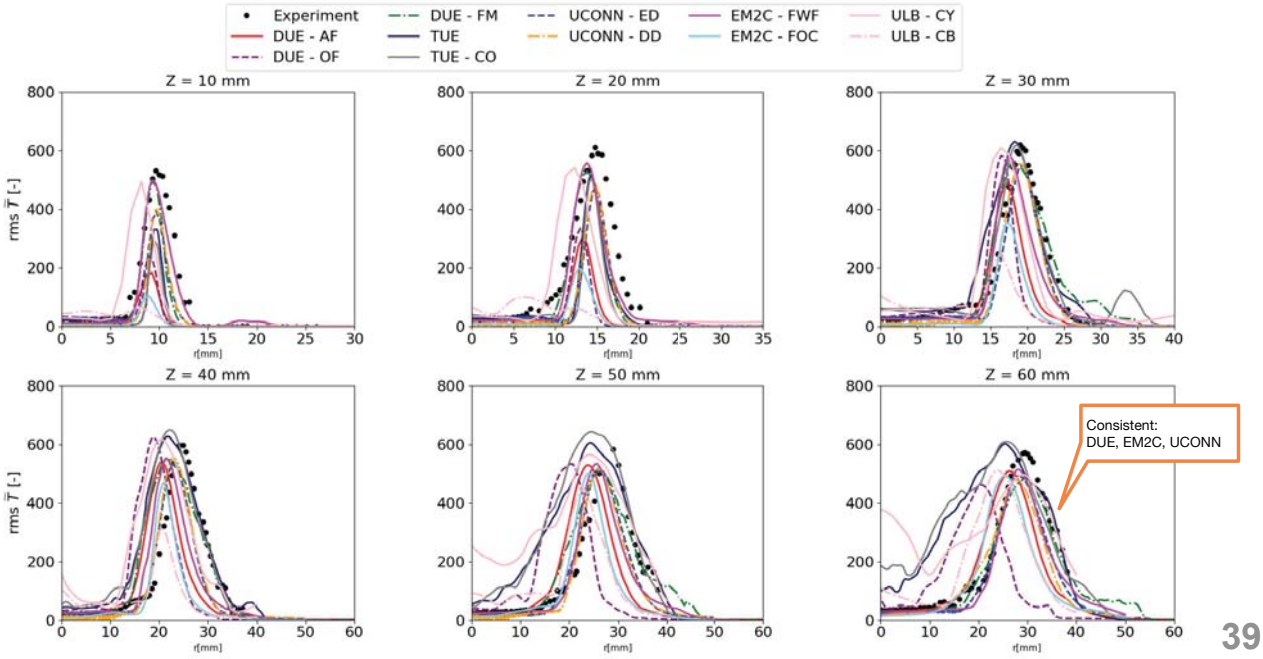

39

SwB3 - H_2O Mass Fraction

Mean

Not all species with virtual chemistry (EM2C)

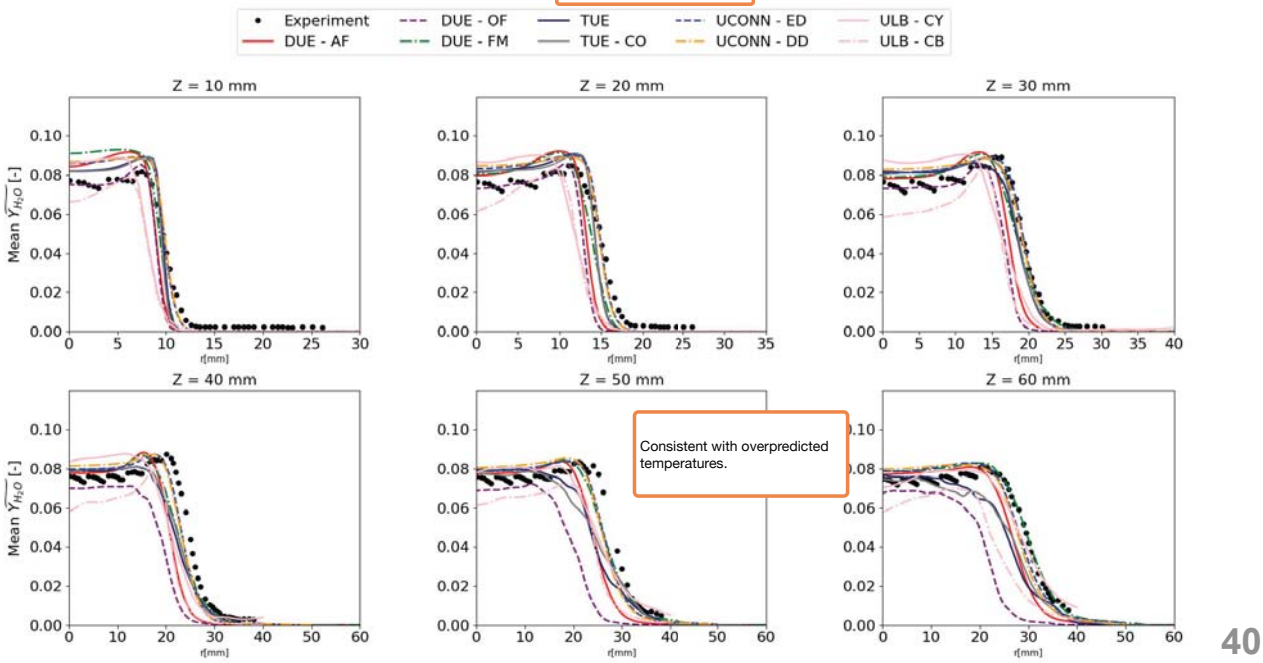

40

SwB3 - H_2O Mass Fraction

RMS

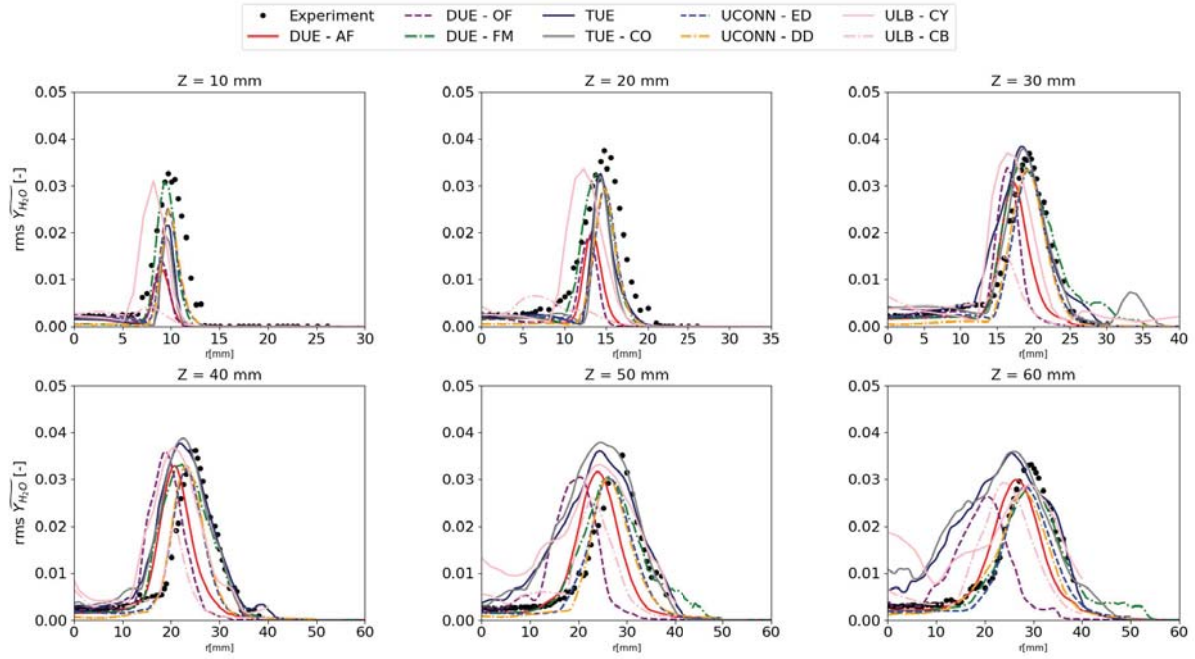

41

SwB3 - O_2 Mass Fraction

Mean

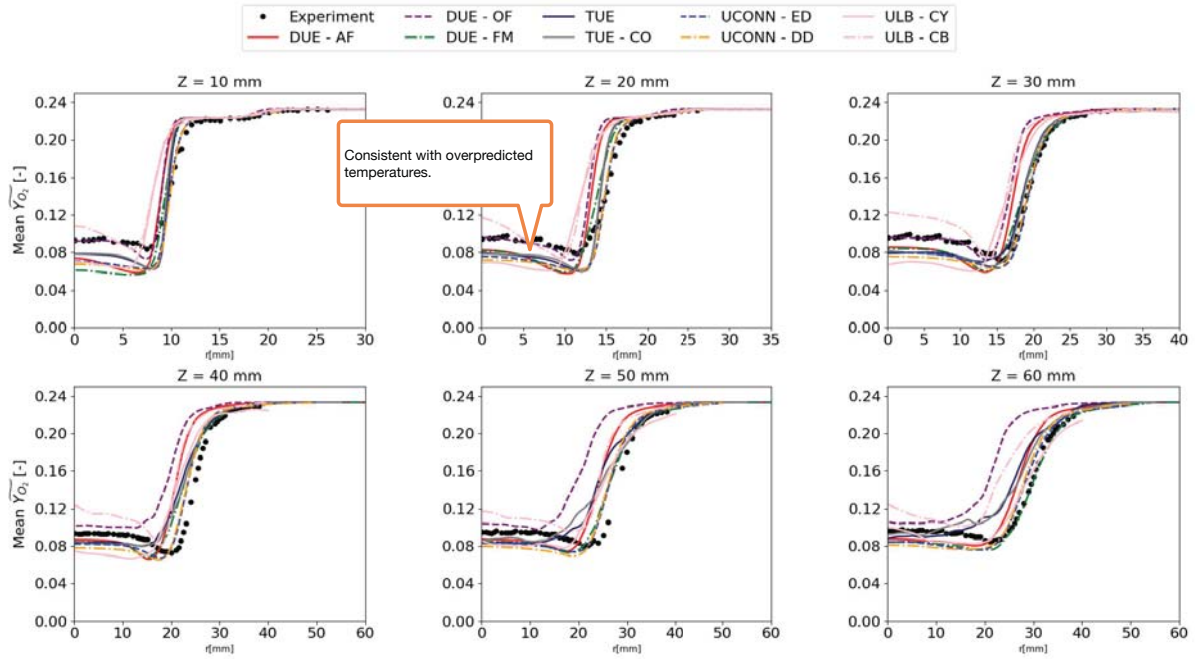

42

SwB3 - O_2 Mass Fraction

RMS

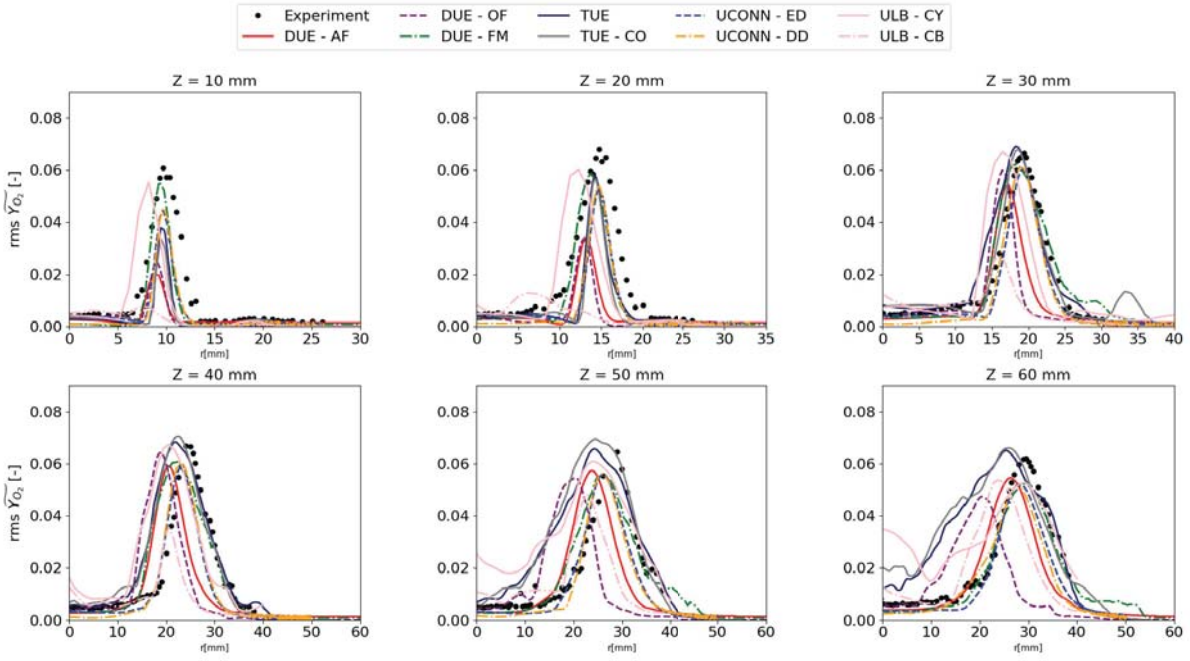

43

SwB3 - CH_4 Mass Fraction

Mean

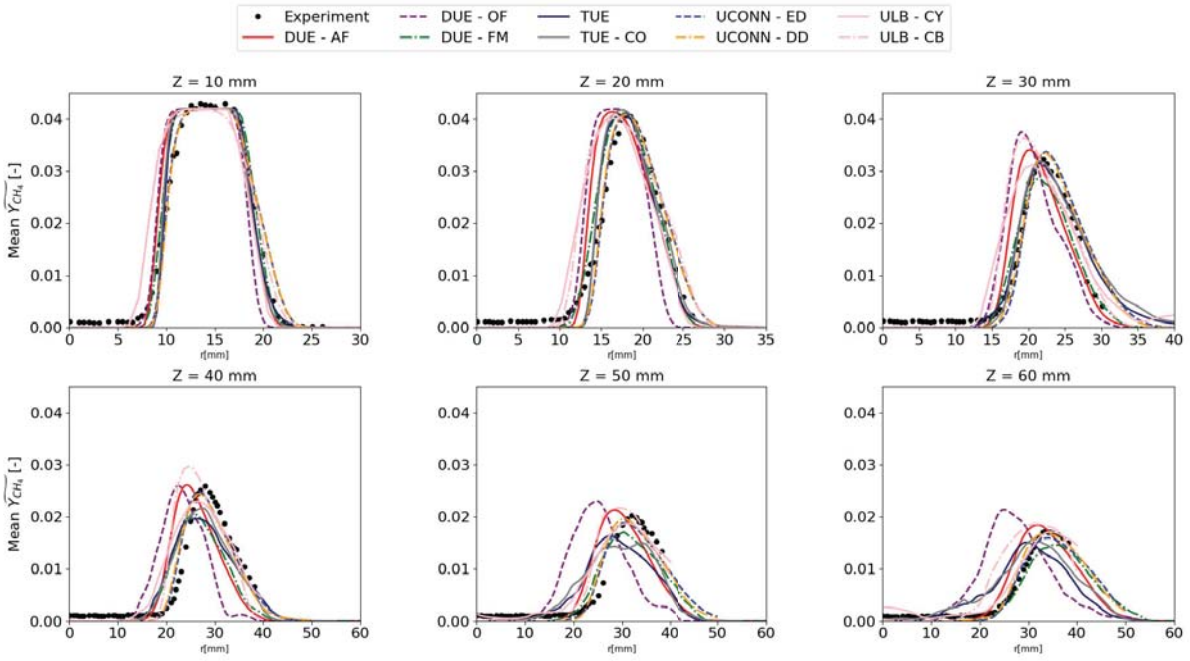

44

SwB3 - CH_4 Mass Fraction

RMS

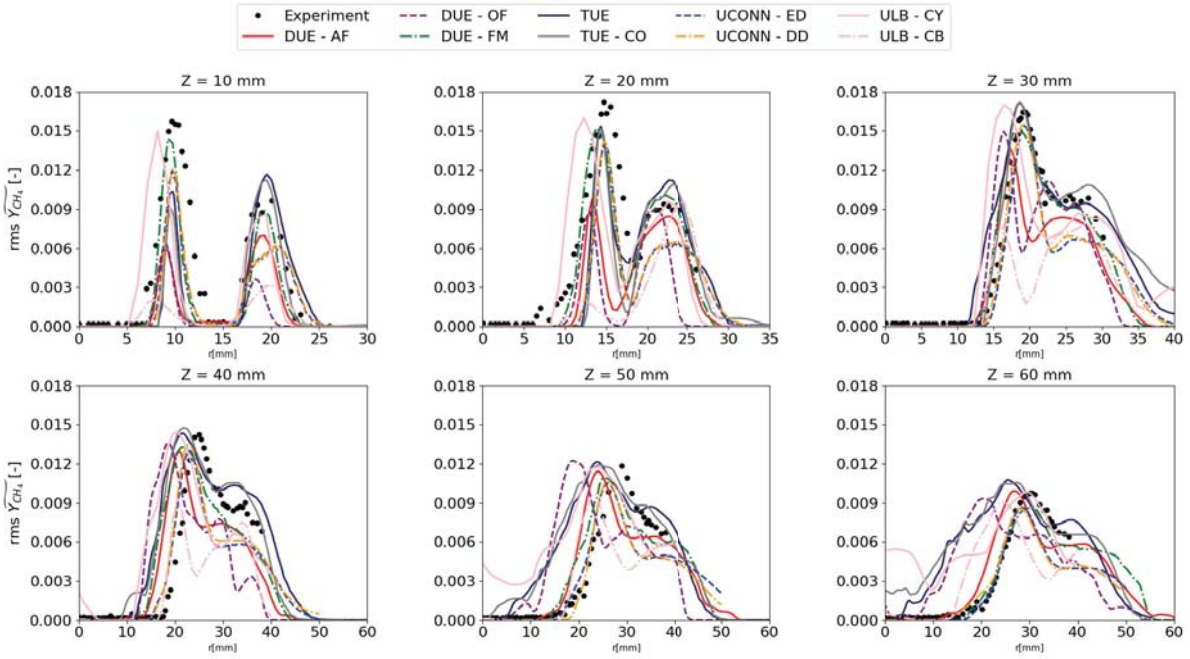

SwB3 - CO_2 Mass Fraction

Mean

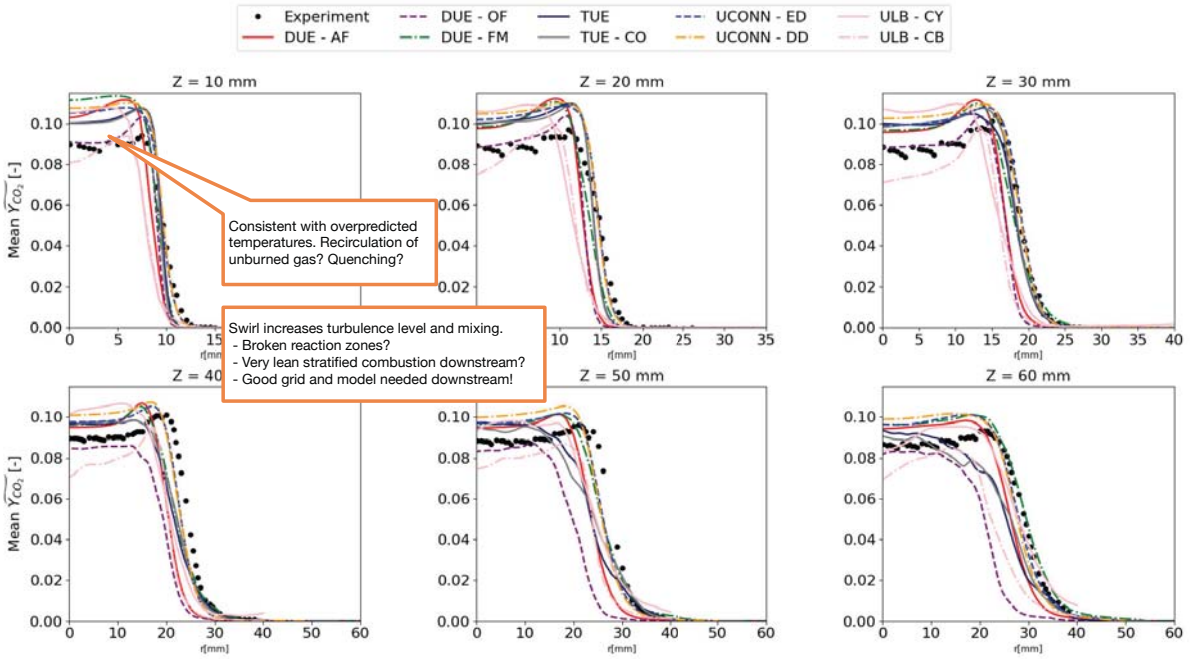

SwB3 - CO_2 Mass Fraction

RMS

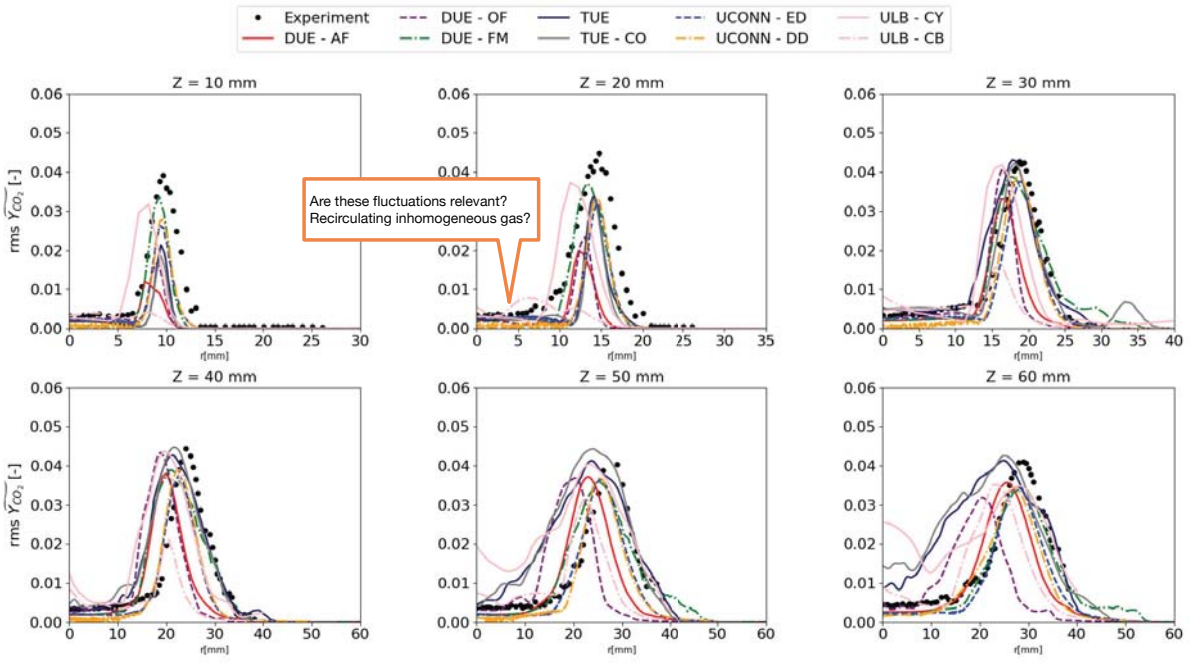

47

SwB3 - CO Mass Fraction

Mean

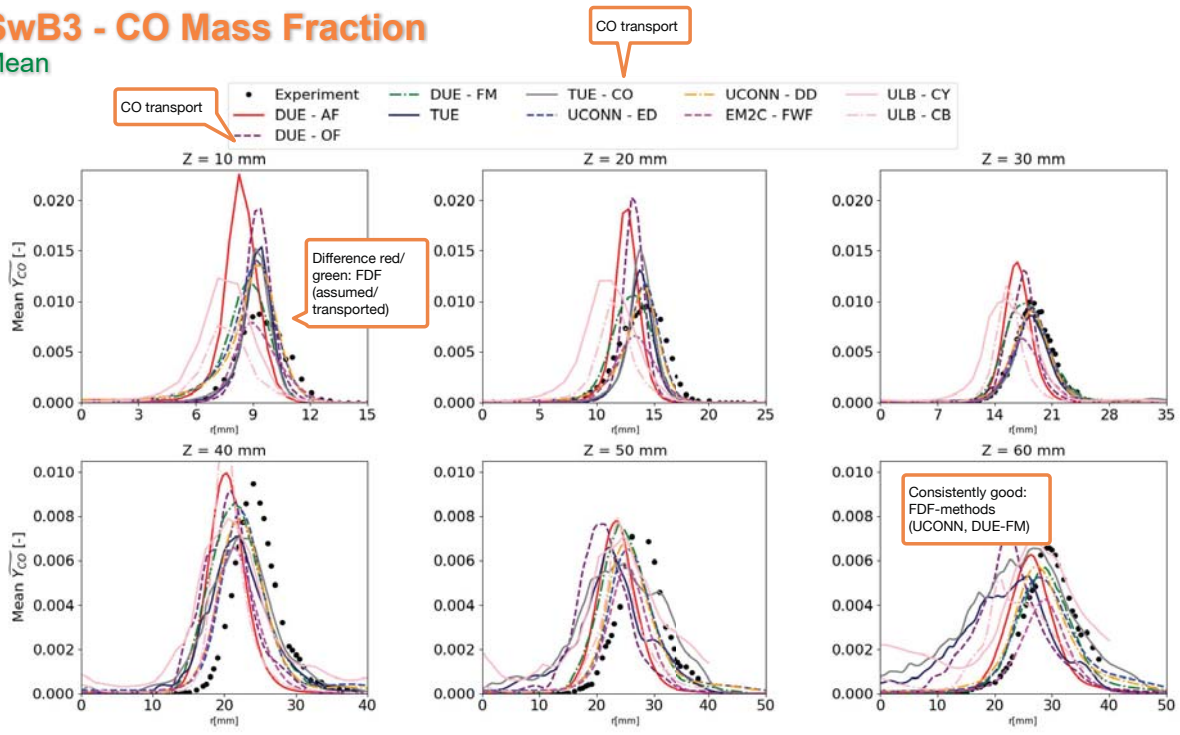

48

SwB3 - CO Mass Fraction

RMS

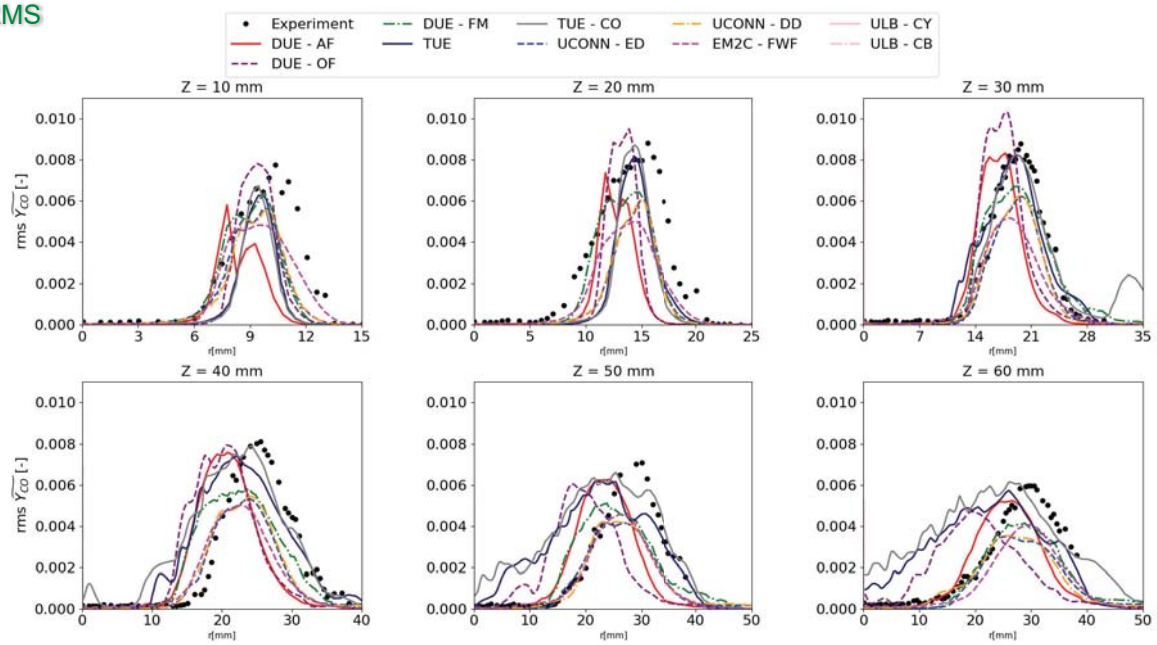

49

Simulation of Cambridge SWB3 configuration, EM2C

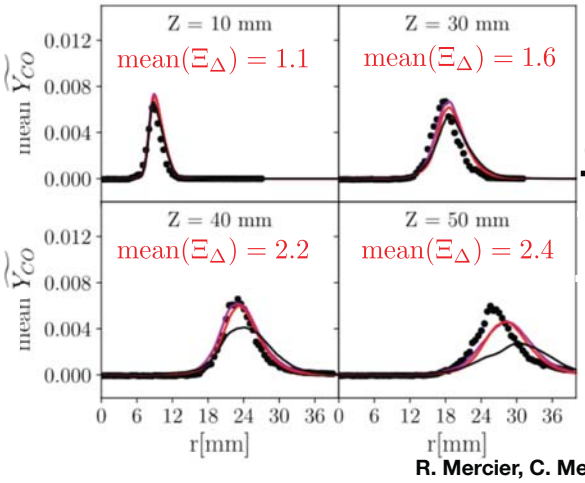

- Experiments

LES with Filtered Tabulated Chemistry

- Filtered Planar Flamelets
- Filtered Wrinkled Flamelets n_Δ=1
- Filtered Wrinkled Flamelets n_Δ=3

R. Mercier, C. Mehl, B. Fiorina and V. Moureau. Submitted (2018)

Recirculation Zone

Initialization issues and stabilization duration

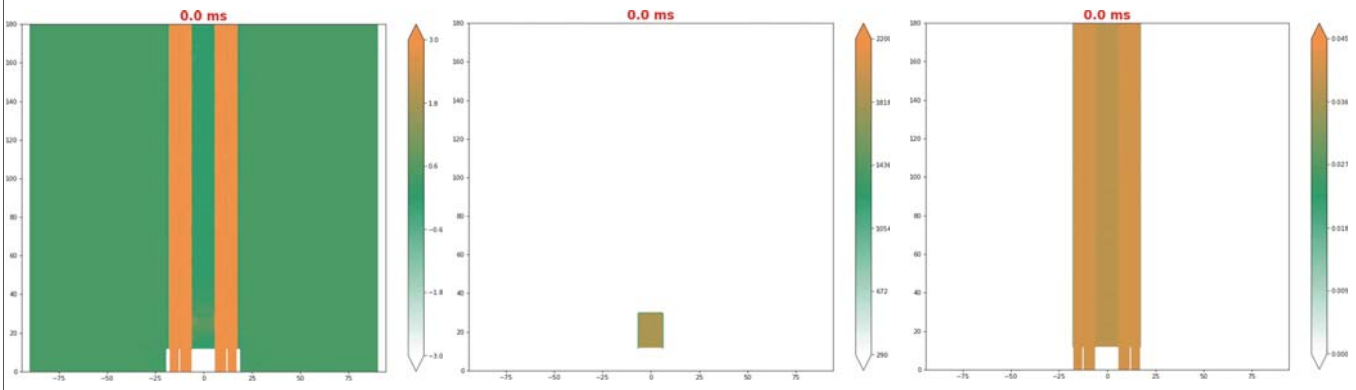

Axial Velocity | Temperature | Mixture fraction

Flame quenches at 105 ms near the inlet

Sufficient inhomogeneity to explain deviations in bluff body wake?

51

Recirculation Zone

Initialisation issues and stabilisation duration

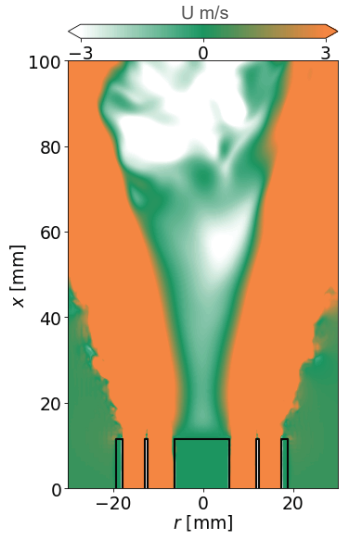

- Different initialization ideas could solve this issue (remapping etc.)
- 300 ms is needed to achieve a stable flame
- Recirculation zone is important
  - Transports co-flow air to the bluff-body
  - A large computational domain is needed
  - Heat-losses could be important upstream (x < 10 mm)
  - Possible quenching (lean) downstream may recirculate unburned reactants
    - Only possible without „mild“ combustion - i.e. large, unmixed structures would have to recirculate. → Big challenge for *flow* simulation.

52

SwB3 - Conclusions

- SwB3 is reasonably captured by most groups
- SwB3 is more sensitive for CO than non-Swirled SwB1
- Recirculation zone needs a large computational domain
- Sampling should start after the recirculation zone builds up, which is longer than for SwB1
- Equivalence ratios at the centreline are also under-predicted with differential diffusion included model, as in SwB1
- Heat losses near the bluff-body could be a more important issue than for SwB1, Swirl brings more air into the recirculation zone
- Lean quenching downstream? Recirculation of unburned reactants?

53

SwB7

Swirled - weak stratification

Contributions and their legends:

Experiments Sweeney et al. C&F 2012

- UDE AF, Inanc et al., ATF/PFGM
- UDE SB, Baik et al., Hybrid FDF/Flamelet

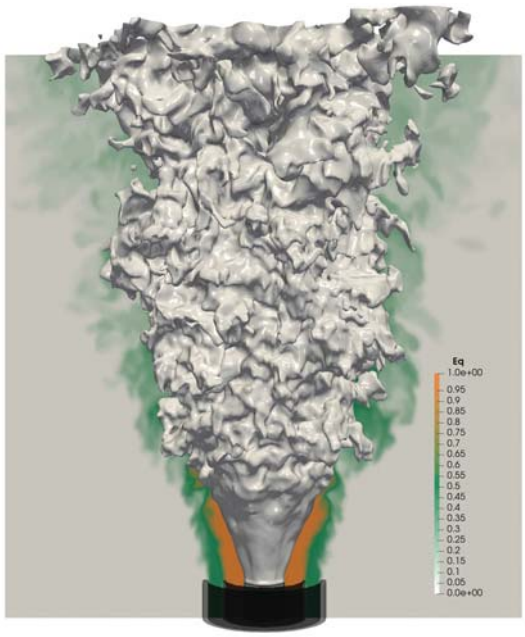

Isosurface of reaction rate. Slice colored by fresh gas equivalence ratio for the SwB7 case.

54

Overview SwB7

LES by E. Inanc, Δ = 0.5 mm

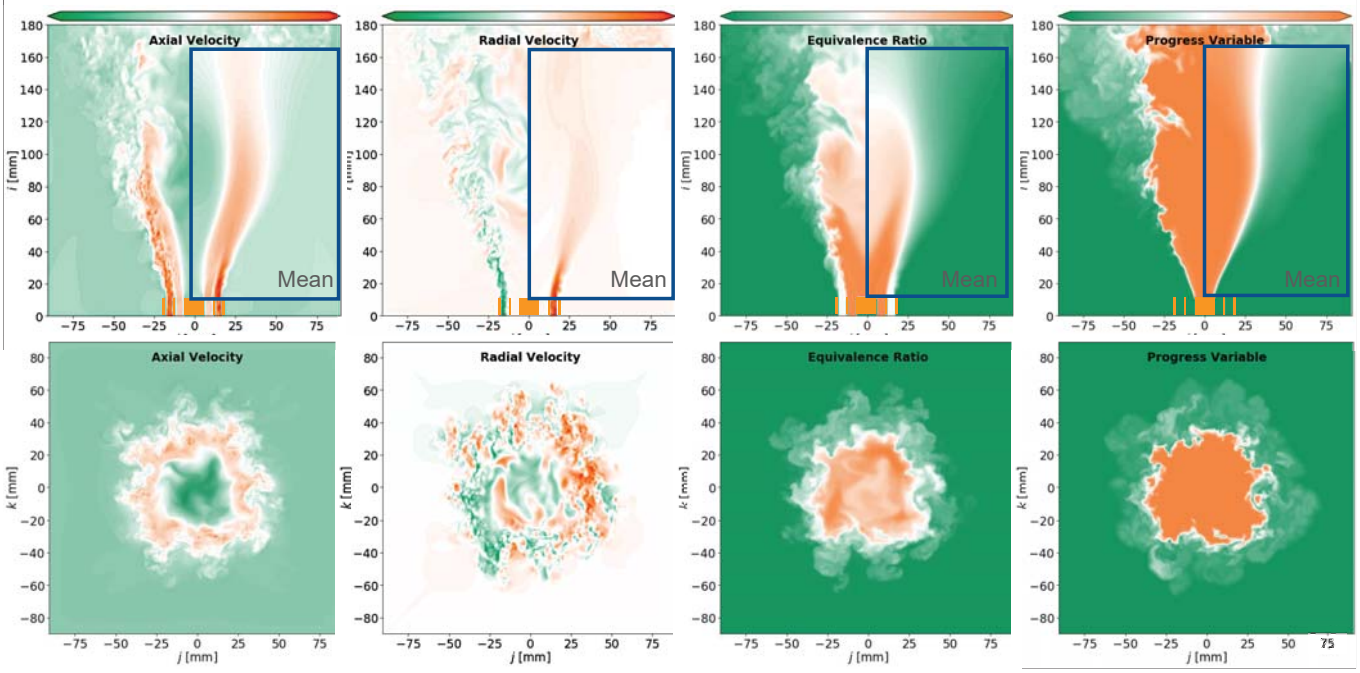

SwB7 - Axial Velocity

Mean

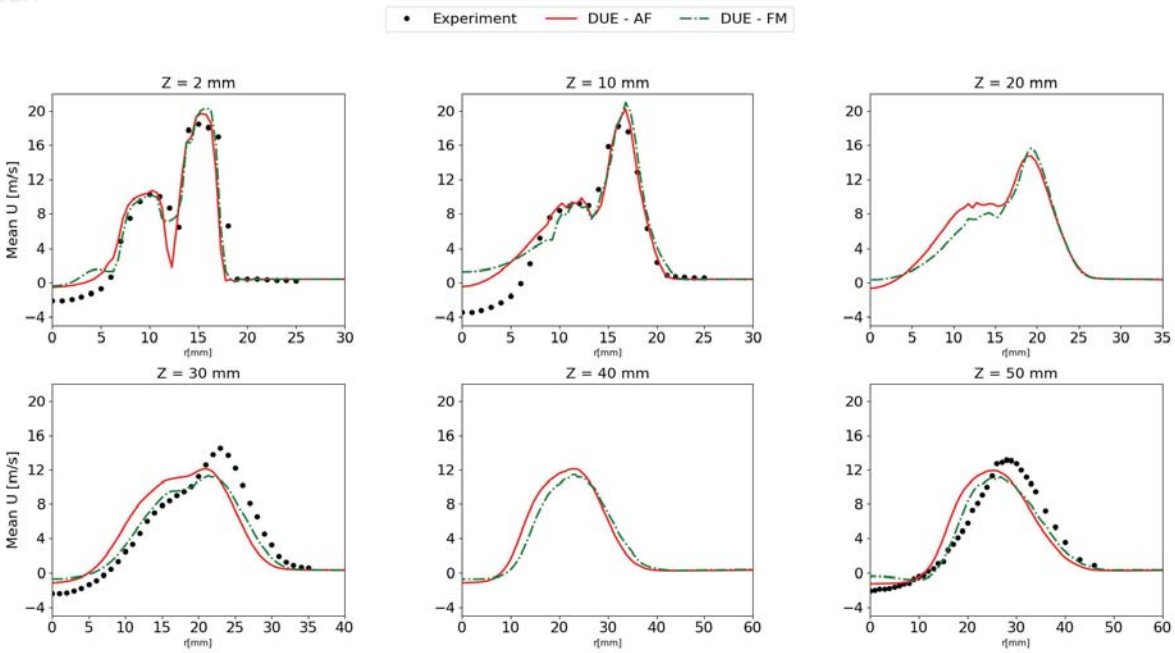

SwB7 - Axial Velocity

RMS

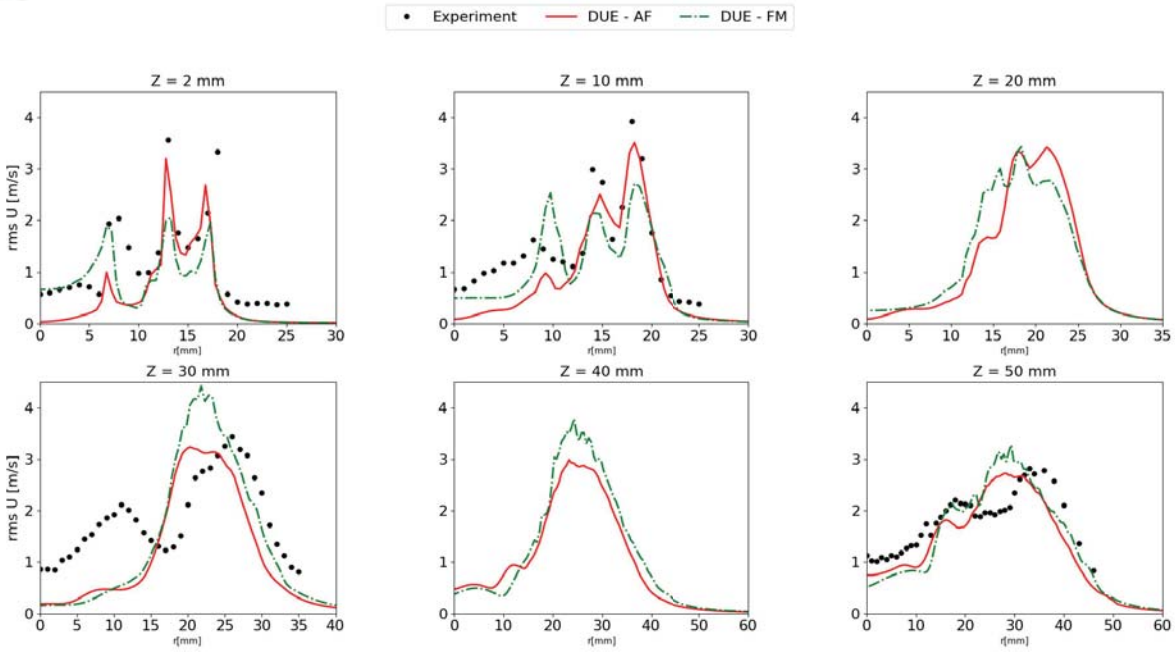

57

SwB7 - Tangential Velocity

Mean

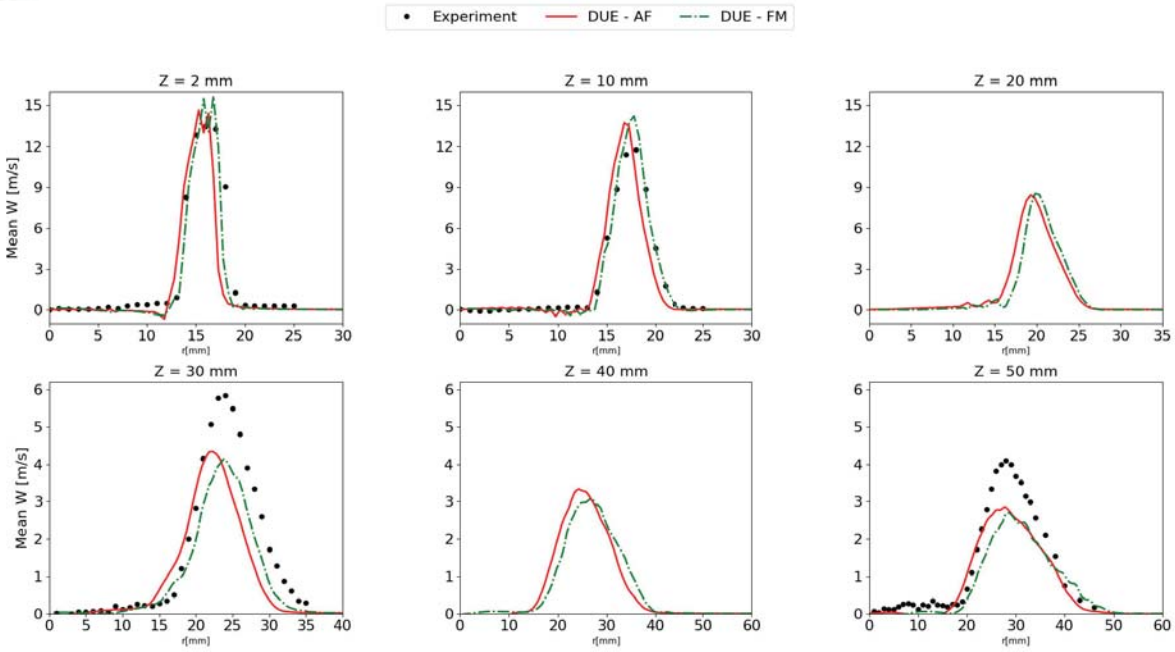

58

SwB7 - Tangential Velocity

RMS

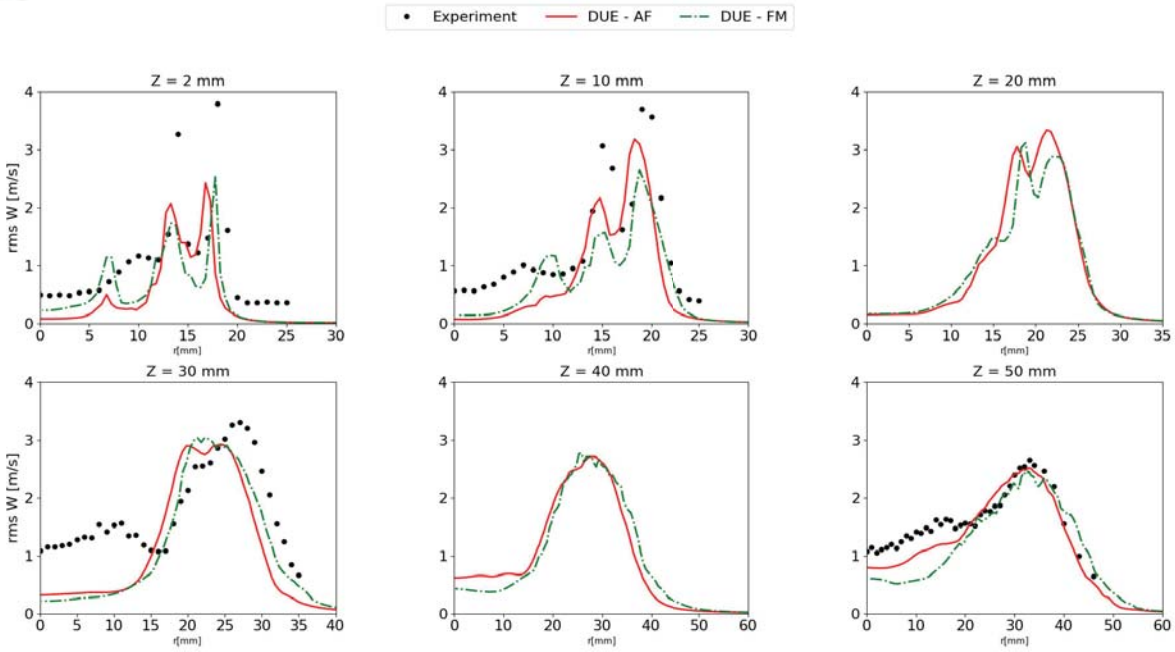

59

SwB7 - Equivalence Ratio

Mean

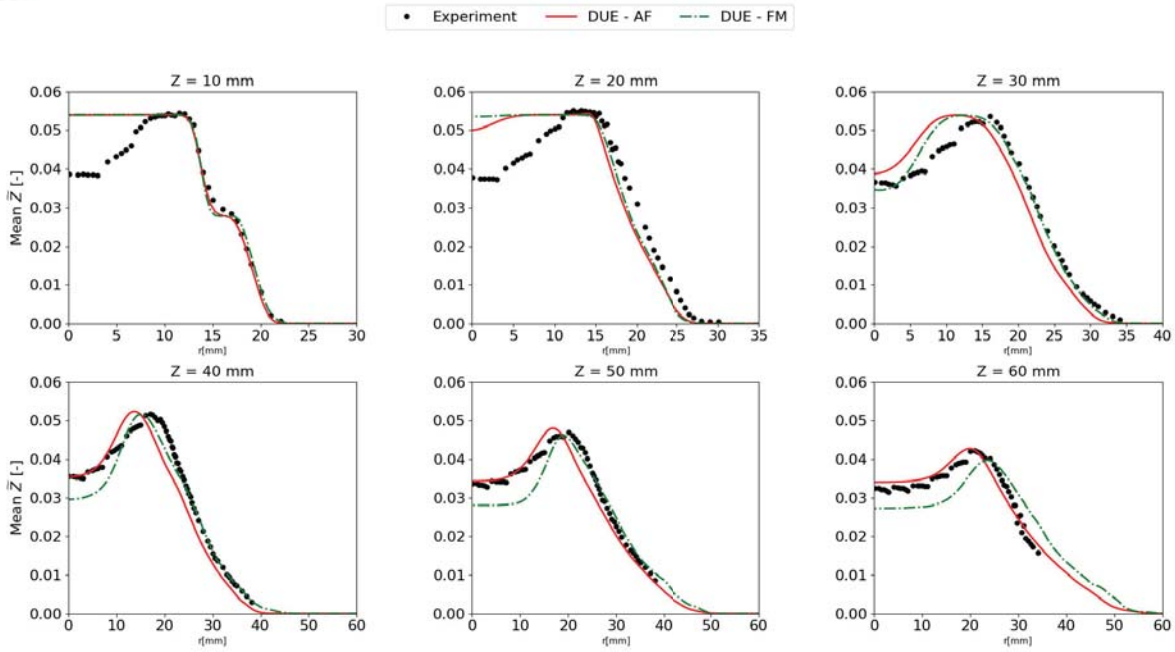

60

SwB7 - Temperature

Mean

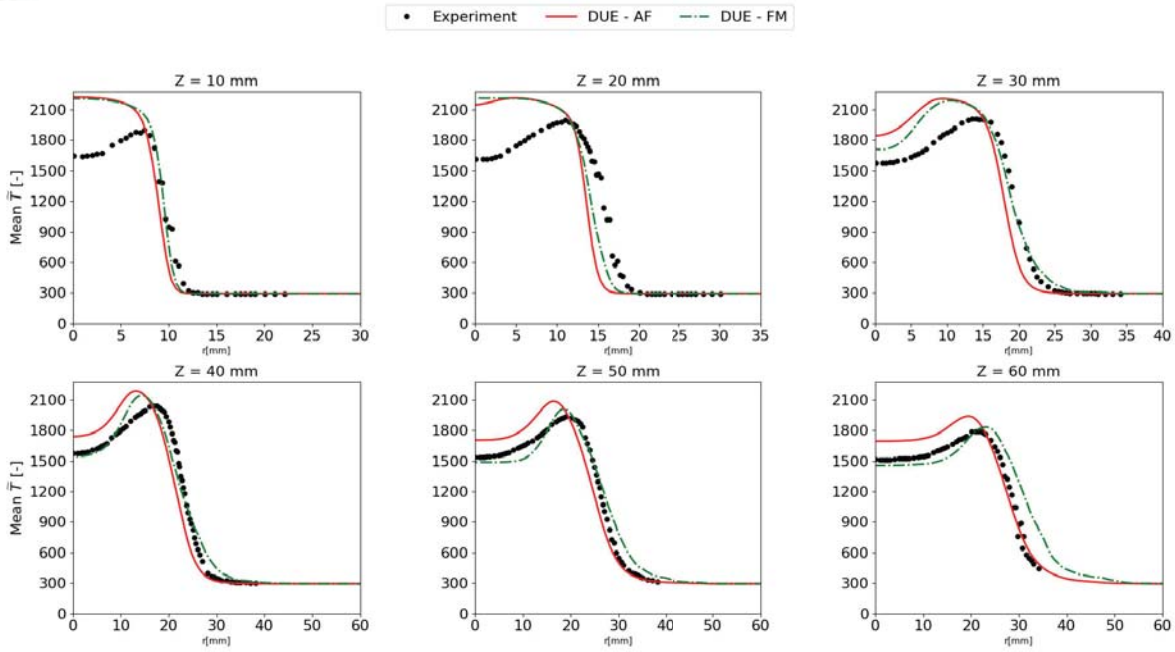

61

SwB7 - CO_2 Mass Fraction

Mean

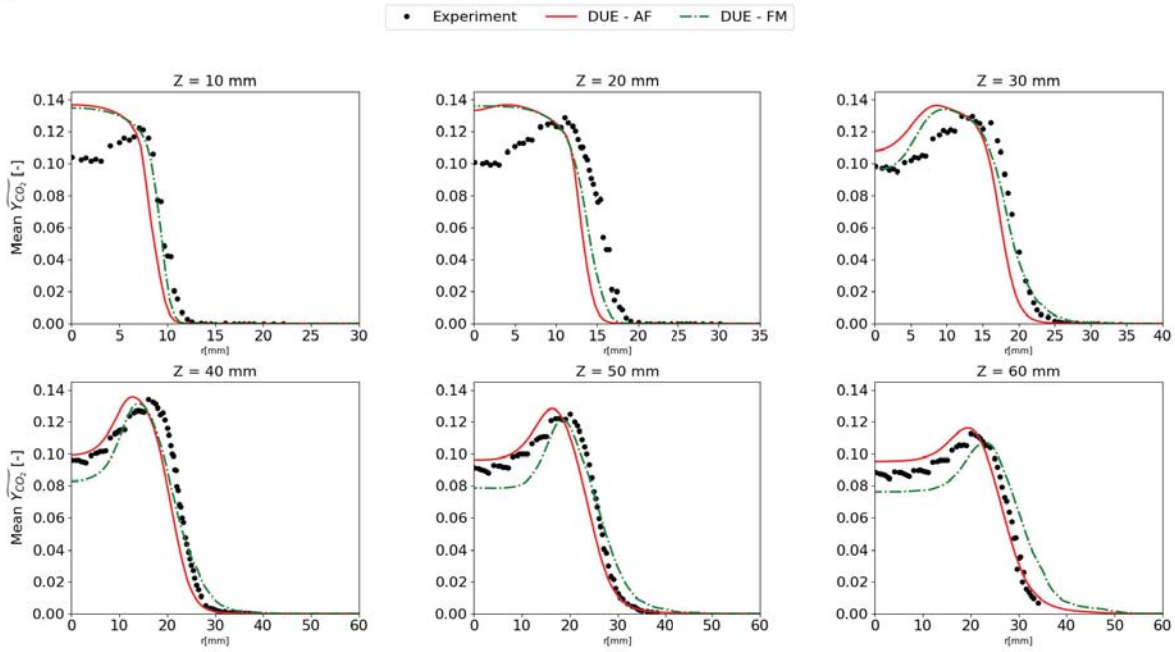

62

SwB7 - CO Mass Fraction

Mean

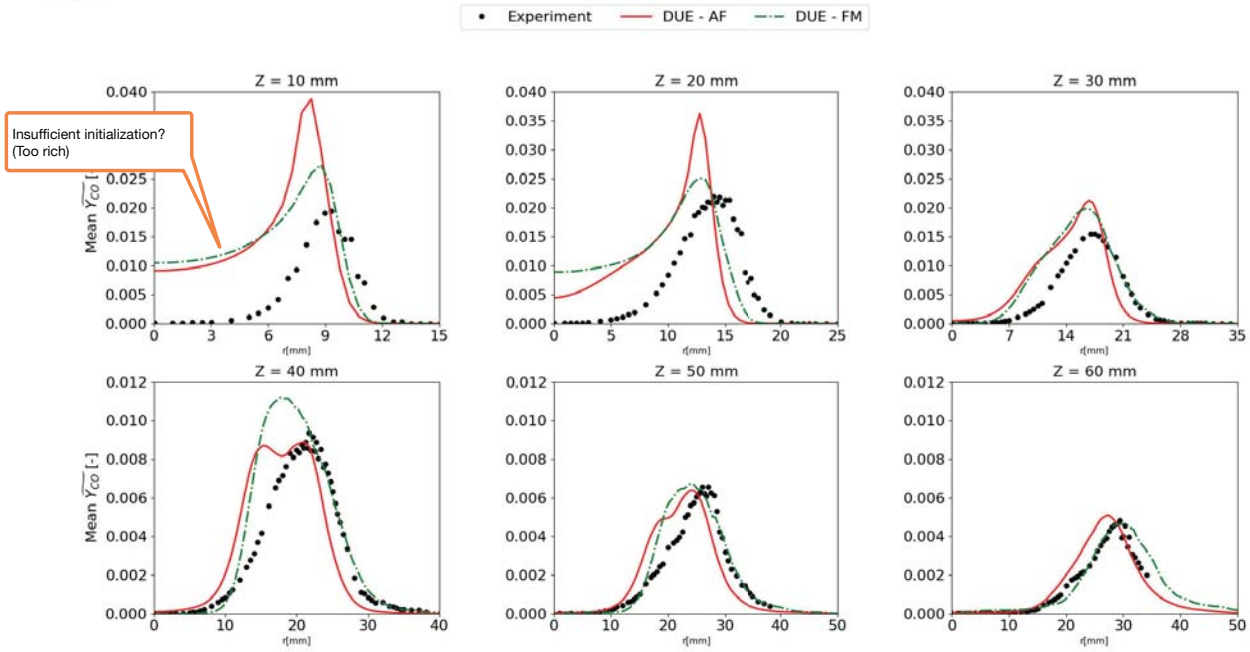

63

SwB7 - Conclusions

- SwB7 is reasonably captured
- Issues about CO in stratified cases persist and are more visible
- Recirculation zone issues persist
- A better FDF of the combustion model clearly helps
- Unity Lewis number assumption could be problematic
  (mentioned more detailedly in SwB11)

64

SwB11

Swirled - high stratification

Contributions and their legends:

Experiments Sweeney et al. C&F 2012

- UDE AF, Inanc et al., ATF/PFGM
- UDE SB, Baik et al., Hybrid FDF/Flamelet

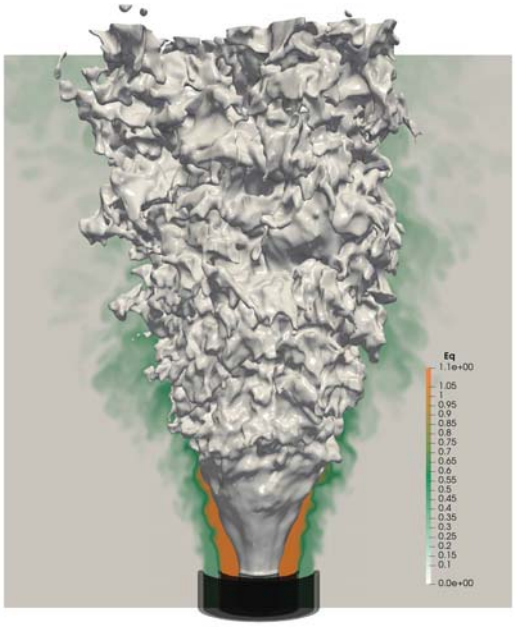

Isosurface of reaction rate. Slice colored by fresh gas equivalence ratio for the SwB11 case.

65

Overview SwB11

LES by E. Inanc, Δ = 0.5 mm

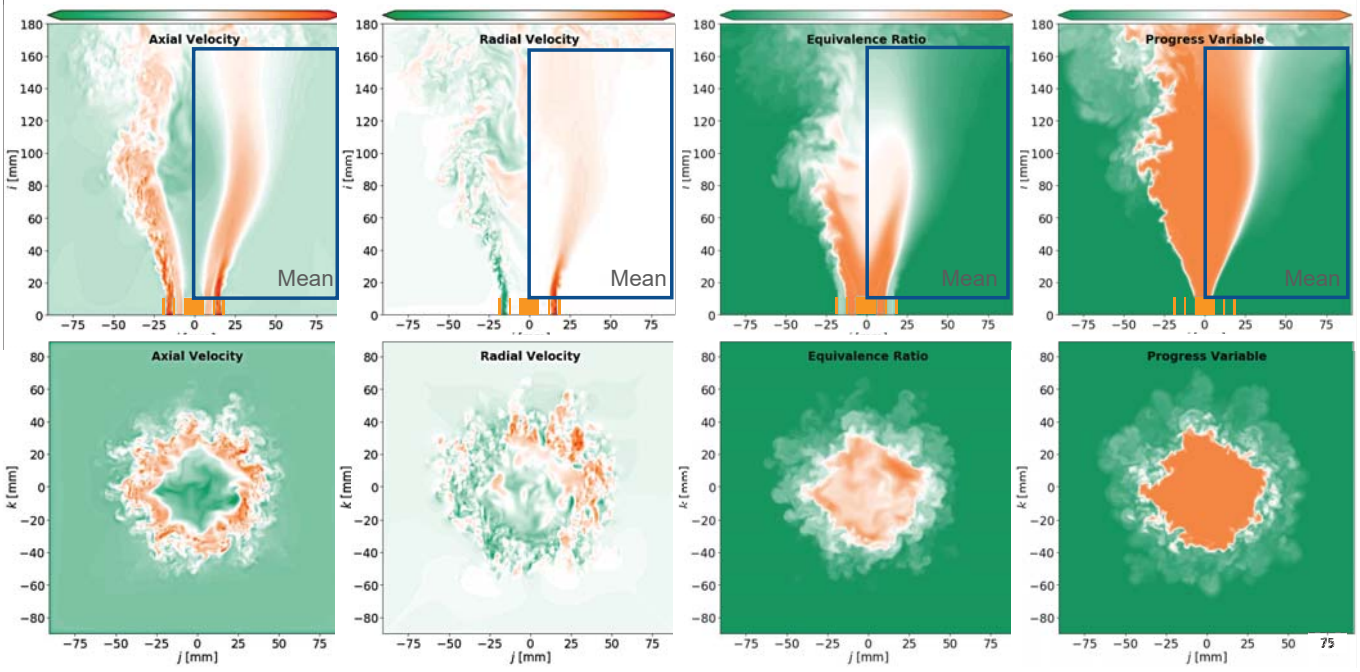

SwB11 - Axial Velocity

Mean

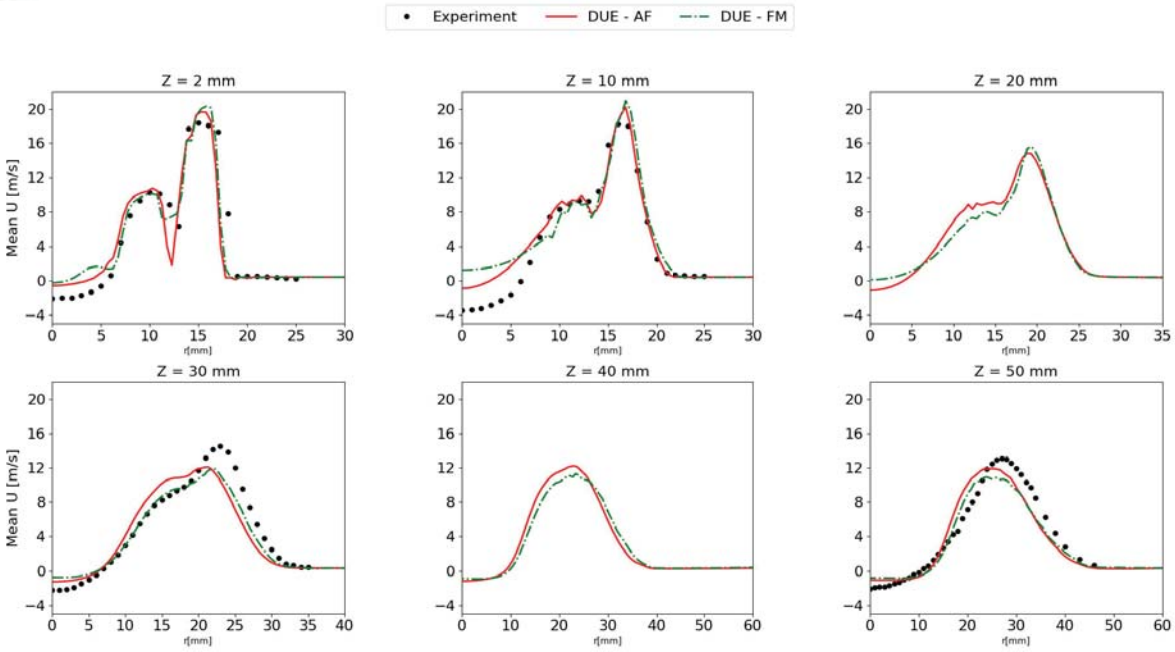

67

SwB11 - Axial Velocity

RMS

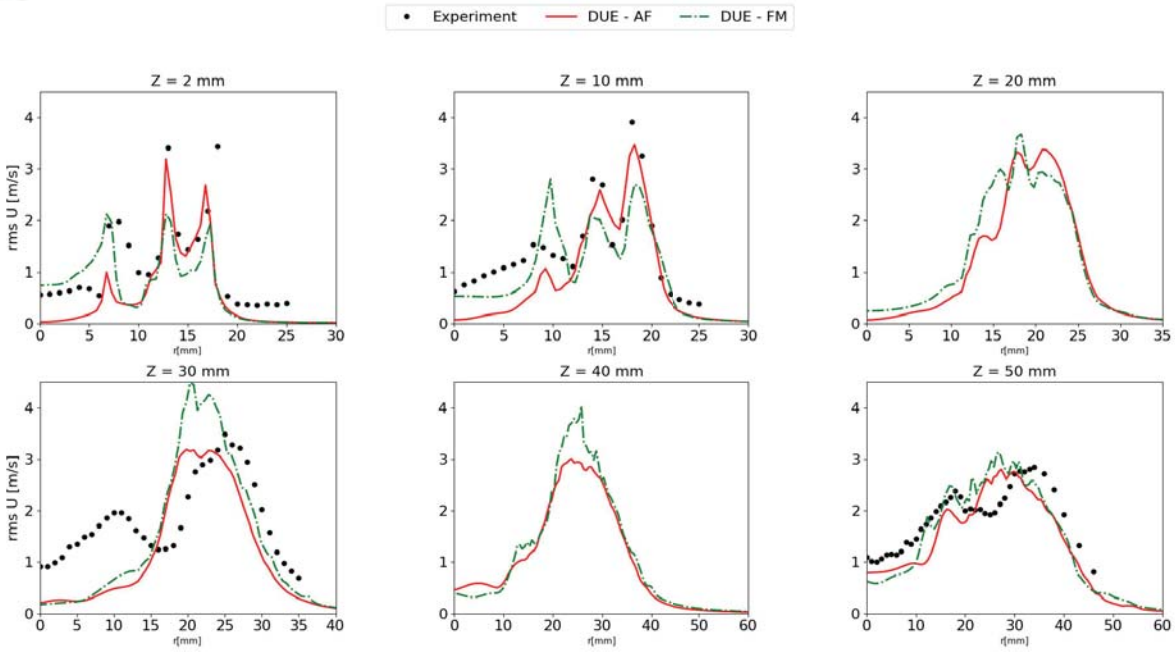

68

SwB11 - Tangential Velocity

Mean

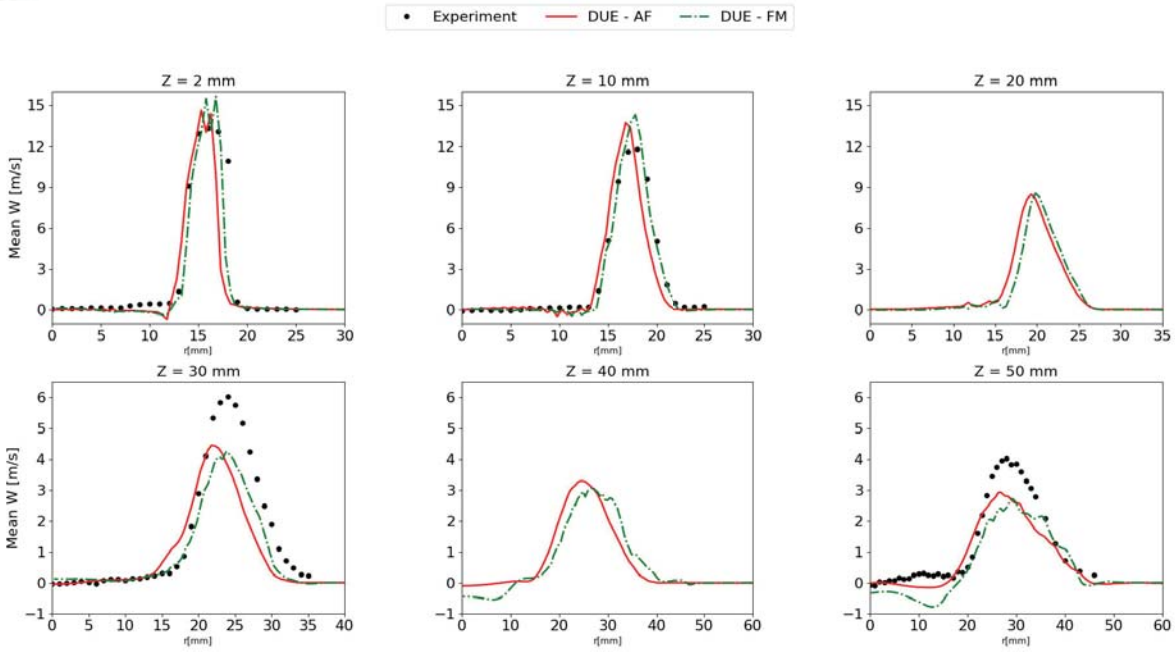

69

SwB11 - Tangential Velocity

RMS

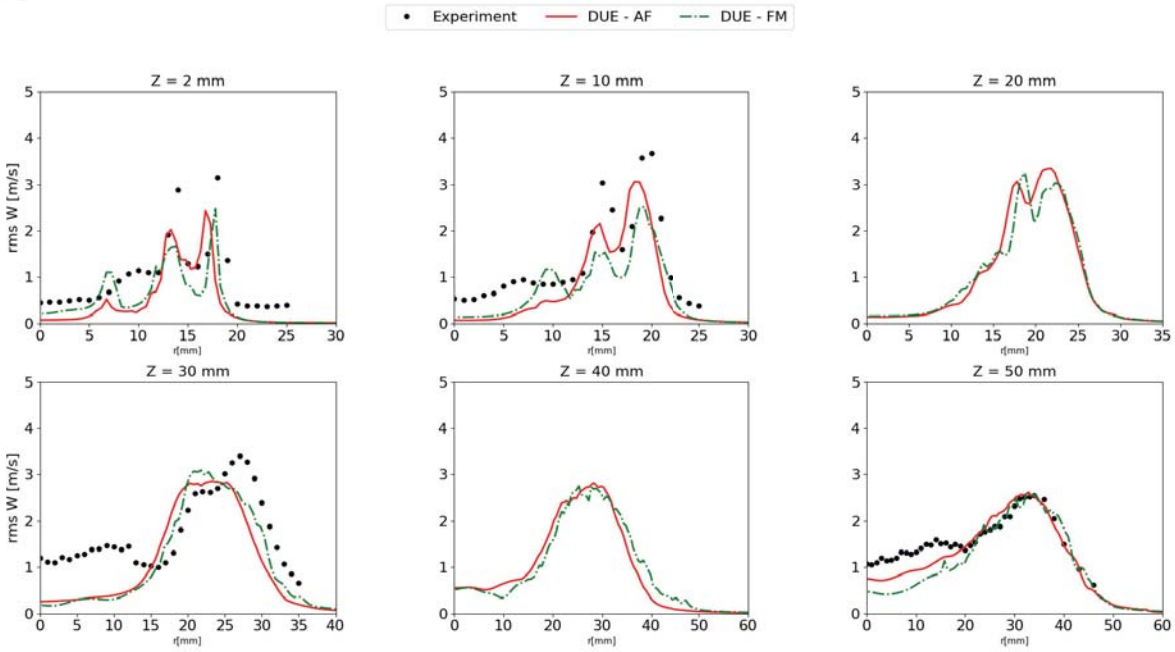

70

SwB11 - Equivalence Ratio

Mean

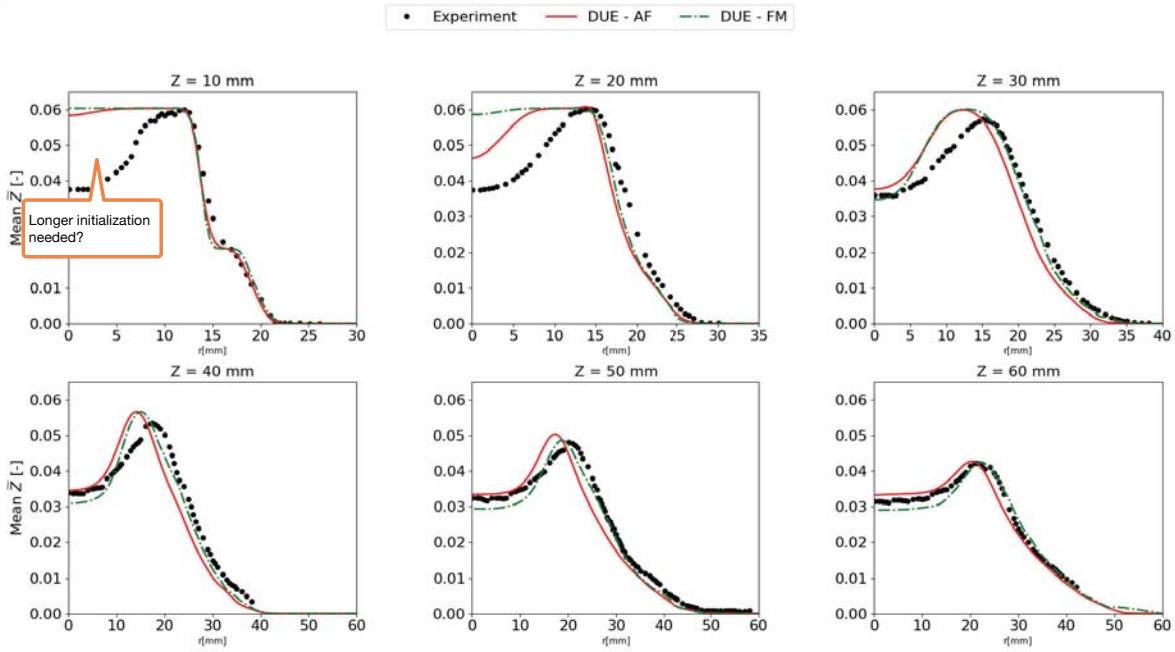

71

SwB11 - Temperature

Mean

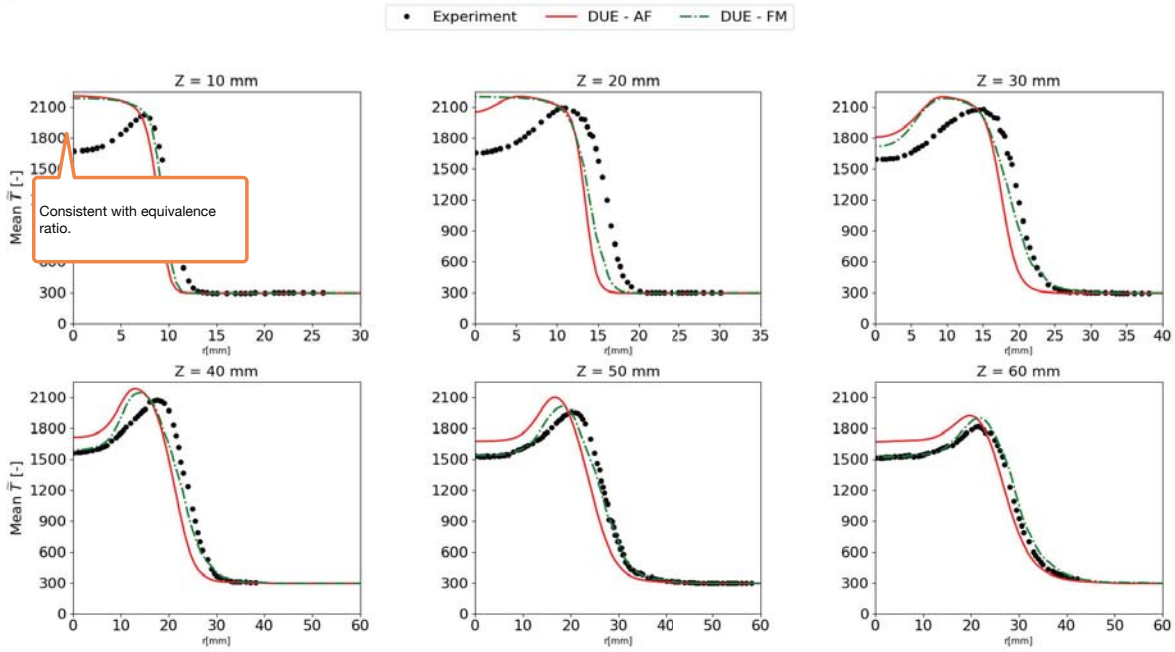

72

SwB11 - CO_2 Mass Fraction

Mean

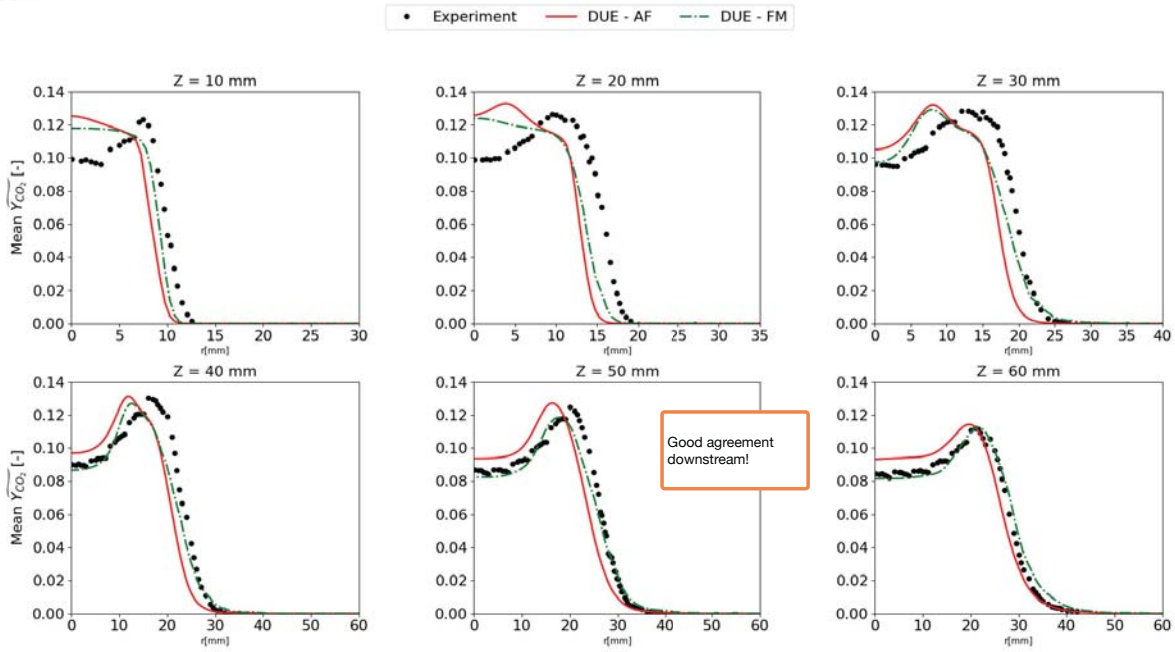

Good agreement downstream!

73

SwB11 - CO_2 Mass Fraction

RMS

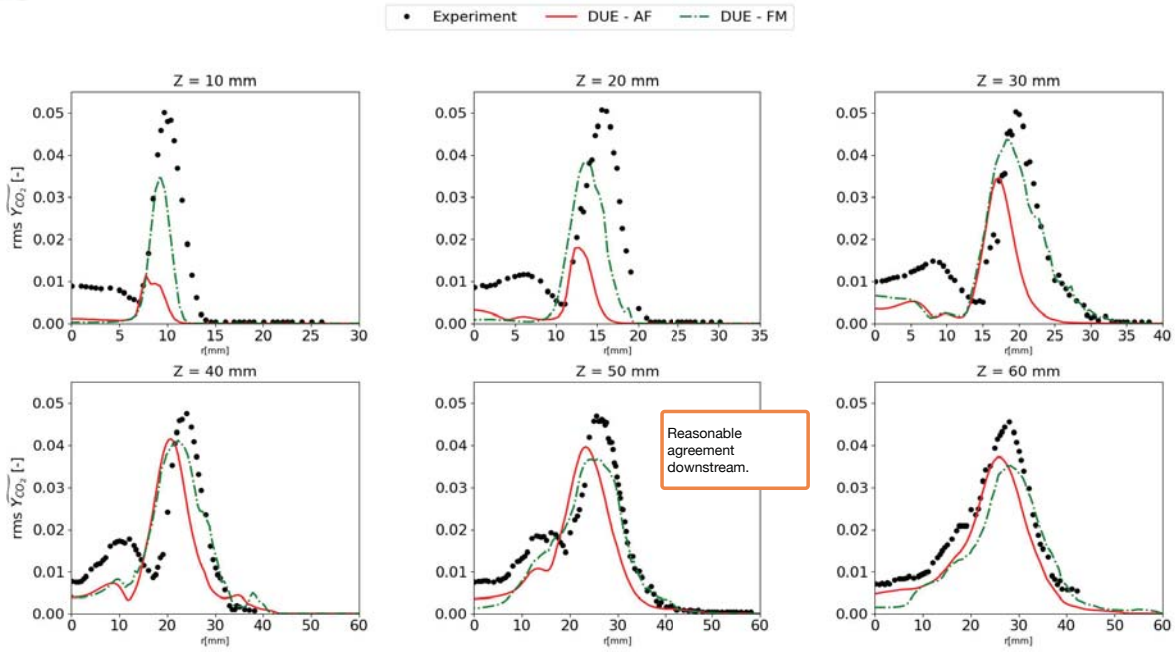

Reasonable agreement downstream.

74

SwB11 - CO Mass Fraction

Mean

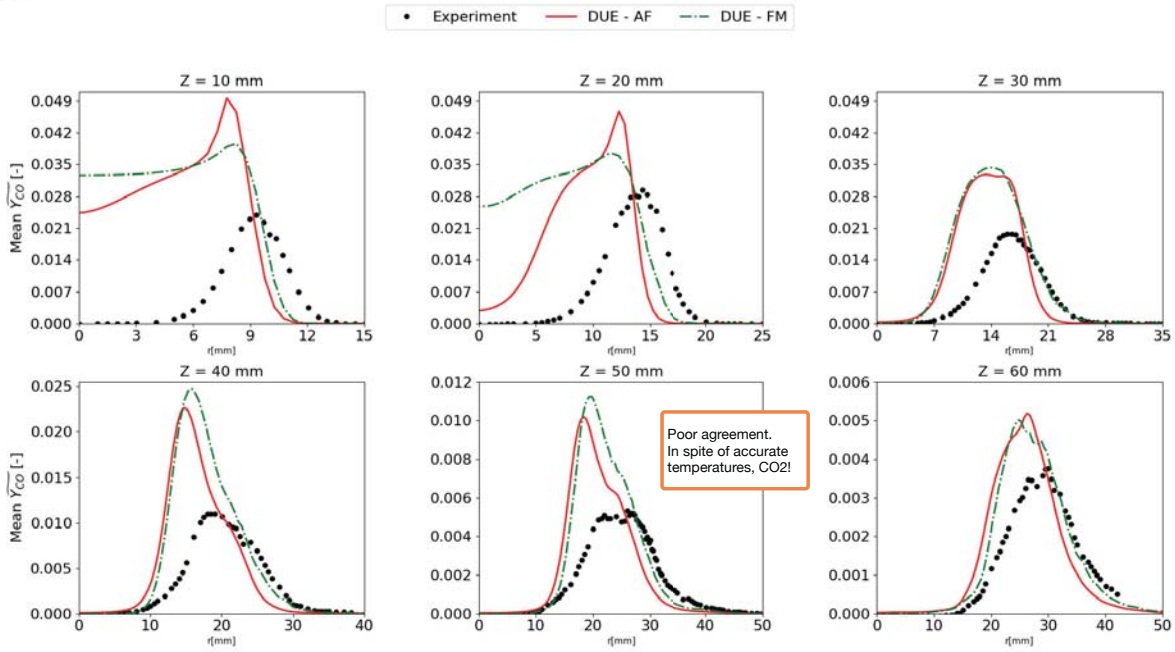

75

Lewis number

Problems in rich mixtures

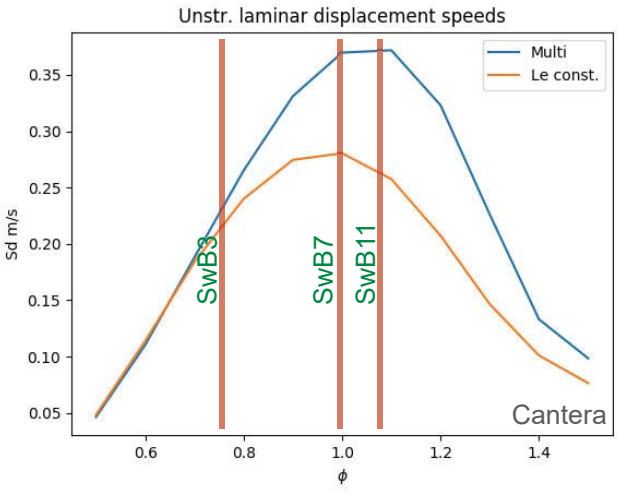

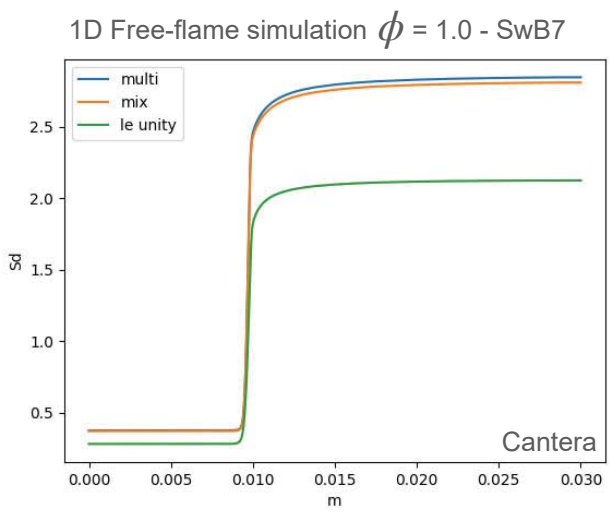

Flame speeds start to differ for richer mixtures (ϕ > 0.8)

76

Lewis number
Problems in rich mixtures

Mixture Fraction over 5 ms

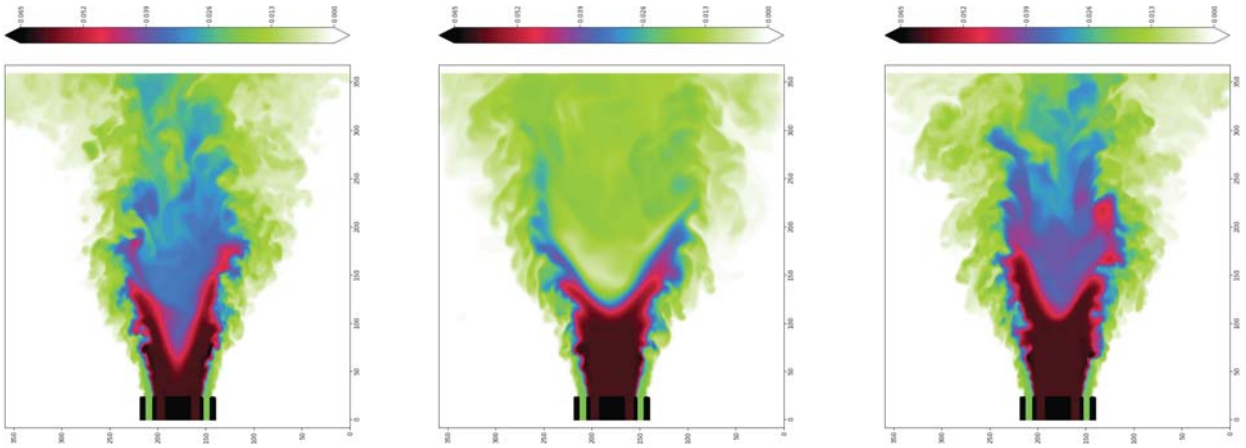

SwB11
Le = 1.0

SwB11
Le = 0.3

SwB11
Quasi Multi Le

77

Lewis number
Problems in rich mixtures

Temperature over 5 ms

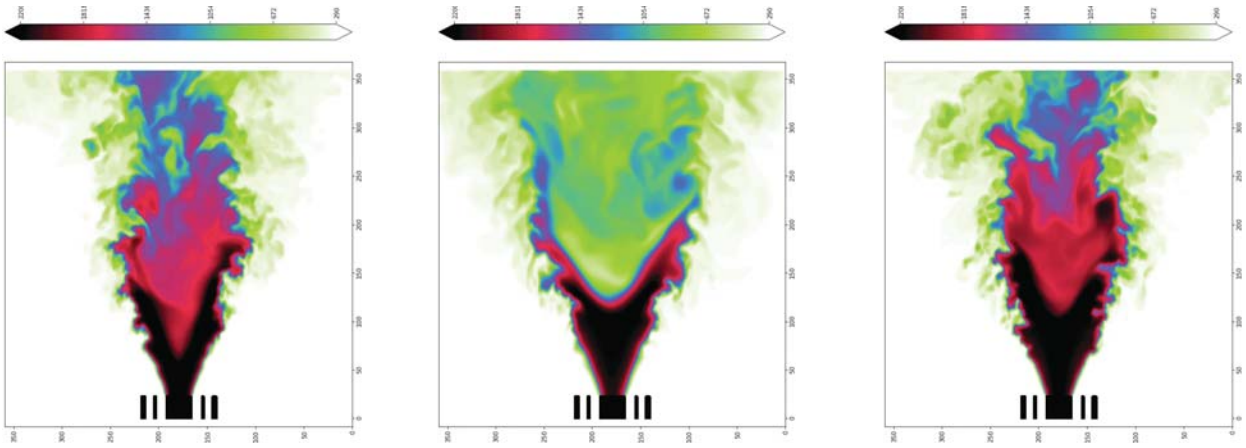

SwB11
Le = 1.0

SwB11
Le = 0.3

SwB11
Quasi Multi Le

78

SwB11 - Conclusions

- Probably strong Lewis number effects
- A model that includes differential diffusion could be very useful

79

Progress from TNF14

Cambridge Flame

- New cases (swirled)
- Focus on species concentration
- More contributions
- Advanced combustion models
- But: long runtime for some flames leads to questionable convergence

80

Special Acknowledgement

Thank you for your attention!

Many thanks to Eray Inanc for gathering and plotting the data.

Big thanks to Mr. Alvin Surjana, who spent many hours to process all of this data!

81

blank

Modeling CO in turbulent flames

Giampaolo Maio, Constantin Nguyen Van, Andreas Kempf, Robert Barlow and Benoît Fiorina

The objectives of this session are to discuss and illustrate issues relative to the prediction of CO in Large Eddy Simulation of turbulent flames. By comparison with the temperature or major species mass fractions, the CO prediction is more sensitive to the modeling of detailed combustion chemistry and to the subgrid scale flame wrinkling modeling. This is specific to the wide range of time scales covered by the CO chemistry. To establish a state-of-the-art of CO modeling in turbulent flames, the three following target flames are selected:

- The **Preccinsta combustion chamber**. The retained configuration corresponds to the stable regime with an equivalence ratio equal to 0.83

- The **Cambridge stratified burner** SwB3 configuration (detailed in TNF session "Cambridge swirled flames")

- The **Inhomogeneous inlet burner,** also investigated within the "Sydney Compositionally Inhomogeneous Flames" TNF session. Both FJ200-5GP-Lr75-57 and FJ200-5GP-Lr75-80 operating conditions are retained.

The session consists of three major parts. First a short review of experimental issues in measuring CO has been presented. Then a discussion on modeling challenges to predict CO formation in turbulent flames has been proposed. Finally, the results obtained in computing the three targets flame have been presented and analyzed.

For most of the TNF target flames investigated at Sandia, CO is measured both by Raman scattering and by two-photon LIF. CO LIF measurements are less affected by hydrocarbon fluorescence interference and can yield higher precision (lower noise), especially at low CO concentrations. However, the CO Raman measurements are considered more reliable in flames with low levels of fluorescence interference, such as lean premixed or stratified flames, due the linearity and relative simplicity of the Raman technique. The same calibration methods have been used for both techniques over the past twenty years, so there should be reasonable consistency across different data sets.

Through the analysis of canonical planar and wrinkled flame configurations, the presentation then highlighted the great sensibility of the CO formation/consumption to three physical phenomena: i) the flame enthalpy (or heat losses), ii) the flame regimes (premixed, non-premixed, stratified, etc.) iii) the subgrid scale flame wrinkling. An accurate prediction of the CO formation requires a fine description of all these phenomena. Each of these issues are illustrated on the three target flames.

The Preccinsta combustor, extensively studied in an LES context, is here investigated by three groups: EM2C, CORIA and Jiansgu University. All simulations have been performed using a Low Mach number solver. Chemistry has been modeled by different level of accuracy, including a global step, a virtual and a detailed mechanism. The experimental

conditions are subject to convective heat transfers occurring through the injector system and quartz windows. Wall temperature Dirichlet boundary conditions have been identified by CORIA group to match the experimental measurements of temperature and the species in the near wall region. Both adiabatic and non-adiabatic simulation have been conducted. In addition, four meshes made of 4 to 900 million of cells have been used. All simulations track the flame front by using a Thickened Flame model for LES approach. The Charlette analytical model is used to account for the influence of unresolved flame wrinkling on the flame propagation speed. The impact of turbulence on the CO prediction is however neglected. Comparison between numerical and experimental data shows that the temperature is well captured by non-adiabatic simulations unlike to adiabatic computations that over predict the temperature in the near wall region. In addition, heat losses have also a strong impact on the CO formation (adiabatic simulations strongly overestimate measured profiles). A strong effect of the mesh refinement is also observed. This behavior his attributed to the lack of modeling of the impact of subgrid scale flame wrinkling on the CO mass fraction.

The CO results from the simulations of the **Cambridge burner SwB3** configuration have been then analyzed. Significant scattering in the mean CO profiles prediction are observed. In particular, the overestimation of the CO production by the Thickened Flame model for LES is evidenced. Simulations conducted using a filtered wrinkled flamelet table show that accounting for the subgrid scale flame wrinkling impact on filtered species quantities improves the CO prediction.

Finally, CO profiles predicted from the **piloted Inhomogeneous Jet Flame Burner** are presented. Discussion within the “Sydney Compositionally Inhomogeneous Flames” TNF session, highlighted difficulties in predicting the mixing and temperature fields, especially downstream of the pilot-coflow shear layer. It is therefore difficult to draw clear conclusions on the origins of the CO deviation. However, the results appear sensitive to the flame regime assumption made to tabulate the chemistry. In particular, premixed flamelet based models tends to overestimate the CO profiles, whereas tabulation based on non-premixed flame archetype are more adapted to this jet flame configuration.

CO Raman and LIF measurements and uncertainty: Brief overview

Rob Barlow
Sandia National Laboratories

TNF 2018
DUBLIN IRELAND JULY 27-28

CO Raman scattering

- Non-resonant process (weak) requires high laser energy for single-shot measurements
- Scattering signal is linear with laser energy
- Temperature dependent response and crosstalk from N_2 based on theoretical calculations of Raman spectra (Fuest et al. PCI 2011)
- Main problem is with HC fluorescence interference; measurements limited to Raman friendly flames (premixed and partially premixed CH_4 and DME flames)

TNF 2018
DUBLIN IRELAND JULY 27-28

LIF of CO as applied at Sandia (Carter, Fiechtner)

- Two photon excitation at 230.1 nm using ns Nd:YAG/dye lasers
- Detection at ~484 nm (10-nm bandpass)
- 3rd photon can ionize the excited state CO
- With increasing laser intensity, ionization becomes dominant loss mechanism over quench
- Close to linear ($S_f \propto I_L^b$; b ~ 1.2)
  - Can assume linear if low laser energy fluctuations
- Reduces sensitivity to quenching environment
  - Can ignore quenching variations in "Raman friendly" CH_4 flames (Settersten et al. J Chem Phys 2002)
  - This did not work in oxy-fuel study (Sevault et al. CNF 2012)

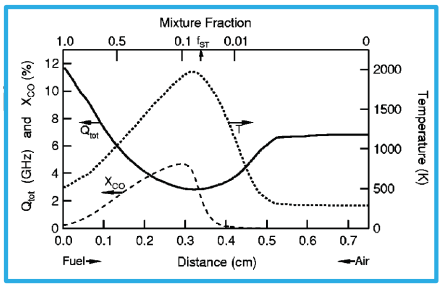

Advantages of CO LIF over Raman scattering

- Much less affected by HC fluorescence interference

DLR-A CH4/H2/N2 flame (Meier et al., CNF 2000)

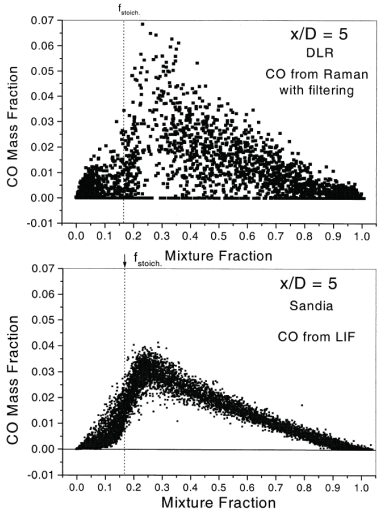

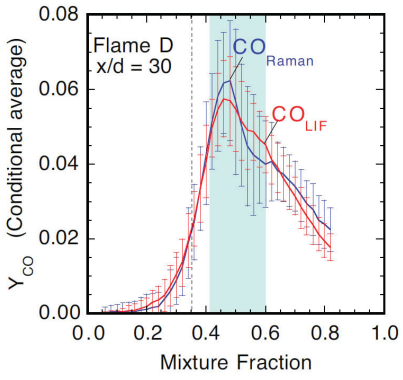

Piloted flame D (Barlow & Frank, PCI 1998)

Advantages over CO Raman scattering

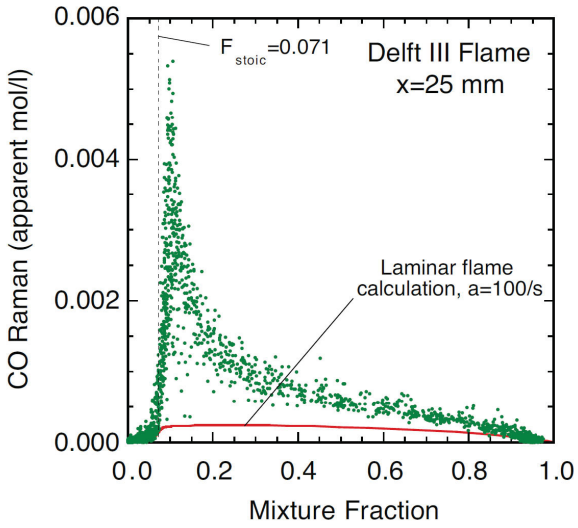

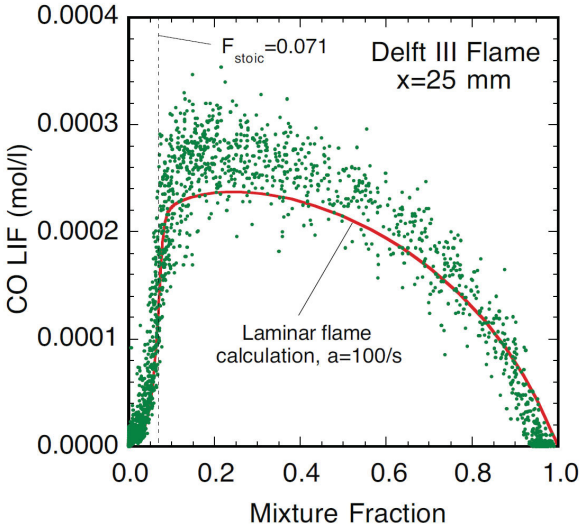

- Delft III nonpremixed natural gas jet flame

TNF 2018 DUBLIN IRELAND JULY 27-28

Advantage over CO Raman scattering

- Lower noise at low CO levels
  - N_2 Raman crosstalk onto CO
- Data shown for the old point measurement system
- Not a big difference in noise for the line measurement system at peak CO levels in premixed and stratified methane flames

CO/H2/air flat flame (Hencken burner)

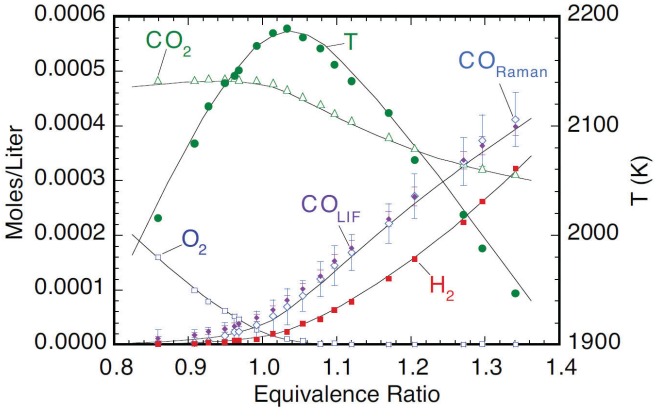

TNF 2018 DUBLIN IRELAND JULY 27-28

Disadvantages of CO LIF

- Added complexity
  - Hardware
  - Nonlinear process
- MUST be measured after the Raman measurement
  - 5 μs delay in Sandia setup to allow Raman shutter to fully close
  - Becomes useless in high speed flows (1 mm displacement in 200 m/s flow)
- Some unresolved mysteries with the Sandia system
  - Calibration sometimes drifts during a day, sometimes rock steady in reference to CO Raman mean values
  - CO Raman (linear process, linear detection) is considered more reliable
  - Adjust CO LIF multiplier to match CO Raman mean at peak levels when there is a discrepancy

TNF 2018 DUBLIN IRELAND JULY 27-28

Calibration and uncertainty

- Same calibration procedure for both techniques
- Series of CH_4/air flat flames
- Equilibrium at $T = T_{ad} - 35K\ (\pm 25K)$
- Estimated uncertainty in mean: ±10%
  - Uncertainty in T, ϕ, repeatability
  - Several data sets (4.4% rms)
  - Calibration optimization code (Magnotti, Hartl) will facilitate more complete analysis
- Higher uncertainty for:
  - CO Raman in flames with HC interference

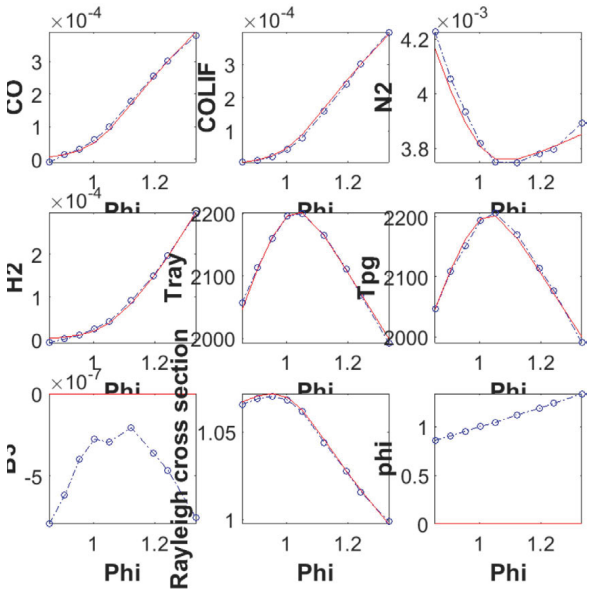

TNF 2018 DUBLIN IRELAND JULY 27-28

Modeling CO in turbulent flames

Giampaolo Maio, Constantin Nguyen Van, Benoît Fiorina
EM2C - CNRS
CentraleSupélec
University of Paris-Saclay

Andreas Kempf
Duisburg Essen University

TNF 2018
DUBLIN IRELAND JULY 27-28

Content

1. Experimental issues in measuring CO *(R. Barlow)*
2. Modeling issues to predict CO formation in turbulent flames *(B. Fiorina)*
3. Analysis of three target flames *(B. Fiorina)*
   1. Preccinsta burner
   2. Inhomogeneous inlet burner
   3. Cambridge swirled flame
4. Conclusions

CO chemistry apparently simple …

- CO is produced by the hydro-carbon oxydation mechanism FAST
- Then oxided through a very simple mechanism SLOW

$$CO + O + M \rightarrow CO_2 + M \quad R1$$

$$CO + O_2 \rightarrow CO_2 + O \quad R2$$

$$CO + OH \rightarrow CO_2 + H \quad R3$$

$$CO + HO_2 \rightarrow CO_2 + OH \quad R4$$

3

… CO covers then a wide range of time and length scales

Isothermal, constant pressure plug flow reactor (Courtesy from Alberto Cuoci)

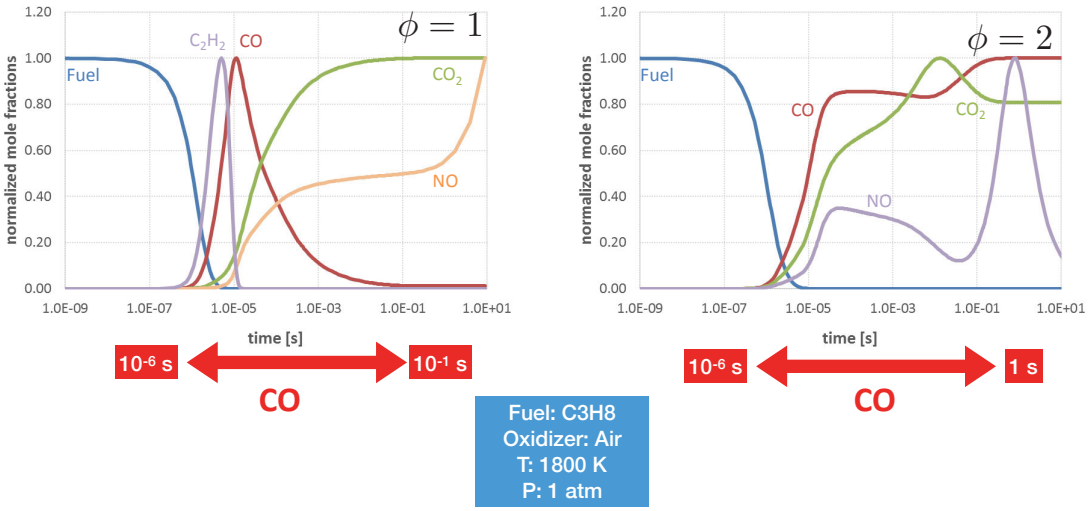

Fuel: C3H8
Oxidizer: Air
T: 1800 K
P: 1 atm

CO modeling is very sensitive to:

- **Heat losses or flame enthalpy**
- **The flame regime (premixed, non-premixed, stratified)**
- **Flame turbulence interactions (LES):**
  - **(subgrid scale) flame wrinkling**

Sensibility of CO formation-consumption to the flame enthalpy

CO tends to decrease with enthalpy at equilibrium

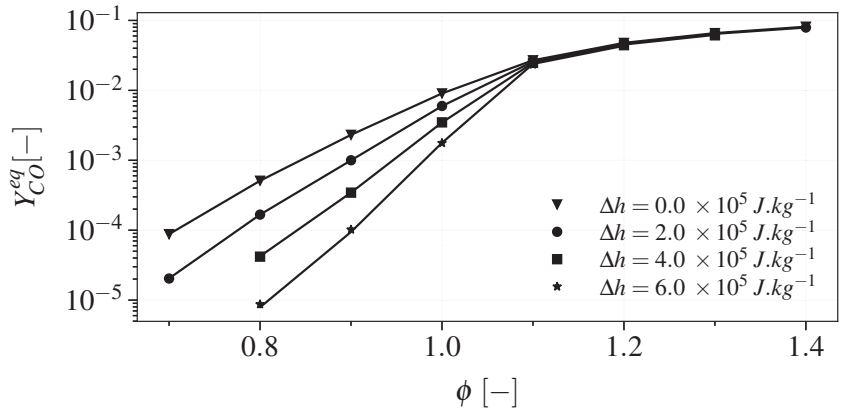

Equilibrium values of CO mass fraction as a function of equivalence ratio, for different enthalpy defect $\Delta h = h^{ad} - h$

CO chemistry is affected by heat losses in flames

$$H^{eq} = H^{f} - \left[\frac{\lambda}{\dot{m}}\frac{\partial T}{\partial x}\right]$$

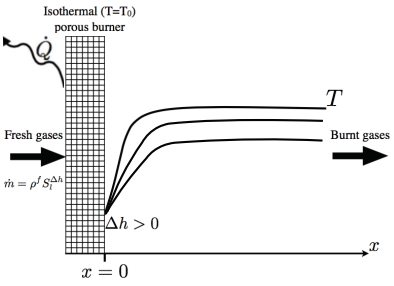

Burner stabilized flame configuration

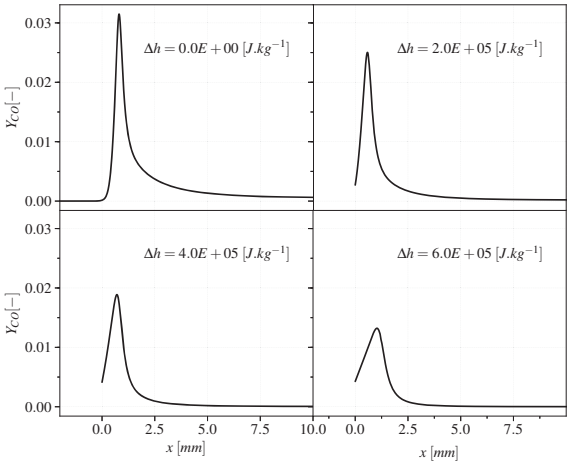

CO mass fraction from 1-D Burner-stabilized flames computed for different enthalpy level.

But too low temperature promote extinction, incomplete combustion and therefore more CO

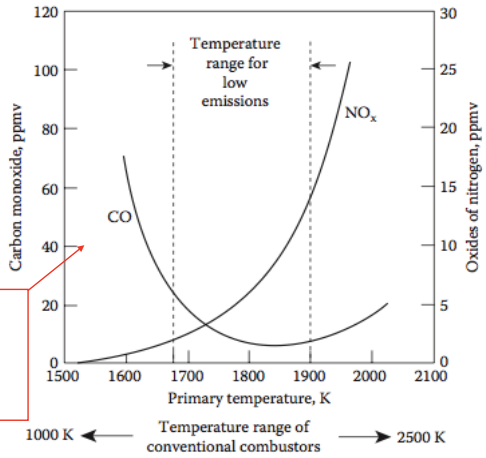

Unburnt hydrocarbons and CO production

From Lefebvre and Ballal, 2010

Sensibility of CO modeling to the flame regime

Chemistry reduction reduces the range of application of the kinetics scheme

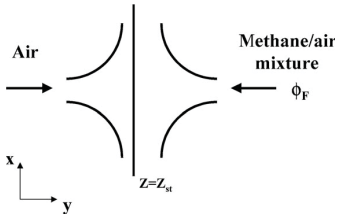

1) compute a 1D diffusion flamelet
2) *a priori* test chemistry tabulation strategies

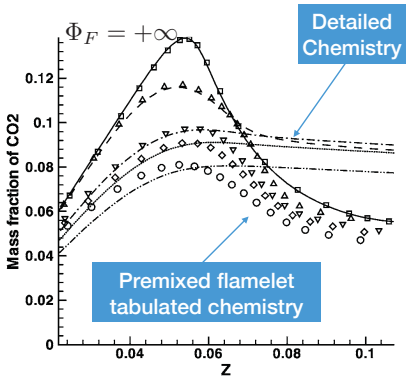

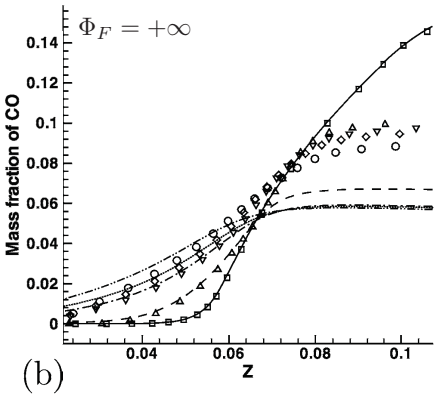

1-D methane-air diffusion flame simulations with detailed and tabulated chemistry for different strain rates. (Fiorina et al, Comb & Flame, 2005)

11

Simulation of hybrid flame regime with reduced chemistry is therefore challenging

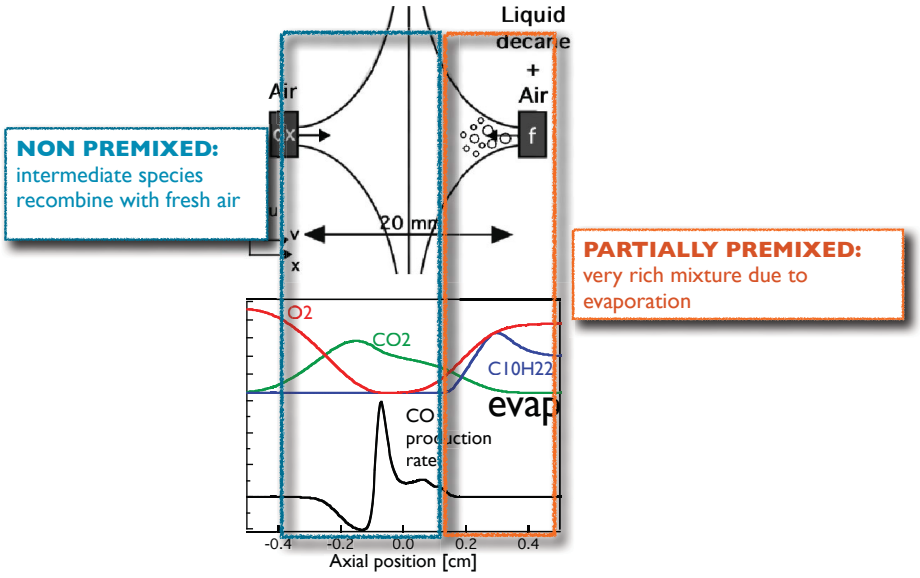

Franzelli et al. (PROCI, 2013)

12

Tabulated chemistry for spray flames

◯ Detailed chemistry

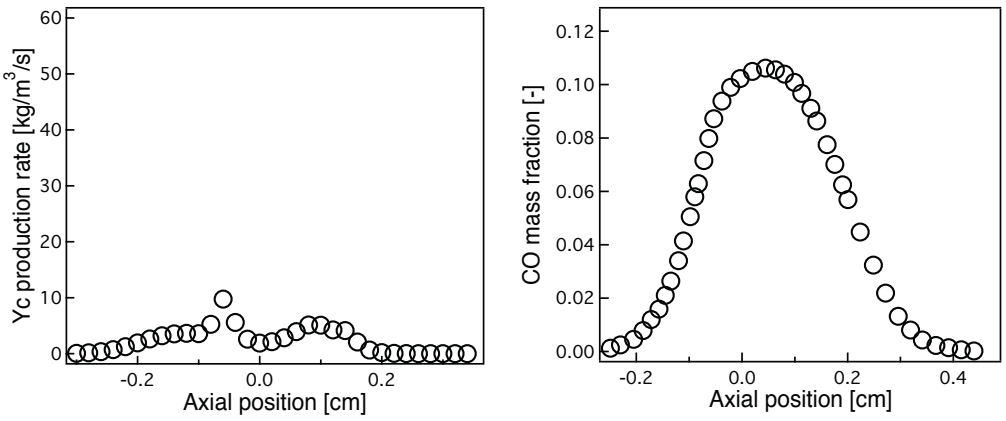

Franzelli et al. (PROCI, 2013)

Tabulated chemistry for spray flames

◯ Detailed chemistry

— Premixed Flamelet Tabulation

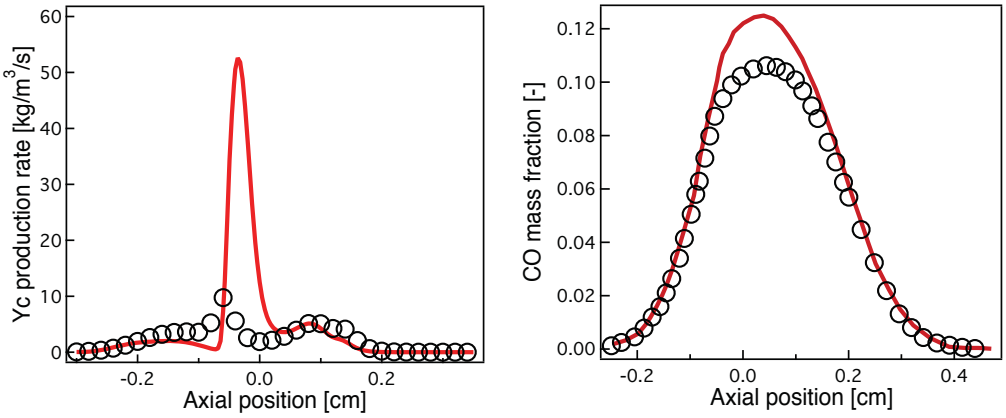

Franzelli et al. (PROCI, 2013)

Tabulated chemistry for spray flames

Detailed chemistry

Premixed Flamelet Tabulation

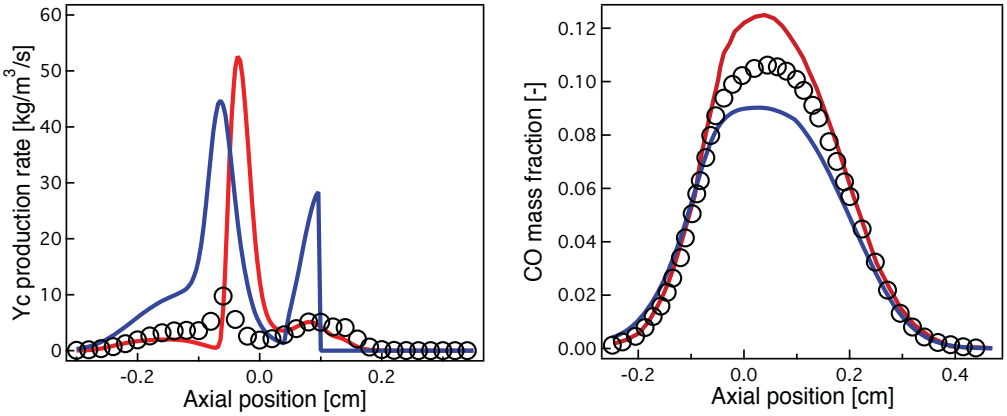

Diffusion flamelet tabulation

Franzelli et al. (PROCI, 2013)

Tabulated chemistry for spray flames

Detailed chemistry

Premixed Flamelet Tabulation

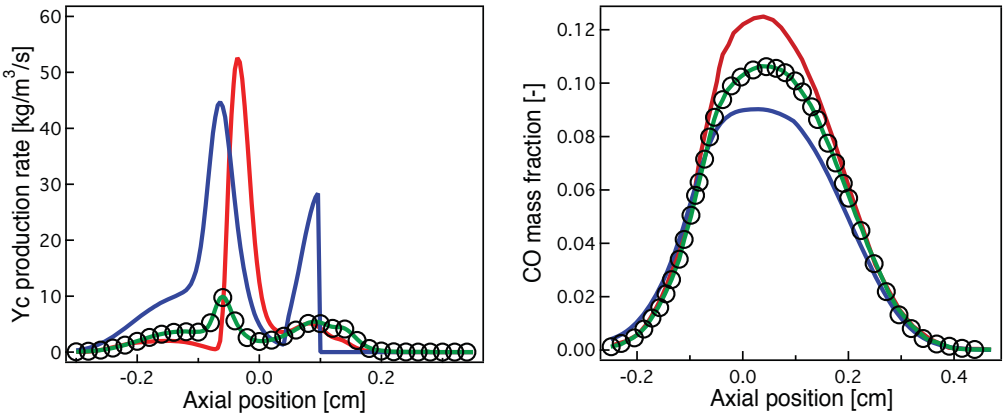

Diffusion flamelet tabulation

Partially premixed flamelet tabulation

Franzelli et al. (PROCI, 2013)

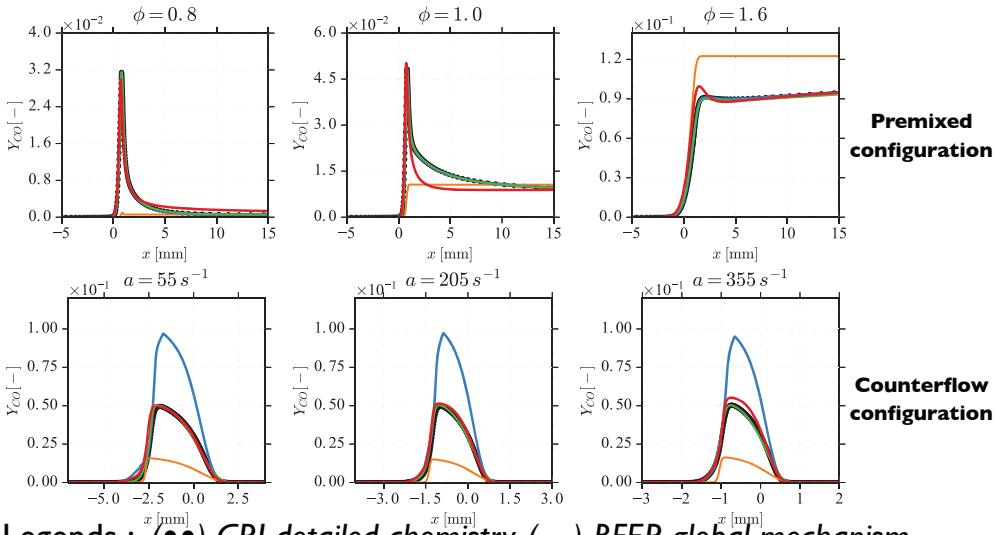

Legends : (••) *GRI detailed chemistry,* (—) *BFER global mechanism,*
(—) *FPI premixed tabulated,* (—) *LU19 analytic scheme,*
(—) *CO-PREM-DIFF virtual mechanism* [17]

M. Cailler et al. submitted (2018)

Subgrid scale flame wrinkling impact on filtered CO quantities

Modeling the chemical flame structure in an LES context

Laminar

No subgrid flame wrinkling

$$\Xi_\Delta = \frac{S_\Delta}{S_l^0} = 1$$

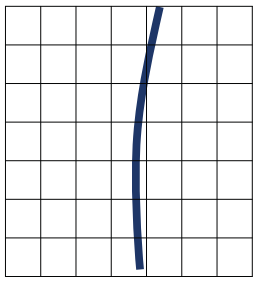

LES Grid

PREMIXED FLAME (FLAMELET REGIME)

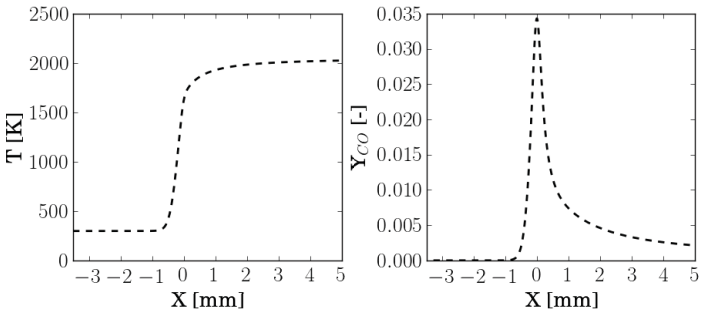

[1] Colin et al., Physics of Fluids, 2000
[2] Kuenne et al., Combustion and Flame, 2011

Modeling the chemical flame structure in an LES context

Laminar

LES solution

Thickened Flame Model for LES [1,2] TFLES

- Thickening by F of the 1D flamelet:

$$\widetilde{Y}_{\mathrm{CO}}(x) = Y_{\mathrm{CO}}^{\mathrm{1D}}(\mathrm{F}x)$$

- Same peak of intermediate species as in the laminar flame

No subgrid flame wrinkling

$$\Xi_\Delta = \frac{S_\Delta}{S_l^0} = 1$$

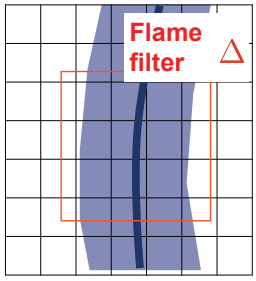

LES Grid

PREMIXED FLAME (FLAMELET REGIME)

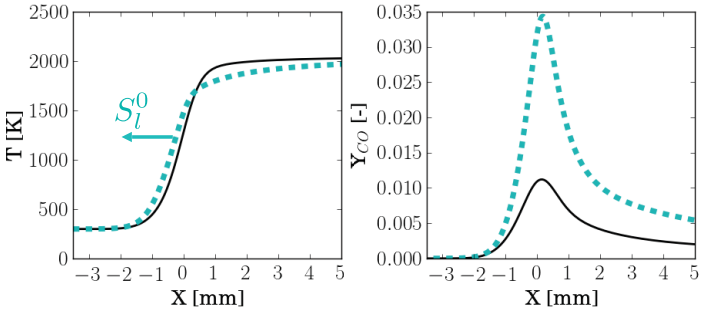

[1] Colin et al., Physics of Fluids, 2000
[2] Kuenne et al., Combustion and Flame, 2011

Filtered species modeling using geometrical approaches

F-TACLES

LES solution

TFLES

No SGS wrinkling

$$\Xi_\Delta = \frac{S_\Delta}{S_l^0} = 1$$

Filtered flame models [1, 2, 3]

- Explicit filtering of the 1D flamelet:

$$\widetilde{Y}_{\mathrm{CO}}(x) = \widetilde{Y}^{\mathrm{1D}}_{\mathrm{CO}}(x)$$

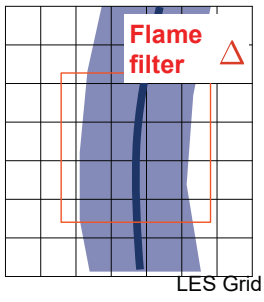

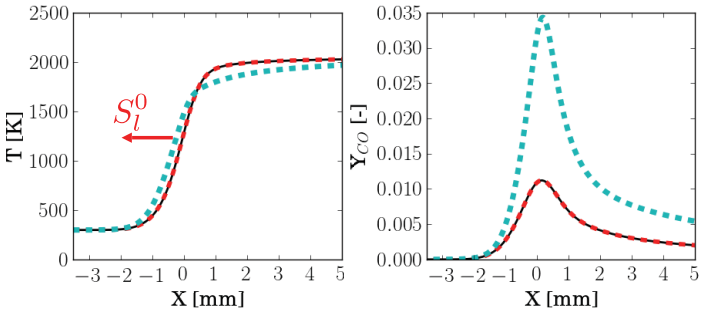

[1] Duwig, Combustion Theory and Modelling, 2009.
[2] Fiorina et al., Combustion and Flame, 2010.
[3] Moureau et al., Combustion and Flame, 2011.

Filtered species modeling using geometrical approaches

What happens when

$$\Xi_\Delta = \frac{S_\Delta}{S_l^0} > 1 \ ?$$

LES solution

TFLES

- The turbulent flame consumption speed accounts for the effect of subfilter scale wrinkling:

$$S_\Delta = \Xi_\Delta S_l^0$$

- Species ?

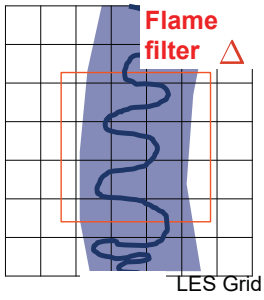

Filtered species modeling using geometrical approaches

What happens when

$$\Xi_\Delta = \frac{S_\Delta}{S_l^0} > 1 \ ?$$

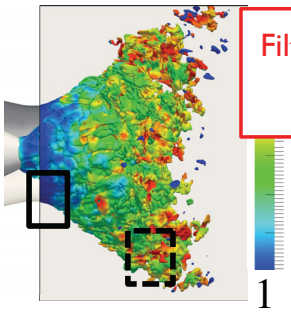

[1] Moureau et al., Combustion and Flame, 2011.
[2] Meier et al., Combustion and Flame, 2007.

TFLES

Filtered laminar flamelet

$\Xi_\Delta \approx 1.2$

$\Xi_\Delta \approx 2.0$

Filtered DNS

Filtered species mass fraction depends on the level of SGS wrinkling Ξ_Δ

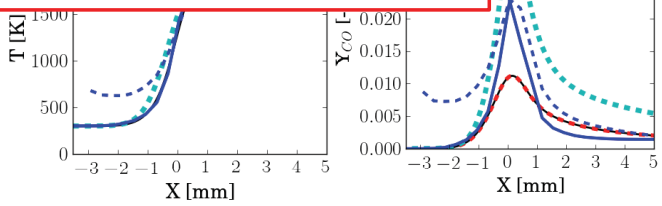

- A priori estimation of $\widetilde{Y}_{CO}$ from the DNS [1] of the lean turbulent premixed burner PRECCINSTA [2]

R. Mercier, C. Mehl, B. Fiorina and V. Moureau. Filtered Wrinkled Flamelets model for Large-Eddy Simulation of turbulent premixed combustion, Submitted (2018).

23

Comprehensive analysis by filtering manufactured wrinkled flames

R. Mercier, C. Mehl, B. Fiorina and V. Moureau. Submitted (2018)

1) Manufacture wrinkled flamelets

Comprehensive analysis by filtering manufactured wrinkled flames

R. Mercier, C. Mehl, B. Fiorina and V. Moureau. Submitted (2018)

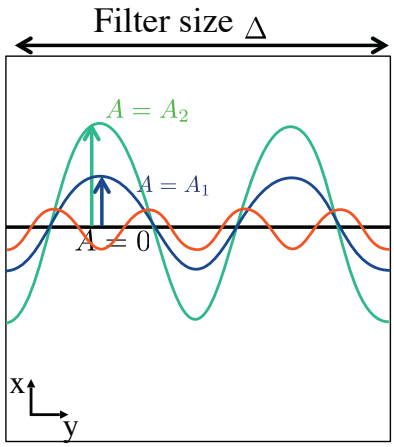

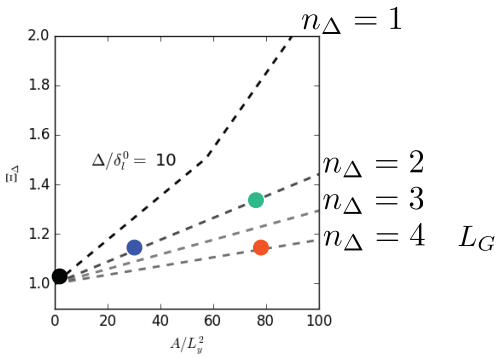

1) Manufacture wrinkled flamelets

Comprehensive analysis by filtering manufactured wrinkled flames

R. Mercier, C. Mehl, B. Fiorina and V. Moureau. Submitted (2018)

2) Filter the manufactured wrinkled flamelets

Comprehensive analysis by filtering manufactured wrinkled flames

R. Mercier, C. Mehl, B. Fiorina and V. Moureau. Submitted (2018)

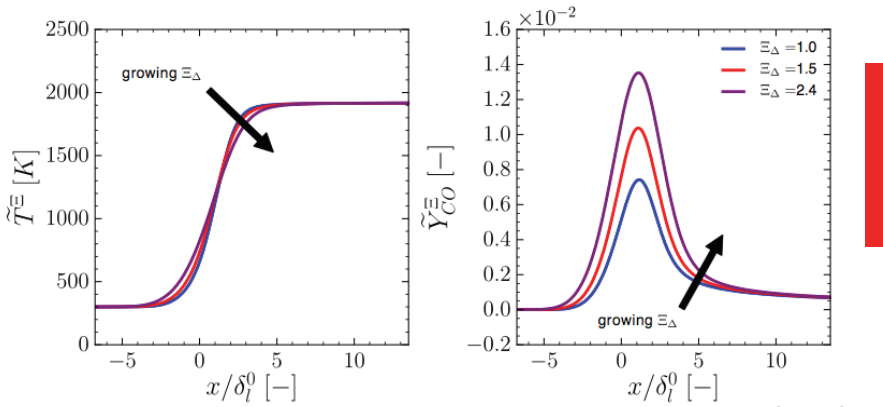

Flamelet assumption: flame structure is even not altered by turbulence !

$$\overline{Y}_{CO} = \Xi \overline{Y}_{CO}^{1DFlamelet} \quad ?$$

2) Filter the manufactured wrinkled flamelets

Normalized mass of CO in the filter volume in terms of flame wrinkling

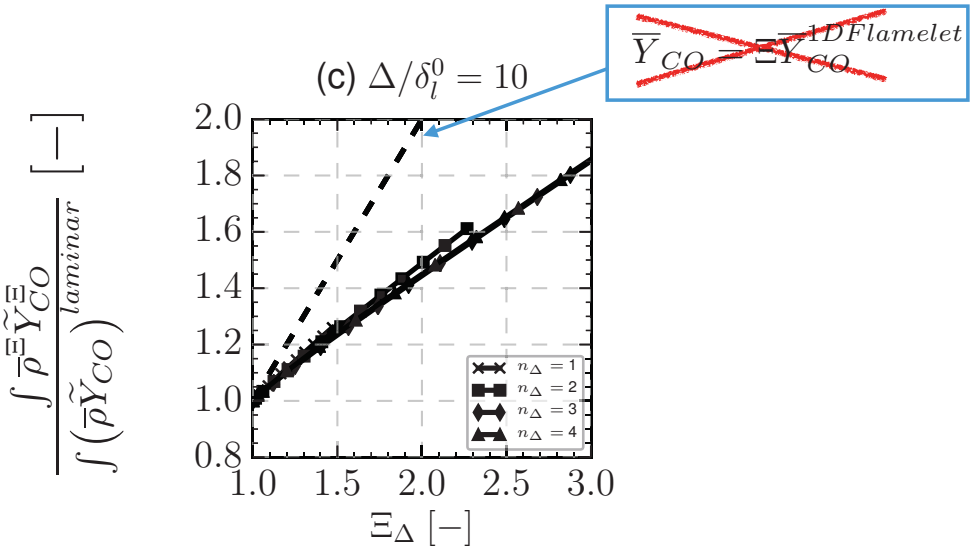

28

Target flames

1. **Preccinsta burner**
2. **Inhomogeneous inlet burner**
3. **Cambridge flame**

PRECCINSTA: turbulent (quasi) premixed flame

Air + CH_4 (assumed perfectly premixed)

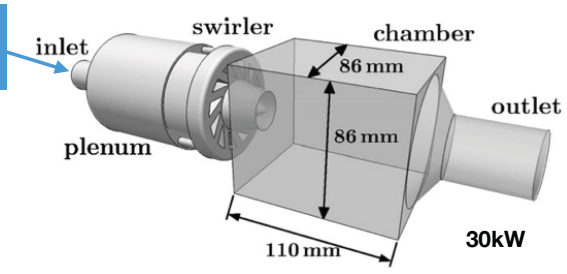

Geometry of the Preccinsta burner (Moreau et al., Combust. Flame, 2011)

Available diagnostics:

- Velocity components (LDV)
- Temperature and major species mass fractions (RAMAN)

- Previous numerical works reproduce fairly well flow dynamics as well as the mean flame front position but problems for Temperature and CO prediction in the ORZ

B. Franzelli, E. Riber, L.Y. Gicquel, T. Poinsot, Combust. Flame 159 (2012) 621–637
S. Roux, G. Lartigue, T. Poinsot, U. Meier, C. Bérat, Combust. Flame 141 (2005) 40–54
V. Moureau, P. Domingo, L. Vervisch, Combust. Flame 158 (2011) 1340–1357
B. Fiorina, R. Vicquelin, P. Auzillon, N. Darabiha, O. Gicquel, D. Veynante, Combust. Flame 157 (2010) 465–475
R. Mercier, V. Moureau, D. Veynante, B. Fiorina, Proc. Combust. Inst. 35 (2015) 1359–1366
P. S. Volpiani, T. Schmitt, D. Veynante, Combust. Flame 180 (2017) 124–135

Non-adiabatic condition

Determination of the wall thermal condition

- Iterative process
  1. Modification of wall thermal condition
  2. Convergence of LES results
  3. Comparison of temperature profile to experiments
  4. Back to 1.
- On 14M and 110M meshes
- Obtained Dirichlet condition
  - External injector wall
    + chamber base
    + chamber windows
  - Start at T=300K
  - Slight rise of temperature in injector
  - T=500K on chamber base
  - High rise up to 1800K on windows

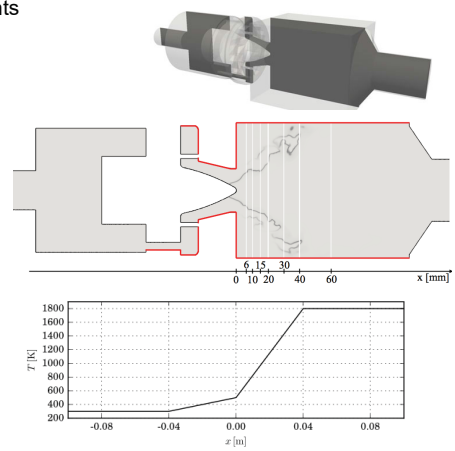

Benard, P., Lartigue, G., Moureau, V., and Mercier, R., Proceedings of the Combustion Institute, 2018.

3 groups for PRECCINSTA

Ping Wang

Giampaolo Maio and Benoît Fiorina

Pierre Bénard and Vincent Moureau

Codes

Group	Code type	Grid	Spatial scheme	temporal scheme	Turbulence
JIA	LESOCC2C Low Mach	Multibloc Structured	2nd	2nd	Dyn. Smag.
EM2C	YALES2 Low Mach	Unstructured	4th	4th order explicit	Wale
CORIA	YALES2 Low Mach	Unstructured	4th	4th order explicit	Dyn. Smag.

33

Simulations performed

Group	Turb. Comb. Model	Chemistry	Heat losses	Mesh
JIA	- TFLES - Ξ anal. model (Colin)	2-steps mechanism	ADIAB.	4M cells (struct.)
		REDIM (tabulated)	ADIAB.	4M cells (struct.)
EM2C	- TFLES - Ξ anal. model (Charlette)	Virtual optimized chemistry	ADIAB.	14M cells (unstr.)
		Virtual optimized chemistry	NON ADIAB.	14M cells (unstr.)
CORIA	- TFLES - Ξ anal. model (Charlette)	Skeletal (19 species)	ADIAB.	14M cells (unstr.)
		Skeletal (19 species)	NON ADIAB.	14M cells (unstr.)
		Skeletal (19 species)	NON ADIAB.	110M cells (unstr.)
	- Resolved flame front	Skeletal (19 species)	NON ADIAB.	900M cells (unstr.)

INERT COLD SIMULATIONS

Cold case, velocity profiles

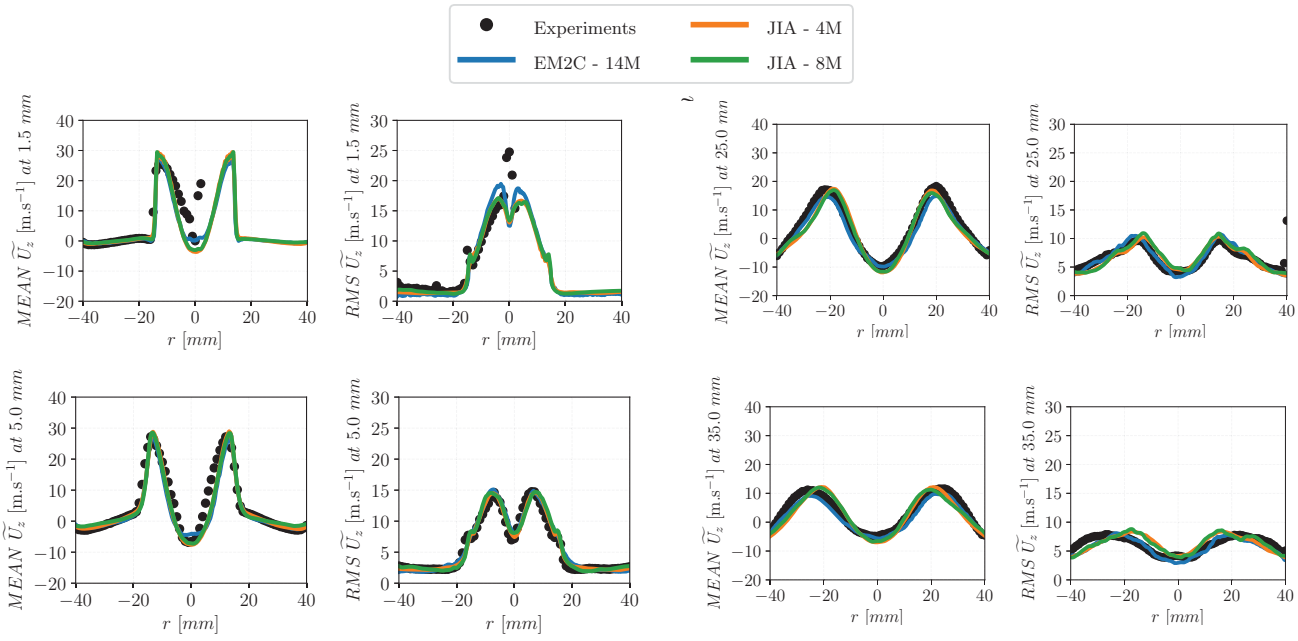

REACTIVE SIMULATIONS

Temperature - Adia VS Non-Adia

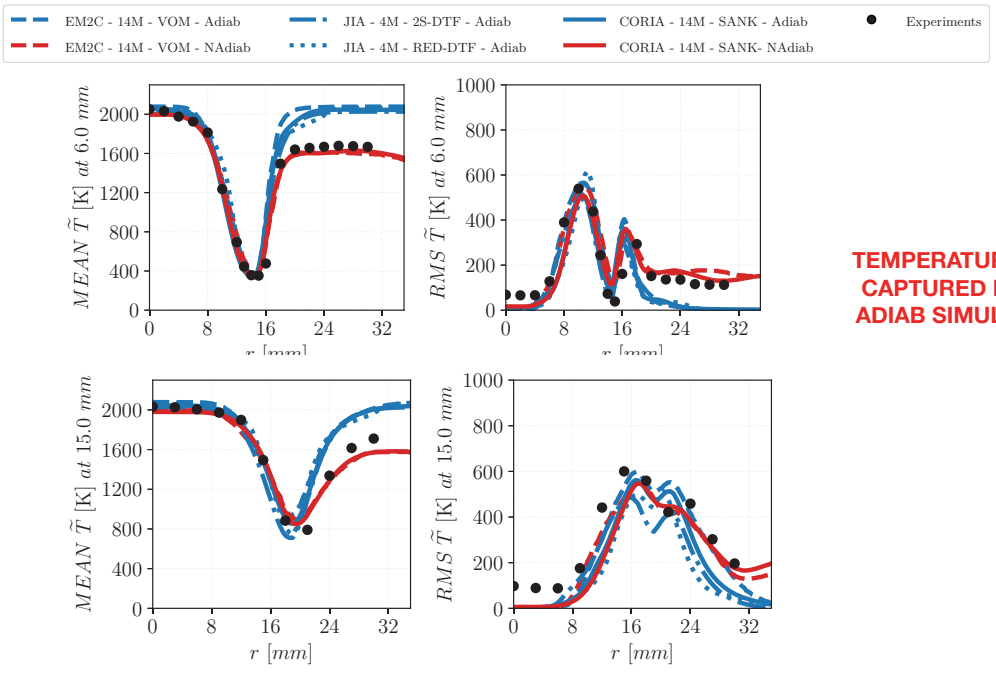

TEMPERATURE WELL CAPTURED BY NON ADIAB SIMULATIONS

Temperature - Adia VS Non-Adia

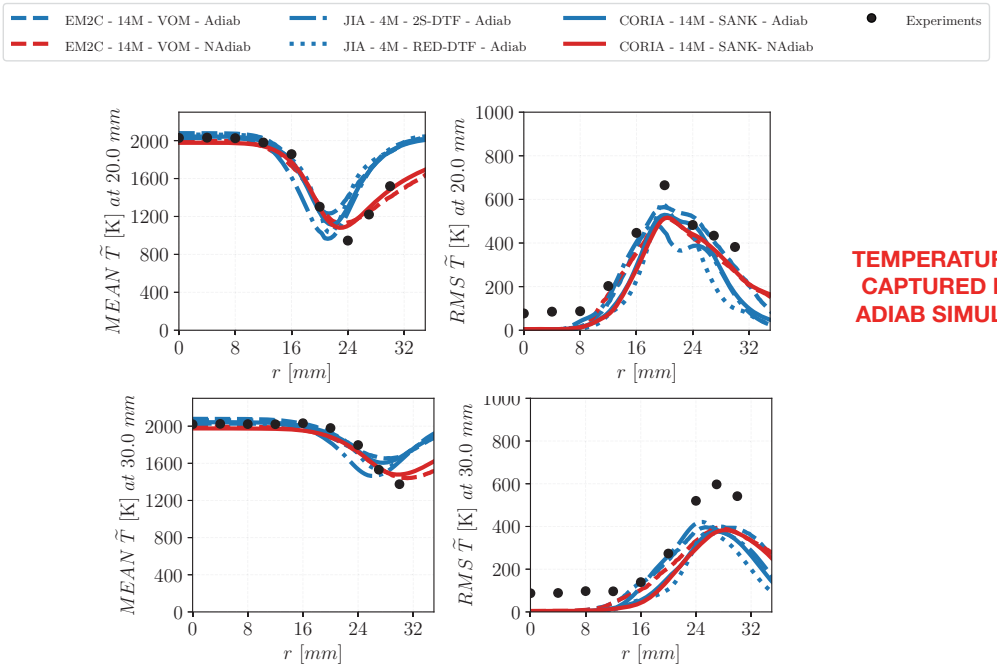

TEMPERATURE WELL CAPTURED BY NON ADIAB SIMULATIONS

CO - Adia VS Non-Adia

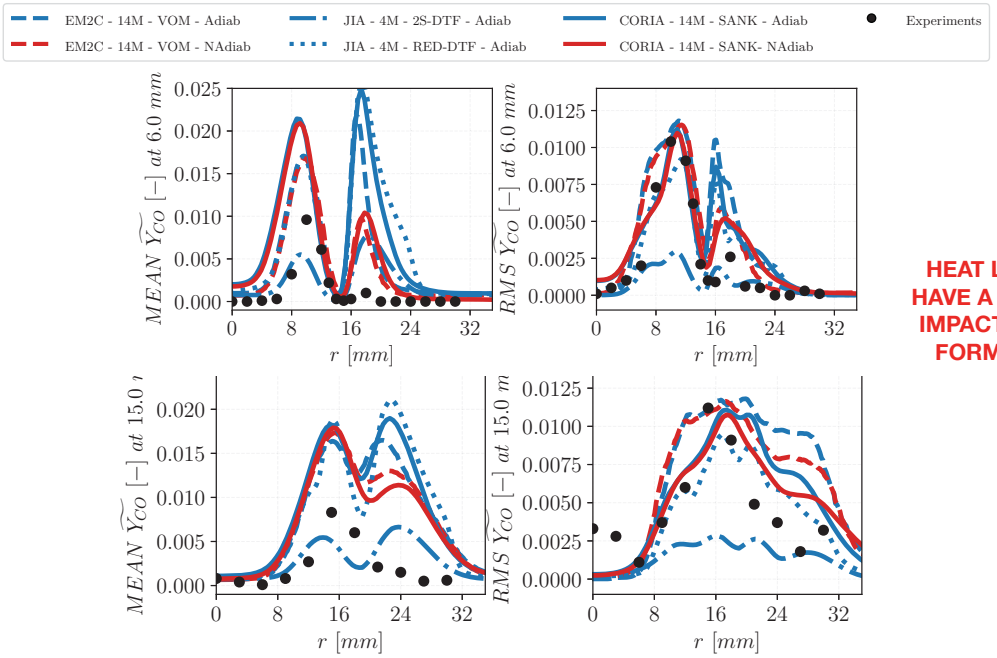

HEAT LOSSES HAVE A STRONG IMPACT ON CO FORMATION

CO - Adia VS Non-Adia

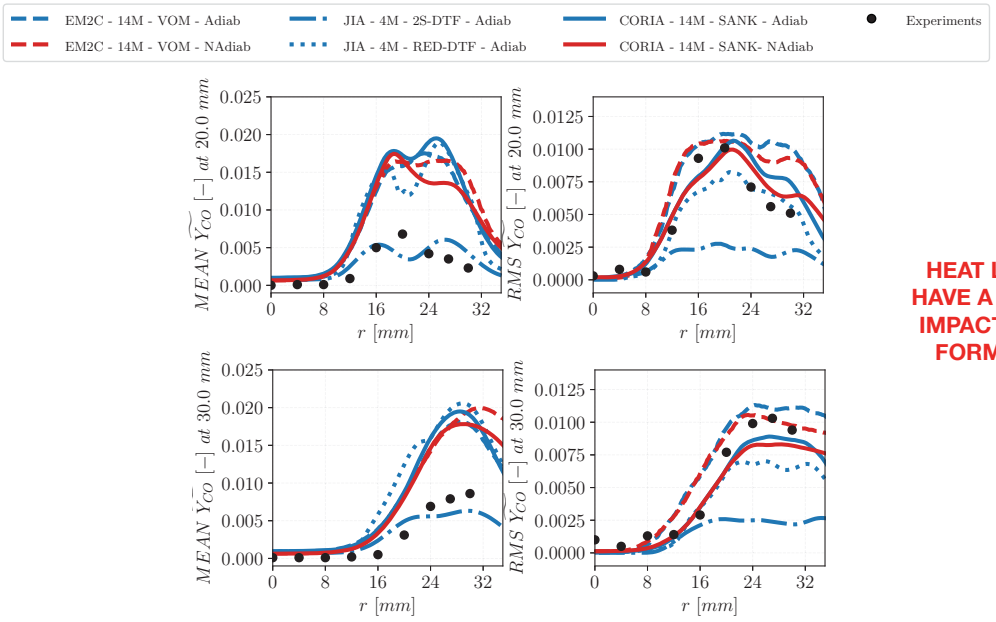

HEAT LOSSES HAVE A STRONG IMPACT ON CO FORMATION

Temperature - Mesh refinement

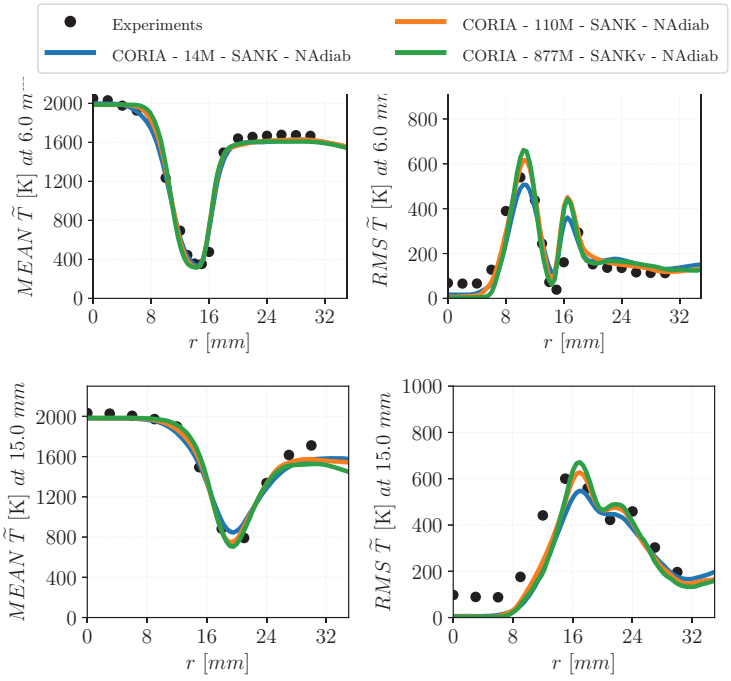

NO SIGNIFICANT EFFECT OF GRID REFINEMENT ON TEMPERATURE

Temperature - Mesh refinement

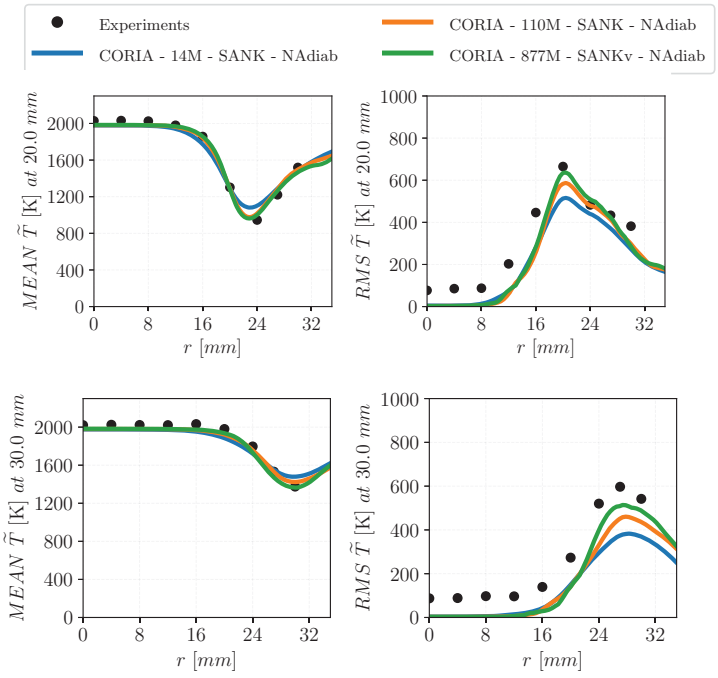

NO SIGNIFICANT EFFECT OF GRID REFINEMENT ON TEMPERATURE

CO - Mesh refinement

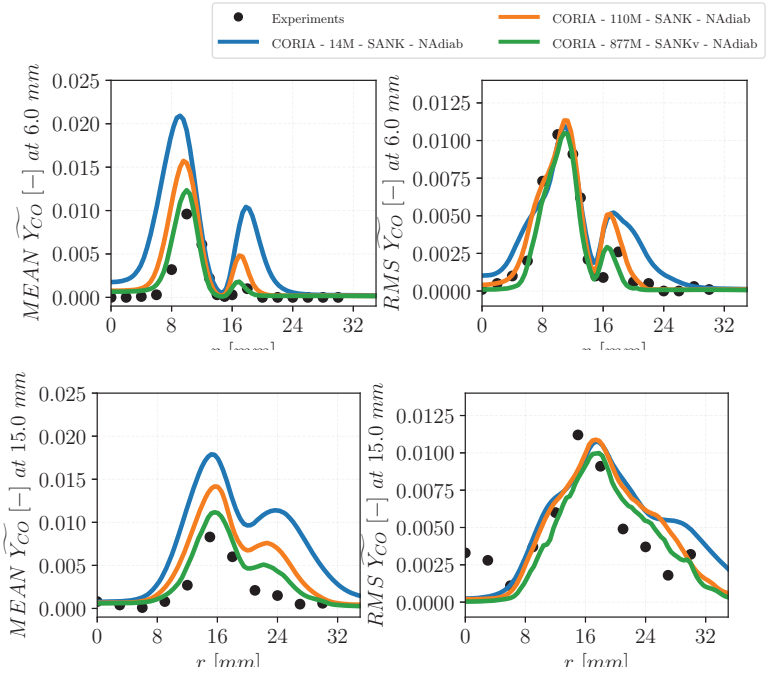

STRONG EFFECT OF MESH REFINEMENT:

IMPACT OF SGS FLAME WRINKLING ON FILTERED CO MASS FRACTION IS NOT MODELED

CO - Mesh refinement

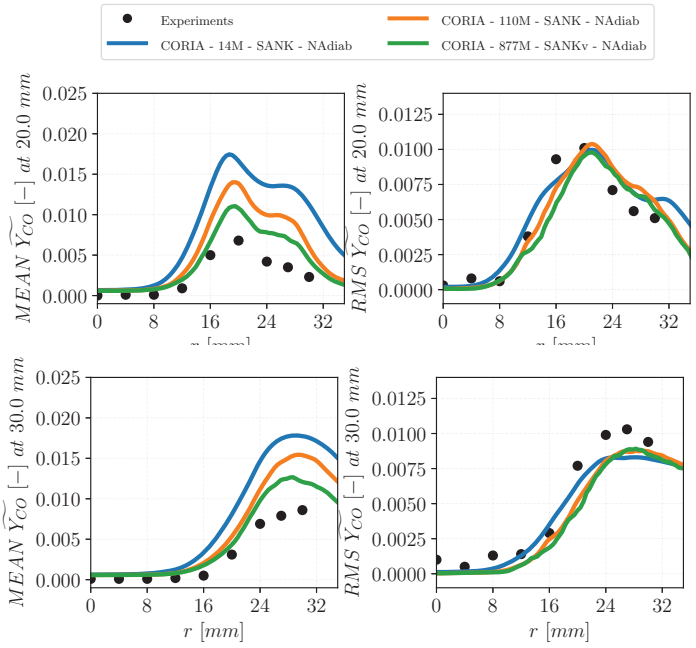

STRONG EFFECT OF MESH REFINEMENT:

IMPACT OF SGS FLAME WRINKLING ON FILTERED CO MASS FRACTION IS NOT MODELED

Go back to Piloted Inhomogeneous Jet Flame Burner

Group	Turbulent Combustion Model	Chemistry	
JIA	Presumed FDF	Tab. Chem. (hybrid flamelets - REDIM)	MULTI REGIMES
KIT	None	Skeletal (19 species)	MULTI REGIMES
PRI	FPV 2 mixt. Pres. FDF	Tab. Chem. (non-premixed)	NON PREMIXED
EM2C	TFLES Ξ anal. model	Tab. Chem. (premixed)	PREMIXED

Group	Turbulent Combustion Model	Chemistry	
STA	FPV + ??	Tab. Chem. (non-premixed)	NON PREMIXED
UBM	Eulerian Stochastic field	Skeletal (19 species)	MULTI REGIMES
CAM	Presumed FDF	Tab. Chem. (hybrid flamelets)	MULTI REGIMES
DUE	Transport & presumed FDF	skeletal &Tab. Chem. (premixed)	MULTI REGIMES

46

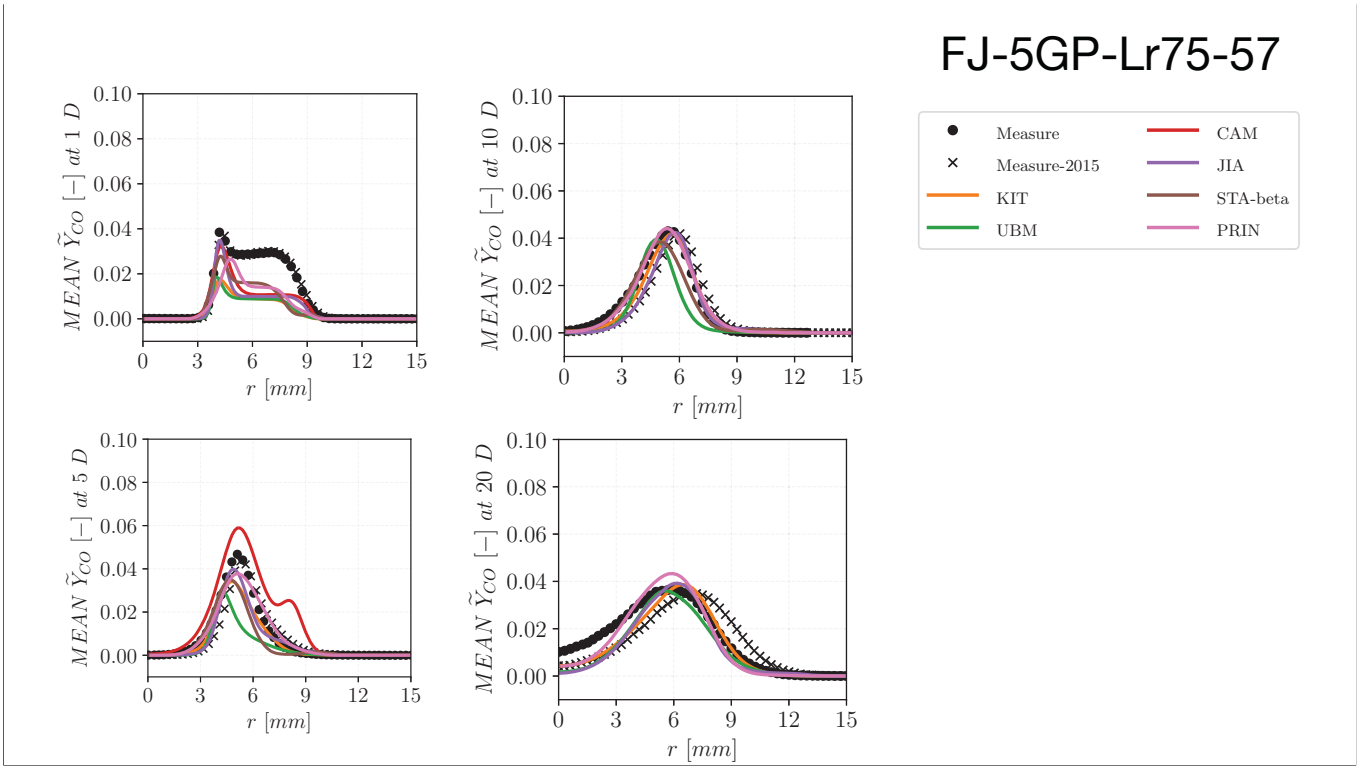
FJ-5GP-Lr75-57
MEAN $\tilde{Y}_{CO}$ [–] at 1 D
MEAN $\tilde{Y}_{CO}$ [–] at 10 D
MEAN $\tilde{Y}_{CO}$ [–] at 5 D
MEAN $\tilde{Y}_{CO}$ [–] at 20 D
r [mm]
Measure
Measure-2015
KIT
UBM
CAM
JIA
STA-beta
PRIN

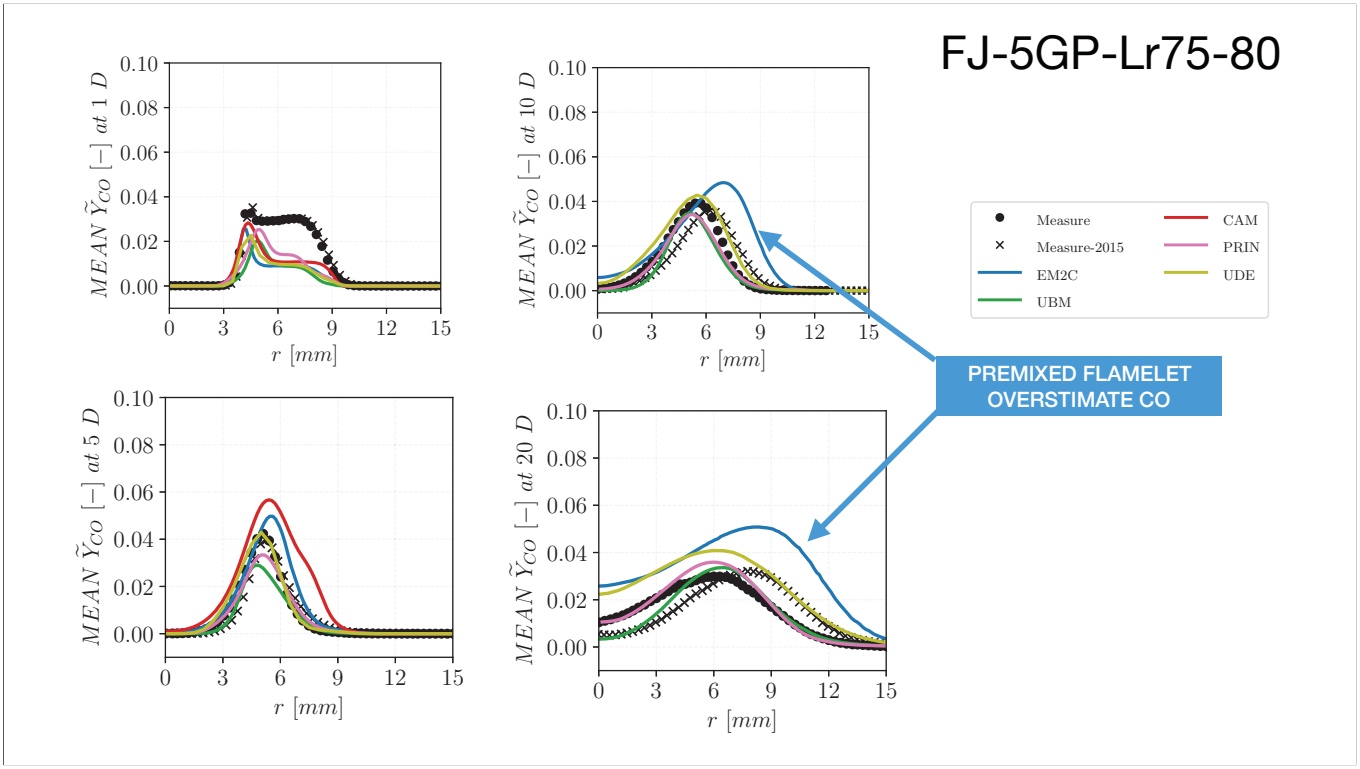
FJ-5GP-Lr75-80
MEAN $\tilde{Y}_{CO}$ [–] at 1 D
MEAN $\tilde{Y}_{CO}$ [–] at 10 D
MEAN $\tilde{Y}_{CO}$ [–] at 5 D
MEAN $\tilde{Y}_{CO}$ [–] at 20 D
r [mm]
Measure
Measure-2015
EM2C
UBM
CAM
PRIN
UDE
PREMIXED FLAMELET OVERSTIMATE CO

SwB3 - CO Mass Fraction

Mean

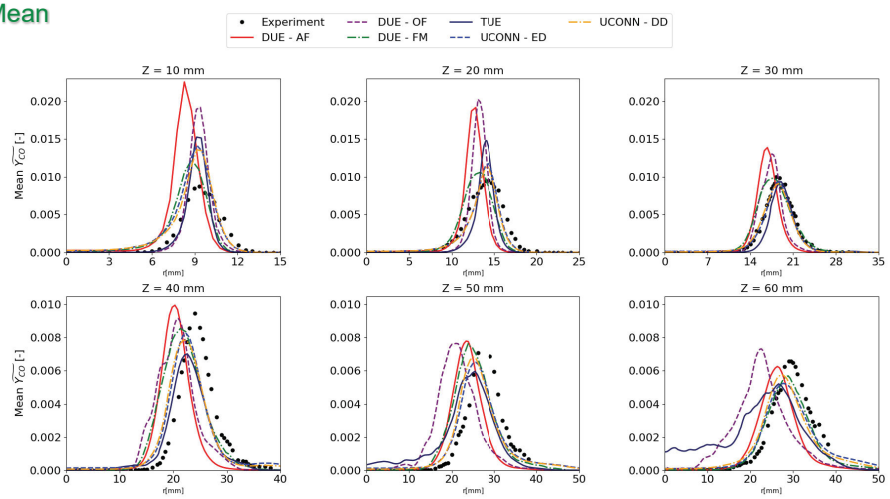

49

Simulation of Cambridge SWB3 configuration

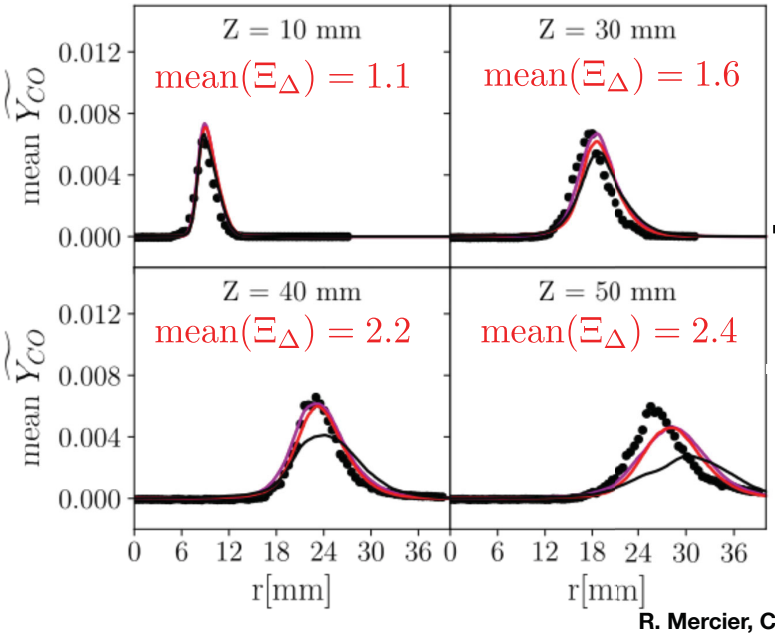

● ● ● **Experiments**

LES with Filtered Tabulated Chemistry

Filtered Planar Flamelets

Filtered Wrinkled Flamelets n_Δ=1

Filtered Wrinkled Flamelets n_Δ=3

R. Mercier, C. Mehl, B. Fiorina and V. Moureau. Submitted (2018)

Conclusions

- Discuss some modeling issues for CO
  - Specific to the wide range of time scales covered by CO chemistry
  - List is not exhaustive

- Show examples
  - Need more target flames (stratified non-adiabatic flames)
  - Compensating errors are easy to obtain but not trivial to detect
    - Thickened flame model overestimate CO …
    - … but neglecting the impact of SGS flame wrinkling underestimate CO

PTF/TNF Joint Session on Highly Turbulent Premixed Flames

Cordinators: A. Steinberg, P. Hamlington, L. Vervisch, M. Ihme, E. Hawkes, J. Sutton

This joint session between the PTF and TNF workshops focused on various issues pertaining to the physics, measurement, and simulation of "highly turbulent" premixed flames. The first talk by A. Steinberg and P. Hamlington focused on recent observations made through experiments and direct numerical simulations (DNS). Subsequent talks by L. Vervisch and M. Ihme focused on modeling capabilities and gaps. The final two talks by E. Hawkes and J. Sutton discussed future directions in DNS and experiments.

Summary by A. Steinberg and P. Hamlington

Experiments in flames with high Karlovitz numbers have predominantly been performed through multi-dimensional imaging techniques such as planar laser-induced fluorescence (PLIF) and Rayleigh scattering. The most prevalent configurations have been jet- and Bunsen-flames issuing into a large co-flow of combustion products, although some results from bluff-body flames and expanding flames were noted. The vast majority of experiments have focused on methane/air combustion at 1 atm; some data at up to 20 bar and other data with propane and ethylene were highlighted.

Imaging results show a prevalence of broadened preheat zones (or CH_2O zones) while maintaining thin regions of high heat release rate, although broadened reaction zones have also been observed. There is a discrepancy between the reported Karlovitz numbers at which reaction zone broadening occurs between different burners, which may be due to different definitions of Karlovitz number or the influence of geometry. Despite the prevalence of thin reaction zones, there is a discrepancy between the turbulent burning velocity and the reaction zone area.

Results from DNS and from multi-scalar imaging experiments using Raman/Rayleigh diagnostics indicate a complicated interplay between mixing and chemistry, leading to a large number of thermochemical states and reaction rates. This is clearly evidenced by premixed flames at a given equivalence ratio issuing into a co-flow of products at a different equivalence ratio. Both DNS and experiments show significant stratification at the reaction zone due to mixing of the co-flow products. Hence, many flames that have been reported to be premixed in the literature may actually be better classified as stratified.

Another key area of interest is the influence of combustion on the structure and dynamics of turbulence. This has primarily been studied through DNS of isotropically forced turbulence. The flame influences the structure of the turbulence by suppressing small scales through increased temperature/viscosity, and by enhancing large scales through pressure-dilatation effects. The flame also induces anisotropy in the direction of the flame normal and changes the alignment of vorticity and strain rate. Both of these effects diminish with increasing Karlovitz number.

Backscatter – viz. net up-scale transfer of kinetic energy – has been observed in DNS through analyses in physical space, Fourier space, and wavelet space. This process can lead to energization of large scale turbulent motions in some DNS. Enstrophy transport budgets indicate a range of moderate Karlovitz numbers over which flame-scale baroclinic vorticity production is significant, which may provide the necessary injection of small-scale turbulence to drive backscatter. Experiments have noted that large-scale pressure gradients – e.g. induced by swirling flows or confinement geometry – may play an important role in flame-scale turbulence production through baroclinic torque, and hence of the dynamics of reacting turbulence.

Summary by L. Vervisch, P. Domingo, G. V. Nivarti, R. S. Cant and S. Hochgreb

In the practice of real burners featuring a limited range of variation of their turbulent Reynolds number, it was discussed how high Karlovitz combustion actually goes with a drastic reduction of the

Damköhler number. Then, two routes have been examined to support the existence of low Damköhler combustion.

The discrepancy between the enhancement in overall burning rate and the enhancement in flame surface area measured for high-intensity turbulence has been reported in the context of scaling laws for diffusivity enhancement from eddies smaller than the flamelet thickness. The factor quantifying this discrepancy is formalized as a closed-form function of the Karlovitz number.

The relation between the dilution by burnt gases and the apparition of high Karlovitz flames was also discussed. Basic scaling laws have been presented which suggest that the overall decrease of the burning rate due to very fast mixing can indeed be compensated by the energy brought to the reaction zone by burnt gases. The results confirm the possibility of reaching, with the help of a vitiated mixture, very high Karlovitz combustion before quenching occurs.

Summary by M. Ihme

In coordination with the presentation flame experiments at high-Karlovitz number conditions, this presentation focused on three aspects, namely the analysis of the flame-structure from direct numerical simulations, the evaluation of the current state-of-the-art in modeling these flame conditions, and a discussion on potential pathways for directly integrating measurements and experimental observations into simulations.

In the first part, three different canonical DNS-configurations at large Ka-conditions were examined. By modulating the initial conditions and stratification, notional conditions of premixed, non-premixed and stratified flames were considered. A Lagrangian flamelet analysis was performed to identify whether these high-Ka flames retain an inherent flamelet characteristics. Despite simplifying assumptions about transport properties, scale separation, and chemical complexity employed in this DNS, this Lagrangian analysis showed the presence of an intact but weakened inner core flamelet structure that is well represented by 1D elongated flame-elements. Entrainment of hot combustion products by turbulent transport leads to mixing of the unburned reactants that can be well represented by a partially premixed reactor. Since the flame-structure and burning intensity is controlled by the upstream reactant mixture, it is unlikely that unstrained premixed flamelet methods are able to describe such flame regimes without taking into account the reactant mixing at the subgrid.

The second part of this presentation reviewed LES-modeling efforts on simulating vitiated flames. Progress and challenges in predicting general flame structure, heat-release and emissions were discussed. Significant efforts have been made in modeling the Sydney partially-premixed jet burner (PPJB), employing different modeling strategies that include “implicit” finite-rate chemistry, thickened flame models, transported PDF-methods, and flamelet modeling strategies employing multistream non-premixed and stretched premixed methods, and more recent models such as the conditional dissipation mapping closure and were presented. It was concluded that current combustion models capture the main features of turbulent flame-structure at moderate Ka-regimes; in general, models were found to over predict the reactivity at higher Ka; and extensions of flamelet models show promise but lack key-physical aspects. In regard to outstanding research issues, opportunities arise by extending the flame-structure analysis beyond statistical and conditional analyses. Inherent to vitiated flame configurations considered, it is noted that simulations can be overwhelmed by sensitivities to boundary conditions.

In the last part, potential merits of combustion model adaptation and data assimilation techniques were discussed to improve predictions and take advantage of extensive measurements that are generated from high-speed, simultaneous, and multi-dimensional measurements. An example was showcased in which data assimilation was employed to integrate simultaneous PIV/PLIF-measurements into LES with the goal to improve state-estimates in predicting local ignition events.

Other, and perhaps more useful, opportunities arise in utilized assimilation techniques for model evaluations and the direct assessment of the model performance in capturing the instantaneous flame-structure at high turbulent conditions.

Summary by E. Hawkes

Needs for further improvements, specifically in application of DNS for model development, were discussed. It was argued that the development of practical combustion models that industry can use should arguably be the primary objective of DNS work going forwards, however there have been generally only low levels of DNS work targeted at this objective. Particularly, there are low levels of work targeting *a posteriori* tests, with almost all studies offering only fundamental information or a priori tests, despite *a posteriori* tests offering the most definitive conclusions regarding the performance of a model. New opportunities were identified in conducting partial *a posteriori* tests, where some model inputs are taken directly from DNS, in order to focus attention of the performance of specific sub-models.

Parameter regimes and configurations were discussed. Recent experiments carried out at Michigan at higher Re than previous work show major, qualitative and quantitative differences to lower Re conditions, suggesting that higher Re needs (somehow) to be accessed by DNS. In high Re, high Da conditions in particular, there may be a significant separation between the scales of the thickened local flame structure and large scales of flame wrinkling, which may have as yet unknown effects on many aspects, such as the influence of heat release on scalar transport, scaling of terms in the flame surface density balance equation and the implications for modelling them, etc.

In terms of configurations, recent work from Alexei Poludnenko demonstrates a lack of convergence of large-scaled quantities in DNS of flame-in-a-box cases as the dimension of the box was increased, with fixed forcing length scales. This potentially invalidates the use of these simulations to assess models of large-scaled quantities such as the turbulent velocity (at least in steady state conditions). A need to increase effort on cases with less trivial geometries was identified; e.g. having recirculation zones, mean shear, etc; these cases should have parametric sets and also preferably involve flows that be computed straightforwardly with LES at resolutions where the models are actually doing some work, which will be challenging due to the required scale separation. Such configurations also avoid the problem of convergence with scale observed in flame-in-a-box cases, by only allowing a finite development time or length, which limits the attainable flame growth.

Summary by J. Sutton

The overall discussion was on needs for further improvements in experiments with a focus on current knowledge gaps. These include the understanding of configuration effects (i.e., geometry, pressure, turbulence generation, fuel type, etc.), characterization of the internal structure of turbulent flames, the effects of turbulence-induced stratification, etc. It was argued that specific measurement needs include quantitative multi-scalar measurements, high-resolution velocity measurements, simultaneous velocity/scalar measurements, and heat release rate measurements, and the coordination of new burner designs with modeling efforts. In terms of configuration needs, it was discussed that multiple turbulence generation mechanisms (shear, decaying turbulence, other?) should be tested and to analyze whether measurements in different setups including jets, Bunsen flames, swirl flames are consistent. The need to study more realistic or at least more complex fuels was discussed. Finally, Mach number and compressibility effects were discussed. New measurements in turbulent, compressible flames have shown that turbulence is not attenuated through the flame, but rather flame-generated turbulence is observed.

The final portion of the session focused on emerging capabilities. A collaboration between Darmstadt and Sandia presented a new method to approximate chemical explosive mode and heat release rate using only major species, temperature, and OH. Test data in the Lund premixed jet

flame showed sufficient accuracy in the new methodology. A new high-resolution velocimetry approach being developed at Ohio State was presented. Results from turbulent synthetic flows and tracer particle fields showed much improved results and an order-of-magnitude increases in spatial resolution as compared to traditional particle imaging velocimetry.

Structure and Dynamics of Highly Turbulent Premixed Flames

Adam M. Steinberg[1] and Peter E. Hamlington[2]
[1]Guggenheim School of Aerospace Engineering, Georgia Institute of Technology
[2]Department of Mechanical Engineering, University of Colorado Boulder

*Not a comprehensive review

Overview

- In highly turbulent premixed flames, turbulence time scales are short relative to flame time scales
- $\frac{u_\ell}{s_l^0}$ $Re_T = \frac{u_\ell \ell}{\nu}$ $Ka_\delta = \left(\frac{\delta_l^0}{\eta}\right)^2$ $Ka_r = \left(\frac{\delta_r}{\eta}\right)^2$ etc.
- The intensity of the turbulence results in some behavior that is different from would occur at lower intensity

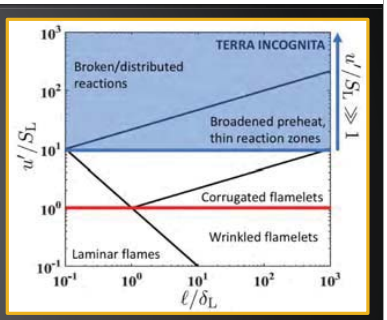

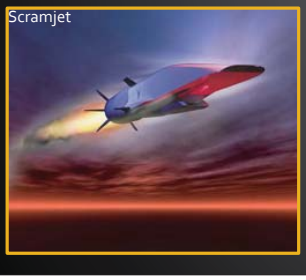

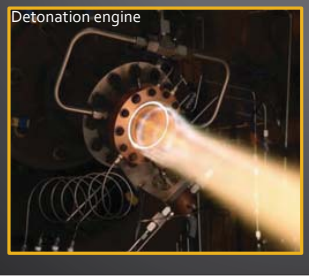

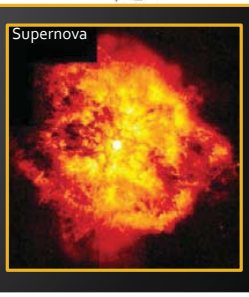

Overview

- Physical aspects – A. Steinberg and P. Hamlington
- Modeling aspects – L. Vervisch and M. Ihme
- Looking forward – E. Hawkes and J. Sutton

Overview

- **What is the 'structure' of highly turbulent flames?**
  - o Local thermo-chemical states
  - o Location of states relative to each other
- **What are the 'dynamics' of highly turbulent flames?**
  - o Local and global flame speeds

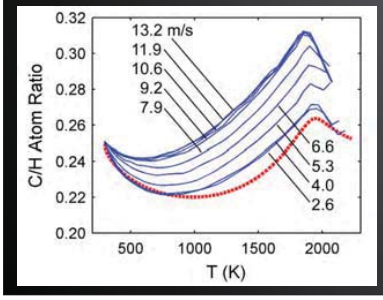

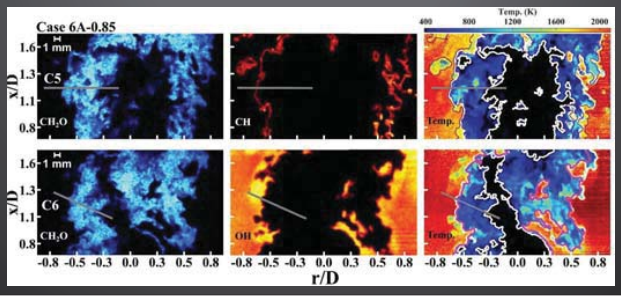

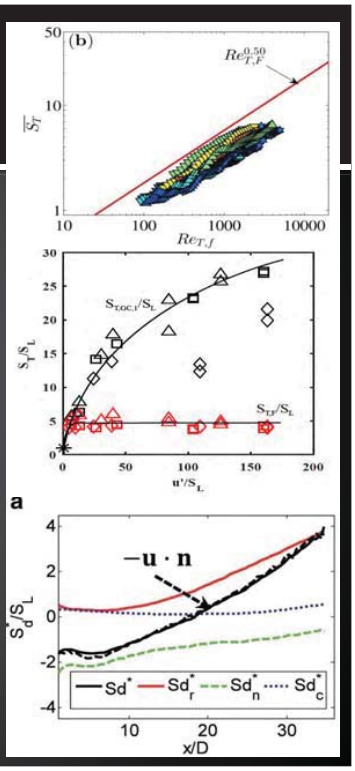

Overview

- **What is the 'structure' of turbulence at high intensities?**
  - o Vorticity variations through flame
  - o Spectra and scales of motion
- **What are the 'dynamics' of turbulence at high intensities?**
  - o Enstrophy dynamics and baroclinic torque production
  - o Kinetic energy transfer dynamics and backscatter

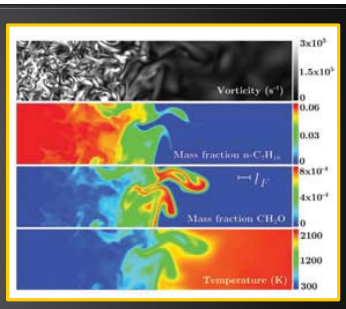

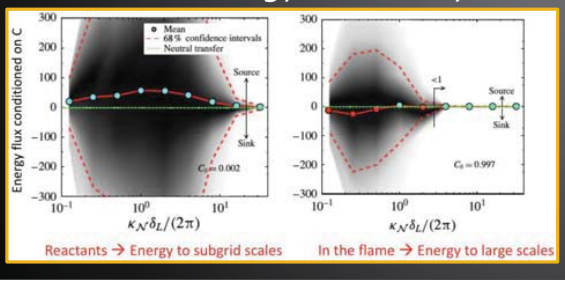

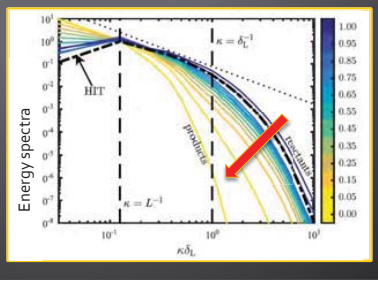

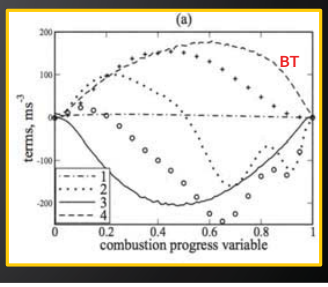

Effects of Turbulence on Combustion

Flame images, regimes, and thermo-chemical states

Flame Structure: Images and Regimes

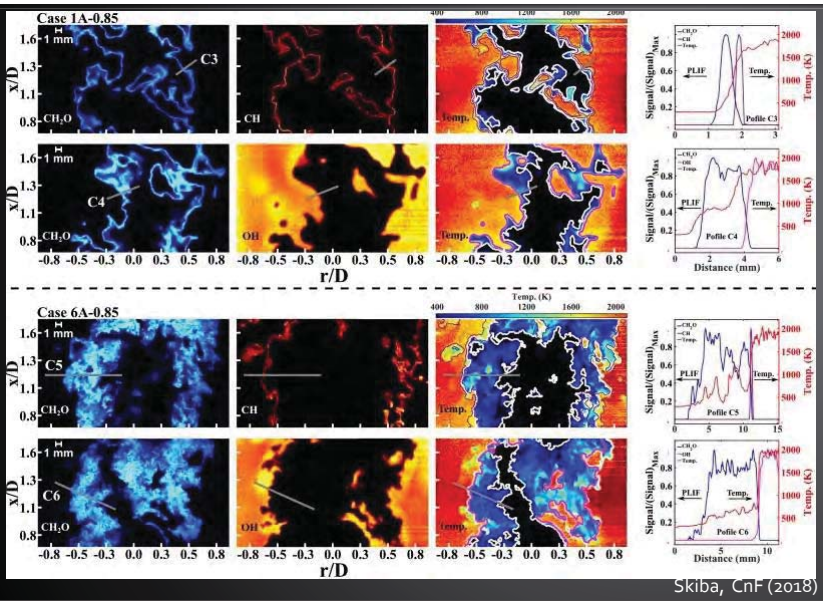

Skiba, CnF (2018)

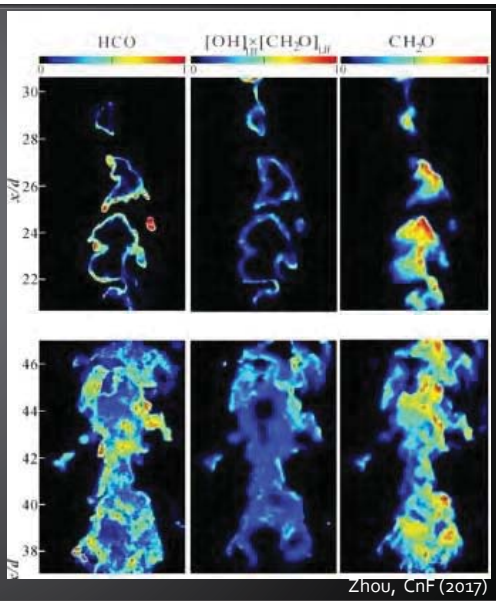

Zhou, CnF (2017)

Flame Structure: Images and Regimes

Large-scale decaying turbulence

Small-scale shear-driven turbulence

Small-scale shear-driven and forced turbulence

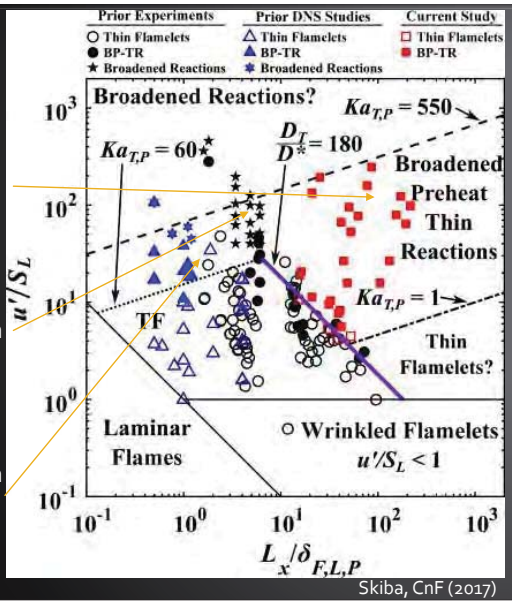

Skiba, CnF (2017)

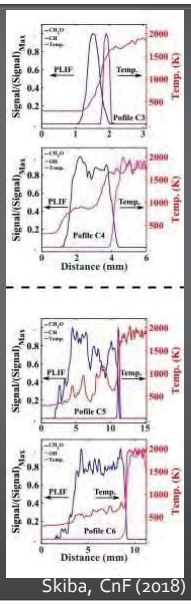

Skiba, CnF (2018)

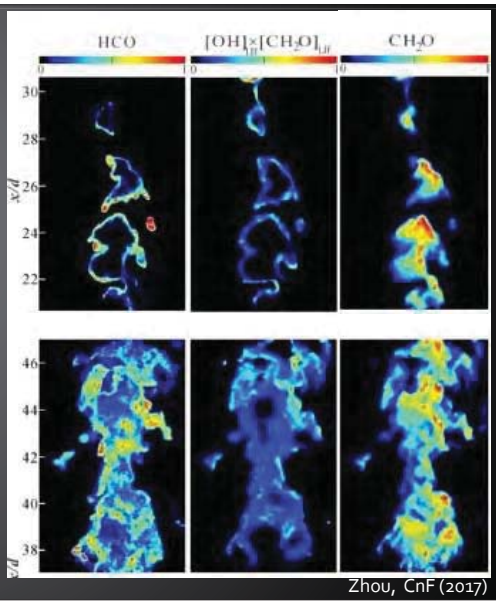

Zhou, CnF (2017)

Flame Structure: Images and Regimes

Large-scale decaying turbulence

Small-scale shear-driven turbulence

Small-scale shear-driven and forced turbulence

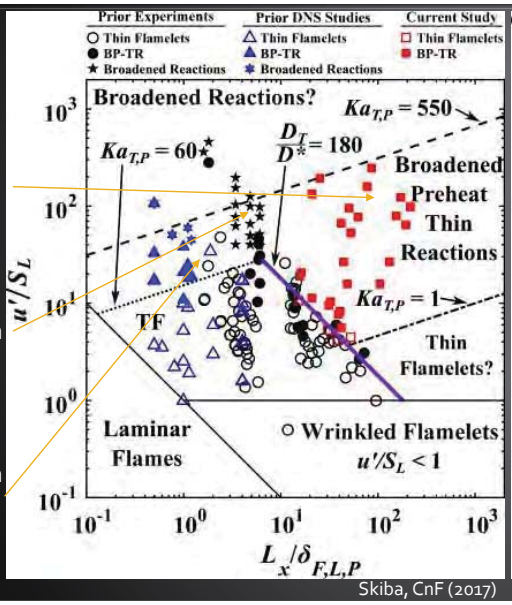

Skiba, CnF (2017)

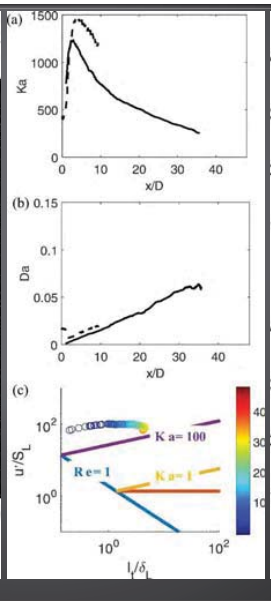

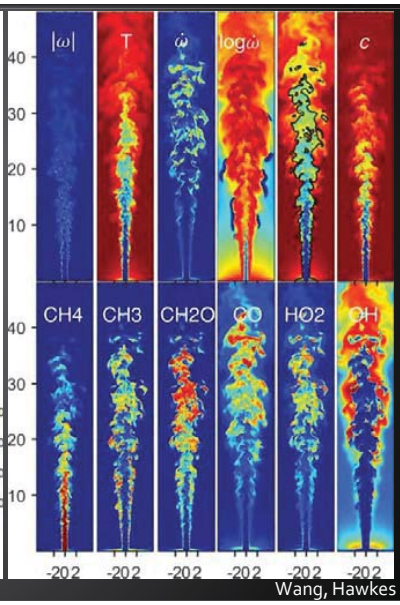

Wang, Hawkes

Flame Structure: Images and Regimes

Large-scale decaying turbulence

Small-scale shear-driven turbulence

Small-scale shear-driven and forced turbulence

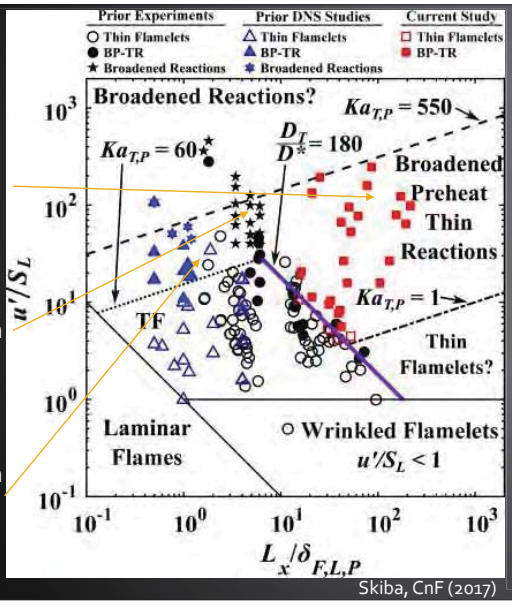

Skiba, CnF (2017)

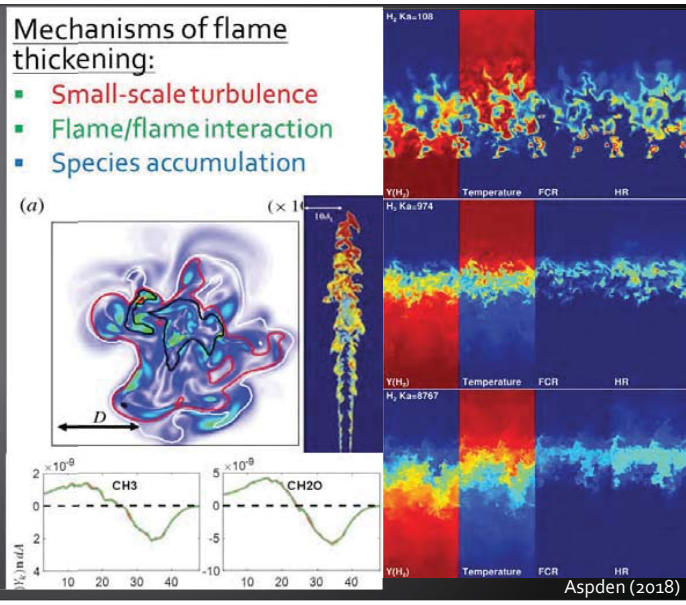

Aspden (2018)

Flame Structure: Not CH_4 or H_2, BRZ

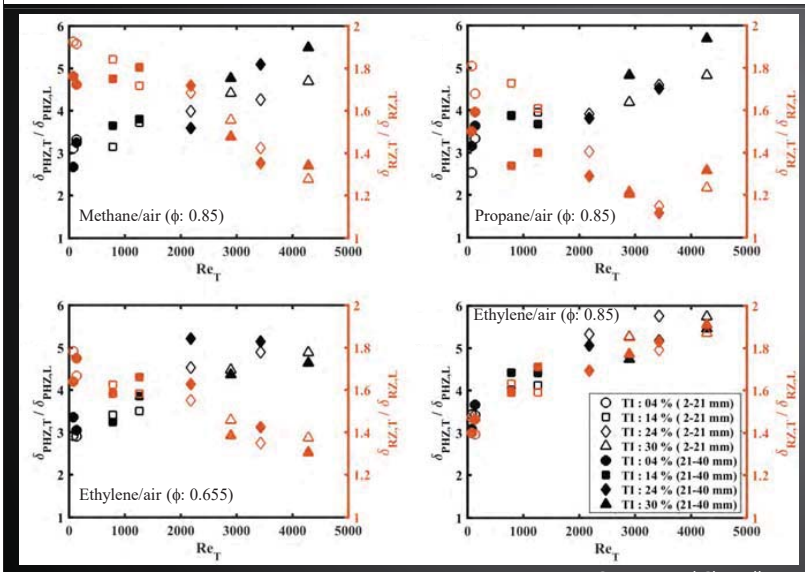

Cetegen and Chowdhury

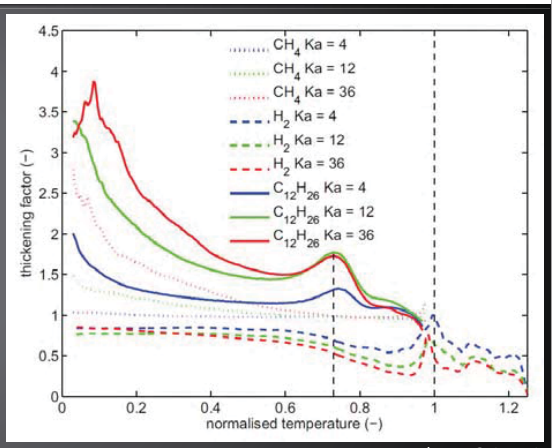

Aspden, PCI (2017)

Flame Structure: Not CH_4 or H_2, BRZ

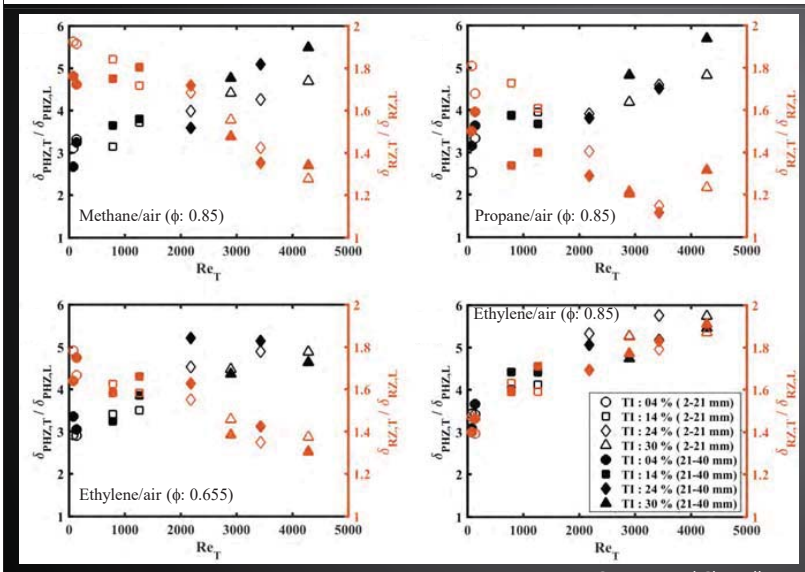

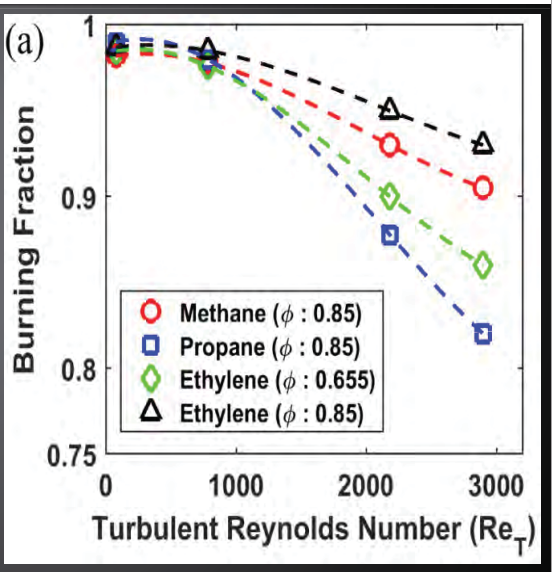

Cetegen and Chowdhury

Flame Structure: Not CH_4 or H_2, BRZ

- Broken reaction zones
  - Mean shear
  - Turbulence
  - Reactant composition
  - Back-support (pilot)
- Well characterized by fluid strain-rate and extinction strain rate of burning mixture (?)

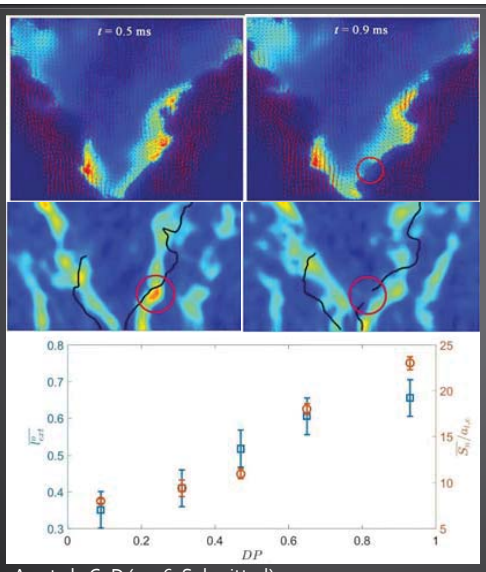

An et al., CnD (2016, Submitted)

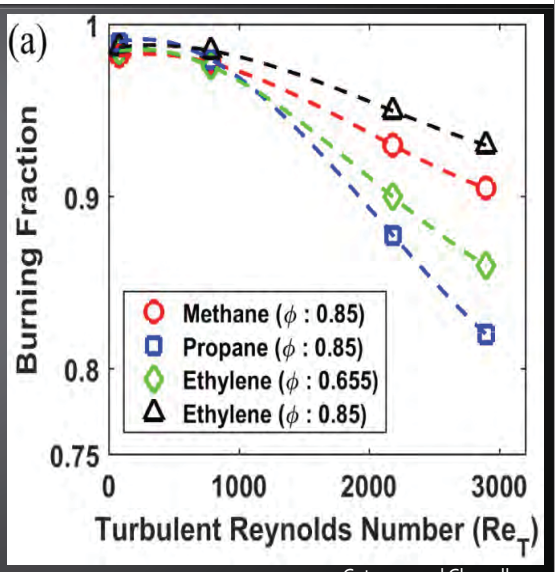

Cetegen and Chowdhury

Flame Structure: State

- Differential diffusion important, but saturates
- Mixing/entrainment of surrounding gas (products, coflow) into premixture
- Range of temperature/composition ⇒ range of reaction rates
- Measuring 'flame surface areas' may not be sufficient
- Data on mixture, temperature, reaction rate very important

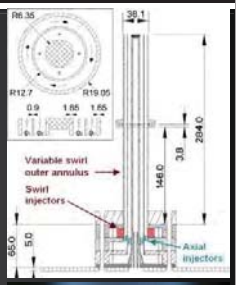

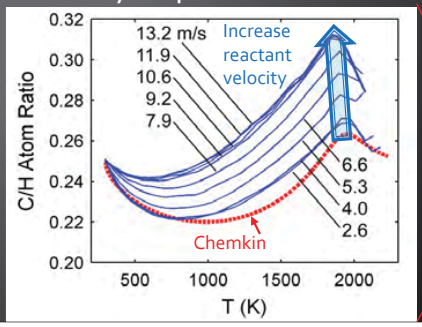

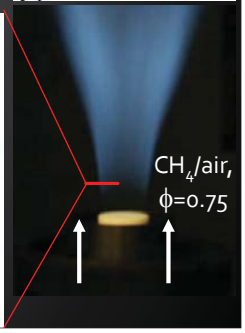

Flame Structure: State

- Differential diffusion important, but saturates
- Mixing/entrainment of surrounding gas (products, coflow) into premixture
- Range of temperature/composition ⇒ range of reaction rates
- Measuring 'flame surface areas' may not be sufficient
- Data on mixture, temperature, reaction rate very important

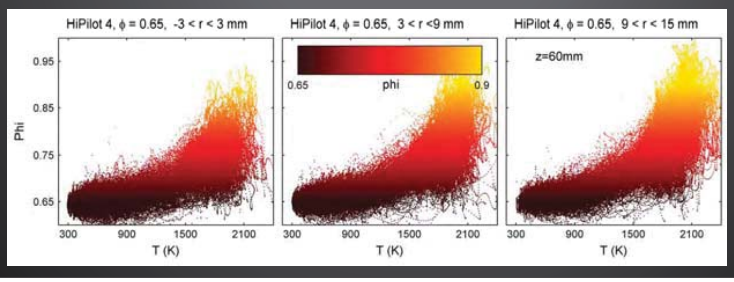

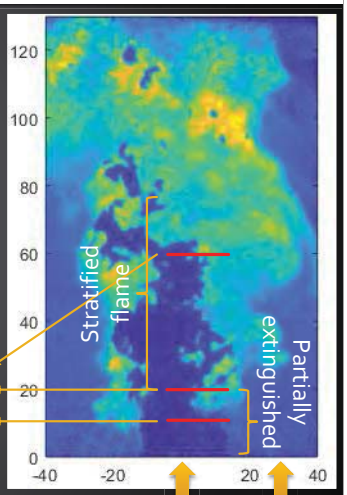

$Ka \approx 400$ $\phi = 0.65$ $\phi = 0.9$

Flame Structure: State

- Differential diffusion important, but saturates
- Mixing/entrainment of surrounding gas (products, coflow) into premixture
- Range of temperature/composition ⇒ range of reaction rates
- Measuring 'flame surface areas' may not be sufficient
- Data on mixture, temperature, reaction rate very important

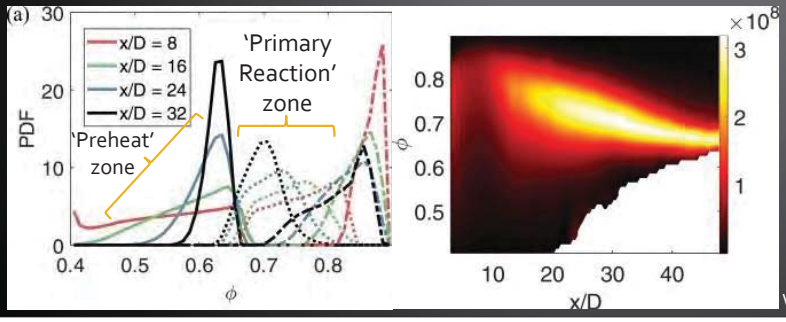

No heat release occurs with mixtures at the jet equivalence ratio

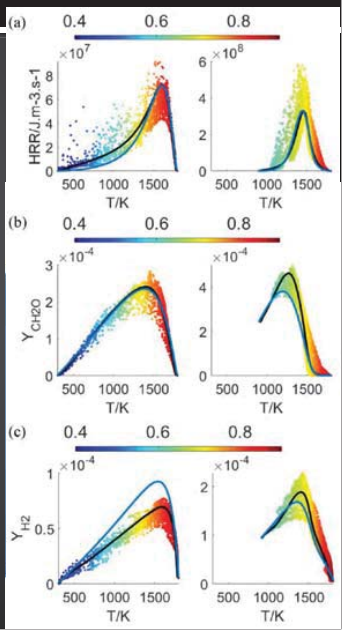

Wang, Hawkes

Flame Dynamics: Global

Measured global consumption speed

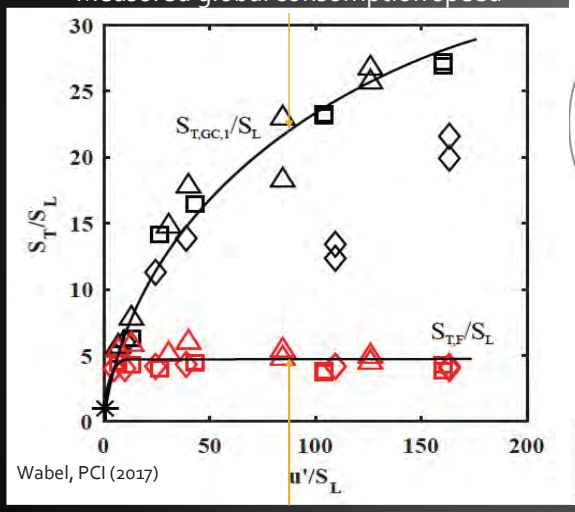

Wabel, PCI (2017)

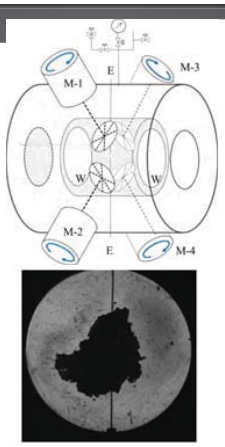

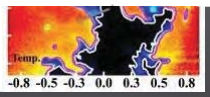

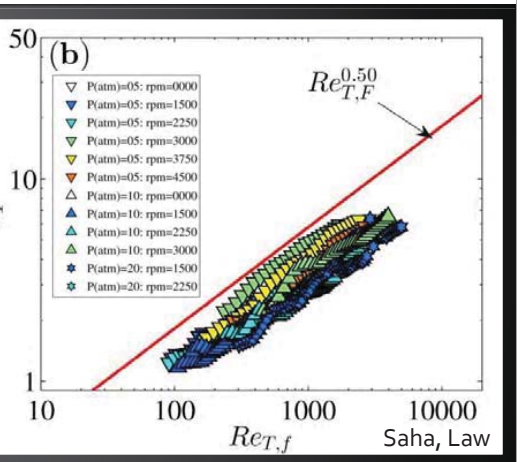

Saha, Law

Expectation based on flame area and speed

$\mathrm{Re}_{t,f} = (u'R)/(S_L\delta_L)$ R= mean flame radius

$S_T = dR/dt$

$R = \sqrt{A/\pi}$

$\overline{S}_T = S_T / S_L \approx \mathrm{Re}_{T,f}^{1/2}$

Flame Dynamics: Global

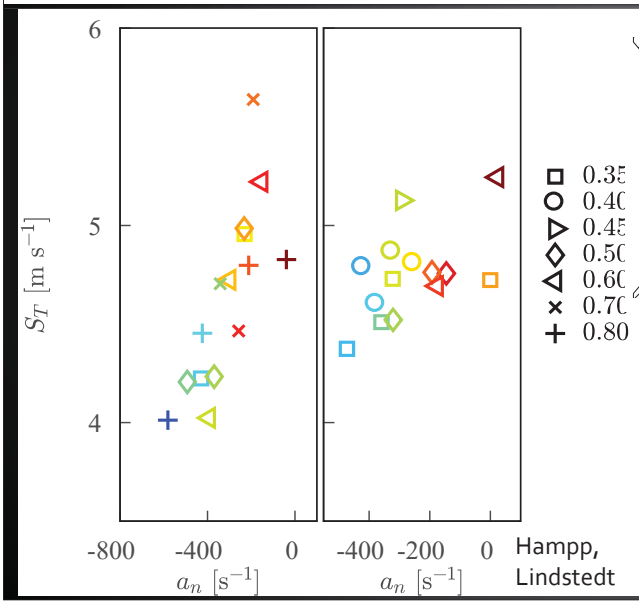

Hampp, Lindstedt

Constant Re_t
Varying strain rate

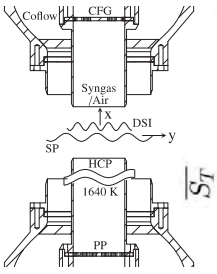

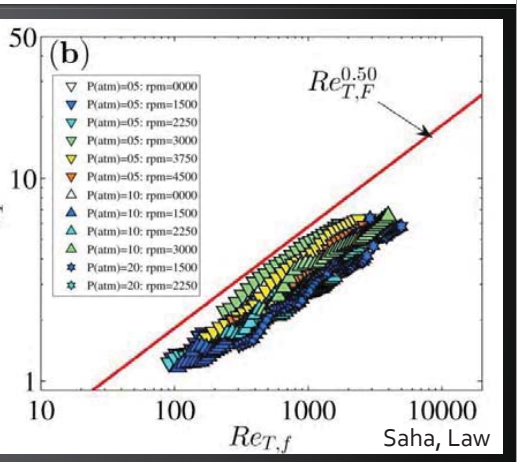

Saha, Law

$\mathrm{Re}_{t,f} = (u'R)/(S_L\delta_L)$ R= mean flame radius

$S_T = dR/dt$

$R = \sqrt{A/\pi}$

$\overline{S}_T = S_T / S_L \approx \mathrm{Re}_{T,f}^{1/2}$

Flame Dynamics: Local

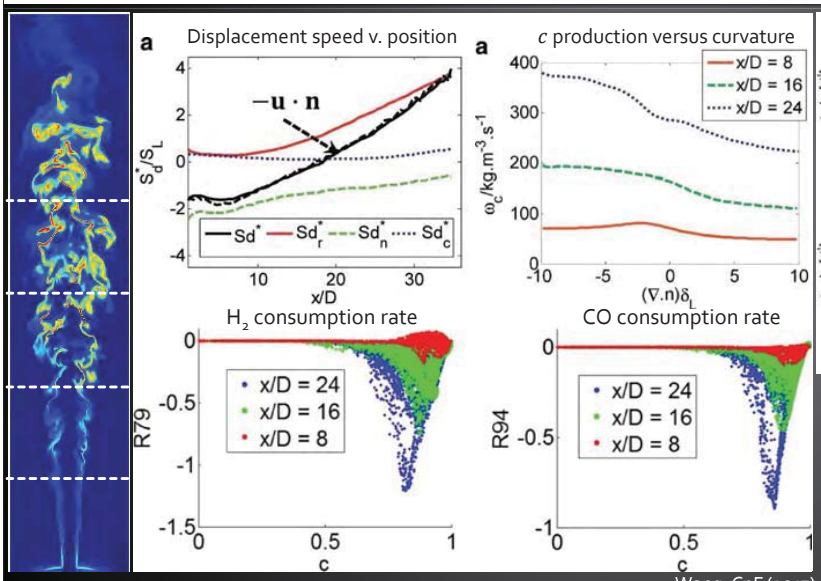

Wang, CnF (2017)

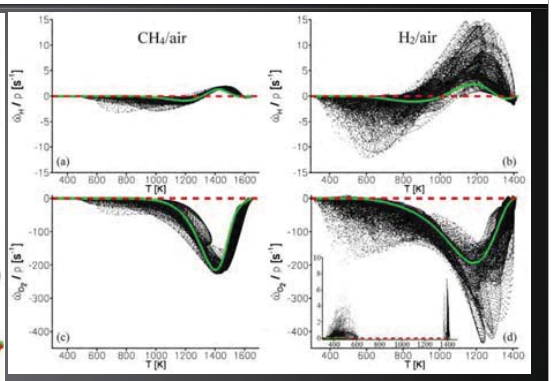

Carlsson, PCI (2015)

Flame Dynamics: Local

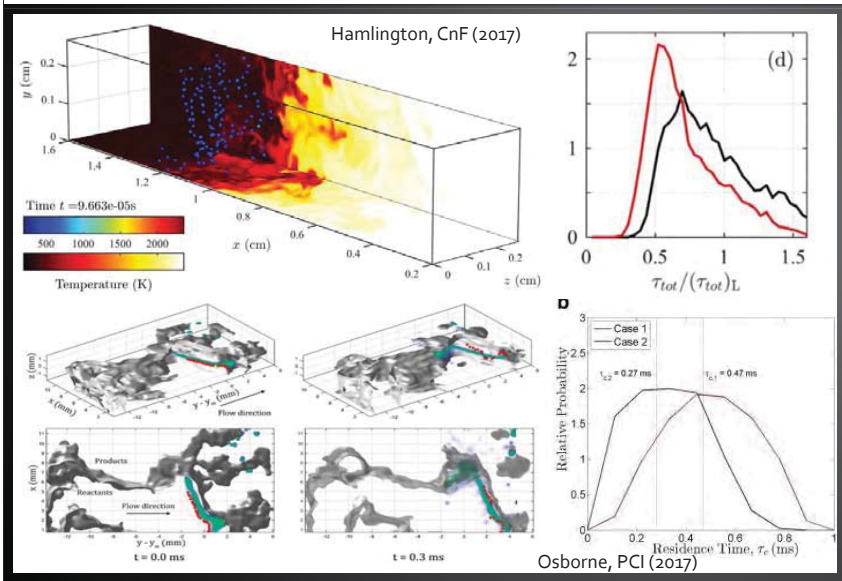

Hamlington, CnF (2017)

Osborne, PCI (2017)

Case-1
T_0 = 350K isotherm
Evolution of leading flame particles in time.
Taylor-scale Reynolds number Re_λ = 86

Dave, Mohan, Chauduri

Summary

- Large variety of states and rates
  - Mixing of gasses from different regions of the flame
  - Complicated fuel effects likely
  - Flame speeds and surface areas may have limited utility(?)
- Regimes are very configuration dependent
  - Broadened reaction zones very hard to achieve in DNS of HIT boxes, but readily achieved in jet flames
  - Broken reaction zones depend on back-support, mean strain-rate, etc.

Effects of Combustion on Turbulence

Structure, flame-scale turbulence, inter-scale energy transfer

Turbulence Structure: Vorticity

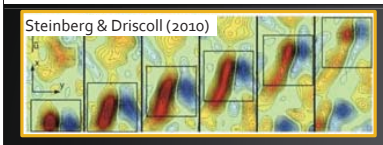

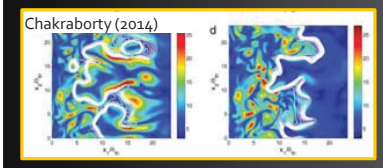

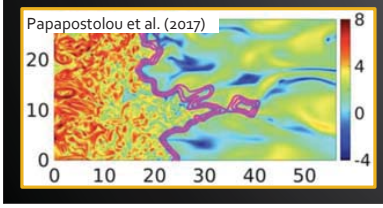

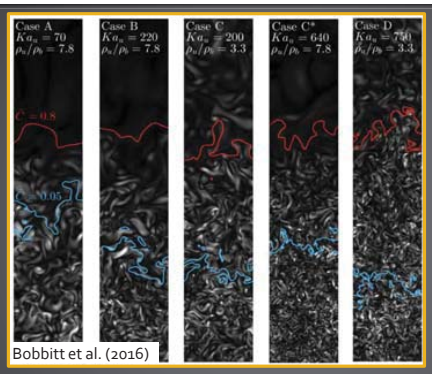

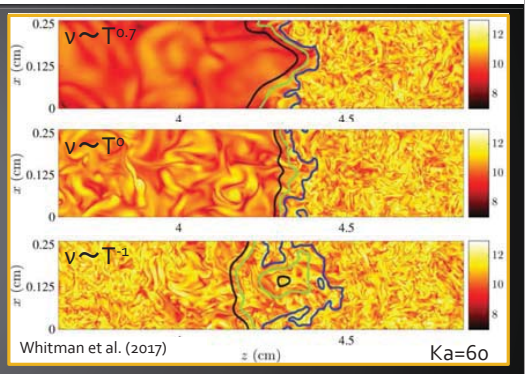

- Vorticity suppression occurs for all Ka; the spatial region over which the suppression occurs increases in size with Ka
- Temperature/density/viscosity ratio determines the extent to which vorticity is suppressed

Turbulence Structure: Anisotropy/Alignment

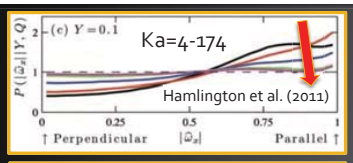

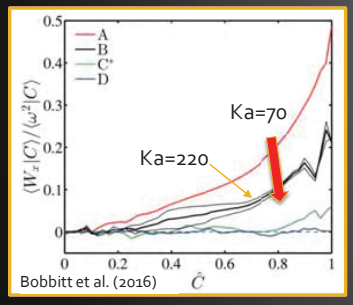

Anisotropy in direction of mean flame normal, reduces as Ka increases

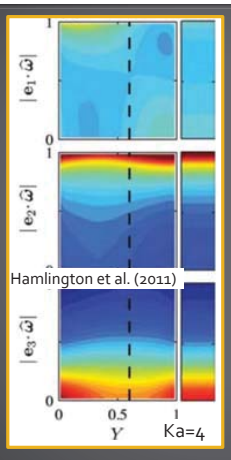

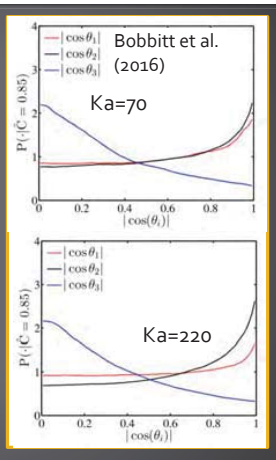

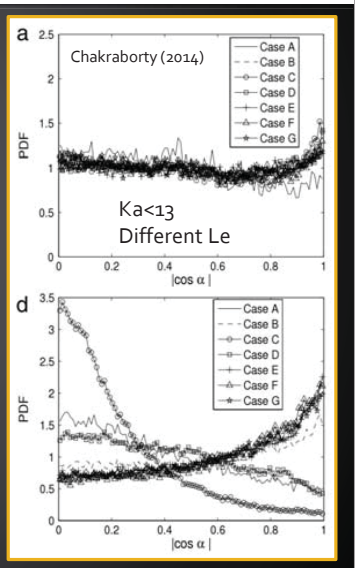

At low Ka in reaction zone, vorticity is more aligned with extensional strain eigenvector; vortex stretching altered

Turbulence Structure: Scale Space

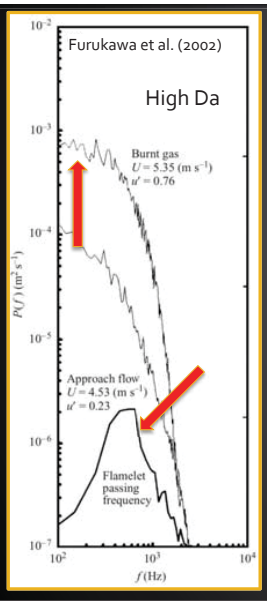

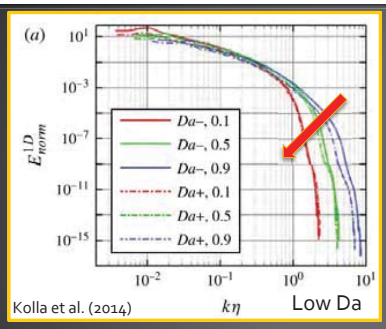

Kolla et al. (2014)

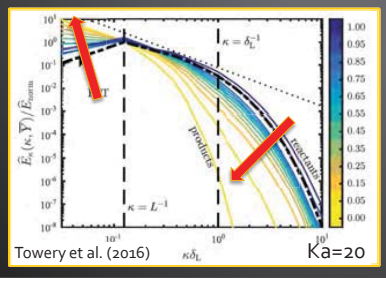

Towery et al. (2016) Ka=20

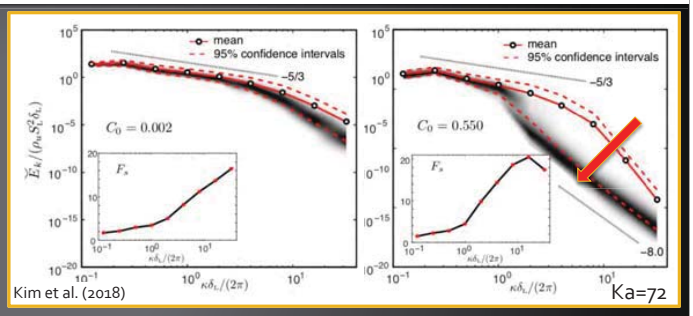

Kim et al. (2018) Ka=72

- Small-scales are suppressed by premixed flames, although there is little dependence on Ka/Da at high intensities
- Large-scales are enhanced, either in the mean or at scales larger than the flame

Turbulence Structure: Summary

- **At high Ka, vorticity magnitude is suppressed through premixed flames from reactants to products**
  - Points to the importance of viscous diffusion
- **Anisotropy generated by premixed flames for low Ka in direction of mean flame normal**
  - Effect weakens as Ka increases and initially isotropic turbulence remains isotropic
- **Alignments between strain rate eigenvectors and vorticity (hence vortex stretching) are altered**
  - Nonlinear forward cascade may be affected at low Ka
- **Small-scale turbulent motions are suppressed, large scales are enhanced**
  - Effect is present for all Ka/Da studied to date

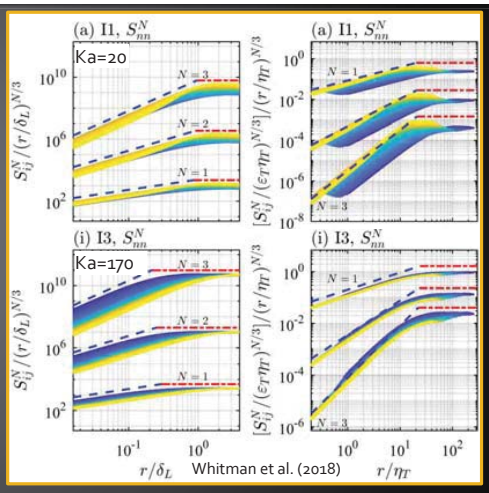

Whitman et al. (2018)

Implication: The structure of turbulence at high Ka is that of non-reacting turbulence at lower Reynolds numbers *

Turbulence Dynamics: Vorticity

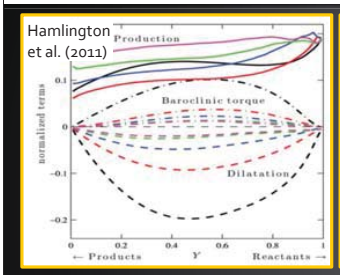

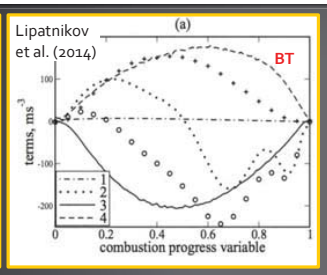

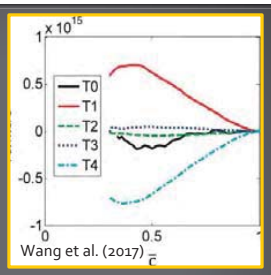

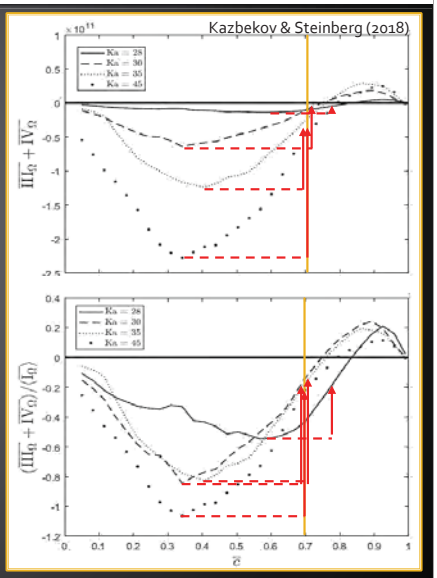

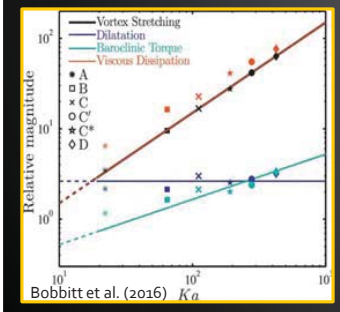

- At high Ka, enstrophy dynamics are a balance of stretching and dissipation
- At low Ka, baroclinic torque and dilatation have larger relative effects
- Vorticity/strain rate interactions are the source of anisotropy

Turbulence Dynamics: Backscatter

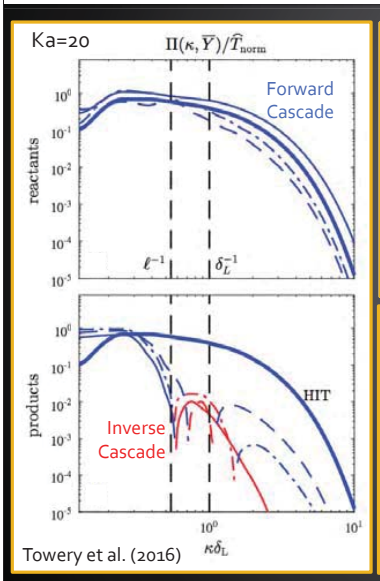

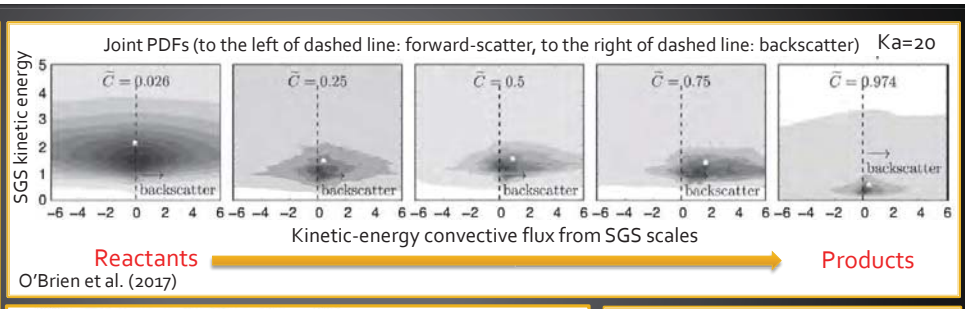

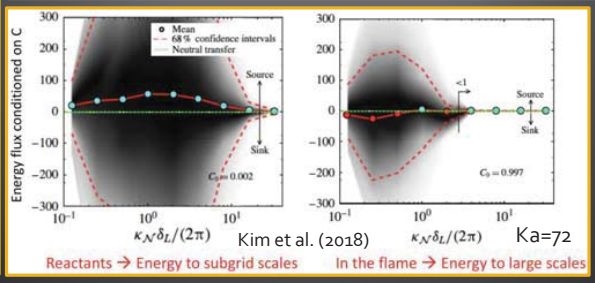

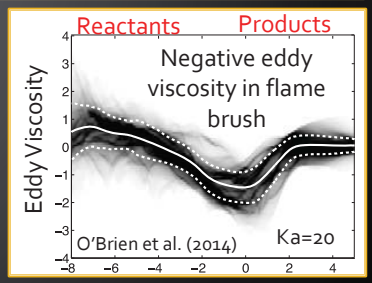

Turbulence Dynamics: Kinetic Energy

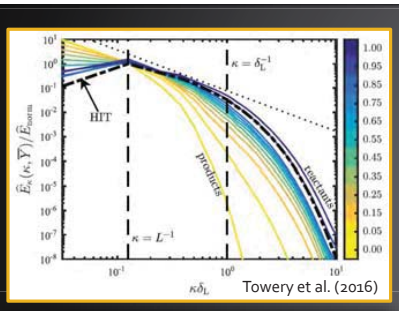

Towery et al. (2016)

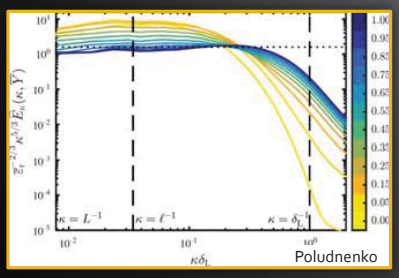

Poludnenko

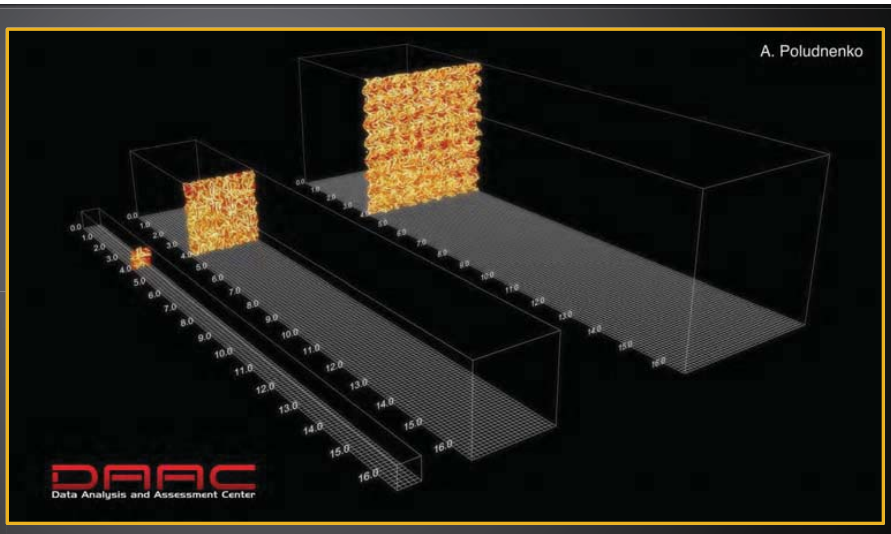

Kinetic energy is transferred to the largest available scale

Turbulence Dynamics: Kinetic Energy

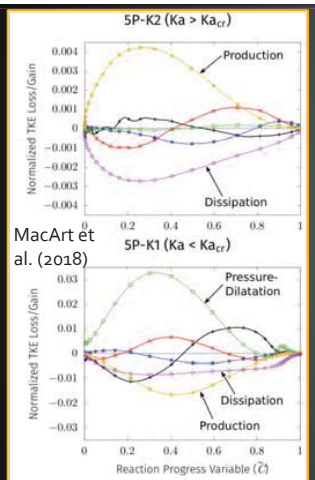

MacArt et al. (2018)

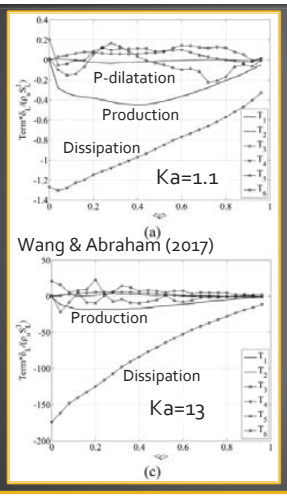

Wang & Abraham (2017)

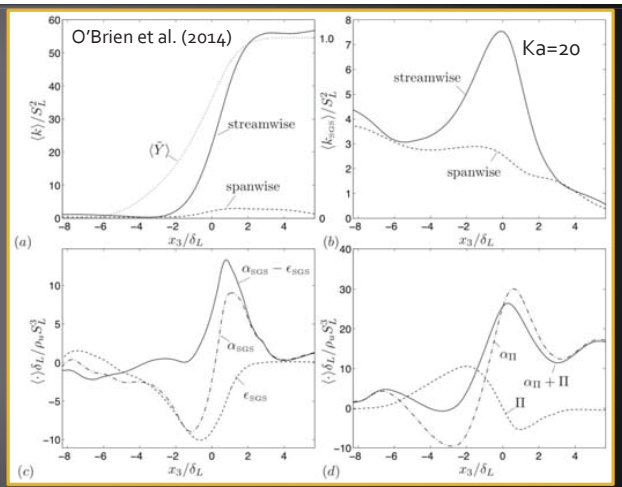

$$\underbrace{\frac{\partial \overline{\rho}\widetilde{k}}{\partial t}}_{\text{Unsteady}} + \underbrace{\frac{\partial \overline{\rho}\widetilde{u}_j\widetilde{k}}{\partial x_j}}_{\text{Advection}} = \underbrace{-\frac{1}{2}\frac{\partial}{\partial x_j}\left(\overline{\rho u_j'' u_i'' u_i''}\right)}_{\text{Turbulent Transport}} + \underbrace{\frac{\partial}{\partial x_j}\left(\overline{u_i'' \tau_{ij}'}\right)}_{\text{Viscous Transport}} - \underbrace{\overline{u_i''}\frac{\partial p'}{\partial x_i}}_{\text{Vel.-Pressure}} - \underbrace{\overline{\rho} u_i'' u_j''\frac{\partial \widetilde{u}_i}{\partial x_j}}_{\text{Production}} - \underbrace{\overline{\tau_{ij}'}\frac{\partial u_i''}{\partial x_j}}_{\text{Dissipation}}$$

Pressure-dilatation is significant for low Ka

Turbulence Dynamics: Summary

- **The balance of terms in enstrophy dynamics depends on Ka**
  - o Low Ka: stretching, dissipation, baroclinic torque, dilatation
  - o High Ka: stretching, dissipation
- **There is significant backscatter of kinetic energy from small to large scales due to pressure-dilatation, nonlinear advection, and viscous diffusion**
  - o Relative balance for different Ka still unclear
  - o Suggests negative eddy viscosity for low Ka
- **At low Ka, pressure-dilatation can become significant in kinetic energy dynamics**

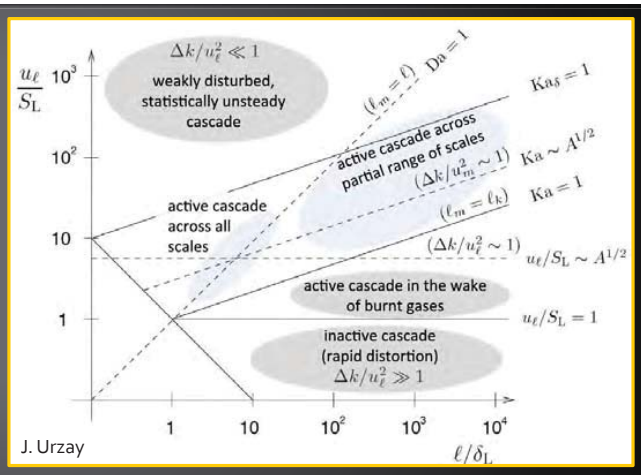

J. Urzay

Implication: **The dynamics of turbulence at high Ka is that of non-reacting turbulence at lower Reynolds numbers ***

*** Baroclinic torque remains significant at high Ka for imposed pressure gradients; configuration matters!**

Part 3: Open Problems

What needs to be done next?

3: Open Problems

- **How do turbulence-flame interactions depend on configuration?**
  - Shear, stratification, back-support, swirl, pressure gradients?
  - Are simulation results for idealized configurations relevant in more realistic systems?
- **How do structure and dynamics change for high Ma_t (not just high Ka)?**
  - Deflagration to detonation transition, shocklets?
- **Do LES models need to account for kinetic energy backscatter, and how does this change with intensity?**
  - Do we need sophisticated models at high intensities?
- **How can spectral structure and dynamics be probed through premixed flames?**
  - Is this even a reasonable question to ask (i.e., uncertainty principle)?

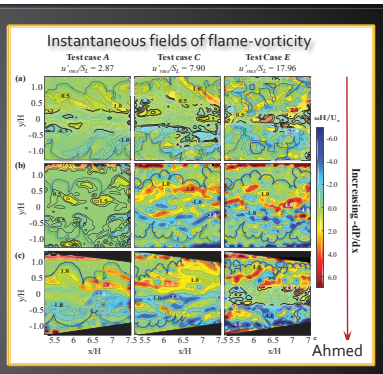

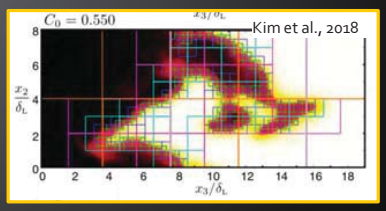

3: Open Problems

- **How is thermochemical phase space affected by high intensity turbulence?**
  - Do SGS turbulence models (e.g., flamelets) and reduced chemical mechanisms need to be revisited?
- **How prevalent are extinction, ignition, and pocket formation events for high intensity turbulence?**
  - What are the formation/destruction mechanisms, dynamically?
- **Do we ever approach fully distributed burning?**
  - Are there flame holes and localized extinction?
- **Do classical regime diagrams need to be revisited/reformulated?**
  - Configuration, Mach number, other axes added?
  - Are labels correct?

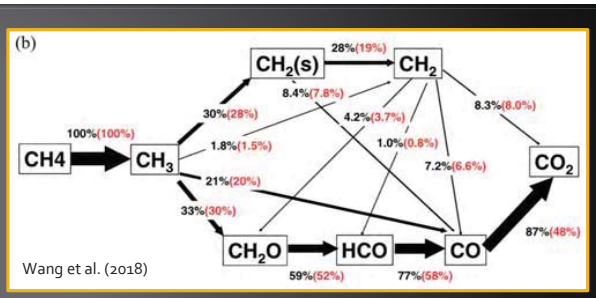

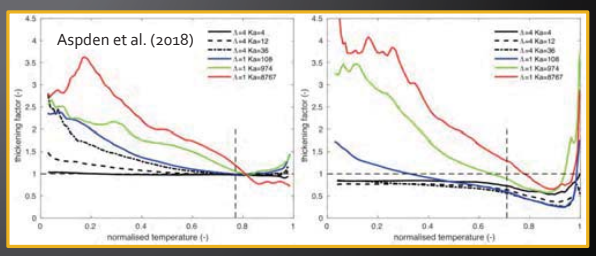

3: Open Problems

- **How can turbulent flame speed be parameterized at high intensities?**
  - Surface area dependence?
  - Differences between local/global flame speeds?
- **What can be accomplished experimentally?**
  - Thermochemistry, chemical pathways, turbulence, etc.?
  - What conditions/configurations can be explored?
- **What can be accomplished computationally?**
  - What conditions/configurations can be explored?
  - How do we deal with necessary computational cost?
- **How can experiments and DNS leverage each other?**
  - Assessment of experimental techniques
  - Filling in gaps in desired parameter space

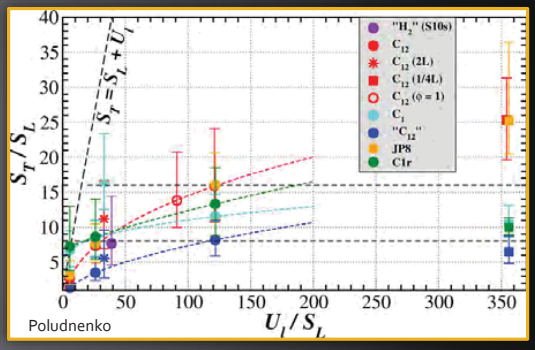

Poludnenko

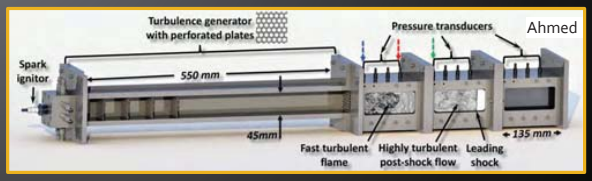

Ahmed

TNF & PTF joint session 2018

TNF&TPF 2018 DUBLIN IRELAND JULY 27-28

14th INTERNATIONAL WORKSHOP ON MEASUREMENT & COMPUTATION OF TURBULENT FLAMES

Modeling of highly turbulent flames

Luc Vervisch

INSA Rouen Normandy, IUF & CNRS-CORIA

- G.V. Nivari, R. S. Cant & S. Hochgreb Engineering Dept, Cambridge, UK
- B. Zhou, C. Brackmann, Z. Li, M. Aldén, X. S. Bai, Lund, Sweeden
- F.T. C. Yuen & Ö. Gülder, Inst. Aerospace Studies, U. Toronto, Canada
- T. M. Wabel, A. W. Skiba & J. F. Driscoll, Aerospace Eng., U. Michigan
- A Bouaniche, L. Vervisch & P. Domingo CNRS-CORIA, INSA Rouen Normandy, France
- H. Wang, E. R. Hawkes, B. Savard & J. Chen, China, Australia, USA
- Z. M. Nikolaou, C. Chrysostomou, L. Vervisch, S. Cant

Highly turbulent flames?

- Increasing the turbulent Reynolds number

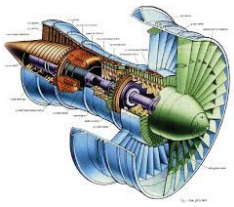

$$Re_{\mathrm{T}} = \frac{u' \ell_{\mathrm{T}}}{\nu}$$

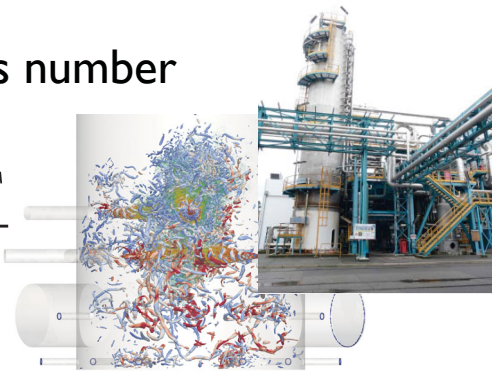

Farcy et al. AIChE Journal 62(3): 928-938 (2016)
Farcy et al. Chem. Eng. Sci. 139 (2016)

- In the practice of combustion systems, it is mainly u' that will increase, lengths being limited by design

$$Re_{\mathrm{T}}^{1/2} = \left(\frac{u' \ell_{\mathrm{T}}}{\nu} \right)^{1/2} = \frac{\tau_{\mathrm{T}}}{\tau_k} = Da \times Ka$$

Three parameters: Da, Ka, Re_T

$$\mathrm{Da} \times \mathrm{Ka} = \sqrt{\mathrm{Re_T}}$$

- Can we fix Da at which combustion occurs?

$$\mathrm{Re_T} \approx \mathrm{Ka}^2$$

- For a fixed value of Da, increasing the Karlovitz by 10 means increasing the turbulent Reynolds number by 100 (increase u' by a 100!)
- In practice, the turbulent Reynolds number stays limited and when Ka goes up Da does down

Karlovitz, Damköhler and Reynolds $Da = \frac{\tau_T}{\tau_c}$ $Ka = \frac{\tau_c}{\tau_k}$

$$Da \times Ka \approx \frac{k}{\sqrt{\nu\epsilon}} = \left(\frac{k^{1/2}k^{3/2}}{\nu\epsilon}\right)^{1/2} = Re_T^{1/2}$$

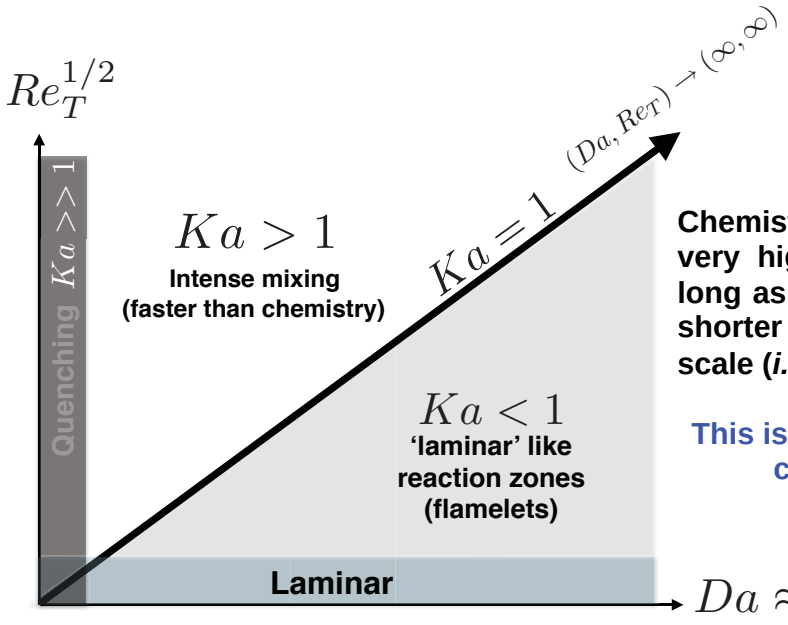

Chemistry can be fast (large Da) at very high Reynolds numbers, as long as the chemical time scale is shorter than the smallest flow time scale (*i.e.* Ka stays moderate).

This is the case in most practical combustion systems.

The 2010 Karlovitz number's bubble

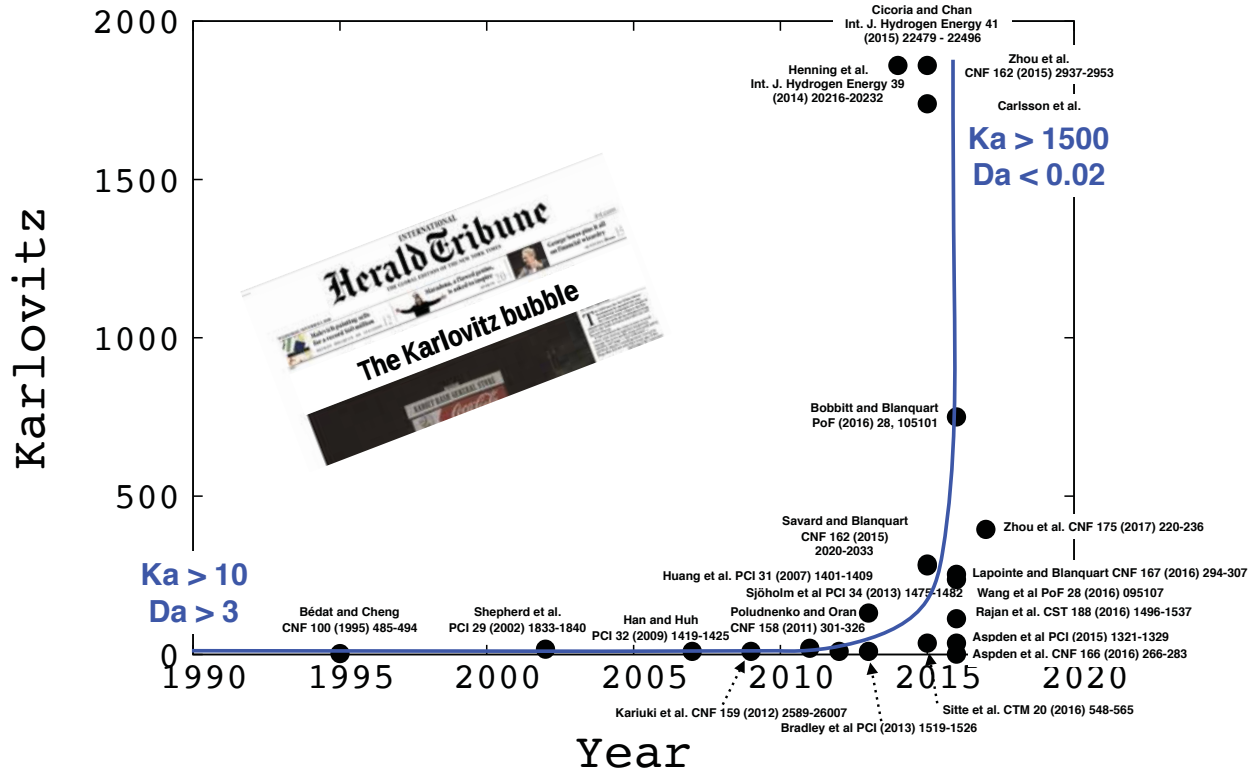

The 2010 Damköhler number crisis

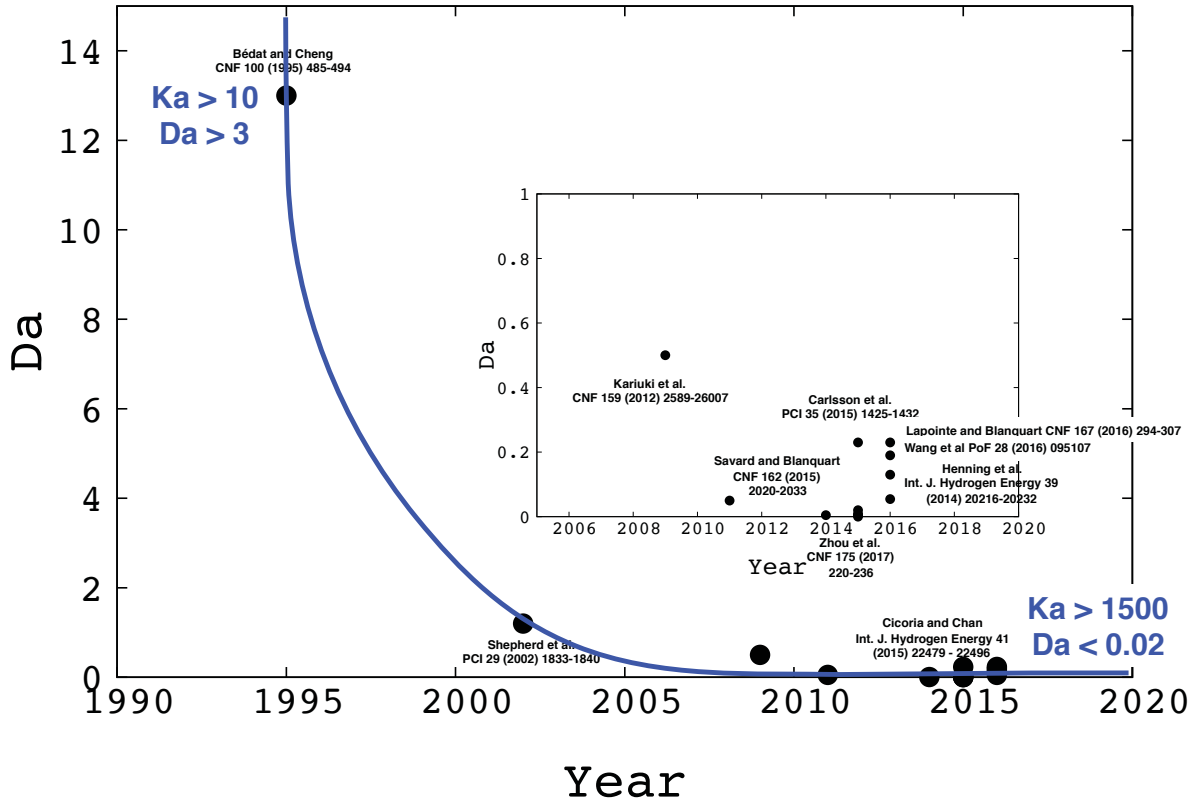

How can the flame just exist? — Two scenarios:

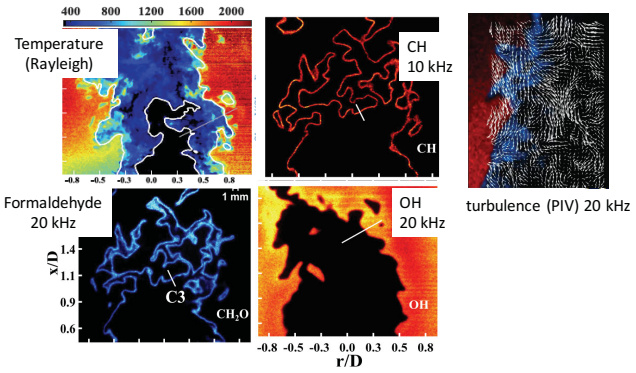

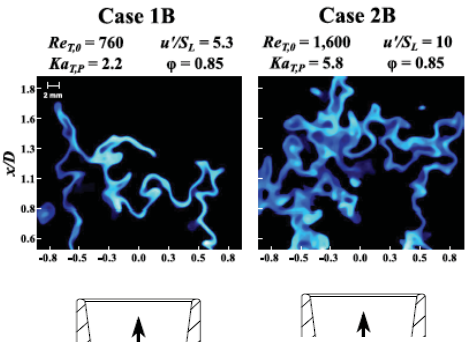

Wabel et al. PCI 36: 1801-1808

1. Increase of burning rate and flame surface due to enhanced scalar diffusivity in small-scale turbulence (between flame and Kolmorogov scales)

2. Increase of flame robustness because of dilution by burnt gases: High-Ka flames cannot exist without significant vitiation of fresh gases

Measured discrepancy between burning velocity and flame surface area

- Damköhler's first hypothesis $\frac{s_T}{s_L} \sim \frac{A_T}{A} = \left(1 + \frac{\Delta A}{A}\right)$

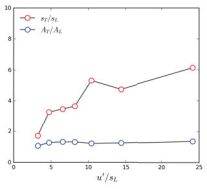

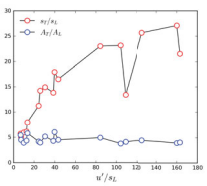

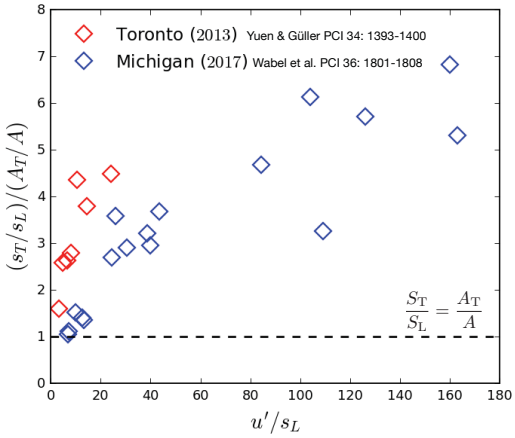

UNIVERSITY OF CAMBRIDGE

- Nivarti et al. propose to introduce Damköhler's second hypothesis, with a boost in diffusivity at small scales

$$\frac{s_T}{s_L} = \underbrace{\left(1 + \frac{\Delta A}{A}\right)}_{\text{large-scale}} \underbrace{\left(1 + \frac{\Delta D}{D}\right)^{1/2}}_{\text{small-scale}}$$

Nivarti, Cant & Hochgreb

Measured discrepancy between burning velocity and flame surface area

- Prandtl's scaling $D_\ell = \ell u_\ell$

UNIVERSITY OF CAMBRIDGE

- Model spectrum to calibrate velocity distribution vs scales

$$\hat{E}(\hat{\kappa}) = C\hat{\varepsilon}^{2/3}\hat{\kappa}^{-5/3}\hat{f}_L(\hat{\kappa})\hat{f}_\eta(\hat{\kappa})$$

- Contribution from diffusivity enhancement

$$\frac{\Delta D}{D} = \int_1^{\frac{\delta_L}{\eta}} \frac{\hat{u}(\hat{\kappa})}{\hat{\kappa}}\, d\hat{\kappa} \quad \Rightarrow \quad \frac{\Delta D}{D} = (2C)^{1/2}\hat{\varepsilon}^{1/3}\int_1^{\sqrt{\mathrm{Ka}}} \hat{\kappa}^{-11/6} e^{-\beta\hat{\kappa}/(2\sqrt{\mathrm{Ka}})}\, d\hat{\kappa}$$

Numerical Evaluation

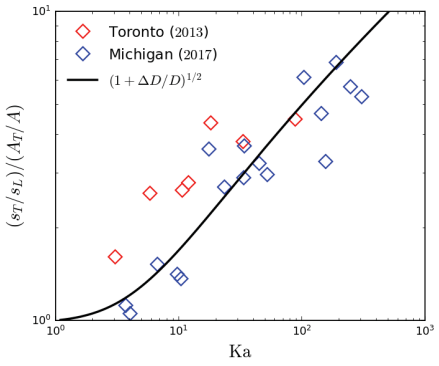

Analytical Scaling

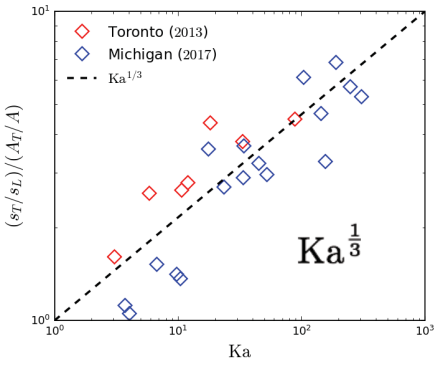

Nivarti, Cant and Hochgreb (2018) *JFM Rapids* (under review)

How can the flame just exist? — Second scenario:

- Any other basic properties of these burners influencing the reaction zones?

- Yes, these burners have a huge pilot of burnt gases!

Zhou et al. CNF 162 (2015) 2937-2953

Fuel/air Jet
d = 1.5 mm
Phi = 0.4
66 m/s < u < 418 m/s

Pilot flame

d = 61 mm
Phi = 0.9
u = 0.3 m/s

Case#-U(m/s)	Re_T	Ka x/d = 30	Da x/d = 30	Power pilot W	Power jet-flame W	Contribution of high Ka jet-flame to burner power
LUPJ3-66	138	136	0.09	2486	154	5,8 %
LUPJ3-165	267	417	0.04	2486	386	13 %
LUPJ3-220	356	567	0.03	2486	832	25 %
LUPJ3-418	676	1739	0.02	2486	978	28 %

Calibration of the response of high Ka flame to burn gases dilution

Unburnt — Dilution factor

$$\phi_u = \phi_o(1 - f_b) + f_b\phi_b$$

Fresh — Burnt

- The dilution by burnt gases makes the flame robust to high Ka (and low Da)
- Asymptotic analysis shows that dilution by burnt gases compensate strain effects:

Strain

$$S_L = S_L^o \left[\frac{1 - \mathcal{K}}{1 - f_b} \right]$$

Dilution factor

Bouaniche et al. FTaC (in press)

Calibration of the impact of burnt gases

- One-dimensional unstrained flame diluted by its burnt gases:

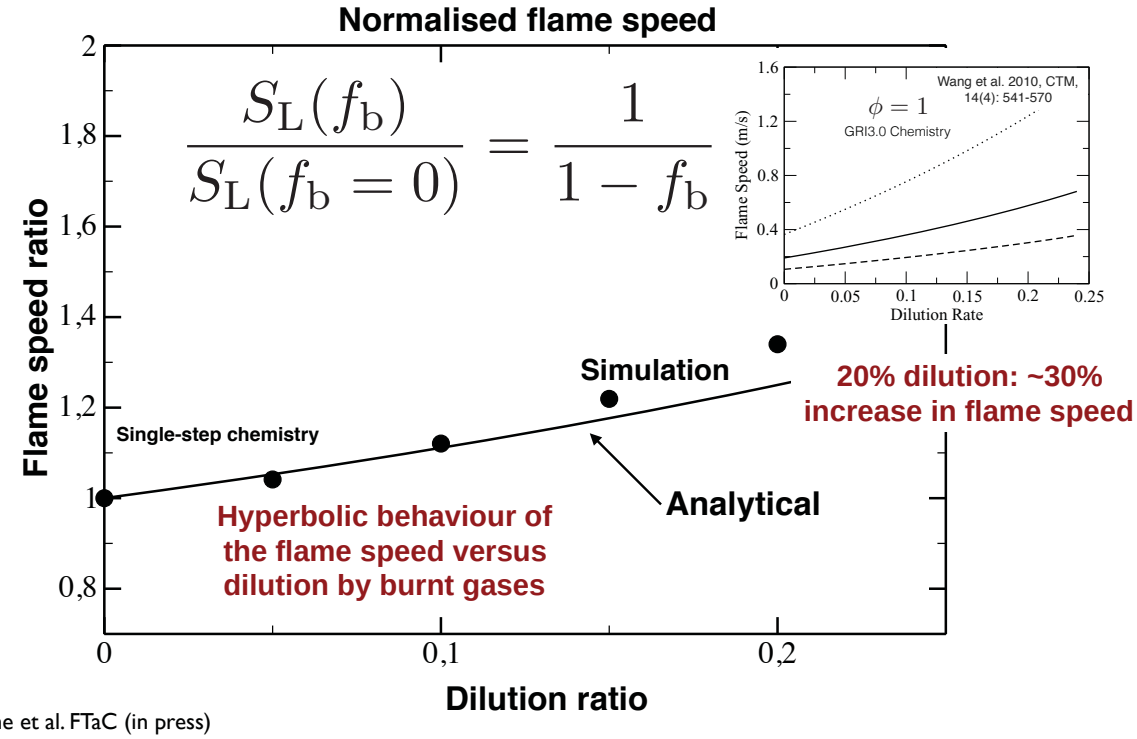

Bouaniche et al. FTaC (in press)

TNF&TPF DUBLIN IRELAND 2018 JULY 27-28 19th INTERNATIONAL WORKSHOP ON MEASUREMENT & COMPUTATION OF TURBULENT FLAMES

- Closing the gap between premixed and non-premixed: Quenching characteristic mixing time of diffusive/reacting layers:

N. Peters, Turbulent Combustion, Cambridge U. Press

$$\frac{1}{\tau_{m_q}} = \frac{Z_{st}^2(1-Z_{st})^2}{a_T/S_L^2}$$

$$S_L = S_L^o \times \frac{1}{1-f_b}$$

- The quenching Ka increases with dilution

$$\mathrm{Ka}_q(f_b) \approx \left(\frac{1}{1-f_b}\right)^2$$

Bouaniche et al. FTaC (in press)

Response of kerosene spray flame to high Ka

- For conditions close to a real combustion chamber, what is the minimum amount of energy required to secure burning at high Ka?
- Aeroengine conditions:
  - Kerosene chemistry: 26 transported species and 24 QSS, 180 reactions (detailed chemistry reduced by ORCh, Jaouen et al. Combust. Flame 177 (2017)109-122).
  - Composition space trajectories mimicking multi-point injection (P = 9.63bar):
    - Inlet 1: Liquid kerosene (T= 450K). 3.1% of Q_m (total mass flow rate)
    - Inlet 2: Air (T= 703K). 52% Q_m (With secondary air progressively introduced for t > 0)
    - Inlet 3: Burnt gases at equilibrium for the equivalence ratio of the combustion chamber (T = 1877K). Nominal condition: 44.9% Q_m

Bouaniche et al., FTaC (in press)

Minimum characteristic mixing time before quenching

- Ratio of energy introduced vs produced equal to 0.35

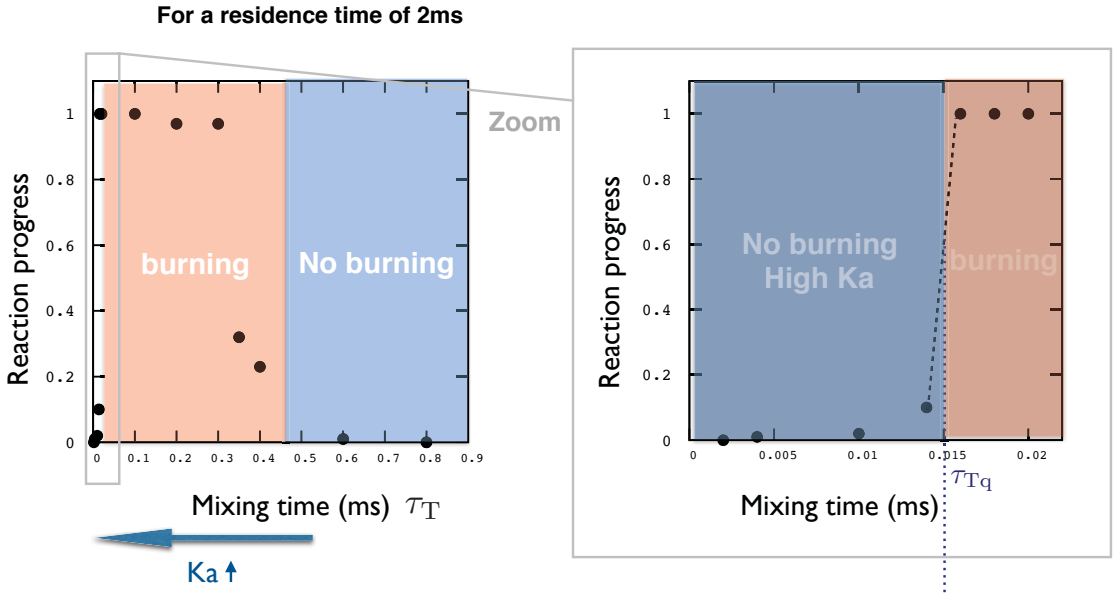

This operation is repeated for various levels of burnt gases to determine $Ka_q = Ka_q(f_b)$

Bouaniche et al. FTaC (in press)

Scaling for Ka at quenching

- Dilution by burnt gases significantly enhances the quenching Ka

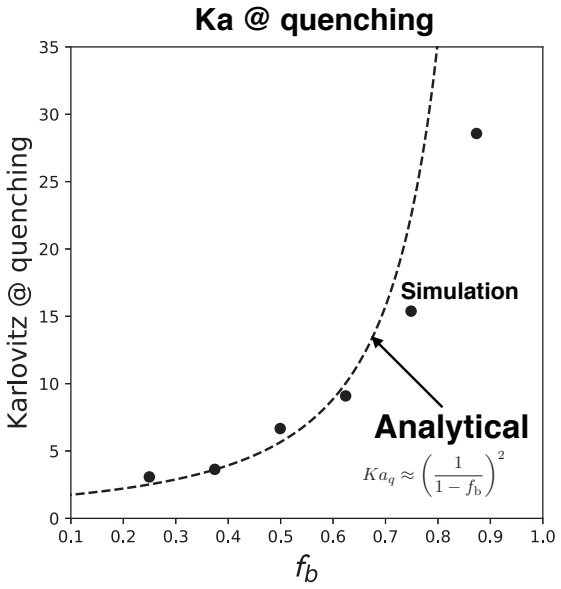

f_b ~ Energy ratio recirculating/produced

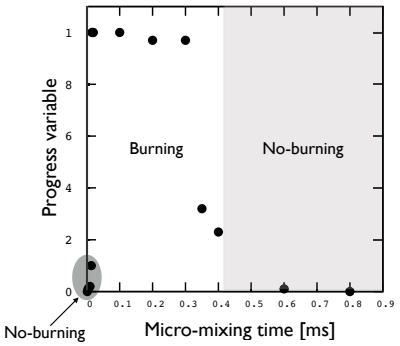

(a) Full range

Burning within the range

$0.015 \text{ ms} < \tau < 0.1 \text{ ms}$

Re_T	Re_λ	ℓ_T	τ_T	η_k	τ_k
1480	149	7 mm	2 ms	29 µm	0.051 ms

Typical GT swirling flame

Bouaniche et al. FTaC (in press)

Is SGS modeling needed for low Da flame?

$$\overline{\dot{\omega}_i(Y_1, \cdots, Y_N, T)} \underset{?}{=} \dot{\omega}_i(\widetilde{Y}_1, \cdots, \widetilde{Y}_N, \widetilde{T})$$

Is SGS modeling needed for low Da flames?

- DNS by Wang et al CNF 193 (2018) 229–245

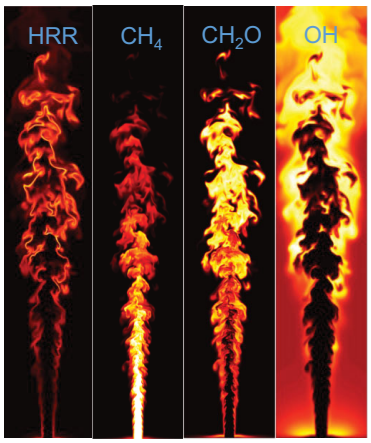

Instantaneous distributions of heat release rate and species mass fractions of CH_4, CH_2O and OH (Wang et al., CNF, 2018)

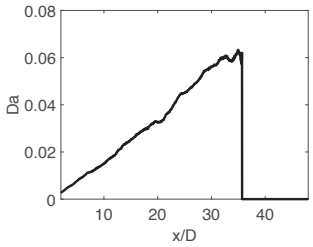

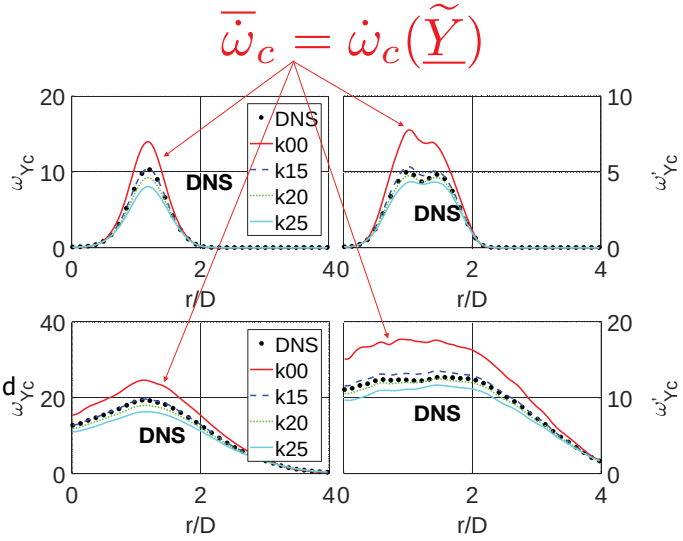

Towards regime-free turbulent combustion modeling

- With the progress of computing power, a large part of scalar signal is now resolved in the simulation of turbulent flames
- However, accounting for the fluctuations remaining unresolved is mandatory to calculate the non-linear terms
- High-order methods provide direct ways for approximating signals within mesh-cells, which are easily combined with signal reconstruction

Coarse mesh — Approximate deconvolution

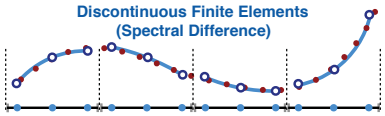

$$\underline{\varphi}(\underline{x},t) = \mathcal{L}_{\Delta}^{-1}\left[\overline{\underline{\varphi}(\underline{x},t)}\right]$$

Towards regime-free turbulent combustion modeling

- Signal reconstruction has been tested with success for the simulation of turbulent flames

- A.W. Vreman, R.J.M. Bastiaans, B.J. Geurts (2009), A similarity sub-grid model for premixed turbulent combustion, Flow Turbulence Combust. 82 (2): 233–248
- P. Domingo, L. Vervisch (2017) DNS and approximate deconvolution as a tool to analyse one-dimensional filtered flame sub-grid scale modeling, Combust. Flame, 177: 109-122.
- P. Domingo, L. Vervisch (2015) Large Eddy Simulation of premixed turbulent combustion using approximate deconvolution and explicit flame filtering. Proc. Combust. Inst., 35(2): 1349-1357.
- C. Mehl, J. Idier, and B. Fiorina, Evaluation of deconvolution modelling applied to numerical combustion, Combust. Theory Modell. 22, 38 (2017).
- Q. Wang and M. Ihme, Regularized deconvolution method for turbulent combustion modeling, Combust. Flame 176, 125 (2017).
- Z. Nikolaou, L. Vervisch (2018) A priori assessment of an iterative deconvolution method for LES sub-grid scale variance modelling, Flow Turbulence and Combust. 101(1): 33-53.
- Z. Nikolaou, R. S. Cant, L. Vervisch (2018) Scalar flux modelling in turbulent flames using iterative deconvolution, Phys. Rev. Fluids. 3(4): 043201.

- Construct an approximation of the scalar signal:

$$\phi(\underline{x},t) = \mathcal{L}_{\Delta}^{-1}[\widetilde{\phi}(\underline{x},t)]$$

Unresolved **Resolved**

- Use it to compute the non-linear terms, then filter explicitly:

$$\overline{\dot{\omega}}(\underline{x},t) = \overline{\dot{\omega}(\mathcal{L}_{\Delta}^{-1}[\widetilde{\phi}(\underline{x},t)])}$$

Towards machine learning based turbulent combustion modeling

- Applied to DNS of a planar turbulent premixed flame

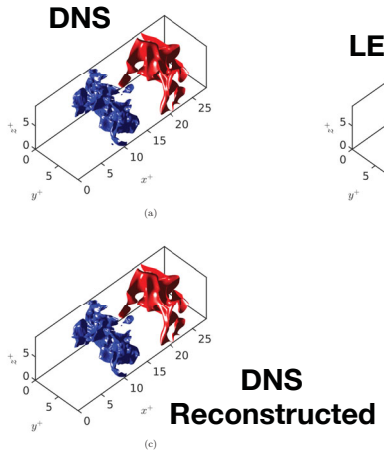

Fig. 3: Iso-surfaces of progress variable field (0.1-blue, 0.9-red) on the LES mesh for $\Delta^+ = 1$: (a) original field c, (b) filtered field $\tilde{c}$, and (c) deconvoluted field c^* using the trained CNN. Note the pronounced loss of small-scale information due to the the filtering in (b) on the reactant (blue) side where turbulence is more intense, and the recovery of the small-scales in the deconvolution step in (c).

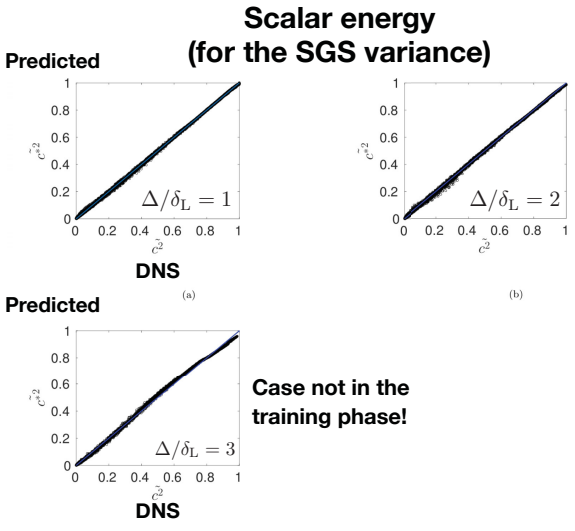

Fig. 4: Instantaneous scatter plot of $\widetilde{c^{*2}}$ as obtained using the convolutional network against the actual value for: (a) $\Delta^+ = 1.0$, (b) $\Delta^+ = 2.0$ and (c) $\Delta^+ = 3.0$. The blue line corresponds to $y = x$.

Z. Nikolaou et al. (submitted)

SUMMARY

- New scaling for turbulent flame speed including effect of enhanced scalar diffusivity
- Scalings for Ka at quenching in the presence of strong vitiation (high Ka flames do not exist otherwise, is this really practical? To be discussed!)
- SGS models still needed at low Da
- Machine learning could be helpful for multiple-regime modeling.

Modeling of Turbulent Flames in the High-Ka Combustion Regime

MATTHIAS IHME

WITH CONTRIBUTIONS FROM: HAO WU, JEFF LABAHN, XINYU ZHAO, LUC VERVISCH, EVATT HAWKES

Stanford University

Outline

Do flamelets exists at high-Ka?

Experimental configuration for model evaluation: PPJB

- Status on model performance
- Current development
- Progress and limitations

Integration of experiments and simulations

- State estimate
- Model assessment

Conclusions and open research issues

Stanford University

Flame Structure Analysis

Objective

- Flame structure analysis
- Presence of flamelets, effects of product-gas recirculation, flame broadening

Approach

- Flamelet analysis of idealized series of flame configurations, covering premixed, partially premixed, and non-premixed conditions

Configuration and chemistry

- Periodic box (1 cm^3) with 256^3 equidistant structural mesh
- Skeletal CH4 mechanism

Turbulence Initialization

- Initialized with VKP spectrum with:
  - Ret=100
  - Integral length scale: $l = 10\,\mathrm{mm}$
  - Kolmogorov length scale: $\eta = 0.025\,\mathrm{mm}$

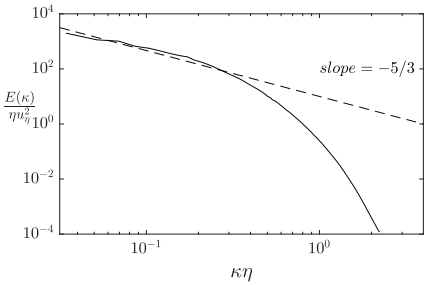

Stanford University

Flame Structure Analysis

	Premixed	Partially-premixed	Non-premixed
Scalar field	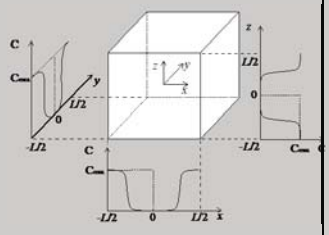	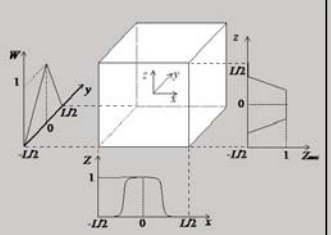	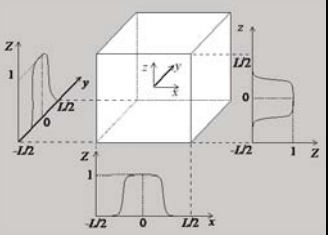
TKE	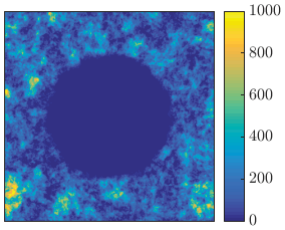	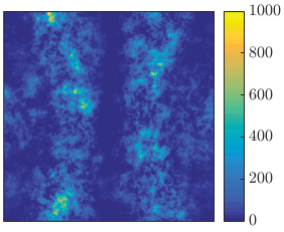	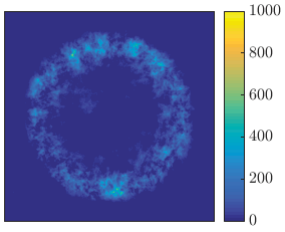

Stanford University

Simulation results

	Premixed	Partially-premixed	Non-premixed
Temperature	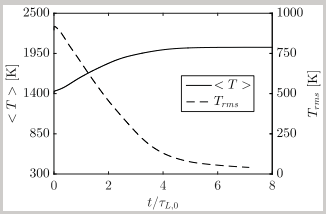	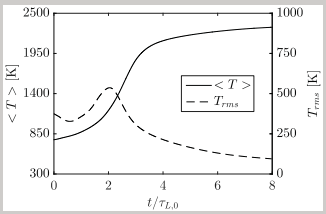	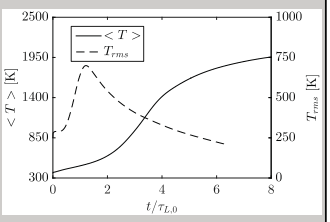
Temporal evolution	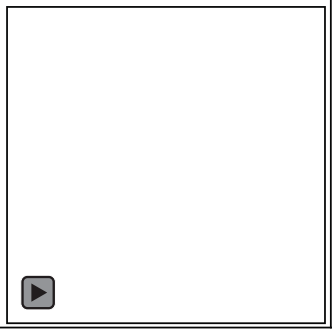	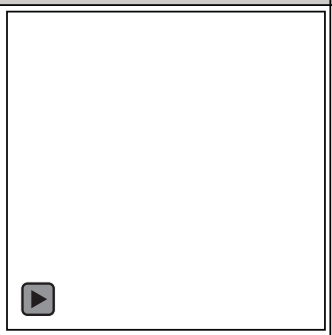	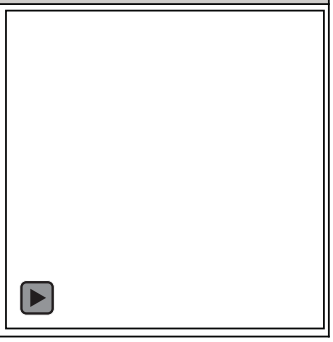

Stanford University

Regime diagrams

Flow and flame related quantities

- Integral length scale: $l = 10\,\mathrm{mm}$
- Flame thickness, $l_f = \dfrac{T_{\max} - T_{\min}}{\max(|\nabla T|)}$
- Reynolds number $Re_t = \dfrac{v' l}{\nu}$
- Damkoehler number $Da_L = \dfrac{\tau_L}{\tau_c}$
  - Characteristic turb. timescale $\tau_L = \dfrac{l}{v'}$
  - Combustion timescale $\tau_c = \dfrac{1}{\dot{\omega}_{\mathrm{O_2}}}$
- Karlovitz number $Ka = \dfrac{Re_t^{1/2}}{Da_L}$

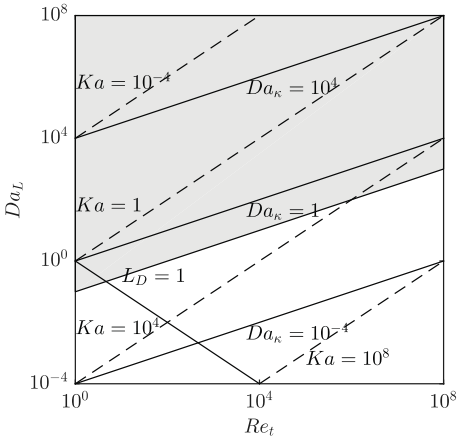

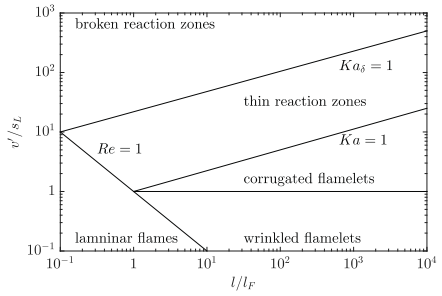

1. Williams, *AIAA Aero. Sci. Meeting & Exhibit*, 2006
2. Peters, *Cambridge University Press*, 2000

Stanford University

Regime diagrams

- All flames are in “broken reaction zones” regime with Ka > 100
- Ka first decays then increases as the flow evolves
  - Re_t decays with time
  - Da_L first reduces as combustion takes places; then increases as combustion approaches equilibrium
- Trajectory in Williams diagram for partially-premixed flame falls between premixed and non-premixed flame

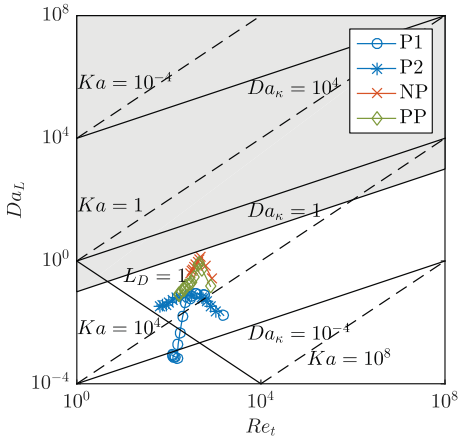

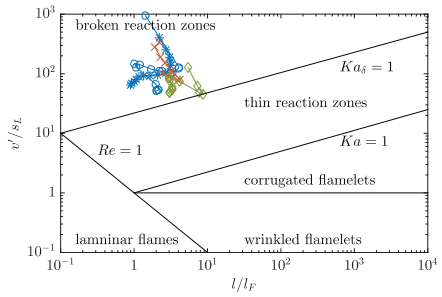

Stanford University

Flamelet extraction

- Isosurface: $C = C_{max}/2 = 0.14$
- Flamelet transformation

$$\nabla \rightarrow \nabla C \frac{\partial}{\partial C} + \nabla_\perp$$

$$\frac{\partial}{\partial t} \rightarrow \frac{\partial}{\partial \tau} + \frac{\partial C}{\partial t}\frac{\partial}{\partial C} - (\boldsymbol{v} - (\boldsymbol{v}\cdot\boldsymbol{n})\boldsymbol{n})\cdot\nabla$$

- Premixed flamelet equations

$$\rho\frac{\partial Y_k}{\partial \tau} + \frac{\partial Y_k}{\partial C}\dot{\omega}_C = \rho\chi_{CC}\frac{\partial^2 Y_k}{\partial C^2} + \dot{\omega}_k$$

$$\rho\frac{\partial T}{\partial \tau} + \frac{\partial T}{\partial C}\left[\dot{\omega}_C - \frac{\rho\chi_{CC}}{c_p}\left(\frac{\partial c_p}{\partial C} + \sum_{k=1}^{N} c_{p,k}\frac{\partial Y_k}{\partial C}\right)\right] = \rho\chi_{CC}\frac{\partial^2 T}{\partial C^2} - \frac{1}{c_p}\sum_{k=1}^{N_s} h_k\dot{\omega}_k$$

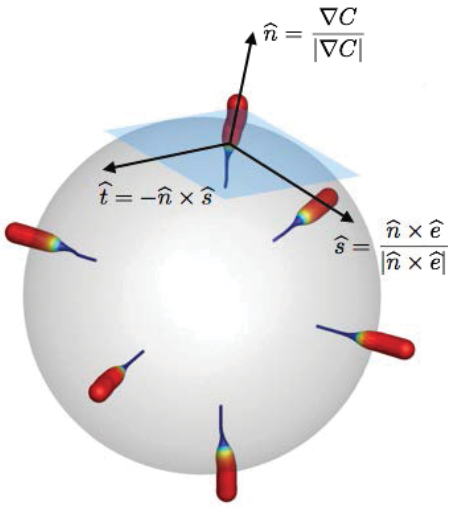

Stanford University

9

Premixed Flame: Local Flame Structure

$t/\tau_{L,0} = 0.0$ $t/\tau_{L,0} = 0.4$ $t/\tau_{L,0} = 0.8$ $t/\tau_{L,0} = 1.2$

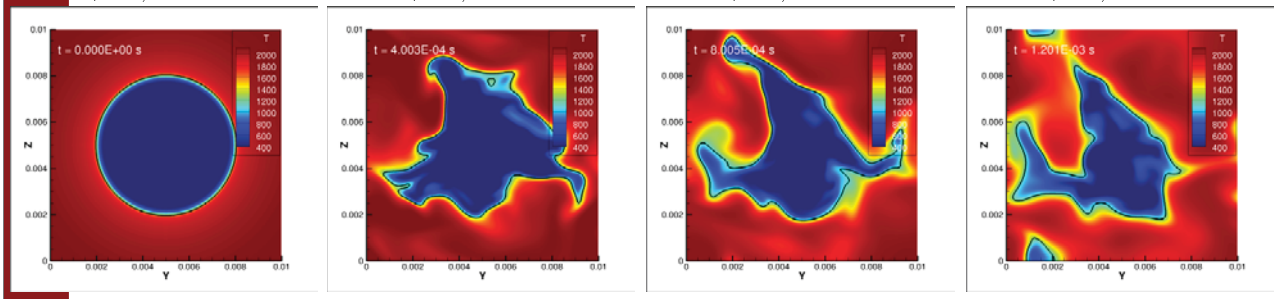

$t/\tau_{L,0} = 2.0$ $t/\tau_{L,0} = 3.0$ $t/\tau_{L,0} = 4.0$ $t/\tau_{L,0} = 5.0$

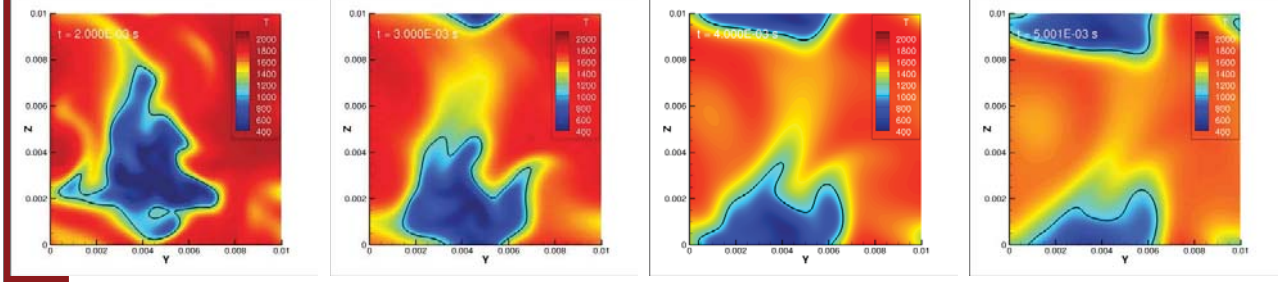

Stanford University

10

Premixed Flame: Local Flame Structure

$t/\tau_{L,0} = 0.0$ $t/\tau_{L,0} = 0.4$ $t/\tau_{L,0} = 0.8$ $t/\tau_{L,0} = 1.2$

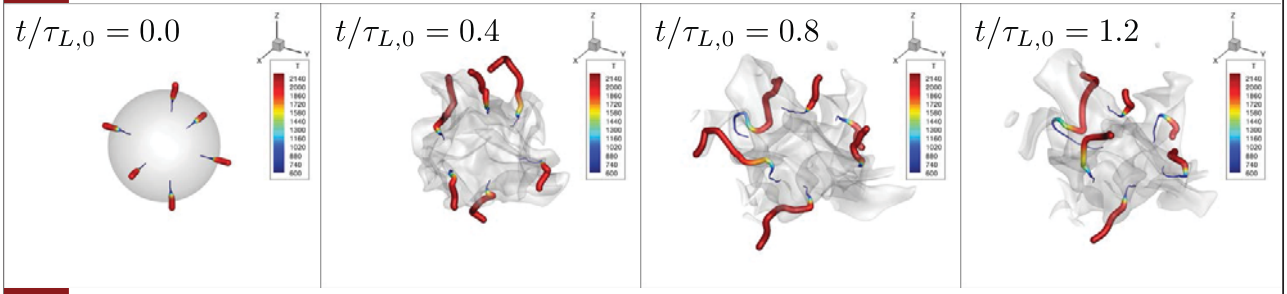

$t/\tau_{L,0} = 2.0$ $t/\tau_{L,0} = 3.0$ $t/\tau_{L,0} = 4.0$ $t/\tau_{L,0} = 5.0$

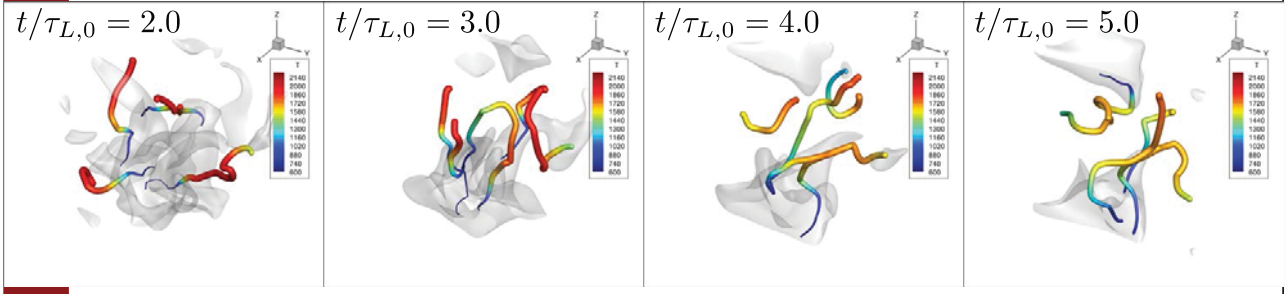

Stanford University

Premixed Flame: Local Flame Structure

Flame/turbulence interaction

- Phase 1 (t/τ< 0.5): Initialization and flame relaxation
- Phase 2 (t/τ< 2.0): broadening of preheat/reaction zones, product-gas recirculation
- Phase 3 (t/τ>2): broken flamelet, product-gas dilution and reactant vitiation

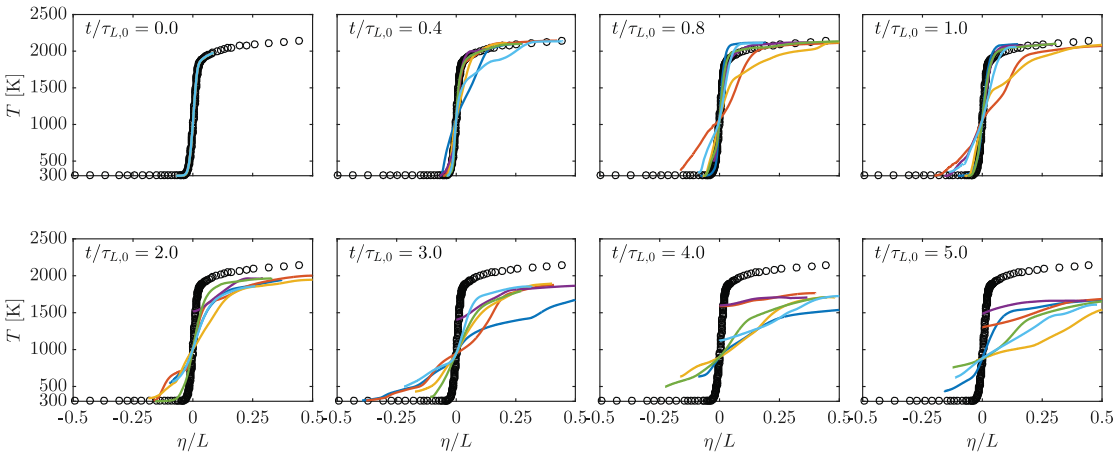

Stanford University

Flame front pinch-off and union of flamelets

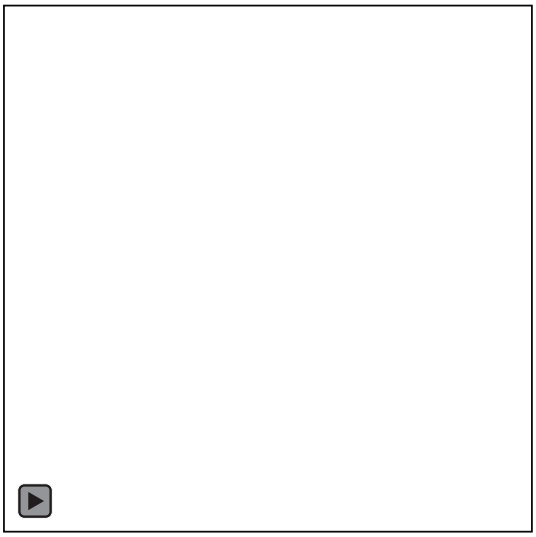

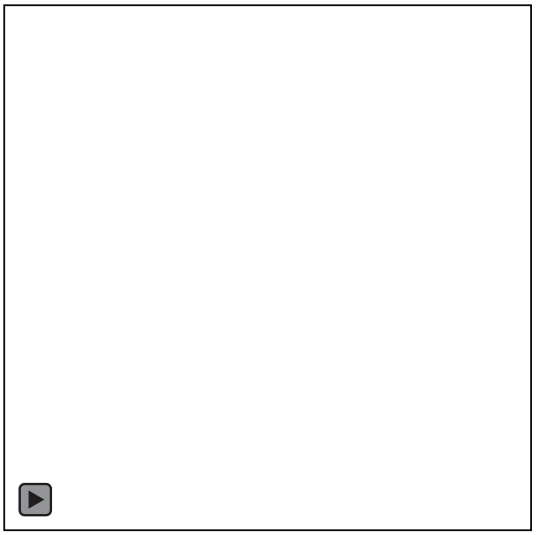

Stanford University

Model Implications

- Persistence of inner-core (weakened) flamelet-structure ➔ quasi-1D elongated element
- Diffusion and entrainment of hot products in reactant mixture by turbulent motion
- Non-equilibrium flamelet structure
- Highly wrinkeled flame-surface

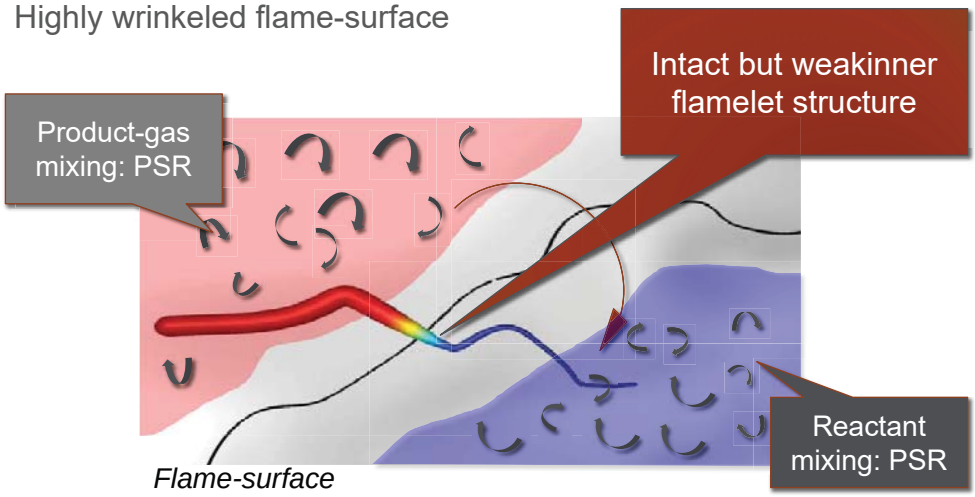

Stanford University

Model Implications

- Persistence of inner-core (weakened) flamelet-structure ➔ quasi-1D elongated element
- Diffusion and entrainment of hot products in reactant mixture by turbulent motion
- Non-equilibrium flamelet structure
- Highly wrinkeled flame-surface

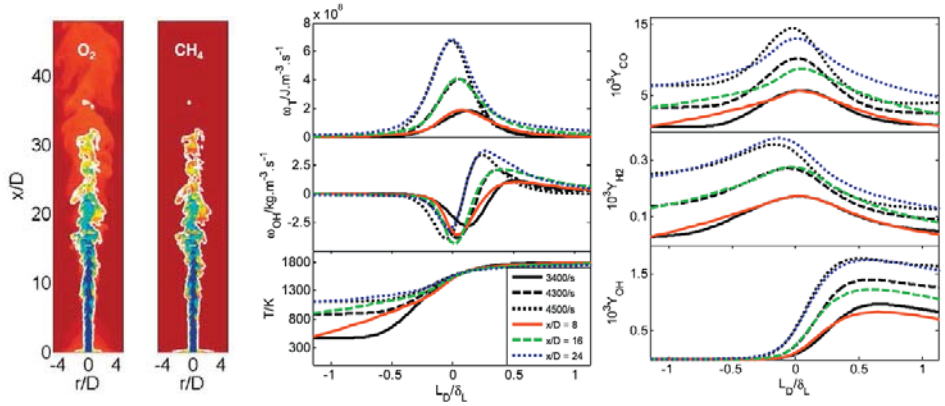

H. Wang, E. Hawkes, J. H. Chen, Combust. Flame, 180, 110-123, 2017.

Stanford University

Model Implications

- Persistence of inner-core (weakened) flamelet-structure ➔ quasi-1D elongated element
- Diffusion and entrainment of hot products in reactant mixture by turbulent motion
- Non-equilibrium flamelet structure
- Highly wrinkeled flame-surface

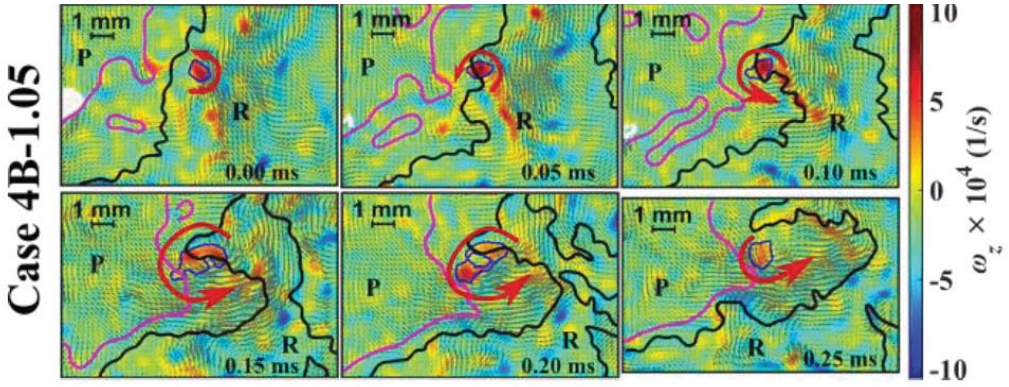

Skiba, Driscoll, CNF

Stanford University

Modeling Challenges

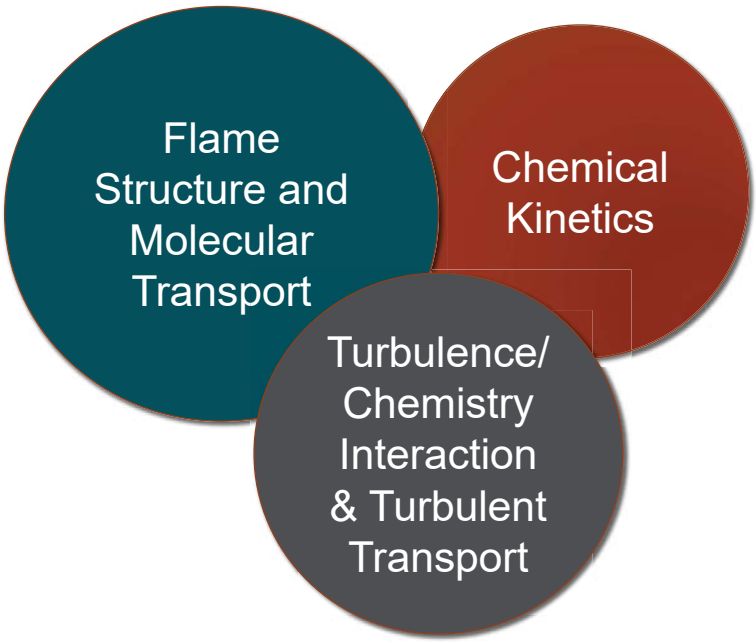

Stanford University

Combustion Modeling

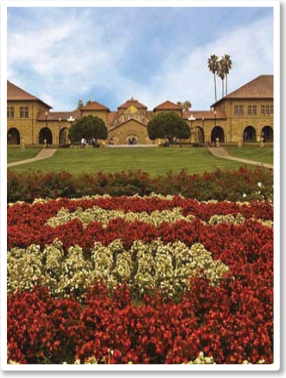

Stanford University

Measurements for Model Development

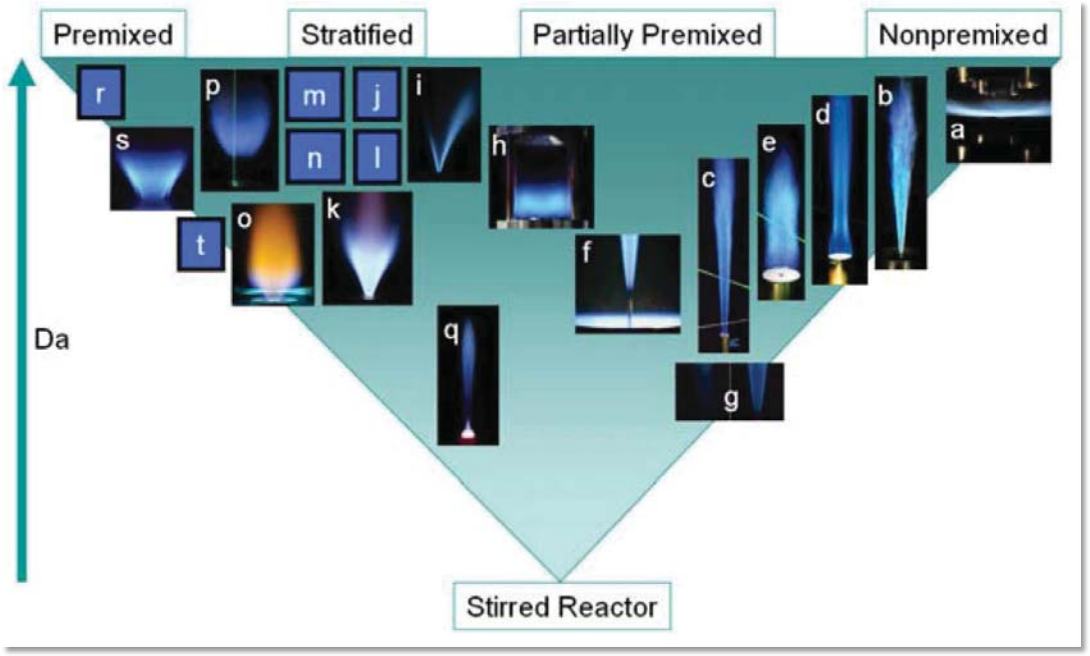

TNF9, 2008

Stanford University

Measurements for Model Development

TNF9, 2008

Stanford University

Sydney Partially-Premixed Jet Burner (PPJB)

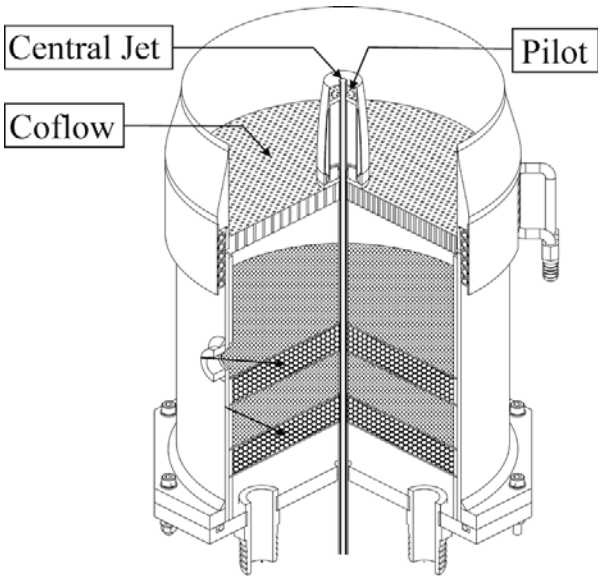

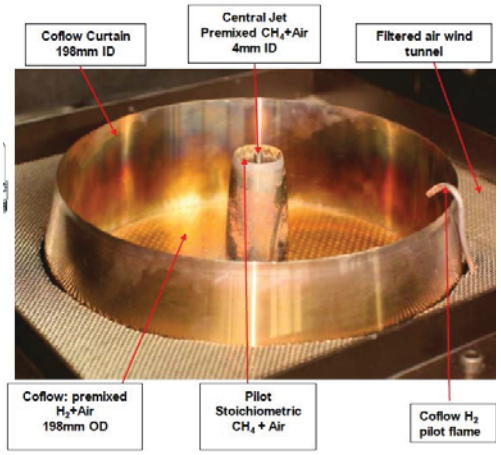

Variable	Unit	Jet	Pilot	Coflow
D	mm	4.0	23.5	197.0
U	m/s	Varies	5.2	3.98
T	K	290	2274	1493
Mixture	–	CH_4–Air	CH_4–Air	H_2–Air
ϕ	–	0.5	1.0	0.43

Case	U_j (m/s)	Re	Ka
PM1-50	50	12,500	100
PM1-100	100	25,000	1600
PM1-150	150	37,500	2500
PM1-200	200	50,000	3500

Dunn, M., Masri, A., and Bilger, R., "A new piloted premixed jet burner to study strong finite-rate chemistry effects," Combustion and Flame, 151, 2007, 46–60.
Jeff Sutton, OSU
Fokion Egolfopoulos, USC

Stanford University

Sydney Partially-Premixed Jet Burner (PPJB)

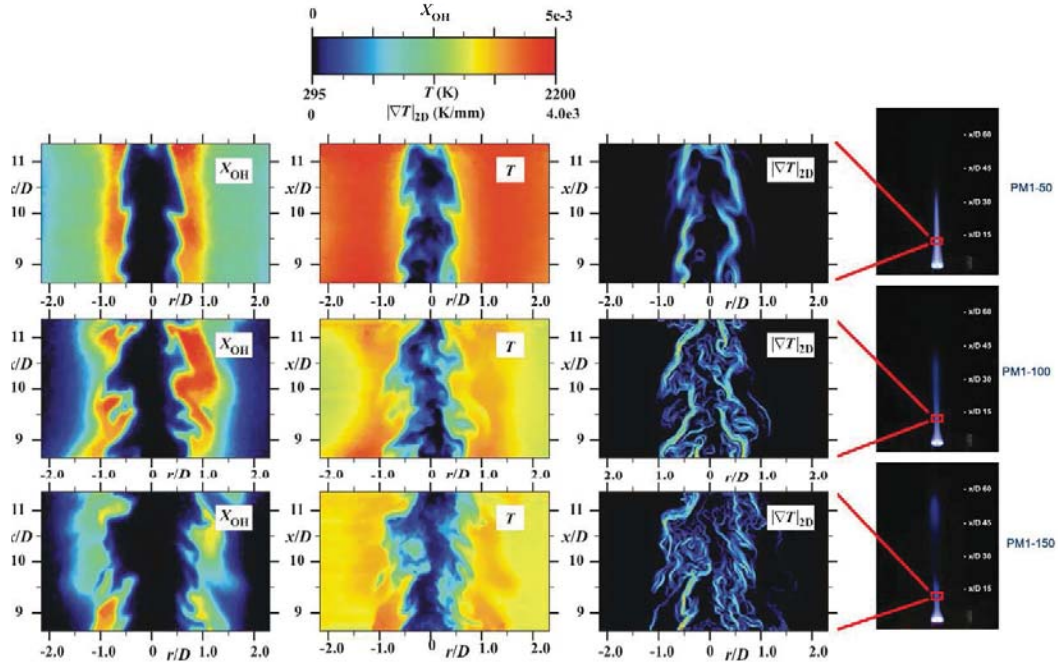

Dunn, M., Masri, A., and Bilger, R., "A new piloted premixed jet burner to study strong finite-rate chemistry effects," Combustion and Flame, 151, 2007, 46–60.

Stanford University

Sydney Partially-Premixed Jet Burner (PPJB)

BR zones vs. BP-TR zones regimes

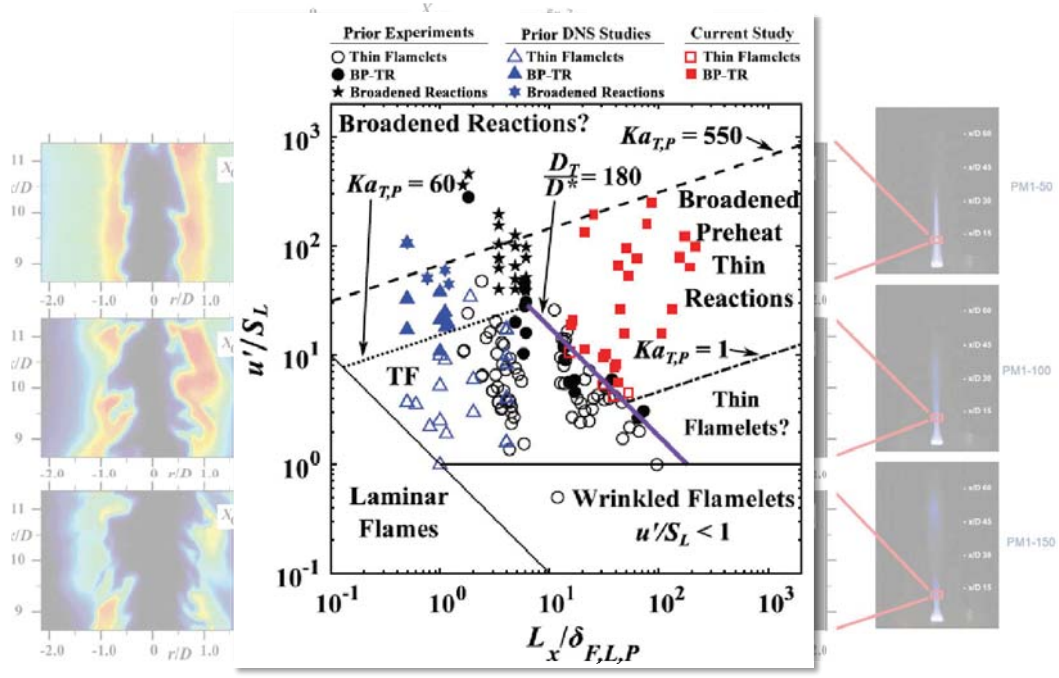

Dunn, M., Masri, A., and Bilger, R., "A new piloted premixed jet burner to study strong finite-rate chemistry effects," Combustion and Flame, 151, 2007, 46–60.

Stanford University

Sydney Partially-Premixed Jet Burner (PPJB)

Modeling Strategies (TNF10/11)

- "Implicit" FR LES without TCI-source term closure (Lund)
- Thickened flame model (Lund)
- Transported PDF-method (Cornell)
- Stochastic field methods (IC London)
- Flamelet formulations
  - Steady unstretched premixed (Aachen)
  - Steady multistream non-premixed (UM)

Analysis

- Statistical results, CO-T conditions
- Deviation with increasing downstream distance

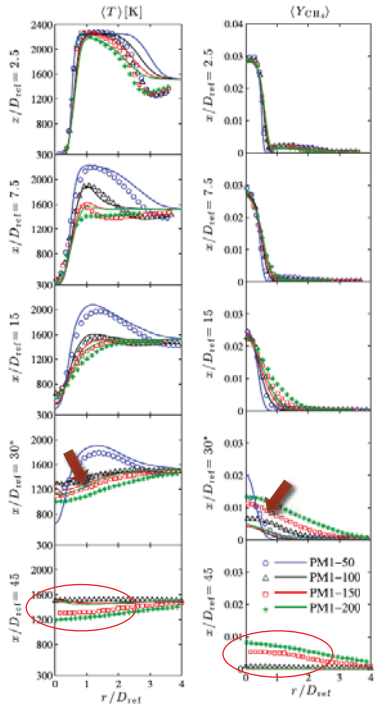

Stanford University

Sydney Partially-Premixed Jet Burner (PPJB)

TNF10/11 Findings

- PM1-50/100: Encouraging results for HH and major species
- PM1-150/200: deficiency of numerical models in capturing degree and impact of the finite rate chemistry effects
- Computational sensitivity analysis by Rowinski & Pope (CTM 2013)
  - Sensitivity of reaction progress to pilot velocity
  - Mixing models and differential diffusion
  - Pilot composition and pilot temperature

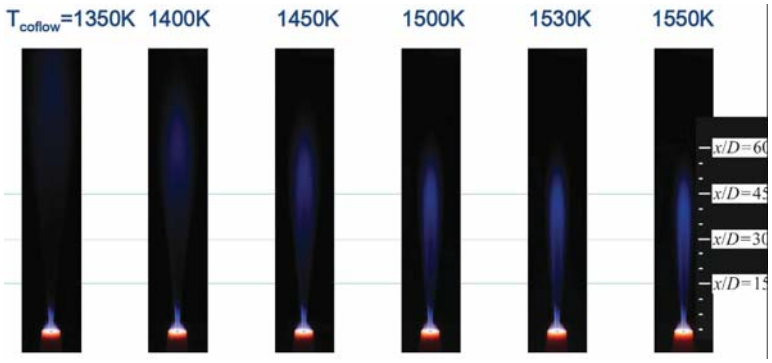

Stanford University

Mesh resolution and SGS contributions (Z. Ren, Tsinghua)

- **Objective:** Investigate the effect of grid resolution on LES-TPDF simulation of the PM1-150
  ➔ $\delta_L/\Delta r$ increases from 1.0 to 2.0 (0.1m → 2m CVs)

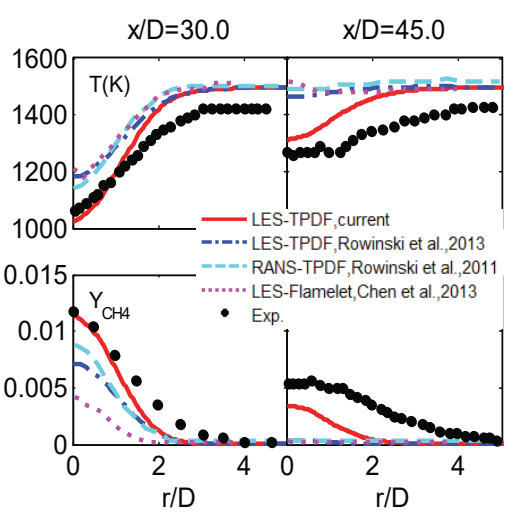

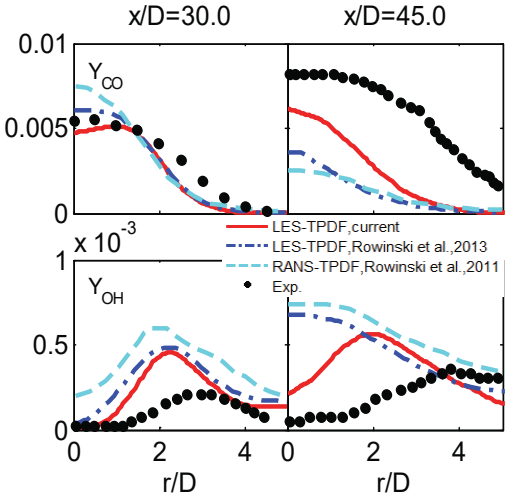

Stanford University

Mesh resolution and SGS contributions (Z. Ren, Tsinghua)

Mixing-Reaction Budgets: Net production rate ($d\boldsymbol{\phi}^*(t)/dt$):

$$d\boldsymbol{\phi}^*(t)/dt = \underbrace{\left(\nabla\cdot\left(\bar{\rho}\tilde{\Gamma}\nabla\tilde{\boldsymbol{\phi}}\right)/\bar{\rho}\right)^*}_{\text{Molecular diffusion rate}} + \underbrace{\Omega_M^*\left(\widetilde{\boldsymbol{\phi}^*}-\boldsymbol{\phi}^*\right)}_{\text{Subgrid mixing rate}} + \underbrace{\boldsymbol{S}(\boldsymbol{\phi}^*)}_{\text{Reaction rate}}$$

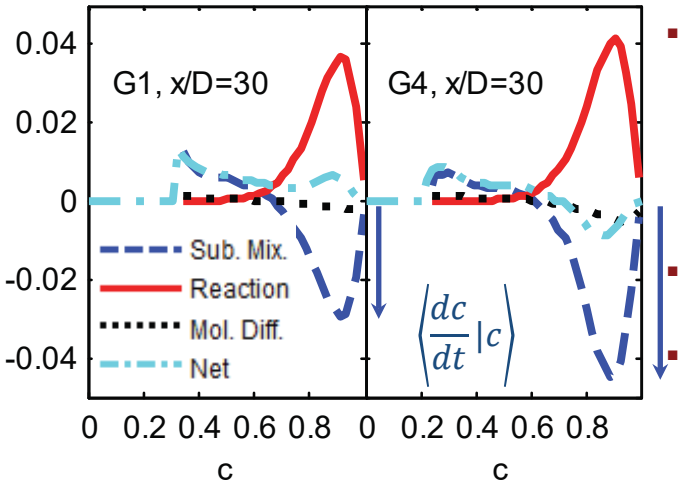

- Increasing grid resolution enhances negative subgrid mixing rate, resulting in the alleviation of the overpredicted combustion progress
- Subgrid mixing rate shows strong grid dependency
- Mesh resolution improves results

Stanford University

Turbulence/Chemistry Interaction

Presumed PDF-closure models

- mixing between multiple streams of different intensity: x/D = 15, r/D=1.1

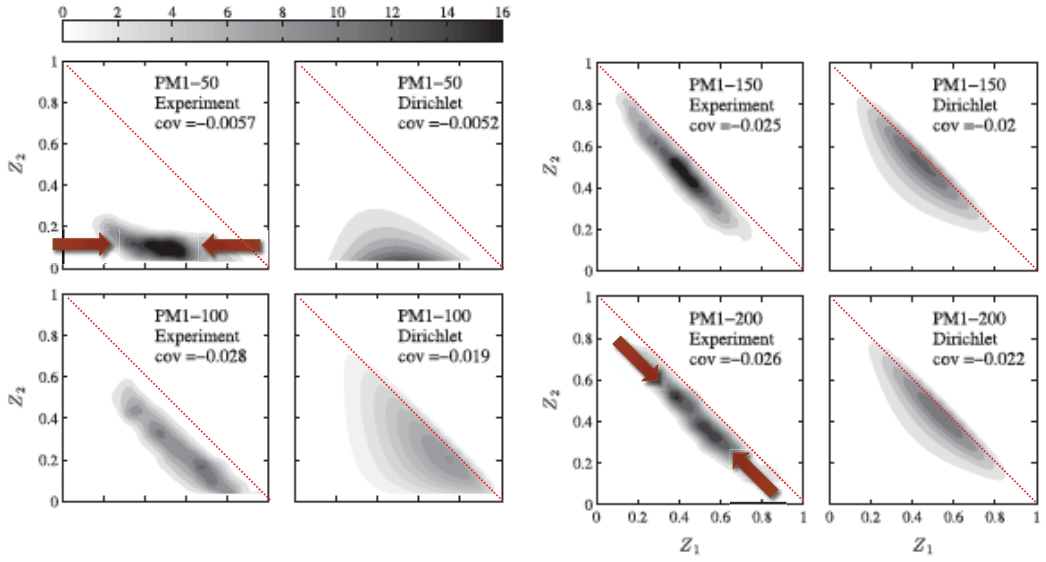

Stanford University

Turbulence/Chemistry Interaction (Steve Pope)

Conditional Dissipation Mapping Closure (CDMC)

- Closure for the PDF, *f(c),* and conditional dissipation (CD), $\chi(c)$, of the progress variable
- Key idea: Perform a straining- and mapping transformation to produce surrogate process c_s with same PDF and CD
  - Consideration of coupling between reaction and diffusion
  - Satisfies boundedness, realizability – each instant describes exactly the evolution of the statistics of a set of realizable fields
  - Evolution equations for the mapping functions, from which the PDF and CD can be obtained
- Ongoing work: extend to turbulent combustion, inhomogeneous cases, solution method

Stanford University

Turbulence/Chemistry Interaction (Steve Pope)

Conditional Dissipation Mapping Closure (CDMC)

- Statistically-homogeneous,1D reaction-diffusion equation

$$\partial_t c = \Gamma \partial_{xx} c + S(c)$$

- Initial condition: uniform PDF
- Damkoehler number: Da = 0.17 (distributed)

- Results:
  - Initially, mixing towards the mean
  - Conditional dissipation decreases with tim
  - More slowly, reaction moves probab towards *c=1*

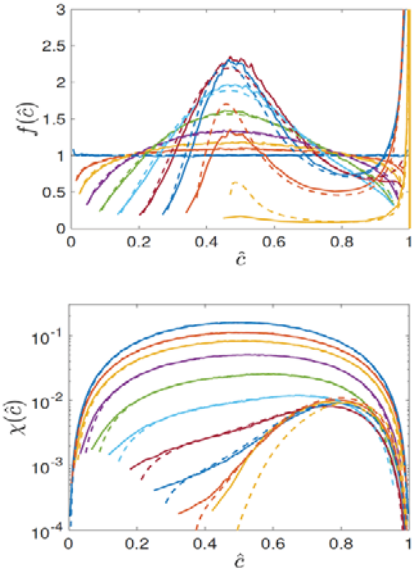

Solid: DNS; dashed: CDMC

Stanford University

Combustion Model Evaluation (Yang, Peking, Han et al. TUD, Sandia)

A posteriori model evaluation through DNS of Lund burner

- LES-TPDF
- LES/DTF+FRC
- LES/DTF+strained premixed flamelets
- LES-resolution: > $2\Delta_{DNS}$ (65μm)

Key findings:

- LES/DFT/FRC capture key features of high-Ka flame-statistics
- Consideration of detailed strain effects necessary for tabulation methods
- Thickening factor: <3
- Comparison with DNS eliminates ambiguity in boundary conditions

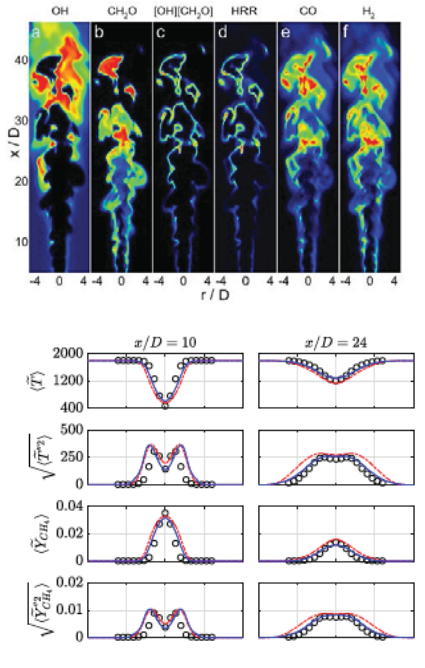

Red: LES/DTF/SPF, blue: LES/DTF/FRC

Han, Wang, Kuenne, Hawkes, Chen, Janicka, Hasse,Combust. Symp. 2018

Stanford University

Summary

Modeling progress on high-Ka flames

- Combustion models capture main features of turbulent flame structure at moderate Ka-regimes
- Overprediction of reactivity at high-Ka regimes
- Extension of flamelet models show promise but lack key physical aspects
- Resolution one cure to improve predictions

Research needs

- LES comparison restricted to statistical comparisons
- Simulations overwhelmed by sensitivity to boundary conditions
- Lack of quantitative and systematic evaluation of model performance
  - What are quantities of interest? States, processes …
  - Required and achievable accuracies of a model?
  - Error control …
- Quantitative Comparison of Flame Structure

Stanford University

Combustion Model Adaptation

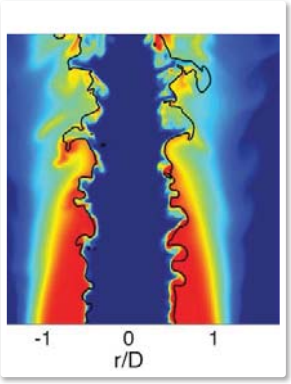

Stanford University

Adaptive Combustion Models

Hierarchy of combustion models available to represent majority of relevant combustion process

- "One model fits all …"
- Augment models to address deficiencies

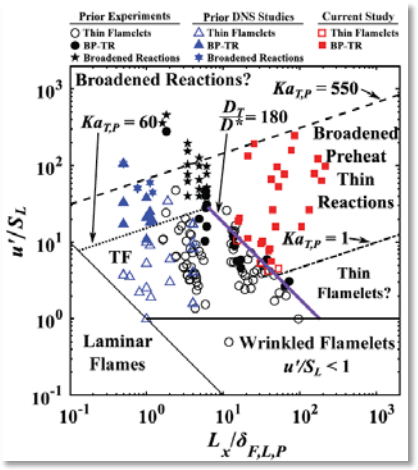

- Model accuracy depends on
  - Quantities of interest
  - Combustion-physical processes
  - Combustion regimes: premixed, non-premixed, multiphase

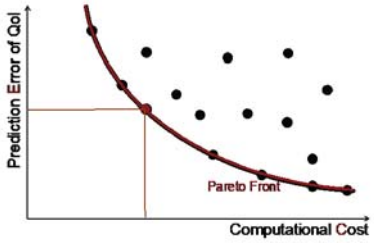

Stanford University

Adaptive Combustion Models

Problem formulation:

- Set of quantities/processes of interest
- Direct error control of solution
- Set of candidate combustion models
  - Reaction-transport manifolds
  - Chemistry manifold
- Control of cost/accuracy

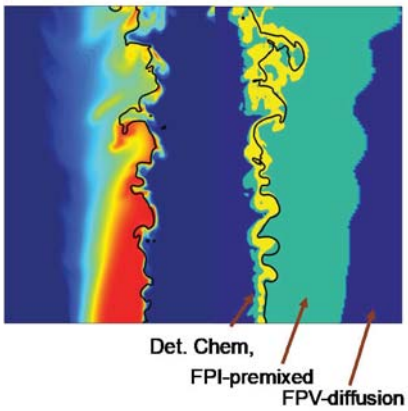

Local model adaptation

- Dynamic adaptive chemistry (Lu, Sun, Pepiot)
- Mixed-model combustion (Knudsen)
- Pareto-efficient combustion (Wu, Wang)

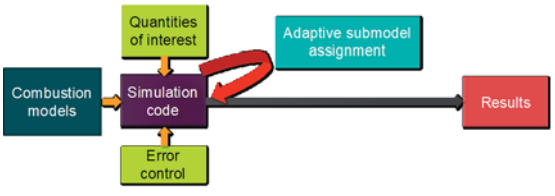

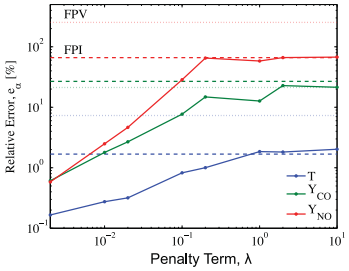

Stanford University

Integration of Experiments and Simulations

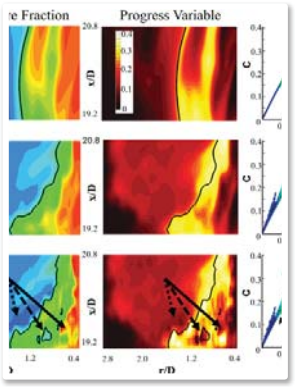

Incorporate experimental data into simulations

- Take advantage of high-speed high-resolution simultaneous measurements to inform combustion models

Key idea: Combine incomplete experimental measurements with erroneous high-fidelity simulation models to improve state predictions

- State estimate
- Model evaluation
- Parameter estimate

Assimilation methods:

- Nudging, Optimal Interpolation, 3D/4D-var, Ensemble Kalman Filter

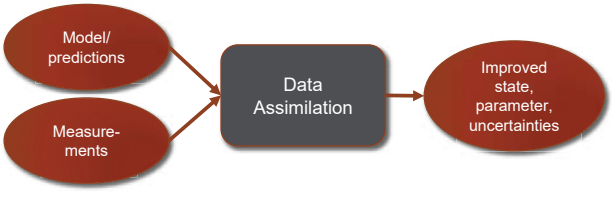

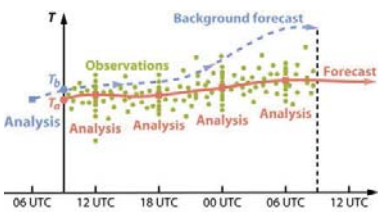

Incorporate experimental data into simulations: Example

Experimental data

- DME/Air jet flame
- Data: OH-PLIF and tomographic PIV (TPIV) data available at x/D = 20
  - Probe volume of 11.4x16.9x3.3 mm^3
  - Data acquired at 10kHz

Computational method

- Ensemble Kalman filter for assimilation
- Dynamic thickened-flamelet model
- 4 million cells
- 12 ensemble members
- Background-error covariance matrix localization

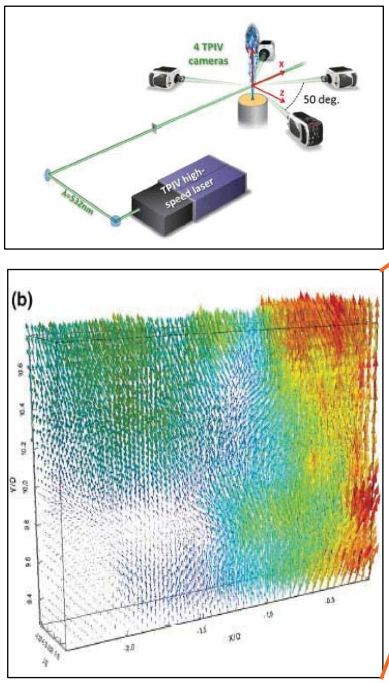

Stanford University

Incorporate experimental data into simulations: Example

State estimate: Capturing extinction and reignition

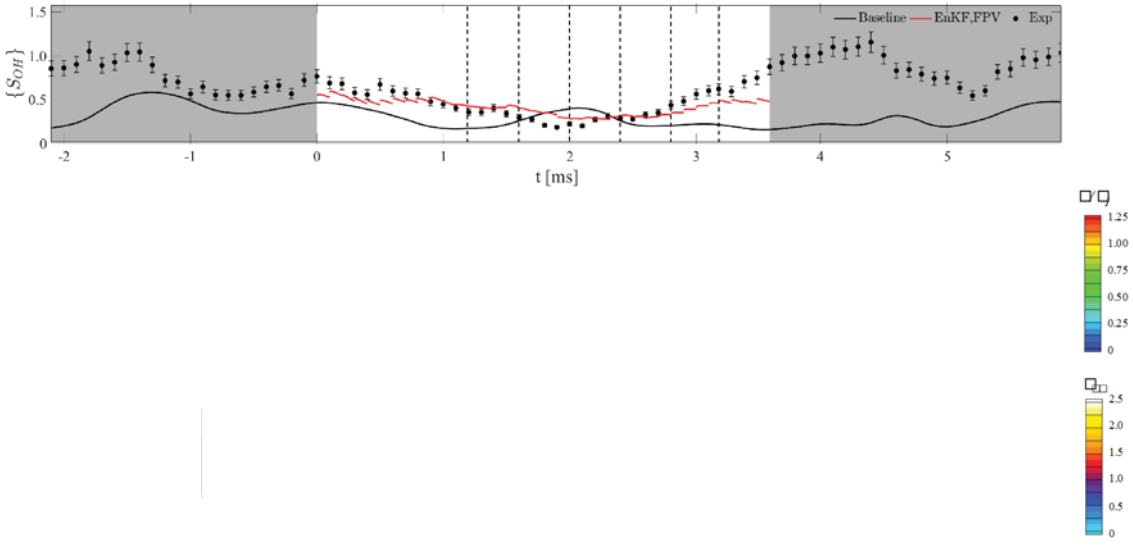

Stanford University

Incorporate experimental data into simulations: Example

Model evaluation: examining model response → erroneous representation of extinction and reignition by scalar unmixing!

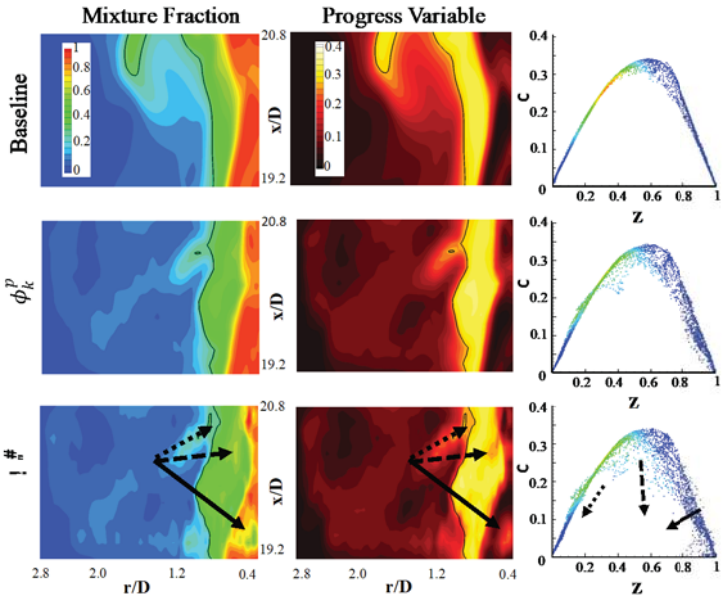

Summary and Conclusions

Experimental evaluation of combustion models limited

- Few experimental configurations and limited number of operating points and fuels
- Statistical comparisons
- Sensitivity to boundary conditions and tuning parameters

Model performance

- Models capture trends in reaction progress at low/moderate Ka at varying degree
- Physical mechanism are contained in models at varying level of fidelity and rigor
  - Strain and transient effects
  - Finite-rate chemistry
  - Dilution and mixing of reactants and products
  - SGS-models

Opportunities and needs

- Fine-scale analysis of model performance
- Data assimilation for combustion-model evaluation and state estimate
- Quantitative evaluation of model performance
  - Model accuracy, quantities of interest, conditions of applicability, bootstrapping

PTF/TNF joint session

Highly turbulent premixed flames

Needs for further improvement (specifically DNS)

Evatt Hawkes, UNSW Sydney

evatt.hawkes@unsw.edu.au

Scope

Needs for further improvement...

Three things to highlight

- Objectives of our work – what are we hoping to achieve with DNS?
- Parameter regimes – need to go to higher Re as key priority
- Configurations – need to create databases useful for model validation, for which isotropic turbulence cases offer only a part of the solution

Main paradigms of using DNS for models

Fundamental investigation

- Learn about what controls turbulence – chemistry interaction & hence what needs to be built into a model

Inventing the models

- Somehow the fundamentals are digested and turned into models

A priori tests

- Test individual assumptions, specific sub-model propositions, determine constants / fits

A posteriori tests

- Somebody picks up the model, runs it, assess outcomes & improves

UNSW SYDNEY

DNS to model – we're doing it wrong

Main issue – our work is lacking in translation

Vast majority of DNS work

Fundamental studies that never get incorporated into models or have any other impact on industry

- Lots of a priori tests with no translation into a posteriori tests
- Lots of a posteriori tests (mostly against experiments) without serious efforts to isolate causes of problems and improve

… Translation to industry…?

UNSW SYDNEY

Using DNS to improve mixing timescale model in TPDF simulation of premixed combustion

Mike Kuron (U.Conn. lead author), **Zhuyin Ren** (Tsinghua), T.F. Lu (U Conn.), H. Zhou (Tsinghua), J.H. Chen (Sandia), J.C.K. Tang (UNSW)

Particle equations for composition transported PDF approach

Mean advection Turbulent diffusion

$$dx = \left[\tilde{u} + \frac{1}{\bar{\rho}}\frac{\partial(\bar{\rho}\widetilde{\Gamma_t})}{\partial x}\right]dt + \sqrt{2\widetilde{\Gamma_t}}\,dW$$

$$d\phi = dM(\Omega) + dR$$

Mixing (model) Chemistry (closed)

Particle equations – TPDF approach, traditional method

Turbulence model

$$dx = \left[\tilde{u} + \frac{1}{\bar{\rho}}\frac{\partial(\bar{\rho}\widetilde{\Gamma_t})}{\partial x}\right]dt + \sqrt{2\widetilde{\Gamma_t}}\,dW$$

$$d\phi = dM(\Omega) + dR$$

$$\Omega \sim c_\phi \frac{\tilde{\varepsilon}}{\tilde{k}}$$

Order unity (?) parameter Turbulence model

UNSW SYDNEY

Particle equations – TPDF approach – using DNS to eliminate some model assumptions

Provide from DNS

$$dx = \left[\tilde{u} + \frac{1}{\bar{\rho}}\frac{\partial(\bar{\rho}\widetilde{\Gamma_t})}{\partial x}\right]dt + \sqrt{2\widetilde{\Gamma_t}}\,dW$$

$$d\phi = dM(\Omega) + dR$$

$$\Omega \sim c_\phi \frac{\tilde{\varepsilon}}{\tilde{k}}$$

Provide from DNS Provide from DNS

UNSW SYDNEY

Micro-mixing models

- IEM
  - Particle compositions evolve by linearly decaying to the local mean

$$d\phi \sim -\frac{1}{2}\,\Omega\left(\phi - \tilde{\phi}\right)$$

- Modified Curl
  - Pairwise exchange model mixing particles at rate consistent with mixing frequency:

$$\phi^{(p,\,\mathrm{new})} = \phi^{(p)} + \frac{1}{2}\,a\,(\phi^{(q)} - \phi^{(p)})$$

$$\phi^{(q,\,\mathrm{new})} = \phi^{(q)} + \frac{1}{2}\,a\,(\phi^{(p)} - \phi^{(q)}),$$

- EMST
  - Each particle is connected to its neighbour in composition space
  - Particles can only mix with their neighbors along the EMST edges
  - Particles selected to mix undergo a mixing event in a similar manner to the MC model

DNS test cases

- Temporally evolving premixed H_2-Air slot jet (Hawkes et al., CNF 2012)
  - Two cases in the “thin reaction zones” regime:
    - Da-: Da<1, Ka~92
    - Da+: Da>1, Ka~22
  - Statistically 1-D, time dependent flames

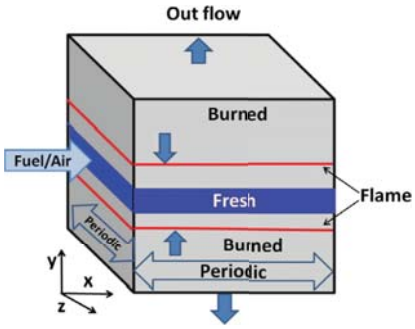

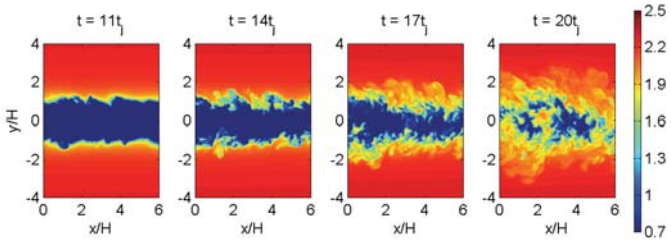

Case Da- representative temperature (T/1000 K) iso-contours

Mixing model performance

- Progress variable based on H_2 mass fraction used to define diffusion coefficient and mixing timescale… (others were tested, H_2 optimal)
- IEM & MC under-predict the flame speed
- EMST demonstrates superior performance, accurately capturing the flame

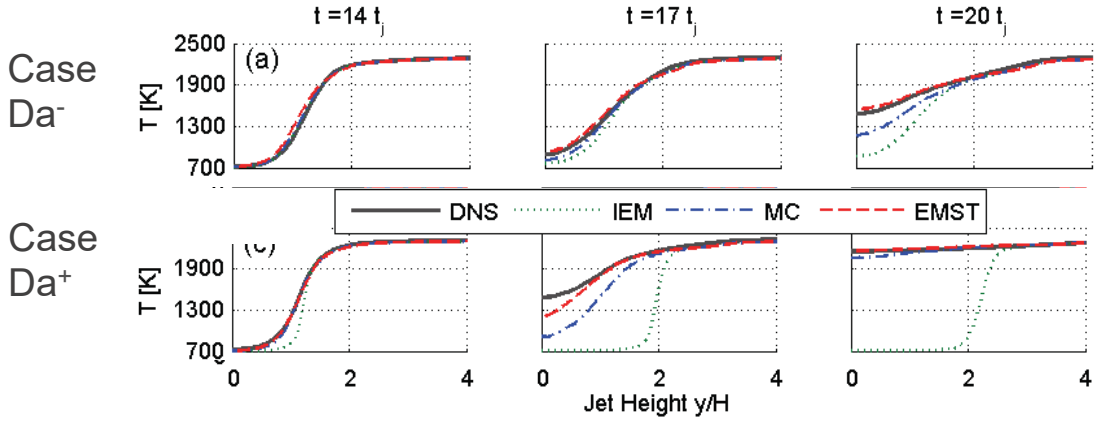

Kuron, M., Hawkes, E.R., Ren Z., Tang, J., *et al.* (2017), *Proceedings of the Combustion Institute* 36, pp. 1987–1995.

UNSW SYDNEY

Particle equations

Provide from DNS

$$dx = \left[\tilde{u} + \frac{1}{\bar{\rho}}\frac{\partial(\bar{\rho}\widetilde{\Gamma_t})}{\partial x}\right]dt + \sqrt{2\widetilde{\Gamma_t}}\,dW$$

$$d\phi = dM(\Omega) + dR$$

$$\Omega \sim c_\phi \frac{\tilde{\varepsilon}}{\tilde{k}}$$

~~Provide from DNS~~ Provide from DNS
Set as constant

UNSW SYDNEY

Mechanical-to-scalar timescale ratio

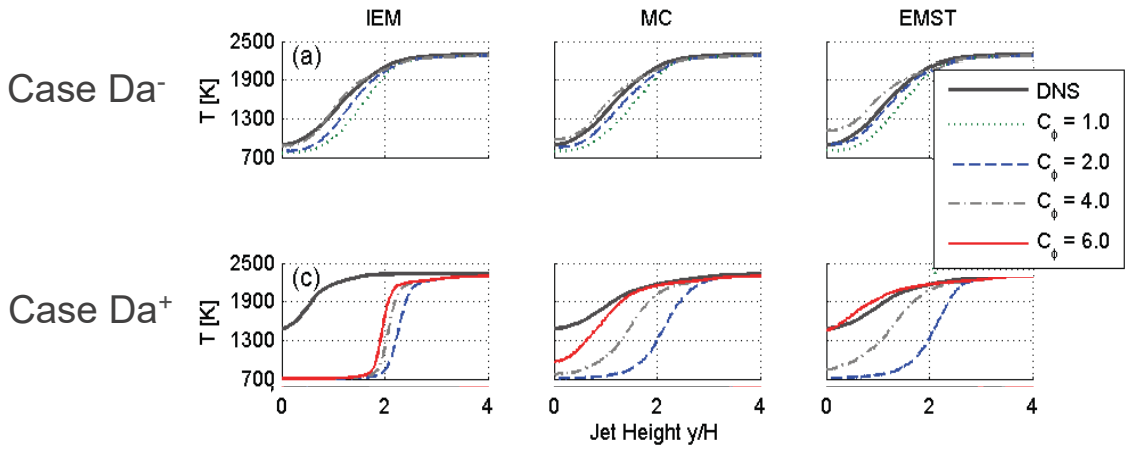

- The optimal value of the timescale ratio is ~2.0 for Case Da- and ~6.0 for Case Da+
  - No single value of the mechanical-to-scalar timescale ratio is optimal for all cases, even in the same geometric configuration. **PROBLEM!!!**

Scalar dissipation rate model development

- A hybrid model is constructed by locally blending a flamelet limit with the turbulence timescale limit using a segregation factor s

$$\chi = \Omega \widetilde{c''^2} \sim (1-s) c_\phi \frac{\tilde{\varepsilon}}{\tilde{k}} \widetilde{c''^2} + s \int \chi_l(c)\, P(c) dc; \qquad s = \frac{\widetilde{c''^2}}{\tilde{c}(1-\tilde{c})}$$

- To close the model, the conditional scalar dissipation rate is reconstructed from a 1D, freely propagating premixed flame

Kuron, Ren, **Hawkes**, Zhou, Kolla, Chen, Lu, (2017), *Combustion and Flame* 177, pp. 171-183.

Scalar dissipation rate *a priori* comparison to DNS

- Using the H_2-Air premixed slot jet DNS, the hybrid model is reconstructed and compared to the dissipation rate of the progress variable, a priori

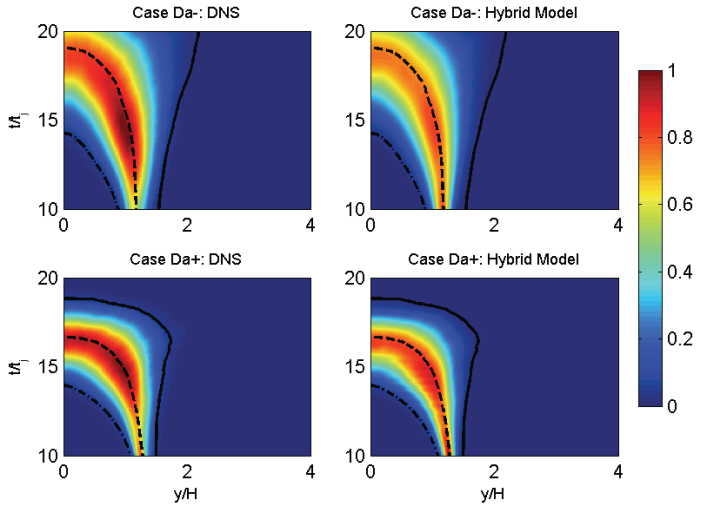

$\chi/\max(\chi_{DNS})$

Hybrid mixing rate model *a posteriori* TPDF comparison

- The hybrid mixing model shows superior performance to the turbulent mixing rate and laminar flamelet closure (Pope and Anand) approaches

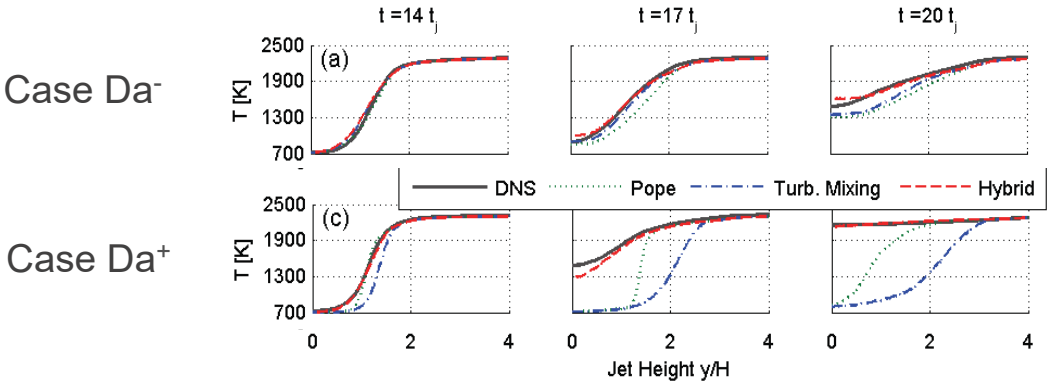

Kuron, Ren, **Hawkes**, Zhou, Kolla, Chen, Lu, (2017), *Combustion and Flame* 177, pp. 171-183.

Synposis – premixed cases

- Error isolation – eliminated turbulence model and other parameters
- Demonstrated EMST can work, with correct mixing timescale input
- Traditional approach of constant c_ϕ demonstrated to fail
- Focused theoretical work to revise the timescale model
- Demonstrated in a priori test
- Confirmed in a posteriori test

UNSW SYDNEY

Parameter regimes
Re as a key priority

DNS - limitations

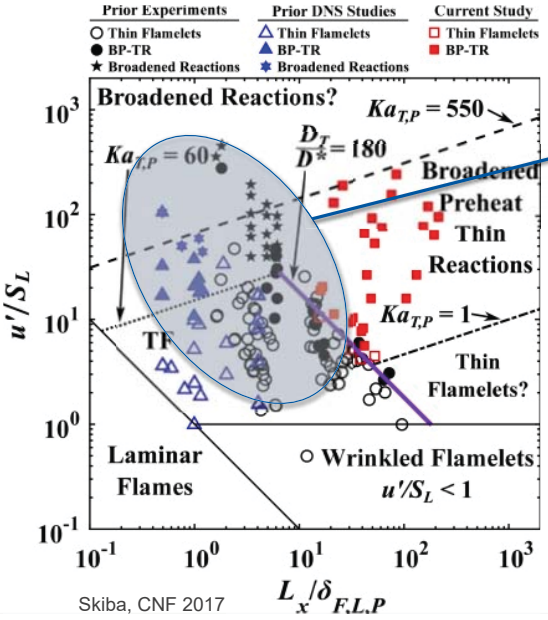

Skiba, CNF 2017

- DNS for high Ka is turbulence-limited, thus limited by Re
- Almost all high Ka DNS have low Da
  - Vervisch - Karlovitz bubble, Damkohler crisis!
- A high Da, high Ka flame might be qualitatively different…

DNS - limitations

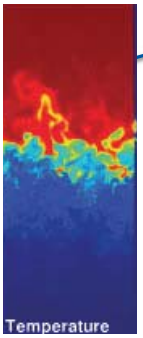

DNS
Aspden, 2018
arXiv
~2.5 x thickening at Ka 1,000
~ 3.5 x at Ka 10,000

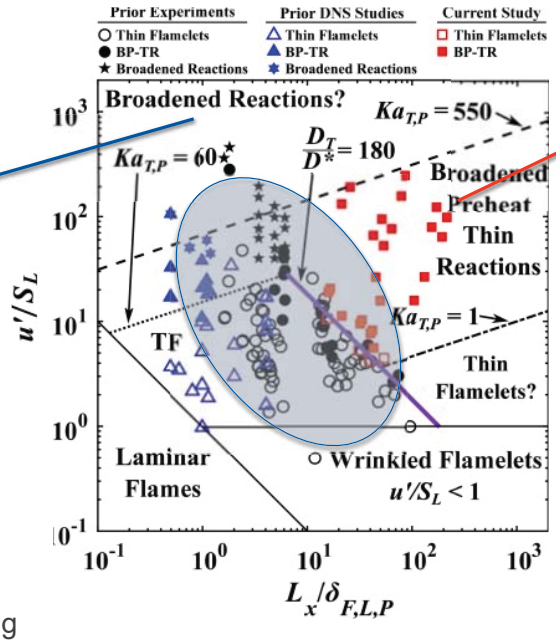

Skiba, CNF 2017

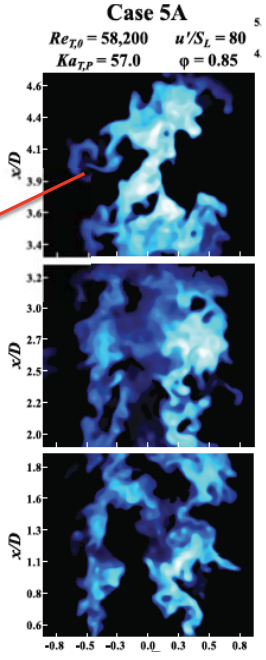

Experiments
Skiba, CNF 2018
16 x thickening at Ka ~ 100

Jet flames at similar Ka and increasing Re number

Stefano Luca, Antonio Attili, Fabrizio Bisetti et al. 37th International Symposium on Combustion
- Talk 1A01 on Monday, 10:05, turbulent combustion

- 4 spatially evolving jet, with Jet Re number from 2800 to 22400
- Constant U bulk at the inlet (100 m/s)
- Increasing Re obtained increasing the jet width, therefore increasing the turbulence integral scale
- At constant u' and increasing integral scale, the Kolmogorov scale increases slightly (Ka~Re^-0.5 in fresh gases)

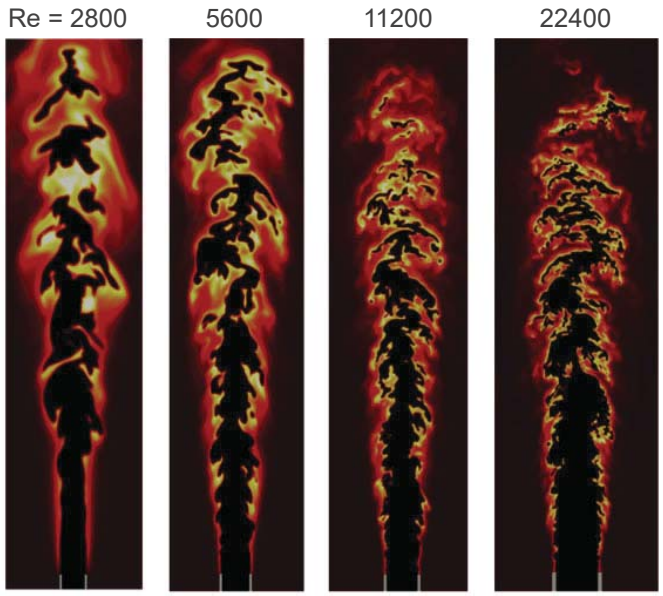

	R1-K1	R2-K1	R3-K1	R4-K4
Jet Reynolds Number	2800	5600	11200	22400
Jet Bulk Velocity, U_{bulk}	100 m/s	100 m/s	100 m/s	100 m/s
Inlet temperature	800 K	800 K	800 K	800 K
Slot width, H	0.6 mm	1.2 mm	2.4 mm	4.8 mm
Grid Size	720×480×256	1440×960×256	2880×1920×512	5760×3844×1024
Total number of points	88 Million	350 Million	2.8 Billion	22 Billion

Regime diagram & flame length for the 4 flames

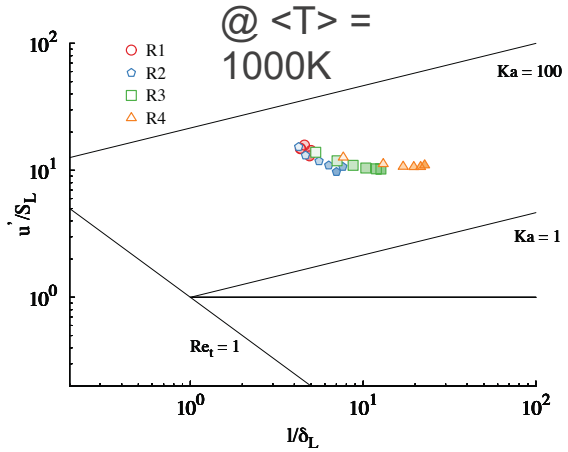

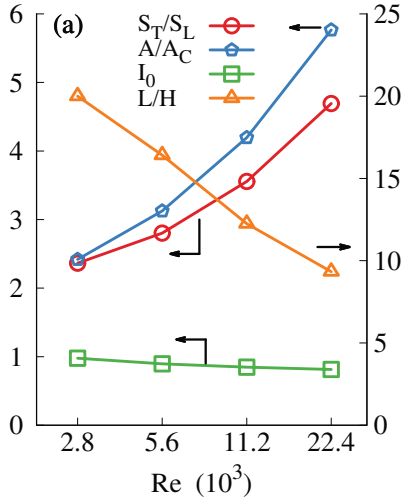

- Re varied by a factor of 10
- Flame length in H units continuously decreasing, no sign of limit behaviour either way…

Scaling of the source term of the FSD equation

$$\nabla \cdot (\langle \mathbf{u} + S\mathbf{n} \rangle_s \Sigma) = \langle a + S \nabla \cdot \mathbf{n} \rangle_s \Sigma = \langle \mathrm{K} \rangle_s \Sigma$$

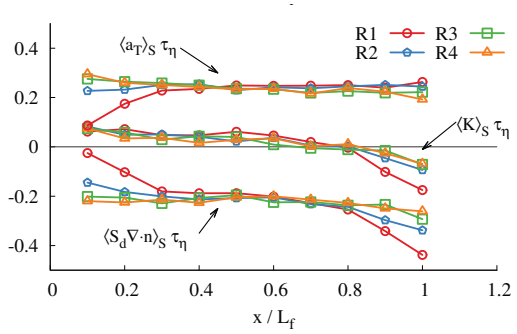

- Source terms are Kolmogorov scaled, in contrast to prevailing thought and models
- Serious implications for whole approach of modelling the FSD

Heat Release Effects on Turbulent: The Most "Interesting" Regime

Jonathan F. MacArt, Michael E. Mueller

Computational Turbulent Reacting Flow Laboratory (CTRFL)
Department of Mechanical and Aerospace Engineering
Princeton University

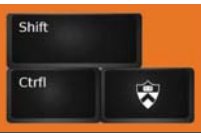

TNF/PTF Joint Session on Highly Turbulent Premixed Combustion
Dublin, Ireland
July 27, 2018

Dilatation Effects

- Physical Arguments
  - Dilatation effects from heat release dominate turbulence dynamics when the dilatation is faster than turbulent dissipation.
    - From Bilger[1], requires $Ka < Ka_{\mathrm{cr}} = \tau = T_b/T_u - 1$
  - Results in counter-gradient transport effects for both the turbulent scalar flux and the Reynolds stresses
    - Confirmed via our DNS of planar jet flames at low Karlovitz number[2]
    - Gradient transport dominates in our DNS at high Karlovitz number[2]
    - More recent work has shown that this holds true for the subfilter fluxes and subfilter stresses irrespective of filter width for these datasets[3]
  - However, our high Karlovitz DNS database is at low Damköhler number, so all scales of turbulence are faster than the flame.
    - High Ka, high Da: Some scales faster, some slower than flame.
    - Large scales in counter-gradient and small scales in gradient transport?

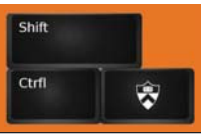

[1]R.W. Bilger, Flow Turb. Combust. 72 (2004) 93-114
[2]J.F. MacArt, T. Grenga, M.E. Mueller, Combust. Flame 191 (2018) 468-485
[3]J.F. MacArt, O. Shende, M.E. Mueller, Combust. Flame (2018) in preparation

Dilatation Effects

- Regime Diagram

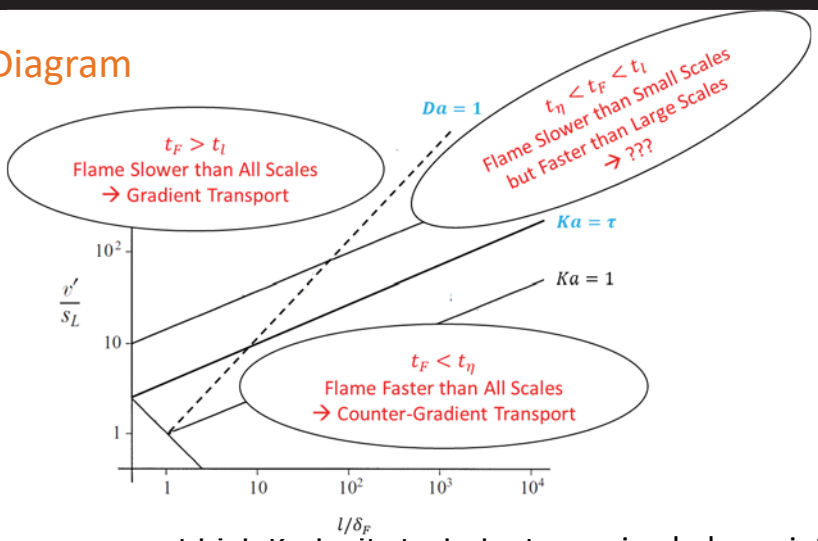

- To scale our current high Karlovitz turbulent premixed planar jet flame DNS database ($Ka \sim 50 = 6.5\tau$) from $Da = 0.06 \rightarrow 1.0$ at same Ka:
  - $Re_0 \approx 1{,}280{,}000;\ Re_t \approx 26{,}000$
  - 59 trillion grid points!

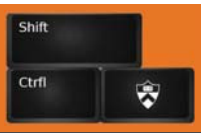

Configurations

AEROSPACE ENGINEERING
TEXAS A&M UNIVERSITY

Flame-generated turbulence and up-scale kinetic-energy transport

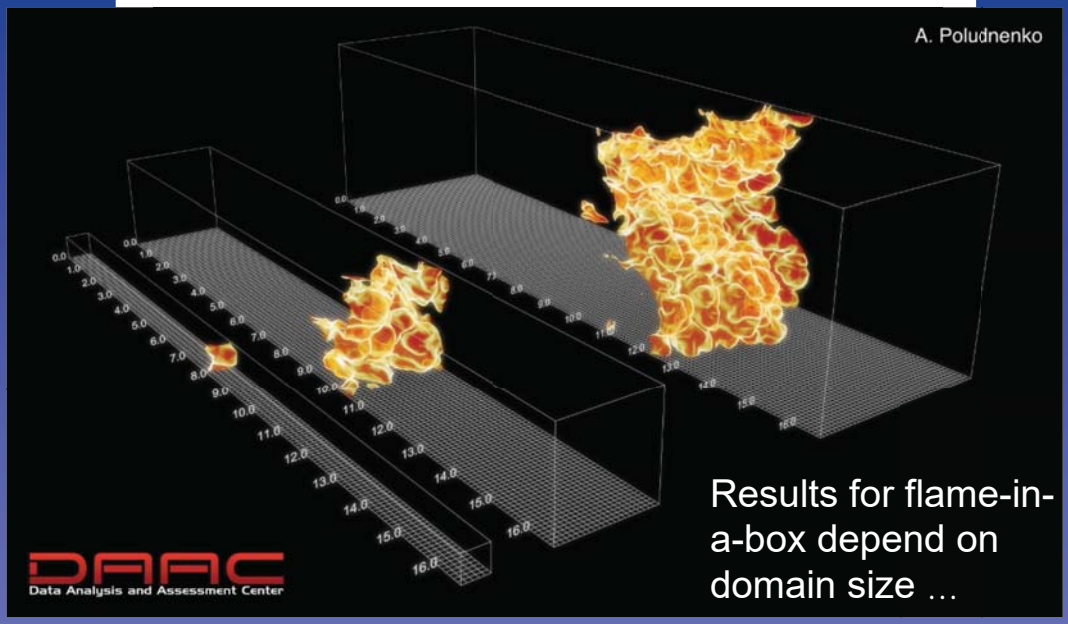

Largest domain: 2,048 × 2,048 × 8,192 ⇒ 32 billion cells

High Ka premixed jet flame

Haiou Wang (now at Zhejiang U) in collaboration with Jackie Chen (Sandia), Bo Zhou, Zhongshan Li, Marcus Aldén (Lund)

Wang et al. Proc. Combust. Inst. 2017

Wang et al. J. Fluid Mech., 2017

UNSW THE UNIVERSITY OF NEW SOUTH WALES

LUND UNIVERSITY

UNSW SYDNEY

Upstream flame weakening

Experimental chemiluminescence

Experimental OH PLIF

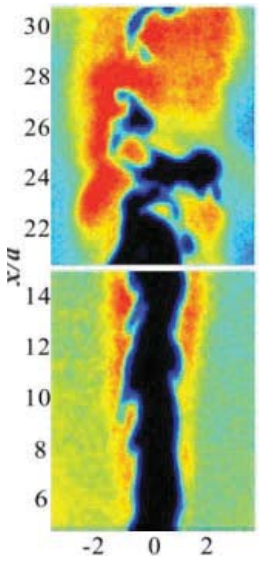

DNS OH

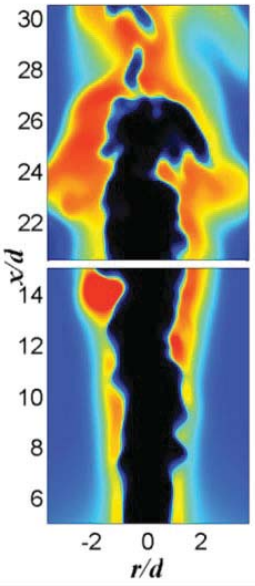

29

UNSW SYDNEY

Stretch factor, I_0, turbulent flame area ratio, A', and turbulent burning rate ratio, S_T/S_L

$$\frac{S_T}{S_L} = \frac{\iint \omega_c dydz \;\; \delta x}{\rho_u \delta A_L(x)} = I_0 \frac{\delta A_T(x)}{\delta A_L(x)} = I_0 A'(x)$$

- The burning rates considerably reduced upstream
- Sensitive to the choice of the species defining c
  - Very small I_0 for CO_2, related to quenching of the oxidation layer
  - Reduced but non-zero for fuel, oxygen, water

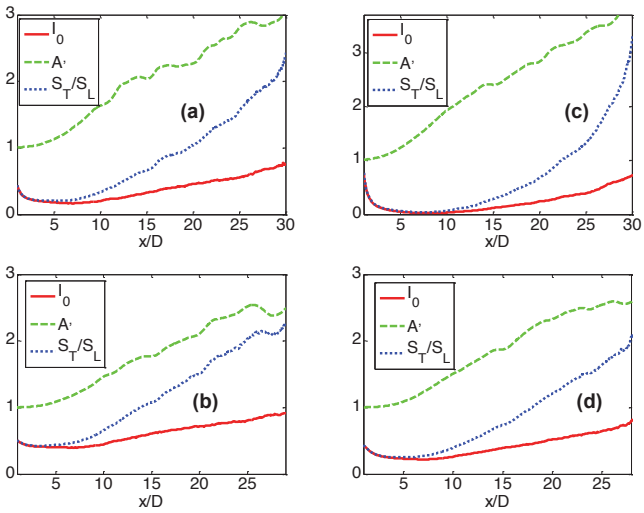

Progress variable, c, defined based on (a) O_2, (b) CH_4, (c) CO_2, and (d) H_2O

What causes this reduced reaction? – comparison to strained laminar flame

- Strain rate selected such that of the strained laminar flame matches that of the turbulent flame
  - Required strain rate found to be close to the strain rate of the **mean** flow

$$\left(\delta_{ij} - \langle N_i N_j \rangle_s\right) \frac{\partial \tilde{u}_i}{\partial x_j}$$

- Note: good agreement was obtained by also accounting for local changes of boundary conditions accounted for in laminar flames

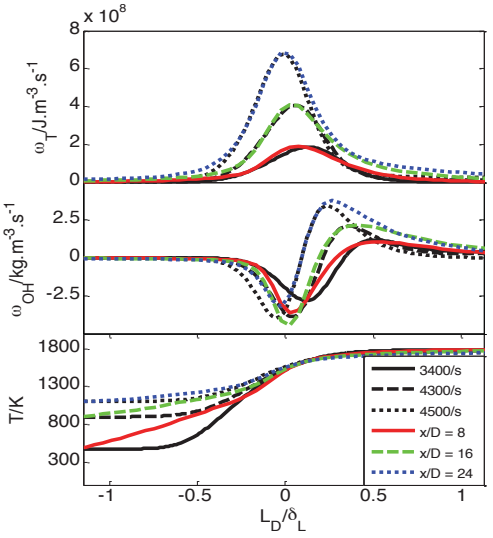

Profiles of heat release rate, OH reaction rate, and temperature

Wall heat transfer in « highly turbulent » swirl flames

- **Wall heat transfer has on strong impact on swirl flame topology [1]**
  - M-flame shape versus V-flame

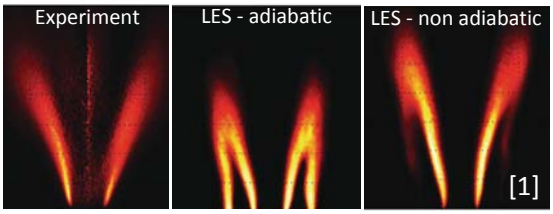

- **The same is observed in the lean-premixed PRECCINSTA burner [2]**
  - High sensitivity of the outer flame lift-off to the mesh resolution

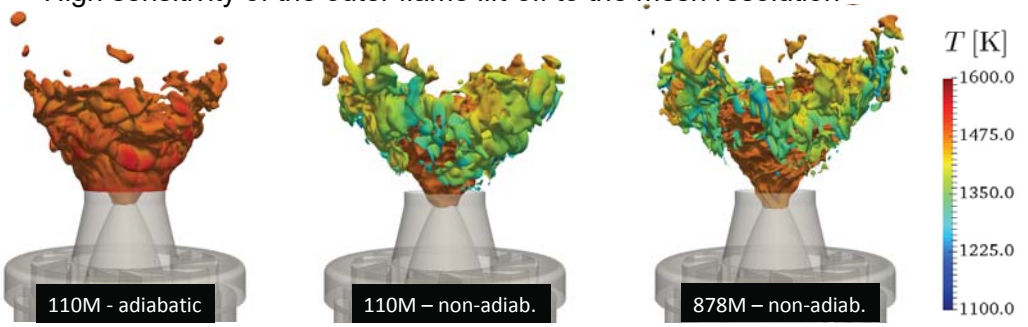

[1] Mercier et al., Combust. Flame, 2016
[2] Bénard et al., PCI, 2019

32

Premixed flame anchored on a backward-facing step

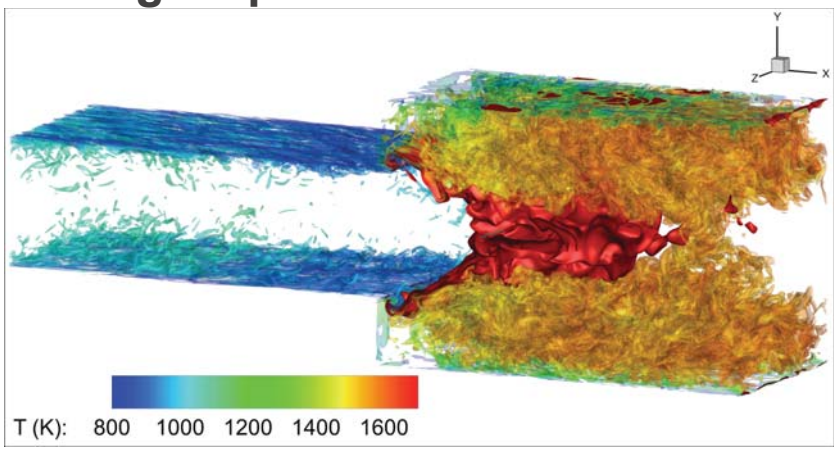

- Konduri, Chen et al., see talk 4A06, 11:50 am, Tuesday
- Completely opposite situation to usual – more turbulence in products than reactants

Main points

Objectives

- Development of models that industry use can is arguably a primary objective with DNS work, however:
  - Generally low levels of DNS work really targeted at models
  - A posteriori tests provide the most definitive conclusions about models, yet almost all DNS works are a priori tests or only fundamental studies

Parameter regimes

- Recent experiments at higher Re show major differences to lower Re conditions => we need to increase DNS Reynolds numbers
  - In high Ka we are constrained in cost by Re, at fixed Ka a factor of 10 increase in Re costs 1000x and only changes Da by a factor sqrt(10)!
- Also pressure, density ratio, compressibility, fuel especially those fuels with low-T activity are parameters of interest

Configurations

- Recent DNS suggest flame in a box cases exhibit large scale results that depend on the size of the box, invalidating their use for some purposes, e.g. as a validation database for a RANS model, and raising important questions about spectral transfer
- Need to increase effort on cases with less trivial geometries; e.g. recirculation zones, mean shear, etc; these cases should have parametric sets and also preferably involve flows that be computed straightforwardly with LES at resolutions where the models are actually doing some work, which may be challenging due to required scale separation

UNSW SYDNEY

Acknowledgements

Evatt Hawkes acknowledges the following support.

Australian Government
Australian Research Council

Funding:

- Australian Research Council
- Australian Renewable Energy Agency

Australian Government
Australian Renewable Energy Agency
ARENA

Computational time:

- National Computational Infrastructure, Australia
- Pawsey Supercomputing Centre, Australia
- NERSC, USA

NCI
PAWSEY supercomputing centre
NERSC

UNSW SYDNEY

Needs for Further Improvements : An Experimental ("Forward-Looking") Viewpoint

Jeffrey A. Sutton

Department of Mechanical and Aerospace Engineering
Ohio State University

Joint PTF-TNF Session

Friday, July 27, 2018

Brief Overview (or Reminder) of Some Knowledge Gaps

- Configuration effects on turbulence-flame interaction: (1) geometry, (2) pressure, (3) turbulence generation (4) fuel type, (5) pilot/back support (6) etc…
- What is the internal structure of highly turbulent flames? Is the fundamental thermo-chemical state very different from that of a laminar flame?
- What is the effect of turbulence-induced stratification (concentration gradients in cold reactants and/or entrainment of hot products)?
- Others? Please add to discussion at the end!

What's Needed?

- Measurements across various configurations – is the reaction zone structure and/or turbulence-flame interaction the same for the same thermo-chemical environment? Does pressure, fuel type, turbulence-generation mechanism, etc. make a difference?
- Quantitative multi-scalar measurements (thermo-chemical state)
- High-resolution, 3D (or 4D) velocity measurements (turbulence dynamics)
- Simultaneous velocity/scalar measurements. Quantitative scalar measurements preferred, but structural topography from imaging yields useful information (i.e., broadened preheat layers, but thin RZ)
- Heat-release rate and burning mode measurements (if partially premixed)
- Local flame/consumption speed

Need for Databases (in the context of models)

- There exist very detailed databases for non-premixed flames that can aid the assessment and development of combustion models
- Quantitative velocity and multi-scalar measurements are available
- Measurements generally have good boundary condition characterization
- Databases cover a broad range of conditions with varying levels of complexity

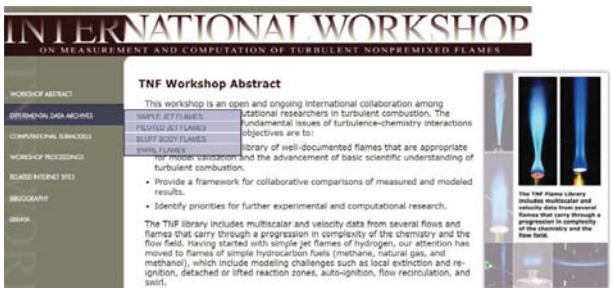

Need for Premixed Databases

- There is data available for premixed flames…but the type of data available varies from experiment to experiment (largely structural and topological information)
- Quantitative velocity and multi-scalar measurements with well-characterized boundary conditions are not readily available for high-Ka premixed flames
- There are some recent pushes in this direction…
- However, many expts. were not designed (nor never intended) to be used for model assessment
- There is a need to plan experiments and burner design with the intent for model "validation"

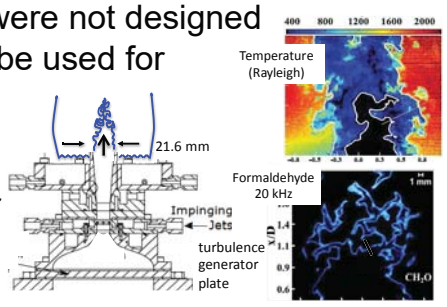

U of M Hi-Pilot Burner

Y_{CO} vs. T

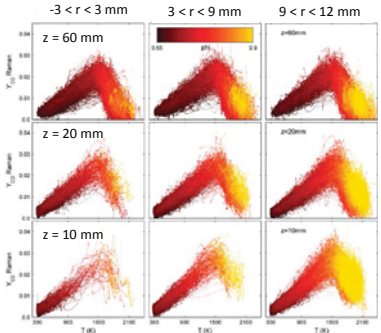

Wabel, Steinberg, Barlow

Configurations and Test Conditions

- High turbulence levels (Ka, u'/S_L, Re_T,…)
- Multiple turbulence-generation mechanisms (shear, decaying, etc). Are measurements in jets, Bunsen flames, swirl flames, etc. consistent?
- Elevated pressure (is this just higher Re # or something else?)
- Real or (at least) more complex fuels ($CH_4 \rightarrow C_3H_8 \rightarrow C_4H_{10} \rightarrow \rightarrow$ kerosene)
- Mach number/compressibility effects
- Other aspects central to practical configurations
  - Large-scale coherent disturbances
  - Transient problems?
  - Sprays flames?

High-Reynolds Numbers and High-Intensity Turbulence

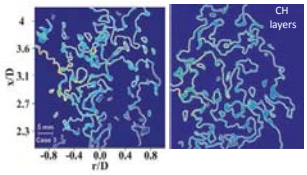

Hi-Pilot Bunsen (Mich)

$u'/S_L > 240$; $Re_T \rightarrow 10^5$
$L_{11}/\delta > 100$

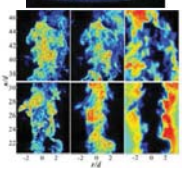

Premixed Jet Flame (Lund)

$u'/S_L \rightarrow 200$; $Re_T \rightarrow 700$
$L_{11}/\delta \approx 10$

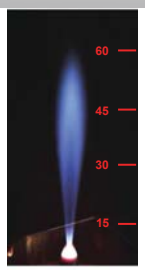

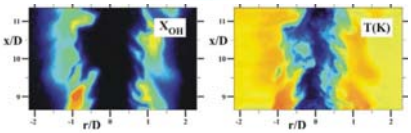

Premixed Jet Flame (Sydney)

$u'/S_L > 200$; $Re_T > 5000$
$L_{11}/\delta \approx 2$

Modified version (OSU)

$u'/S_L \rightarrow 100$; $Re_T > 10^4$
$L_{11}/\delta > 20$

Swirl flames?

Other?

Recommendations for Canonical, Turbulent Premixed Flame Facilities (Lieuwen, GT)

- Combustion regimes at high u'/S_L conditions may be very different in many practical applications (high pressure, larger size) than what is observed in atmospheric pressure, lab scale burners

- An illustrative calculation of u'/S_L for Ka = 1 and Da = 1 limits for CH_4-air at 50 m/s; $\phi = 1$:

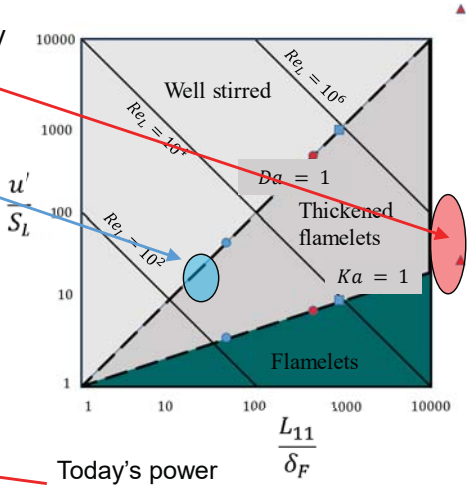

Today's power generation facilities

Today's aircraft engines

Passing out of flamelet regime in atmospheric, lab scale facility at $u'/S_L = 4$

Ka=1

L_{11}	1 atm	20 atm	50 atm
2 cm	4	10	13
20 cm	8	21	29

Da=1

L_{11}	1 atm	20 atm	50 atm
2 cm	46	924	2310
20 cm	462	9238	23095

Recommendations for Canonical, Turbulent Premixed Flame Facilities

- Perhaps there should be identification of higher Reynolds number platforms for high turbulence intensity experiments
- Would likely require a pressurized facility (should we develop a common design that could be shared?)
- This would allow an increase in length scales (due to device size) and decrease of flame thickness (due to pressure).
- Will we see the same basic results as 1-atm, laboratory-scale experiments?

Fuel Type

- *Just a quick summary from Fokion's update this morning at PTF…*
- An analysis of 3276 published turbulent flame studies revealed that < 2% were carried out at pressures ≠ 1 atm; only 0.1% used pre-vaporized fuels
- There are certain flame phenomenon that are sensitive to kinetics (i.e., extinction/re-ignition) and these kinetics can be sensitive to fuel and pressure.
- For heavy fuels: fuel diffusivity and chemistry are certainly different as compared to CH_4. This will change the preheat zone structure!
- There needs to be systematic investigations of fuel type effects. While there may be little difference between 'light' and 'heavy' fuels for the same aero-thermochemical state, the pathway to this particular state and the interaction with turbulence along the way may be very different!

Mach Number and Compressibility Effects (K. Ahmed)

Standing Turbulent Flame in the Compressible Regime

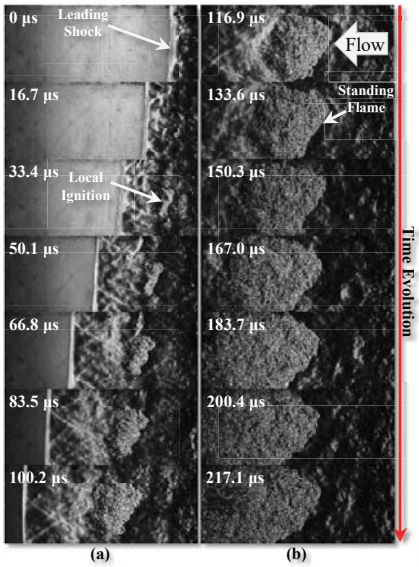

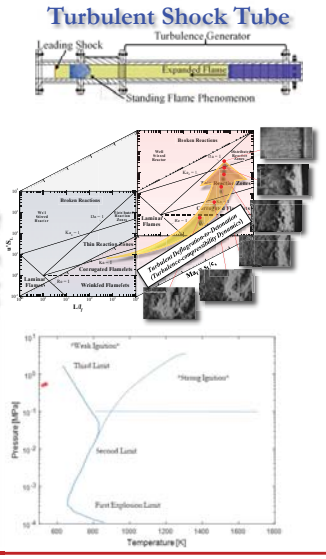

- Turbulent, compressible flames can be explored in the TST, ranging from low compressibility to detonation using shock-driven turbulence
- A standing turbulent, compressible flame is established for 0.1 ms
- Without turbulence, the flow is below auto-ignition regime; turbulence leads to auto-ignition and flame generation

Mach Number and Compressibility Effects (K. Ahmed)

DNS simulations by Towery et al. (2017) reported that as the Mach number increases beyond 0.3, the flow transitions from linear to non-linear compressibility and develops locally supersonic flows giving rise to small-scale eddy shocklets producing energy.

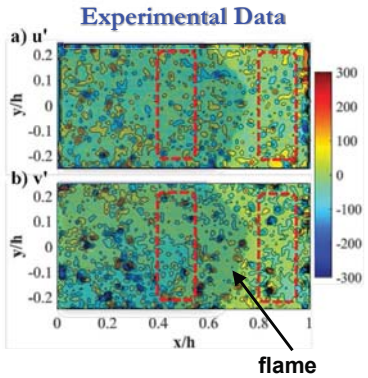

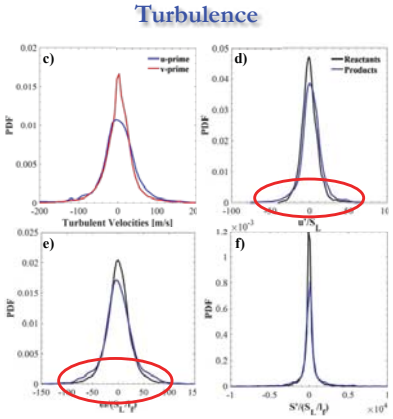

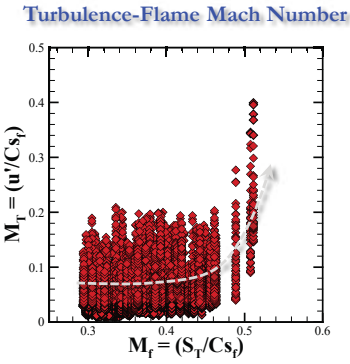

- Turbulence is not attenuated through flame, but rather the data shows flame-generated turbulence
- There is a transition into non-linear compressible regime above $M_f = 0.4$ and evidence of the mechanism of flame-generated turbulence in high compressibility regime

Shear Flow Configurations (Lieuwen, GT)

- In realistic environments, flames exist in hydronamically unstable, shear flows. The flames are subjected to coherent large-scale strain and curvature. This can induced large-scale coherent pressure gradients on fine-scale (stochastic) turbulence
- GT has introduced a geometry that generates large-scale disturbances by utilizing an upstream turbulent generator (variable, 5-25%) that introduces coherent, fluctuating curvature
- Results show that S_L is coherently modulated in time; there is coupling between strain and flame curvature

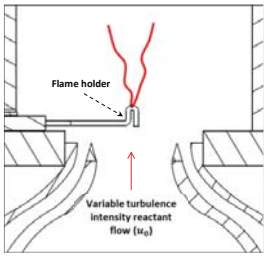

Humphrey, L. J., Emerson, B., and Lieuwen, T. C., 2017, "Premixed turbulent flame speed in an oscillating disturbance field," J. Fluid Mech., 835, pp. 102-130.

Shear Flow Configurations (Steinmetz et al., Sydney)

- Sydney has a platform for investigating highly shear flames with shear inhomogeneity
- Shear is introduced at jet exit plane for the same mixture; concentric jet and annulus tubes allow control of turbulence profiles through: (1) variation of jet velocities and varying relative velocities of jet and annulus (2) Recession of central jet (up to 40 diameters)
- With increasing shear, CH remains thin, but does become increasingly broken (maybe different from what has been observed with configs like HiPilot?)
- What types of data do modelers need/want from this type of system?

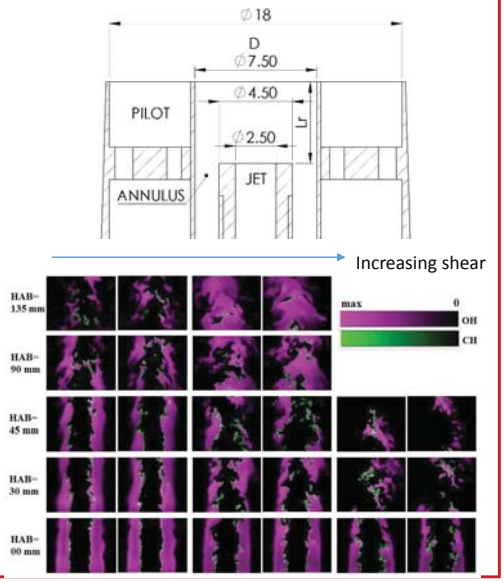

Experimental Challenges

- Quantitative scalar measurements (Raman/Rayleigh/LIF) are difficult. For premixed flames, resolving scalars over 'thin' flame thickness is a major challenge
- Overwhelming majority of measurements are at 1 atm with CH_4 as fuel; moving to more complex fuels leads to significant interference in measurements. How does the uncertainty grow as fuel increases in complexity? What is the fuel type 'limit', C2, C3, C4,…?
- Increasing pressure increases Re # and decreases smallest turbulence length scales and flame thickness (δ) → L_{11}/δ increases. This changes 'position' on Borghi diagram and also creates a measurement dynamic range problem
- High-pressure measurements require facility with walls/windows. Many diagnostics which are 'friendly' in open environments are very difficult in enclosed configurations.

Emerging Diagnostics and Capabilities

- Quantitative heat release measurements
- High-resolution velocimetry
- High-speed imaging uses for model assessment?

Method to Approximate CM and HRR from Major Species, T, and OH (Hartl, Zhao, Barlow, Geyer, Hasse, Dreizler)

Approximation method:

Reduced thermochemical state (T and 7 major species + OH)

CO_2 N_2 CO O_2 CH_4 H_2O T OH H_2

Constrained 0D simulation (temporal evolution to quasi steady state)

GRI Mech 3.0

Approximated full thermochemical state

CO_2 N_2 CO HO_2 O_2 OH CH_3 H_2O CH_2O O CH_4 HCO H_2O_2 T (etc.) H H_2

CM and HRR are calculated from the approximated full state

Hartl et al. CNF (2018)

Options:

- Allow Y_{major} to evolve within bounds of experimental uncertainty (original approach with experimental data)
- Keep T, Y_{major} fixed as minor species evolve to quasi steady state (approach used with DNS data)
- Add OH as fixed input for improved accuracy on HRR

Method to Approximate CM and HRR from Major Species, T, and OH (Hartl, Zhao, Barlow, Geyer, Hasse, Dreizler)

Lund flame DNS

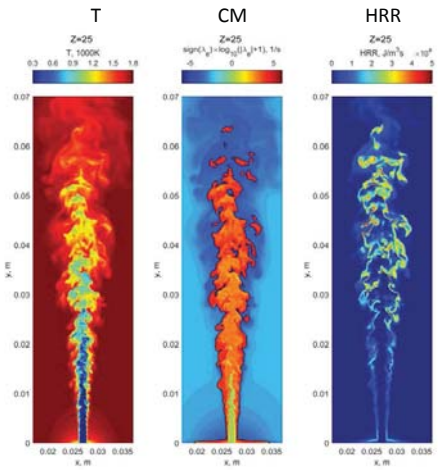

*DNS by: H. Wang, et al., PCI (2017), **36**:2045-2053*
*H. Wang, et al., JFM (2017), **815**:511536*
CEMA by: Xinyu Zhao, Tianfeng Lu, Chao Xu, Ji-Woong Park

Test of Approximation

Extract 1D "slices" from two DNS cases

- ϕ_{jet} = 0.7; ϕ_{coflow} = 0.9; x/D = 8, 16, 24
- ϕ_{jet} = 0.4; ϕ_{coflow} = 0.9; x/D = 8, 16, 24

- Use T, Y_{major} from DNS as input
- Compare CM and HRR from the approximation to those from full DNS
- Repeat using T, Y_{major}, and OH

Preliminary Results

ϕ = 0.7, 24D rightside

- fully resolved DNS results
- approximated results (Raman species fixed)
- approximated results (Raman species, OH fixed)

- Good agreement on CM (except at low T)
- Good agreement on CM crossing location and ΔCM (magnitude of change at the crossing)

- Close agreement on HRR when OH is included, but some deviations (diffusion effects? mechanism?)

- Examples of high HRR not associated with zero crossing

- Similar results for ϕ = 0.4 case.

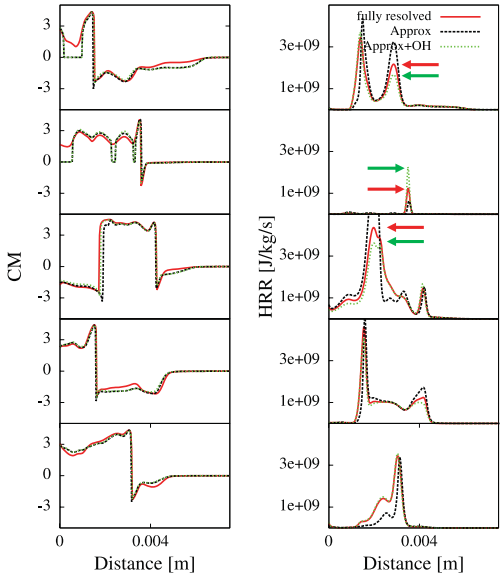

High-Resolution Velocimetry (Sutton)

- Particle Imaging Velocimetry (PIV) is the *de facto* velocity measurement in flows and flames, but it is a "non-dense" estimate of the velocity field since you get one velocity vector per interrogation window (IW) and $N_{IW} << N_{pixels}$
- The relative lack of spatial resolution of PIV leads to errors in high-gradient flow regions and in the estimation of important derivative quantities
- We introduce a wavelet-based optical flow (WOF-X) method for high-resolution velocity imaging (still based on tracer particle fields for right now)
- Find velocity field $\underline{v}$ that transforms particle image I_0 to I_1 in time interval Δt

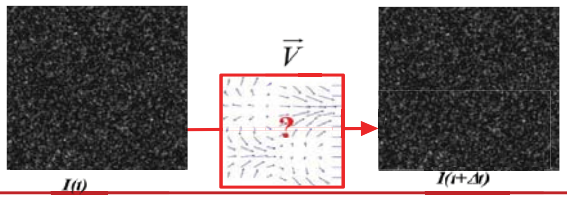

High-Resolution Velocimetry (Sutton)

- For optical flow methods, image intensity or 'brightness' is assumed as a conserved quantity

$$\frac{\partial I\left(\underline{x},t\right)}{\partial t}+\underline{v}\left(\underline{x},t\right)\cdot\nabla I\left(\underline{x},t\right)=0$$ Optical flow eqn.

$$I_0\left(\underline{x}\right)-I_1\left(\underline{x}+\underline{v}\left(\underline{x}\right)\right)=0$$ Displaced frame difference (DFD) eqn.

$$\hat{\underline{v}}=\underset{\underline{v}}{\operatorname{argmin}}\ J_D\left(I_0,I_1,\underline{v}\right)+\lambda J_R\left(\underline{v}\right)$$

Solved via minimization problem
J_D is a penalty function integrated over the image
λ is a regularization parameter

- There are more *unknowns* than equations, so the problem does not have a unique solution (under constrained). **Reduce number of unknowns using wavelets**
- Multi-resolution strategy that is not sensitive to individual pixel intensity

Test Case – 2D DNS (Sc = 0.7, Re = 3000 isotropic turbulence)

Synthetic particle field

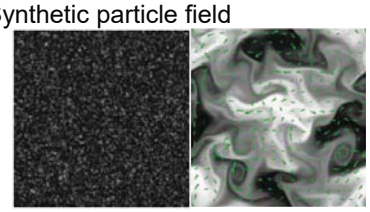

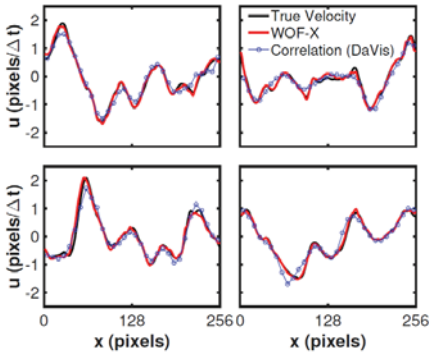

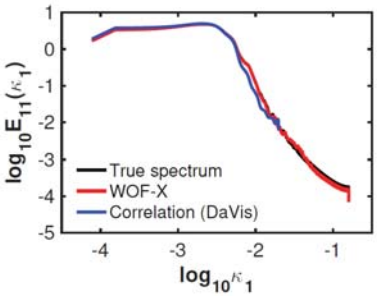

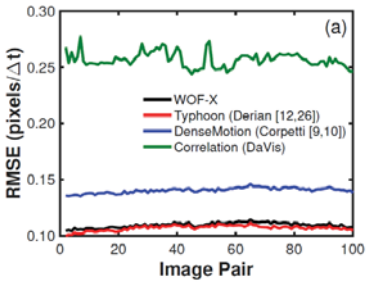

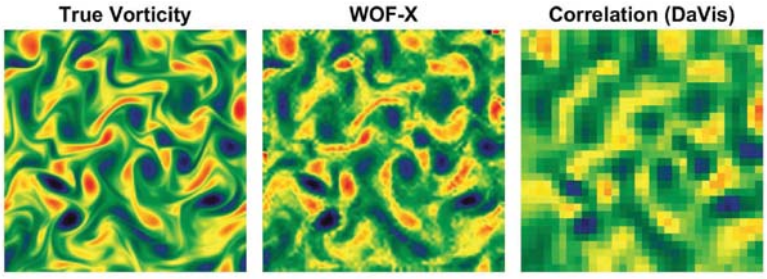

First Attempt on Experimental Reacting Flow

- Took non-optimized (for WOF-X) PIV particle data from Aaron Skiba from Hi-Pilot Burner

Correlation | **WOF-X** | **Non-reacting**

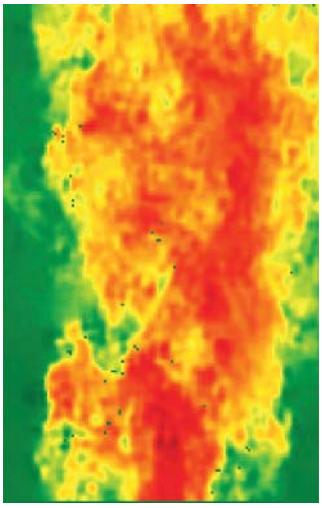

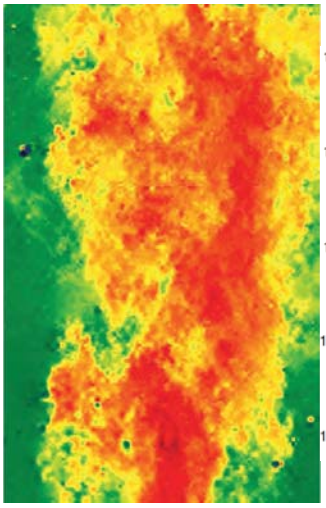

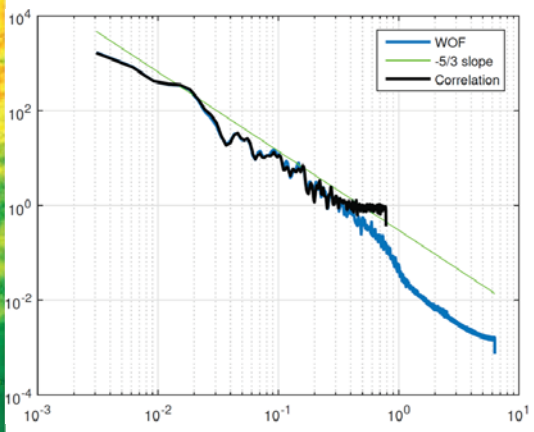

First Attempt on Experimental Reacting Flow

- Took non-optimized (for WOF-X) PIV particle data from Aaron Skiba from Hi-Pilot Burner

Correlation | **WOF-X** | **Reacting**

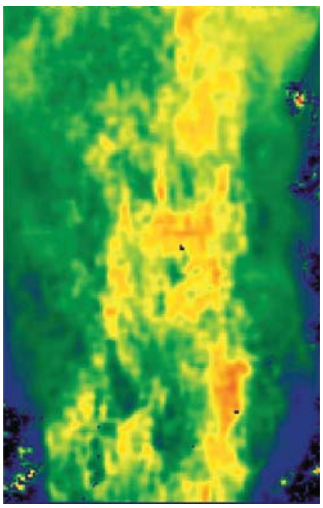

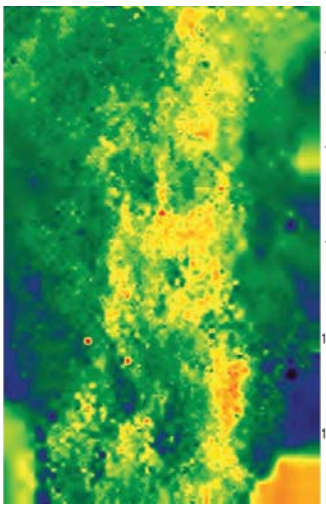

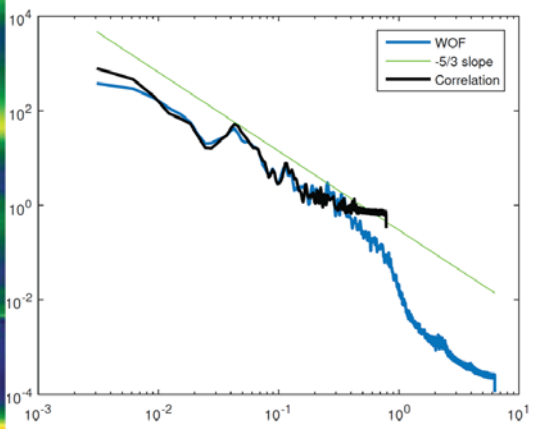

High-Speed Imaging

- Over the last decade there has been a large surge of kHz-rate imaging in both premixed and non-premixed flames. Beyond more ‘typical’ applications of high-speed PIV and OH PLIF, there continue to be advances…

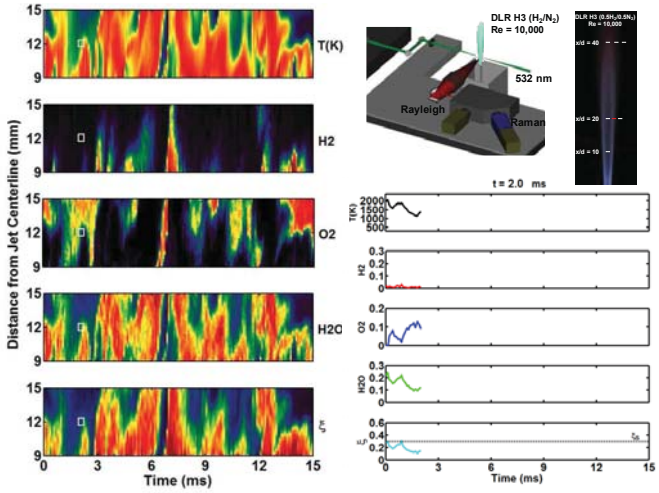

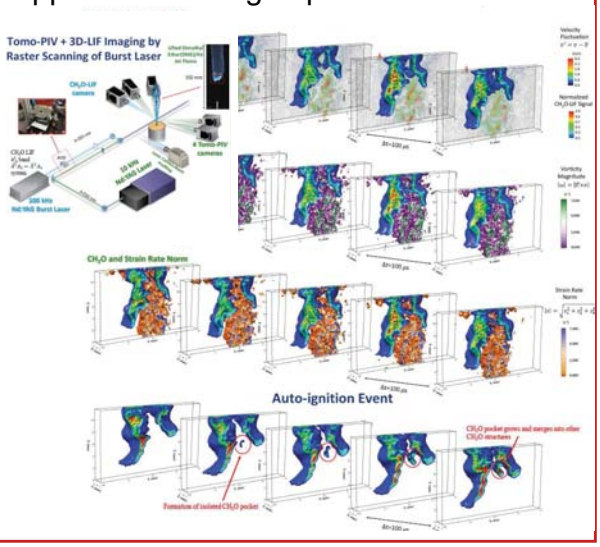

High-Speed Imaging

- While time-resolved imaging and measurements clearly have value in understanding flow and combustion dynamics (especially in the context of transient and/or unsteady events), and open question is:

  “how to use them for model assessment and/or validation”?

- One can not compare any single realization, so it needs to be a time-based statistic…

Comments and Open Questions – You Discuss!

- First, let's agree on some terminology (e.g., Ka, stratification, etc.)
- Should we move to higher pressures? This may be a nightmare for experimentalists, but perhaps DNS can….(although keeping the same L_{11}/δ is not what happens in a real system)
- Fuels??? CH_4 is still good when just assessing fundamental flame physics. Should we at least move to C2-C4 to assess fuel effects? Pre-vaporized fuels?
- How to coordinate new burner designs with modeling efforts?
- Other thoughts????

Joint TNF/ISF Session: Progress on Turbulent Sooting Flames

Coordinators: Bassam B Dally, Michael E Mueller

Panelists: Simone Hochgreb, William L Roberts, Venkat Raman

The objective of the session was to bring together the TNF and ISF turbulent flames communities to discuss common challenges and strategies for addressing experimental and computational challenges in turbulent sooting flames. The session began with an overview of recent ISF turbulent flames progress followed by comments from three panelists and discussion.

An overview and objectives of the ISF Workshop was briefly presented to the TNF community. An overview of current experimental capabilities for turbulent sooting flames was then presented including (Time-Resolved) Laser Induced Incandescence for soot volume fraction and primary particle size, Coherent Anti-Stokes Rayleigh Scattering and non-linear Two-Line Atomic Fluorescence for temperature, and krypton Planar Laser Induced Fluorescence for mixture fraction. The emphasis of the overview was on the accuracy of the measurement techniques and their suitability for lightly versus highly sooting turbulent flames. An overview of target flames and computational comparisons was then presented. ISF target flames include both jet flames and recirculating flows (bluff body flames and confined swirl flames) with parametric sweeps including Reynolds number, global strain rate, fuel composition, pressure, and overall equivalence ratio. The two types of targets accentuate different aspects of soot-turbulence-chemistry interactions, with jet flames stressing small-scale interactions including slow PAH chemistry and recirculating flows stressing large-scale interactions, notably the residence time at different mixture fractions where different growth mechanisms dominate. For comparisons with experimental measurements, progress between consecutive Workshops has been rapid with decreasing variance between models with detailed model improvements being made based on insights from limited experimental measurements and DNS data. However, the fundamental challenge in understanding the underlying physics and uncovering the source of discrepancies is a fundamental lack of data, particularly (simultaneous) data on flame structure, including temperature and speciation, with soot measurements.

Three panelists then spoke on the experimental and computational challenges. Simone Hochgreb discussed the range of experimental configurations being investigated in the community, ranging from simple flames to more technical combustion devices, and recent advances in diagnostics for turbulent sooting flames including multi-species Raman, krypton PLIF, CARS, and LIGS. Challenges in making measurements in turbulent sooting spray flames were highlighted. Bill Roberts highlighted recent progress at KAUST in making high-pressure measurements in turbulent sooting flames. Venkat Raman discussed the differences in the modeling challenges between jet flames and recirculating flows with respect to small-scale and large-scale intermittency. The importance of history in soot evolution was also discussed and the need to identify canonical configurations that match the history of soot evolution in technical combustion systems. Fundamental differences between detailed, PAH-based soot models and semi-empirical, acetylene-based soot models were also highlighted with a suggestion to design experiments to stress each class of models.

Subsequent discussion focused on the feasibility in various measurement strategies and identified a number of experimental groups starting to look into turbulent sooting flames. All agreed that the challenge is significant from both computational and experimental perspectives with much working remaining.

Joint TNF/ISF Session: Progress on Turbulent Sooting Flames

Bassam B. Dally
School of Mechanical Engineering
University of Adelaide

Michael E. Mueller
Department of Mechanical and Aerospace Engineering
Princeton University

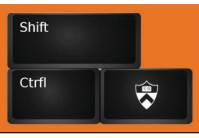

Joint ISF/TNF Session
Dublin, Ireland
July 28, 2018

ISF Workshop

- Brief History and structure
  - Established in 2012 as a satellite meeting to the combustion symposium;
  - Managed by an Organising Committee and guided by an Advisory Scientific Committee;
  - Scientific committee meets yearly;
  - ISF4 workshop is organized in two themes: Laminar and Turbulent; each have a leader and co-leader
  - Database is organized on the workshop website: https://www.adelaide.edu.au/cet/isfworkshop/data-sets/

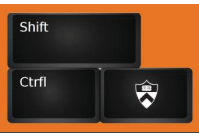

ISF Workshop Aims

- Aims of Workshop
  - To advance understanding and predictive capability of flames with soot, to identify gaps in this understanding and to coordinate research programs to address them;
  - To identify well defined target flames and coordinate additional experiments that provide suitable data for model development and validation, spanning a variety of flame types and fuels in each of the research programs;
  - To establish an archive of the detailed data sets of target flames with defined accuracy and to provide a forum for the exchange and dissemination of these data.

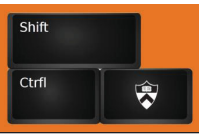

Experimental Challenges

- Laminar Flames
  - Traditionally involved gas sampling, line of sight extinction, soot particulate sampling, thermocouples measurements and CARS point measurements;
  - Data was essential to development of soot models, sampling interfered with flames, measurements sometime were limited to low sooting flames
- Turbulent Flames
  - Strong radiation emission from the flame, beam steering, signal absorption, strong Mie scattering signal, highly intermittent measurements, interdependency is critical requiring simultaneous measurements, planar measurements are essential to measure gradients, soot is highly dependent on flow dynamics, etc..

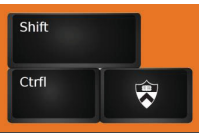

Methodology Advancement

- Soot Volume Fraction
  - Laser Induced Incandescence, LII, has been developed to provide temporal and spatially resolved planar measurements of soot. Choice of wavelength, calibration and quantification are still under investigation.
  - The minimum detection limit is 3ppb, on a shot by shot basis;
  - Measurement uncertainty on the mean values is ~25%, due to uncertainty in the extinction and calibration constants;
  - The laser sheet thickness in the flame is measured to be 0.75 mm. [Adelaide Group]

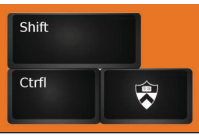

Methodology Advancement

- Primary Soot Particles' Size
  - Time Resolved Laser Induced Incandescence, Ti-ReLII, has been developed to provide two dimensional soot particles size distribution. Its precision depends on the temporal resolution of the signal decay, model used to estimate the size and estimating the soot particles' temperature.
  - The minimum detection limits for dp is 5 nm and the uncertainties is ~10 nm. [Adelaide Group]

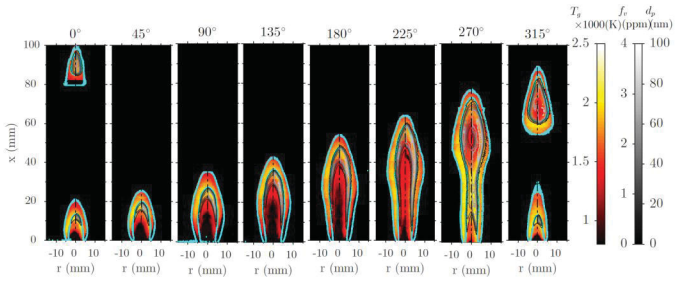

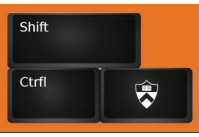

Methodology Advancement

- Gas Temperature Measurement - CARS
  - Coherent Anti-Stokes Rayleigh Scattering, CARS was the technique of choice to measure gas temperature in particle laden flows. These measurements were restricted to point measurements and low sooting intensity. Planar CARS (including fs - Ps excitation) measurements have been attempted lately, but is yet to be a technique of choice;
  - Accuracy is report to be estimated ~2 - 3% across the entire spatial domain [Campbell et al. 2016]
  - Reported spatial resolution of <40 µm

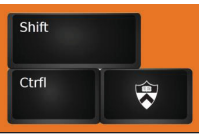

Methodology Advancement

- Gas Temperature Measurement - nTLAF
  - The non-linear Two-Line Atomic Fluorescence, nTLAF Technique relies on the excitation of a seeded metal into the flame, the ratio of two LIF signals and predetermined calibration constants to calculate the gas temperature. Indium atoms were generated in the flame by seeding Indium tri-chloride and Indium nano-particles into gaseous and liquid fuels;
  - This technique is not suitable to measuring temperatures below 800K due to low anti-stokes signals at these temperature. Resolution of 500 µm.
  - Precision is 4.1% or ~65-75K see paper by [Sun in symposium]

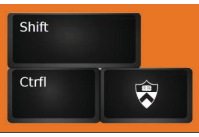

Methodology Advancement

- Gas Temperature Measurement - nTLAF
  - Using Gallium instead of Indium as the seed in the nTLAF technique have the potential to cover the whole temperature range from 300K-2500K. The group at Lund have successfully applied this technique to laminar sooting flames using Gallium tri-Chloride in gaseous form.;
  - The Adelaide group has plans to apply this technique to turbulent flames this year.
  - Precision was report 1% and the accuracy 2-3% (20-30 K); [Jesper Borggren, Doctoral thesis, (2018), Lund, Sweden]

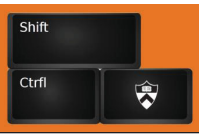

Methodology Advancement

- Gas Temperature Measurement – nTLAF - Ga

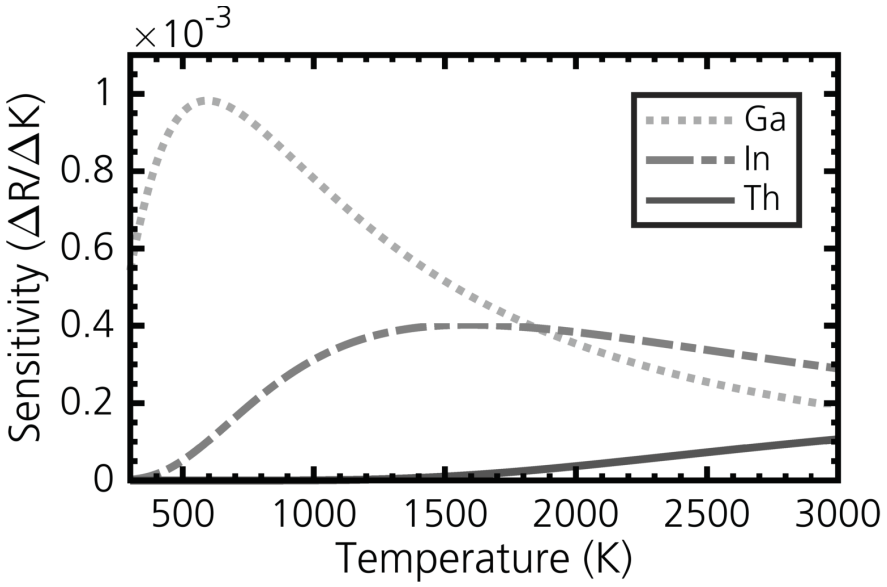

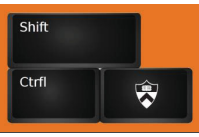

Jesper Borggren,
Doctoral thesis, (2018), Lund, Sweden

Methodology Advancement

- Gas Temperature Measurement - nTLAF - Ga

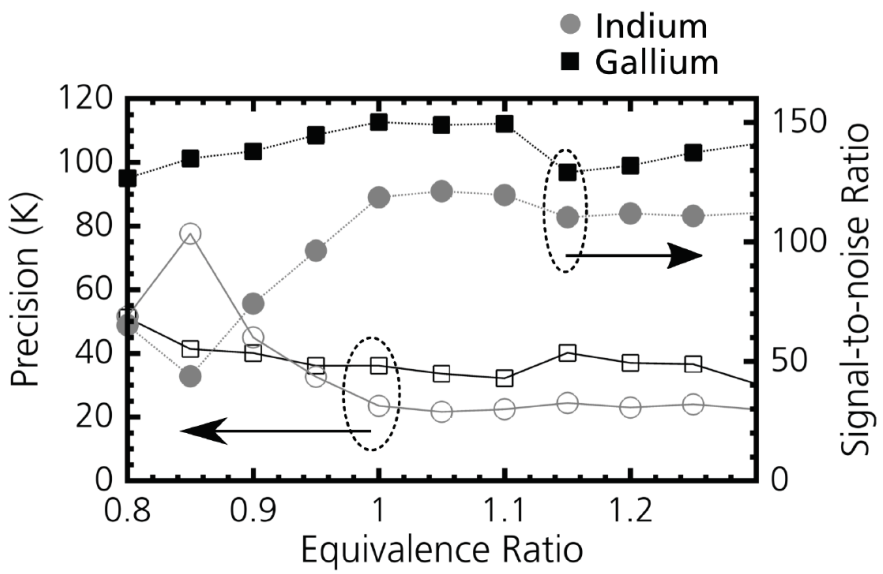

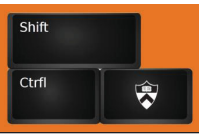

Jesper Borggren,
Doctoral thesis, (2018), Lund, Sweden

Methodology Advancement

- Mixture Fraction Measurements
  - The mixture fraction is inferred from laser-induced fluorescence of krypton gas seeded into the fuel stream. To obtain mixture fraction from the fluorescence signal, the signal must be corrected for density and fluorescence quenching effects. This correction is accomplished by invoking an assumed state relationship that is derived from a laminar strained-flame calculation. Once properly calibrated, the krypton planar laser-induced fluorescence data give the mixture fraction, temperature and major species near the regions of soot formation. The krypton is seeded into the fuel jet at a mole fraction of approximately 4%.
  - Low signal to noise ratio, line measurements only.
  - Limited use in highly sooting flame.

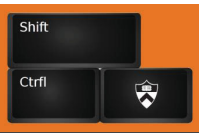

Target Flames

- Type I: Jet Flames
  - Adelaide Jet Flames
    - Nonpremixed simple jet flames
      - Fuel: $C_2H_4/H_2/N_2$ (40/40/20)
    - Two parametric sweeps:
      - Variation in Reynolds number at fixed global strain rate
      - Variation in global strain rate at fixed Reynold number
    - Data: Exit velocity, soot volume fraction (LII), centerline temperature (thermocouple), and radiant heat flux
  - Sandia Jet Flame
    - Nonpremixed piloted jet flame
      - Fuel: C_2H_4
    - Data: Soot volume fraction (LII), soot temperature, OH PLIF, PAH PLIF, and radiant intensity

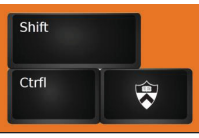

Target Flames

- Type II: Recirculating Flows
  - Adelaide Bluff Body Flames
    - Nonpremixed bluff body flames
      - Fuels: Various C_2H_4/H_2 mixtures and LPG
    - Parametric sweeps
      - Variation in C_2H_4/H_2 ratio at constant thermal power
    - Data: Soot volume fraction (LII)
  - DLR Combustor
    - Nonpremixed confined swirl flames
    - Parametric sweeps
      - Variation in pressure at volume flow rates
      - Inclusion/exclusion of secondary air injection
    - Data: Soot volume fraction (LII), temperature (CARS), velocity (PIV), OH PLIF, PAH PLIF

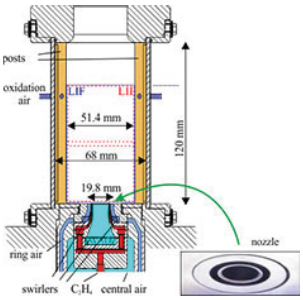

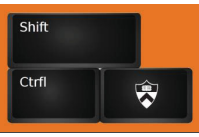

Target Flames

- Why two distinct sets of target flames?

Jets

Diesel Engines

Furnaces

Recirculating Flows

Aviation Turbines

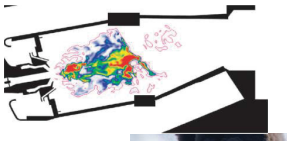

Fires

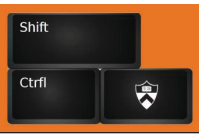

Target Flames

- Why two distinct set of target flames?
  - Jet Flames
    - Role of Polycyclic Aromatic Hydrocarbons (PAH) is critical in the formation and growth of soot.
    - PAH chemistry is slow and extremely sensitive to turbulent straining.
  - Recirculating Flows
    - Growth of soot is dictated by residence times at various mixture fractions.
    - Different growth mechanisms dominate at different mixture fractions.

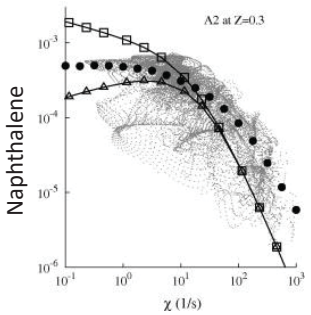

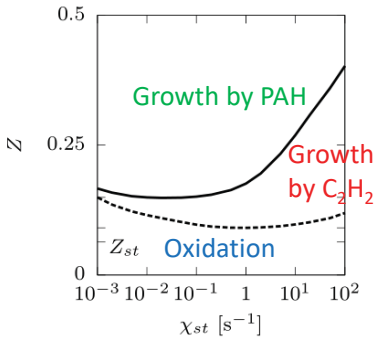

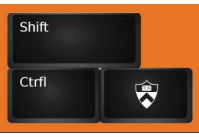

Target Flames

- Progress from ISF-3 to ISF-4
  - Example: Sandia Jet Flame
    - For ISF-3, the results for soot volume fraction were somewhat scattered.
      - However, the consistent trend was that most detailed models tended to underpredict the soot volume fraction and significantly so.
    - For ISF-4, the results were less scattered and in better agreement with the experimental measurements but still work to do.
      - Some differences between soot models.
      - Improvements in detailed models derived based on insights from both experiments and DNS.

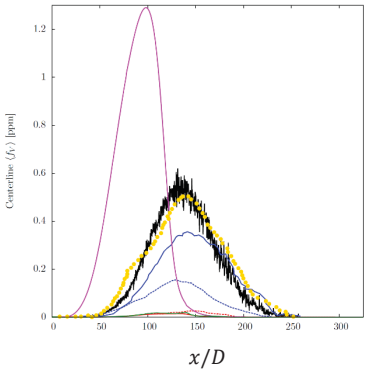

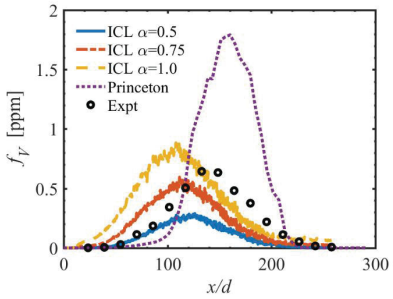

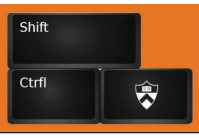

Challenges

- Why are our predictions wrong?
  - Since we have relatively sparse data, currently limited to primarily soot volume fraction and perhaps limited measurements of some temperature, uncovering the sources of discrepancies is a challenge.
    - Is something fundamentally wrong with the turbulent flame structure?
      - Velocity, mixture fraction, temperature, major species
    - Is something fundamentally wrong with modeling the small hydrocarbon fragments and their interactions with turbulence?
      - Acetylene mass fractions
    - Is something fundamentally wrong with modeling PAH and their interactions with turbulence?
      - PAH mass fractions
    - Is soot, etc. correctly correlated with other quantities?
      - Would simultaneous measurements help?

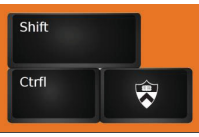

Challenges

- Information via DNS
  - Since measurements can be difficult, tremendous insight has been drawn from large-scale DNS.
    - Sensitivity of PAH to strain (turbulence-chemistry interactions)
    - Mechanistic explanation for the criticality of PAH-based processes in turbulent jet flames (turbulent transport)
  - Challenges with DNS
    - Many species required to describe even two-ring aromatics (> 50 species)
    - Very long run times required to access soot evolution time scales (and any slow recirculation time scales)
    - Increased reliance on subcontinuum chemistry and soot ***models***
  - Bottom Line: DNS is invaluable for physical insight and detailed data for model evaluation but does not replace experiments.

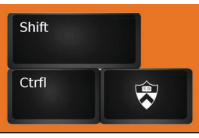

Challenges

- What should be measured?
  - How do we make "TNF" measurements in sooting flames?
    - Maybe this is not even possible…
    - Are there lesser techniques not utilized in non-sooting flames that would be appropriate for sooting flames?
  - Should we make measurements in a family of flames ranging from non-sooting to sooting with the same basic flame structure?
    - "TNF" measurements in the non-sooting flames
    - "ISF" measurements in the sooting flames
    - What would be a suitable flame series in terms of configurations, fuels, etc. considering both experimental and computational constraints?
    - What would be the best parameter to vary from sooting to non-sooting?

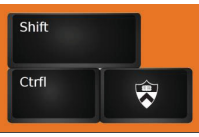

Challenges

- What should be measured?
  - How do we make "TNF" measurements in sooting flames?
    - Maybe this is not even possible…
    - Are there lesser techniques not utilized in non-sooting flames that would be appropriate for sooting flames?
  - Should we make measurements in a family of flames ranging from non-sooting to sooting with the same basic flame structure?
    - "TNF" measurements in the non-sooting flames
    - "ISF" measurements in the sooting flames
    - What would be a suitable flame series in terms of configurations, fuels, etc. considering both experimental and computational constraints?
    - What would be the best parameter to vary from sooting to non-sooting?

UNIVERSITY OF CAMBRIDGE

A range of flame experiments

	non-premixed ..premixed	Examples	Measurements	Fuel	Pressure
jet		TUD, Sandia, DLR	T Y_i U OH NO	CH_4 H_2	
piloted jet/bluff		Sandia/TUD C-F, Cabra PPJB, DJHC	T Y_i U OH NO	CH_4 H_2 DME CO CH_3OH	
stratified		TUD, CAM, Sydney	T Y_i U OH CH2O	CH_4 CH_4 H_2	
technical		TECFLAM, PRECCIINSTA, GTMC, Siemens,	T Y_i U OH CH2O	CH_4 H_2	P
soot		NASA LDI DLR-Adelaide DJHC, DLR-RQL	T f_v OH	CH_4 C_2H_4	P
spray		Sydney, Cambridge, DLR, DHSC, NASA LDI, CORIA	T* U d OH CH2O	Ethanol, methanol, alkanes, jet A1	P

50,000 <Re <100,000

10 <Ka <5000

Radiant background!

Measurement techniques for radiant backgrounds

				Resolution	Pros/Cons	Cost	Expertise
correlation	PIV	**u**	velocity	kHz, µm..mm (image)	High signal *Radiant interference*	$$	-
	LDA	**u**	velocity	kHz, µm..mm (point)	High signal *Radiant interference*	$$	-
	LIF	Y,T	selected species mass fraction temperature	kHz, 0.1-1 mm	Good signal *Species specific* *Quenching, calibration*	$$	+
scattering	Rayleigh	T,ρ	density, temperature	(k)Hz, 0.1-1 mm	Simple bulk technique *Low signal*	$$	++
	Raman	**Y**, T	major species mass fraction, temperature	Hz, 0.1-1 mm	Multiple species *Low signal* *Many interferences*	$$$	+++
coherent	CARS	**Y**, T	major species mass fraction, temperature	(k)Hz, 1 mm	Coherent *Alignment*	$$$$	+++
	LIGS LIEGS	T	temperature	Hz, 1-5 mm	Coherent *Needs absorber/low signal* *Alignment*	$$	++
	DFWM	Y	selected species mass fraction	Hz, 1-5 mm	Coherent *Species specific* *Alignment*	$$	++

Polarization separation – remove C_2 bands

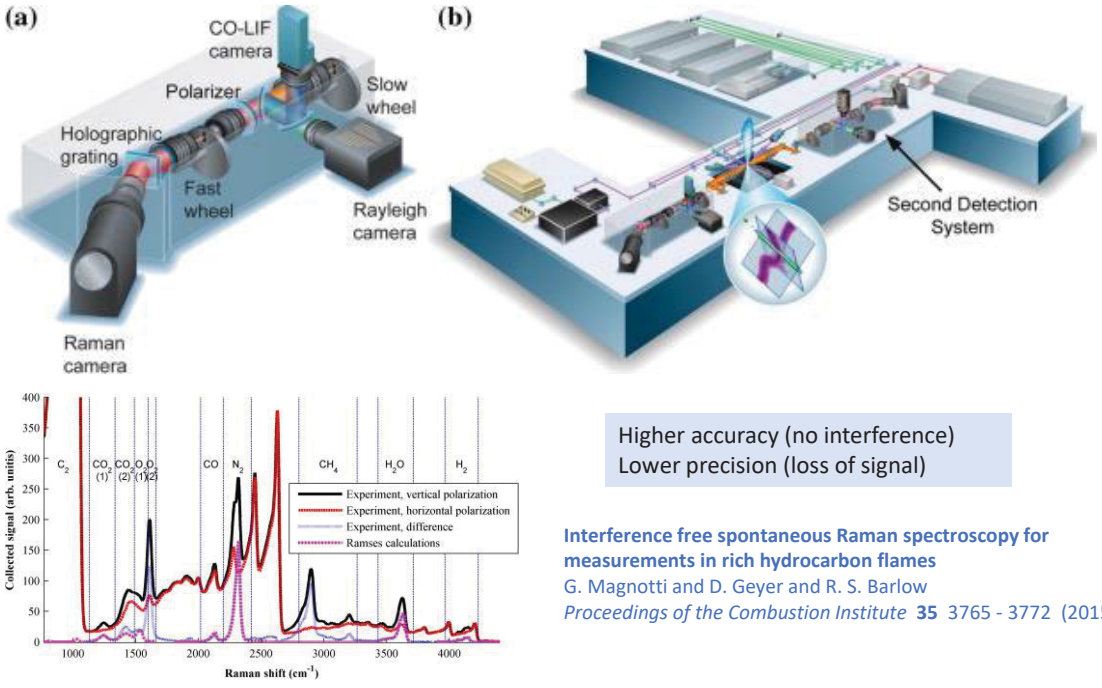

Higher accuracy (no interference)
Lower precision (loss of signal)

Interference free spontaneous Raman spectroscopy for measurements in rich hydrocarbon flames
G. Magnotti and D. Geyer and R. S. Barlow
Proceedings of the Combustion Institute **35** 3765 - 3772 (2015)

Dual SBG Raman spectroscopy + polarization

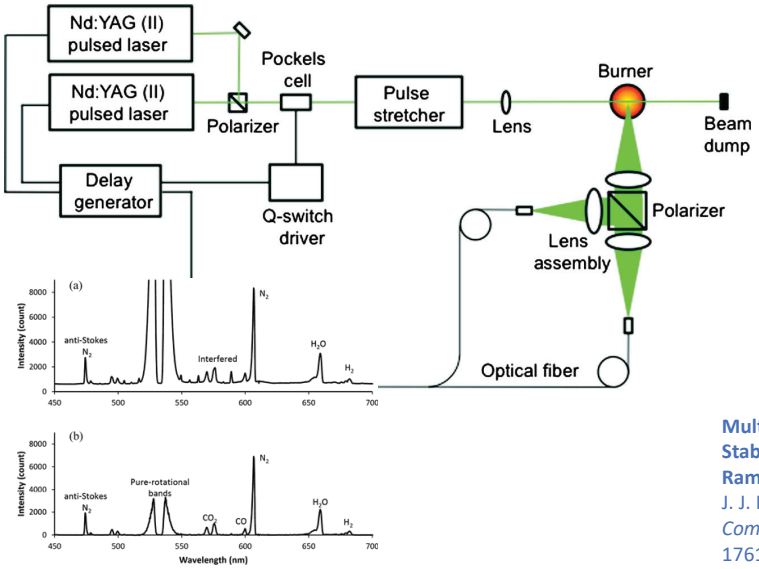

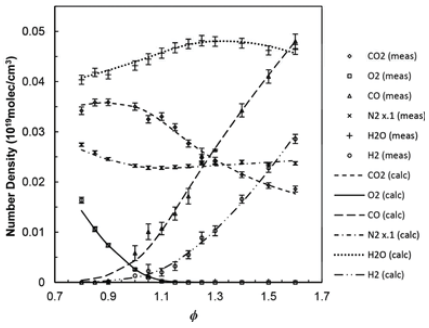

Multiscalar Analyses of High-Pressure Swirl-Stabilized Combustion via Single-Shot Dual-SBG Raman Spectroscopy
J. J. Kojima and D. G. Fischer
Combustion Science and Technology **185** 1735-1761 (2013)

Subframe burst gating (stokes+anti-stokes)
Removal of interferences from fluorescence

Kr-LIF (soot and mixture fraction)

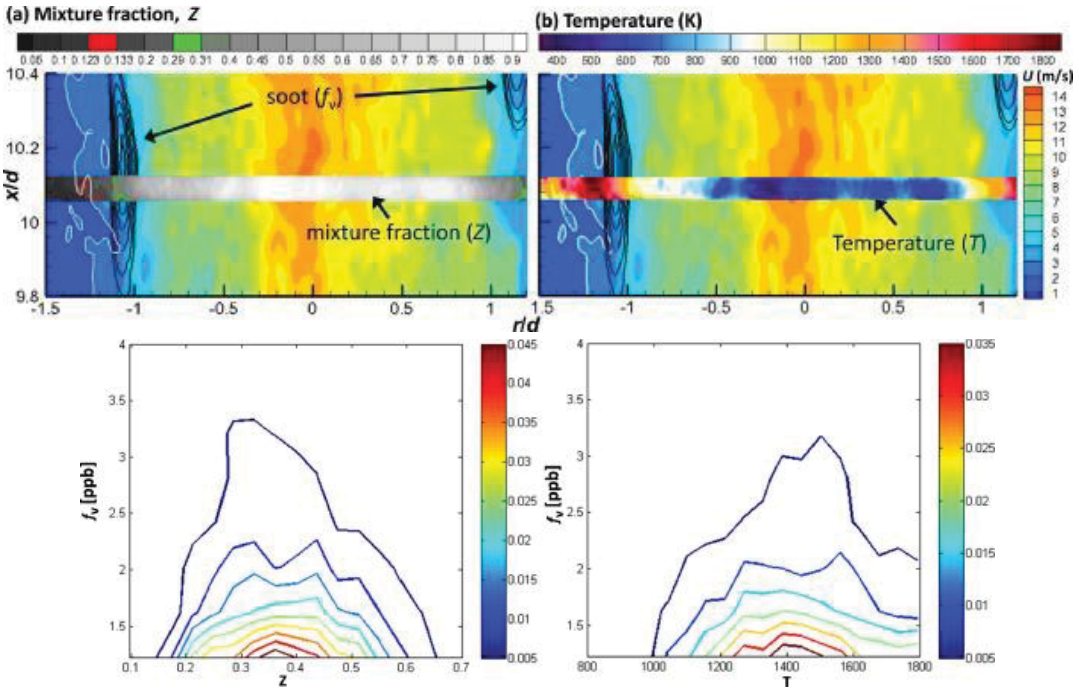

O. Park and R. A. Burns and O. R. H. Buxton and N. T. Clemens
Proceedings of the Combustion Institute **36** 899-907 (2017)

Dual pump and PS/FS CARS

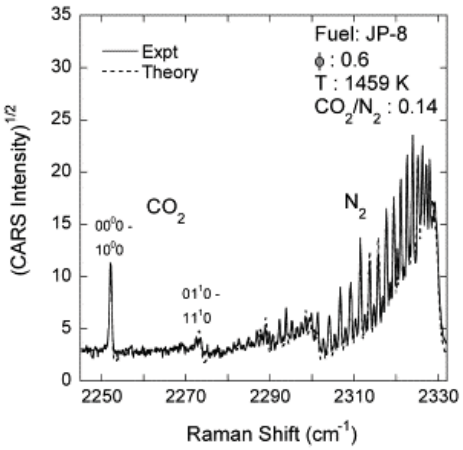

S. Roy and T. R. Meyer and R. P. Lucht and V. M. Belovich and E. Corporan and J. R. Gord
Combustion and Flame **138** 273 - 284 (2004)

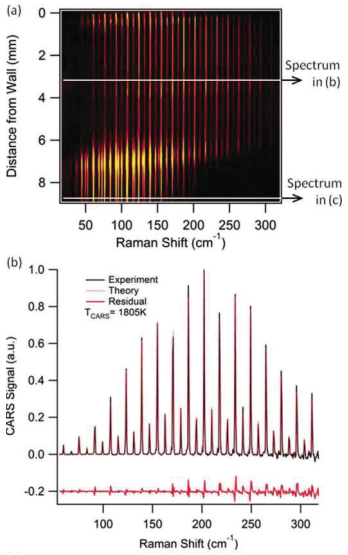

A. Bohlin and B. D. Patterson and C. J. Kliewer
The Journal of Chemical Physics **138** (2013)

Dual pump: downstream of flame

PS/FS: possibly workable in sooty flames

LIGS in flames

Pump energy = 100-200 mJ, Probe power = 2 W

$$SIGNAL\ INTENSITY:\ I \leftrightarrow \rho^2 = \left(\frac{P}{RT}\right)^2$$

$$DAMPING\ RATE:\ \Gamma \leftrightarrow \frac{1}{\rho} = \frac{RT}{P}$$

ABSORBERS:

Non-sooty flames: water

Sooty flames: soot

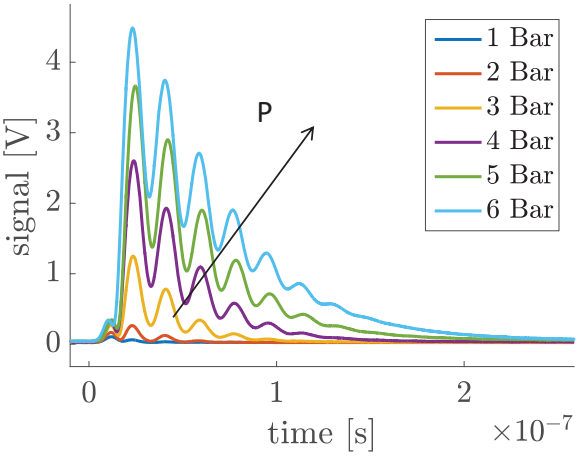

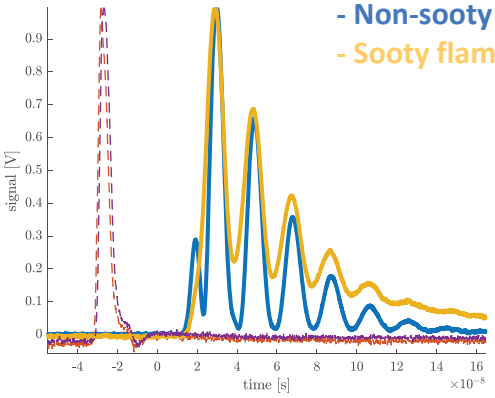

KAUST-Cambridge, unpublished
De Dedomenico, 2018

Differences:
- Rising time
- Contrast
- Damping rate

Not many measurements of scalars + soot in *liquid* spray flames

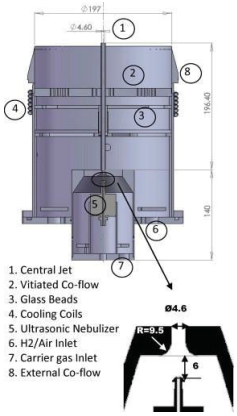

W. O'Loughlin and A. R. Masri
Combustion and Flame **158** 1577 - 1590 (2011)

U | d | OH | CH2O

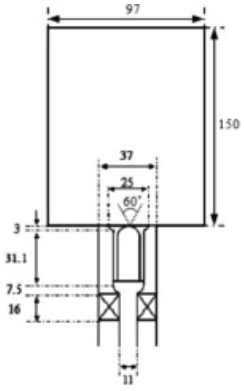

R. Yuan and J. Kariuki and A. Dowlut and R. Balachandran and E. Mastorakos
Proceedings of the Combustion Institute 35 1649-1656 (2015)

U | d | OH | CH2O

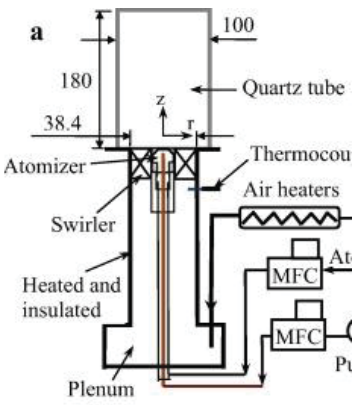

C. T. Chong and S. Hochgreb
Applied Energy 185 1383-1392 (2017)
C. T. Chong and S. Hochgreb
Fuel 115 551-558 (2014)

U | d | OH*

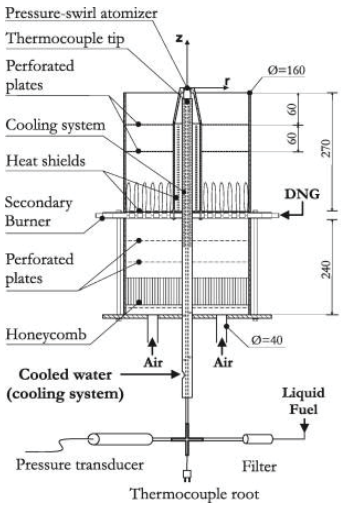

H. Correia Rodrigues and M. J. Tummers and E. H. van Veen and D. J. E. M. Roekaerts
International Journal of Heat and Fluid Flow 51 309-323 (2015)

T | U | d

Technical/high pressure spray flames

NASA-LDI atmospheric

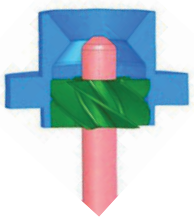

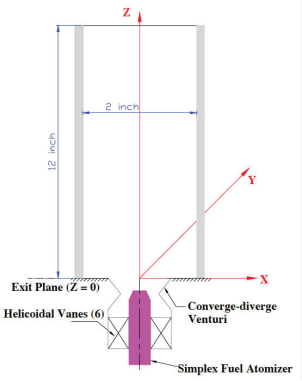

CORIA pressure

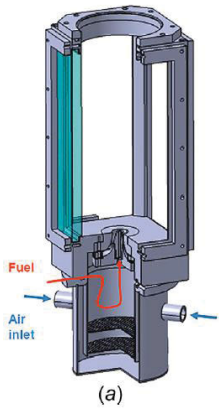

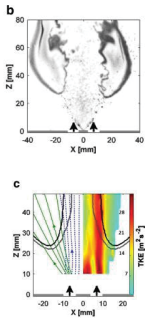

A. Iannetti, N.-S. Liu, F. Davoudzadeh
The Effect of Spray Initial Conditions on Heat Release and Emissions in LDI CFD Calculations
NASA Report No. NASA/TM—2008-214522, NASA Glenn Research Center, Cleveland, OH (2008)

The Structure of a Swirl-Stabilized Reacting Spray Issued from an Axial Swirler ,
J. Cai and S. M. Jeng and R. Tacina
AIAA 2005-1424 43rd AIAA Aerospace Sciences Meeting, Reno, Nevada (2005)

J. Marrero-Santiago and A. Verdier and C. Brunet and A. Vandel and G. Godard and G. Cabot and M. Boukhalfa and B. Renou
J. Eng. Gas Turbines Power 140 (2018)

A. Verdier and J. M. Santiago and A. Vandel and S. Saengkaew and G. Cabot and G. Grehan and B. Renou
Proceedings of the Combustion Institute 36 2595 - 2602 (2017)

Dilute spray flames DHSC: sensible place to start?

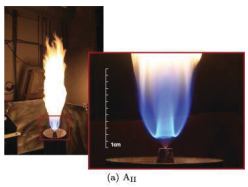

air (A)

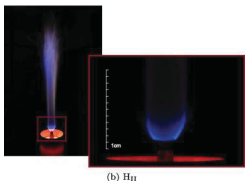

hot pilot (H)

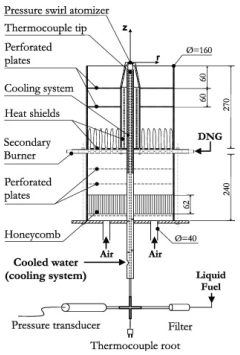

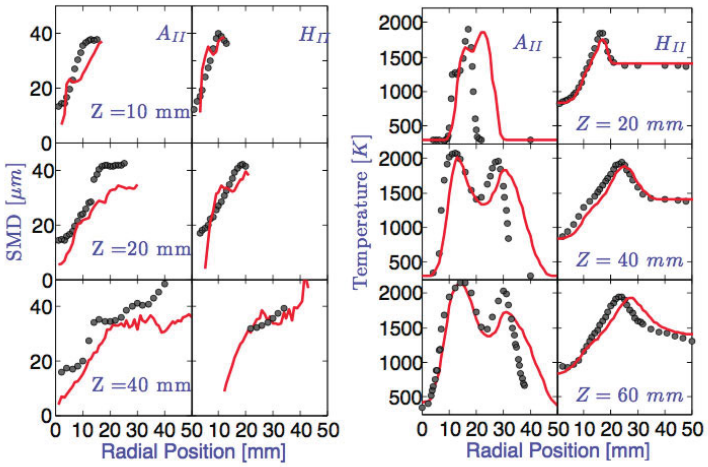

H. Correia Rodrigues and M. J. Tummers and E. H. van Veen and D. J. E. M. Roekaerts
Combustion and Flame 162 759-773 (2015)

L. Ma and D. Roekaerts
Proceedings of the Combustion Institute 36 2603-2613 (2017)

Soot/spray measurement needs: Input from industry and collaborators

Fuels and operating conditions

- CH_4/C_2H_4: significantly higher discrepancy with CH_4 : kinetic pathways probably not well worked out.
- Liquid fuels: approaching real kerosene (perhaps synthetic). Intermediate step could be addition of liquid fuels to C_2H_4
- Pressure: Need further validation mechanisms including total soot and soot size (common needs with IC engines), primary but also agglomerates. PAH measurements and techniques needed at pressure.
- Temperature: mechanisms are typically validated for low pressure flames, which do not reach high temperatures (unlike high pressure flames, up to 2300 K)
- Laminar vs. turbulent: residence time at microscale key: experiments in vitiated JSR (i.e. not flames) at high T possibly useful

Soot/spray measurement needs: Input from industry and collaborators

Geometries:

- Swirl stabilized flames (such as DLR): more representative
- Fully characterized boundary conditions

Soot as an issue:

- Top of the radar for e.g. Rolls-Royce
- Not on the radar for e.g. GE, Siemens, P&W

Atmospheric pressure turbulent flames

- The "simple" configuration of unconfined turbulent jet flames has been used extensively to study important aspects of flames:

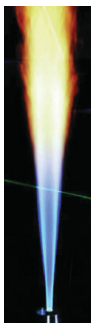
Delft/Sandia flame III


Sydney inhomogeneous inlets flame


Adelaide jet flame


Sandia/ETH syngas flame


DLR lifted flame

- Piloted or non-piloted,
- Attached or lifted,
- Sooty or blue,
- Large range of fuels

- These flames allow isolating effects and are amenable to modeling.
- However, they are not compatible with most available pressure rigs because they need to be vertical to preserve symmetry and tall (> 2m)

High pressure flames

- One of the most successful features of TNF was ability to replicate the different burners
  - Confirmation of measurements by applying different diagnostic techniques
- With the complexities of high pressure facilities, this model doesn't work any more
  - Need to bring burners and diagnostics to the few facilities available
  - High cost dictates very judicious choices of experiments
  - Employ as many simultaneous diagnostics as possible to maximize data yield
  - High rep rate diagnostics highly advantageous (but do you get statistically independent data?)
- Only go to pressure when necessary

High Pressure Combustion Duct

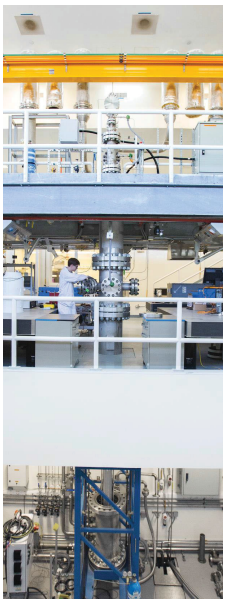

- KAUST high pressure combustion lab
  - Supply of high air & nitrogen flow rates (0.56 kg/s continuous, higher for intermittent)
  - High pressure (45 bar)
- KAUST high pressure combustion duct (HPCD)
  - Designed for turbulent non-premixed flames at high pressure
  - Wide inner diameter (~ 400 mm) allows wide variety of burners
  - Height (~ 9 m) allows very long flames
  - Design pressure: 40 atm
  - Optical access: 6 UV fused silica windows

Vessel and Facility Mods

- Now placing collection optics inside duct. Will be an issue for very radiant flames.
- Adding y and z translation capability to burners (60 mm)
- 200 kg of air storage for short duration runs with higher mass flux
- Will have liquid fuel capability soon
- Redesigning exhaust to allow higher power and also better atmospheric pressure environment
- Continually expanding suite of diagnostic tools available

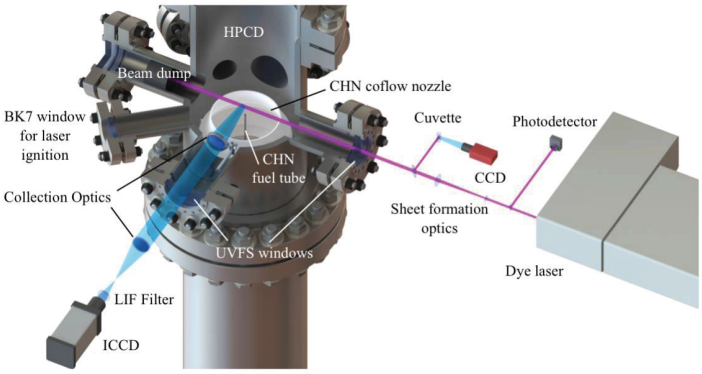

KAUST's HPCD timeline

Flames

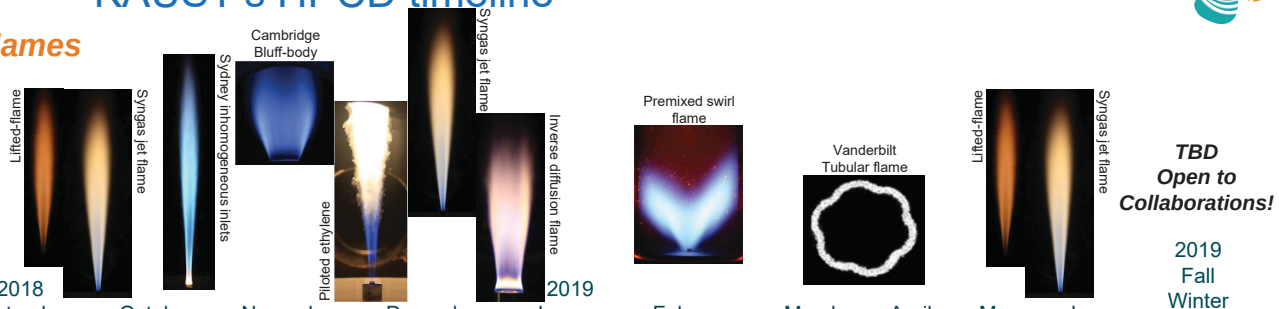

2018 September | October | November | December | 2019 January | February | March | April | May | June

TBD
Open to Collaborations!

2019
Fall
Winter

2-D scalar imaging
Raman (CH_4/N_2)
OH/CH_2O PLIF

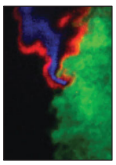

Velocimetry
PIV

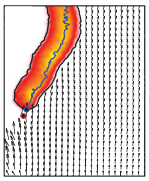

2-D scalar imaging
CH PLIF

Thermometry
Thermographic phosphors
LIGS

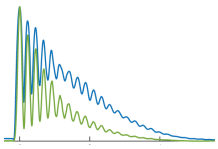

2-D scalar imaging
Raman (CH_4/N_2)
CH PLIF

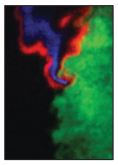

2-D scalar imaging
Raman ($CH_4/N_2/H_2/CO_2$)
Filtered Rayleigh scattering

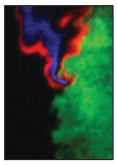

Diagnostics

HP Turbulent Sooting Flames

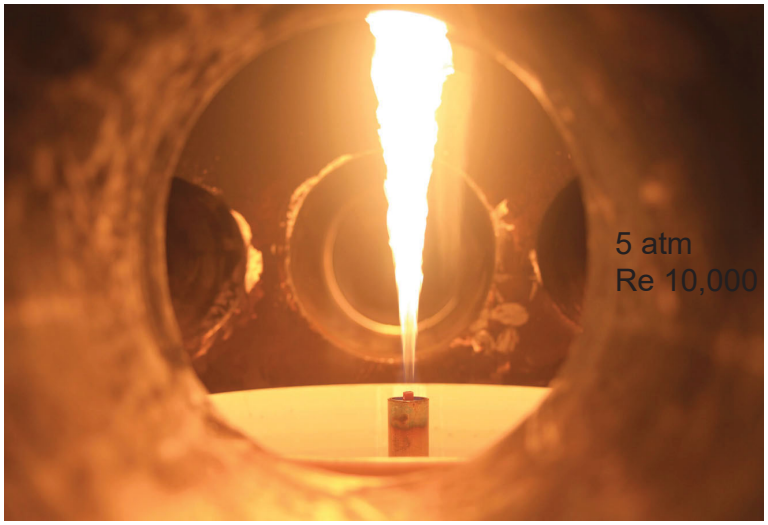

Issues to discuss

- Better linkage between laminar and turbulent flames;
  - Unsteady (forced) co-flow and counterflow flames offer many advantages
- Is nitrogen dilution preferable way to suppress soot at high pressures? Adding Hydrogen? Changing H/C ratio problematic.
- Partial premixing? Sydney inhomogeneous burner at pressure?
- Liquid fuels? (n-Heptane? Multi-component surrogate?) Spray flames or pre-vaporized?
- Is there still utility is in pushing jet flames to higher power and Re? Lifted vs piloted?
- Adelaide ethylene/hydrogen/nitrogen attached flames to high pressure?
- Turbulent counter-flow flames? Much smaller physical region, more amenable to DNS
- How necessary is confinement for swirl flames? Removing confinement simplifies diagnostics and the prescription of thermal boundary conditions.

Simulation View

- Turbulent jet flames seem more difficult than swirl combustion
- Jet flames
  - Almost no sensitivity to typical model variations (chemistry, turbulence model etc.)
  - Highly sensitive to small-scale soot structure description
- Swirl combustor
  - Follows normal rules for soot: chemistry matters, turbulence model does not matter; Good solution of flow field is important
  - Also sensitive to small-scale soot structure description
- More importantly, what works for one does not work for the other

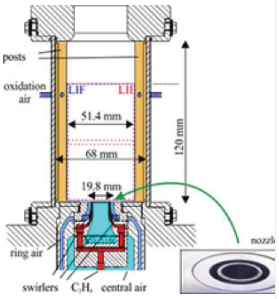

Macroscopic and Microsopic Intermittency

- Swirl combustors are driven by large scale variations in flow path for fuel molecules
  - LES-type models are good at predicting these variations
  - Simulation results are good
- Jet flames dominated by small scale intermittency
  - Persistence of dissipation rates may be important
  - No turbulence modeling framework can capture this (at present)
  - Simulations are insensitive to typical changes

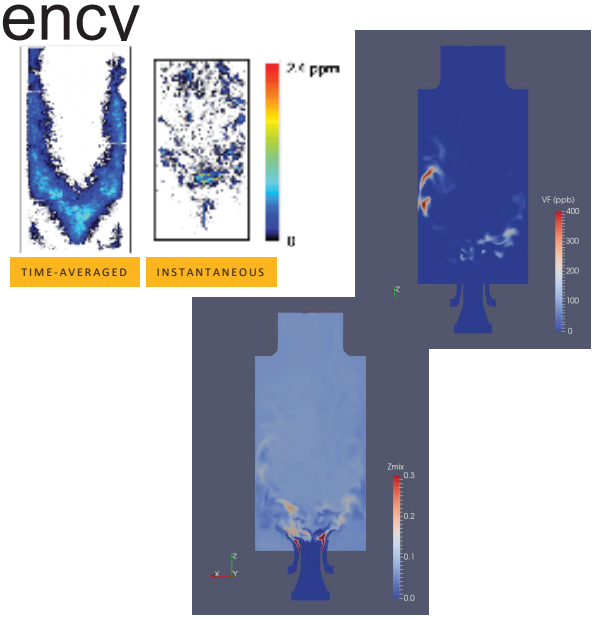

Are Canonical Flames Canonical Enough?

- Canonical flames were designed for gas-phase processes
  - Provides simpler theoretical, numerical and experimental view
- Soot depends on flow history
  - The weakness of canonical flames is they can never reproduce the right history
  - Different from gas-phase processes
    - Short history, confined to diffusion scales (not for NOx)
    - Only the small scale structure needs to be reproduced
- Are other configurations possible?
  - For instance, a diffusion flame and a premixed flame in series

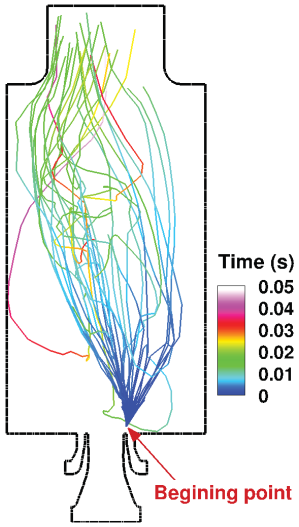

Some Comments

- Semi-empirical model and PAH-based model provide the two most contrasting results
  - Everything else (turbulence model, combustion model, moment methods) a wash
- Validation experiments should focus on this difference
  - Can there be a range of experiments that go from PAH model friendly to semi-empirical model friendly environments?

Jet Intermittency

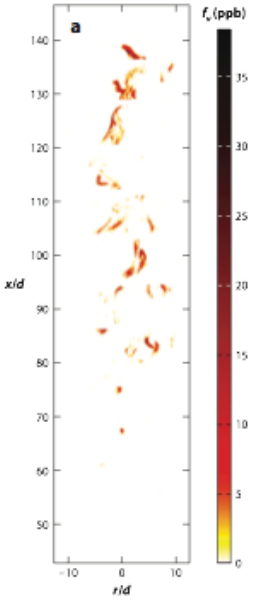

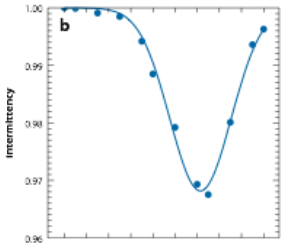

Adelaide/Delft Methane Flame

KAUST High Pressure *Direct images (top) and OH-PLIF (bottom) for KEN flames. Note: Different scales*

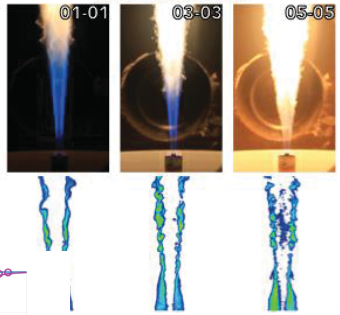

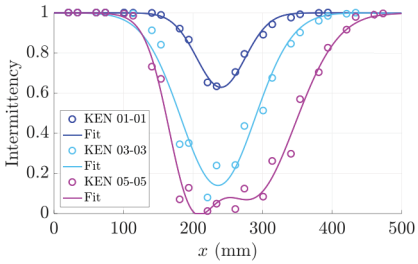

Session: Enclosed Flames and Elevated Pressure

Session Coordinators: Christoph Arndt, Wolfgang Meier (DLR Stuttgart)

In this session, recent experiments and simulations of enclosed flames and flames at elevated pressure, as well as challenges both on the experimental and on the simulation side, were discussed. The session was structured in two parts.

In the first part of the session, the following contributions on experiments and simulations of swirl combustors at atmospheric and elevated pressure as well as a test case of a jet flame at elevated pressure were presented.

- "Experimental Study on Dynamics of Lean Premixed Swirl Flames" from Shanghai Jiao Tong University. A swirl flame was operated with and without enclosure, and several high repetition rate laser diagnostics (Fuel Tracer PLIF, CH2O PLIF and PIV as well as TDLAS) were applied.
- "Experimental and numerical investigation of the response of a swirled flame to flow modulations in a non-adiabatic combustor" from Centrale Supélec. A joint experimental and numerical effort was undertaken to study the response of a swirl flame to flow modulations.
- "SFB 606 Gas Turbine Model Combustor" from DLR Stuttgart. A dual-swirl gas turbine model combustor was studied in detail in different operating regimes (technically premixed, perfectly premixed, and stratified flames).
- "LES Studies on Enclosed Swirl Flames in Laboratory Combustors" from the University of Cambridge. Simulations of the DLR Gas Film were conducted, the corresponding experiments were performed at DLR Stuttgart.
- "High-Pressure Syngas Jet Flames (CHN)" from KAUST. A joint experimental and numerical study of a jet flame at elevated pressure at different pressures and Reynolds numbers was carried out by KAUST in collaboration with the University of Rome.
- "LES Studies on Enclosed Swirl Flames in Industrial Combustors" from the University of Cambridge. Simulations of an industrial swirl burner at elevated pressure were performed, the corresponding experiments were performed at DLR Stuttgart.

The second part of the session focused on FLOX® and MILD combustion. The following contributions were presented:

- "Flameless combustion in a lab-scale furnace" from TU Delft, with experimental and numerical results from a lab-scale MILD combustor at atmospheric pressure fired with Dutch natural gas.
- "Confined and Pressurized Jet in Hot & Vitiated Coflow Burner" from Adelaide and Sydney showing initial results of C_2H_4 and NG:H_2 jet flames at various ratios up to 5 bar pressure.
- "High-Pressure Enclosed Jet Flames" from DLR Stuttgart with detailed experimental results from a single nozzle FLOX® burner for premixed NG jet flames at 8 bar and ~1 MW thermal power.
- "Investigation of a high pressure jet flame with heat losses using tabulated and finite rate chemistry" from University Duisburg-Essen showing results from LES simulations of the enclosed jet flame that was experimentally studied at DLR.

Enclosed Flames and Elevated Pressure

Session Coordinators: Christoph Arndt, Wolfgang Meier
German Aerospace Center (DLR), Institute of Combustion Technology

TNF 2018 DUBLIN IRELAND JULY 27-28

14th INTERNATIONAL WORKSHOP ON MEASUREMENT & COMPUTATION OF TURBULENT FLAMES

DLR

Contributions

Atmospheric Pressure
- Lean Premixed Swirl Flame (Shanghai Jiao Tong / Cambridge)
- Thermo-Acoustically Excited Swirl Flame (Centale Supélec / CNRS)
- SFB Dual Swirl Burner (DLR Stuttgart)
- DLR Gas Film Nozzle (Cambridge)

Elevated Pressure
- High Pressure Jet Flame (KAUST)
- Siemens GT Combustor (Cambridge)

DLR

Experimental Study on Dynamics of Lean Premixed Swirl Flames

Zhi X. Chen [a], Ivan Langella [a,b], N. Swaminathan [a]
Guoqing Wang [c], Sirui Wang [c], Xunchen Liu [c], Lei Li [c], Fei Qi [c]

[a] Cambridge University, Department of Engineering, UK
[b] Loughborough University, Department of Aeronautical & Automotive Engineering, UK
[c] Shanghai Jiao Tong University, Key Laboratory for Power Machinery and Engineering of MOE, China

TNF2018 DUBLIN IRELAND JULY 27-28

Experimental Study on Dynamics of Lean Premixed Swirl Flames

– enclosed vs. open, lift-off & re-attaching, and acoustic forcing

❑ **Burner configuration**

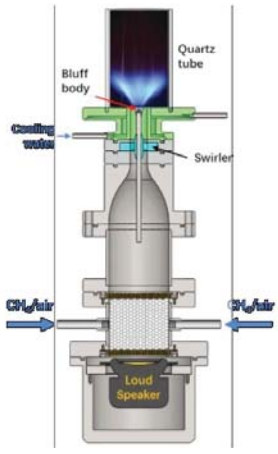

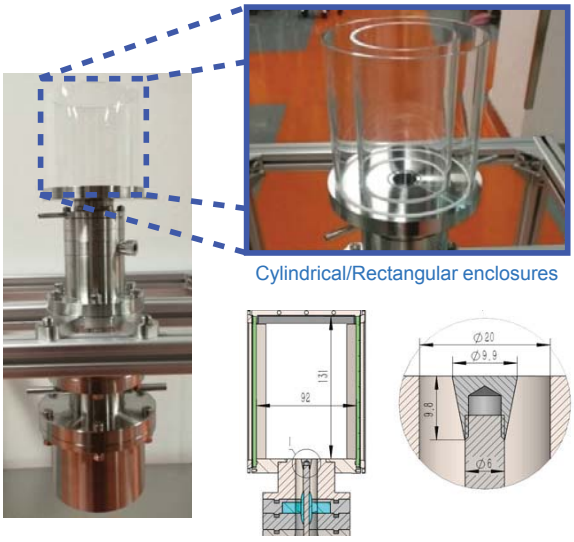

Cylindrical/Rectangular enclosures

Dimensions/Operating conditions

Bluff-body diameter: 9.9 mm

Enclosure diameter/height: 92/131 mm

Premixed mixture flow rate: 0 – 500 SLM

Temperature/pressure: 300 K / 1 atm

Fuel: methane, acetone, DME, etc.

Equivalence ratio: 0.5 – 2.0

Acoustic excitation: 100 – 400 Hz

TNF2018 DUBLIN IRELAND JULY 27-28

UNIVERSITY OF CAMBRIDGE

Measurement techniques – in operation, in progress

❑ **High-rep (10 to 100 kHz) burst-mode Nd:YAG laser (Spectral Energies, QuasiModo1000)**

➢ Single beam (266nm: Acetone-PLIF / 355nm: CH_2O-PLIF + 532nm: PIV)

➢ Two simultaneous beams + OPO (390.3nm: CH-PLIF + 282.8-286.4nm: OH-PLIF)

➢ Tuneable diode laser absorption spectroscopy (TDLAS) for quantitative measurement for mean temperature and CO_2/H_2O concentrations

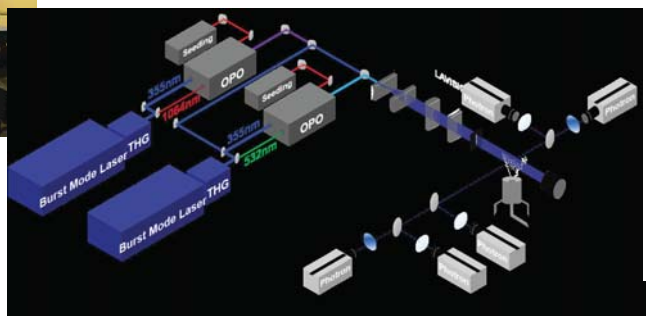

BD: beam damp; BS: beam splitter; CL: cylindrical lens; DM: diachronic mirror; F: short band pass filter; OPO: optical parametric oscillator; M: mirror; THG: third harmonic generator

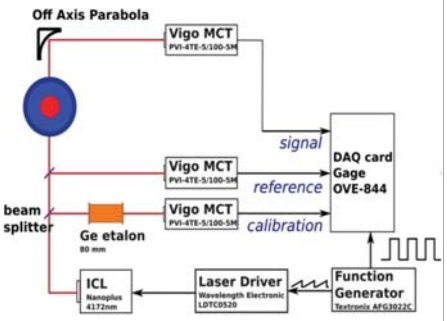

TNF 2018 DUBLIN IRELAND JULY 27-28

UNIVERSITY OF CAMBRIDGE

Preliminary results: DME–air swirl flames at phi = 0.8

❑ **20kHz CH_2O-PLIF + PIV:**

with (left) vs. without enclosure (right)

➢ Shorter flame & large spread angle with enclosure

➢ Additional reaction branch close to outer recirculation zone

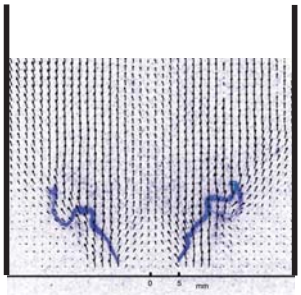

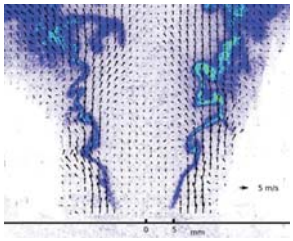

❑ **Sudden lift-off and reattaching observed for the enclosed flame**

➢ Flame shape changes between V and M

➢ Flame-vortex interaction based stabilization mechanism

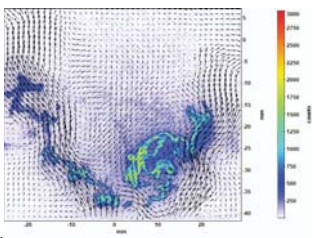

❑ **Phase resolved 2D TDLAS temperature measurement for acoustically forced flame**

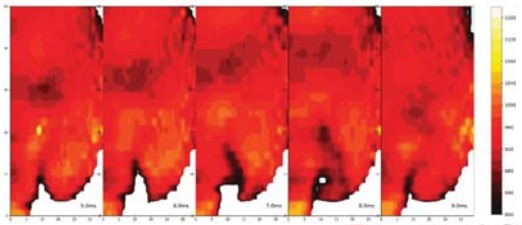

TNF 2018 DUBLIN IRELAND JULY 27-28

Experimental and numerical investigation of the response of a swirled flame to flow modulations in a non-adiabatic combustor

CentraleSupélec

cnrs

CentraleSupélec

Experimental and numerical investigation of the response of a swirled flame to flow modulations in a non-adiabatic combustor

cnrs

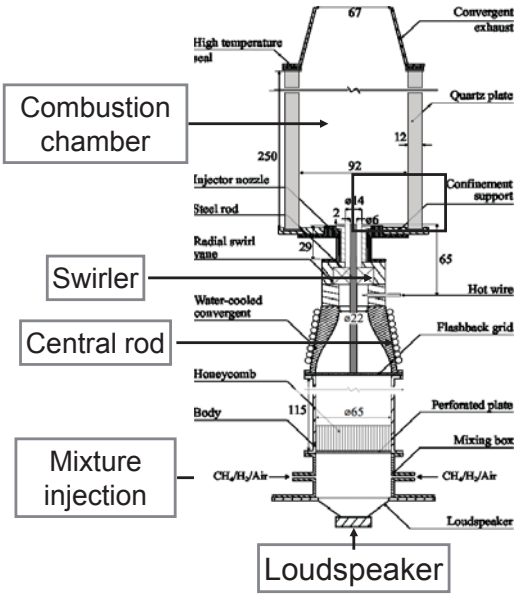

Diagnostics under stationary operation

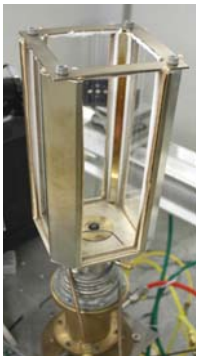

- OH* chemiluminescence
- PIV under cold conditions (transverse/longi)
- Simultaneous OH-LIF and PIV under reacting conditions (transverse/longi)
- **LIP for solid wall temperature measurements**

Guiberti, T., Durox, D., Scouflaire, P., and Schuller, T. (2015). Proceedings of the Combustion Institute

Wall Temperature Measurements

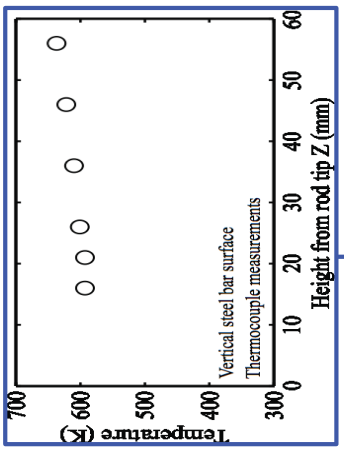

Thermocouple measurements

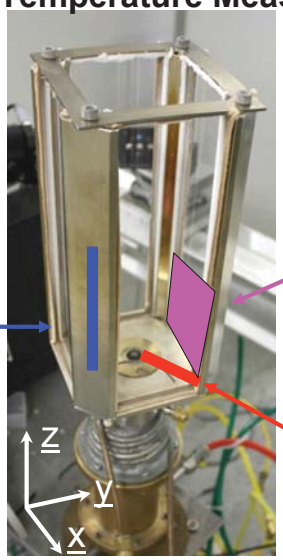

Laser Induced Phosphorescence (LIP)

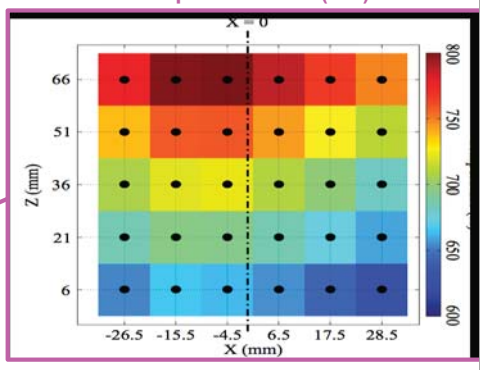

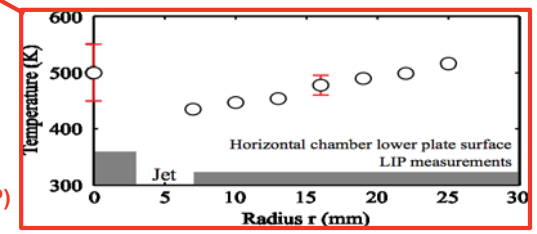

Laser Induced Phosphorescence (LIP)

Guiberti, T., Durox, D., Scouflaire, P., and Schuller, T. (2015). Proceedings of the Combustion Institute

Steady configuration (no accoustic forcing)

Numerical set-up:

- YALES 2 solver
- Non-adiabatic F-TACLES model (Mercier et al. 2014)

Quenching due to joint strain and heat losses not captured by the chemical table

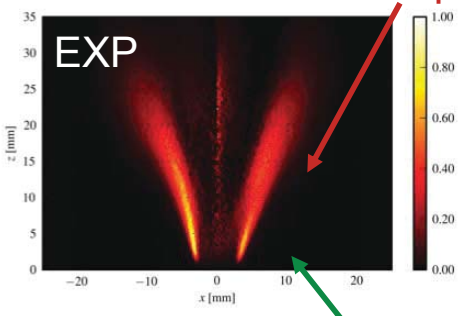

OH*

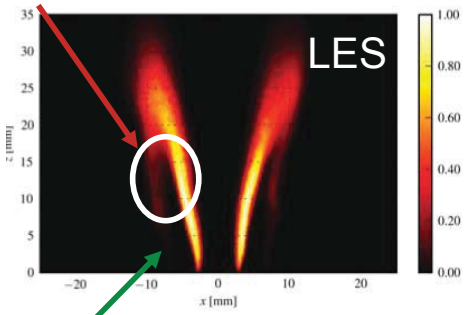

Heat release

Quenching due to heat losses at the wall handled by the LES

R.Mercier, T.Guiberti, A.Chatelier, D.Durox, O.Gicquel, N.Darabiha, T.Schuller, B.Fiorina, Combustion and flame 171, 42 (2016)

Comparison between experimental and numerical Flame Describing Function (Noiray et al. 2008)

Experiments and simulations have been conducted for different forcing frequencies **f** and modulation levels $\mathbf{u'_z / u_z}$

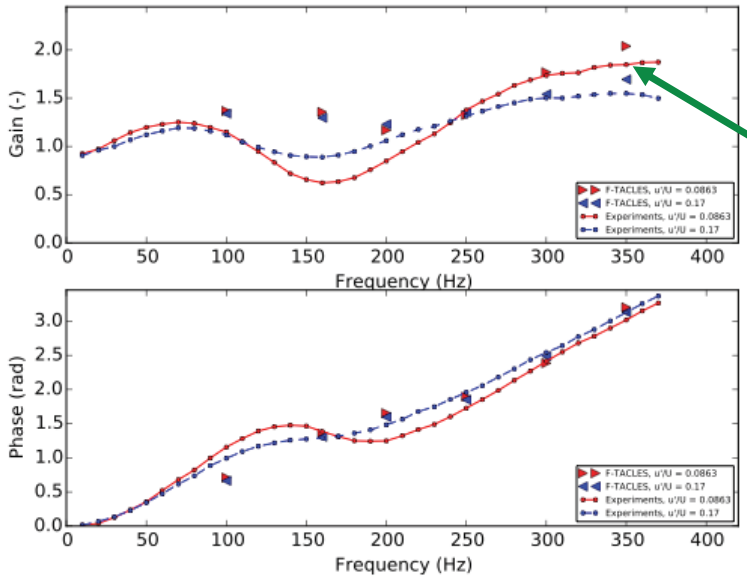

Each symbol corresponds to one LES

A.Chatelier, T.Guiberti, R.Mercier, T.Schuller, N. Bertier, B.Fiorina, T. Schuller. Flow Turbulence and Combustion (2018)

Comparison between experimental and numerical Flame Describing Function

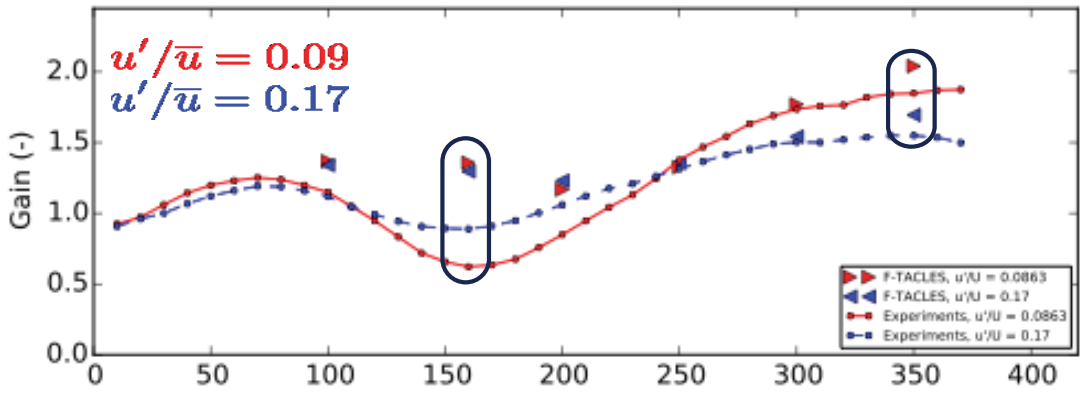

- No drop of gain around 160 Hz: weak destructive interferences
- Good tendency above 250 Hz: correct constructive interferences

A.Chatelier, T.Guiberti, R.Mercier, T.Schuller, N. Bertier, B.Fiorina, T. Schuller. Flow Turbulence and Combustion (2018)

Post-processing

Phase average heat release (OH*)

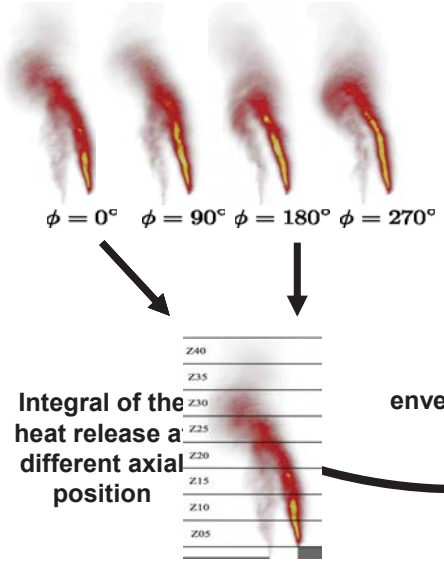

Integral of the heat release at different axial position

envelope of the signal

f = 350 Hz, u'/U = 0.17

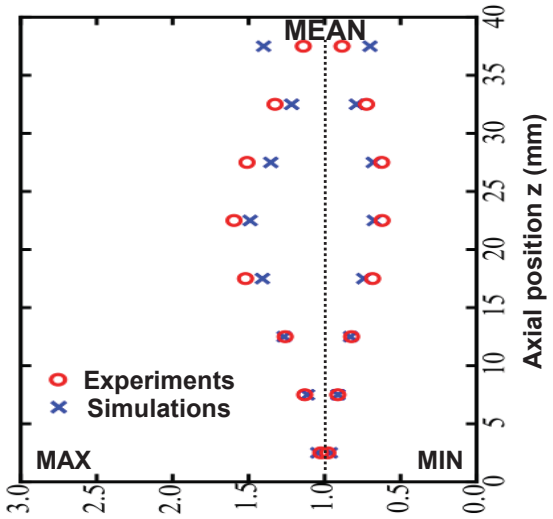

Extrema of the normalized phase-averaged integral heat release (LES) and OH* (EXP)

A.Chatelier, T.Guiberti, R.Mercier, T.Schuller, N. Bertier, B.Fiorina, T. Schuller. Flow Turbulence and Combustion (2018)

Two different flame responses to incoming perturbations in the simulations

f = 350 Hz, u'/U = 0.17

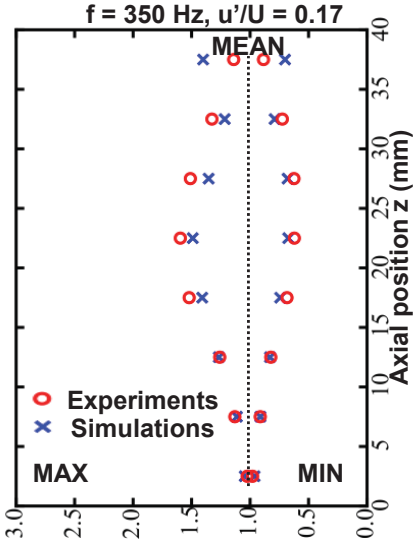

Extrema of the normalized phase-averaged integral heat release (LES) and OH* (EXP)

May be due to a mis-prediction of the influence of the strain rate on the flame response

f = 160 Hz, u'/U = 0.17

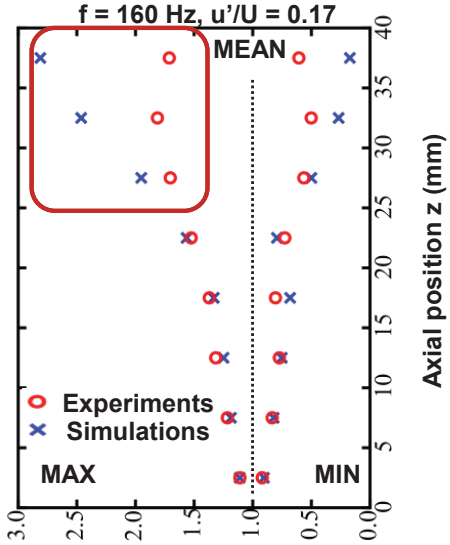

Extrema of the normalized phase-averaged integral heat release (LES) and OH* (EXP)

A.Chatelier, T.Guiberti, R.Mercier, T.Schuller, N. Bertier, B.Fiorina, T. Schuller. Flow Turbulence and Combustion (2018)

SFB 606 Gas Turbine Model Combustor

C.M. Arndt[1], M. Severin[1], C. Dem[1,2], Y. Gao[1], J. Böhnke[1], R. Hadef[3], A.M. Steinberg[4,5], W. Meier[1]

[1] German Aerospace Center (DLR), Institute of Combustion Technology, Stuttgart, Germany
[2] Present Address: Karlsruhe Institute of Technology (KIT) , Institute for Chemical Technology and Polymer Chemistry, Karlsruhe, Germany
[3] Université Larbi Ben M'Hidi, Faculté des Sciences et de la Technologie, Oum El Bouaghi, Algeria
[4] University of Toronto, Institute for Aerospace Studies, Toronto, Canada
[5] Present Address: Georgia Institute of Technology, Guggenheim School of Aerospace Engineering, Atlanta, GA, USA

christoph.arndt@dlr.de

TNF 2018 DUBLIN IRELAND JULY 27-28 — 14th INTERNATIONAL WORKSHOP ON MEASUREMENT & COMPUTATION OF TURBULENT FLAMES

DLR

SFB Dual Swirl Combustor
Operating Regimes and Geometry

- Dual Swirl Gas Turbine Model Combustor (GTMC)
- Separate air plenums for each swirler
  → Air Split Ratio $L = \frac{\dot{m}_{air,o}}{\dot{m}_{air,i}}$ freely variable
- Fuel injection into inner air stream through 60 holes (0.5 mm diameter)
- Optical combustion chamber for laser-based measurements
- Technically premixed (15 kW < P_{th} < 35 kW)
  Perfectly premixed (P_{th} = 25 kW)
  Stratified (P_{th} = 25 kW)
  Liquid fuel operation (prevaporized and liquid) possible

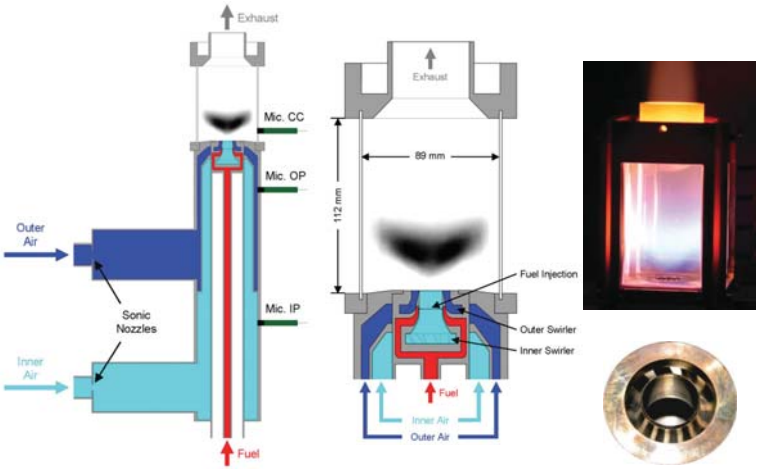

C.M. Arndt et al., Exp. Fluids 56 (2015)

DLR

Thermo-Acoustically Stable Flame – Flame Shape, Flow Field and Species

φ = 0.63, P_{th} = 22.5 kW

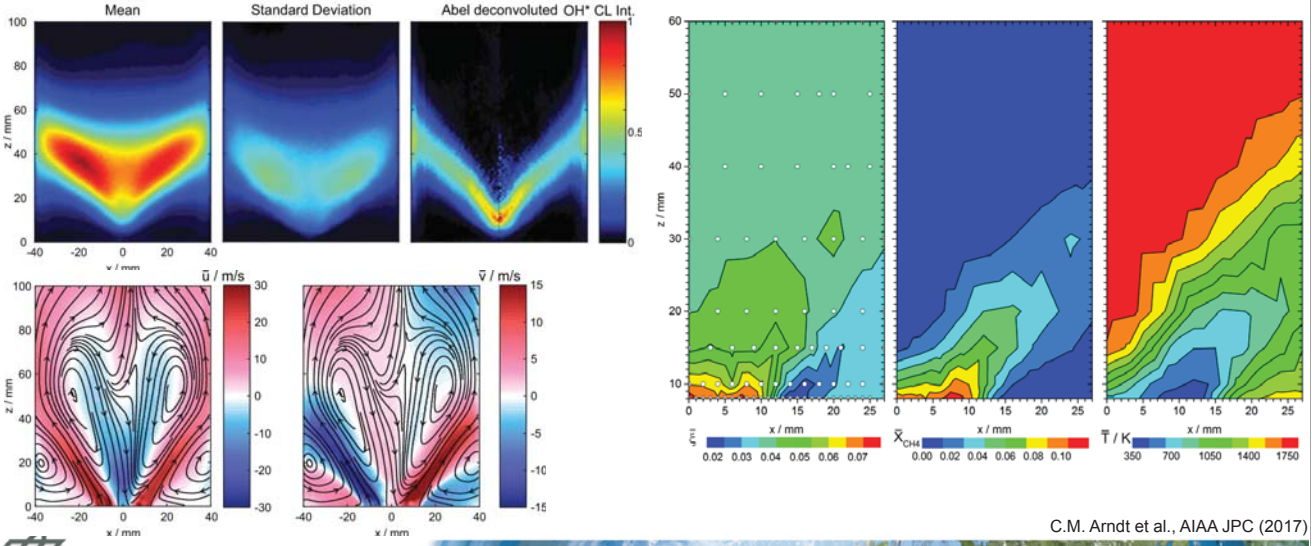

C.M. Arndt et al., AIAA JPC (2017)

Thermo-Acoustically Instable Flame – Acoustic Spectra

φ = 0.7, P_{th} = 25 kW

- Several acoustic modes, only one coupled with heat release

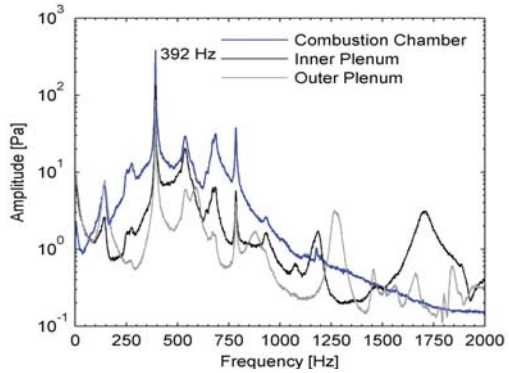

- Thermo-acoustic oscillation at f ≈ 400 Hz
- Corresponds to resonance: λ/2 = length of inner plenum

C.M. Arndt et al., Exp. Fluids 56 (2015)

Thermo-Acoustically Instable Flame– Scatterplots T-f at h=8 mm

φ = 0.7, P_{th} = 25 kW

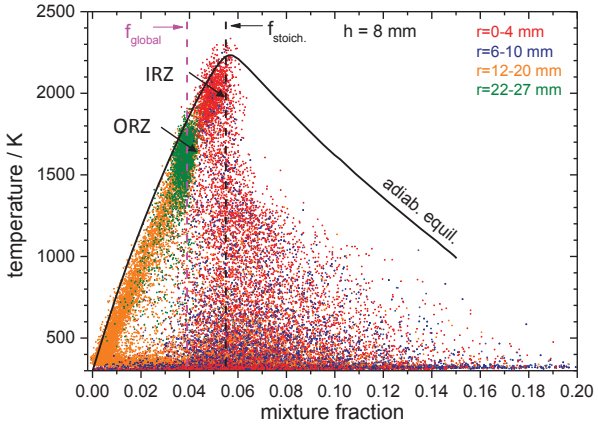

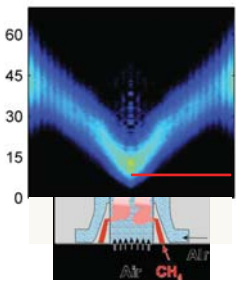

Hardly any reaction below h=8 mm, state mainly determined by mixing.

- Large variation of thermochemical states

W. Meier et al., Exp. Therm. Fluid Sci. 73 (2015)

Thermo-Acoustically Instable Flame– Cyclic Variations

φ = 0.7, P_{th} = 25 kW

- Scatterplots T-f at h=8 mm, r ≤ 10 mm (close to flame zone), 4 phases

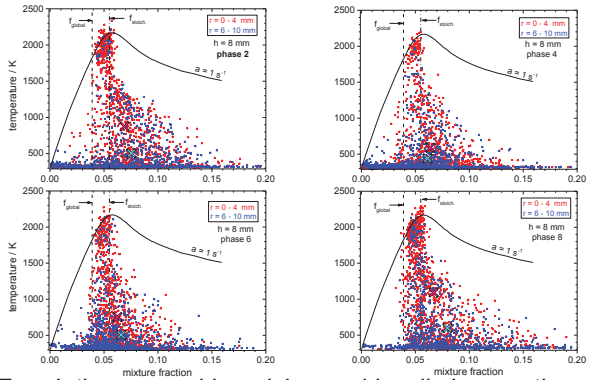

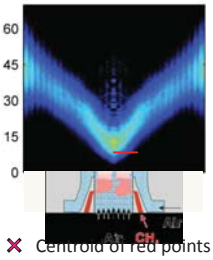

Centroid of red points

Centroid of blue points

- T-variation caused by mixing and hardly by reactions.
- f-variation due to changes of inflowing composition.

W. Meier et al., Exp. Therm. Fluid Sci. 73 (2015)

Stratified Flame – Overview

φ_{global} = 0.75, P_{th} = 25 kW, φ_{in} = 1.0, φ_{out} = 0.6, S = φ_{in} / φ_{out} = 1.67

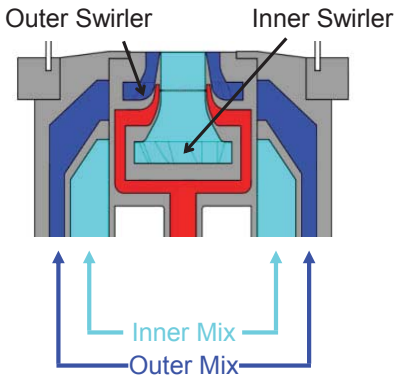

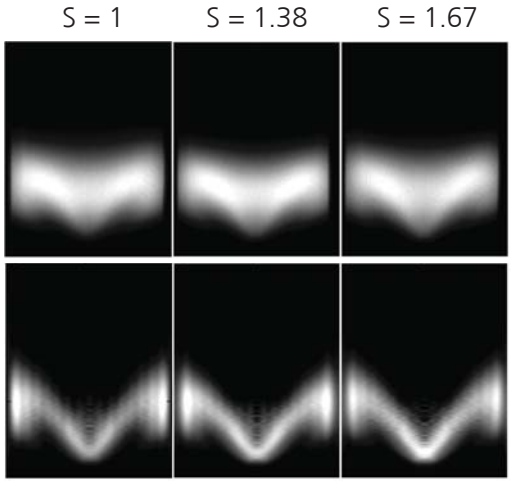

Stratified Flame – T-f Scatterplots

φ_{global} = 0.75, P_{th} = 25 kW, φ_{in} = 1.0, φ_{out} = 0.6, S = φ_{in} / φ_{out} = 1.67

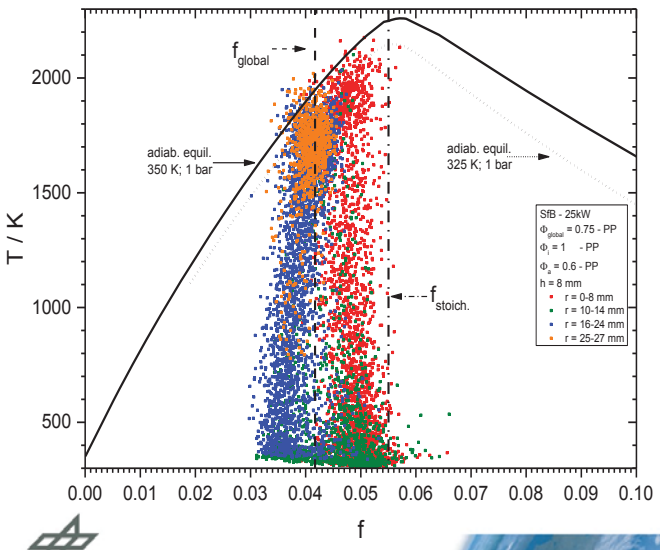

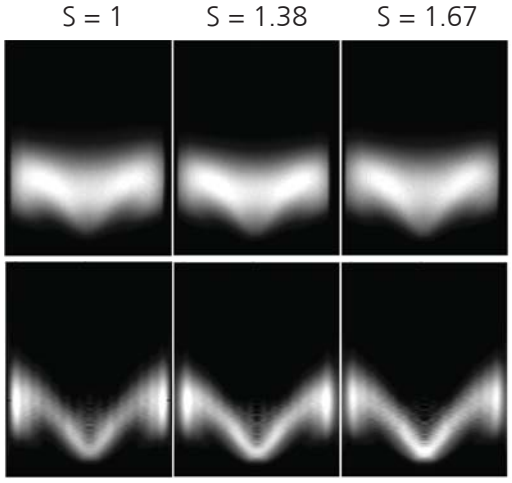

Outlook
Prevaporized Liquid Fuels - Ethanol

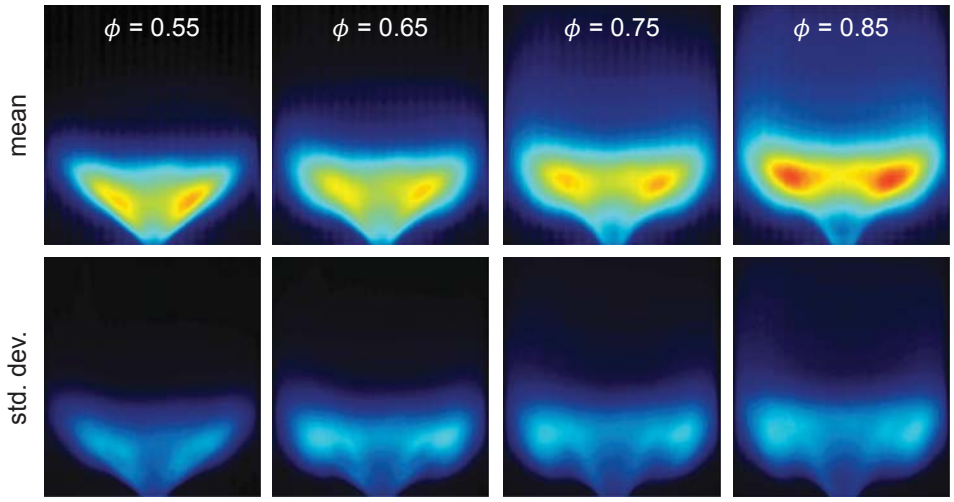

C.M. Arndt et al., AIAA SciTech (2019), submitted

DLR

UNIVERSITY OF CAMBRIDGE

Loughborough University

LES Studies on Enclosed Swirl Flames in Laboratory Combustors

Zhi X. Chen[a], Ivan Langella[a,b], N. Swaminathan[a]

[a] Cambridge University, Department of Engineering, UK

[b] Loughborough University, Department of Aeronautical & Automotive Engineering, UK

TNF 2018 DUBLIN IRELAND JULY 27-28

DLR Dual Swirl Gas Turbine Model Combustor

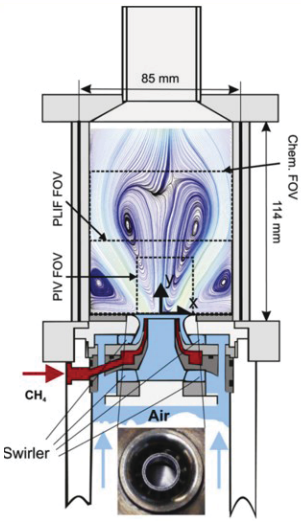

*swirl number

Table 1: Operating conditions for the cold flow and two flames considered.

Case	Φ_{glob}	Z_{glob}	$\dot{m}_p$ (g/s)	$\dot{m}_j$ (g/s)	SN*	P_{therm} (kW)
Non-reacting	—	—	19.74	1.256 (Air)	0.9	—
Flame A (stable)	0.65	0.037	18.25	0.697	0.9	34.9
Flame B (unstable)	0.75	0.042	4.68	0.205	0.55	10.3

❑ **Major modelling challenges**

- ➢ Mass split between the two air swirlers sharing the same plenum
- ➢ Flow separation at the contoured nozzle lip
- ➢ Partially premixed lifted swirl flame interacting with the precessing vortex core (PVC)
- ➢ Pronounced thermoacoustic instability at 290 Hz for Flame B
- ➢ Flame shape change from conical (stable) to flat (unstable)

UNIVERSITY OF CAMBRIDGE

Weigand *et al.*, *Combust. Flame* 144 (2006) 205-224.
Meier *et al.*, *Combust. Flame* 144 (2006) 225-236.

TNF 2018 DUBLIN IRELAND JULY 27-28

LES/flamelet modelling & OpenFOAM compressible solver

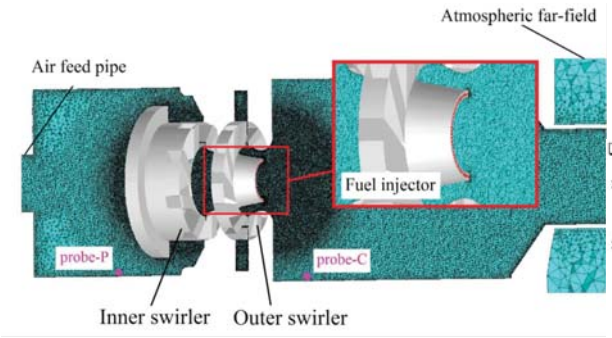

Outlet: $\bar{p} = p_{atm} - \frac{1}{2}\bar{\rho}|\tilde{u}_i|^2$ & $\frac{\partial \tilde{u}_i}{\partial n} = 0$

Non-slip walls: $\frac{\partial \bar{p}}{\partial n} = 0$ & $\tilde{u}_i = 0$

Inlets: $\frac{\partial \bar{p}}{\partial n} = 0$ & $\tilde{u}_i$ = fixed values from $\dot{m}$

Second-order schemes
Time-step: 1e-7s
Grid size: 20M tetrahedral
For physical time 0.15s, wall-clock 210 hrs with 1080 ARCHER cores ~ 3,400 kAUs

❑ **A flamelet model for partially premixed combustion**

- ➢ Chemistry tabulation (GRI 3.0) using a collection of premixed flamelets

$$\varphi = \mathcal{F}(Z, c)$$

- ➢ First two moments are transported along with enthalpy

$$\bar{\rho}\frac{D\widetilde{\varphi}}{Dt} = \nabla\cdot\left[\left(\bar{\mu} + \frac{\mu_t}{Sc_t}\right)\nabla\widetilde{\varphi}\right] + \overline{S_\varphi^*} - \overline{S_\varphi}$$

$$\widetilde{\varphi} = \left\{\widetilde{Z}, \widetilde{Z''^2}, \widetilde{c}, \widetilde{c''^2}, \widetilde{h}\right\},$$

$$\overline{S_\varphi^*} = \left\{0, 2\frac{\mu_t}{Sc_t}|\nabla\widetilde{Z}|^2, \overline{\dot{\omega}_c^*}, 2\frac{\mu_t}{Sc_t}|\nabla\widetilde{c}|^2 + 2\left(\widetilde{c\dot{\omega}_c^*} - \widetilde{c}\,\widetilde{\dot{\omega}_c^*}\right), \frac{D\bar{p}}{Dt}\right\},$$

$$\overline{S_\varphi} = \left\{0, 2\bar{\rho}\widetilde{\chi}_{Z,sgs}, 0, 2\bar{\rho}\widetilde{\chi}_{c,sgs}, 0\right\}.$$

$$\overline{\dot{\omega}_c} \simeq \bar{\rho}\int_0^1\int_0^1 \frac{\dot{\omega}_c(\xi,\zeta)}{\rho(\xi,\zeta)}\widetilde{P}(\xi,\zeta)\,d\zeta\,d\xi$$

$$+$$

$$\overline{\dot{\omega}_{hp}} \simeq \widetilde{c}\left(\bar{\mu}|\nabla\widetilde{Z}|^2 + \bar{\rho}\widetilde{\chi}_{Z,sgs}\right)\int_0^1 \frac{1}{\psi^{Eq}}\frac{d^2\psi^{Eq}}{d\xi^2}\widetilde{P}_\beta(\xi)\,d\xi$$

UNIVERSITY OF CAMBRIDGE

TNF 2018 DUBLIN IRELAND JULY 27-28

LES/flamelet modelling & OpenFOAM compressible solver

– Typical comparisons for Flame A (stable) and B (unstable)

❑ **Mean radial profiles**

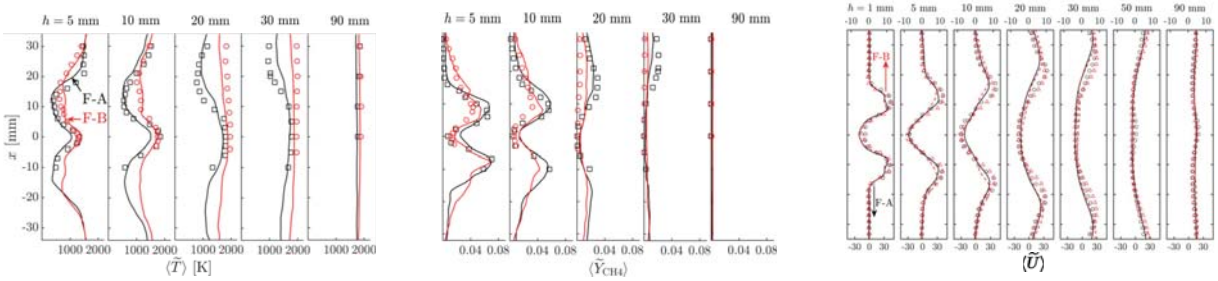

❑ **Flame shape (CH concentration)**

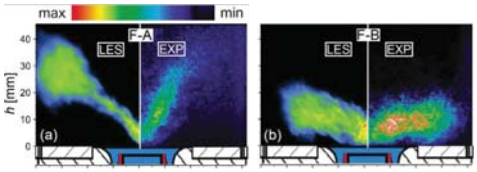

❑ **Acoustic power spectra**

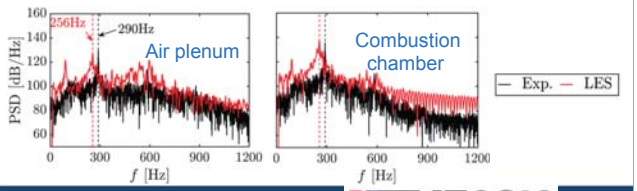

UNIVERSITY OF CAMBRIDGE

Z. X. Chen, N. Swaminathan, M. Stöhr, W. Meier, *Proc. Combust. Inst.* (2018) submitted.

TNF2018 DUBLIN IRELAND JULY 27-28

TNF2018 DUBLIN IRELAND JULY 27-28

19th INTERNATIONAL WORKSHOP ON MEASUREMENT & COMPUTATION OF TURBULENT FLAMES

SAPIENZA UNIVERSITÀ DI ROMA

جامعة الملك عبدالله للعلوم والتقنية
King Abdullah University of Science and Technology

High-Pressure Syngas Jet Flames (CHN)

Experimental effort:

W.R. Boyette[1], T.F. Guiberti[1], G. Magnotti[1], W.L. Roberts[1]

Numerical effort:

P.P. Ciottoli[2], B.J. Lee[3], P.E. Lapenna[2], R.M. Galassi[2], E. Martelli[4], F.E. Hernandez Perez[1], M. Valorani[2], H.G. Im[1]

1 King Abdullah University of Science and Technology (KAUST), Saudi Arabia

2 Sapienza University of Rome, Rome, Italy

3 Gwangju Institute of Science and Technology, Gwangju, South Korea

4 Campania University L. Vanvitelli, Aversa, Italy

Target description

- Baseline case identical to Sandia/ETH-Zürich chnA TNF target flame (non-premixed - *ID* = 4.6 mm - 40% CO, 30% H_2, 30% N_2 by vol.)

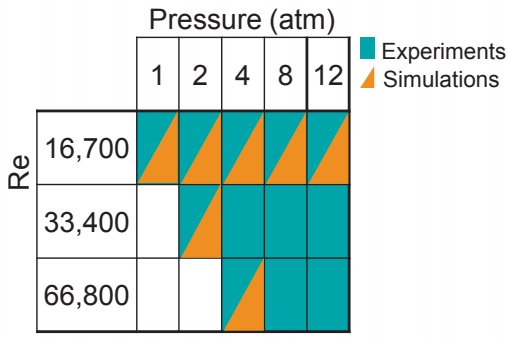

- OH-PLIF at 12 experimental conditions
- PIV (non-reactive) at conditions P < 8 atm
- LES at 5 constant Re and 3 constant velocity conditions

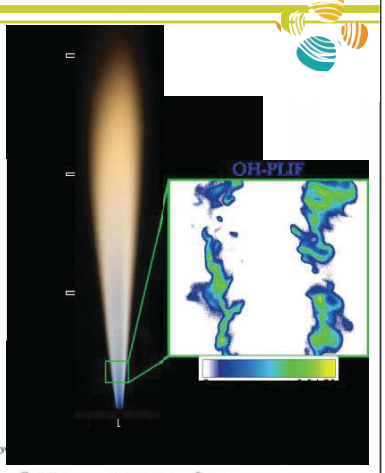

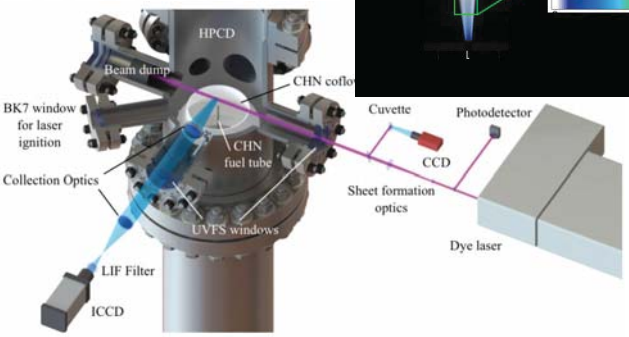

Schematic of the high-pressure combustion duct (HPCD)

Modelling Framework

- **Large eddy simulations (LES)** using **Smagorinsky** model for **subgrid stresses**
- **Steady laminar flamelet model** (SLFM) for modeling combustion
- Transport equations for resolved mixture fraction Z and its variance Z''
- Favre-filtered governing equations are solved using a **finite volume pressure-based** solver of **OpenFOAM**
- A presumed **(beta)** probability density function **(PDF)** approach is employed to represent the subgrid-scale (SGS) turbulence-chemistry interaction

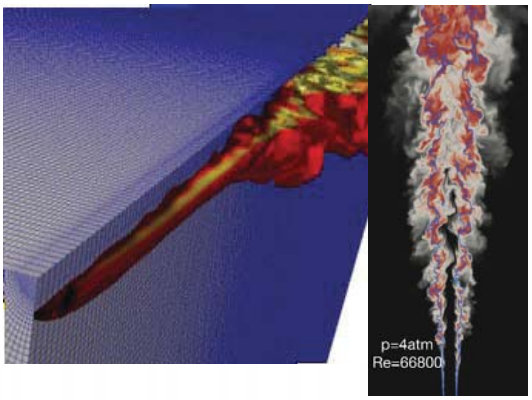

- Flamelet library for species and temperature is constructed and parameterized in terms of the resolved scalar dissipation rate **χ**, resolved mixture fraction **Z**, and its variance **Z''**
- Flamelet solution using **12 species and 33** reactions (Li *et al.*, 2007)
- Cylindrical computational domain (R = 169 mm, L = 960 mm)

Results

- To assess effects of pressure and turbulence, quantitative comparisons b
  experiments and simulations are based on the features of the OH layer:

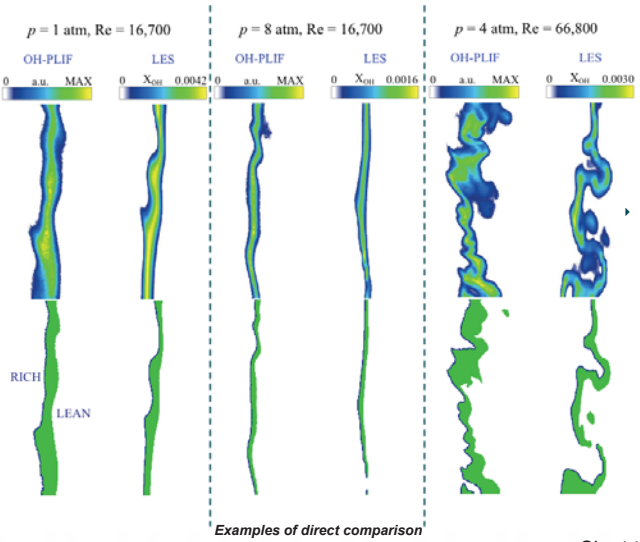

Examples of direct comparison

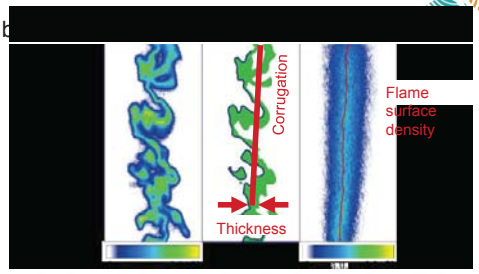

- Non-reactive PIV is also available to prescribe proper inflow conditions and assess turbulence properties:

P (atm)	U_j (m/s)	Integral scale (mm)	Taylor scale (μm)	Taylor Re	Kolmogorov scale (μm)
1	77.3	2.0	570	160	23
2	38.7	2.1	500	190	19
2	77.3	2.0	340	270	11
4	19.3	2.1	490	190	18
4	38.7	2.0	340	270	10
4	77.3	2.1	240	400	6

- Short-term plans include reactive PIV measurements (fall 2018) for validation of LES predictions of mean and r.m.s flow characteristics.

King Abdullah University of Science and Technology

UNIVERSITY OF CAMBRIDGE

Loughborough University

LES Studies on Enclosed Swirl Flames in Industrial Combustors

Zhi X. Chen[a], Ivan Langella[a,b], N. Swaminathan[a]

[a] Cambridge University, Department of Engineering, UK

[b] Loughborough University, Department of Aeronautical & Automotive Engineering, UK

TNF 2018 DUBLIN IRELAND JULY 27-28

Siemens SGT-100 Industrial Gas Turbine Combustor

– Flamelet modelling of a technically premixed CH_4/air combustion at 3 bar

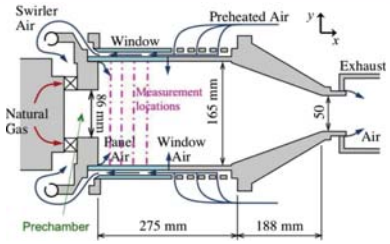

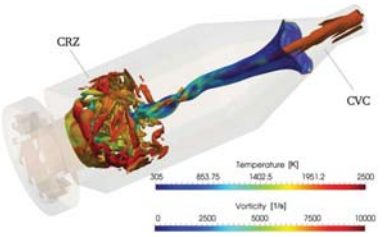

❑ **Effect of mixture stratification (A) and SGS variance (B)**

➢ Neither considered (– –), A (——), A+B (– · –)

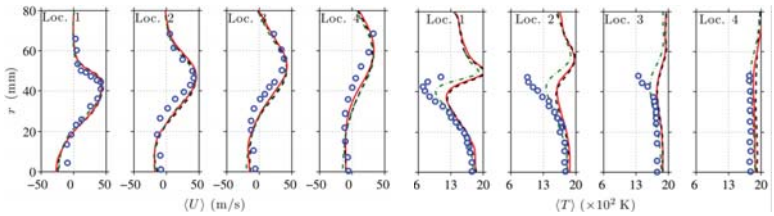

- Mixture stratification has only marginal effect on the results
- The effect of SGS variance of mixture fraction is significant for temperature predictions
- SGS strain may be the responsible for the overprediction of temperature

UNIVERSITY OF CAMBRIDGE

Stopper *et al.*, *Combust. Flame* 160 (2013) 2103-2118.
I. Langella, Z. X. Chen, N. Swaminathan and S. K. Sadasivuni, *J. Propul. Power* (2018) in press.

TNF2018 DUBLIN IRELAND JULY 27-28

Flameless combustion in a lab-scale furnace

Xu Huang, Eric van Veen, Mark Tummers and Dirk Roekaerts
Delft University of Technology

Contribution to TNF workshop, Dublin, 2018

TU Delft
Challenge the future

Lab-scale furnace for study of flameless combustion

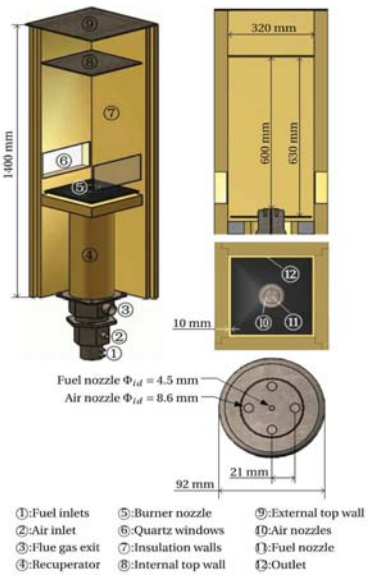

Objectives:
- Experimental study to gain understanding of flameless combustion
- Development and validation of computation model describing effects of dilution by recirculation of products and enthalpy loss.

Setup:
- Furnace with REKUMAT 150 recuperative Flame-FLOX burner.
- Side walls fixed in lab-frame and vertically movable burner and top wall.
- Side walls insulated and cooling mainly via top wall.
- Flue gas exit to recuperator via slit in bottom plane

- Fuel: Dutch natural gas.
- Power: 9 kW
- Equivalence ratio: three cases: 0.7, 0.8, 0.9

- Diagnostics: OH* chemiluminescence, LDA, CARS, wall thermocouples

Acknowledgement: X. Huang received a scholarship from CSC and Technology Foundation STW for financed the experimental setup.

X. Huang et al, Energy Procedia, 120, 395-402 (2017)
X. Huang, PhD Thesis, TU Delft, to be published

TU Delft
Challenge the future

Experimental results

Flameless combustion

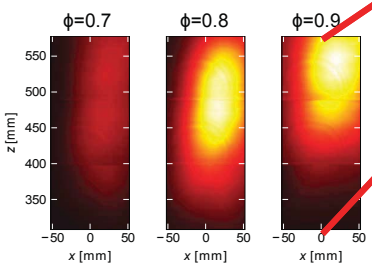

Flameless regime all three cases.
Mean OH* chemiluminescence: high in upper part.

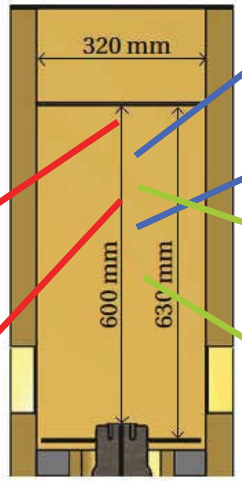

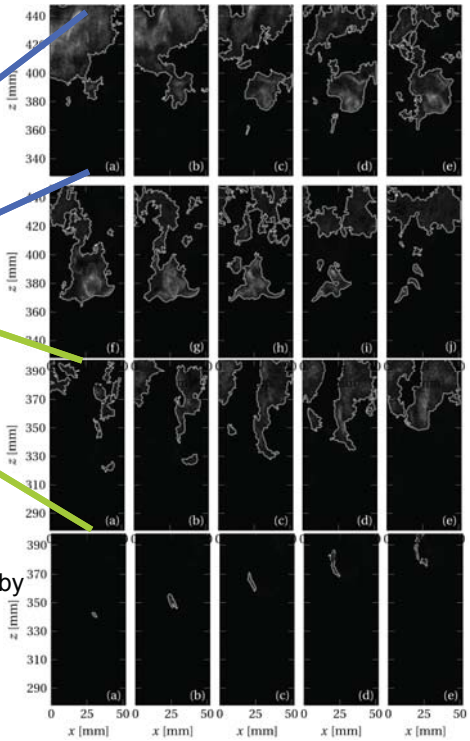

Turbulent combustion process sustained by
- Single and multiple ignition kernels
- Growth/decay
- Merger into clusters
- Occasional flame propagation

Experimental results

Fuel: Dutch natural gas
Power: 9 kW
Equivalence ratio: 0.7, 0.8, 0.9

LDA in forward scatter configuration
Data rate of at least 50 Hz
Measurement locations
on horizontal traverses at
z=3,50,100,200,300,400,500 mm.
Provides joint one-points statistics of two components of velocity.

CARS
Measurement locations
on horizontal traverses at
z=3,25, 50,100,200,300,400,500 mm
Per location
1600 single-shot CARS spectra
collected at 10 Hz.
Provides one-point PDF of temperature

Thermocouples
(Super OMEGACLADTM XL sheathed ungrounded type K)
At centre of internal top wall, in burner head, at side wall

Flue gas analyser (Testo 335)

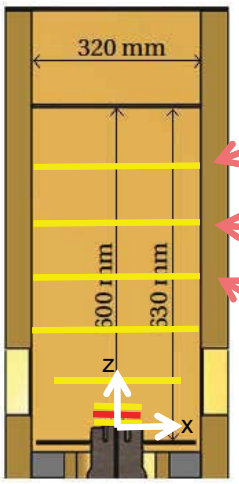

PDF of temperature at several positions

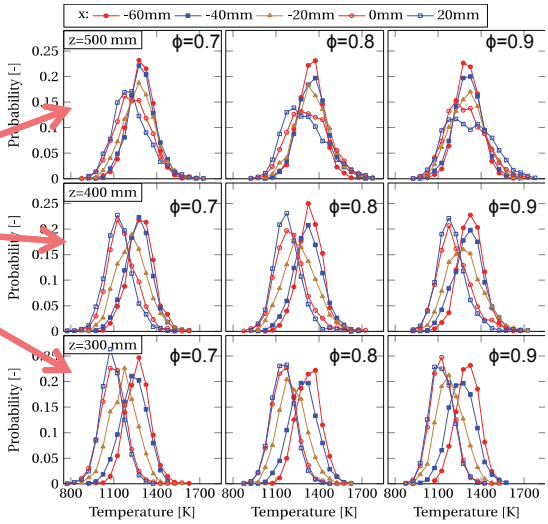

Relevant PDF feature: tail of moderately high temperature values becoming larger with heigth z

CARS System (van Veen and Roekaerts, 2003, 2005)
Single-shot imprecision 1%-4% (2000 to 300 K) . Inaccuracy estimated to be 20 K

Numerical modeling and simulation

So far the furnace has been simulated using:

- RANS with modified Eddy Dissipation Concept model (ANSYS-Fluent) (H.Bao, N. Romero Anton)
- RANS with FGM based on fuel – air flamelets, including heat loss (ANSYS-Fluent) (N.Romero Anton)
- RANS with Diluted Air FGM: based on fuel – diluted air flamelets, including heat loss (OpenFOAM) (X. Huang)

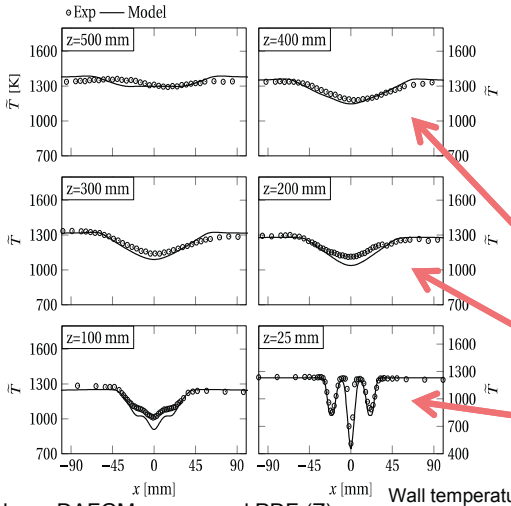

k-ε + DAFGM + assumed PDF (Z)

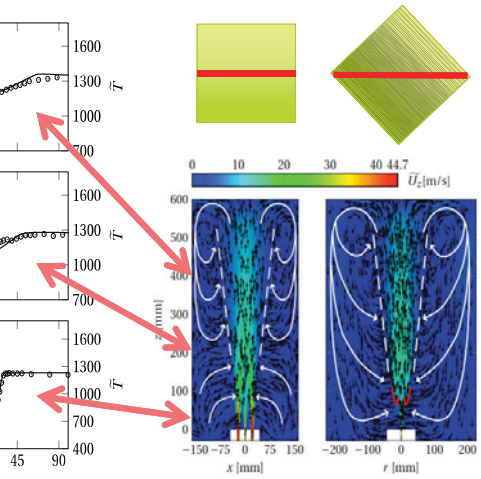

Wall temperature is assumed to be a piecewise linear profile inspired by near wall CARS data.

Challenges:
- Trends with equivalence ratio
- Representation of ignition kernel dynamics
- Prediction of temperature PDF

Experimental data base will become available for model validation studies.

d.j.e.m.roekaerts@tudelft.nl

X. Huang, PhD Thesis, TU Delft, to be published
X. Huang et al, poster presentation, TNF 2018

Confined and Pressurised Jet in Hot & Vitiated Coflow Burner

M.J. Evans[a], P.R. Medwell[a], Q.N. Chan[b]
[a]The University of Adelaide [b]The University of New South Wales

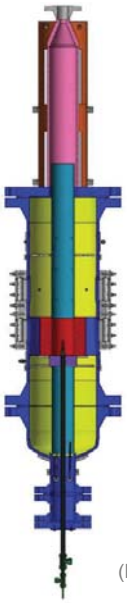

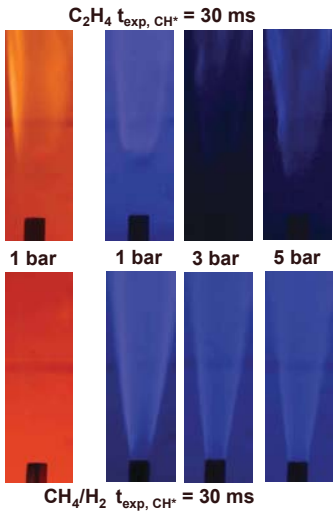

Instantaneous (top, C_2H_4) and averaged (bottom, CH_4/H_2) images of CH* emissions and photographs from initial testing

- 4.6 mm ID central jet
- 95 mm ID, non-premixed coflow burner
  - Ceramic flow straightener 80 mm upstream of jet exit
- 300 mm ID stainless steel pressure vessel
  - 10 bar design pressure
  - thermally insulated walls
  - approx. 3.5 m tall, 1000 kg total mass
- Water cooled exhaust with digital pressure control
- Up to eight 48 × 107 mm (W × H) windows, at two axial locations
- Similar operational envelope to JHC burner
- Initial test cases:
  - Coflow: natural gas/H_2 with T_{ad} 1590 K; 9% O_2
  - both C_2H_4 and NG:H_2 jet flames at various ratios
  - up to 5 bar

High-Pressure Enclosed Jet Flames

German Aerospace Center (DLR)
Institute of Combustion Technology, Stuttgart

SIEMENS

DLR

Single Nozzle FLOX® Burner for Premixed Enclosed Jet Flames

- Model combustor with relationship to gas turbine combustor with multiple nozzles
- Design by DLR/Siemens
- Operation in DLR high-pressure test rig
- Goals: component development: injector and mixing concept at realistic scale

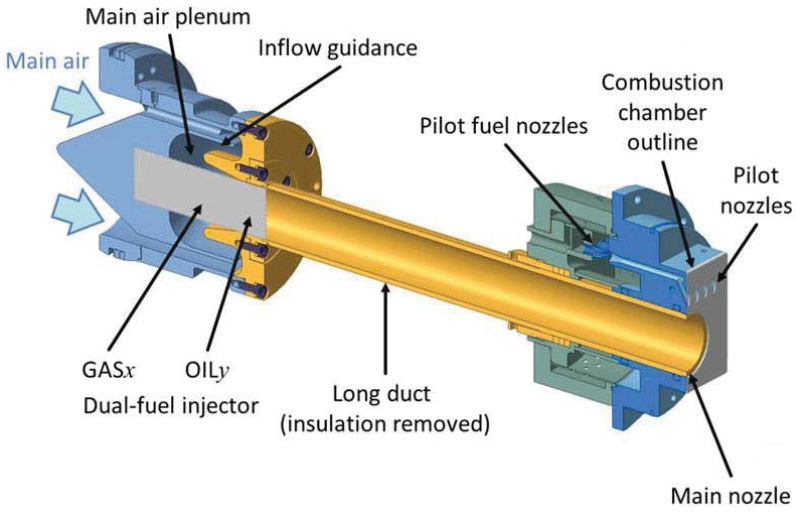

DLR

Single Nozzle FLOX® Burner

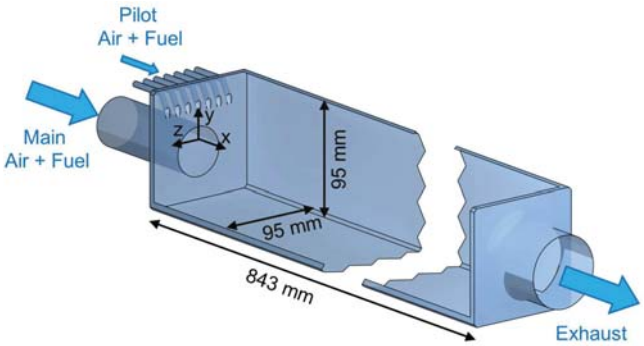

- Main nozzle off-centered at y = -10 mm
- Main nozzle diameter 40 mm
- Fuel (natural gas) injected at x = -400 mm

- Large quartz glass windows
- Burner head rotateable ±90°

Operating Conditions and Measurement Techniques

- Operation with and without pilot flames
- Pressure 4-12 bar
- Jet exit velocity 80-120 m/s
- Thermal Power 416-1482 kW
- Air excess ratio λ = 1.4-3.6
- Air preheat temperature 623-823 K

- OH chemiluminescence imaging
- OH laser induced fluorescence (also for 2D T)
- Particle image velocimetry
- Multispecies Raman measurements
- CARS temperature measurements
- Commercial exhaust gas analysis
- Dynamic pressure measurements
- Further measurement techniques for liquid fuel

Examplary Experimental Results

Gaseous fuel – unpiloted flame, 8 bar, v_{jet} = 111 m/s

Mean chemiluminescence and velocity distributions from 2 different direction

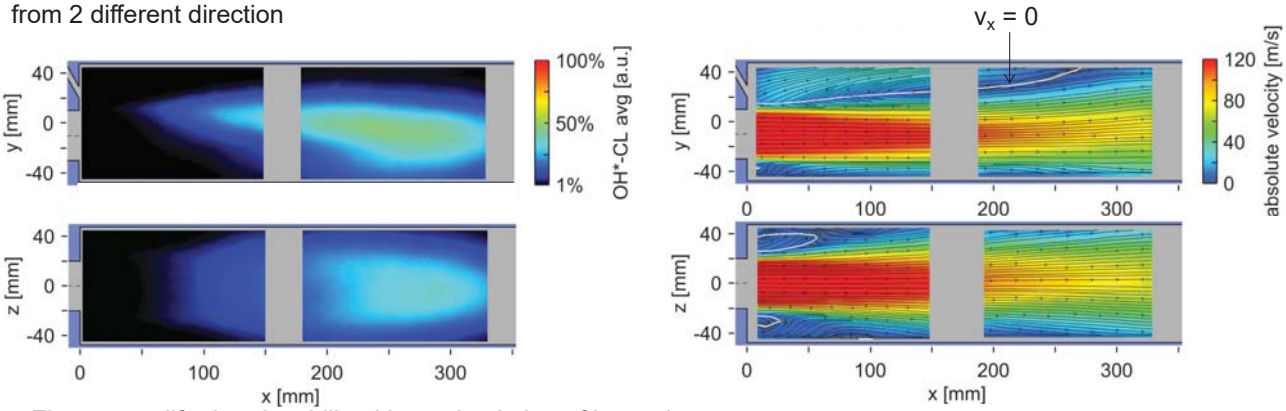

- Flames are lifted and stabilized by recirculation of burned gas
- Large recirculation zone on side with larger distance to wall

Mean Distributions of T, Fuel and Water

Gaseous fuel – unpiloted flame, 8 bar, v_{jet} = 111 m/s

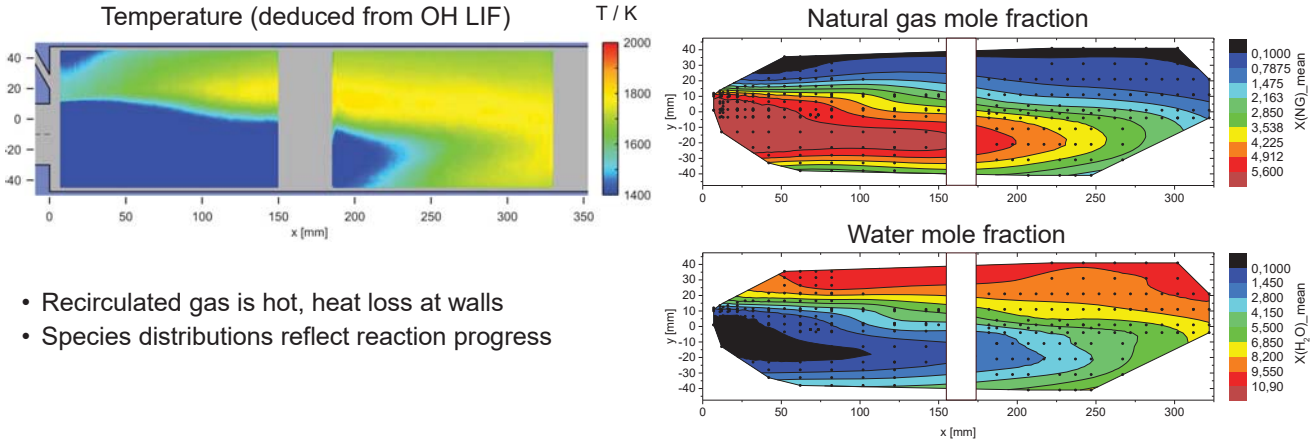

- Recirculated gas is hot, heat loss at walls
- Species distributions reflect reaction progress

Results from Simultaneous OH PLIF / PIV Single Shot Measurements

Gaseous fuel – unpiloted flame, 8 bar, v_{jet} = 111 m/s

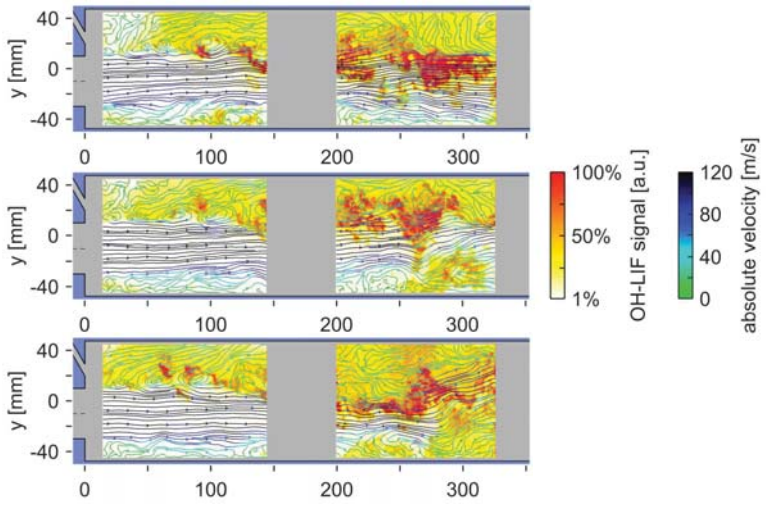

- Vortices in shear layer generate mixing of fresh gas from the jet and recirculating burned gas.
- Auto-ignition is frequently observed in the starting region of the jet (verified by high-speed chemiluminescence imaging).

References

- Oliver Lammel et al., High Momentum Jet Flames at elevated pressure, A: Experimental and Numerical Investigations for Different Fuels, Proc. ASME Turbo Expo, GT2017-64615
- Michael Severin et al., High Momentum Jet Flames at elevated pressure, B: Detailed Investigations of Flame Stabilization with Simultaneous PIV and OH-LIF, Proc. ASME Turbo Expo, GT2017-64556

Institute for Combustion and Gas Dynamics
Fluid Dynamics

SIEMENS

UNIVERSITÄT DUISBURG ESSEN
Offen im Denken

Investigation of a high pressure jet flame with heat losses using tabulated and finite rate chemistry

P.Gruhlke, H. Janbazi, I. Wlokas, C. Beck, A. Kempf
pascal.gruhlke@uni-due.de

Lehrstuhl Fluiddynamik, Institut für Verbrennung und Gasdynamik
Universität Duisburg-Essen, Germany

Combustion modelling

UNIVERSITÄT DUISBURG ESSEN
Offen im Denken

- Comparison of two combustion models:
  - Finite rate chemistry (FRC) combustion model using extended DRM19[1] (by OH* sub-mechanism[2]) and inhouse skeletal reaction mechanism (developed for chamber inlet conditions; optimized for flame speed, temperature, CO and NOx).
  - Premixed flamelet generated manifold (PFGM) combustion model (table generation using GRI-Mech 3.0[3]).
- Thickened-flame approach including Charlette model[4] to compensate reduced flame wrinkling.

Institute for Combustion and Gas Dynamics
Fluid Dynamics

1. Kazakov et al., http://www.me.berkeley.edu/drm (1994)
2. Kathrotia et al., Appl. Phys. B (2012)
3. Smith et al., www.me.berkeley.edu/gri_mch/ (2000)
4. Charlette et al., Combust. Flame (2002)

Numerical setup

UNIVERSITÄT DUISBURG ESSEN
Offen im Denken

- LES simulations using OpenFOAM with two different combustion models.
- Blended temporal discretization (0.3 explicit/0.7 implicit).
- Convection discretized by TVD scheme[5].
- Sub-grid viscosity computed with transported sub-grid kinetic energy model[6].
- **Non-adiabatic** simulation: **heat losses in experiments** modelled by iso-thermal chamber walls calculated from coolant mass flows and temperatures.
- Mesh: 8.7 M cells (Δ_F= 1.0 mm).
- Sampling after 6 flow-through times for another 10 flow-through times.
- Computational cost on fine grid: FRC(DRM19) 1,440,000 CPUh,
  FRC(Skel. Mech.) 360,000 CPUh,
  FGM 64,000 CPUh.

5. Windén, PhD Thesis (2014)
6. Yoshizawa et al., J. Phys. Soc. Jpn. (1985)

IVG Institute for Combustion and Gas Dynamics
Fluid Dynamics

3

Instantaneous fields

UNIVERSITÄT DUISBURG ESSEN

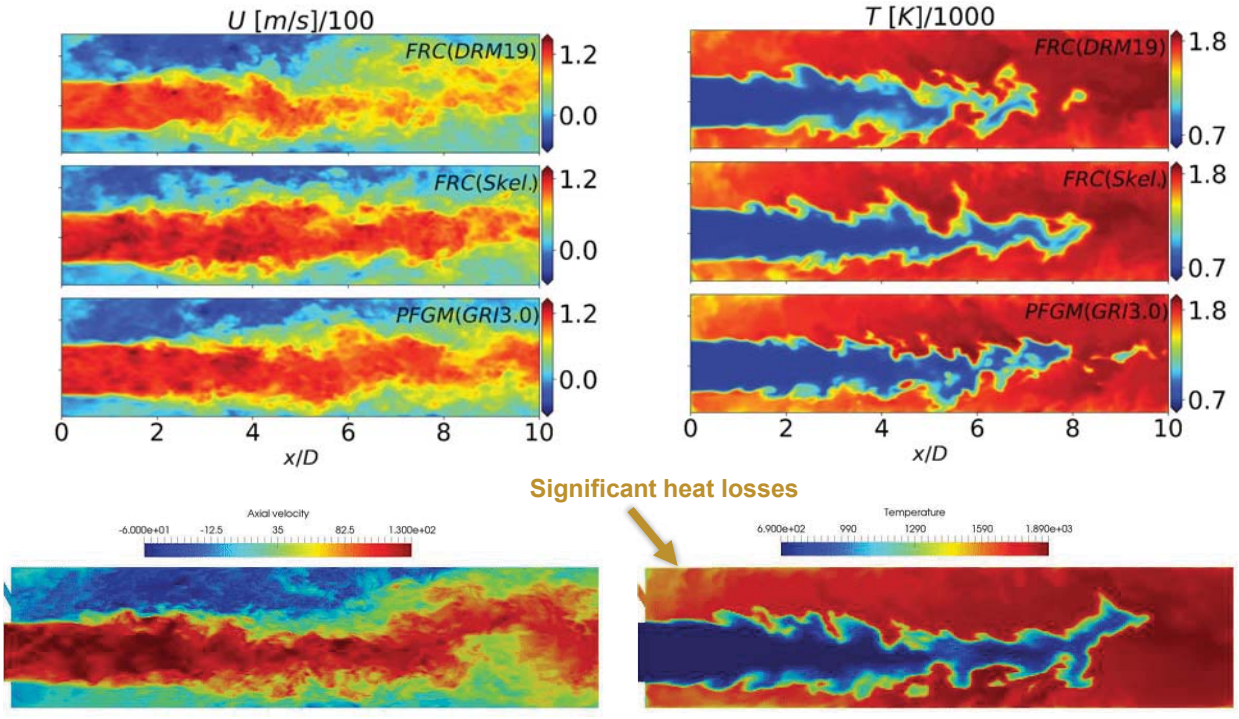

Animations from FRC(DRM19)

4

Quantitative results

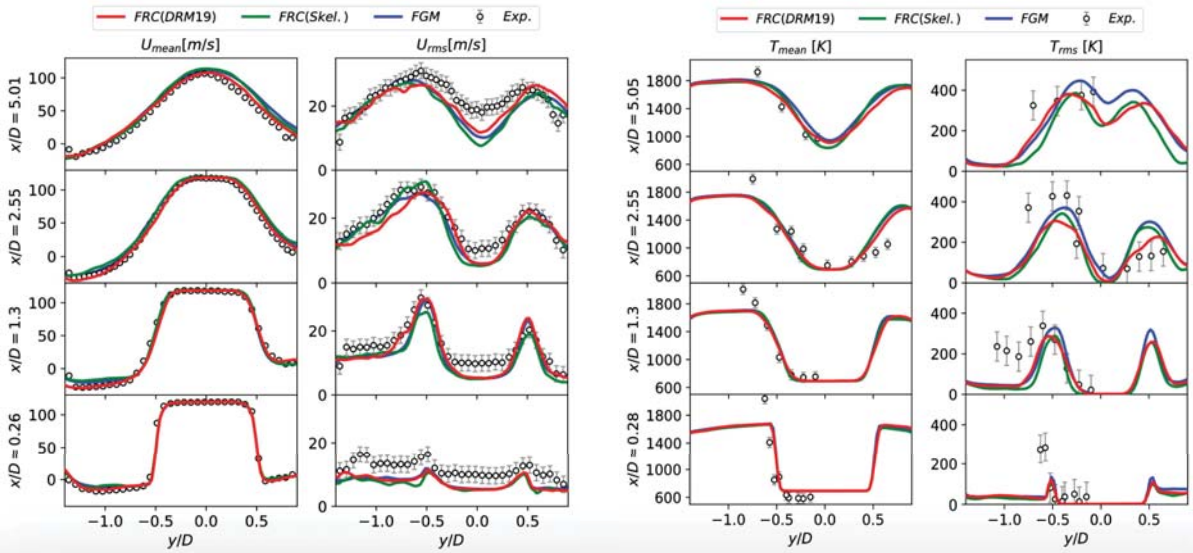

Flow field and temperature profiles well captured by both combustion models.
Results improve using DRM19.

Analysis of flame stabilization based on most detailed simulation: comparison with experiment

Line-of-sight integrated results

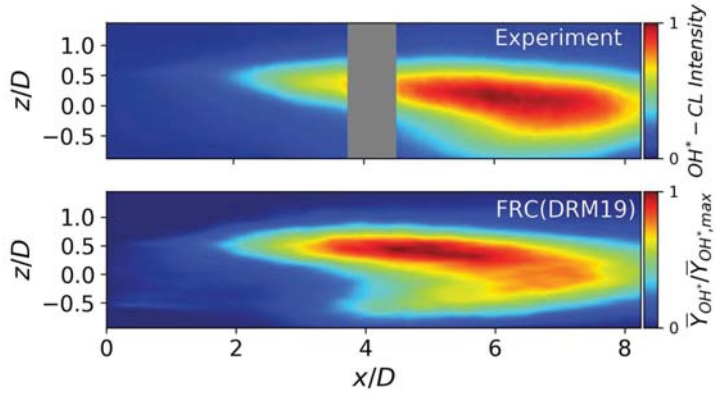

DRM19 simulation with OH* is very close to experiment.
Other simulations do not include OH*.

Analysis of flame stabilization based on most detailed simulation: comparison with experiment

UNIVERSITÄT DUISBURG ESSEN
Offen im Denken

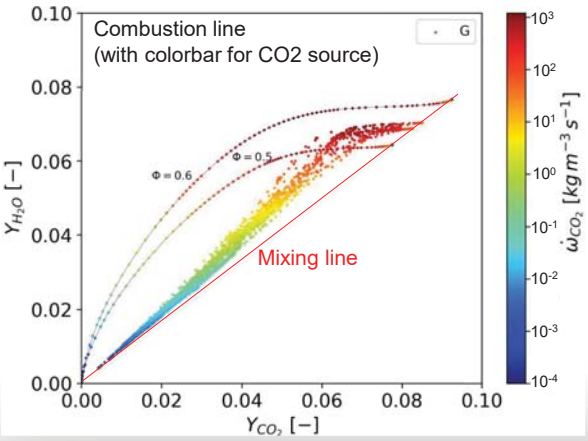

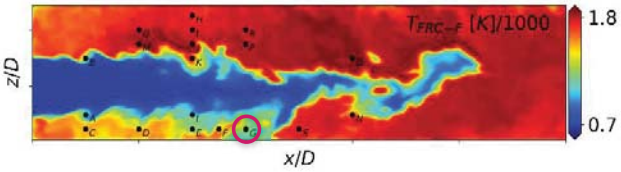

Mixture composition at lower degrees of reaction progress close towards non reacting mixture
→ mixing of recirculated hot gas appears to be faster than reaction.
Mixing with hot gases induces auto-ignition effects stabilizing the flame.

Analysis of prediction capability of PFGM regarding flame lift off

UNIVERSITÄT DUISBURG ESSEN

Line-of-sight integrated results

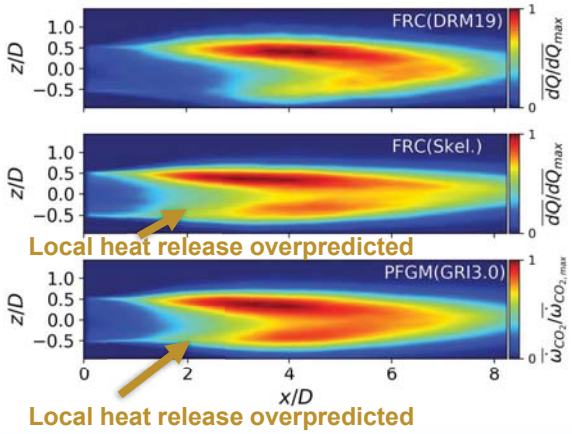

Plug flow analysis of kinetic models

- Ignition delay times of a homogenous mixture of fresh gas and burnt products with different portions for a plug flow reactor (ζ=1 pure fresh gas, ζ=0 pure burnt products).

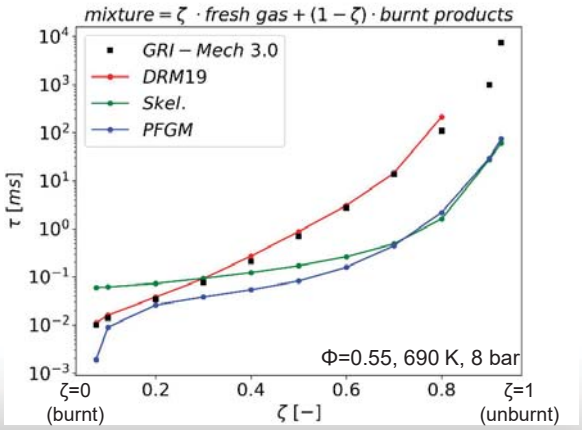

Difference in ignition time scales at low reaction progress can explain poor prediction of flame lift off by PFGM.

References

1. Kazakov, Andrei, and Michael Frenklach. "Reduced reaction sets based on GRI-Mech 1.2." University of California at Berkeley, Berkeley, CA, http://www. me. berkeley. edu/drm (1994).
2. Kathrotia, T., Riedel, U., Seipel, A., Moshammer, K., & Brockhinke, A. (2012). Experimental and numerical study of chemiluminescent species in low-pressure flames. Applied Physics B, 107(3), 571-584.
3. Smith, G. P, Golden, D. M., Frenklach, M., Moriarty, N. W., Eiteneer, B., Goldenberg, M., Bowman, C. T., Hanson, R. K., Song, S., Gardiner, W. C., Lissianski, V. V., and Qin, Z., 2000, www.me.berkeley.edu/gri_mch/.
4. Charlette, F., Meneveau, C., & Veynante, D. (2002). A power-law flame wrinkling model for LES of premixed turbulent combustion Part I: non-dynamic formulation and initial tests. *Combustion and Flame*, *131*(1-2), 159-180.
5. Windén, B. (2014). Powering performance of a self-propelled ship in waves (Doctoral dissertation, University of Southampton).
6. Yoshizawa, A., & Horiuti, K. (1985). A statistically-derived subgrid-scale kinetic energy model for the large-eddy simulation of turbulent flows. Journal of the Physical Society of Japan, 54(8), 2834-2839.

Institute for Combustion and Gas Dynamics
Fluid Dynamics

Acknowledgments:

We acknowledge financial support through BMWi (funding reference number 03ET7011L) and computing time granted by CCSS of the University of Duisburg-Essen and provided on the supercomputer magnitUDE (DFG grant INST 20876/209-1 FUGG).

Thank you for your attention!

Flame-wall interactions

Coordinators: Andreas Dreizler, Johannes Janicka

Background

Flame-wall interaction (FWI) is a topic of the TNF Workshop since 2014. The primary issue is to gain a deeper understanding of turbulent flames in the vicinity of walls as urgently needed to improve combustion modelling. Confined flames are of high practical relevance as walls impose boundary conditions with significant impact on physical-chemical processes at micro and macro scales of turbulent flames. This impact leads to flame quenching related to heat losses and incomplete combustion causing primary pollutant formation such as carbon monoxide (CO) and unburnt hydrocarbons (UHC). To understand these processes, the influence of walls on turbulence-chemistry interaction as one of the primary fields of interest in the TNF must be studied in much more detail.

Following the TNF strategy, a target flame has been introduced in TNF 13 [1]. Briefly, it is a side-wall quenching (SWQ) geometry operating at atmospheric conditions. The fully premixed flame is anchored at a ceramic rod generating a V-shaped flame brush where one of the two branches is interacting with a temperature-controlled wall. Flow conditions are either laminar or turbulent by inserting a turbulence grid inside the burner nozzle.

Based on the previous TNF sessions and recent research efforts, the objective of the FWI-session at TNF was twofold:

1. Provide an update on recent experimental efforts including the TNF-target geometry and a new FWI-burner concept from Melbourne University and provide new phenomenological insights into FWI
2. Show the progress made in numerical simulations of near-wall combustion phenomena and identify next steps of combustion modelling FWI

Experimental studies on Flame-Wall interactions

Contributors:

- Jacob E. Rivera, Rahul Palluli, Bin Jiang, Robert L. Gordon, Mohsen Talei, University of Melbourne
- Hidemasa Kosaka, Florian Zentgraf, Benjamin Böhm, Andreas Dreizler, TU Darmstadt

The **University of Melbourne** introduced a Forced Laminar Axisymmetric Quenching (FLAQ) Burner suitable to study Flame-Wall Interaction and the interaction of cooling jets with flames [2-4]. On a long term, mechanisms will be investigated that are responsible for changes in exhaust CO, e.g. transient FWI, the influence of cooling rates, surface reactivity and dilution. The FLAQ-burner provides an axisymmetric, optically accessible flame with a concave FWI-zone. Present studies focus on the influence of local effects such as heat loss, quenching mode, flame geometry, and transient effects on the exhaust gas composition. The exhaust gas composition is analysed with respect to the concentrations of CO, CO_2, O_2, NO_x and unburnt hydrocarbons using extractive measurement methods. In the slides, selected results are discussed showing the formation of M- and V-shaped flames depending on the inflow and boundary conditions, stability limits, and radial profiles of mean temperatures and CO concentrations. Future research will focus primarily on wall reactivity and thermal boundary conditions (thermal barrier coating, annealing), turbulence, fuel effects, and the impact of cooling jets.

The group at **TU Darmstadt** has significantly enlarged the data base of the SWQ-target flames. It comprises the following aspects:

- Effects of the local flow field on flame quenching [5]

- Influence of the wall on CO concentrations and temperature [6] and multi-scalar imaging [7]
- Influence of varying wall temperatures and fuels on thermochemical states near walls [8]
- Reaction rates in FWI [9] and heat release imaging [10]

In the FWI-session the discussion was focused on selected issues with the following conclusions:

- Studying the influence of varying wall temperatures shows how the quenching distance is decreased for increasing wall temperatures causing an enhanced heat transfer rate. This counter-intuitive observation is restricted to the FWI-zone. Further downstream in the post-flame region higher wall temperatures are associated with reduced heat transfer as expected for chemically non-reacting flows.
- For a fixed wall temperature CO/T scatter plots show for stoichiometric methane/air flames an impact on the CO-formation for wall distances below 0.2 mm whereas the CO-oxidation at high temperatures (T > 1500 K) is influenced already for wall distances up to ~1 mm. This observation is explained by different chemical time scales for CO-formation and oxidation in relation to physical time scales for heat transfer. This explanation was confirmed by 2D DNS [11]. For DME/air flames the CO-formation is even less strongly influenced due to its chemical time scales that are shorter compared to methane combustion.
- Heat release zones of premixed flames in the near wall region have been imaged by simultaneous imaging of formaldehyde and hydroxyl radicals. From instantaneous realizations flame curvatures have been deduced. Correlations of normalized heat release and curvature indicate the influence of Lewis-number effects [10].

Future research directions comprise the influence of more complex fuels, higher Reynolds-numbers and pressures. In terms of diagnostics, multi-scalar imaging appears to be most important to further understand the impact of solid walls on the thermochemical state.

Modelling and numerical simulation

Contributors:

- Mahmoud Jafargholi, Christos E. Frouzakis, George K. Giannakopoulos, Konstantinos Boulouchos LAV, ETH Zürich
- Umair Ahmed, Nilanjan Chakraborty, Jiawei Lai, Markus Klein, School of Engineering, Newcastle University and LRT and Universität der Bundeswehr München
- Andrea Gruber, Jacqueline H. Chen, SINTEF, Trondheim and Sandia National Laboratories, Livermore
- Michael Pfitzner, Christian Mundt, Institut für Thermodynamik, Universität der Bundeswehr München
- J. Sellmann, J. Lai, A. Kempf, N. Chakraborty, IVG, Universität Duisburg-Essen and Newcastle University
- Johannes Janicka et al., TU Darmstadt

Compared to TNF 13 a larger group of researchers contributed to the FWI-session, and the research focus was more aligned along the SWQ-target configuration.

The **ETH-group** performed Direct Numerical Simulations to study premixed flame propagation in confined geometries and flame-wall interactions. Using a spectral element low Mach number reactive flow solver based on Nek5000, premixed syngas/air mixtures at an equivalence ratio of 0.3 ($CO:H_2$ = 3:1) have been simulated in 2D and 3D using detailed chemistry and transport. Homogeneous isotropic turbulence at atmospheric pressure has been prescribed in addition to an initial gas temperature of 820 K and a wall temperature of 550 K. Varying u'/s_l, the temporal evolution has been investigated for flames approaching the wall. The findings can be summarized as follows:

- Confinement affects flame propagation through varying thermodynamic conditions, modifications of the flow field, and flame/wall interactions:
    - The flame 'feels' the wall early: significant variation of the local displacement speed, quenching distance and heat fluxes
    - initial (kernel growth) and final (FWI) consumption of the fuel need 3 to 5 times longer to consume the first and last 10% of the fuel
- Early flame kernel growth:
    - u' plays the dominant role
    - for the same u', smaller turbulent length scale l_t leads to faster initial fuel consumption
- Fuel consumption rate:
    - increases with turbulence intensity and saturates at high u'
    - no discernible trend vs. turbulent length scale
    - turbulence pushes the flame closer to the walls than the laminar quenching distance
    - mean distance of the flame from the wall decreases with u'

The joined studies of the universities of **Newcastle** and of the Federal Armed Forces at **Munich** focused on a fundamental understanding and modelling of flame-wall interactions using Direct Numerical Simulations (DNS). For head-on quenching, single-step chemistry is compared to detailed chemistry including modifications proposed by Sellmann et al. [12.] and Lai et al. [13]. The conclusions drawn are:

- The quenching distance for turbulent condition decreases and the magnitude of the maximum wall heat flux increases in comparison to the corresponding laminar HOQ values for cases with Le<1.
- All the modelling assumptions associated with high Damköhler number (i.e. $Da \gg 1$) and presumed bi-modal PDF of c are rendered invalid close to the wall.
- Both conventional Flame Surface Density (FSD) and Scalar Dissipation Rate (SDR) closures for mean reaction rate break down in the near-wall region.

At **SINTEF/Sandia** the focus was on Direct Numerical Simulations of turbulent flame-wall interactions in a constant volume vessel. A new data base has been introduced to investigate turbulent flame-wall interaction at constant volume conditions. Most important features are:

- The data enables comparison of the FWI-process for hydrogen-air and methane-air flames at different Ka-numbers but for the same wall quenching time
- Cases are initialized in a closed box for isothermal walls at 750K and relaxed for 10 integral time scales before spark ignition

Primary findings are:

- All flames exhibit some degree of radical recombination at the wall: its role is minimal for the lean hydrogen flame, but more important for the stoichimoetric methane flame and greatest for the stoichiometric hydrogen flame
- Flame velocity seems to be the governing parameter in the turbulence-chemistry interaction more than flame thickness vs turbulence length scales
- The hydrogen stoichiometric flame shows the largest wall heat flux and the largest heat release rate due to radical recombination
- The hydrogen lean flame shows the least heat release rate due to radical recombination (wall heat flux is also low due to the lower flame temperature)
- Total mass of CO peaks at quenching but it successively burned out after the FWI

In **Munich** the heat transfer coefficient in reactive boundary layers was investigated which is proposed as $\dot{q}_{react} = -\lambda \frac{\rho_W}{\rho_\infty} \sqrt{\frac{\rho_\infty u_\infty}{2 \rho_W x}} \left.\frac{\partial Z^*}{\partial \zeta}\right|_{\zeta=0} \frac{1}{1-Z_{st}} (T_{ad} - T_W)$ [14]. In the slides, boundary layer profiles are compared for chemically reactive and non-reactive conditions. In addition, a tabulation

method is proposed suitable for FWI-combustion modelling. Its application is demonstrated for wall-heat flux predictions of methane-oxygen combustion at rocket-like conditions.

The collaborative research of **Newcastle** University and University of **Duisburg-Essen** is devoted to flame surface density (FSD) based modelling of head-on quenching of turbulent premixed flames. The objective of the study is an a priori analysis of the mean reaction rate closure and modelling of the unclosed terms based on existing models. Findings are drawn from a parametric DNS-study including three different Lewis numbers and five different initial turbulent intensities. Head-on quenching is simulated in 3D using the compressible code SENGA 11 on a Cartesian grid, a no-slip isothermal inert wall, and one-step reaction kinetics. Whereas a detailed discussion of the results can be found in [12], the most important results are:

- A modified FSD-based closure for mean reaction rate in terms of flame-wall interaction has been proposed
- Existing models for the unclosed terms of the FSD transport equation have been modified
- The modified models are capable for a Lewis number range of Le = 0.8 - 1.2 and different turbulent initial values

Recent result of **TU Darmstadt** comprise 2D Direct Numerical Simulation (DNDS) and 3D Large Eddy Simulation (LES) of the SWQ-target flames. Comparing detailed chemistry and the FGM-based tabulated chemistry approach show similar wall-normal temperature profiles that compare very well with experimental observations. In contrast, predictions of the CO-concentrations differ strongly in the near-wall region. Based on a budget-analysis it is revealed that close to the wall diffusion dominates with large contributions from scalar dissipation rates which is not reflected in unbounded flamelet calculations that are the base for the FGM-approach. Solving chemical reactions in the state-space and imposing estimated gradients from DNS, the REDIM approach matches the CO-profiles from the DNS in physical and state-space [15]. Using the LES-FGM-approach and restricting to global features of the flow and scalar fields, flame brush and probability of the flame close to the wall are very well covered [16].

In the discussion, future research directions in FWI were identified as:

- Increased pressure
- Sustainable fuels
- Partially premixed/stratified flames near walls

References

[1] C. Jainski, M. Rißmann, B. Böhm, A. Dreizler: Experimental investigation of flame surface density and mean reaction rate during flame-wall interaction; Proc. Combust. Inst. 36, 1827 – 1834 (2017)

[2] J. E. Rivera, R. L. Gordon, M. Talei: Flame-Wall Interaction of a Forced Laminar Premixed Propane Flame: Flame Dynamics and Exhaust CO Emissions; Proceedings of the Combustion Institute 37, https://doi.org/10.1016/j.proci.2018.07.030

[3] J. E. Rivera, R. L. Gordon, M. Talei: Flame Chemiluminescence Measurements of a Laminar Forced Flame Interacting with a Cold Wall; Proceedings of the 11th Asia-Pacific Conference on Combustion, Sydney, Australia, 2017

[4] J. E. Rivera, R. L. Gordon, M. Talei, M. J. Brear: A Novel Burner for Investigating End-Gas Effects of Transient Flame-Wall Interaction; Proceedings of the 20th Australasian Fluid Mechanics Conference, Perth, Australia, 2016

[5] C. Jainski, M. Rißmann, S. Jakirlic, B. Böhm, A. Dreizler: Quenching of premixed flames at cold walls: effects on the local flow field; Flow Turbulence and Combustion 100, 177 – 196 (2018)

[6] C. Jainski, M. Rißmann, B. Böhm, J. Janicka, A. Dreizler: Sidewall quenching of atmospheric laminar premixed flames studied by laser-based diagnostics; Combustion and Flame 183, 271 – 282 (2017)

[7] A. Bohlin, C. Jainski, B.D. Patterson, A. Dreizler, C.J. Kliewer: Multiparameter spatio-thermochemical probing of flame-wall interactions advanced with coherent Raman imaging; Proc. Combust. Inst. 36, 4557 – 4564 (2017)

[8] H. Kosaka, F. Zentgraf, A. Scholtissek, L. Bischoff, T. Häber, R. Suntz, B. Albert, C. Hasse, A. Dreizler: Wall heat fluxes and CO formation/oxidation during laminar and turbulent side-wall quenching of me-thane and DME flames; International Journal of Heat and Fluid Flow 70, 181 – 192 (2018)

[9] C. Jainski, M. Rißmann, B. Böhm, A. Dreizler: Experimental investigation of flame surface density and mean reaction rate during flame-wall interaction; Proc. Combust. Inst. 36, 1827 – 1834 (2017)

[10] H. Kosaka, F. Zentgraf, B. Böhm, A. Dreizler: Heat Release Rate Imaging During Side-Wall Flame Quenching Using Laser-Induced Fluorescence Of Formaldehyde And Hydroxyl Radicals; 19th Lisbon laser Conference 2018

[11] S. Ganter, A. Heinrich, T. Meier, G. Kuenne, C. Jainski, M.C. Rißmann,A. Dreizler, J. Janicka: Numerical analysis of laminar methane–air side-wall-quenching; Combustion and Flame 186, 299-310 (2017)

[12] J. Sellmann, J. Lai, A.M. Kempf, N. Chakraborty: Flame Surface Density based modelling of head-on quenching of turbulent premixed flames; Proc. Combust. Inst. 36, 1817-1825 (2017)

[13] J. Lai, M. Klein, N. Chakraborty: Direct Numerical Simulation of Head-On Quenching of Statistically Planar Turbulent Premixed Methane-Air Flames Using a Detailed Chemical Mechanism; Flow Turbulence Combustion 101, 1073–1091 (2018)

[14] G. Frank, M. Pfitzner: Investigation of the heat transfer coefficient in a transpiration film cooling with chemical reactions; International Journal of Heat and Mass Transfer 113, 755-763 (2017)

[15] S. Ganter, C. Straßacker, G. Kuenne, T Meier, A. Heinrich, U. Maas, J. Janicka: Laminar near-wall combustion: Analysis of tabulated chemistry simulations by means of detailed kinetics; International Journal of Heat and Fluid Flow 70, 259-270 (2018)

[16] A. Heinrich, G. Kuenne, S. Ganter, C. Hasse, J. Janicka: Investigation of the Turbulent Near Wall Flame Behavior for a Sidewall Quenching Burner by Means of a Large Eddy Simulation and Tabulated Chemistry; Fluids 3(3), 65 (2018)

Flame wall interactions
New Target Configuration for TNF

Institute Reactive Flows and Diagnostics RSM,
TU Darmstadt

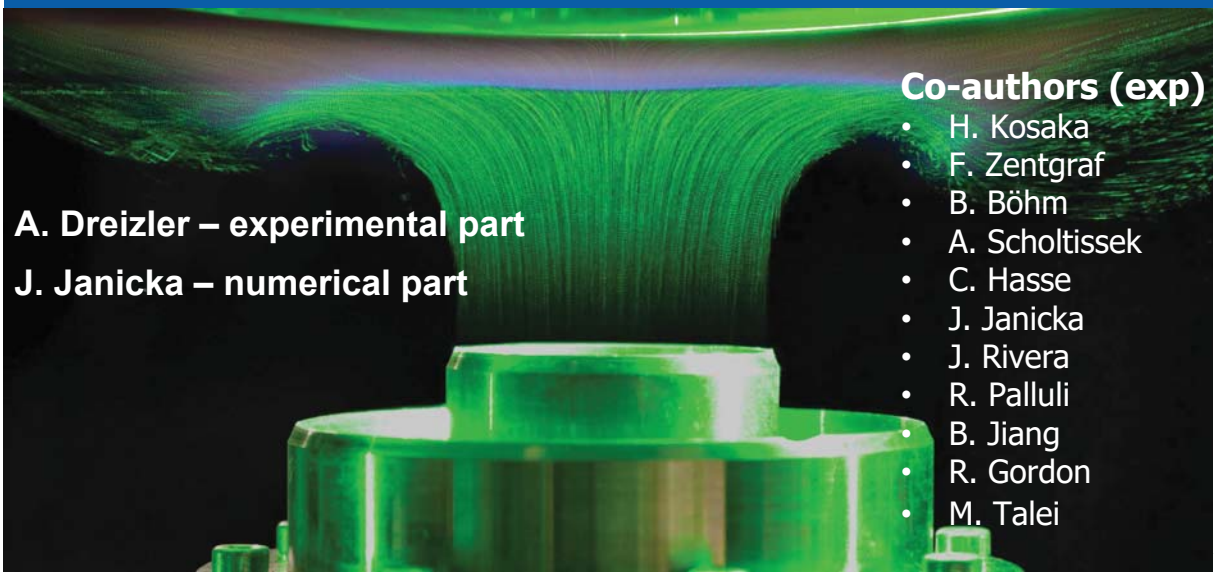

A. Dreizler – experimental part

J. Janicka – numerical part

Co-authors (exp)

- H. Kosaka
- F. Zentgraf
- B. Böhm
- A. Scholtissek
- C. Hasse
- J. Janicka
- J. Rivera
- R. Palluli
- B. Jiang
- R. Gordon
- M. Talei

Outline

- Motivation
- Experimental Approach at University of Melbourne
- Experimental Approach at TU Darmstadt
- Side Wall Quenching
  - Flow field and flame front
  - Quenching distances and wall-heat flux
  - Thermo-chemical states: CO versus T
  - Heat release rate imaging
- Next steps
- Johannes presentation on numerical simulation of FWI

Flame-wall interaction (FWI)

TECHNISCHE UNIVERSITÄT DARMSTADT

- Topical subject with relevance for
  - Safety technology: flame arresters
  - Catalytically assisted combustion

J. Hermann et al., TU Darmstadt
Pressurized combustor
Interaction of flame-flow-effusion cooling

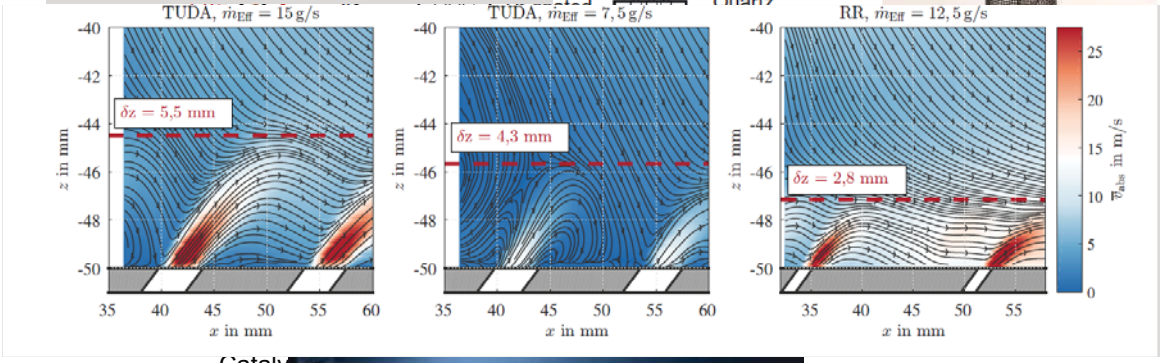

Cataly

Mantzaras et al., Combust. Flame 2013

RSM

Flame-Wall Interaction

TECHNISCHE UNIVERSITÄT DARMSTADT

- Example: Spark ignition engines

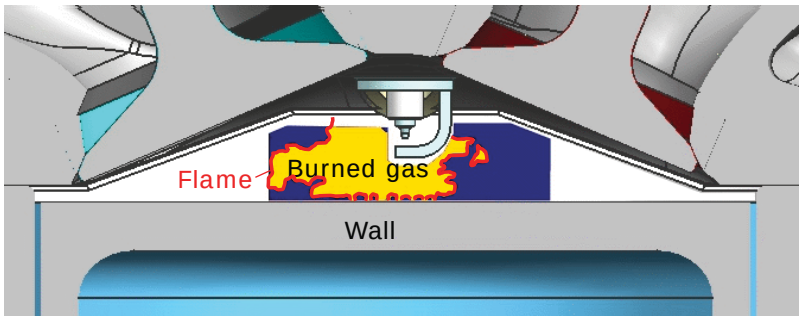

Burned gas : 1500~2500 K

⇕

Wall surface: 350~700 K

- Flame quenching
- Large heat loss to wall
- Sources of UHC and CO

→ **Advanced combustion models & turb-chemistry interactions models**

RSM

FWI for turbulent conditions

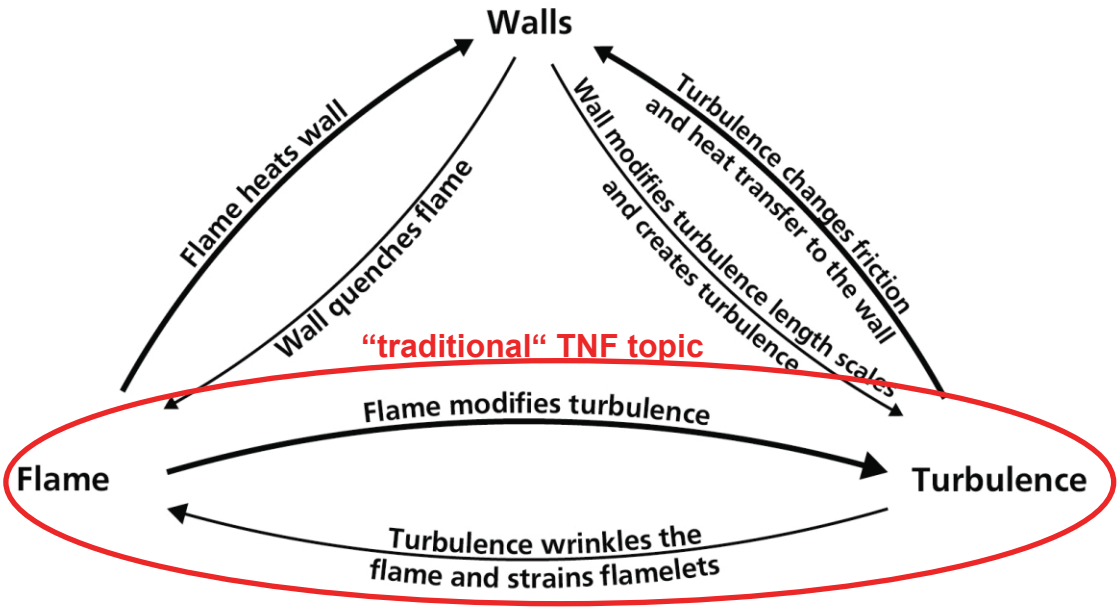

Source: T. Poinsot and D. Veynante, Theoretical and Numerical Combustion 2005

FWI for turbulent conditions

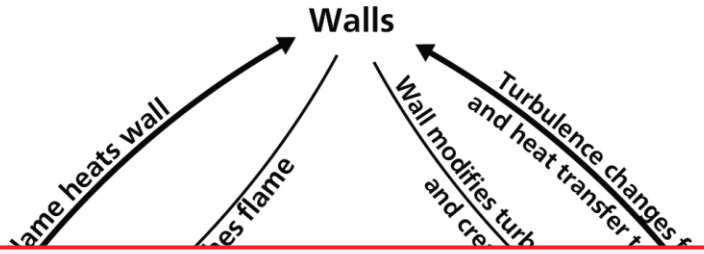

Studied by DNS (Poinsot, Haworth, Bruneaux, Rutland, Chen, Gruber, …)

Very limited number of comprehensive experimental studies going beyond quenching distances and heat transfer

See review article A. Dreizler, B. Böhm, PCI 35, 2015

→ DNS and new experimental data available for model developing and testing

Great topic for TNF: extension of turbulence-chemistry interaction

Outline

TECHNISCHE UNIVERSITÄT DARMSTADT

- Motivation
- Experimental Approach at University of Melbourne
- Experimental Approach at TU Darmstadt
- Side Wall Quenching
  - Flow field and flame front
  - Quenching distances and wall-heat flux
  - Thermo-chemical states: CO versus T
  - Heat release rate imaging
- Next steps
- Johannes presentation on numerical simulation of FWI

RSM

Turbulent Non-Premixed Flames (TNF) 2018

THE UNIVERSITY OF MELBOURNE

Forced Laminar Axisymmetric Quenching (FLAQ) Burner: Flame-Wall Interaction and Cooling Jet-Flame Interaction

FWI at UoM:

Jacob E. Rivera, Rahul Palluli, Bin Jiang, Robert L. Gordon, Mohsen Talei

Publications:

J. E. Rivera, R. L. Gordon, M. Talei, *Flame-Wall Interaction of a Forced Laminar Premixed Propane Flame: Flame Dynamics and Exhaust CO Emissions,* Proceedings of the Combustion Institute 37, **Presentation: Thursday 10:20 Wicklow Hall 2b**

J. E. Rivera, R. L. Gordon, M. Talei, *Flame Chemiluminescence Measurements of a Laminar Forced Flame Interacting with a Cold Wall*, Proceedings of the 11th Asia-Pacific Conference on Combustion, Sydney, Australia, 2017

J. E. Rivera, R. L. Gordon, M. Talei, M. J. Brear, *A Novel Burner for Investigating End-Gas Effects of Transient Flame-Wall Interaction*, Proceedings of the 20th Australasian Fluid Mechanics Conference, Perth, Australia, 2016

Research Aims

- Part of a long term study to quantify the different mechanisms responsible for **changes in exhaust CO**, e.g.
  - Transient FWI
  - Cooling rate
  - Surface reactivity
  - Cooling holes and dilution
- FLAQ Burner provides an axisymmetric, optically accessible flame with a concave FWI.
- Aims to provide repeatable, self-consistent data sets of local effects (heat loss, quenching mode, flame geometry, transient effects), in-chamber effects connected to impact on exhaust.

Flame-Wall Interaction Configuration

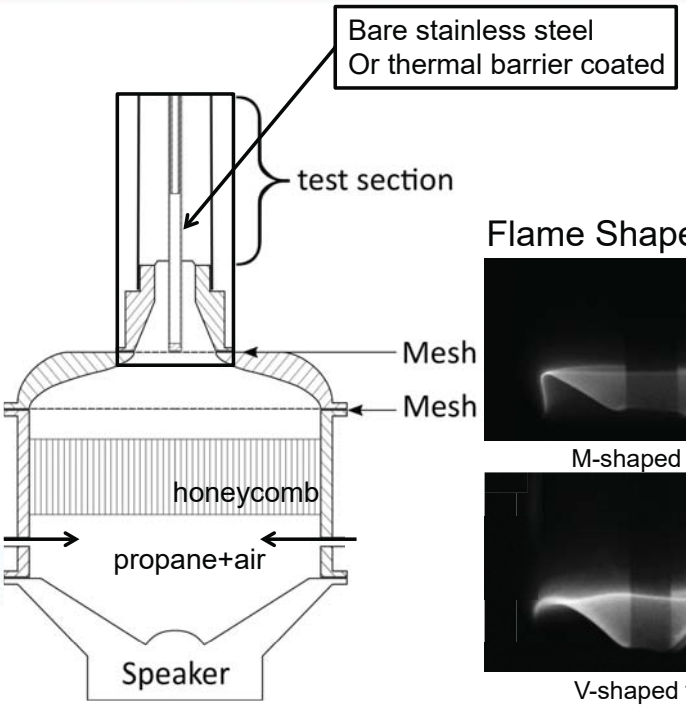

Flame Shapes:

M-shaped flame

V-shaped flame

Flame-Wall Interaction Configuration

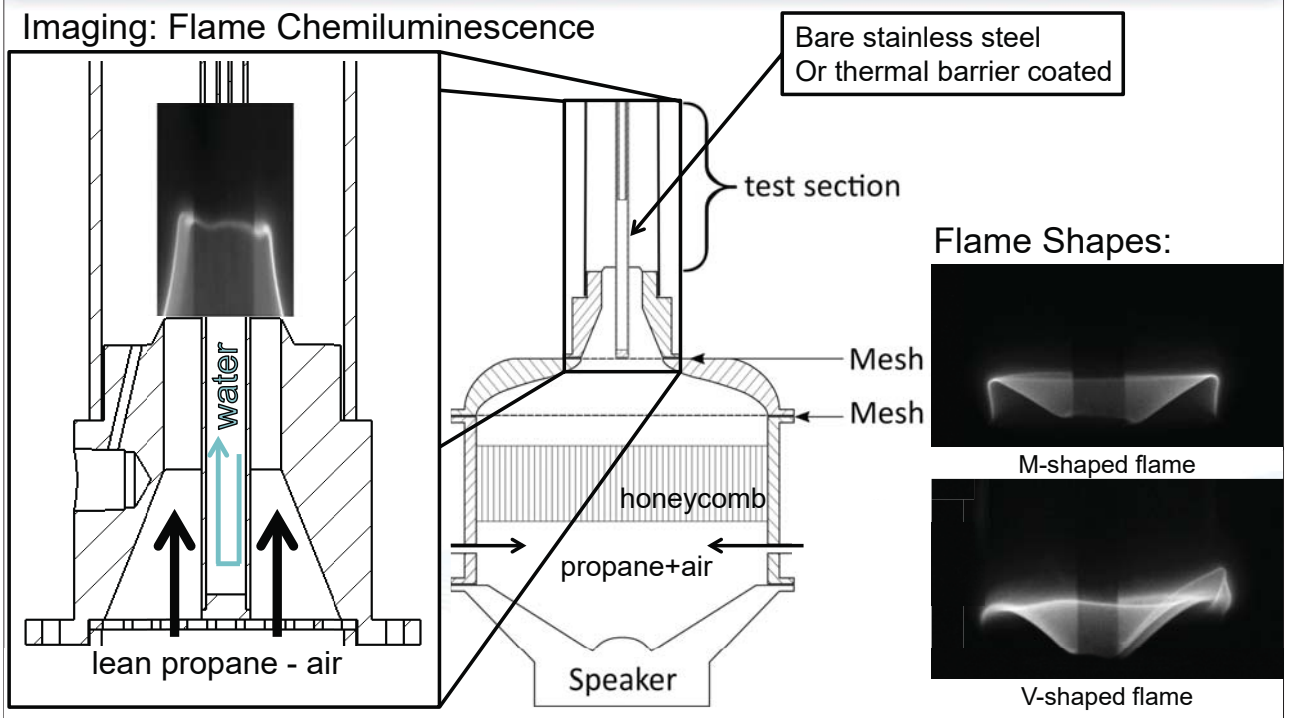

Boundary Conditions

Flow Conditions	
Re_D	< 1000
$\bar{u}$	$0 - 3\ m/s$
$\dot{Q}_T$	$\sim 10\ kW$
$Fuel$	C_3H_8
$\dot{m}_{air}$	$0 - 5\ g/s$
$\dot{m}_{fuel}$	$0 - 0.5\ g/s$

Coolant Conditions	
$Coolant$	$water$
$\dot{m}_c$	$0 - 3\ g/s$
$T_{c,in}$	$300\ K$
$T_{c,out}$	$320 - 373\ K$

Sample flame shape map at $\dot{Q}_c \approx 200\ W$

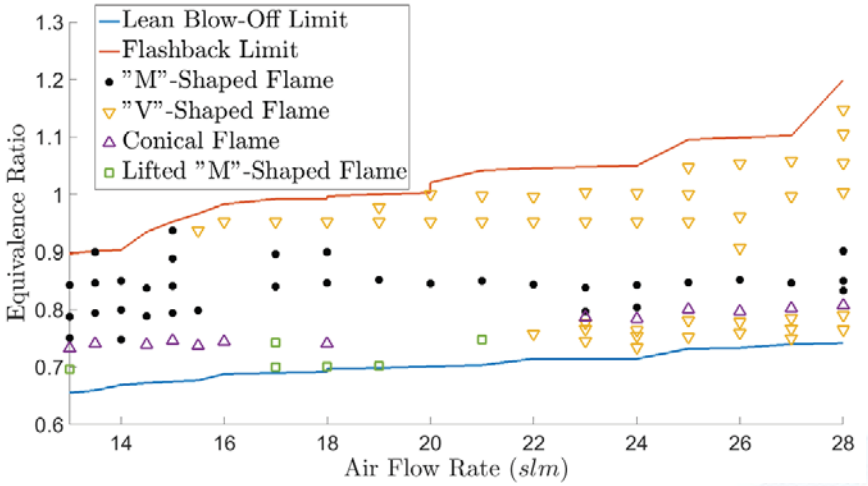

Dimension Summary	
Nozzle Diameter	$25\ mm$
Quenching Wall Diameter	$9.53\ mm$
Enclosure Diameter	$50\ mm$

Flame-Wall Interaction Configuration

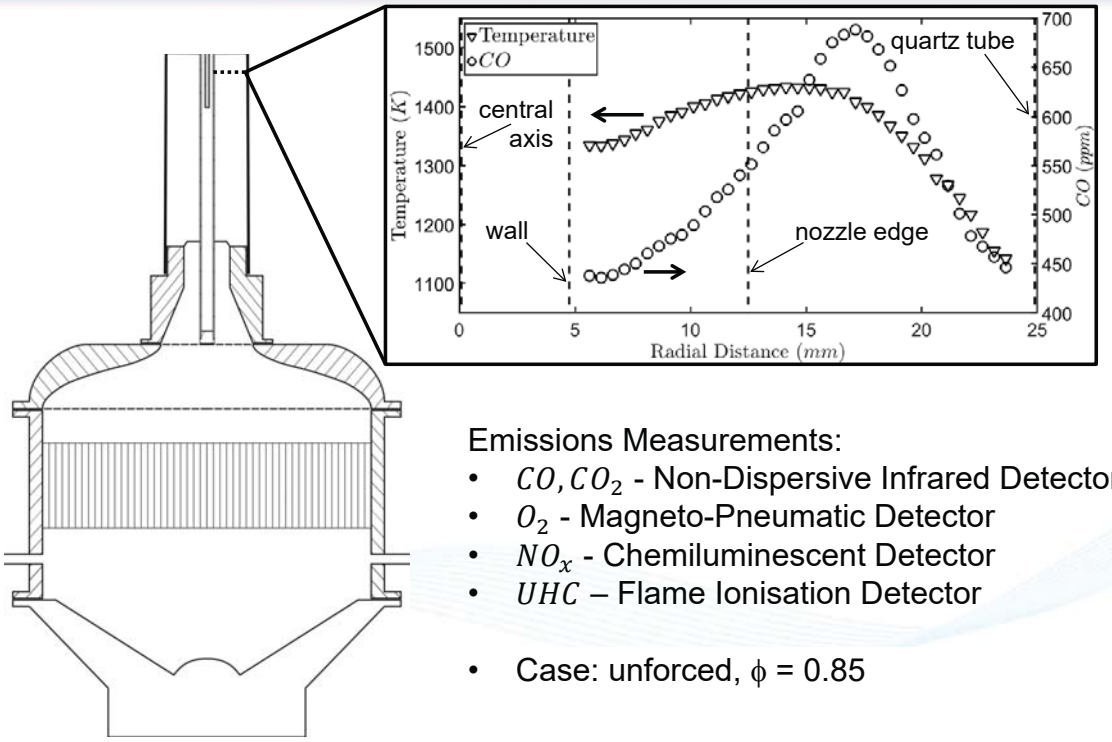

Emissions Measurements:

- CO, CO_2 - Non-Dispersive Infrared Detector
- O_2 - Magneto-Pneumatic Detector
- NO_x - Chemiluminescent Detector
- UHC – Flame Ionisation Detector

- Case: unforced, ϕ = 0.85

Cooling Jet-Flame Interaction Configuration

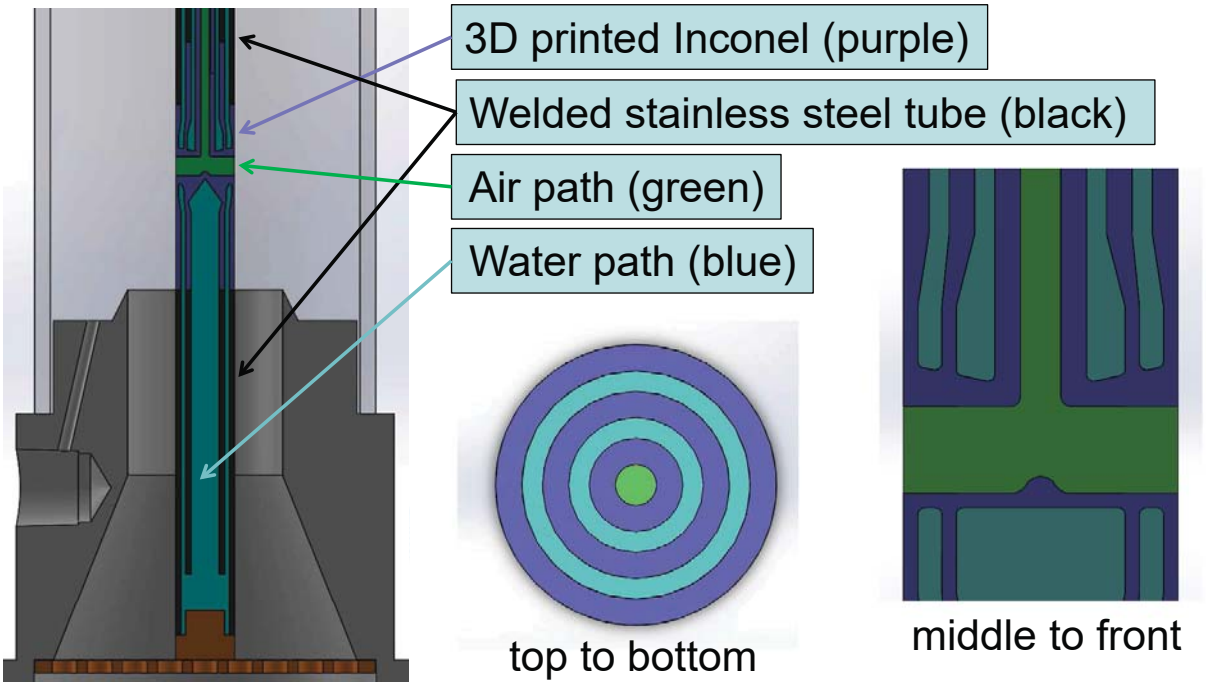

Cooling Jet-Flame Interaction Configuration

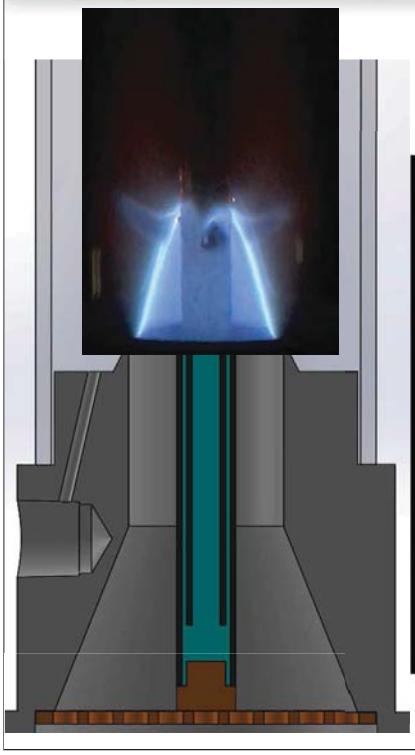

Video at one condition:

Video from $u_{jet} = u_{high} \rightarrow u_{low}$:

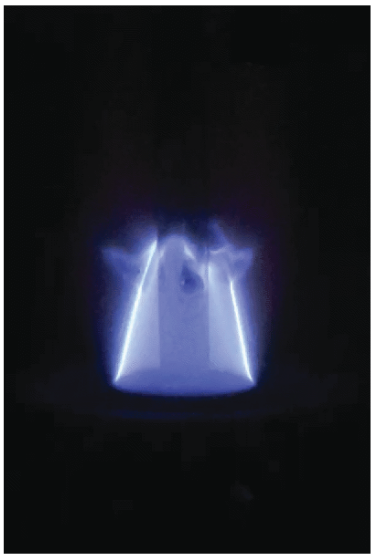

Future Work

- Local wall and flame measurements, and boundary condition quantification.
- Wall reactivity and thermal boundary conditions (thermal barrier coating, annealing).
- Turbulence
- Flame stabilisation/geometries
- Fuel effects
- Cooling jet impact
- Numerical Simulation

Outline

TECHNISCHE UNIVERSITÄT DARMSTADT

- Motivation
- Experimental Approach at University of Melbourne
- Experimental Approach at TU Darmstadt
- Side Wall Quenching
  - Flow field and flame front
  - Quenching distances and wall-heat flux
  - Thermo-chemical states: CO versus T
  - Heat release rate imaging
- Next steps
- Johannes presentation on numerical simulation of FWI

RSM

Fundamental types of Flame-Wall Interaction

TECHNISCHE UNIVERSITÄT DARMSTADT

Head-on quenching

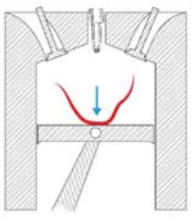

HOQ Burner

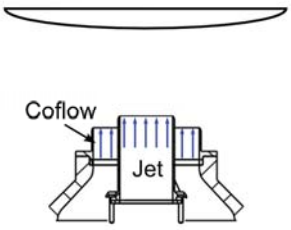

- transient
- 1D when laminar
- flame ignited by laser spark
- low sample number

Side-wall Quenching

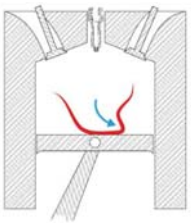

SWQ Burner

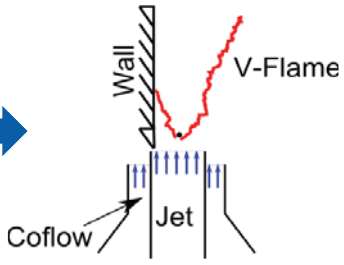

- Statistically stationary
- 3D
- high sample number

28.07.2018 | TNF 14 | FWI-Session | Andreas Dreizler | 24

RSM

Burner setup

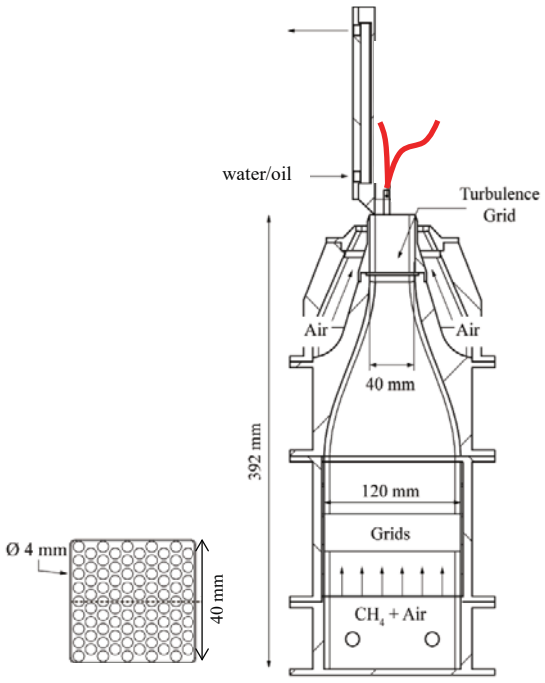

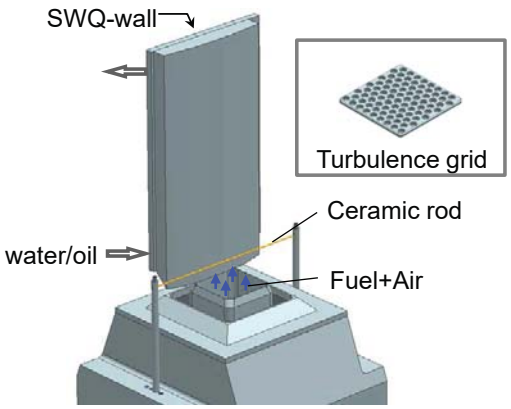

- Premixed V-flame (fuel: methane, DME)
- Φ = 0.83, **1**, 1.2
- Re = 5000
- Laminar and turbulent (by turb. grid)
- Temperature controled wall

Literature

- Jainski, C., Rißmann, M., Jakirlic, S., Böhm, B., Dreizler, A.: Quenching of premixed flames at cold walls: Effects on the local flow field. Flow Turbulence Combustion 100, 177 – 196 (2018).
- Kosaka, H., Zentgraf, F., Scholtissek, A., Bischoff, L., Häber, T., Suntz, R., Albert, B., Hasse, C., Dreizler, A.: Wall heat fluxes and CO formation/oxidation during laminar and turbulent side-wall quench-ing of methane and DME flames. International J. of Heat and Fluid Flow https://doi.org/10.1016/j.ijheatfluidflow.2018.01.009 (2018).
- Jainski, C., Rißmann, M., Böhm, B., Janicka, J., Dreizler, A.: Sidewall quenching of atmospheric laminar premixed flames studied by laser-based diagnostics. Combustion and Flame 183, 271 – 282 (2017).
- Rißmann, M., Jainski, C., Mann, M., Dreizler, A.: Flame-flow interaction in premixed turbulent flames during transient head-on quenching. Flow Turbulence Combustion 98, 1025 – 1038 (2017).
- Jainski, C., Rißmann, M., Böhm, B., Dreizler, A.: Experimental investigation of flame surface density and mean reaction rate during flame–wall interaction. Proceedings of the Combustion Institute 36, 1827 – 1834 (2017). 1
- Bohlin, A., Jainski, C., Patterson, B.D., Dreizler, A., Kliewer, C.J.: Multiparameter spatio-thermochemical probing of flame–wall interactions advanced with coherent Raman imaging. Proceedings of the Combus-tion Institute 36, 4557 – 4564 (2017).

Parameters of interest to better understand FWI

TECHNISCHE UNIVERSITÄT DARMSTADT

- Quenching distances, visualization of flames near walls
- Wall temperature and heat flux $\dot{Q}$
- Flow fields near walls
  - Velocity boundary layers **u**
- Thermo-chemical states during FWI
  - Thermal boundary layers **T**
  - Concentration boundary layers **X**
- Local heat release rates near walls
- Reaction rates

Focus today

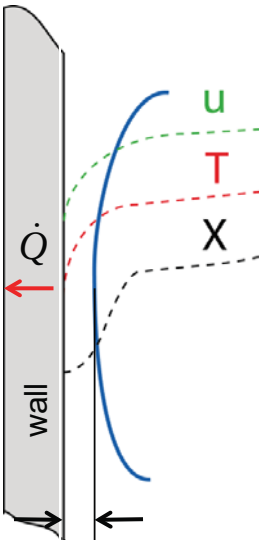

Quenching distance

RSM

Outline

TECHNISCHE UNIVERSITÄT DARMSTADT

- Motivation
- Experimental Approach at University of Melbourne
- Experimental Approach at TU Darmstadt
- Side Wall Quenching
  - Flow field and flame front
  - Quenching distances and wall-heat flux
  - Thermo-chemical states: CO versus T
  - Heat release rate imaging
- Next steps
- Johannes presentation on numerical simulation of FWI

RSM

High-speed PIV/OH-PLIF: Experimental setup

TECHNISCHE UNIVERSITÄT DARMSTADT

Gas velocity	Flame front position
Particle Image Velocimetry (**PIV**)	Planar **LIF** of **OH** radical Flame front from OH gradient
2 D Rep. Rate: 10 kHz and 10 Hz	2 D Rep. Rate: 10 kHz and 10 Hz

- Two fields of view (18x18 mm^2)
- 2C-PIV (AL_2O_3 particles)
- OH-PLIF
  - High-speed dye laser system (35 µJ/pulse)
  - $Q_1(6)$-line
  - Canny-edge filter for flame front detection

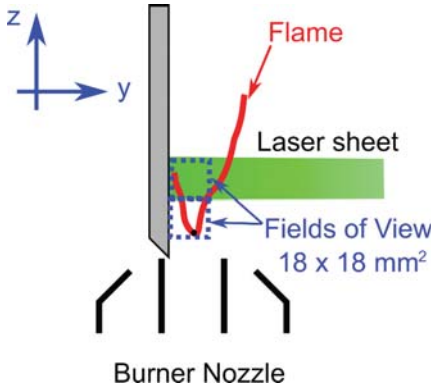

RSM

Experiments on FWI: parameters of interest

TECHNISCHE UNIVERSITÄT DARMSTADT

- Visualization of flow field and flames near walls

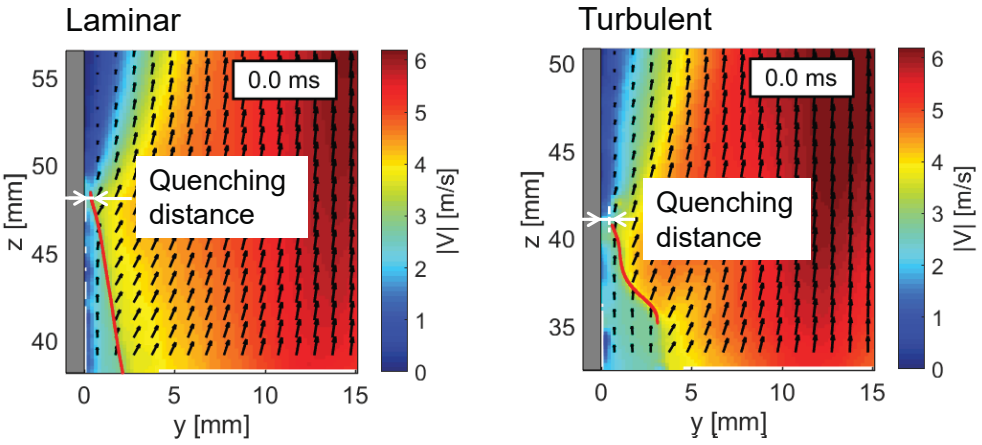

RSM

Outline

TECHNISCHE UNIVERSITÄT DARMSTADT

- Motivation
- Experimental Approach at University of Melbourne
- Experimental Approach at TU Darmstadt
- Side Wall Quenching
  - Flow field and flame front
  - Quenching distances and wall-heat flux
  - Thermo-chemical states: CO versus T
  - Heat release rate imaging
- Next steps
- Johannes presentation on numerical simulation of FWI

RSM

CARS/ CO-LIF/ OH-PLIF/ Phosphor Thermometry Experimental setup

TECHNISCHE UNIVERSITÄT DARMSTADT

Gas Temperature	CO Concentration	Wall Temperature	Flame front position
ro-vibrational ns-**CARS**	Two Photon **LIF** of **CO** molecule	Phosphor thermometry	Planar **OH-LIF**
0 D Rep. Rate: 10 Hz	0 D Rep. Rate: 10 Hz	2 D Rep. Rate: 10 Hz	2 D Rep. Rate: 10 Hz

Front view

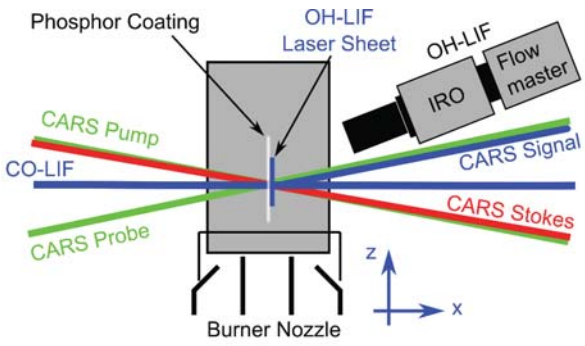

Side view

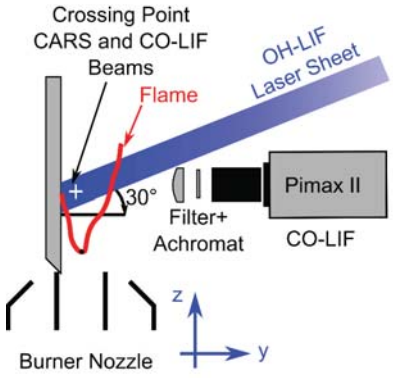

28.07.2018 | TNF 14 | FWI-Session | Andreas Dreizler | 32

RSM

Gas phase and wall surface temperature
(Re = 5000, Φ = 1.0, laminar)

TECHNISCHE UNIVERSITÄT DARMSTADT

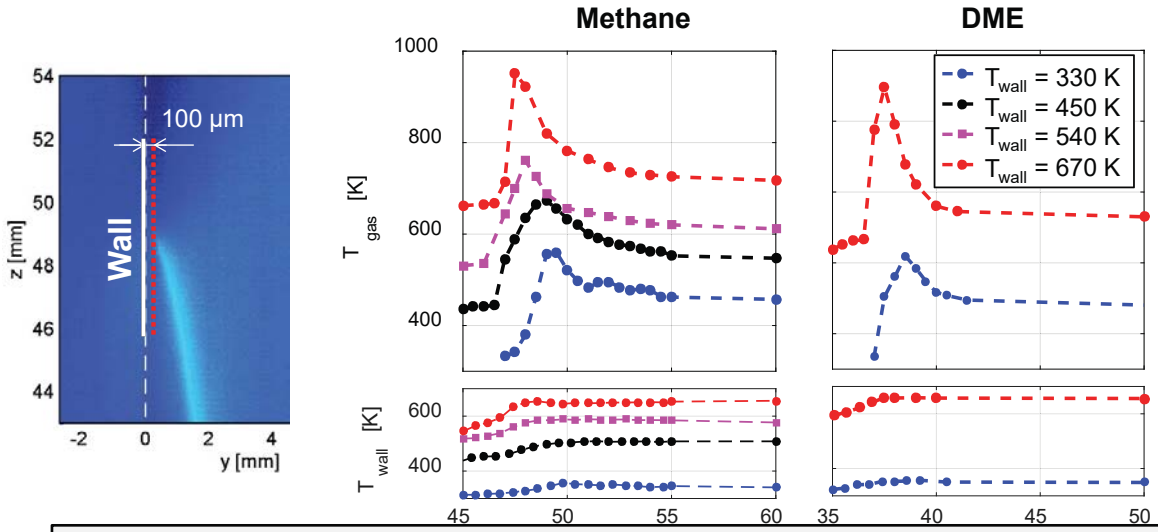

- **DME** flames: quench further upstream than methane flames
- Higher T_{wall} → increased T_{gas} within boundary layer
  → flame burns further upstream due to increased laminar burning velocity

RSM

Wall-heat flux
(Re = 5000, Φ = 1.0, laminar)

TECHNISCHE UNIVERSITÄT DARMSTADT

$$q = \lambda \frac{(T_{gas} - T_{wall})}{\Delta y}$$

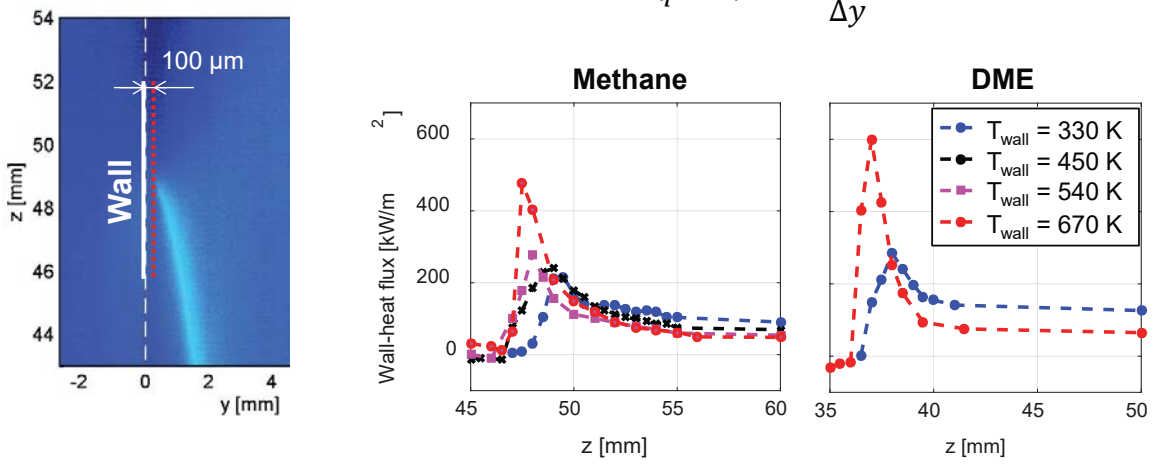

RSM

Quenching distance and wall-heat flux
(Re = 5000, Φ = 1.0, laminar)

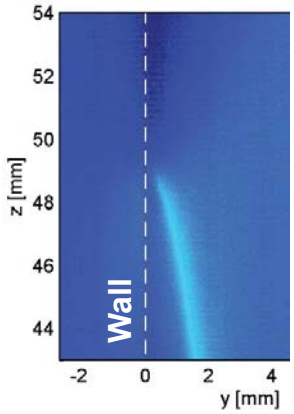

Quenching position

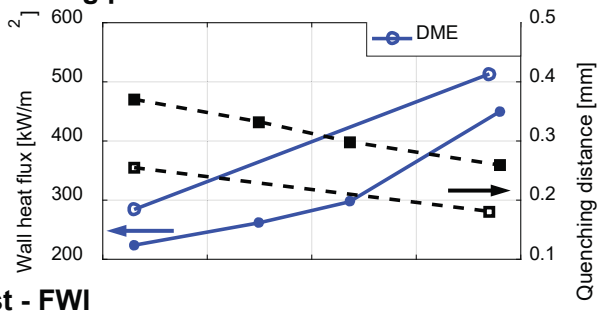

Post - FWI

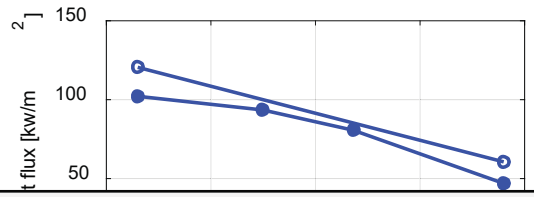

With **higher T_{wall}**
- **Maximum heat flux** increases due to decreasing **quenching distances**
- **Heat flux in post-flame region** decreases as expected for non-reacting flows

Outline

- Motivation
- Experimental Approach at University of Melbourne
- Experimental Approach at TU Darmstadt
- Side Wall Quenching
  - Flow field and flame front
  - Quenching distances and wall-heat flux
  - Thermo-chemical states: Physical space and CO versus T
  - Heat release rate imaging
- Next steps
- Johannes presentation on numerical simulation of FWI

Physical space: Temperature & CO-profiles
(Re = 5000, Φ = 1.0, laminar)

TECHNISCHE UNIVERSITÄT DARMSTADT

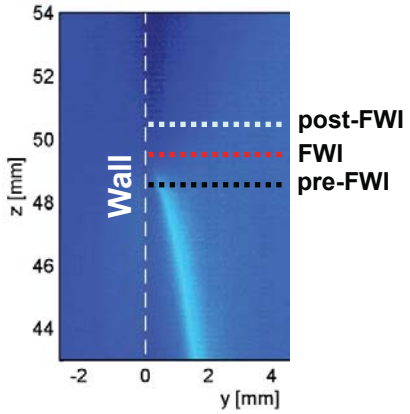

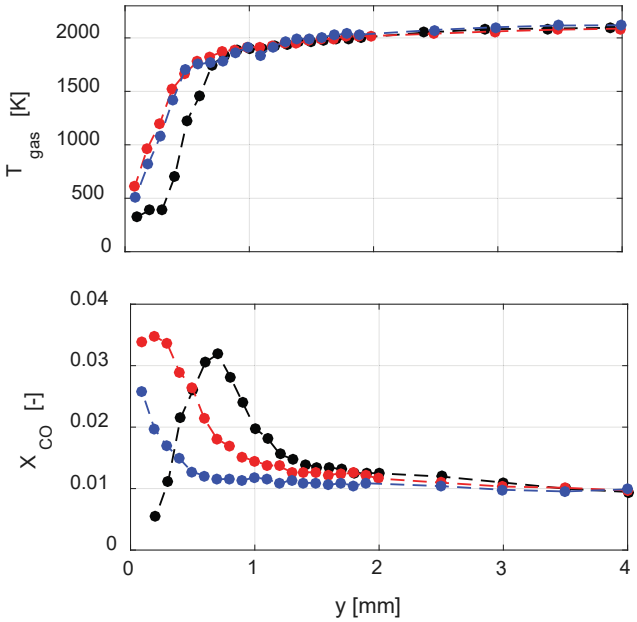

RSM

State space: CO-temperature correlations

TECHNISCHE UNIVERSITÄT DARMSTADT

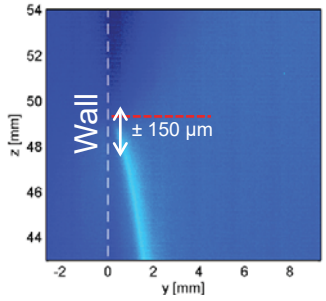

- Spatial **conditioning (axial & wall-normal)**
- Flame tip **fluctuates** up and down (± 150 µm)

→ Different **thermo-kinetic states** at one measurement location

z = 48 mm, laminar
Upstream quenching position, various y-positions

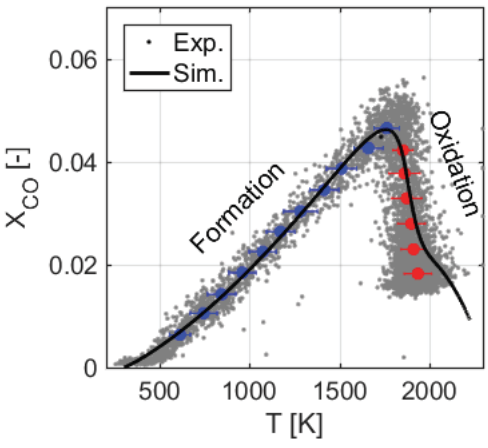

RSM

Thermo-chemical states for z = 49.5 mm @ quenching position
(Re = 5000, Φ = 1.0, laminar)

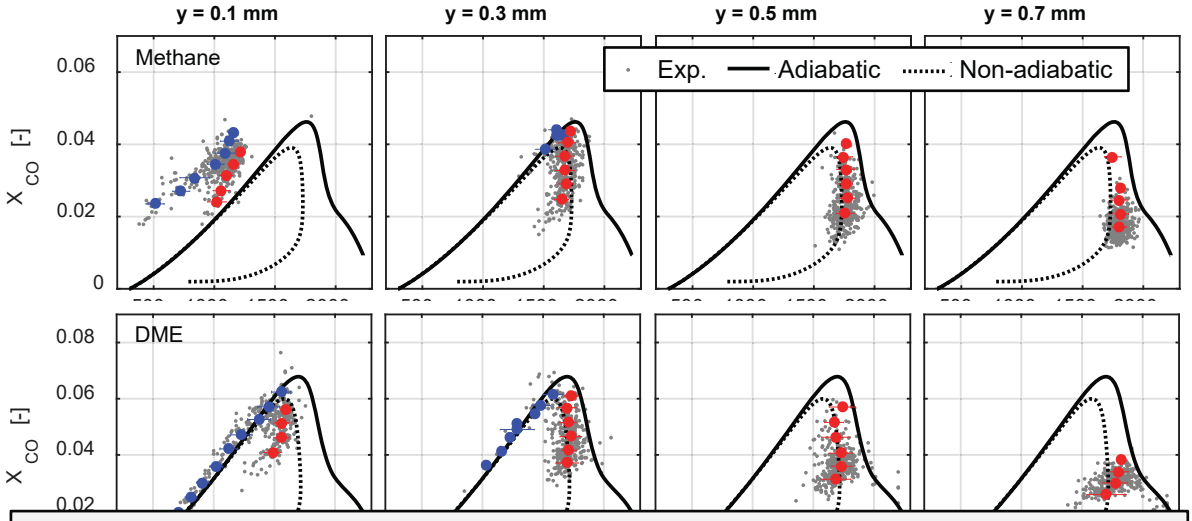

- **CO formation** branch: strongly influenced for *y* < 0.3 mm for **methane** flame
- **CO consumption** branch: shifted to lower temperatures for entire near-wall region with both fuel types

Time scale analysis
(Re = 5000, Φ = 1.0, laminar)

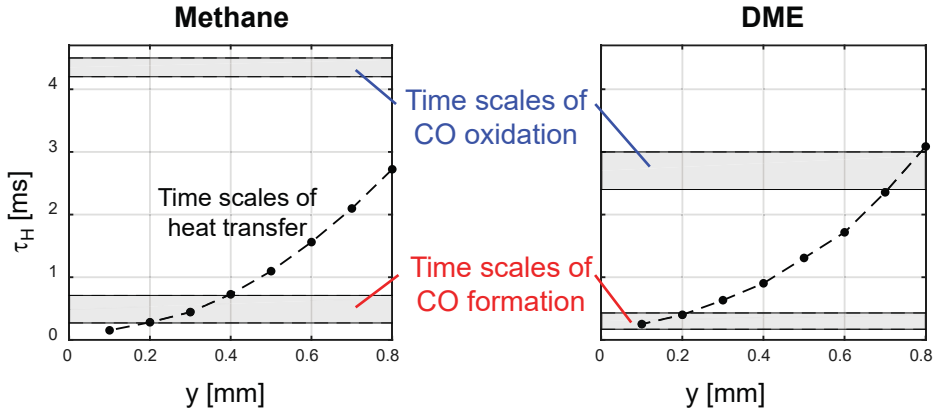

- **CO-formation**: slower than heat transfer for y ≤ 0.2 mm (methane), y < 0.1 mm (DME)

→ Only for **methane at y ≤ 0.2 mm** influence of wall heat loss

- **CO-oxidation**: both fuels are influenced by heat loss in near-wall region

[1] E. Marín, Characteristic dimensions for heat transfer, Latin-American Journal of Physics Education 4 (2010) 56–60

Thermo-chemical states for z = 42.5 mm
(Re = 5000, Φ = 1.0, turbulent)

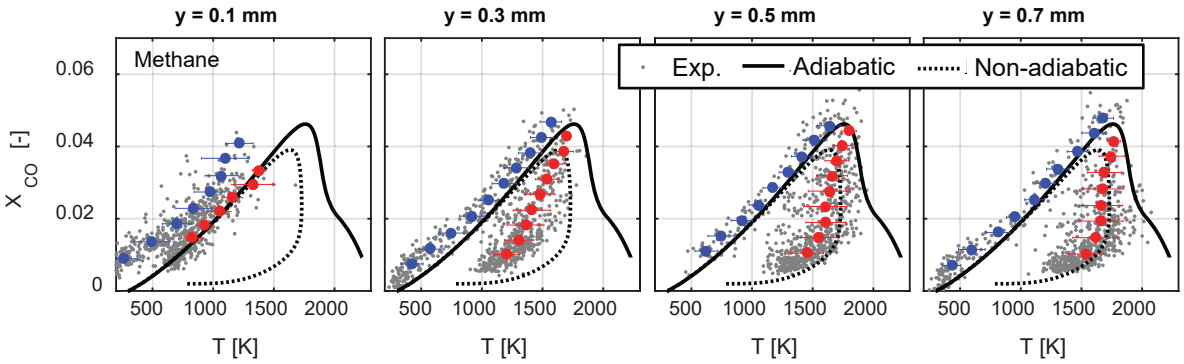

- **Both branch are influenced** for entire near-wall region
- **Intermediate states** between both branches are observed

→ Increased wall heat transfer due to turbulence

Outline

- Motivation
- Experimental Approach at University of Melbourne
- Experimental Approach at TU Darmstadt
- Side Wall Quenching
  - Flow field and flame front
  - Quenching distances and wall-heat flux
  - Thermo-chemical states: CO versus T
  - Heat release rate imaging
- Next steps
- Johannes presentation on numerical simulation of FWI

Experimental HRR imaging for DME flame

- Dominant reaction path for HRR:

$$\mathbf{CH_2O} + \mathbf{OH} \rightarrow HCO + H_2O$$

- Correlation of $[CH_2O]$ x $[OH]$ and HRR

Wall normal profiles
(1D simulation)

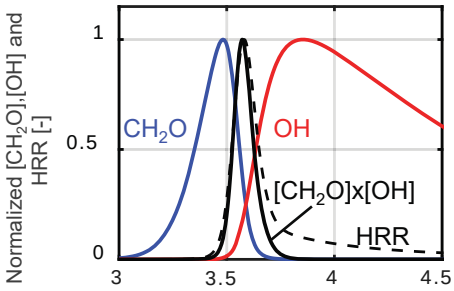

Correlation of
$[CH_2O]$ x $[OH]$ and HRR

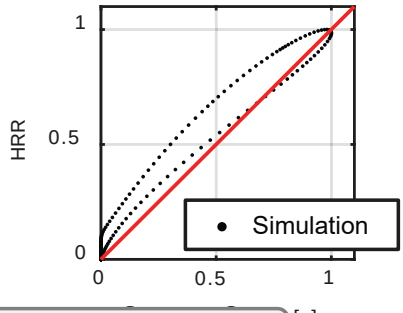

$[CH_2O]$ x $[OH]$ is well correlated to HRR

Averaged CH_2O/OH-LIF and HRR images
Laminar flames

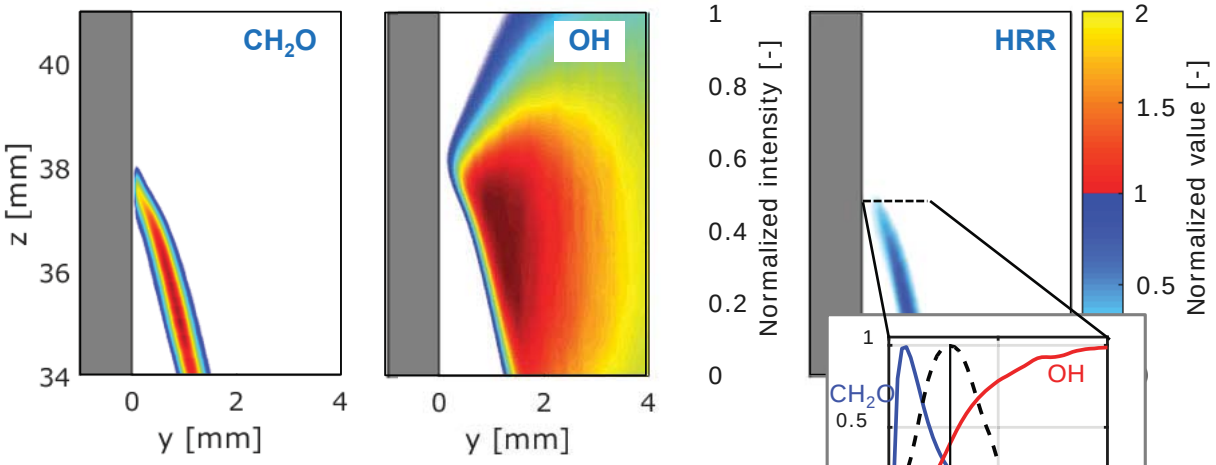

- HRRs decrease approaching wall
- Quenching distance δ_Q deduced from peak HRR

Instantaneous CH_2O/OH-LIF and HRR images
Turbulent flames

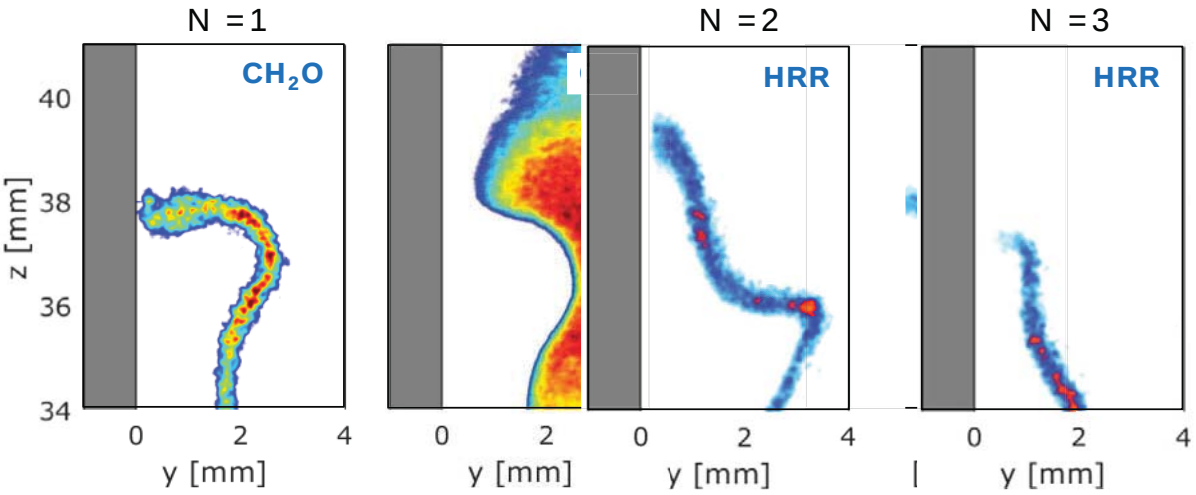

- HRRs decrease approaching wall
- HRRs spatially and temporally fluctuate

  ⇨ Statistical analysis with flame curvature

Flame curvature for turbulent flames

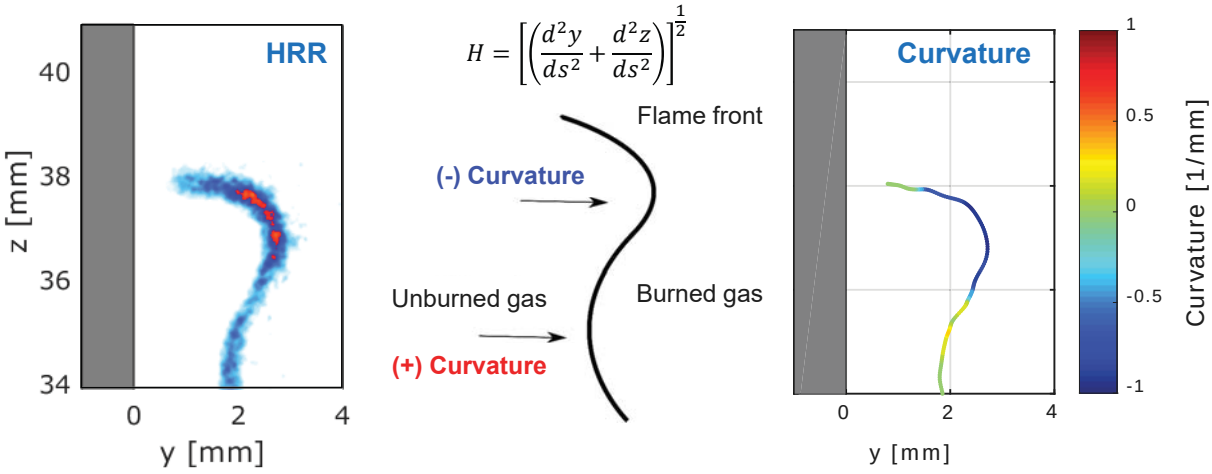

Flame curvature in turbulent flame

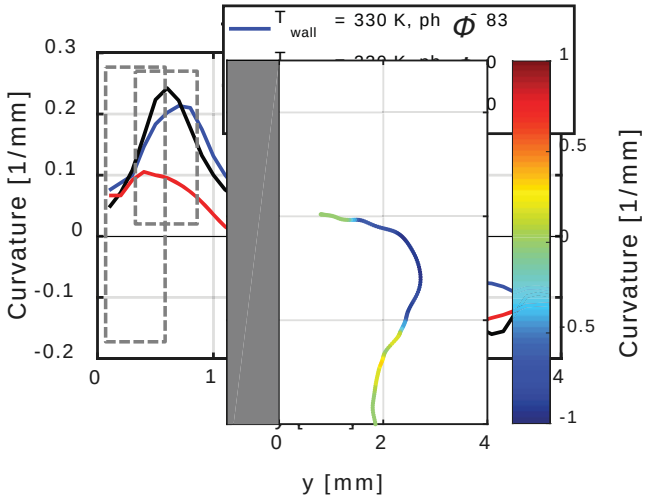

- Due to laminarization/ wall topology
- Due to increased viscosity for higher T_{wall}

Correlation flame curvature – HRR Turbulent flame

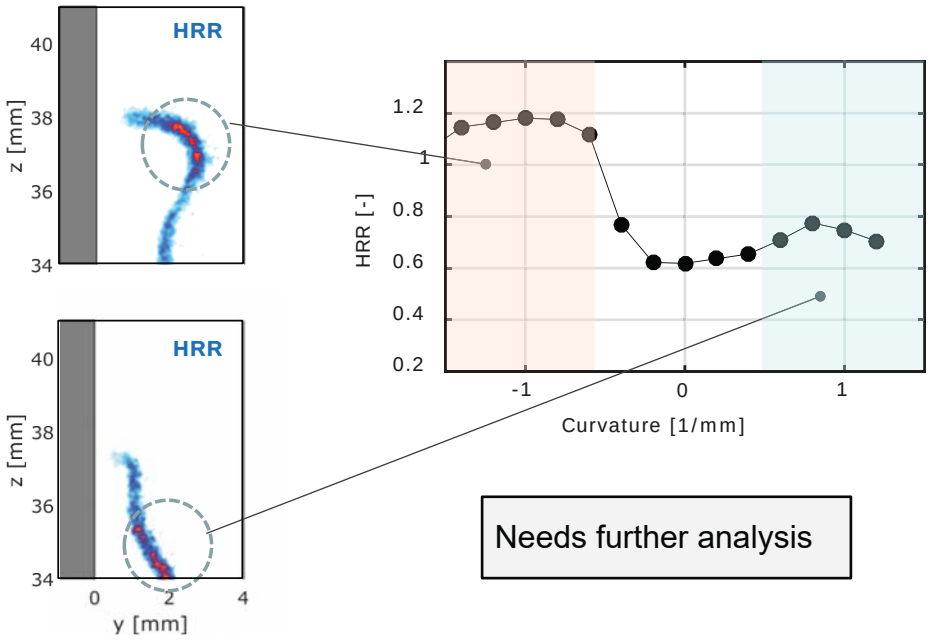

Needs further analysis

Next steps

TECHNISCHE UNIVERSITÄT DARMSTADT

Variation of process parameters

- Higher Reynolds-numbers
- Higher pressures
- More complex fuels

Diagnostics

- Measurement of additional species

RSM

TECHNISCHE UNIVERSITÄT DARMSTADT

Thank you for your kind attention

RSM

TNF 14
Flame-Wall Interactions
Simulation and Modelling

Contributors

1) Mahmoud Jafargholi, Christos E. Frouzakis, George K. Giannakopoulos, Konstantinos Boulouchos LAV, ETH Zürich

2) Umair Ahmed, Nilanjan Chakraborty, Jiawei Lai and Markus Klein
School of Engineering, Newcastle University | LRT, Universität der Bundeswehr München

3) Andrea Gruber et al.
SINTEF, Trondheim, Norway

4) Michael Pfitzner, Christian Mundt
Institut für Thermodynamik, Universität der Bundeswehr München

5) J. Sellmann, J. Lai, A. Kempf, N. Chakraborty
IVG, Universität Duisburg-Essen

6) Johannes Janicka
EKT, TU Darmstadt

TNF 14
Flame-Wall Interactions
Simulation and Modelling

Contributors

1) Mahmoud Jafargholi, Christos E. Frouzakis, George K. Giannakopoulos, Konstantinos Boulouchos LAV, ETH Zürich

2) Umair Ahmed, Nilanjan Chakraborty, Jiawei Lai and Markus Klein
School of Engineering, Newcastle University | LRT, Universität der Bundeswehr München

3) Andrea Gruber et al.
SINTEF, Trondheim, Norway

4) Michael Pfitzner, Christian Mundt
Institut für Thermodynamik, Universität der Bundeswehr München

5) J. Sellmann, J. Lai, A. Kempf, N. Chakraborty
IVG, Universität Duisburg-Essen

6) Johannes Janicka
EKT, TU Darmstadt

ETH zürich

DNS of Premixed flame propagation in confined geometries and flame-wall interactions

Mahmoud Jafargholi

Christos E. Frouzakis, George K. Giannakopoulos, Konstantinos Boulouchos

Financial support: Swiss National Science Foundation (SNSF)
Computational resources: Swiss Supercomputing Center (CSCS) / ETHZ cluster

LAV

ETH zürich

Nek5000 + LAV plugin

- Spectral element low Mach number reactive flow solver based on Nek5000
- High-order spliting *(Tomboulides, Lee, Orszag, JSC, 1997)* :
  - thermochemistry: species and energy equations
  - flow: continuity and momentum equations

  Preserves overall time integration order *(Tomboulides, Orszag, JCP, 1998)*
- Accurate and efficient time integration techniques for the two subsystems
  - Hydrodynamic subsystem: semi implicit (Nek5000)
  - Thermochemistry subsystem: adaptive timestepper for thermochemistry (CVODE)

LAV

ETH zürich

Numerical setups in 2- and 3-D

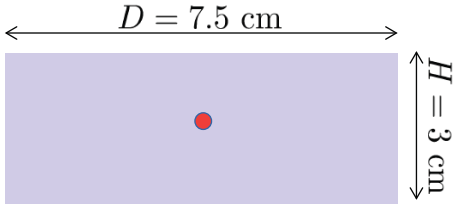

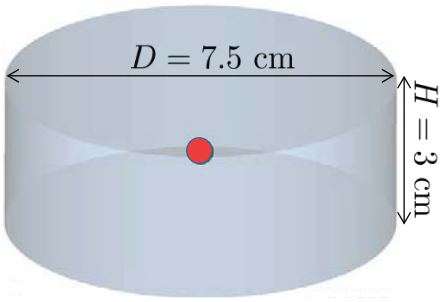

- Premixed syngas/air: φ=0.3, CO:H_2 = 3:1
- Detailed chemistry and transport: 12 species, 35 reactions (Keromnes et al., CF, 2013)

	T_u [K]	p_0 [atm]	S_L^0 [cm/s]	δ_f^0 [cm]	t_{ref} [s]	T_w [K]	T_b [K]	δ_f^0/δ_l^0
2D	822.7	4.49	54.96	2.37e-2	4.31e-4	550	1713.4	4.3
3D	822.7	1.00	138.02	1.15e-1	8.32e-4	550	1713.3	11.5

$$\delta_f^0 = \frac{T_b^0 - T_u}{max(dT/dx)} \qquad \delta_l^0 = \frac{\alpha}{S_L^0}$$

LAV

ETH zürich

3D flames: Numerical setup and cases

Flow:
Homogeneous, isotropic turbulence
prescribed u', l_t

Unburned mixture:
T_u=820 K
p_0=1 atm
$\phi = 0.3$
CO:H_2=3:1
T_{wall}=550 K

S_L= 138 cm/s
$\delta_L = 0.115$ cm
$t_{ref} = S_L/\delta_L = 0.83$ ms

Hot kernel:
$D_k = 0.45$ cm
$T_k = T_{af}$ =1713 K

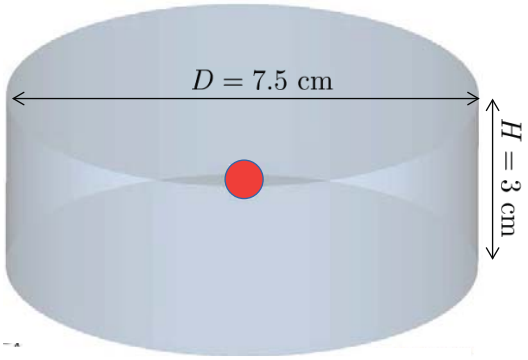

	Case 3D	l_t/δ_f^0	u'/S_L^0
1	L0U0 (laminar)	0	0
2	L1U6	1	3.46
3	L2U2	2	1.15
4	L2U4	2	2.31
5	L2U6	2	3.46
6	L2U12 ×3	2	6.93
7	L2U18	2	10.39
8	L2U24	2	13.86

LAV

ETH zürich

Laminar quenching distances (top wall)

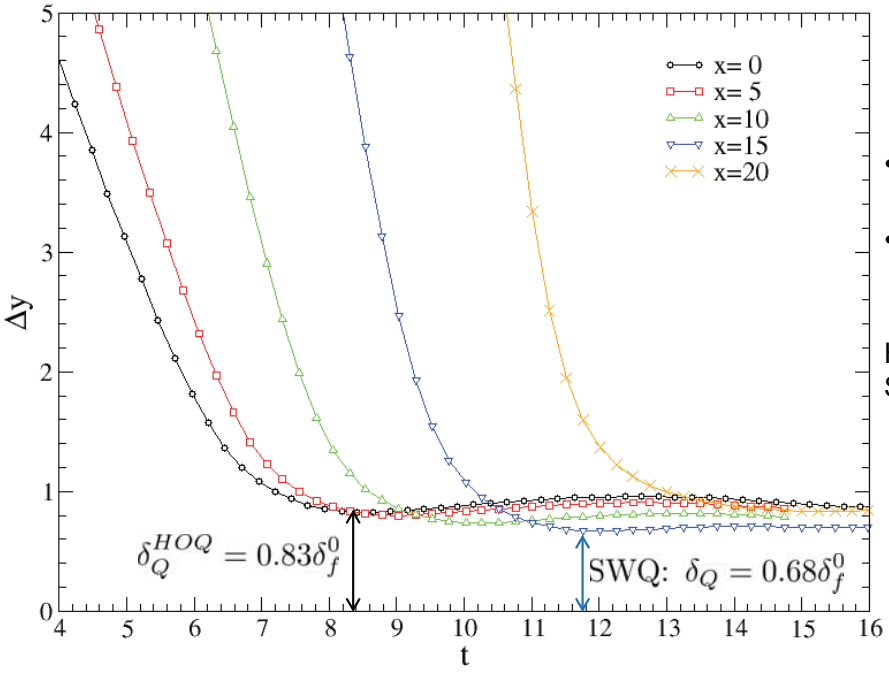

- Flame front defined by T=1500 K
- Δy=distance of flame from upper wall

HOQ: head-on quenching
SWQ: side-wall quenching

LAV

ETH zürich

Flame propagation: effect of u'

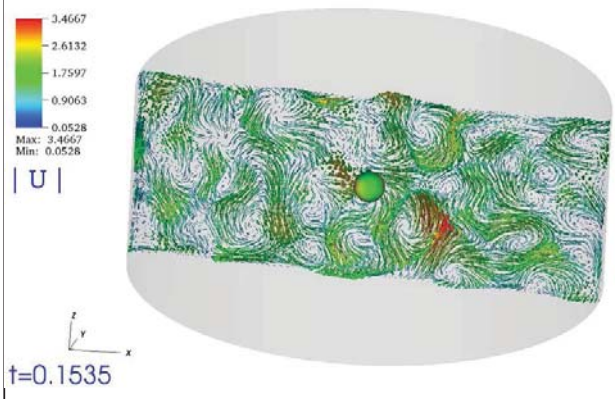

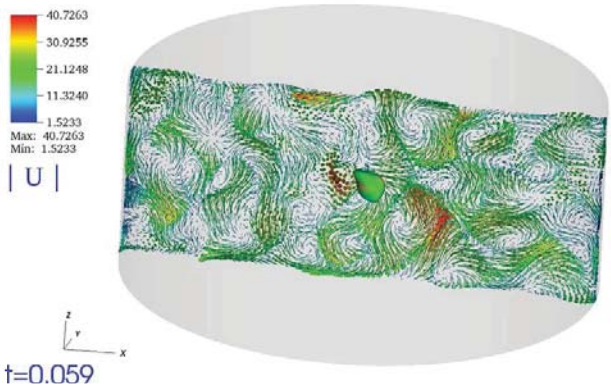

$l_t=2\delta_f$, u'=1.15S_L

$l_t=2\delta_f$, u'=13.86S_L

$$U_{ref} = 1.38 \text{ m/s}$$
$$t_{ref} = 0.83 \text{ ms}$$

LAV

ETH zürich

Flame propagation: effect of u’

$l_t=2\delta_f$, $u'=1.15S_L$ $l_t=2\delta_f$, $u'=13.86S_L$

$$U_{ref} = 1.38 \text{ m/s}$$
$$t_{ref} = 0.83 \text{ ms}$$

LAV

ETH zürich

Pressure and integral heat release rate (non-dim)

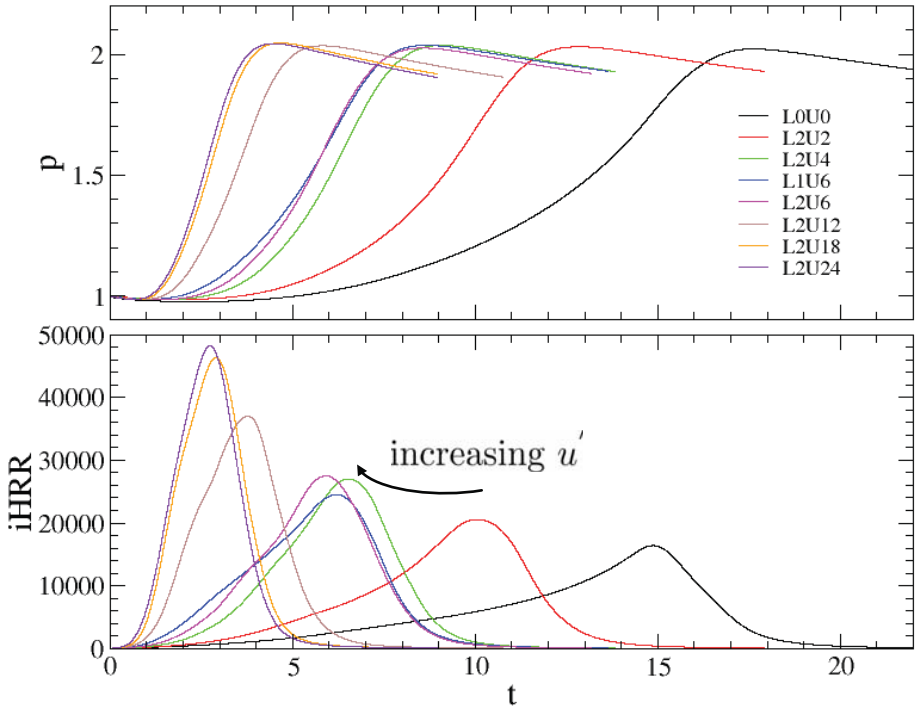

LAV

ETH zürich

Turbulent “quenching distances”

Flame front within $5\delta_f^0$ from horizontal walls

- Flame gets closer to the wall compared to the laminar case
- Mean distance decreases with increasing turbulence intensity

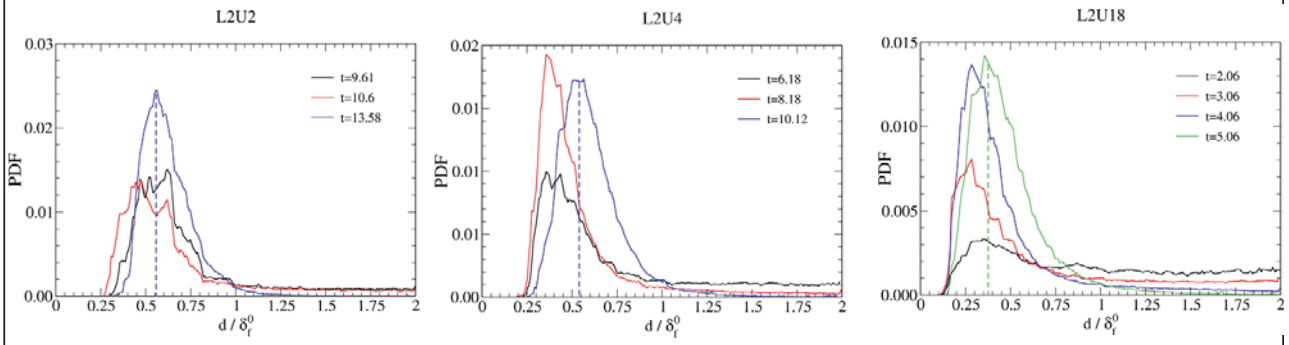

LAV

ETH zürich

Summary

- Confinement affects flame propagation through varying thermodynamic conditions, modification of the flow field and flame/wall interactions (FWIs)
  - flame ‘feels’ the wall early: significant variation of the local displacement speed quenching distance and heat fluxes
  - initial (kernel growth) and final (FWI) consumption of the fuel need 3 to 5 times longer to consume the first and last 10% of the fuel
- Early flame kernel growth:
  - u’ plays the dominant role
  - for the same u’, smaller l_t leads to faster initial fuel consumption
- Fuel consumption rate:
  - increases with turbulence intensity and saturates at high u’
  - no discernible trend vs. turbulent length scale
  - turbulence pushes the flame closer to the walls than the laminar quenching distance
  - mean distance of the flame from the wall decreases with u’

LAV

TNF 14
Flame-Wall Interactions
Simulation and Modelling

Contributors

1) Mahmoud Jafargholi, Christos E. Frouzakis, George K. Giannakopoulos, Konstantinos Boulouchos LAV, ETH Zürich

2) Umair Ahmed, Nilanjan Chakraborty, Jiawei Lai and Markus Klein
School of Engineering, Newcastle University | LRT, Universität der Bundeswehr München

3) Andrea Gruber et al.
SINTEF, Trondheim, Norway

4) Michael Pfitzner, Christian Mundt
Institut für Thermodynamik, Universität der Bundeswehr München

5) J. Sellmann, J. Lai, A. Kempf, N. Chakraborty
IVG, Universität Duisburg-Essen

6) Johannes Janicka
EKT, TU Darmstadt

Newcastle University

der Bundeswehr Universität München

Fundamental understanding and modelling of Flame-Wall Interaction using Simple and Detailed chemistry based Direct Numerical Simulations (DNS)

Umair Ahmed[1], Nilanjan Chakraborty[1], Jiawei Lai[1] and Markus Klein[2]

[1]School of Engineering, Newcastle University, Newcastle upon Tyne, NE1 7RU, UK

[2]Universität der Bundeswehr München, Werner Heisenberg Weg 39, D-85577 Neubiberg,Germany

1-D single step head-on quenching

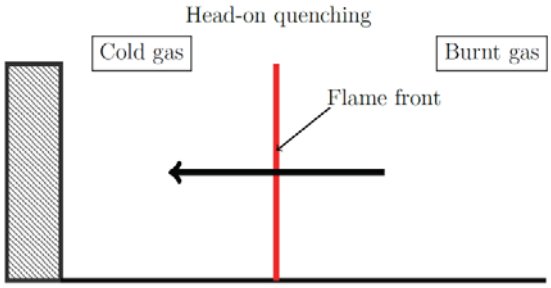

- Reaction progress variable $c = \frac{Y_{R_0} - Y_R}{Y_{R_0} - Y_{R_\infty}}$
- Non-dimensional temperature $T = \frac{\hat{T} - T_0}{T_{ad} - T_0}$
- Non-dimensional wall heat flux :
  $\Phi = \frac{|q_w|}{\rho_0 C_P S_L (T_{ad} - T_0)}$ where $q_w = -\lambda \left(\frac{\partial \hat{T}}{\partial x}\right)_w$
- Peclet number $Pe = \frac{X}{\delta_Z}$

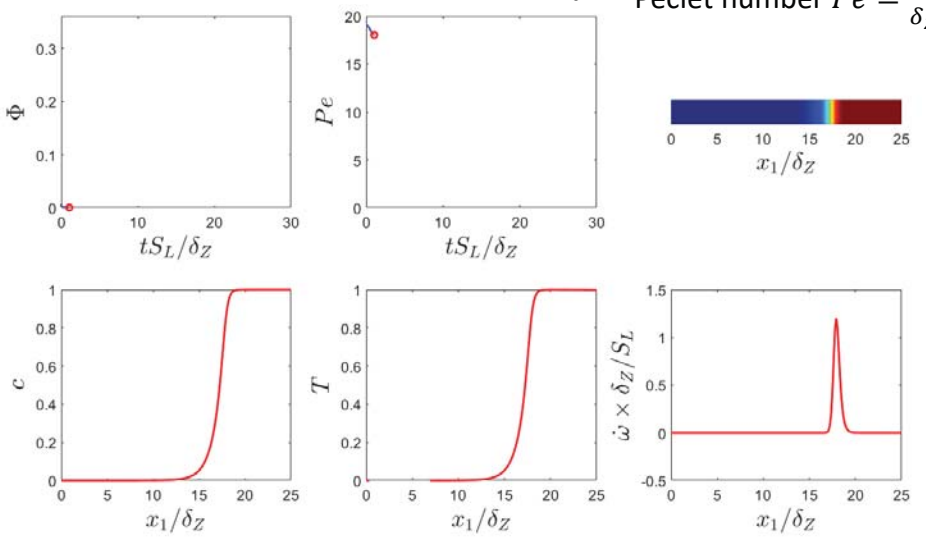

Comparison of chemistry head-on quenching

1-Step chemistry

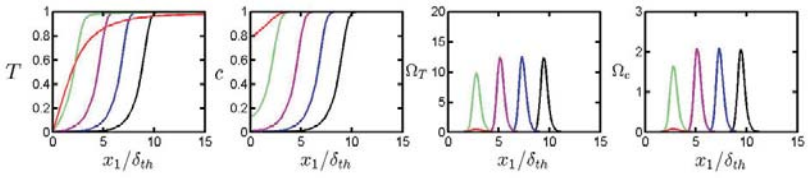

tS_L/δ_{th} = (—)4.0 (—)4.5 (—)5.0 (—)5.5 (—)6.0

Detailed chemistry

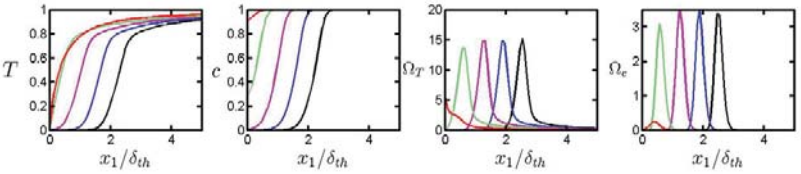

tS_L/δ_{th} = (—)1.50 (—)2.04 (—)2.65 (—)3.16 (—)3.95

- Two laminar cases are simulated one with single step chemistry and the other with a skeletal mechanism proposed by Smooke and Giovangigli (1991).

- Normalised heat release :
  $\Omega_T = \dot{\omega}_T \times \frac{\delta_{th}}{[\rho_0 S_L C_{p_0} T_0]}$
  where $\dot{\omega} = -\sum_{i=1}^{16} \dot{\omega}_i h_{fi}^0$
- Normalised reaction :
  $\Omega_c = \dot{\omega} \times \frac{\delta_{th}}{\rho_0 S_L}$
  $= -\frac{\dot{\omega}_{CH_4}}{Y_{R_0} - Y_{R_\infty}} \times \frac{\delta_{th}}{\rho_0 S_L}$

Smooke, M. D. & Giovangigli, V. (1991) Premixed and nonpremixed test problem results, 29–47. Springer Berlin Heidelberg, Berlin, Heidelberg.

3-D Head-on quenching

Chemical Mechanism	u'/S_L	l/δ_{th}	Da	Ka	τ
16 species, 25 reactions	7.5	2.5	0.34	13.0	6.0
1-step irreversible	7.5	2.5	0.34	13.0	6.0

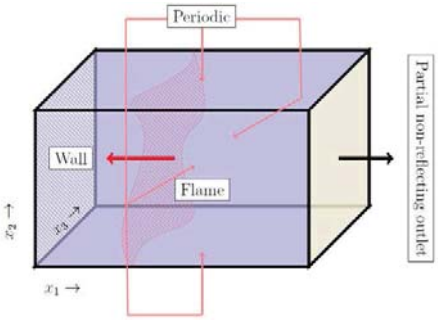

- Two turbulent cases are simulated one with single step chemistry and the other with a skeletal mechanism proposed by Smooke and Giovangigli (1991).
- The flow in the domain is initialised by isotropic turbulence using the method proposed by Rogallo (1981).
- Normalised methane mass fraction is used to define the progress variable for the detailed chemistry case

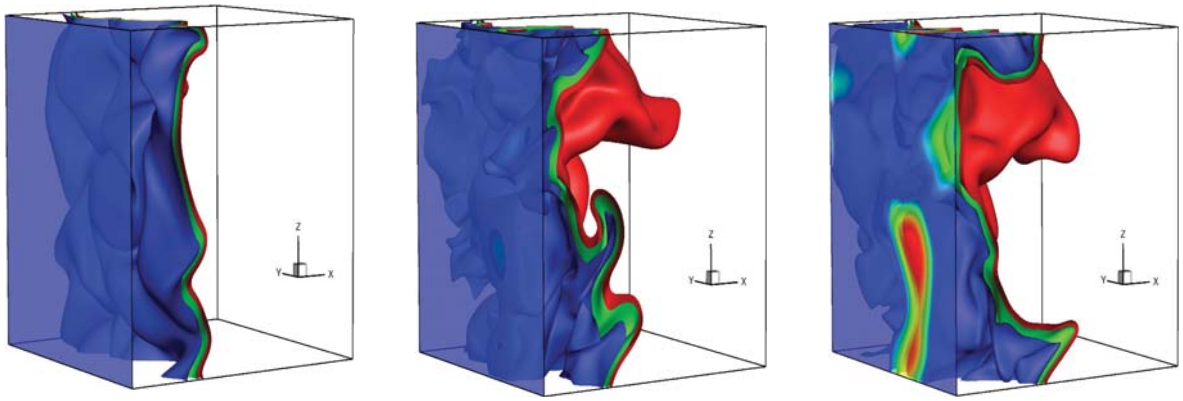

Rogallo, R.S. (1981), Numerical experiments in homogeneous turbulence, Technical report, NASA AMES.
Smooke, M. D. & Giovangigli, V. (1991) Premixed and nonpremixed test problem results, 29–47. Springer Berlin Heidelberg, Berlin, Heidelberg.

3-D single step head-on quenching

- Further details for single step chemistry head-on quenching are available in Lai and Chakraborty (2016)

Lai, J. & Chakraborty, N. (2016) Flow Turbulence Combust

Detailed chemistry head-on quenching

Laminar conditions

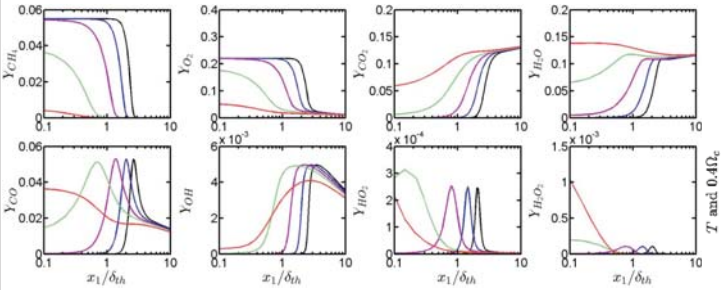

Turbulent conditions

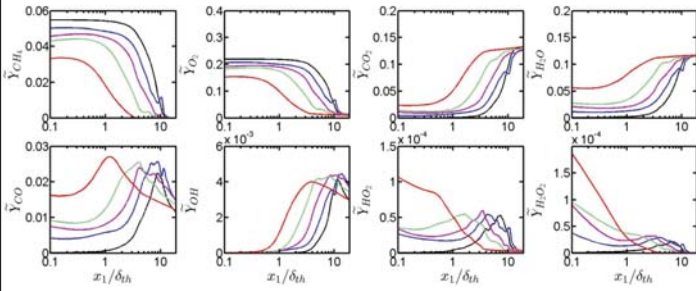

tS_L/δ_{th} = (—)1.50 (—)2.04 (—)2.65 (—)3.16 (—)3.95

Comparison of detailed and 1-Step chemistry

- $CO + OH \rightarrow CO_2 + H$
- $O_2 + H + M \rightarrow HO_2 + M$
- $2HO_2 \rightarrow H_2O_2 + O_2$

1-Step chemistry **Detailed chemistry**

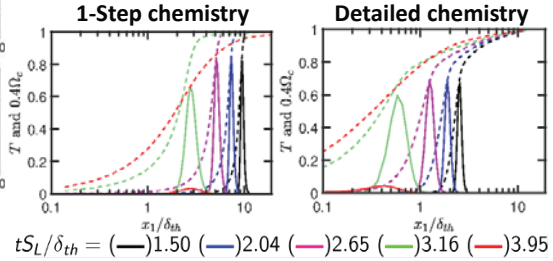

tS_L/δ_{th} = (—)1.50 (—)2.04 (—)2.65 (—)3.16 (—)3.95

Wall heat fluxes 1-Step chemistry

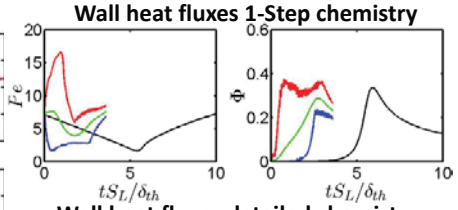

Wall heat fluxes detailed chemistry

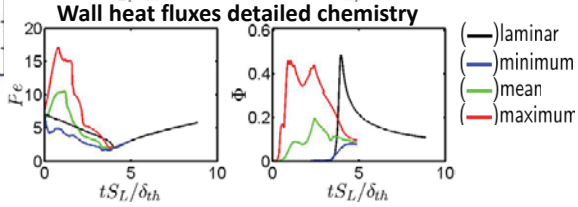

Model development for head-on quenching

1-Step chemistry Standard model

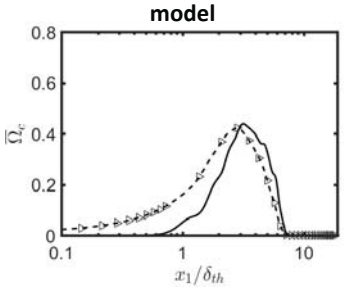

1-Step chemistry Sellmann et al. (2017) model

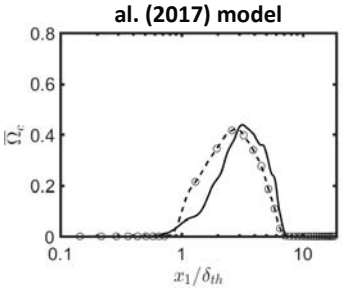

Detailed chemistry Standard model

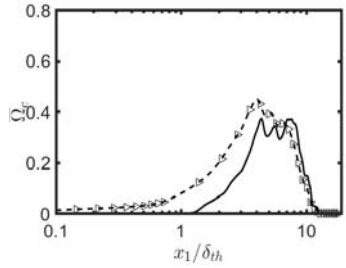

Detailed chemistry Sellmann et al. (2017) model

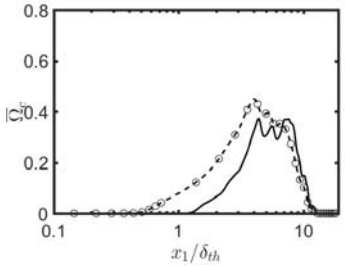

- $\Sigma_{gen} = \overline{|\nabla c|}$
- $\bar{\dot{\omega}}_c = \rho_0 S_L \Sigma_{gen}$ represented by $(-\Delta -)$
- $\bar{\dot{\omega}}_c = A_1 \rho_0 S_L \Sigma_{gen}$ represented by $(-\mathrm{O} -)$
  where
  $A_1 = 0.5[\mathrm{erf}\left(\frac{x_1}{\delta_{th}} - 0.7\Pi\right) + 1]$
  and $\Pi = (Pe_{min})_L \delta_{th}/\delta_Z$
- Similar models have been proposed for the scalar dissipation rate based reaction rate closure and further details can be found in Lai et al. (2018)

Sellmann, J. Lai, J., Kempf, AM. & Chakraborty N. (2017), Proc. Combust. Ins
Lai, J., Klein, M. & Chakraborty, N. (2018) Flow Turbulence Combust

Ongoing work on flame-wall interaction

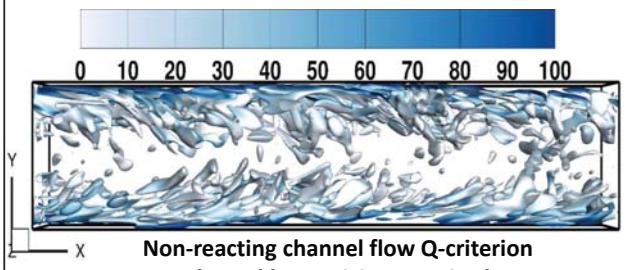

Non-reacting channel flow Q-criterion coloured by vorticity magnitude

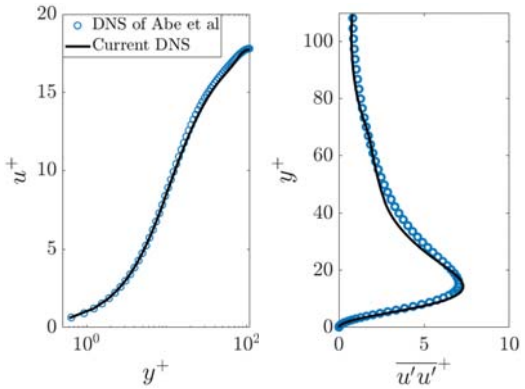

Non-reacting channel flow mean velocity and Reynolds stress profiles

- Currently flame wall interaction simulations in fully developed turbulent channel flow are underway.
- $Re_\tau = 110$ channel flow is used for the non-reacting channel.
- V-flame is being investigated in the $Re_\tau = 110$ channel flow.
- Three wall conditions are being simulated :
  - Isothermal walls
  - Adiabatic walls
  - Walls at an elevated temperature

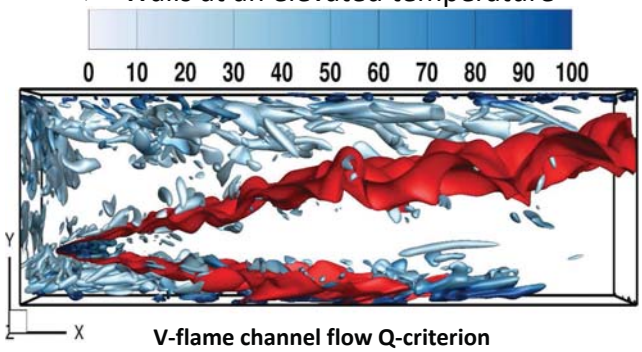

V-flame channel flow Q-criterion coloured by vorticity magnitude

DNS data of Abe et al is available at http://www.rs.tus.ac.jp/~t2lab/db/index.html

Conclusion

The quenching distance for turbulent condition decreases and the magnitude of the maximum wall heat flux increases in comparison to the corresponding laminar HOQ values for cases with $Le < 1$.

All the modelling assumptions which are associated with high Damköhler number (i.e. $Da \gg 1$) and presumed bi-modal PDF of c are rendered invalid close to the wall.

Both conventional Flame Surface Density (FSD) and Scalar Dissipation Rate (SDR) closures for mean reaction rate break down in the near-wall region.

TNF 14
Flame-Wall Interactions
Simulation and Modelling

Contributors

1) Mahmoud Jafargholi, Christos E. Frouzakis, George K. Giannakopoulos, Konstantinos Boulouchos LAV, ETH Zürich

2) Umair Ahmed, Nilanjan Chakraborty, Jiawei Lai and Markus Klein
School of Engineering, Newcastle University | LRT, Universität der Bundeswehr München

3) Andrea Gruber et al.
SINTEF, Trondheim, Norway

4) Michael Pfitzner, Christian Mundt
Institut für Thermodynamik, Universität der Bundeswehr München

5) J. Sellmann, J. Lai, A. Kempf, N. Chakraborty
IVG, Universität Duisburg-Essen

6) Johannes Janicka
EKT, TU Darmstadt

Direct Numerical Simulation of Turbulent Flame-Wall Interactions in a Constant Volume Vessel

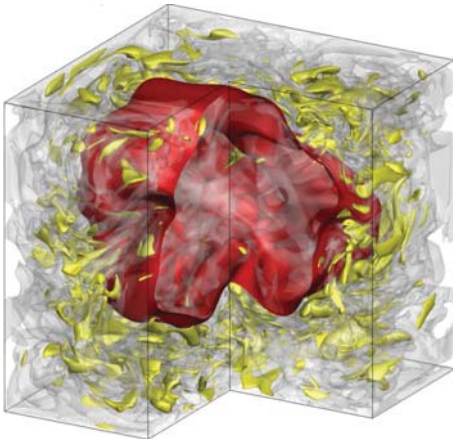

Andrea Gruber **SINTEF Energy Research**

in collaboration with Jacqueline H. Chen
Sandia National Laboratories

Overview

A new DNS database on turbulent FWI is (very) recently established

Aims to investigate turbulent flame-wall interaction at constant volume conditions:

- Compares the FWI process for hydrogen-air and methane-air flames at different Ka but for the same wall quenching time
- Case is initialized with HIT (see below) in a closed box (isothermal walls at 750K) and relaxed for 10 t_{l11} before spark ignition
- Grid is 700^3 with mild stretching towards from wall to center (6 microns to 20 microns)

Case	Fuel	ϕ	S_l (m/s)	Ka	T_{ad} (K)	ChemKin
H2S	Hydrogen	1.0	12.05	2.64	2586	Li et al
H2Sb	Hydrogen	1.0	12.05	0.88	2586	Li et al
H2L	Hydrogen	0.25	2.45	13	1473	Li et al
CH4S	Methane	1.0	2.42	7	2436	Smooke & Giovangigli

Initial turbulence characteristics (before relax): L_t = 5 mm, l_{11} = 0.907 mm, η_k = 0.036 mm
t_{l11} = 0.00084 s, t_k = 0.000017 s, u' = 10.8 m/s, Re_t = 715

FWI of stoichiometric CH4-air vs lean H2-air flame (matching flame speed)

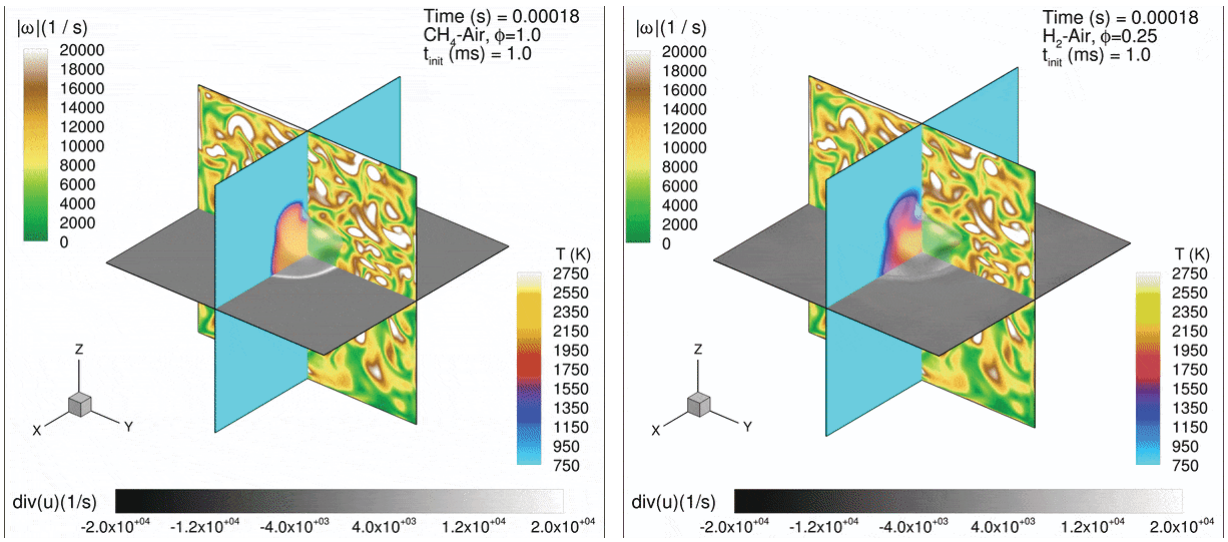

In spite of the considerable difference in T_{ad} and δ_l = (0.287 vs 0.541 mm) the flames exhibit similar propagation characteristics and quench on the wall simultaneously (the hydrogen flame is slightly more wrinkled/curved)

FWI of stoichiometric hydrogen-air flames for different turbulence levels (longer decay)

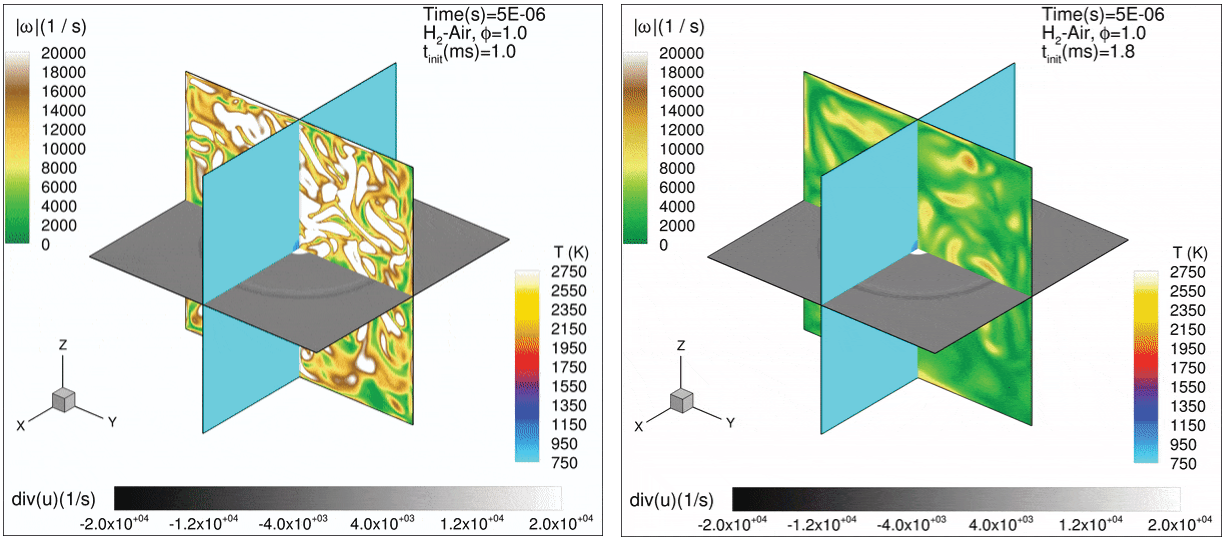

The stoichiometric (very fast) hydrogen flames «ignore» the underlying turbulence field (squashing turbulence structures against the wall), more so after a longer turbulence decay

Role of radical recombination at the wall

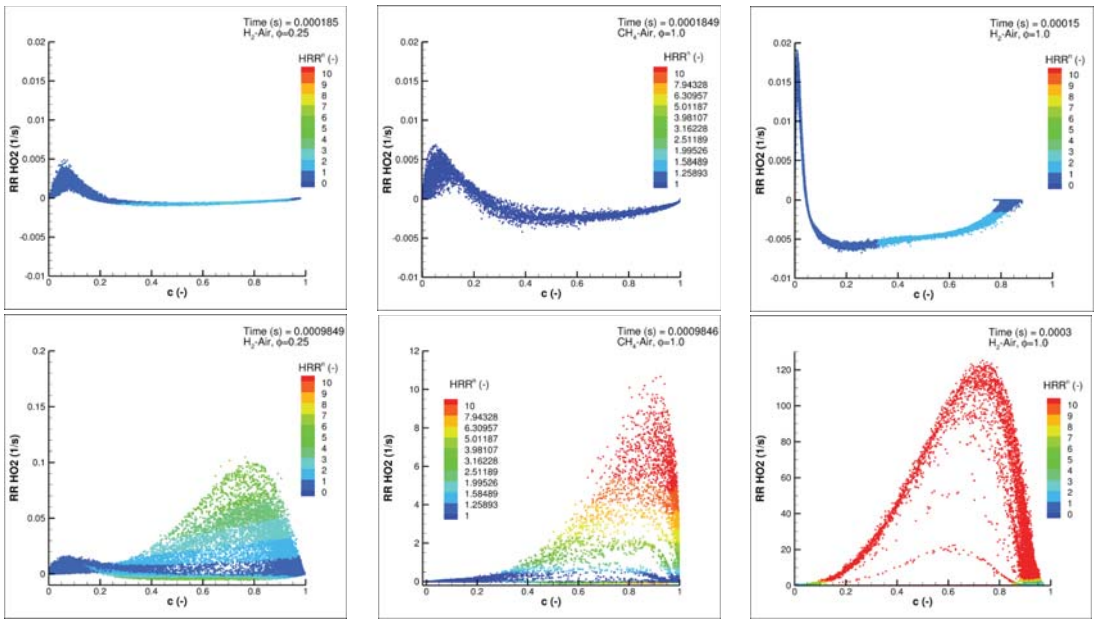

All flames exhibit some degree of radical recombination at the wall: its role is minimal for the lean hydrogen flame, more important for the stoichimoetric methane flame and greatest for the stoichiometric hydrogen flame

CO chemistry is strongly affected by the FWI

Before FWI

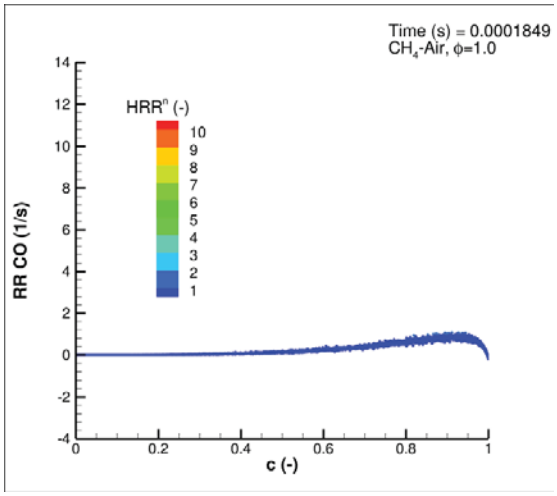

During FWI

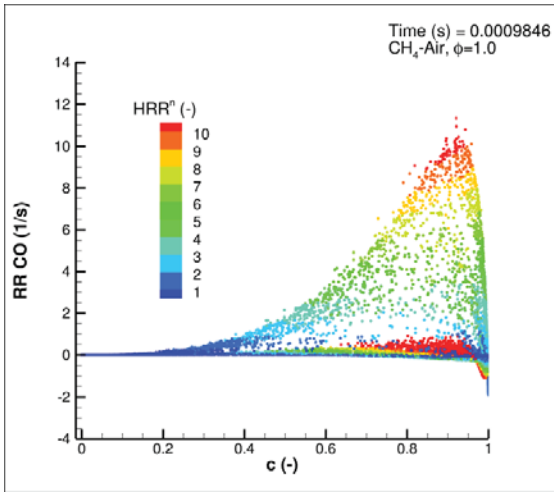

Conclusions

- Analysis of DNS database is in initial phase and results are preliminary
- Flame velocity seems to be the governing parameter in the turbulence-chemistry interaction more than flame thickness vs turbulence length scales
- Radical recombination during quenching seems to be important also for methane combustion (although to a lesser extent than for hydrogen)
- The hydrogen stoichiometric flame shows the largest wall heat flux and the largest heat release rate due to radical recombination
- The hydrogen lean flame shows the least heat release rate due to radical recombination (wall heat flux is also low due to the lower flame temperature)
- Total mass of CO peaks at quenching but it successively burned out after the FWI

TNF 14
Flame-Wall Interactions
Simulation and Modelling

Contributors

1) Mahmoud Jafargholi, Christos E. Frouzakis, George K. Giannakopoulos, Konstantinos Boulouchos LAV, ETH Zürich

2) Umair Ahmed, Nilanjan Chakraborty, Jiawei Lai and Markus Klein
School of Engineering, Newcastle University | LRT, Universität der Bundeswehr München

3) Andrea Gruber et al.
SINTEF, Trondheim, Norway

4) Michael Pfitzner, Christian Mundt
Institut für Thermodynamik, Universität der Bundeswehr München

5) J. Sellmann, J. Lai, A. Kempf, N. Chakraborty
IVG, Universität Duisburg-Essen

6) Johannes Janicka
EKT, TU Darmstadt

Heat transfer coefficient in reactive boundary layers

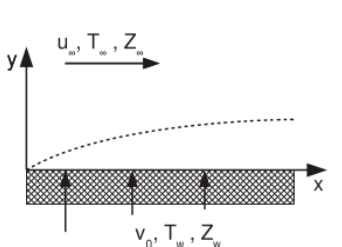

Test case: laminar flow over a porous plate.[1]

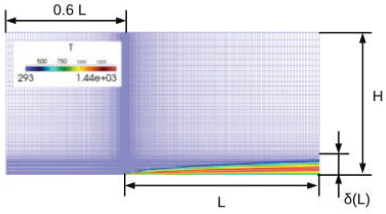

2D computational domain.[1]

- ∞: inflow properties, W:coolant properties
- Lewis numbers = 1, Sc = 1
- Boundary layer theory + Dorotnitzyn Stewartson transformation: (x,y) → (ξ, ζ)

[1] G.Frank, M. Pfitzner, "Investigation of the heat transfer coefficient in a transpiration film cooling with chemical reactions", International Journal of Heat and Mass Transfer, 113, 2017, pp-755-763

Free stream	**Coolant 1**	**Coolant 2**
Air (273K, 1bar, 2m/s)	3.1%H2+96.9%N2	CH4

Inert BL

$$T_{inert}(Z) = T_\infty + \frac{Z - Z_\infty}{Z_W - Z_\infty}(T_W - T_\infty)$$

$$\dot{q}_{inert} = -\lambda \frac{\rho_W}{\rho_\infty} \sqrt{\frac{\rho_\infty u_\infty}{2\,\rho_W x}} \left.\frac{\partial Z^*}{\partial \zeta}\right|_{\zeta=0} (T_W - T_\infty)$$

Reactive BL

Burke-Schumann solution:

$$T_{react}(Z) = \begin{cases} T_0 + \dfrac{Z}{Z_{st}}(T_{ad} - T_0) & Z \le Z_{st} \\ T_F + \dfrac{1-Z}{1-Z_{st}}(T_{ad} - T_F) & Z > Z_{st} \end{cases}$$

$$\dot{q}_{react} = -\lambda \frac{\rho_W}{\rho_\infty} \sqrt{\frac{\rho_\infty u_\infty}{2\,\rho_W x}} \left.\frac{\partial Z^*}{\partial \zeta}\right|_{\zeta=0} \frac{1}{1-Z_{st}} (T_{ad} - T_W)$$

BL without pressure gradient

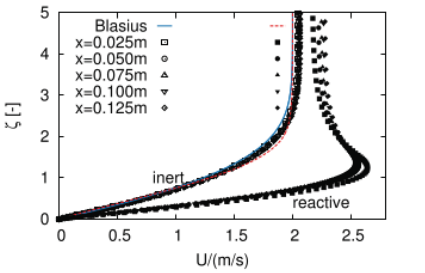

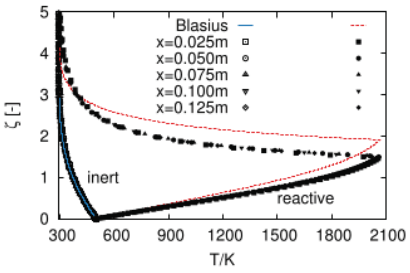

BL without pressure gradient for coolant CH4. Top : Ux, bottom: T.

BL with pressure gradient

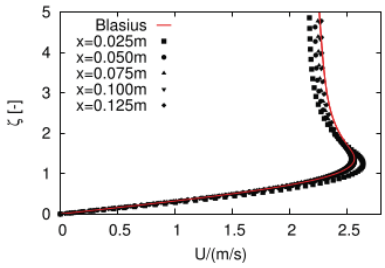

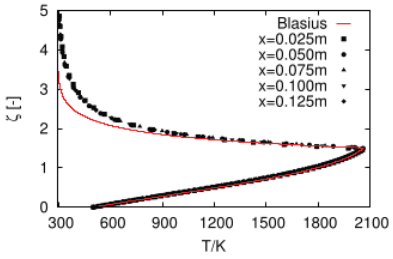

BL with pressure gradient for coolant CH4. Top : Ux, bottom: T.

Nusselt number

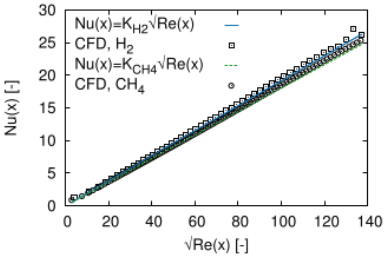

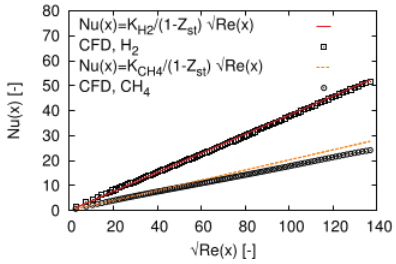

Nusselt numbers. Top: inert case. Bottom: reactive case.

Blasius inert Blasius reactive CFD inert CFD reactive

Chemistry tabulation methods

Chemical equilibrium

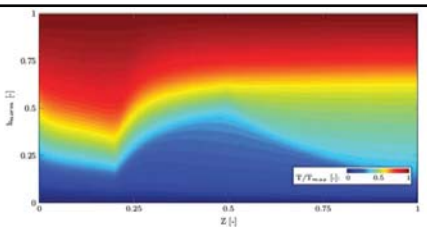

- S-shape curve filled ✓
- No nonequilibrium wall quenching ✗

Frozen chemistry

[2] Frank et al. 2016
„Construction of Libraries for Non-Premixed Tabulated chemistry Combustion Models including Non-Adiabatic Behaviour due to Wall Heat Losses"

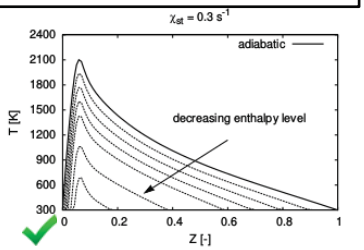

- Strain rate ✓
- S-shape curve filled ✓
- FWI affects T, not Y_k (frozen) ✗

Convective heat sink term (Lee, Ihme 2011)

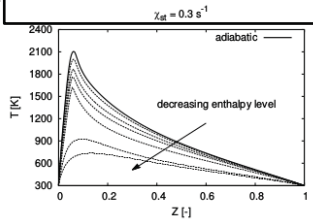

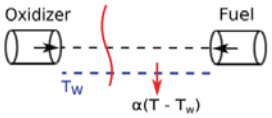

$$\dot{q} = \frac{\rho}{\tau_C}(T(Z) - T_W)$$

- Head-on quenching
- Artificial convective heat loss term ✗
- FWI affects both T and Yk. ✓ Strain rate ✓
- S-shape curve partially filled -> interpolation ✗

Specified fuel boundary temperature

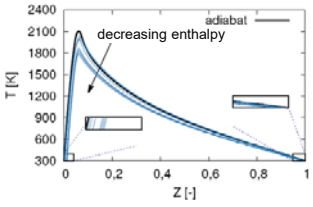

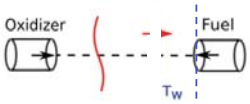

- Fixed temperature wall
- FWI affects both T and Yk. ✓
- Strain rate ✓

Efficient wall-heat flux prediction for methane-oxygen combustion at rocket-like conditions

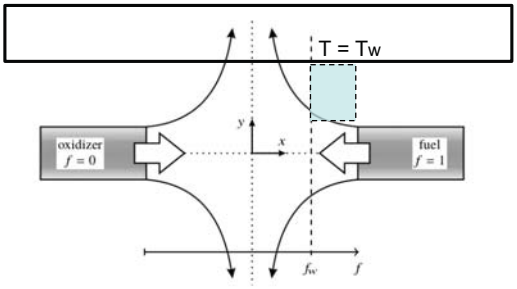

Non-adiabatic tabulation
(Wu, Ihme 2015, Ma et al. 2018)

- Permeable isothermal wall at f=fw
- O_2-CH_4, 20 bar
- 13 species, 73 reactions
- 3D thermochemical library

Consideration of strong heat losses

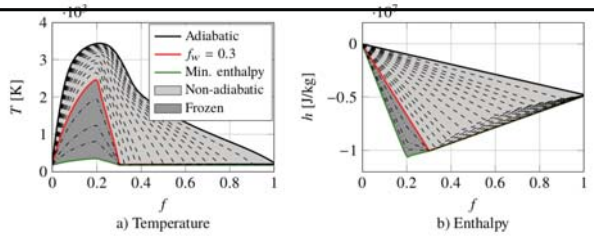

Incorporation of flame-wall interaction

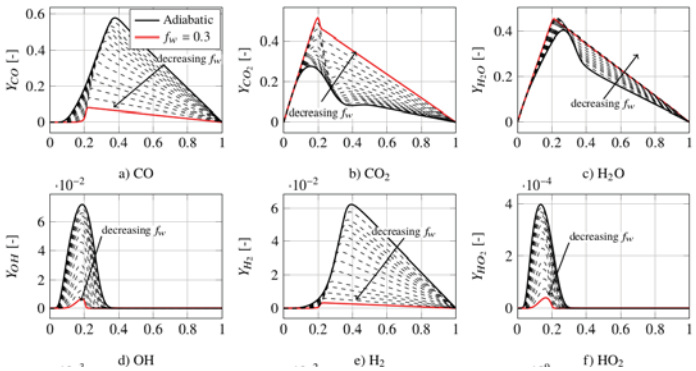

LES of 7-element GOX/GCH$_4$ subscale rocket combustor [4]

Temperature field

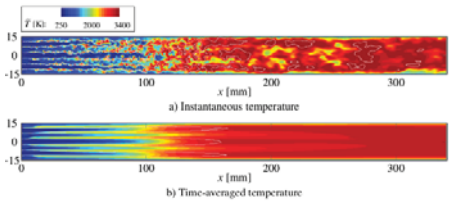

Axial influence of enthalpy loss

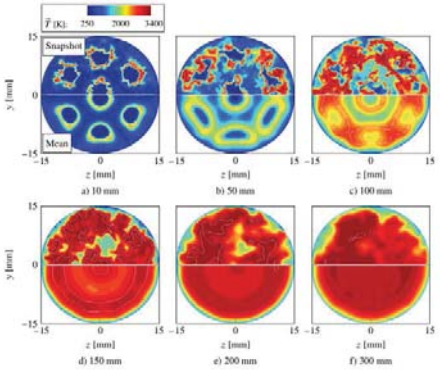

[3] Valino FTAC 1998. [4] Experiment by Haidn et al. 2017

State space

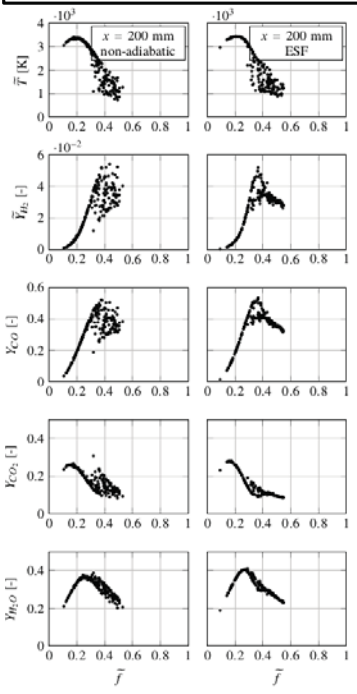

Comparison with experiment

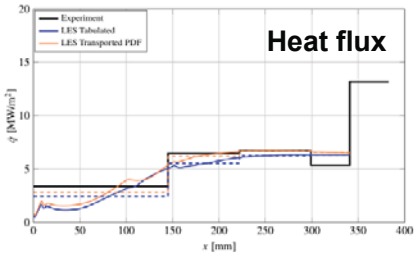

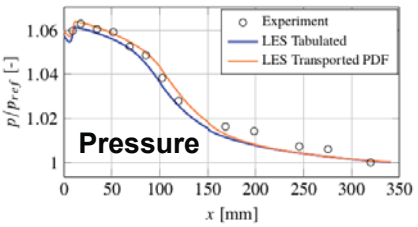

Normalized CPU cost

- Tabulated: 1
- Transported PDF (Eulerian Stochastic Fields [3]): 53

TNF 14
Flame-Wall Interactions
Simulation and Modelling

Contributors

1) Mahmoud Jafargholi, Christos E. Frouzakis, George K. Giannakopoulos, Konstantinos Boulouchos LAV, ETH Zürich

2) Umair Ahmed, Nilanjan Chakraborty, Jiawei Lai and Markus Klein
School of Engineering, Newcastle University | LRT, Universität der Bundeswehr München

3) Andrea Gruber et al.
SINTEF, Trondheim, Norway

4) Michael Pfitzner, Christian Mundt
Institut für Thermodynamik, Universität der Bundeswehr München

5) J. Sellmann, J. Lai, A. Kempf, N. Chakraborty
IVG, Universität Duisburg-Essen

6) Johannes Janicka
EKT, TU Darmstadt

Institute for Combustion and Gas Dynamics
Fluid Dynamics

UNIVERSITÄT DUISBURG ESSEN
Offen im Denken

Newcastle University

Flame Surface Density based Modelling of Head-On Quenching of Turbulent Premixed Flames

- J. Sellmann, J. Lai, A. Kempf, N. Chakraborty
- johannes.sellmann@uni-due.de

Objective

- A priori analysis of:
- the mean reaction rate closure by Flame Surface Density (FSD)[1]
- FSD transport terms[2]
- Modelling, the unclosed terms, based on existing models[3,4,5,6].
- For:
- Three different Lewis number: 0.8, 1.0, 1.2
- Five different initial turbulent values ($\boldsymbol{u'/S_L}$): 5.0, 6.25, 7.5, 9.0, 11.25
- 15 different cases in total

mean reaction rate closure[1]

$$\frac{\partial}{\partial x_i}\left(\bar{\rho}\bar{D}\frac{\partial \tilde{c}}{\partial x_i}\right) + \bar{\dot{\omega}}_c = \overline{(\rho S_d)}_s \Sigma_{gen} \approx \rho_0 S_L \Sigma_{gen}$$

FSD transport[2]

$$\frac{\partial \Sigma_{gen}}{\partial t} + \frac{\partial(\tilde{u}_j \Sigma_{gen})}{\partial x_j} = \underbrace{-\frac{\partial}{\partial x_i}\left[\overline{(u_i)}_s - \tilde{u}_i\right]\Sigma_{gen}}_{\text{Turbulent Transport}} + \ldots$$

$$\ldots + \underbrace{\left(\overline{(\delta_{ij} - N_i N_j)\frac{\partial u_i}{\partial x_j}}\right)_s \Sigma_{gen}}_{\text{Tangential Strain Rate term}} \underbrace{-\frac{\partial}{\partial x_i}\left[\overline{(S_d N_i)}_s \Sigma_{gen}\right]}_{\text{Propagation Term}} + \ldots$$

$$\ldots \underbrace{\left(\overline{S_d \frac{\partial N_i}{\partial x_i}}\right)_s \Sigma_{gen}}_{\text{Curvature Term}}$$

1. Cant et al. Proc. Combust. Inst. 23 (1990)
2. Pope Intl. J. Engng Sci. 26 (1988)
3. Bruneaux et al., J. Fluid. Mech. 349 (1997)
4. Alshaalan and Rutland Proc. Combust. Inst. 27 (1998)
5. Chakraborty and Cant, Combust. Flame 158 (2011)
6. Katragadda et al. Proc. Combust. Inst. 33 (2011)

www.cenide.de

Simulation Setup

- DNS Simulation[7,8]
- Head on quenching (HOQ)[9,10]
- Compressible 3D DNS SENGA[11]
- Cartesian grid: 512 x 256 x 256
- Simulation domain: $70\delta_z \times 35\delta_z \times 35\delta_z$
- No-slip isothermal inert wall (T_w=T_0)
- Periodic in transverse direction
- Partially non-reflecting outlet (NSCBC)[12]
- Heat release parameter
- One step reaction (Arrhenius type)

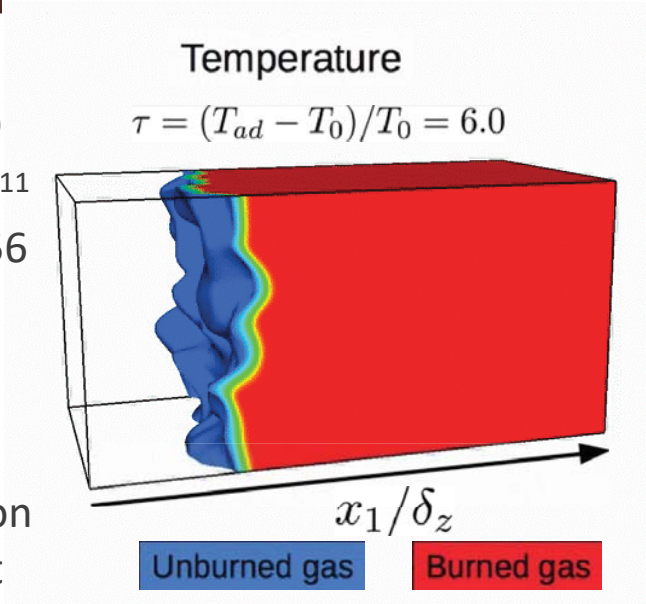

7. Lai and Chakraborty, Combust. Sci. Technol. 188 (2016)
8. Lai and Chakraborty, Flow Turb. Combust. 96 (2016)
9. Poinsot et al., Combust. Flame 95 (1993)
10. Alshaalan and Rutland Proc. Combust. Inst. 27 (1998)
11. Jenkins and Cant, Springer Netherlands (1999)
12. Poinsot and Lele, Comput. Phys. 101 (1992)

www.cenide.de

Important Parameters

- Quenching sensor[3]:

$L_H = c_w - T_w$

$L_H = 0$ Away from the wall

$L_H \neq 0$ When quenching starts

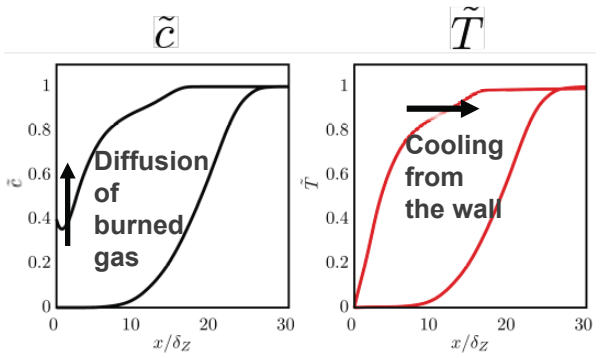

Quenching distance Pe_{min}:

$Pe = X/\delta_Z$ $X \rightarrow$ Distance of iso-surface $\tilde{T}$=0.9

$\delta_z = \alpha_0/S_L \rightarrow$ Zeldovich flame thickness

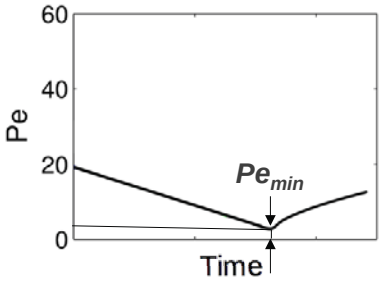

For turbulent cases[13]:

$Pe_{min} = (Pe_{min})_L[erf(8Le - 6.0) + 1]/2$

3. Bruneaux et al., J. Fluid. Mech. 349 (1997)
13. Lai and Chakraborty, Flow Turb, Combust. 96 (2016)

Results

- Only most represented results, compared against previous models are shown. A detailed description of the models and results are published: *Johannes Sellmann, Jiawei Lai, Andreas M Kempf, Nilanjan Chakraborty, Proceedings of the Combustion Institute, Volume 36, Issue 2, 2017*

mean reaction rate closure[1]

$\bar{\omega}_c = \overline{(\rho S_d)}_s \Sigma_{gen} \approx \rho_0 S_L \Sigma_{gen}$

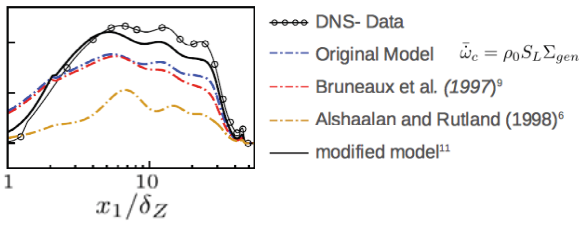

FSD transport[2]

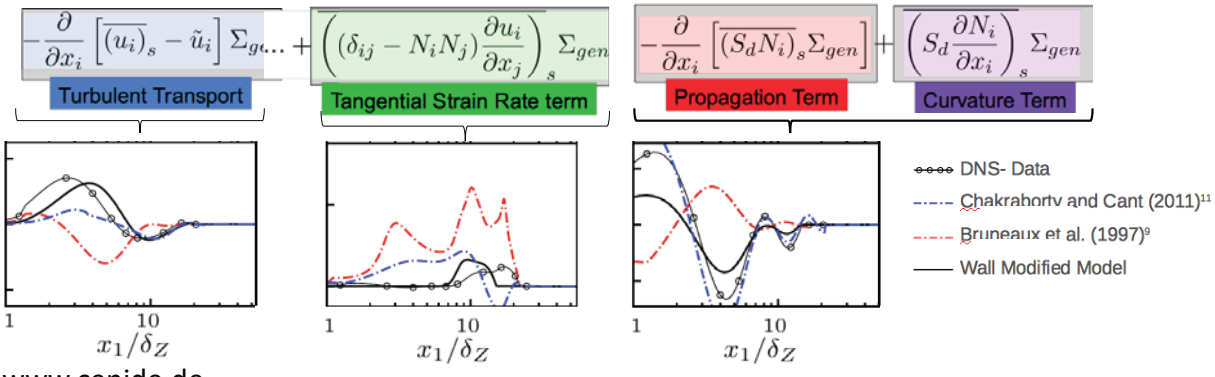

Conclusion

- Modified FSD based closure for mean reaction rate in terms of Flame Wall Interaction has been proposed
- Existing models for the unclosed terms of the FSD transport equation have also been modified
- The modified models are capable for a Lewis number range of Le = 0.8 - 1.2 and different turbulent initial values

TNF 14
Flame-Wall Interactions
Simulation and Modelling

Contributors

1) Mahmoud Jafargholi, Christos E. Frouzakis, George K. Giannakopoulos, Konstantinos Boulouchos LAV, ETH Zürich

2) Umair Ahmed, Nilanjan Chakraborty, Jiawei Lai and Markus Klein
School of Engineering, Newcastle University | LRT, Universität der Bundeswehr München

3) Andrea Gruber et al.
SINTEF, Trondheim, Norway

4) Michael Pfitzner, Christian Mundt
Institut für Thermodynamik, Universität der Bundeswehr München

5) J. Sellmann, J. Lai, A. Kempf, N. Chakraborty
IVG, Universität Duisburg-Essen

6) Johannes Janicka
EKT, TU Darmstadt

Configuration: SWQ-burner

TECHNISCHE UNIVERSITÄT DARMSTADT

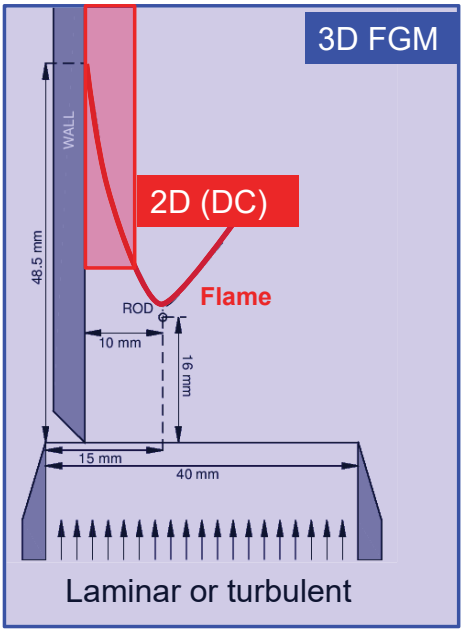

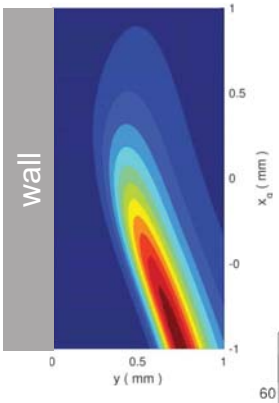

SFB/Transregio 150
Turbulente, chemisch reagierende Mehrphasenströmungen in Wandnähe

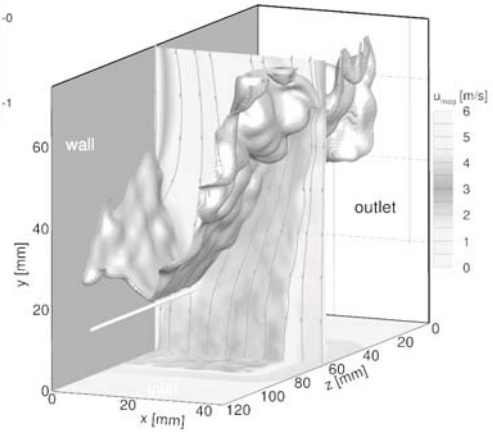

Prediction of near-wall profiles using DC and FGM

TECHNISCHE UNIVERSITÄT DARMSTADT

Observation FGM/DC/Exp

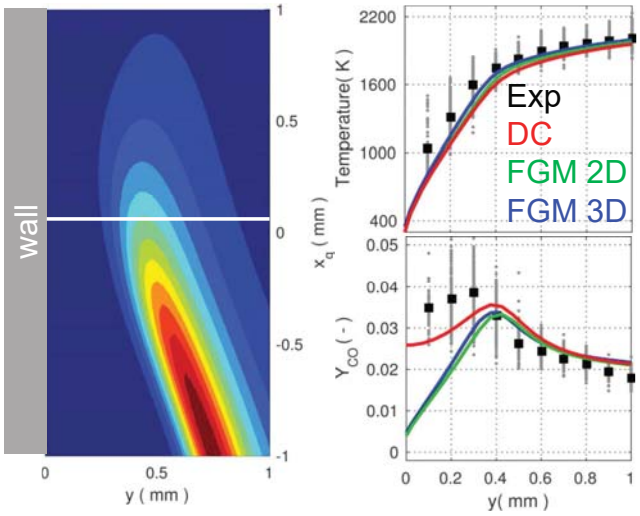

- Temperature ok in DC and FGM
- CO: FGM fails, DC ok

DC budget analysis

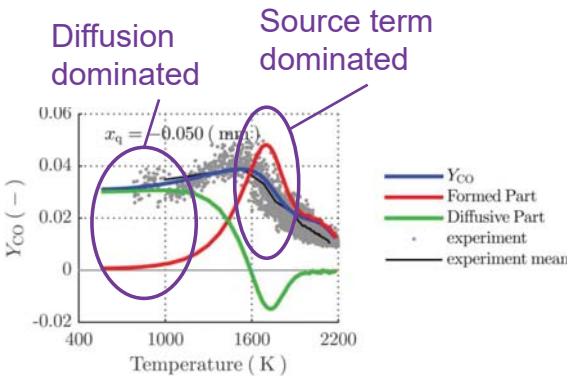

- Wall region dominated by diffusion
- Problem of FGM?

Budget analysis in composition space

TECHNISCHE UNIVERSITÄT DARMSTADT

Rewriting: $Y_k = Y_k(Y_{CO_2}, h)$

$$\rho\chi_{CO_2}\frac{\partial^2 Y_{CO}}{\partial Y_{CO_2}^2} + 2\rho\chi_{CO_2,h}\frac{\partial^2 Y_{CO}}{\partial Y_{CO_2}\partial h} + \rho\chi_h\frac{\partial^2 Y_{CO}}{\partial h^2} + \dot{\omega}_{CO} - \frac{\partial Y_{CO}}{\partial Y_{CO_2}}\dot{\omega}_{CO_2} = 0$$

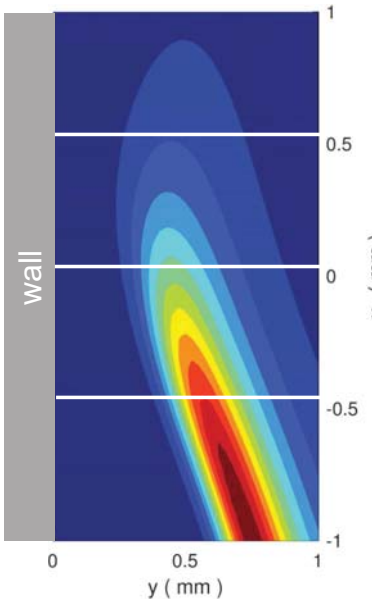

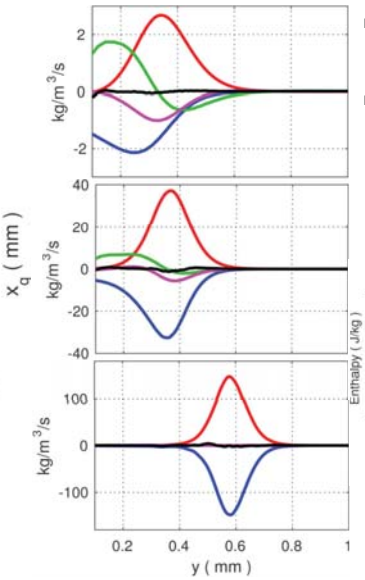

- Neglected in FGM table generation
- At flame-wall attachment large contribution of scalar dissipation term, especially χ_h

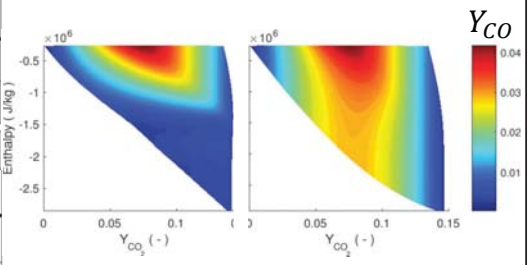

REDIM to account for the full set of χ

TECHNISCHE UNIVERSITÄT DARMSTADT

- Solving reaction mechanism in Θ - space
- Gradients from DC or estimated (e.g. from HOQ)

$$\psi(\theta_i) \longleftrightarrow Y_k(CO_2, h, \ldots)$$

$$\frac{\partial \Psi(\theta)}{\partial t} = \left(I - \Psi_\theta \Psi_\theta^+\right) \cdot \left(F(\Psi) - \frac{1}{\rho} D \left\|\Psi_\theta^T \operatorname{grad}(\Psi)\right\|^2 \frac{1}{m_s}\operatorname{Tr}(A)\right)$$

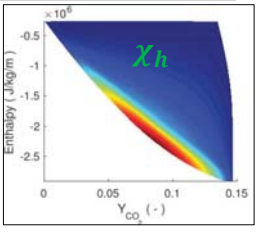

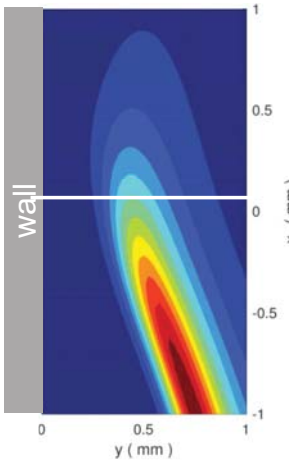

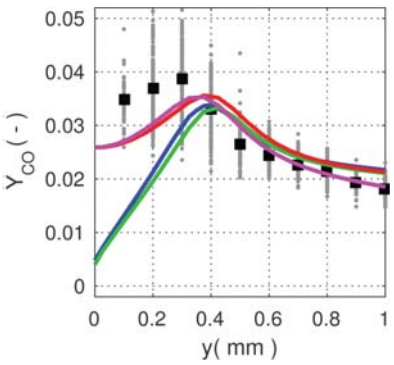

Exp
DC
FGM 2D
FGM 3D
REDIM

- REDIM matches the DC
- However, somehow case specific

Configuration: SWQ-burner

TECHNISCHE UNIVERSITÄT DARMSTADT

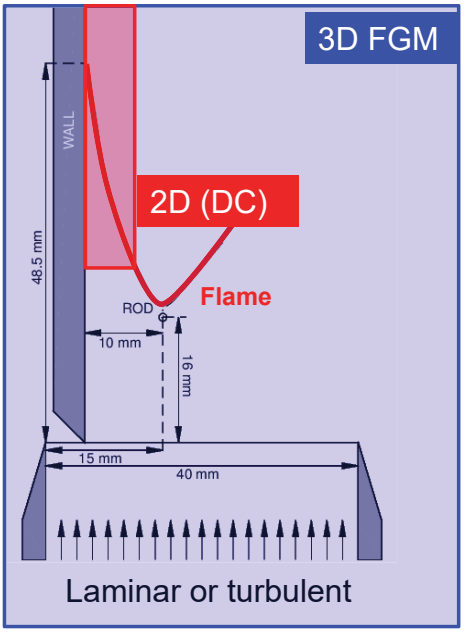

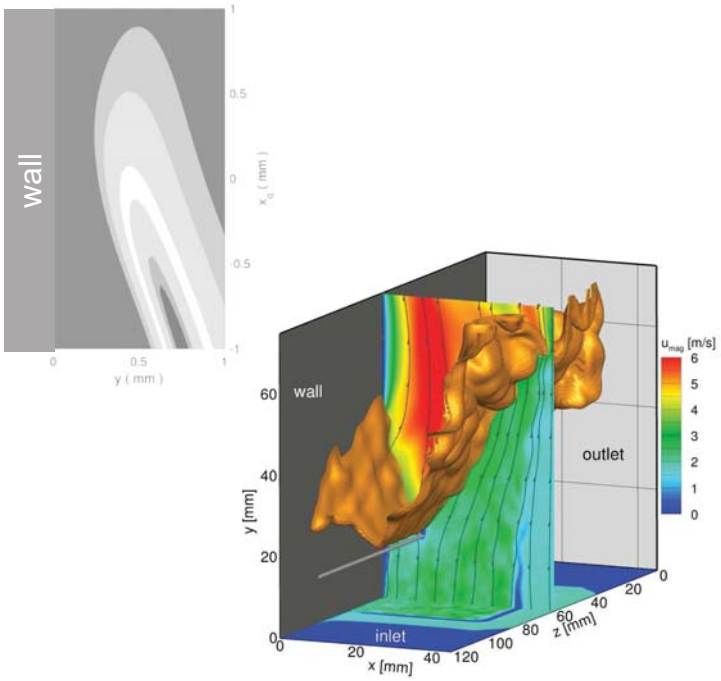

Comparison: LES to measurements

TECHNISCHE UNIVERSITÄT DARMSTADT

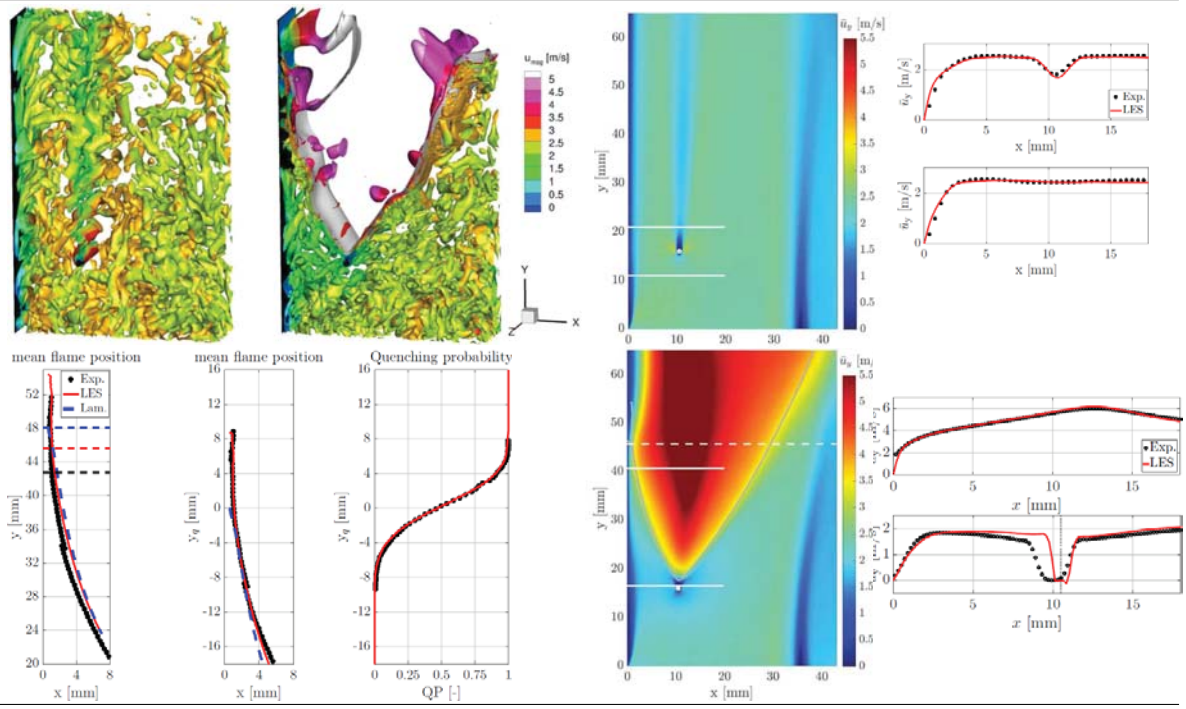

Flame-wall Attachement angle at the quenching point

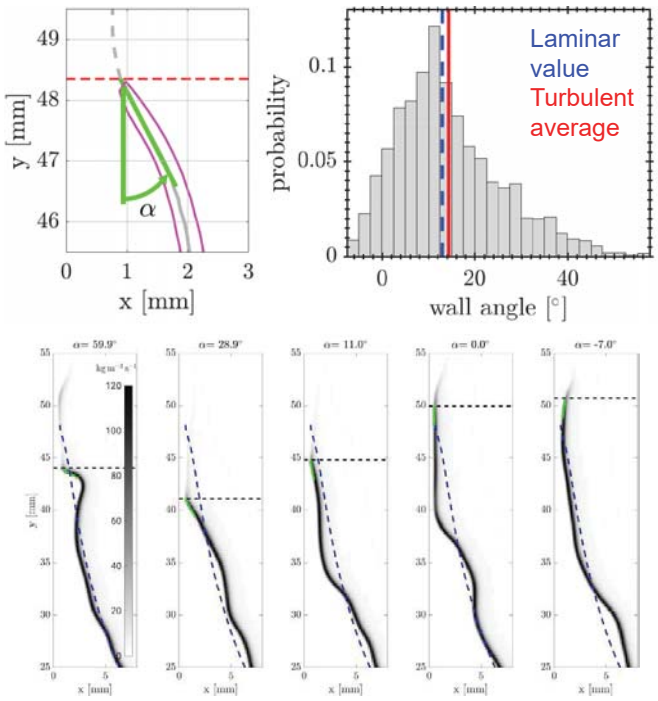

- Large range of attachment angles
- Rare events oft almost pure SWQ alignment (90°)
- Frequent occurrence HOQ regime (~0°)
- Also negative values are observed

Research Fields	Research Group					
	ETH	NCU/ UB	SINTEF	UB	NC/UD	TUD
Scientific challenges (near wall)						
Characterization of mechanism/phenomena						
DNS (dc)	x	x	x		x	x
Modelling						
Detailed Chemistry						
Reduction				x		x
Turbulence-Chemistry-Interaction					x	x
Method Development						
numerical						

Research Fields	Research Group					
	ETH	NCU/ UB	SINTEF	UB	NC/UD	TUD
Scientific challenges (near wall)						
Characterization of mechanism/phenomena						
DNS (dc			x		x	x
Modell						
Detaile						
Reducti				x		x
Turbule					x	x
Metho						
numeri						

Future challenges

- **Pressure**
- **Green fuels**
- **Stratification**
- **Multi mode combustion**
- **…**

Plenty of room for future research

Thank you

SWQ-to-HOQ transition by FTWI

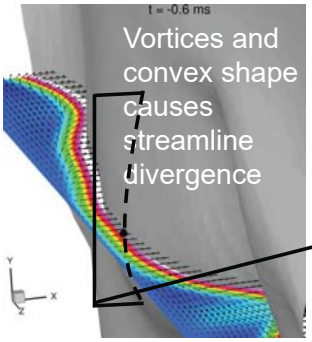

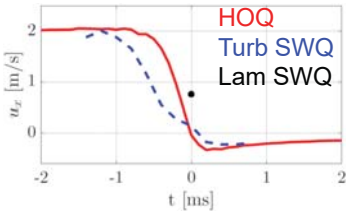

Even below HOQ values,
Near wall they approach each other

Low opposing convection

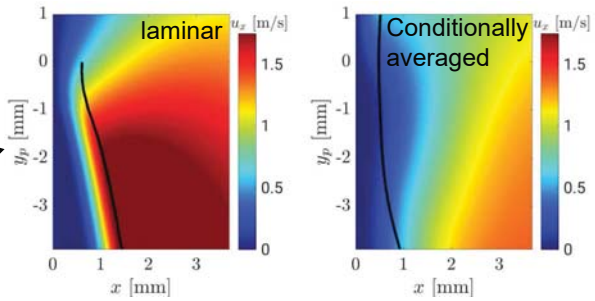

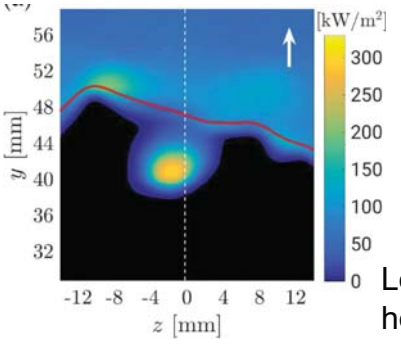

Locally extreme heat fluxes

Multi-mode combustion: Combustion mode analysis, measurement and modelling

Coordinator: Robert Gordon

This session follows on from discussions in TNF13 on combustion regime indicators and reaction progress markers. A brief review of the key information from TNF13 was presented, then the presentation was structured as follows: a review of progress in the identification of combustion mode through numerical and experimental tools; the use of this information in combustion model selection; approaches in modelling combustion with mode flexibility. Combustion mode switching from premixed to non-premixed is discussed, along with combustion mode switching from premixed to autoignition.

Numerical identification of combustion mode: Chemical explosive mode analysis of high-Karlovitz premixed flames
(Xinju Zhao, Ji-Woong Park, Peiyu Zhang, Tianfeng Lu, Haiou Wang, Jacqueline H. Chen, Evatt Hawkes)

This section outlined advances in the use of the Chemical Explosive Mode Analysis (CEMA) with regards to premixed combustion versus autoignition. A decomposition of the effects of chemistry and diffusion on the Chemical Explosive Mode permits identification of assisted ignition, auto-ignition and (local) extinction, noting that while the chemistry always progresses, the diffusion contribution to the reaction can be assisting, negligible, or retarding the progress. These concepts are then applied to the investigation of a high Karlovitz number jet flame, and the observations are intended to aid modellers in determining which approaches to apply for different regimes. This application of CEMA requires a full knowledge of the chemical Jacobian matrix to evaluate.

Experimental identification of combustion mode: Gradient-free regime identification (GFRI)
(S. Hartl, D. Geyer, A. Dreizler, G. Magnotti, R.S. Barlow, C. Hasse, G. Magnotti, R. van Winkle)

In acknowledgement that most numerical markers of combustion regime require knowledge of local scalar gradients, and that these are prohibitive to gather, the experimental investigations of this section were focussed on the identification of the local combustion mode through multi-scalar measurements and then evaluating the most likely local thermochemical state. The four-stage process involves (a) measurement of the local major species and temperature, (b) approximation of the full thermochemical state through a constrained 0D reactor calculation, (c) determination of the most relevant local flame markers, and (d) applying a combination of these markers to determine the local combustion mode (from non-premixed to premixed). The premixed zones are identified from the Chemical Mode zero-crossings that correlate with large heat release rate, and the non-premixed regions are indicated by negative chemical mode, large HRR, significant OH, and non-constant mixture fraction in the vicinity of the stoichiometric mixture fraction. Test cases, validation and examples were presented, as well as information regarding recent and future publications of applications on the topic.

Combustion model selection during modelling: Combustion Regimes
(Matthias Ihme, Hao Wu, Qing Wang)

Having developed numerical tools to determine the chemical modes, the next section explored how one might use this information to select the appropriate combustion model within a zone of a CFD simulation. The concept of the Combustion Model Compliance Indicator is introduced, which evaluates a drift term of the actual evolution of the Quantities of Interest versus the combustion model manifold. This is an estimate of the initial growth rate of errors, and can be evaluated for each applicable combustion model, then the model that would propagate errors the most slowly is

chosen. Application of this approach in a GT-relevant combustor simulation led to a 40% reduction in cost.

Multi-Modal Turbulent Combustion: Recent Modelling Efforts
(Michael Mueller)

Another approach to improving the modelling of multi-modal combustion problems presented was to develop combustion models that are a priori developed for multi-modal combustion. This final section first investigated when such approaches were necessary (e.g. which manifolds significantly depart from each other when premixed or non-premixed combustion is assumed). Typically this arises in the modelling of emissions rather than temperature. A review was presented of recent non-premixed models that permit premixed combustion under certain conditions. This was followed by a postulate that all adiabatic, isobaric two stream combustion problems can be represented on a unit square of two variables if those variables are suitably defined (e.g. mixture fraction and progress variable). What follows is an approach for the development of the two variables and their transport equations to ensure they meet the requirements.

Multi-mode combustion: Combustion Mode analysis, measurement and modelling

TNF14 Workshop, Trinity College, Dublin

Contributors: Matthias Ihme, Michael Mueller, Xinju Zhao, Sandra Hartl, Matthew Dunn and co-workers

28th July, 2018

Overview

What are our strategies for identifying and modelling multi-mode combustion regimes? When is it important?
Which modes: Non-premixed to premixed; premixed to autoignition.

Outline

- Identification of combustion modes:
  - Numerical: CEMA in high Ka flames (UCONN)
  - Experimental: Gradient Free Regime Identification, high rep rate HRR (UASDarmstadt, Sandia, Sydney)
- Combustion model selection: Combustion Model Compliance Indicator (Stanford)
- Combustion modelling with mode flexibility: Generalised Multi-Modal Manifolds (Princeton)

Flame identification and characterization in partially premixed and stratified combustion based on 1D Raman/Rayleigh data

S. Hartl[a], D. Geyer[b] and C. Hasse[a]
(and many contributions through discussions with R. Barlow and A. Dreizler)

Summary

- Flame index/combustion regime index require at least 3D scalar gradients
- Such quantitative information is difficult to obtain experimentally
- Approach to use 1D Raman/Rayleigh line data to
  - detect reaction zones
  - identify mode of burning
- Tested successfully in fully resolved flames accounting for experimental uncertainty and available scalars from Raman/Rayleigh
- First promising tests on stratified (TSF-A) and partially-premixed/stratified (Sydney Sandia w. inh. inlets, DME-D) benchmark flames

Progress Variable and Combustion Regime: Relevance to Modeling

MATTHIAS IHME, HAO WU
TIANFENG LU, CHRISTIAN HASSE, ROB BARLOW

Summary and Conclusions

Combustion regime indicators and model compliance

- Regime indicators/flame indices are useful to guide physical interpretation; lack fine-grained description of species-sensitivities
- Guidance of combustion-model selection requires consideration of target species, flame structure
- Drift term provides potential use for combustion model selection

Combustion Regimes

Regime identifications

- Yamashita-Takeno flame index: $\nabla Y_F \cdot \nabla Y_O$
- Alignment of mixture fraction and progress variable gradient: $\nabla Z \cdot \nabla C$
- FI/Oxi. diff. gradient: $D_O = |\nabla Y_{O,\mathrm{FPI}}|/|\nabla Y_O|$
- Time-scale analysis
- CEMA
- Mode-analysis: curvature, Le-effects, flame-orthogonality, pressure effects

→ Useful for physical interpretation and combustion analysis

- Interpretation of preferential transport
- Ignition and scalar flux

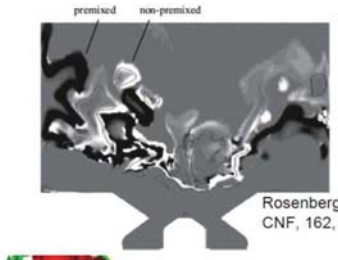

Rosenberg, et al. CNF, 162, 2015

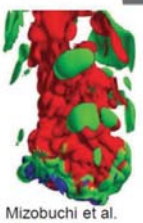

Mizobuchi et al. PCI, 30, 2005

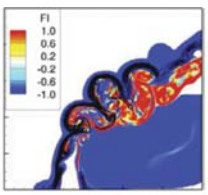

Lyra, et al. CNF, 162, 2015

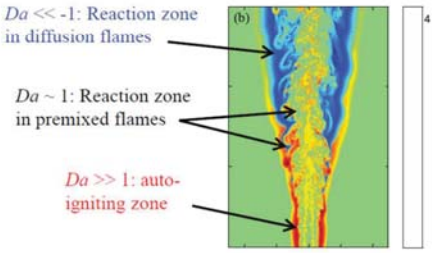

Fiorina et al., CNF, 140, 147, 2005
Yamashita et al. PCI, 26, 27, 1996
Lamouroux et al. CNF, 161, 2120, 2014
Knudsen & Pitsch, CNF, 156, 678, 2009
Lu et al., JFM, 652, 2010

Stanford University

- applied to identify premixed flame fronts in e.g. DNS [1,2] and for characterization of extinction and ignition processes [3,4]
- analysis is local and does not depend on scalar gradients

1. balance equations of chemically reacting system: $\frac{\mathrm{D}\Phi_j}{\mathrm{D}t} = \dot{\omega}_j(\Phi) + S_j(\Phi)$
2. chemical Jacobian: (contains chemistry-related information) $\mathrm{J}_{\dot{\omega}}^{ij} = d\dot{\omega}_i / d\Phi_j$
3. solve eigenvalue problem: $\lambda = \mathbf{b}\mathbf{J}_{\dot{\omega}}\mathbf{a}$
4. the (non-conservative) eigenvalue with max. real part is defined as λ_e (if $\mathrm{Re}(\lambda_e) > 0$, it is called the chemical explosive mode – CEM)

Define **CM** based on eigenvalue: $\mathrm{sign}(\mathrm{Re}(\lambda_e)) \times \log_{10}(1 + |\mathrm{Re}(\lambda_e)|)$

[1] R. Shan et al., Combust. Flame 159 (**2012**)
[2] T. F. Lu et al., Journal of Fluid Mechanics 652 (**2010**)
[3] I. A. Dodoulas and S. Navarro-Martinez, Combust. Theory and Modelling 19 (**2015**)
[4] S. Lyra et al., Combust. Flame 162 (**2015**)

TNF 2018 DUBLIN IRELAND JULY 27-28 | 14th INTERNATIONAL WORKSHOP ON MEASUREMENT & COMPUTATION OF TURBULENT FLAMES

Chemical explosive mode analysis of high-Karlovitz premixed flames

Xinyu Zhao, Ji-Woong Park, Peiyu Zhang, Tianfeng Lu
University of Connecticut
Haiou Wang[a], Jacqueline H. Chen[b], Evatt Hawkes[c]
[a]Zhejiang University
[b] Sandia National Lab
[c] University of New South Wales

7/27/2018

UCONN

Definitions

Chemical Explosive Mode Analysis (CEMA)

- Further quantification of the balance between diffusion and reaction can provide information on the local combustion modes.

$$\boldsymbol{b}\cdot\frac{D\boldsymbol{\omega}}{\lambda_e Dt}=\boldsymbol{b}\cdot\boldsymbol{\omega}+\boldsymbol{b}\cdot\boldsymbol{s}$$

Effects of chemistry vs. diffusion on the CEM

$\phi_\omega=\boldsymbol{b}\cdot\boldsymbol{\omega}$: contribution of chemistry to the CEM

$\phi_s=\boldsymbol{b}\cdot\boldsymbol{s}$: contribution of diffusion to the CEM

Local combustion modes based on $\alpha=\phi_s/\phi_\omega$

$\alpha>1$:	assisted-ignition
$\lvert\alpha\rvert<1$:	auto-ignition
$\alpha<-1$:	extinction

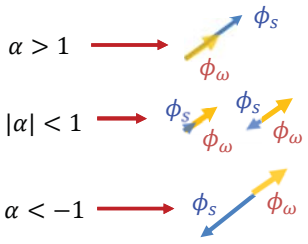

- Chemistry always pushes the mixture in one direction, either by itself (auto-ignition) or assisted by diffusion.
- Diffusion can dilute the mixture and pull it backward along the trajectory (extinction).
- The local modes indicate the local trends/directions, and are different from the finite-scale/global ignition/extinction.

Xu&Lu., PCI 2018

UCONN

CEMA as a diagnostic tool for DNS

Pockets flames and local combustion modes are identified by CEMA

Photograph of the turbulent flame from the Lund experiment (Zhou et al. CNF 2015)

T_j = 300 K
P =1 atm
CH_4/air mixture
Φ_j = 0.4
Re = 15,764
Zhang et al., in preparation

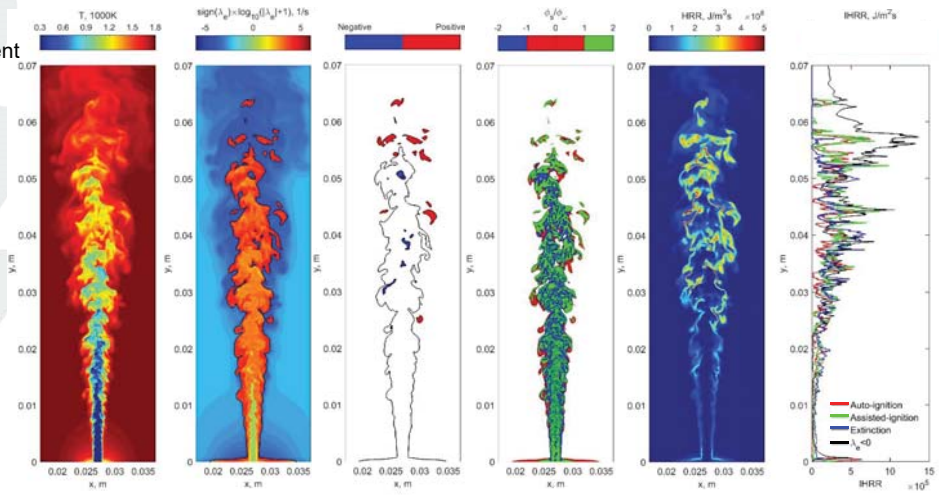

UCONN

CEMA can provide on-the-fly information for modeling.

CEM and local combustion modes can facilitate modeling in partially premixed flames.

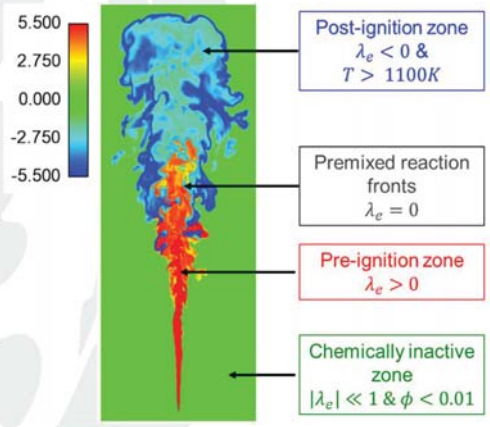

Simulations of the Spray A (*n*-dodecane) flame of the engine combustion network (ECN)

Xu et al., CNF 2018(195) 30-39

- Approximate CEMA approach can be applied as a regime-identification tool in modeling.

$$\lambda_e = \boldsymbol{b}_e \cdot \sum_{r=1}^{I} \mathbf{J}_r \cdot \boldsymbol{a}_e = \sum_{r=1}^{I} (\boldsymbol{b}_e \cdot \mathbf{J}_r \cdot \boldsymbol{a}_e) = \sum_{r=1}^{I} \left(\boldsymbol{b}_e \cdot \boldsymbol{\nu}_r \cdot \frac{\partial \Omega_r}{\partial \boldsymbol{c}} \cdot \boldsymbol{a}_e \right) = \sum_{r=1}^{I} \lambda_r$$

$$\text{where } \frac{\partial \Omega_r}{\partial \boldsymbol{c}} = \left[\frac{\partial \Omega_r}{\partial c_1}, \frac{\partial \Omega_r}{\partial c_2}, \dots, \frac{\partial \Omega_r}{\partial c_{N_s}} \right], \boldsymbol{\nu}_r = [\nu_{1,r}, \nu_{2,r}, \dots, \nu_{N_s,r}]^T$$

$$\lambda_e \approx \sum_{r=1}^{I_r} \lambda_r = \sum_{r=1}^{I_r} \frac{\alpha_r}{\tau_r}$$

- Local combustion mode analysis can facilitate the development of mixing models.

$$d\phi_\alpha^* = -\Omega^* \left(\phi_\alpha^* - \tilde{\phi}_\alpha^* \right) dt + \left[\frac{1}{\bar{\rho}} \frac{\partial \bar{\rho} V_{\alpha,i}}{\partial x_i} \right]^* dt + S_\alpha(\phi^*)\, dt$$

UCONN

Gradient-free regime identification (GFRI)

Idea, method and test cases

TECHNISCHE UNIVERSITÄT DARMSTADT

STFS

Mainly based on:

S. Hartl, D. Geyer, A. Dreizler, G. Magnotti, R.S. Barlow, C. Hasse, Regime identification from Raman/Rayleigh line measurements in partially premixed flames, Combustion and Flame 189 (2018)

S. Hartl, R. Van Winkle, D. Geyer, A. Dreizler, G. Magnotti, C. Hasse, R. S. Barlow, Assessing the relative importance of flame regimes in Raman/Rayleigh line measurements of turbulent lifted flames, Proc. Combust. Inst., accepted

h_da HOCHSCHULE DARMSTADT UNIVERSITY OF APPLIED SCIENCES

KAUST

Sandia National Laboratories

Motivation: Regime identification based on experimental data

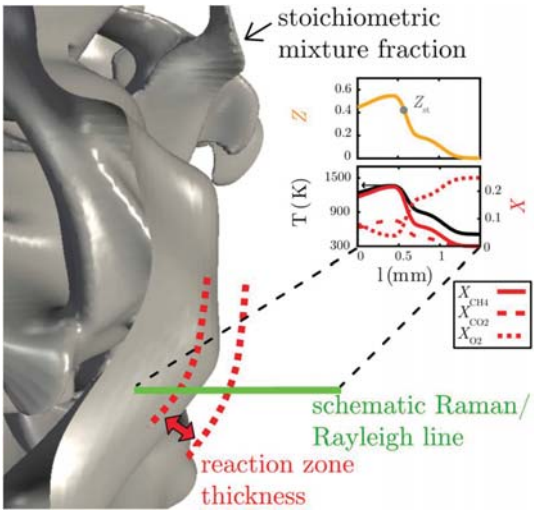

Combined Raman/Rayleigh measurement

- non-resonant laser measurement
  (interaction between light and matter)
- instantaneous data along 1D line
  - Temperature T
  - Raman species:
    Fuel, CO_2, O_2, CO, N_2, H_2O, H_2
    (> 99% of total mass in methane flames)
- unknown orientation of flame and laser

Raman/Rayleigh experimental data $\Phi^{\text{exp,RR}}$

GFRI – gradient-free regime identification (Hypotheses)

1. Major species and temperature from experiment are footprint of thermochemical state — **Experiment**
2. Full thermochemical state can be approximated by constrained 0D simulation — **Approximation**
3. Relevant flame markers can be calculated from approximated state — **Flame markers**
4. Combinations of flame markers reliably detect and characterize reaction zones — **Identification**

GFRI – Identification

Major outcome:
gradient-free regime identification approach which is applicable to (laminar and turbulent) experimental and numerical data

- CM results from approximated thermochemical states in good agreement with the full simulation
- HRR results sufficiently accurate for qualitative assessment of relative importance of different reaction zones

Premixed

- CM zero-crossing
- significant HRR values

Non-premixed

- negative CM
- significant HRR values
- (optional) significant X_{OH}
- non-constant Z in the vicinity of Z_{st}

Published in: S. Hartl, D. Geyer, A. Dreizler, G. Magnotti, R.S. Barlow, C. Hasse, Combustion and Flame 189 (2018)

GFRI - Application to numerical data (laminar counterflow flame)

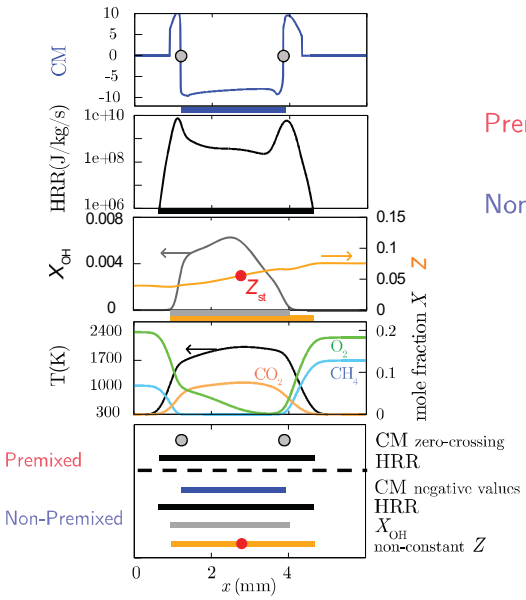

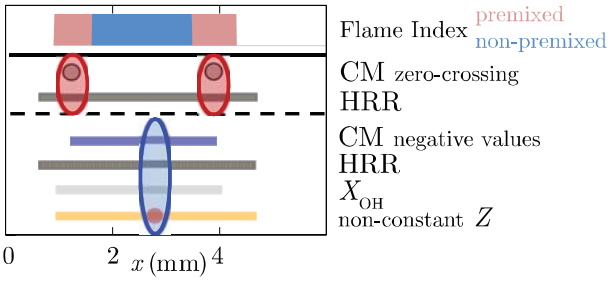

➔ suitable combinations characterize local combustion regime

➔ counterflow flame identification is in agreement with flame index

Published in: S. Hartl, D. Geyer, A. Dreizler, G. Magnotti, R.S. Barlow, C. Hasse, Combustion and Flame 189 (2018)

GFRI: Turbulent lifted flames - identify local reaction zones

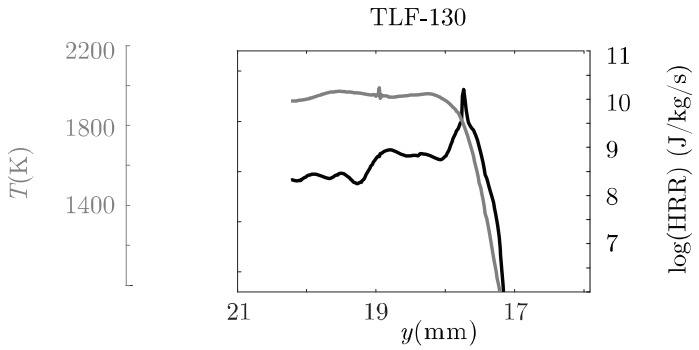

Accepted in: S. Hartl, R. Van Winkle, D. Geyer, A. Dreizler, G. Magnotti, C. Hasse, R. S. Barlow, Proc. Combust. Inst.

GFRI: Turbulent lifted flames - identify local reaction zones

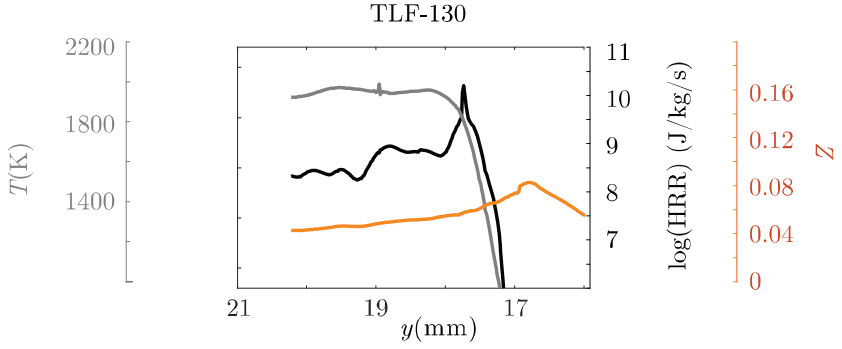

Accepted in: S. Hartl, R. Van Winkle, D. Geyer, A. Dreizler, G. Magnotti, C. Hasse, R. S. Barlow, Proc. Combust. Inst.

GFRI: Turbulent lifted flames - identify local reaction zones

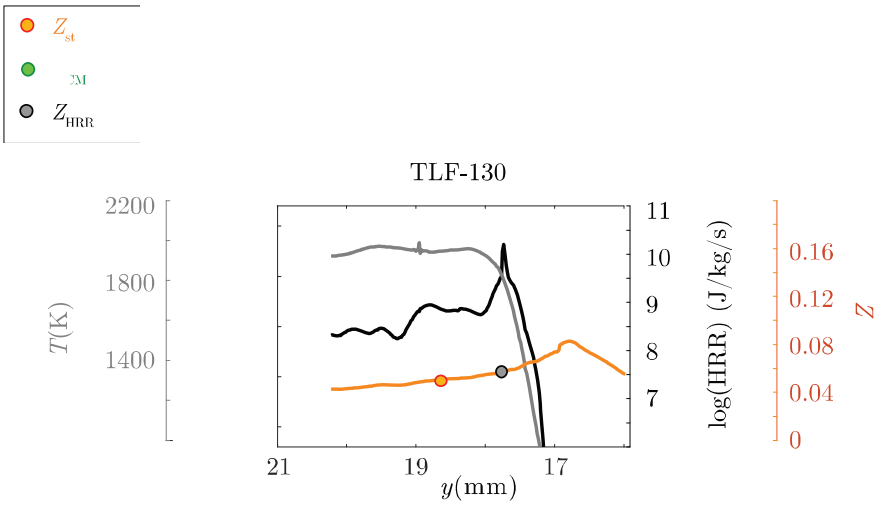

Accepted in: S. Hartl, R. Van Winkle, D. Geyer, A. Dreizler, G. Magnotti, C. Hasse, R. S. Barlow, Proc. Combust. Inst.

GFRI: Turbulent lifted flames - identify local reaction zones

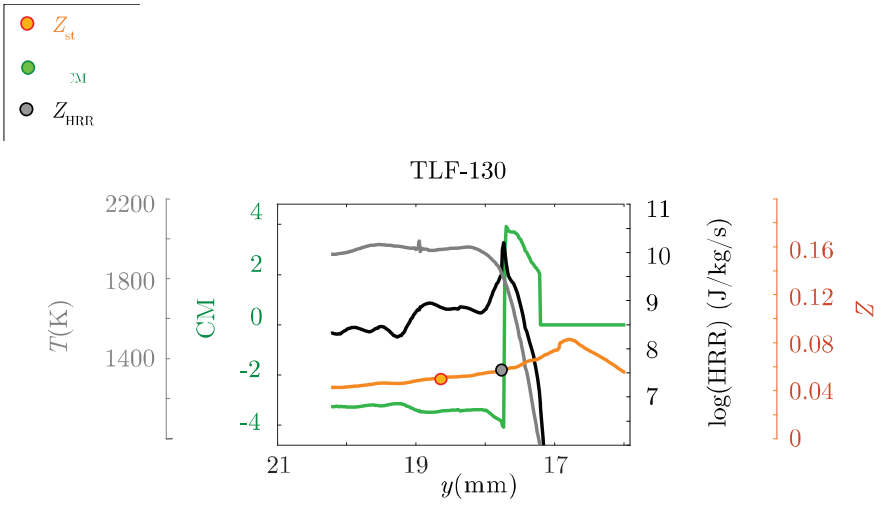

Accepted in: S. Hartl, R. Van Winkle, D. Geyer, A. Dreizler, G. Magnotti, C. Hasse, R. S. Barlow, Proc. Combust. Inst.

GFRI: Turbulent lifted flames - identify local reaction zones

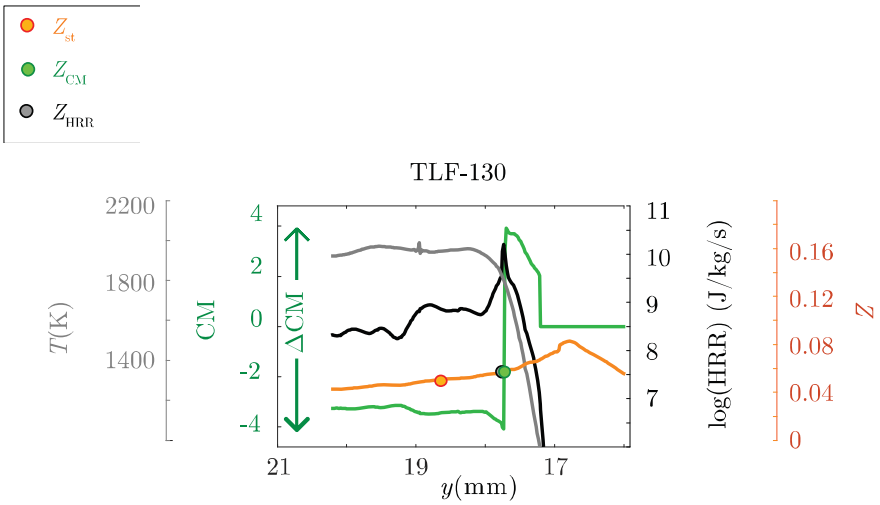

Accepted in: S. Hartl, R. Van Winkle, D. Geyer, A. Dreizler, G. Magnotti, C. Hasse, R. S. Barlow, Proc. Combust. Inst.

GFRI: Turbulent lifted flames - identify local reaction zones

Non-premixed

- negative CM
- significant HRR values
- (optional) significant X_{OH}
- non-constant Z in the vicinity of Z_{st}

Premixed

- CM zero-crossing
- significant HRR values

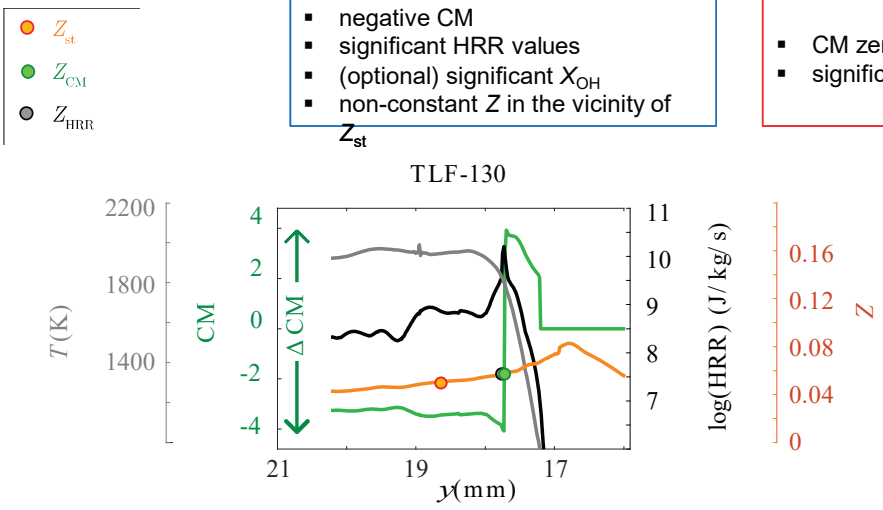

Is this characteristic for all sample lines? Do we get any deeper insight in the flame structure?

Accepted in: S. Hartl, R. Van Winkle, D. Geyer, A. Dreizler, G. Magnotti, C. Hasse, R. S. Barlow, Proc. Combust. Inst.
(see paper Wednesday Morning in Turbulent Flame colloq to hear about the interactions and correlations of these modes)

Combustion Regimes

MATTHIAS IHME, HAO WU, QING WANG

Modeling Combustion Model Compliance Indicator

Model compliance indicator

- Metric for assessing compliance of combustion model manifold and local CFD-solution → departure from combustion manifold
- Incorporate sensitivity to
  - quantities of interest (QoI): CO, NO, H2O
  - flame structure and local manifold representation

- Considers different combustion models:
  - Reaction-transport manifolds: FPV, FPI, FGM, Inert Mixing, …
  - Chemistry manifold: detailed chemistry, skeletal, reduced, …
  - Selects best model that meets requirement on cost and accuracy

- Guide selection of combustion models
- Bootstrapping

Wu, H., See, Y. C., Wang, Q., and Ihme, M., "A Pareto-efficient combustion framework with submodel assignment for predicting complex flame configurations." Combustion and Flame, 162, 4208-4230, 2016.

Combustion model compliance indicator

Drift term: initial growth rate of error

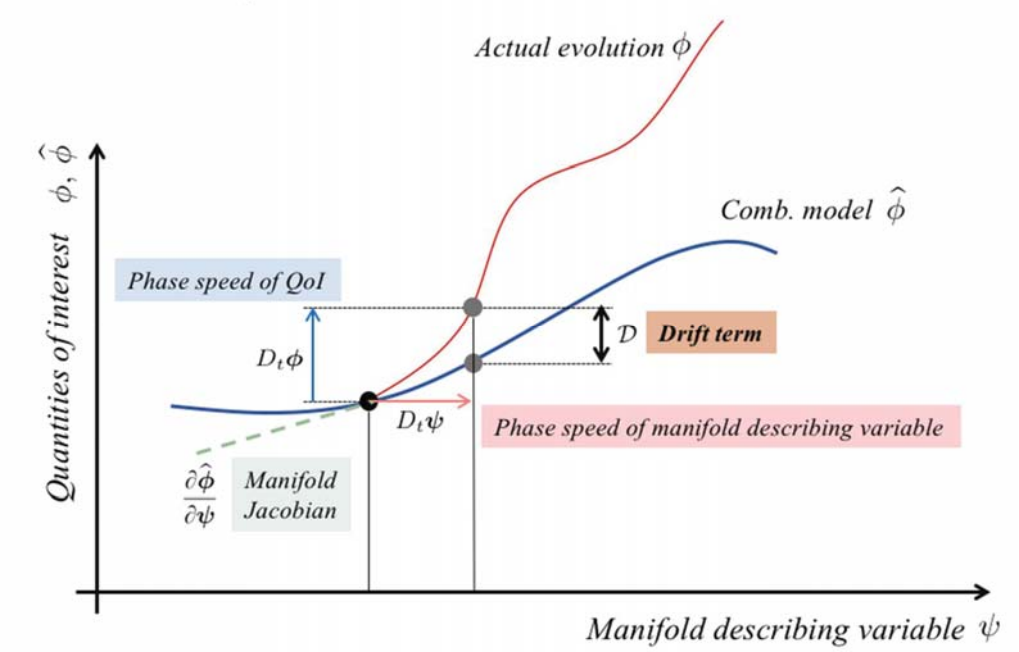

Combustion model compliance indicator

Drift term: initial growth rate of error

Drift from manifold[1] for each QoI and candidate combustion model

$$\boldsymbol{\Delta} = \boldsymbol{\phi} - \hat{\boldsymbol{\phi}}$$

$$\begin{aligned}\boldsymbol{\mathcal{D}} &= D_t\boldsymbol{\Delta}|_{\boldsymbol{\Delta}=0} \\ &= \underbrace{D_t\boldsymbol{\phi}|_{\boldsymbol{\phi}=\hat{\boldsymbol{\phi}}}}_{\frac{1}{\rho}\nabla\cdot(\rho D_\alpha \nabla\phi_\alpha)+\Omega_\alpha^\phi} - \frac{\partial\hat{\boldsymbol{\phi}}}{\partial\boldsymbol{\psi}}\cdot D_t\boldsymbol{\psi}\end{aligned}$$

Tabulated

Calculated

- Relate model error to manifold drift (for QoI's)

$$e^{\mathcal{M}} = \frac{1}{|Q|}\sum_{\alpha\in Q} w_\alpha \mathcal{D}_\alpha^{\mathcal{M}}$$

1 Pope, S. B. "Small scales, many species and the manifold challenges of turbulent combustion, Proc. Combust. Inst. 34, 2013

Combustion Model Compliance Indicator

Piloted turbulent partially-premixed DME jet flame (Lr75)

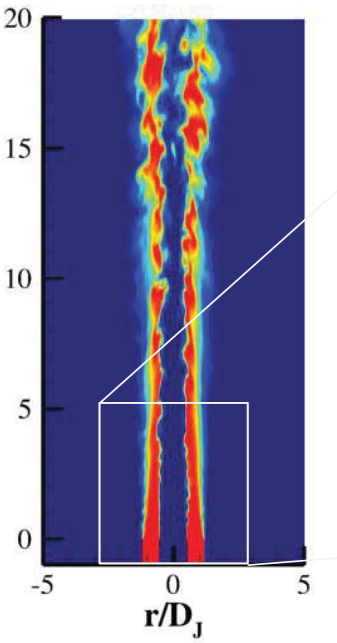

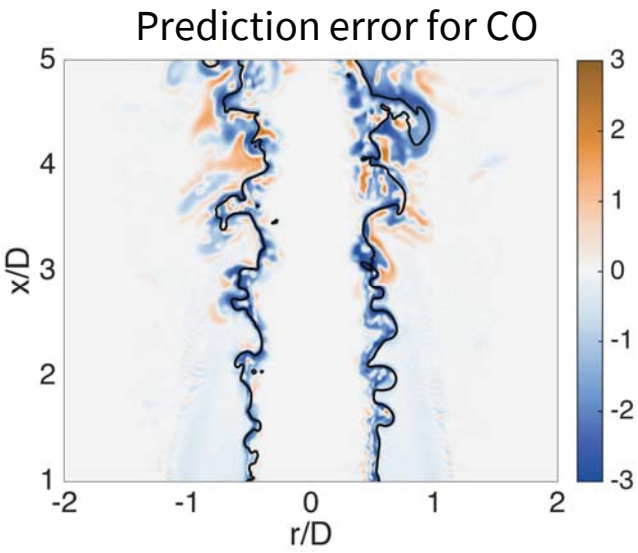

Stanford University

Combustion Model Compliance Indicator

Piloted turbulent partially-premixed DME jet flame (Lr75)

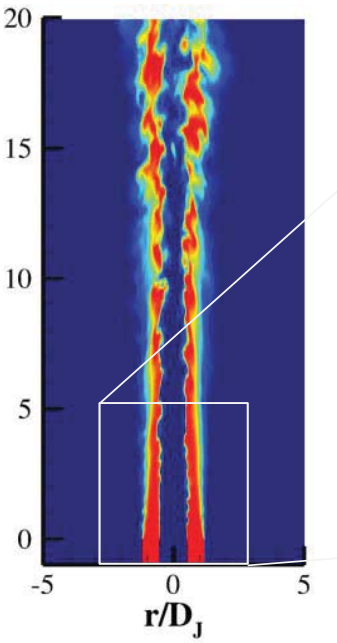

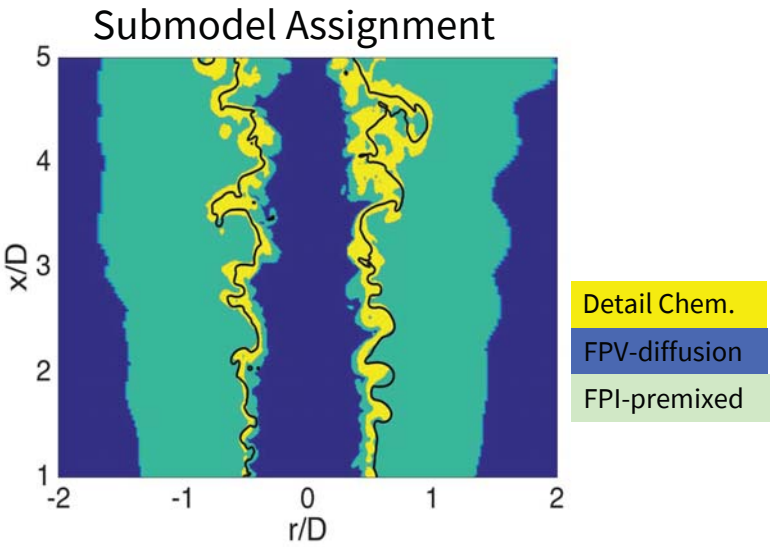

Stanford University

Referee gas turbine combustor

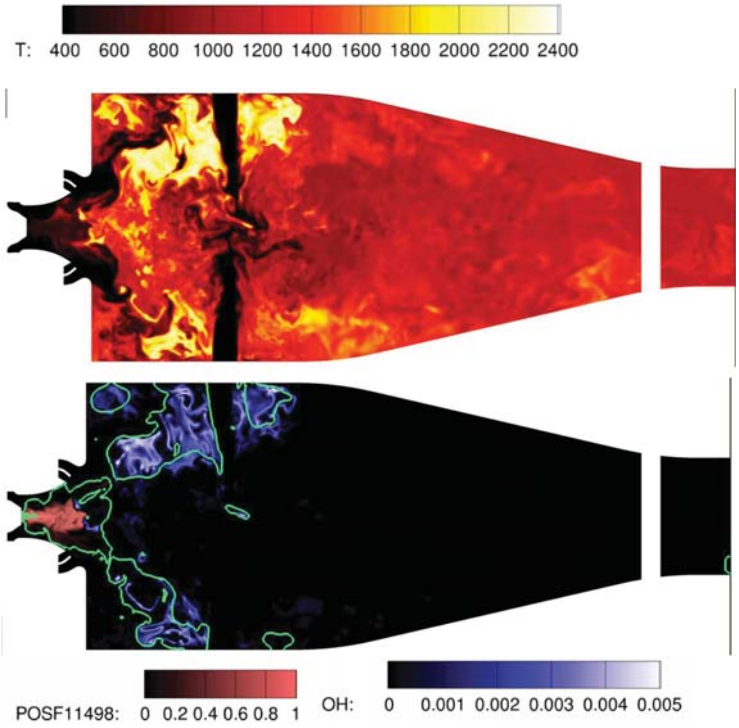

Combustion model

- FPV flamelet model (3 scalars)
- FRC TFLES model (35 scalars)

- 30% FRC (λ=2)
- 40% reduction in cost

Stanford University

Multi-Modal Turbulent Combustion: Recent Modeling Efforts

Michael E. Mueller

Computational Turbulent Reacting Flow Laboratory (CTRFL)
Department of Mechanical and Aerospace Engineering
Princeton University

Multi-Modal Combustion

- Conventional Manifold-Based Approaches
  - Question I: Does the component problem matter?

Nonpremixed

Premixed

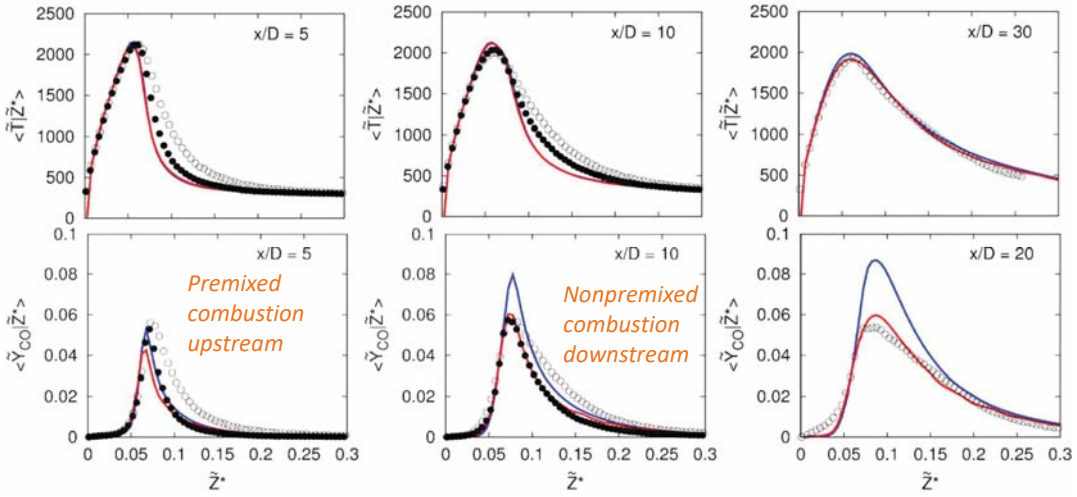

  - CO, in particular, is very sensitive to the combustion mode.

Multi-Modal Combustion

- Mode Switching Manifold-Based Combustion Model
  - Summarily, the component problem matters for any quantity of interest "beyond" the temperature or temperature-like species.
  - Therefore, we want to develop an algorithm to select the locally correct component problem, that is, the local combustion mode.

Use premixed model here…

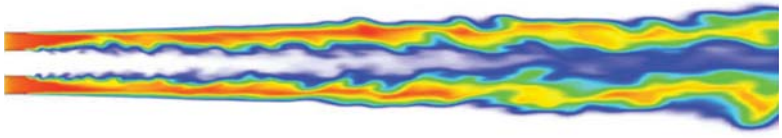

Use nonpremixed model here…

  - Question II: How should the local combustion mode be chosen?

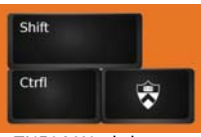

Multi-Modal Combustion

- Mode Switching Manifold-Based Combustion Model
  - Question II: How should the local combustion mode be chosen?
  - Must make an assumption about the ordering of premixed combustion and mixing of central streams with the coflow.

  - Three new models that allow for premixed combustion when:

	Nonpremixed+[1]	Flammability Switching[1]	Time Scale Switching[2]
Central Stream Flammable	Y	Y	Y
Central Stream Unmixed with Coflow	Y	N	N
Slow Local Coflow Mixing Rate	—	N	Y

*Premixed combustion **then** mixing with coflow*

*Premixed combustion **while** mixing with the coflow*

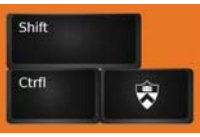

[1]B.A. Perry, M.E. Mueller, Combust. Flame (2018) in preparation
[2]Adapted from: E. Knudsen, H. Pitsch, Combust. Flame 159 (2012) 242-264

Multi-Modal Combustion

- Generalized Multi-Modal Manifolds[1,2]
  - Start by working backward!

- Mueller Postulate of Combustion
  - All[3] combustion processes can be described by two primary quantities on the unit square:

Z, Mixture Fraction

Λ, Generalized Progress Variable

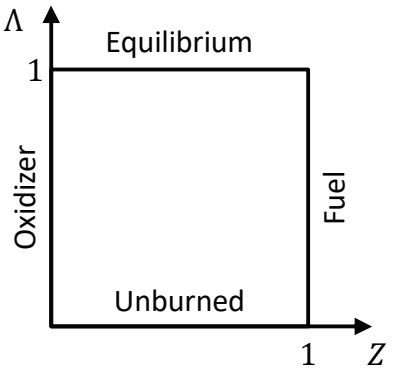

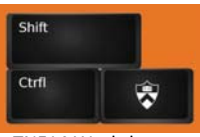

[1]M.E. Mueller, 10th U.S. National Combustion Meeting, April 2017
[2]M.E. Mueller, Combust. Flame (2018) in preparation
[3]Additional variables would be required for variation in enthalpy, pressure, more than two streams, etc.

Multi-Modal Combustion

- Generalized Multi-Modal Manifolds[1,2]
  - Formulation I: "Coordinate Transformation" Approach
    - Similar to conventional "flamelet"-like approaches
    - Define Z as conserved scalar but leave definition of Λ open
    - Start with the governing equations in physical space and change coordinate system to manifold space: $(t, x_j) \rightarrow (Z, \Lambda)$
      - $\frac{\partial}{\partial t} = \frac{\partial Z}{\partial t}\frac{\partial}{\partial Z} + \frac{\partial \Lambda}{\partial t}\frac{\partial}{\partial \Lambda}$
      - $\frac{\partial}{\partial x_j} = \frac{\partial Z}{\partial x_j}\frac{\partial}{\partial Z} + \frac{\partial \Lambda}{\partial x_j}\frac{\partial}{\partial \Lambda}$
    - For unity effective Lewis numbers:

$$\frac{\partial Y_k}{\partial \Lambda}\left[\frac{\partial \Lambda}{\partial t} + u_j\frac{\partial \Lambda}{\partial x_j} - \frac{1}{\rho}\frac{\partial}{\partial x_j}\left(\rho D\frac{\partial \Lambda}{\partial x_j}\right)\right] = \frac{\rho\chi_{ZZ}}{2}\frac{\partial^2 Y_k}{\partial Z^2} + \rho\chi_{Z\Lambda}\frac{\partial^2 Y_k}{\partial Z \partial \Lambda} + \frac{\rho\chi_{\Lambda\Lambda}}{2}\frac{\partial^2 Y_k}{\partial \Lambda^2} + \dot{m}_k$$

      - Scalar Dissipation Rate: $\chi_{\phi\psi} = 2D\frac{\partial \phi}{\partial x_j}\frac{\partial \psi}{\partial x_j}$

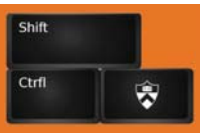

[1]M.E. Mueller, 10th U.S. National Combustion Meeting, April 2017
[2]M.E. Mueller, Combust. Flame (2018) in preparation

Multi-Modal Combustion

- Generalized Multi-Modal Manifolds[1,2]
  - Formulation I: "Coordinate Transformation" Approach
    - Key Idea: Close equation by choosing reference species and rearrange equation to get explicit transport equation for Λ:

$$\frac{\partial \Lambda}{\partial t} + u_j\frac{\partial \Lambda}{\partial x_j} - \frac{1}{\rho}\frac{\partial}{\partial x_j}\left(\rho D\frac{\partial \Lambda}{\partial x_j}\right) = \left[\frac{1}{\partial Y_k/\partial \Lambda}\left(\frac{\rho\chi_{ZZ}}{2}\frac{\partial^2 Y_k}{\partial Z^2} + \rho\chi_{Z\Lambda}\frac{\partial^2 Y_k}{\partial Z\partial \Lambda} + \frac{\rho\chi_{\Lambda\Lambda}}{2}\frac{\partial^2 Y_k}{\partial \Lambda^2} + \dot{m}_k\right)\right]_R \equiv \dot{w}_\Lambda$$

    - Closed equation for evolution of thermochemical state on the manifold:

$$\frac{\partial Y_k}{\partial \Lambda}\dot{w}_\Lambda = \frac{\rho\chi_{ZZ}}{2}\frac{\partial^2 Y_k}{\partial Z^2} + \rho\chi_{Z\Lambda}\frac{\partial^2 Y_k}{\partial Z\partial \Lambda} + \frac{\rho\chi_{\Lambda\Lambda}}{2}\frac{\partial^2 Y_k}{\partial \Lambda^2} + \dot{m}_k$$

  - Formulation II: Conditional Filtering Approach
    - Reveals implicit assumptions of "Coordinate Transformation" approach
      1. Local thermochemical state uniquely parameterizable by Z and Λ.
      2. Flow history effects are negligible.

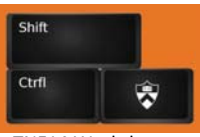

[1]M.E. Mueller, 10th U.S. National Combustion Meeting, April 2017
[2]M.E. Mueller, Combust. Flame (2018) in preparation

Multi-Modal Combustion

- Generalized Multi-Modal Manifolds[1,2]
  - Recovers not only multi-modal behavior but also asymptotic modes in appropriate limits, determined by the scalar dissipation rates
    - Cross-dissipation term can capture alignment effects (e.g., front-supported versus back-supported)
  - Current progress
    - Development of solver **PDRs** (public release soon)
    - Initial, simplified coupling with LES underway
    - Working toward integrated coupling of manifold solver with LES

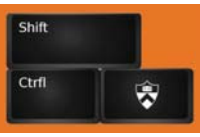

[1]M.E. Mueller, 10th U.S. National Combustion Meeting, April 2017
[2]M.E. Mueller, Combust. Flame (2018) in preparation

TNF 2018
DUBLIN IRELAND JULY 27-28
14th INTERNATIONAL WORKSHOP ON MEASUREMENT & COMPUTATION OF TURBULENT FLAMES

THE UNIVERSITY OF MELBOURNE

Discussion:
(1) Next Steps
(2) Target Flames
(3) Model development
Other ideas

Final Multi-Scalar Measurements at Sandia

Coordinator: Rob Barlow

During the summer of 2017, the management of the Combustion Research Facility at Sandia was informed that the Department of Energy, Office of Basic Energy Sciences had made the decision to realign their Gas Phase Chemical Physics program to focus on very fundamental chemistry. All of the reacting flow work at Sandia, which had been supported by DOE/BES for more than 30 years, was to be zeroed out starting October 1, 2018, and the fiscal year following that date was to be a transition year to phase out those areas of research.

Both the Turbulent Combustion Lab (R. Barlow) and the Advanced Imaging Lab (J. Frank) were affected. At the time, the TCL was undergoing a complete overhaul of data acquisition hardware and software, which was not completed until early in 2018. In order to take maximum advantage of the experimental capabilities of the TCL before its closure, several visitors were invited to run experiments between March and July of 2018.

Visitors, collaborators, and experimental targets included:

• David Butz, Dirk Geyer, Andreas Dreizler	TU Darmstadt Multi-Regime Burner (MRB)
• Tim Wabel, Adam Steinberg	HiPilot Burner
• Matt Dunn, Assaad Masri	new Sydney hot coflow burner piloted ethanol spray flame
• Dirk Geyer, Matt Dunn	Quantitative OH LIF line imaging

The MRB work was a full parametric campaign to characterize several flames using Raman/Rayleigh/CO-LIF and crossed planar OH LIF imaging. See posters by Butz et al. and Hartl et al. for information about the burner and preliminary results.

The HiPilot burner developed at the University of Michigan was designed to push premixed flames to very high levels of turbulence and high Karlovitz number. It has been characterized in several publications using state of the art imaging diagnostics. A major conclusion from the Sandia measurements is that the highest Ka case, which has equivalence ratio 0.65 in the main jet and 0.9 in the pilot flow, actually behaves as a stratified flame. These results were highlighted in the session on highly turbulent flames.

The new hot coflow burner from Sydney University includes active cooling of the central jet and insulation between the central jet and the hot coflow. Several flames were measured, as outlined in the slides, to investigate lifted flame stabilization (auto-ignition vs. flame propagation) and the structure of stratified-premixed jet flames at high Ka.

The piloted ethanol spray flame proved to be a challenge for Raman scattering, and only the outer periphery could be probed.

Work to implement quantitative OH LIF line imaging in combination with Raman/Rayleigh/CO-LIF line imaging was motivated by numerical assessments showing that inclusion of OH, along with measurements of temperature and major species, allows for significant improvements in the accuracy of heat release rate and chemical explosive mode derived from the experimental data. The combined diagnostics were applied to laminar opposed flow flames and turbulent lifted flames.

Last Tango in Livermore:

A five-month marathon of visiting experiments
to make best use of the Turbulent Combustion Lab
before DOE funding was terminated

Rob Barlow, David Butz, Tim Wabel, Matt Dunn, Dirk Geyer

TNF 2018
DUBLIN IRELAND JULY 27-28

Darmstadt MRB – Raman / Rayleigh / LIF & GFRI

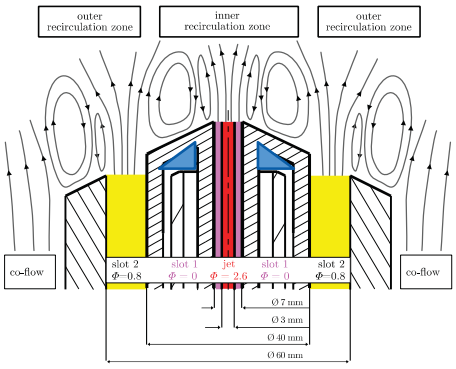

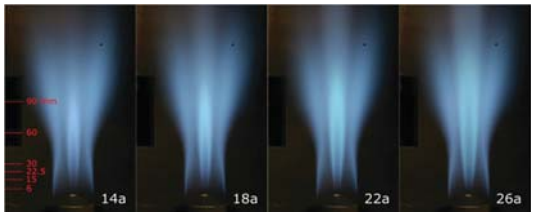

	Jet		Slot 1			Slot 2	
	ϕ	u [m/s]	ϕ	u [m/s] a	u [m/s] b	ϕ	u [m/s]
MRB 14	1.4	105	0	7.5	15	0.8	20
MRB 18	1.8						
MRB 22	2.2						
MRB 26	2.6						

See two posters by Butz and Hartl

Raman/Rayleigh/LIF Experiments on the HiPilot Burner: Preliminary Results

Tim Wabel[1], Adam Steinberg[2], Robert Barlow[3],

[1]University of Toronto
[2]Georgia Tech
[3]Sandia National Laboratories

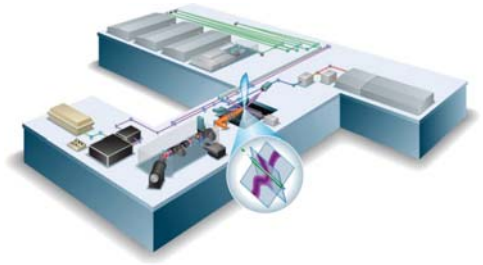

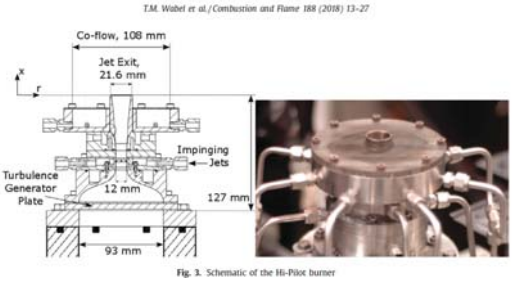

Fig. 3. Schematic of the Hi-Pilot burner

ϕ_{jet} = 0.65, ϕ_{pilot} = 0.9 ϕ vs. T Y_{CO} vs. T

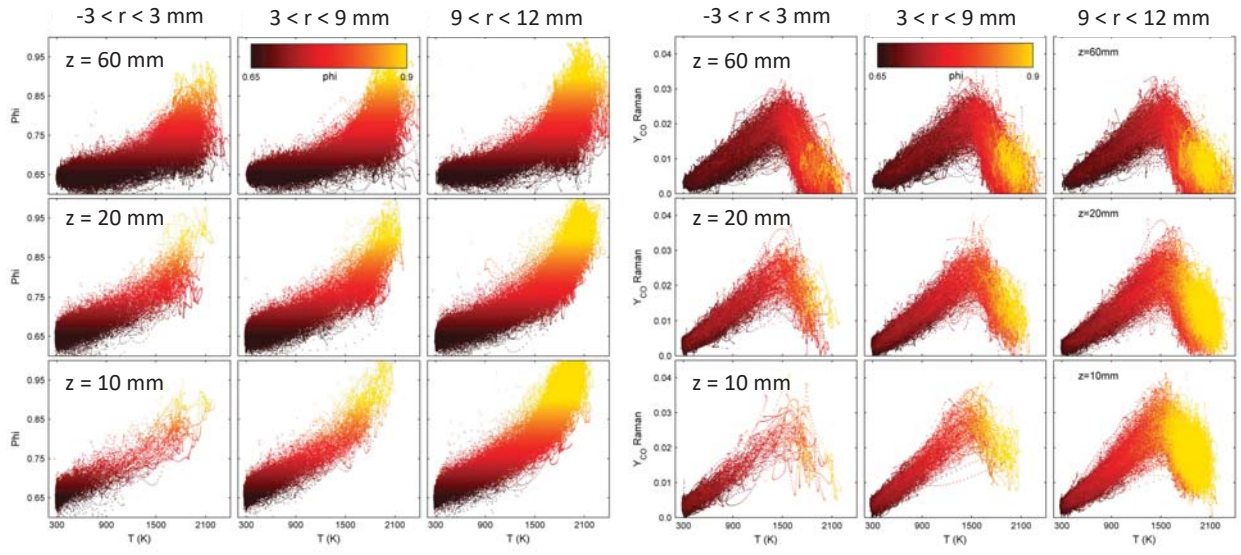

Quantitative line LIF of OH

- Objective: Improved approximation of CM and HRR
- Experimental details: Not important here, but with lots of help from Matt Dunn
- Applied to:
  - Opposed flow laminar CH_4 and CH_4/H_2 partially premixed triple flames
  - Sydney hot coflow burner

TNF 2018 DUBLIN IRELAND JULY 27-28

Familiar jet in hot coflow burner with improvements

- Ceramic heat shield
- Active water cooling of central jet

TNF 2018 DUBLIN IRELAND JULY 27-28

Eight cases measured

- 100m/s 3:1 air:CH_4 jet (1450K and 1550K coflow) (note higher T_{coflow} than Cabra cases)
- CH_4/H_2 jet variant (high and low coflow temperatures)

- Phi=0.6 premixed CH_4 jet, U_j=50 and 200m/s with 1650K coflow
- Phi=0.6 premixed CH_4 with 20% H_2 addition U_j=50 and 200m/s

TNF 2018 DUBLIN IRELAND JULY 27-28

Ethanol Spray Flame

- Dilute ethanol spray in air jet
- Not at all friendly to high-energy pulsed laser beam
- Limited measurements made by bringing the beam in tangentially from the air coflow into the very dilute edge of t he spray flame

TNF 2018 DUBLIN IRELAND JULY 27-28

TNF 2018 Posters

First Author	Poster Title
Christoph Arndt	The SFB Dual-Swirl Combustor – A Versatile Dual-Swirl Gas Turbine Model Combustor for the Study of Technically Premixed, Perfectly Premixed, Stratified and Liquid Fuel Flames
David Butz	A novel burner configuration for multi-regime combustion
Tiernan Casey	Enabling uncertainty quantification and propagation in combustion models using statistical inference of unreported experimental data
Deepak Dalakoti	Flame stabilisation mechanism of a spatially developing n-dodecane jet flame under Spray A thermochemical conditions
Hossam Elasrag	Hybrid Stress Blended Eddy Simulations for Near Blow-out Swilling Spray Flame using the Flamelet Generated Manifold Model
Michael Evans	Confined and Pressurised Jet in Hot & Vitiated Coflow Burner
Fabian Hampp	Turbulent Premixed Syngas Flames
Sandra Hartl	Flame structure analysis of multi-regime combustion processes
X. Huang	Experimental and numerical study of flameless combustion in a furnace
Eray Inanc	Combustion regime investigations of turbulent flames by flame-resolved simulations
Weiqi Ji	Quantifying kinetic uncertainty in turbulent combustion simulations using active subspaces
S. Karaca	LES of Cambridge Stratified Swirl Burner by using the Flamelet Generated Manifold Method
N. Kim	Modeling for Turbulent Piloted Premixed Jet Flames
H. Kosaka	Advanced laser diagnostics for an improved understanding of premixed flame-wall interactions
Zhiyi Li	Large Eddy Simulation of Cambridge Turbulent Stratified Flame with PASR Model: CO Prediction
Zisen Li	Coefficients Specification for a Conceptually Simplified Multiple Mapping Conditioning Model with Mixture Fraction like Reference Variable
Hao Lu	Large-eddy simulation of Sandia Flame F using nonlinear structural subgrid-scale models and partially stirred reactor approach
Giampaolo Maio	Virtual chemistry for temperature and pollutant prediction in numerical simulations of turbulent flames
G. Neuber	Multiple Mapping Conditioning Modelling of a piloted partially-premixed Sandia DME flame series (D - G)
Bruce Perry	Challenges for Large Eddy Simulation of Partially Premixed Turbulent Combustion using Reduced-Order Manifold Flame Structure Models
Steve Pope	The Conditional Dissipation Mapping Closure for all Regimes of Turbulent Premixed Combustion
Jacob Rivera	Novel Burner for Investigating Laminar Forced Premixed Flame-Wall Interaction
Michael Severin	Experimental Analysis of Confined Premixed Recirculation-Stabilized Jet-Flames for Gas Turbine Applications
G. Sorrentino	Modeling of a cyclonic burner under MILD combustion through FGM/IML approach. Effect of radiative heat transfer
A. Unterberger	Instantaneous 3D analysis of the Cambridge stratified swirled flame geometry using computed tomography
Guoqing Wang	Swirling flame dynamics investigated by burst mode laser PLIF/PIV and TDLAS
Tianwei Yang	A Particle Mass-Based Implementation for Mixing Models with Differential Diffusion
Tongxun Yi	Turbulent Flame Structure and Dynamics in Swirling Reacting Flows - Insights from High-Speed Dual-Plane PIV/OH-PLIF Measurements
Jiaping You	Characterization of anisotropic vortex tubes near flame fronts in high-Karlovitz-number turbulent premixed flames
Bo Zhou	On the alignment of strain rate eigenvectors in turbulent premixed counterflow flames

The SFB Dual-Swirl Combustor – A Versatile Dual-Swirl Gas Turbine Model Combustor for the Study of Technically Premixed, Perfectly Premixed, Stratified and Liquid Fuel Flames

C.M. Arndt[1], M. Severin[1], C. Dem[1,2], Y. Gao[1], J. Böhnke[1], R. Hadef[3], A.M. Steinberg[4,5], W. Meier[1]

[1] German Aerospace Center (DLR), Institute of Combustion Technology, Stuttgart, Germany
[2] Present Address: Karlsruhe Institute of Technology (KIT)
Institute for Chemical Technology and Polymer Chemistry, Karlsruhe, Germany
[3] Université Larbi Ben M'Hidi, Faculté des Sciences et de la Technologie, Oum El Bouaghi, Algeria
[4] University of Toronto, Institute for Aerospace Studies, Toronto, Canada
[5] Present Address: Georgia Institute of Technology, Guggenheim School of Aerospace Engineering, Atlanta, GA, USA
email: christoph.arndt@dlr.de

1. Introduction

Most gas turbine (GT) combustors for power generation are equipped with swirl burners and operated with lean premixed or partially premixed flames. While such combustors feature excellent emission levels, serious operational restrictions arise from their susceptibility to thermo-acoustic instabilities, where the unsteady heat release couples with one or more acoustic modes of the combustor. Good progress towards understanding combustion instabilities has been achieved in recent years by the use of GT model combustors. These combustors can feature many phenomena relevant to practical engines, such as self-excited oscillations, swirl-induced vortex breakdown, hydrodynamic instabilities, and time-dependent premixing, while providing well controlled operating and boundary conditions at reasonable costs. Moreover, they can be designed with good optical access to allow for the application of optical and laser measurement techniques capable of determining important quantities like velocity, temperature, and species concentrations with high spatial and temporal resolution.

2. The SFB Dual Swirl Gas Turbine Model Combustor

Within the framework of the collaborative research council ("SFB") 606, a novel dual-swirl gas turbine model combustor was developed for the study of high- and low frequency thermo-acoustic instabilities [1-3], and flame-flame-interaction in a multi-combustor geometry [4,5]. Furthermore, the combustor was adapted for the study of stratified and perfectly premixed flames, as well as for liquid fuel and prevaporized liquid fuel flames [6]. A schematic of the combustor is shown in Figure 1.

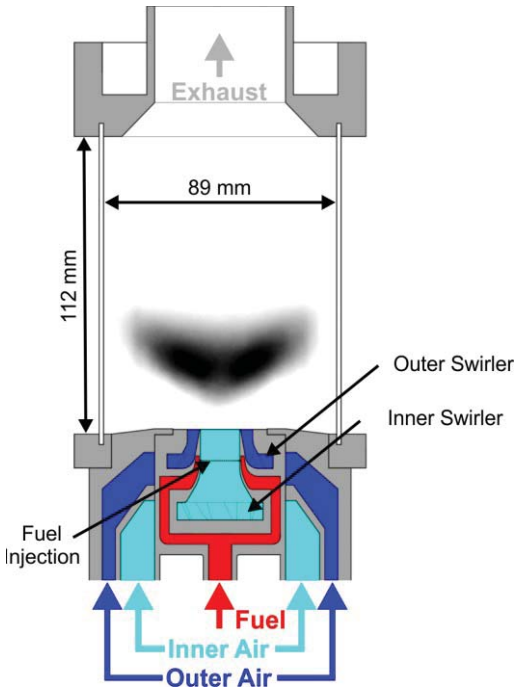

Figure 1: Schematic of the SFB dual swirl burner

The design is based on previously studied dual-swirl-burner configurations, but features several improvements to the boundary conditions. Most importantly, the burner features two swirlers with separate plenum chambers. Thus, the air flow to each plenum can be controlled independently, such that the air split ratio between the inner and outer nozzle can be set exactly. Furthermore, the combustion air can be preheated. The combustion

chamber offers very good optical access and it is equipped with several ports for pressure probes.

For several operating conditions, species data (from laser Raman scattering) [1-3], velocity data (from PIV measurements) [1,3,6] and overall information on flame shape (from OH* chemiluminescence) [1-6] and flow-flame interaction (from high-speed OH PLIF / PIV) [3,6] are available.

3. Sample Results

A sample result on the influence of the stratification level on the flame shape is shown in Fig. 2.

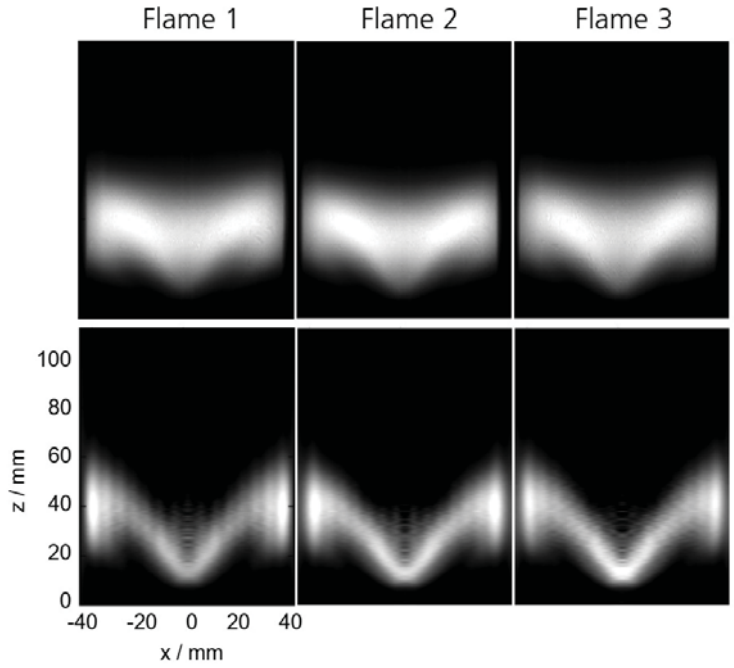

Figure 2. Mean (top row) and Abel deconvoluted (bottom row) chemiluminescence for 3 flames with different stratification ratio. Flame 1 corresponds to a perfectly premixed flame ($\varphi_{in} = \varphi_{out} = 0.75$), Flame 2 to a mild stratification case ($\varphi_{in} = 0.9$, $\varphi_{out} = 0.65$) and Flame 3 to a strong stratification case ($\varphi_{in} = 1.0$, $\varphi_{out} = 0.6$). The global equivalence ratio and thermal power are $\varphi_{global} = 0.75$ and $P_{th} = 25$ kW for all cases.

It is apparent that the overall flame shape and location do not change significantly with increasing stratification ratio. However, the thermo-acoustic properties of the flames change slightly (in terms of amplitude and dominant frequency) with increasing stratification ratio.

4. References

[1] C.M. Arndt, M. Severin, C. Dem, M. Stöhr, A.M. Steinberg, W. Meier, Exp. Fluids 56(4) (2015), 69.

[2] C.M. Arndt, M. Stöhr, M.J. Severin, C. Dem, W. Meier, AIAA Propulsion and Energy Forum (2017), AIAA 2017-4683.

[3] W. Meier, C. Dem, C.M. Arndt, Exp. Therm. Fluid Sci. 73 (2015), 71-78.

[4] C. Kraus, S. Harth, H. Bockhorn, Int. J. Spray Combust. 8(1), pp. 4-26 (2016).

[5] C. Kraus, L. Selle, T. Poinsot, C.M. Arndt, H. Bockhorn, J. Eng. Gas Turbine Power 139 (5) (2016), 051503.

[6] C.M. Arndt, A.M. Steinberg, . Böhnke, R. Hadef, W. Meier, AIAA SciTech Forum (2019), submitted

A novel burner configuration for multi-regime combustion

D. Butz[*,a)], S. Walther[b)], S. Popp[c)], S. Hartl[b),c)], R. Barlow[d)], C. Hasse[c)], A. Dreizler[a)], D. Geyer[b)]

a) FG Reactive Flows and Diagnostics, TU Darmstadt, Darmstadt, Germany
b) Thermodynamics and Alternative Propulsion Systems, University of Applied Sciences, Darmstadt, Germany
c) FG Simulation of Reactive Thermo-Fluid-Systems, TU Darmstadt, Darmstadt, Germany
d) Combustion Research Facility, Sandia National Laboratories, Livermore, CA, USA

** butz@rsm.tu-darmstadt.de*

Combustion processes can be classified as either globally premixed or non-premixed. However, in practical applications, such as gas turbines, aircraft combustors, or direct-injection engines, complex multi-regime combustion scenarios can occur through partial premixing or recirculation. Hence, local flame characteristics can hardly be represented by pure premixed or non-premixed processes [1-3]. In contrast to the conditions in practical applications, the majority of laboratory flames for investigating turbulent combustion phenomena operate with homogeneous fuel compositions, which do not exhibit compositional inhomogeneities leading to multi-regime combustion scenarios. To overcome these limitations Meares et al. introduced an advanced burner design, based on the well-known Sydney/Sandia piloted jet burner, allowing for compositional inhomogeneities at the burner exit [4]. Investigations of the stabilization mechanisms, due to inhomogeneous inlet conditions, confirmed the assumption of different modes of combustion and the important role of multi-mode combustion. While a configuration with near homogeneous inlet conditions exhibited non-premixed flame characteristics, inhomogeneous inflow lead to premix-dominated combustion close to the jet exit and non-premixed-dominated combustion further downstream. Comprehensive experimental data 1D-Raman/Rayleigh scattering in combination with 1D-CO-LIF measurements for different inflow conditions were presented [5, 6]. Mansour et al. [7] introduced slot burner to achieve inhomogeneous conditions at the exit of a conical nozzle. Similar to the configuration by Meares et al. [4], inhomogeneities were varied by moving the axial positions of the central slot of the burner.

Local reaction zones with both premixed and non-premixed characteristics can contribute simultaneously but with varying dominance to the local flame structure. Accordingly, a canonical burner configuration with well-defined boundary conditions is required to gain further insight into the processes of the underlying flame regimes and their interactions. This canonical configuration is the main objective of the current study: the development as well as the experimental and numerical investigation of a novel burner configuration to quantitatively investigate multi-regime combustion processes, the *multi-regime burner* (MRB). In this configuration, inhomogeneous conditions are generated downstream of the nozzle exits by enhanced mixing in strongly interacting shear layers instead of inhomogeneous conditions at the burner's exit. The aim is to ensure well defined boundary conditions at the burner's exit.

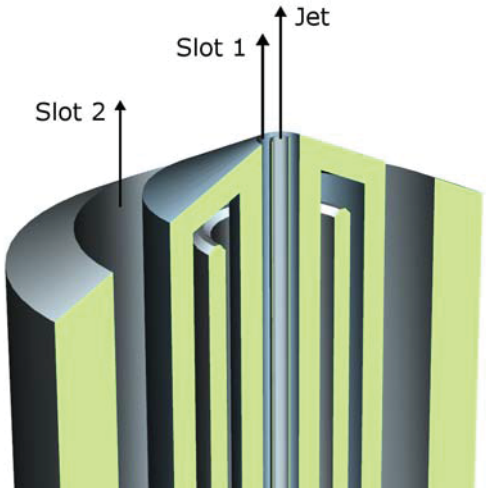

Figure 1: Illustration of the burner geometry

The MRB configuration consists of three inlet streams, which are be operated with different equivalence ratios (see Figure 1) and bulk exit velocities. A central stainless steel jet tube with

an inner diameter of 3 mm and an outer diameter of 3.3 mm is surrounded by an annular slot (slot 1) with an outer diameter of 7 mm. Slot 2 has an inner diameter of 40 mm and an outer diameter of 60 mm. A recirculation zone between slot 1 and slot 2 is stabilized by a bluff body which is kept at a temperature of 80°C by circulation of a tempering liquid to provide a defined temperature at the burner's surface and to prevent for condensation of water at the bluff body. Additionally, swirl up to a swirl number of ~2.0 can be introduced in slot 2 employing a moving block swirl generator located upstream of the exit. The burner slots and the bluff body are staged with an angle of 26° to allow for optical access at the exit plane. An additional air co-flow (1 m/s) around the outer body of the burner (outer diameter of 80 mm) shields the flame and provides well-defined boundary conditions in the area surrounding the burner.

Operating conditions were investigated by utilizing different ranges of lean to rich mixtures which extend beyond the rich flammability limit. The main flame stabilization mechanism of the MRB is the recirculation of flow emanating from slot 2 on the bluff body. A lean premixed methane/air mixture with an equivalence ratio of $\varphi = 0.8$ emanated from slot 2 with a bulk exit velocity of 20 m/s in a first series of experiments. From slot 1 a flow of pure air issued with velocities of 7.5 m/s ("a"-cases) and 15 m/s ("b"-cases) into a narrow region, creating a first (inner) mixing layer in between slot 1 and slot 2. As third flow a rich ($\varphi = 1.4 \div 2.6$) jet flow with a substantially larger bulk velocity (105 m/s, bulk Reynolds number ~20000) emanated at the burners axis, establishing a pronounced second (inner) mixing layer due to the large shear in between the inner jet and slot 1. The inner and the outer mixing layers are clearly visible in the chemiluminescence images in Figure 2. Flames are named according to the equivalence ratio in the jet flow, where case 14 corresponds to $\varphi = 1.4$ and so forth. Jet and slot 2 are separated by a flow of pure air emanating from slot 1 with velocities of 7.5 m/s ("a"-cases) and 15 m/s ("b"-cases). Temperature and species measurements using 1D-Raman/Rayleigh scattering in combination with 1D-CO-LIF and planar OH-PLIF have been performed in the Turbulent Combustion Laboratory at Sandia National Laboratories at various axial positions in a series of methane/air flames.

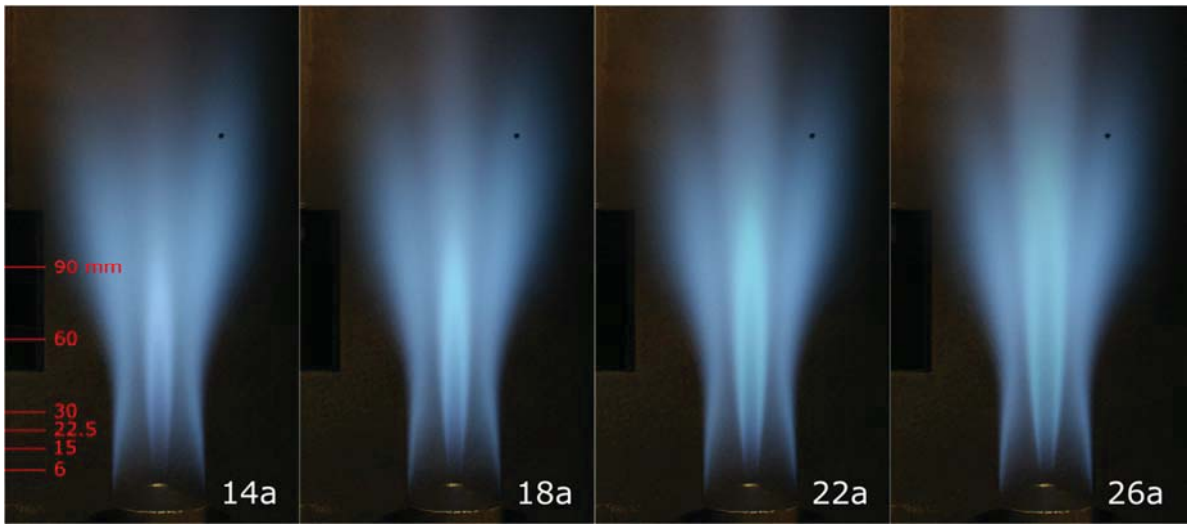

Figure 2: Flame photographs

[1] E. Knudsen, H. Pitsch, Combust. Flame, 156 (2009) 678-696.
[2] E. Knudsen, H. Pitsch, Combust. Flame, 159 (2012) 242-264.
[3] A.R. Masri, Proc. Combust. Inst., 35 (2015) 1115-1136.
[4] S. Meares, A.R. Masri, Combust. Flame, 161 (2014) 484-495.
[5] R.S. Barlow, S. Meares, G. Magnotti, H. Cutcher, A.R. Masri, Combust. Flame, 162 (2015) 3516-3540.
[6] S. Meares, V.N. Prasad, G. Magnotti, R.S. Barlow, A.R. Masri, Proc. Combust. Inst., 35 (2015) 1477-1484.
[7] M.S. Mansour, H. Pitsch, S. Kruse, M.F. Zayed, M.S. Senosy, M. Juddoo, J. Beeckmann, A.R. Masri, Experimental Thermal and Fluid Science, 91 (2018) 214-229.

Enabling uncertainty quantification and propagation in combustion models using statistical inference of unreported experimental data

Tiernan A. Casey*, Habib N. Najm
Combustion Research Facility,
Sandia National Labs, Livermore, CA, USA
*Email: tcasey@sandia.gov

Parameter estimation under uncertainty typically involves performing statistical inference given noisy experimental data, which is unfortunately rarely reported in chemical kinetics experiments used to determine rate parameters for reactions relevant to combustion. The consequences for uncertainty quantification and uncertainty propagation can be fatal, as information about important correlations between parameters can be lost when experiment information is reported in the form of limited data summaries, e.g. statistics of model parameters fit to the underlying data. In situations where data is unreported we can construct an inference for the missing data using maximum entropy (MaxEnt) arguments and approximate Bayesian computation methods to generate a distribution of hypothetical experimental data consistent with the available information [1,2]. We apply this methodology to shock tube experiments, where results are reported in the form of rate constants at various temperatures (Fig. 1) with attached error measures and the underlying concentration decay time series data is unreported.

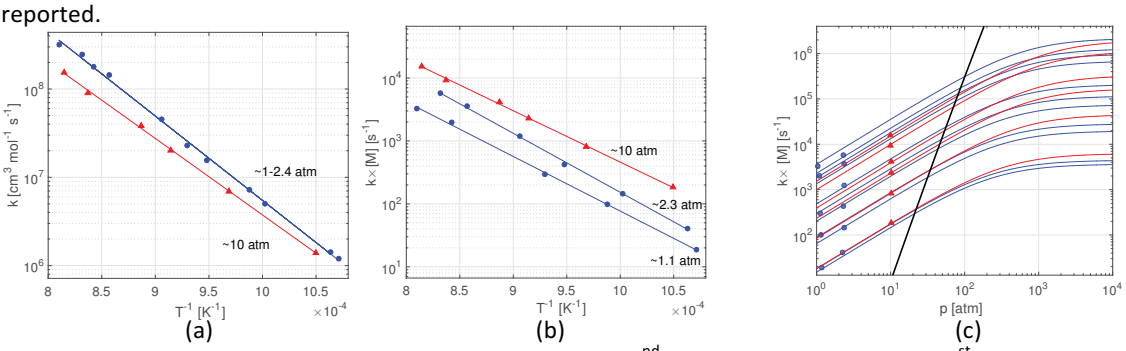

(a) (b) (c)

Fig. 1: Experimental shock tube data of Sajid et al. [3], with 2nd order rate constant fit (a), 1st order rate constant fit, (b) and Lindemann fall-off fit (c)

Once we have arrived at a distribution of noisy experimental data using the data inference method, (Fig. 2) we refit the data using Bayesian inference to determine posterior parameter probability density functions (PDFs) of the Arrhenius parameters of the reaction of interest (H2O2 thermal decomposition) and average over these PDFs to arrive at a maximum entropy estimate of the posterior for the missing data. The original experiment performed measurements at different pressures to study H2O2 thermal decomposition both in the low pressure limit and at pressures where the rate constant is sensitive to pressure. In this context, and having access to a representation of the missing data, we re-analyze the data at different pressures simultaneously to estimate the parameters of the low-pressure limit using Lindemann theory, arriving at an uncertain parametric specification that is ready for deployment in a chemical mechanism.

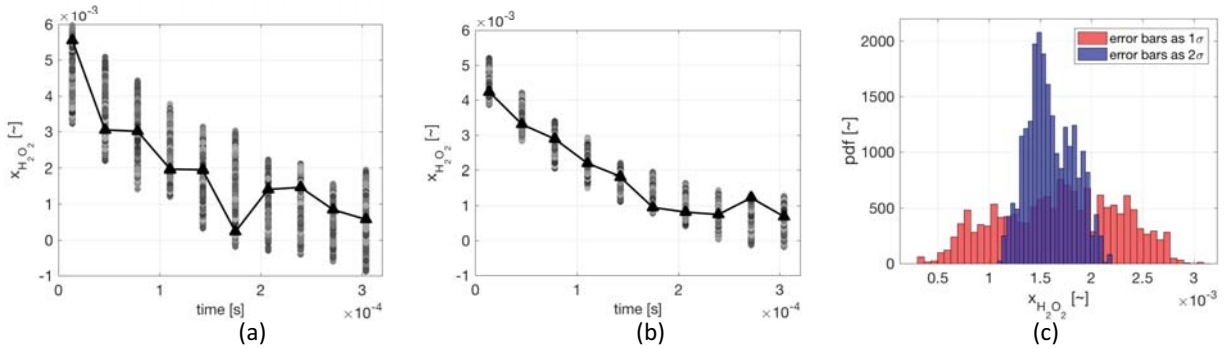

(a) (b) (c)

Fig. 2: Inferred hypothetical data ensemble for a 1 standard deviation interpretation of the reported error bars, (b) 2 standard deviation interpretation. (c) Distribution of data at t=1.35x10^{-4} s

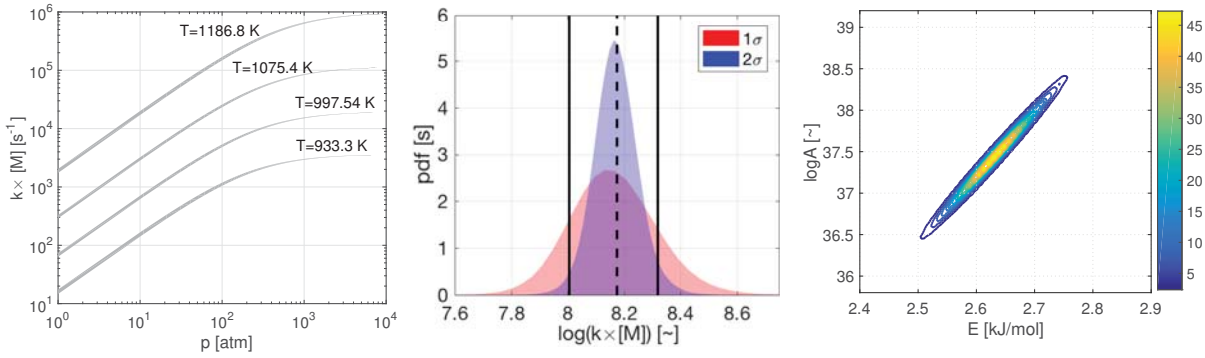

(a) (b) (c)

Fig. 3 (a) Inferred uncertain falloff curves at select temperatures. (b) Inferred comparison of reported means and error bars (lines) to posterior distributions determined from inferred data. (c) Example Arrhenius parameter posterior distribution computed using Bayesian inference using data at multiple temperatures

We employ the estimated Lindemann low-pressure limit parameters (estimated using both low pressure and high pressure data) to propagate uncertainty through a model for predicting the explosion limit curve for stoichiometric hydrogen-oxygen mixtures, quantifying the uncertainty in the Z-curve location given uncertainty in the H2O2 rate parameters, which is expected to essentially dictate the behavior of the 3rd explosion limit.

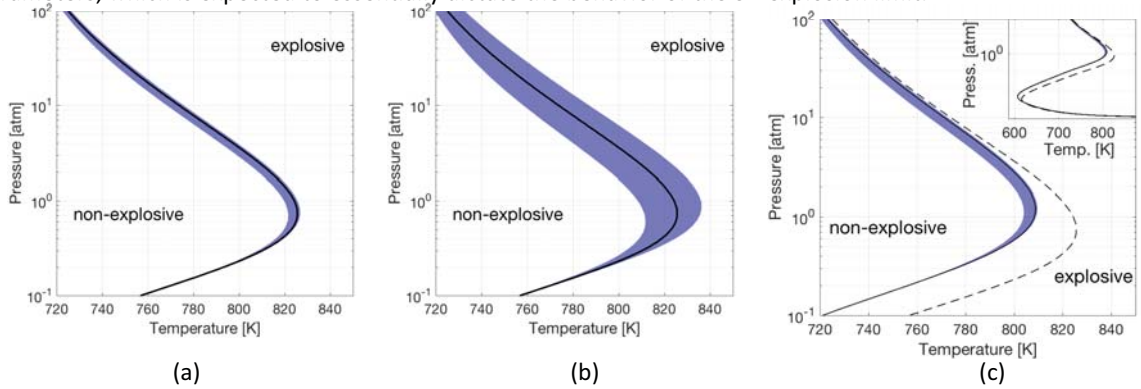

(a) (b) (c)

Fig. 4 (a) explosion limit curve and 90% confidence interval using samples from the MaxEnt posterior, and (b) an equivalent uncorrelated posterior. (c) Comparison of results using a new chemical mechanism to fit the data (dashed line)

Finally, we can compare the estimates of the explosion limit curve when the data is fit using the original calibration mechanism employed by the experimentalists when they analyzed their true raw data to estimates if a different mechanism was used (perhaps a full H2-O2 mechanism for use in predictive simulations). With access to a representation of the original data this is straightforward, and we arbitrarily utilize the mechanism of Li et al. [4] which is often used on large scale simulations of H2-O2 systems. Figure 4 shows that the predictions using both mechanisms can be quite different even though the H2O2 reaction was fit using the same data for both mechanisms, and can obviously be attributed to the differing parameterizations of the remaining reactions in each mechanism which have been constructed using different experimental sources. As such, we advocate construction of chemical models combining available data, and missing data estimated from reported statistics, to arrive at consensus mechanisms that employ all available information in an unbiased data-centric framework.

References:

[1] T. Casey, H. Najm, Estimating the joint distribution of rate parameters across multiple reactions in the absence of experimental data, Proceedings of the Combustion Institute [to appear]

[2] M. Khalil, K. Chowdhary, C. Safta, K. Sargsyan, H. N. Najm, Inference of reaction rate parameters based on summary statistics from experiments, Proceedings of the Combustion Institute 1919 (000) (2016) 1–10. doi: 10.1016/j.proci.2016.08.058.

[3] M. B. Sajid, E. Es-sebbar, T. Javed, C. Fittschen, A. Farooq, Measurement of the rate of hydrogen peroxide thermal decomposition in a shock tube using quantum cascade laser absorption near 7.7 µm, International Journal of Chemical Kinetics 46 (5) (2014) 275–284.

[4] J. Li, Z. Zhao, A. Kazakov, F. L. Dryer, An updated comprehensive kinetic model of hydrogen combustion, International journal of chemical kinetics 36 (10) (2004) 566–575.

Flame stabilisation mechanism of a spatially developing *n*-dodecane jet flame under Spray A thermochemical conditions

Deepak K. Dalakoti[1] Bruno Savard[1] Evatt R. Hawkes[1,2] Armin Wehrfritz[1] Haiou Wang[1,3] Marc S. Day[4] John B. Bell[4]

[1]School of Mechanical and Manufacturing Engineering, The University of New South Wales, Sydney, NSW 2052, Australia
[2]School of Photovoltaic and Renewable Energy Engineering, The University of New South Wales, Sydney, NSW 2052, Australia
[3]State Key Laboratory of Clean Energy Utilization, Zhejiang University, Hangzhou 310027, PR China
[4]Center for Computational Sciences and Engineering, Lawrence Berkeley National Laboratory, Berkeley, CA 94720, USA

One of the most important parameters in diesel engine combustion is the quasi-steady flame lift-off height (distance between the nozzle and the start of the high-temperature flame), which controls the amount of mixing prior to high-temperature combustion and thereby greatly affects the level of NO_x and soot emission as well as unburnt hydrocarbons [1]. To better predict the flame lift-off height in new engine designs, a thorough understanding of the flame stabilisation mechanism is required. To improve our current understanding of the stabilisation mechanism, access to the time- and space-resolved details of the flame structure, which are not available from experiments or from RANS/LES numerical studies, would be beneficial. For this purpose, we present a three-dimensional (3D) direct numerical simulation (DNS) of a spatially developing *n*-dodecane round jet in diesel engine conditions. The ambient pressure (60 atm), oxidiser composition (15% oxygen, 85% nitrogen by volume) and temperature (900 K) were matched to the Engine Combustion Network's (ECN) baseline Spray A flame [2]. The computational domain was initialised with quiescent oxidiser. A fuel jet with peak mixture fraction and temperature of 0.45 and 470 K, respectively, was then injected into the domain with a velocity of 28 m/s. The simulation was conducted for the whole process of two-stage ignition and flame development. In this poster, we present results for the stabilisation mechanism of the statistically-steady flame. To provide a reference for comparison with the turbulent flame, two-dimensional (2D) laminar flame simulations were conducted in a previous study [3] at the same ambient conditions as the present study for several values of inlet velocity and inlet scalar dissipation rate.

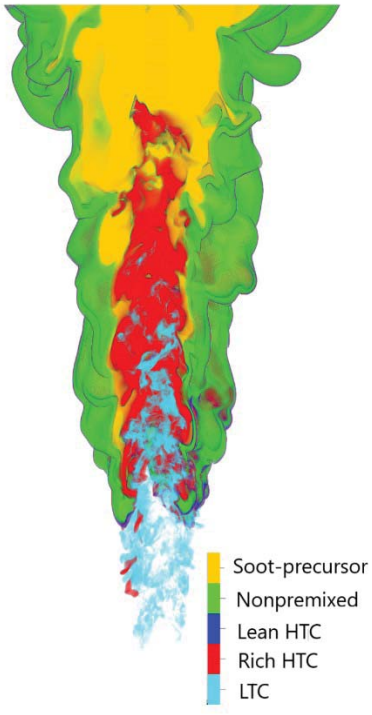

Figure 1 - 3D rendering of the flame coloured by the combustion modes. The figure has been clipped in a quadrant to reveal the internal structure of the flame.

Figure 1 presents a 3D rendering of the flame coloured by the combustion modes and soot-precursor region. Four combustion modes are identified, namely, low-temperature chemistry (LTC), rich high-temperature chemistry (HTC), lean HTC and nonpremixed. LTC starts upstream of HTC near the edge of the jet and persists downstream of the flame base (start of HTC) in the core of the jet. Downstream of LTC, rich HTC can be seen in the core of the jet. Further downstream, the jet is dominated by regions of soot-precursor (identified using acetylene in the present study). A nonpremixed flame shrouds the jet. A few ignition kernels are observed upstream of the flame base.

The flame presents a three-branch structure at the flame base consisting of an LTC branch, a rich HTC branch and a nonpremixed flame branch, which is qualitatively similar to that of propagating, as opposed to autoigniting, 2D laminar flames. Analysis of the transport budget of temperature and the flame displacement speed provides further evidence in support of the propagation stabilisation mechanism, showing significant upstream conduction of heat as expected from a deflagration like structure which is confirmed from the analysis of the 2D laminar reference flames. The turbulent flame displacement speed is of the order of 1 m/s and is close to the values observed for the propagating 2D laminar flames, further supporting the flame propagation stabilisation mechanism. Analysis of the upstream ignition kernels indicates that they have a small contribution to the total heat release rate and do not control the overall flame lift-off height.

References

[1] J. E. Dec, Advanced compression-ignition engines - Understanding the in-cylinder processes, Proceedings of the Combustion Institute 32 II (2) (2009) 2727-2742.

[2] Engine Combustion Network (ECN), www.ecn.sandia.gov (accessed 2/07/2018).

[3] D. K. Dalakoti, A. Krisman, B. Savard, A. Wehrfritz, H. Wang, M. S. Day, J. B. Bell, E. R. Hawkes, Structure and propagation of two-dimensional, partially premixed, laminar flames in diesel engine conditions, Proceedings of the Combustion Institute, 2018

Hybrid Stress Blended Eddy Simulations for Near Blow-out Swilling Spray Flame using the Flamelet Generated Manifold Model

Hossam Elasrag[a*] Shaoping Li[b], and Ellen Meeks[a]

[a]ANSYS Inc., San Diego, CA, USA [b]ANSYS Inc., Lebanon NH, USA

*Hossam.elasrag@ansys.com, ellen.meeks@ansys.com

Simulations for the Cambridge swirl bluff-body spray burner are performed near blow-out conditions. The ANSYS-Fluent hybrid stress blended eddy simulation (SBES) model is used for sub-grid turbulence closure. SBES blends the turbulent stresses and eddy viscosities from different RANS and LES subgrid models. In the current work, the k-ω-SST model [1] is used for RANS turbulence closure near the wall in the boundary layer and the large eddy simulation dynamic Smagorinsky model [2] for turbulence closure in the bulk flow. The injected n-heptane spray droplets are tracked using a Eulerian-Lagrangian approach. Conjugate heat transfer between the bluff-body walls and the gas-flow is accounted for by coupling the solid and gas-phase energy equations. Mixing and chemistry are modeled using the Flamelet Generated Manifold (FGM) model [3]. The study investigates how successful the FGM model is in predicting finite rate effects like local extinction, global extinction, and flame lift-off height. To this end, two near blow-out spray flame; the H1S1 (75% to blow-out) and H1S2 (88% to blow-out), are simulated. Good results are shown matching the spray Sauter mean diameter (SMD) and axial velocity mean and rms experimental data. The results also show that the FGM model captured reasonably well the flame structure and lift-off height as well as the spray pattern. Overall the spray droplets mean D32 and mean axial velocity were under-predicted, while the rms distribution matched reasonably well for the H1S1 flame. The mean flame brush lift-off height is estimated based on the statistically stationary mean flame brush and is estimated to be around 4-6 mm from the bluff-body base. That agrees well with the experiments reported lift-off height of 5mm. Instantaneous local flame extinction is also observed, where islands of OH mass fraction disconnect and reconnect with time. The H1S2 flame, however, showed similar but slightly better match with the measurements for the mean spray data compared to the H1S1 flame, with slight under-prediction for D32 at Z=10 mm and Z=20 mm. As the flame approach blow-out the simulation results were in agreement with the experiments [4], where the flame structure was compressed and shortened towards the bluff-body base as the inflow velocity is increased. SBES-FGM was shown to captured successfully the qualitative and quantitative features of the flow near blow-out.

The conditions for the two flames are shown in Table [1]. The Cambridge swirl bluff-body burner geometry is shown in Fig 1. The experimental setup has two main components; a bluff-body and a square cross sectional enclosure of 150 mm length and 95 mm width. The bluff-body has six 60 degrees' vanes attached to it. The corresponding computational domain is shown in Fig. 2. The bluff-body has a diameter of 25 mm and gives a blockage ratio of 50%. The effective swirl number is about 1.23. As shown in Fig. 1, liquid n-heptane is injected at the centerline and exit from a nozzle of diameter D=0:15mm. Air is injected through the swirl vanes at 298 K.

TABLE 1. Operating gas conditions and liquid fuel properties for the simulated spray n-heptane spray flames[a].

Flame	U_b (m/s)	U_b/U_B	$\phi_{overall}$	Re_g	U_l (m/s)	ρ_l (kg/m^3)	σ (N/m)	$\dot{m}_{fuel}$ (g/s)	We_l	We_g
H1S1	17.1	0.75	0.32	13466	12.64	668.3	0.0201	0.27	1098	1.95
H1S2	20.0	0.88	0.27	15711	12.64	668.3	0.0201	0.27	1098	1.95

[a] Where U_b, U_B, $\phi_{overall}$, and U_l are the air bulk velocity, blow-off velocity limit, overall equivalence ratio, and central liquid jet velocity, respectively. Re_g, $\dot{m}_{fuel}$, ρ_l, and σ are the gas flow Reynolds number, central jet spray mass flow rate, spray density and surface tension,respectively. We_l and We_g are the liquid and gas weber numbers.

The instantaneous flame structure is shown in Fig. [3]. Local holes that presents local extinction can be observed. The same iso-clip mean elevation from the bluff-body is shown in Fig. [4]. In-agreement with

the experiments the mean lift-off height ranges in-between 4-6 mm. Finally, comparisons with the spray mean axial velocity and SMD is shown in Figs. [5], and [6], respectively. Good comparisons are shown.

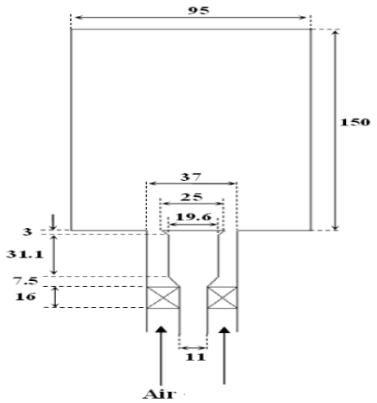

Figure 1Cambridge bluff-body swirling burner

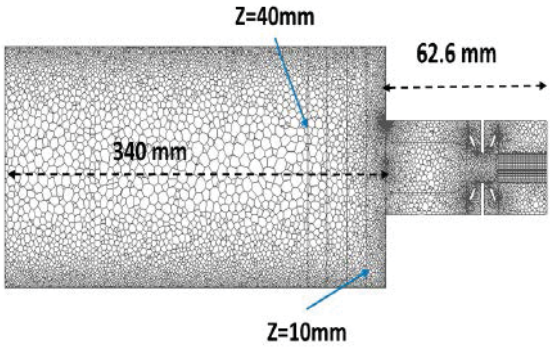

Figure 2 Computational Domain cross-sectional plane

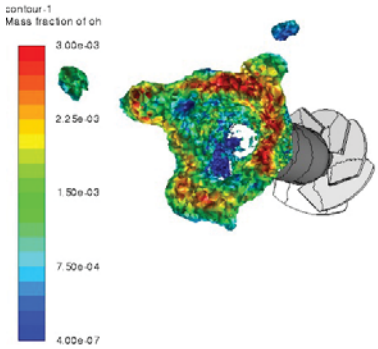

Figure 3 Flame iso-surface T=1600-2200K colored by OH mass fraction

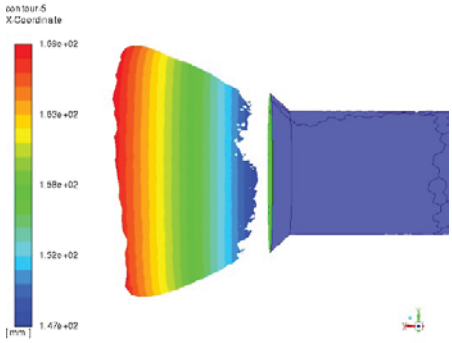

Figure 4 Mean flame brush visualized by iso-clip of mean temperature 1600-2000

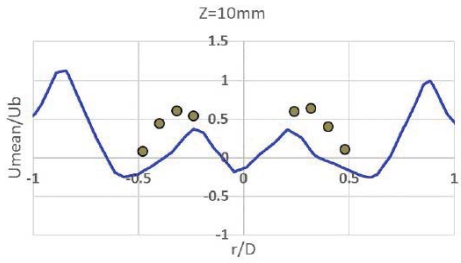

Figure 5 Spray droplets mean axial velocity at Z=10mm for H1S1 flame

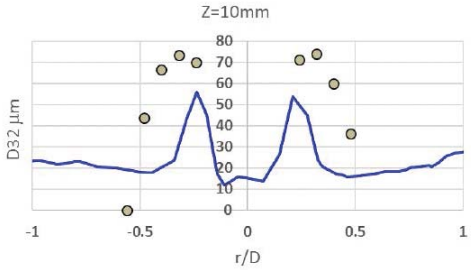

Figure 6 Spray droplets SMD at z = 10mm for H1S1 flame

[1] Menter, F., 2016. "Stress-Blended Eddy Simulation (SBES)-a new paradigm in hybrid rans-les". *6th Symposium on Hybrid RANS-LES Methods*.

[2] M. Germano, U. Piomelli, P. Moin, and W. Cabot, "A dynamic sub-grid scale eddy viscosity model," Phys. Fluids A **3**, 1760 (1991)

[3] Van Oijen, A. J., and De Goey, L. H. P., 2000. "Modelling of premixed laminar flames using flamelet-generated manifolds". *Combust. Sci. Tech., 84*, pp. 439–458.

[4] Yuan, R. Kariuki, J. and Mastorakos, E. "Measurements in Swirling spray flames at blow-off, spray and combustion dynamics, Int. Journal of Spray & Combustion Dynamics 1-26 (1) 2018

Confined and Pressurised Jet in Hot & Vitiated Coflow Burner

M. J. Evans[1], P. R. Medwell[1], Q. N. Chan[2]

[1] *The University of Adelaide, Adelaide, Australia*
[2] *The University of New South Wales, Sydney, Australia*

m.evans@adelaide.edu.au

Moderate or Intense Low oxygen Dilution (MILD) combustion offers practical advantages over conventional combustion. These include reduced soot and NO_x emissions, negligible flame-noise due to lower, more uniform temperatures. Although MILD combustion has been demonstrated in industrial devices, experimental studies at elevated pressures have not been able to separate chemical, mixing and flow-field effects due to complex geometries [1,2]. Consequently, there is still a need for a further understanding of MILD combustion at elevated pressures for future, fuel flexible, low emissions reheat gas-turbines or inter-turbine burners.

The jet-in-hot-coflow (JHC) burner [3,4] and similar the vitiated coflow burner [5] have both been studied extensively and feature a central fuel jet issuing into a coflow of hot combustion products. Data and observations from these burners have been invaluable for gaining insight into flame stabilisation and structure in the MILD and autoignitive regimes, as well as for model validation.

Flames stabilised in hot coflows have been demonstrated as stabilising as either rapidly autoignitive kernels [6-8] or continuous reaction zones, which gradually ignite [8-11]. Although attempts have been made to map the transition between these two mechanisms as part of a comprehensive description of the MILD combustion regime [11-13], these studies have not been able to describe the demonstrated dependency on the underlying flow-field [14]. Hence, the relationship between the MILD combustion regime and Damköhler number is still not fully understood.

The JHC burner configuration allows for systematic experimental variation of the fuel jet properties and oxidant temperature and composition. To extend this research to elevated pressure environments, a confined-and-pressurised JHC (CP-JHC) burner has been developed and recently commissioned with flame testing in progress.

The CP-JHC burner is shown in Figure 1. This burner facilitates studies of flame structure with ambient pressure as an independent variable. This additional parameter influences both turbulence and chemical scales, and hence Damköhler number, which are not achievable in existing JHC burners. Studies using the CP-JHC provide new insight into turbulent flame structure and stabilisation, and also allow experimental investigations of the competition between soot suppression in MILD combustion and enhanced soot formation at elevated pressures.

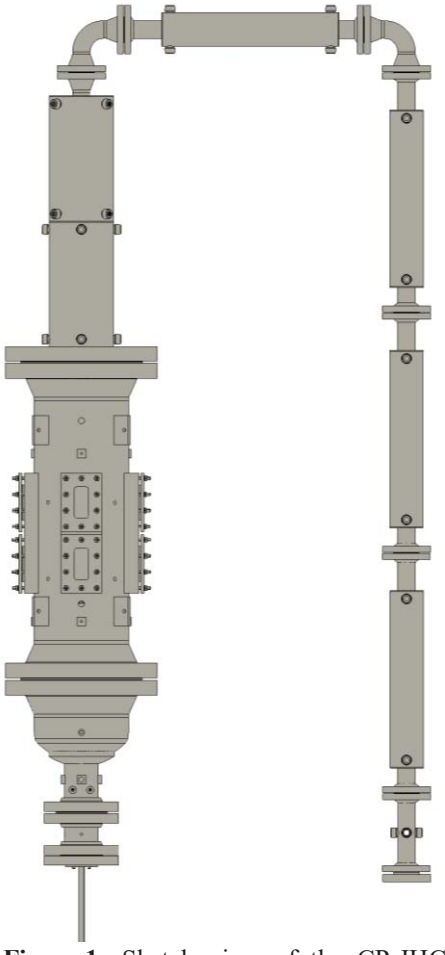

Figure 1: Sketch view of the CP-JHC burner. The main pressure vessel is shown on the left with the water-cooled exhaust on the right.

A coloured cutaway of the CP-JHC is provided in Figure 2, highlighting key features of the burner. The jet flame and hot coflow are contained within a 95 mm (I.D.) cylindrical quartz tube with 2.5 mm wall thickness. This is, in-turn, contained in a section of DN300 (O.D. of 324 mm) pipe with 12.7 mm wall thickness. The void between the quartz and the pipe wall is filled with insulation to allow steady operation at 10 bar with internal temperatures up to 1975 K without a requirement for cooling the main pressure vessel walls. This configuration minimises heat losses in the system, allowing for the investigation of hotter coflow conditions and with minimal thermal boundary layer.

The main fuel stream issues from a 4.6 mm jet, which is readily interchangeable to facilitate measurements with other jet diameters. The 4.6 mm jet is water-cooled to avoid structural damage or thermal decomposition of the fuel. The hot coflow is produced by non-premixed combustion of fuel delivered by ring burners into an air coflow. These rings are situated approximately 600 mm upstream of the jet exit plane, and exhaust gases pass through an externally water-cooled exhaust before an automated pressure-control valve. The pressurised vessel and exhaust stand a total of 3.4 m above the ground.

Optical access to the burner is provided through by eight 20-mm thick, 48 mm × 107 mm sapphire windows, providing four windows (each separated by 90°) at two heights. This configuration allows for imaging and laser diagnostics of jet flames in hot coflows at, and immediately above, the jet exit plane, and further downstream. The inclusion of four windows at each height provides flexibility to study alternative burner configurations such as swirling oxidant streams, or gaseous or spray flames in hot cross-flows. The CP-JHC will facilitate immediate and long-term future studies spanning conditions of interest in fundamental research for novel gas turbine combustor configurations.

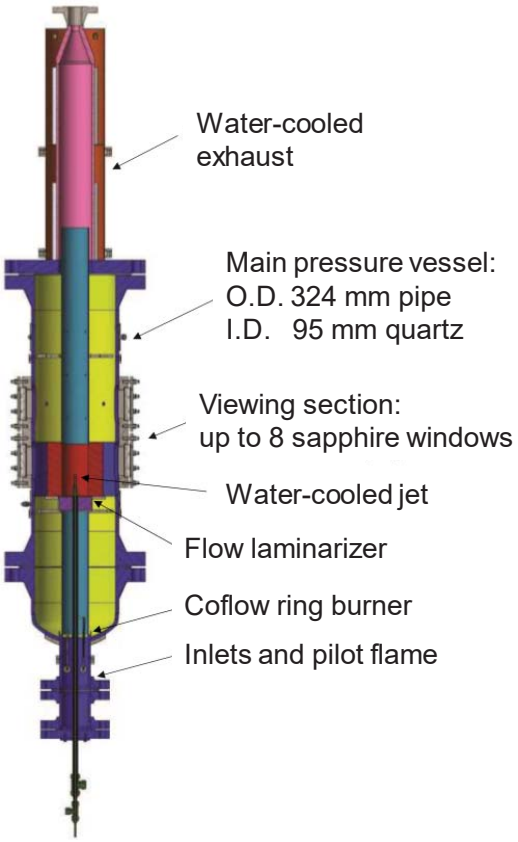

Figure 2: Cross-section of CP-JHC burner showing main burner components

References

[1] Lückerath, R., Meier, W., Aigner, M. (2008) *J. Eng. Gas Turbines Power*

[2] Ye, J.J., Medwell, P.R., Varea, E., Kruse, S., Dally, B.B., Pitsch, H.G. (2015) *Appl. Energy*

[3] Dally, B.B., Karpetis, A.N., Barlow, R.S. (2002) *Proc. Combust. Inst.*

[4] Oldenhof, E., Tummers, M.J., van Veen, E.H., Roekaerts, D.J.E.M. (2012) *Combust. Flame*.

[5] Cabra, R., Myhrvold, T., Chen, J.Y., Dibble, R.W., Karpetis, A.N., Barlow, R.S. (2002) *Proc. Combust. Inst.*

[6] Gordon, R.L., Masri, A.R., Mastorakos, E. (2008) *Combust. Flame*

[7] Yoo, C.S., Richardson, E.S., Sankaran, R., Chen, J.H. (2011) *Proc. Combust. Inst.*

[8] Mastorakos, E. (2012) *Prog. Energy Combust. Sci.*

[9] de Joannon, M., Sabia, P., Cozzolino, G., Sorrentino, G., Cavaliere, A. (2012) *Combust. Sci. Technol.*

[10] Evans, M.J., Medwell, P.R., Tian, Z.F., Ye, J., Frassoldati, A., Cuoci, A. (2017) *Combust. Flame*

[11] Evans, M.J., Medwell, P.R., Wu, H., Stagni, A., Ihme, M. (2017) *Proc. Combust. Inst.*

[12] Medwell, P.R., Dally, B.B. (2012) *Energy Fuels*

[13] Medwell, P.R., Evans, M.J., Chan, Q.N., Katta, V.R. (2016) *Energy Fuels*

[14] Ye, J., Medwell, P.R., Dally, B.B., Evans, M.J. (2016) *Combust. Flame*

Turbulent Premixed Syngas Flames

F. Hampp, R. P. Lindstedt* (p.lindstedt@imperial.ac.uk)
Department of Mechanical Engineering, Imperial College London, Exhibition Road, London SW7 2AZ, UK.

Introduction and Objective

The confluence of climate change, environmental protection and diminishing fossil fuel resources have promoted the development of low carbon footprint and clean energy technologies [1]. The use of hydrogen enriched fuel blends, e.g. syngas, offers great potential in the decarbonisation of gas turbine technologies by substitution and expansion of the lean operation limit. However, the variability of the syngas composition can lead to fuel flexibility concerns for engine manufacturers [2] and the increased hydrogen concentration to safety concerns [3]. Lin et al. [4] evaluated the flashback propensity in gas turbine combustors utilising the turbulent flame speed. The current study uses a back-to-burnt opposed jet configuration to investigate the impact of hydrogen concentration on the turbulent burning velocity and scalar transport.

Experimental Setup

The twin flame variant of the current burner (Fig. 1) was developed by Geyer et al. [5]. The current revised configuration is identical to that of Goh et al. [6] with multi-scale turbulence [7, 8] generated via a cross fractal grid (CFG; [9]). The mixtures contain binary H_2/CH_4 and H_2/CO fuel blends. The binary H_2/CH_4 fuel blend was varied from $\alpha = X_{H2}/(X_{H2} + X_F)$ = 1.0, 0.9, 0.8, 0.7, 0.6, 0.5, 0.4, 0.2 and 0. The binary H_2/CO fuel blend was varied from α = 0.3 – 1.0 in steps of 0.1. The equivalence ratio was adjusted between the mixture specific lower limit of local flame extinction and the upper limit of flashback. The premixed fuel / air mixtures were injected through the upper nozzle (UN) with a constant bulk velocity of U_b = 9.0 m s^{-1} (T_r = 298 K). The CFG was installed 50 mm upstream of the UN exit and provides a constant turbulent flow field with an integral length scale of L_I = 3.9±0.2 mm [10] and a velocity fluctuation of u_{rms} = 1.5±0.11 m s^{-1} at the nozzle exit. The corresponding turbulent Reynolds number (Re_t) was modestly affected (i.e. 286 < Re_t < 320) due to changes in the kinematic viscosity of the reactants (ν_r). The hot combustion products (HCP), emerging from the lower nozzle (LN), were generated from a lean (Φ = 0.60) premixed 50% H_2 / 50% CH_4 flame that was stabilised on a perforated plate (PP). The HCP are in close to thermochemical equilibrium with a nozzle exit temperature of 1640±7.1 K, measured using a 50 μm R-type thermocouple. The HCP composition, including the oxygen residual, does not exert a strong impact on the combustion behaviour of self-sustained flames [11, 12, 13, 14], which are the primary interest in the current study. Particle image velocimetry (PIV) measurements (vector spacing of 0.45 mm with a spatial resolution of 0.92 mm) are combined with a density segregation technique to determine the turbulent burning velocity at the leading edge (e.g. $S_T|\overline{c} = 0.02$ [15]) and the scalar flux, where $\overline{c}$ is the reaction progress variable. For each mixture 1000 repetitions were recorded for statistically independence.

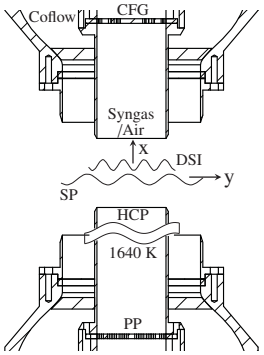

Figure 1: Burner configuration.

Scaling relationships

The wide range of hydrogen concentration results in significant differences in mixture reactivities as well as reactant and burning properties. Li et al. [3] has presented a scaling factor (β, see Eq. 1) based on the amount of air required to fully oxidise the mixture. The β factor has improved the scaling of explosion over-pressures compared to α over a wide range of binary and ternary H_2/CH_4/CO mixtures and is consequently used for the present analysis. Classical theories for turbulent combustion resulting in eddy breakup based models for the reaction rate source term (e.g. Spalding [16, 17]) only provide a scaling of the turbulent burning velocity based on the velocity fluctuations. The latter is kept constant and the results provide a direct indication of the deviation from the classical limit. The turbulent burning velocity has also been analysed theoretically using a Kolmogorov, Petrovskii and Piskunov (KPP) type approach [18] and an eigenvalue analysis [19]. The resulting scaling introduces the ratio of the laminar burning (S_L) and the Kolmogorov (V_κ) velocities along with the Schmidt number σ_{Sc} [20]. Lindstedt et al. [21] has further taken transport effects into account and the derived the correction [22] amounts to a modified value for $C_R = 4.0/e^{\sigma_{Le,r}-1}$, where $\sigma_{Le,r}$ is the Lewis number. The $S_{T,KPP}$ scaling has been used by Goh et al. [8].

$$\beta = \frac{\frac{X_{H2}}{(X_{H2}/X_A)_{st}}}{\frac{X_{H2}}{(X_{H2}/X_A)_{st}} + \frac{X_F}{(X_F/X_A)_{st}}}\,; \qquad S_{T,KPP} \simeq 1.2\sqrt{\frac{1}{e^{\sigma_{Le,r}-1}}\frac{1}{\sigma_{Sc}}\frac{S_L}{V_\kappa}}\cdot u'\,; \qquad \sigma_{Le,r} = \frac{X_{H_2}}{X_{H_2}+X_F}Le_{H_2} + \frac{X_F}{X_{H_2}+X_F}Le_F \quad (1)$$

Results and Discussion

Lean premixed syngas / air flames were stabilised against hot combustion products with the equivalence ratio varied from the extinction to the flashback limit for each specific mixture. The turbulent burning velocity (S_T) was measured based on the leading edge [15] and is depicted in the top of Fig. 2a for all H_2 / CH_4 mixtures. As the amount of CH_4 is increased, a higher Φ is required to stabilise a self propagating flame. For example, the pure H_2-air flame was stabilised at $\Phi = 0.35$ (i.e. upper limit to avoid flashback). A CH_4 blending of merely 20% resulted in a significant decrease in reactivity. This results in a significant drop of S_T and an increase of the upper limit equivalence ratio to $\Phi = 0.50$. A 50% blending with CH_4 allowed an Φ increase up to $\Phi = 0.80$ demonstrating the strong impact of methane addition on the mixture reactivity. Scaling of S_T with the velocity fluctuations collapses the data to a normalised value of $S_T/\sqrt{u_r' u_r'}$ of around 3.1 ± 0.28. The KPP scaling also provides a good scaling (see Eq. (1)) for cases with an assumed "flamelet related" burning mode. For very lean cases it can be expected the latter assumption becomes less reliable. The R^2 value of a linear regression increases from 0.02, 0.01 to 0.33 for S_T, $S_T/\sqrt{u_r' u_r'}$ and $S_T/S_{T,KPP}$, respectively. When removing the case 80% H_2 / 20% CH_4 at Φ = 0.35 (i.e. extinction strain < bulk strain) the R^2 for the $S_T/S_{T,KPP}$ improves to 0.47. The results for H_2 / CO mixtures are shown in Fig. 2b along with

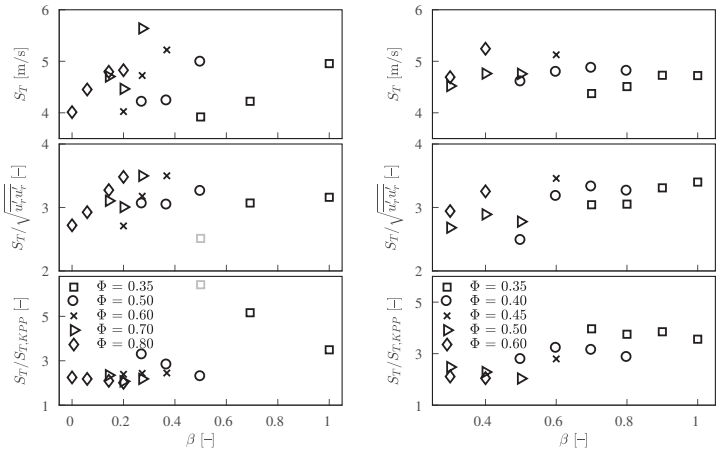

(a) (b)

Figure 2: Turbulent burning velocity at the leading edge ($S_T|\overline{c} = 0.02$) for (a) H_2 / CH_4, (b) H_2 / CO. Top: Measured $S_T|\overline{c} = 0.02$; Middle: normalised by $\sqrt{u_r'u_r'}$; Bottom: normalised by $S_{T,KPP}$. Grey symbols indicate mixtures with an extinction strain below 150% of the bulk strain rate.

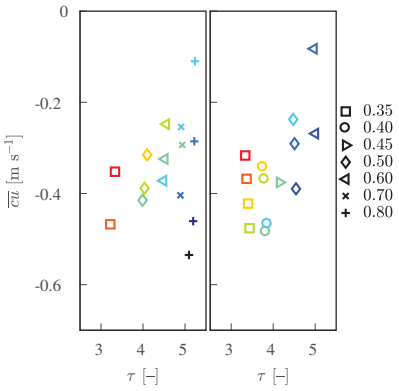

Figure 3: Scalar flux ($\overline{cu}$) at the $\overline{c}$ = 0.50 iso-contour as a function of heat release factor ($\tau = (T_{ad} - T_r)/T_r$). Left H_2 / CH_4; Right H_2 / CO. The legend refers to the equivalence ratio (Φ). The symbol colour code indicates the hydrogen concentration (i.e. black to red – 100% CH_4 or CO to 100% H_2).

the scaled values based on the eddy breakup theory and KPP values. The influence of CO blending on the mixture reactivity is much less profound compared to CH_4, in particular for small blending fractions. The R^2 value of the linear regression increases from 0.02, 0.37 to 0.67 for S_T, $S_T/\sqrt{u_r'u_r'}$ and $S_T/S_{T,KPP}$, respectively. The scalar flux ($\overline{cu} = \overline{c}(1-\overline{c}) \cdot (\overline{U}_p - \overline{U}_p)$, where $\overline{U}_p$ and $\overline{U}_r$ are the condition mean axial product and reaction fluid velocity [23]) is evaluated at the $\overline{c}$ = 0.50 iso-contour for all mixtures in Fig. 3 as a function of the heat release parameter ($\tau = (T_{ad} - T_r)/T_r$). The hydrogen concentration in the binary fuel blends does not affect τ strongly, e.g. τ = 5.1 – 5.2 for 100% CH_4 – 50% H_2 / 50% CH_4 at Φ = 0.8. However, an increased hydrogen concentration results in a strong reduction of the gradient transport, i.e. less negative $\overline{cu}$. For example, $\overline{cu}$ reduces from -0.53 m s^{-1} for 100% CH_4 at Φ = 0.8 to -0.11 m s^{-1} for 50% H_2 / 50% CH_4 at the same Φ. This can be attributed to the increasing detachment of the flame front with S_T where it experiences a reduced compressive strain [13]. Consequently, the dilatation of mixtures with a fast S_T at a given τ is more effective and leads to a stronger acceleration of the products. This results in a more pronounced reduction of the gradient scalar flux. However, the transition to counter-gradient transport was suppressed due to the high turbulence levels.

Conclusions

The present work investigated the impact of hydrogen content of binary methane and carbon monoxide fuel blends on the turbulent burning velocity and scalar transport. The turbulent flow field was maintained constant at $Re_t \simeq 300$. The turbulent burning velocity increases significantly with increasing hydrogen concentration for both CH_4 and CO fuel blends. However, a significantly stronger inhibiting effect of CH_4 on the H_2 chemistry compared to CO is evident. Mixtures with a fast turbulent burning velocity result in a stronger reduction of the gradient scalar flux, yet the transition to counter-gradient transport is suppressed by the high turbulence intensity. The extensive data set provides a great challenge for combustion models.

Acknowledgement The authors gratefully acknowledge the support of the ETI under the High Hydrogen project (PE02162). The support of Dr Robert Barlow and the contribution by Dr Henry Goh are also gratefully recognised.

References

[1] T. Lieuwen, V. Yang, R. Yetter (eds.) Synthesis Gas Combustion, Boca Raton: CRC Press, 2009.
[2] T. Lieuwen, V. McDonell, D. Santavicca, T. Sattelmayer, Comb. Sci. Technol. 180 (2008), pp.1169–1192.
[3] T. Li, F. Hampp; R. P. Lindstedt, Proc. Safety Environ. Prot. 116 (2018) pp. 663–676.
[4] Y.-C. Lin, S. Daniele, P. Jansohn, K. Boulouchos, J. Eng. Gas Turbines Power 135 (2013) 111503.
[5] D. Geyer, A. Kempf, A. Dreizler, J. Janicka, Combust. Flame 143 (2005) pp. 524–548.
[6] K. H. H. Goh, P. Geipel, F. Hampp, R. P. Lindstedt, Proc. Combust. Inst. 34 (2013), pp. 3311–3318.
[7] K. H. H. Goh, P. Geipel, F. Hampp, R. P. Lindstedt, Fluid Dyn. Res. 45 (2013) 061403.
[8] K. H. H. Goh, P. Geipel, R. P. Lindstedt, Combust. Flame 161 (2014) pp. 2419–2434.
[9] K. H. H. Goh, P. Geipel, R. P. Lindstedt, Flow Turbul. Combust. 85 (2010), pp. 397–419.
[10] F. Hampp, S. Shariatmadar, R. P. Lindstedt, Proc. Comb. Inst. (2018), https://doi.org/10.1016/j.proci.2018.06.079.
[11] E. Mastorakos, A. M. K. P. Taylor, J. H. Whitelaw, Combust. Flame 102 (1995), pp. 101–114.
[12] F. Hampp, R.P. Lindstedt, Combust. Flame 182 (2017), pp. 248–268.
[13] F. Hampp, R. P. Lindstedt, Proc. Combust. Inst. 36 (2017), pp. 1911–1918.
[14] F. Hampp, R. P. Lindstedt, Accepted for Publication in Springer Book Chapter (2018).
[15] C. J. Lawn, R. W. Schefer, Combust. Flame 146 (2006), pp. 180–199.
[16] D. B. Spalding, Proc. Combust. Inst. 13 (1971) pp. 649–657.
[17] D. B. Spalding, Proc. Combust. Inst. 16 (1977) pp. 1657–1663.
[18] B. Hakberg, A. D. Gosman, Proc. Combust. Inst. 20 (1985) pp. 225–232.
[19] C. A. Catlin, R. P. Lindstedt, Combust. Flame 85 (1991) pp. 427–439.

[20] R. P. Lindstedt, V. Sakthitharan, 8th Symposium on Turbulent Shear Flows, 1991.
[21] R. P. Lindstedt, V. D. Milosavljevic, M. Persson, Proc. Combust. Inst. 33 (2011) pp. 1277–1284.
[22] N. K. Aluri, S. P. Reddy Muppala, F. Dinkelacker, Combust. Flame 145 (2006), pp. 663–674.
[23] K. N. C. Bray, in N. Swaminathan N, K. N. C. Bray (eds.), Turbulent Premixed Flames, Cambridge University Press (2001), pp. 41–60, ISBN: 978-0-521-76961-7.

blank

Flame structure analysis of multi-regime combustion processes

S. Hartl[*,a),b)], S. Popp[*,b)], D. Butz[c)], C. Hasse[b)], A. Dreizler[c)], D. Geyer[a)], R. Barlow[d)]

a) Thermodynamics and Alternative Propulsion Systems, University of Applied Sciences, Darmstadt, Germany
b) FG Simulation of Reactive Thermo-Fluid-Systems, TU Darmstadt, Darmstadt, Germany
c) FG Reactive Flows and Diagnostics, TU Darmstadt, Darmstadt, Germany
d) Combustion Research Facility, Sandia National Laboratories, Livermore, CA, USA

** hartl@stfs.tu-darmstadt.de, popp@stfs.tu-darmstadt.de*

Laminar and turbulent combustion processes can be classified as either globally premixed or non-premixed. However, in practical applications complex multi-regime combustion scenarios occur locally through partial premixing or recirculation. Flame characteristics in such regions can hardly be represented by pure premixed or non-premixed processes [1,2,3]. Understanding and quantifying the importance of premixed and non-premixed reaction zones within turbulent flames is an important issue for multi-regime combustion [3,4]. The term partially premixed is used here to describe all conditions in between perfectly premixed and perfectly non-premixed. Since premixed and non-premixed flame regimes can contribute simultaneously (with varying dominance) to the total heat release, a detailed knowledge of the underlying flame regimes is required for model selection [1,2,5].

The objective of this study is to analyze and characterize the local flame structure of multi regime combustion processes using experimental data of a novel burner configuration. The so called multi-regime burner (MRB) was designed to allow for a variety of combustion regimes in a single flame configuration with well-defined boundary conditions. Therefore, premixed and non-premixed reaction zones can be addressed and the relative importance of reaction zones can be analyzed.

The novel multi-regime burner configuration consists of three inlet streams, which can be operated with different equivalence ratios. A central jet tube is surrounded by an annular slot (slot 1). A recirculation zone between slot 1 and slot 2 is stabilized by a bluff body. An additional air co-flow around the outer body of the burner shields the flame. The flow from slot 2 was kept at an equivalence ratio of $\varphi = 0.8$ while the jet flow was varied from $\varphi = 1.4$ up to $\varphi = 2.6$. Flames are named according to the equivalence ratio in the jet flow, where case 26 corresponds to $\varphi = 2.6$ and so forth. Jet and slot 2 are separated by a flow of pure air emanating from slot 1 with velocities of 7.5 m/s ("a"-cases) and 15 m/s ("b"-cases). Figure 1 (left) shows a photograph of flame 26b.

Radial temperature and species concentration measurements using 1D-Raman/Rayleigh scattering in combination with 1D-CO-LIF have been performed at various axial positions in a series of methane/air flames. Those radial profiles for temperature and species allow to examine the local thermochemical state as well as specific mixing characteristics.

The poster presents a reliable detection and characterization of local reaction zones using experimental data. Further, the possibility of representing the local flame structure with common numerical models will be discussed. In order to decide if common 1D flame characterizations can be used to describe the local flame structure of the multi-regime burner setup, different pre-evaluation strategies will be investigated. The suitability of look-up tables is first evaluated by means of a prior analysis. The mixture fraction Z and the progress variable Y_c, which fully parameterize the manifold, are used as inputs for flamelet look-up tables. As a second approach, the gradient-free regime identification (GFRI) analysis [6], allowing the local combustion regime to be identified based on Raman/Rayleigh measurements, is utilized.

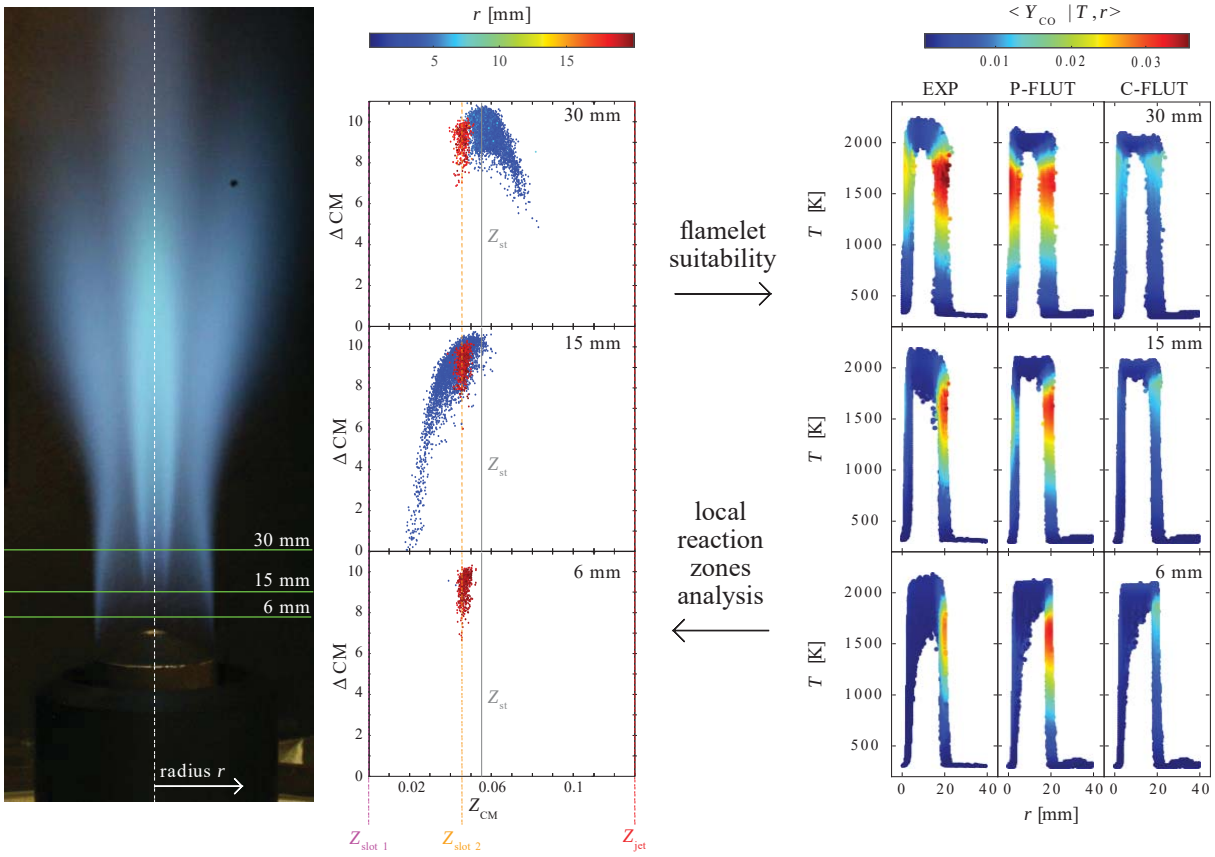

Figure 1: Analysis of flame MRB-26b at three axial positions 6 mm, 15 mm and 30 mm (flame photograph (left), local reaction zone analysis using the chemical mode (middle) and flamelet suitability based on temperature (right)). The color visualizes the radial position in the flame (left) and the CO mass fraction (right).

In the GFRI approach a premixed reaction zone is identified by a zero-crossing of the chemical mode (CM) combined with significant heat release rate (HRR) values at the CM zero-crossing, and a non-premixed reaction zone is identified by negative CM and significant HRR values at the stoichiometric mixture fraction. Note that the results of the GFRI approach are sufficiently accurate to address the relative importance of local premixed and non-premixed reaction zones within partially premixed flames. Figure 1 shows preliminary results of visualizing the strength of premixed flame zones using the chemical mode (middle). Further, the suitability of flamelet manifolds, using flamelet look-up tables based on freely propagating flames (P-FLUT) and 1D counterflow flames (C-FLUT), by comparing CO mass fraction conditioned on temperature and radial location is shown (right). Building on this, the main outcome in respect of the selection of a suitable tabulated manifold will be discussed.

References

[1] E. Knudsen, H. Pitsch, A general flamelet transformation useful for distinguishing between premixed and non-premixed modes of combustion, Combustion and Flame 156 (2009) 678-696.

[2] E. Knudsen, H. Pitsch, Capabilities and limitations of multi-regime flamelet combustion models, Combustion and Flame 159 (2012) 242-264.

[3] A.R. Masri, Partial premixing and stratification in turbulent flames, Proceedings of the Combustion Institute 35 (2015) 1115-1136.

[4] S. Hartl, R. Van Winkle, D. Geyer, A. Dreizler, G. Magnotti, C. Hasse, R.S. Barlow, Assessing the relative importance of flame regimes in Raman/Rayleigh line measurements of turbulent lifted flames, Proceedings of the Combustion Institute, accepted

[5] M. Ihme , Y.C. See , Prediction of autoignition in a lifted methane/air flame using an unsteady flamelet/progress variable model, Combust. Flame 157 (2010) 1850–1862 .

[6] S. Hartl, D. Geyer, A. Dreizler, G. Magnotti, R.S. Barlow, C. Hasse, Regime identification from Raman/Rayleigh line measurements in partially premixed flames, Combust. Flame, 189 (2018) 126-141.

Experimental and numerical study of flameless combustion in a furnace

X. Huang[1], E.H. van Veen, M.J. Tummers, D.J.E.M. Roekaerts[*]

Department of Process and Energy, Delft University of Technology, The Netherlands

*D.J.E.M.Roekaerts@tudelft.nl

The objective of the current research is to characterize flameless combustion in a lab-scale furnace via detailed measurements and modelling. The goal of the experiments is to observe the flame behaviour and obtain velocity and temperature data using high speed imaging and laser diagnostic techniques. The goal of the modelling is to extend the Flamelet Generated Manifolds (FGM) method to take into account the effects of dilution by recirculated burnt gases. One of the cases of the Delft jet-in-hot-coflow (DJHC) burner [1,2] and the new database for the new lab-scale furnace are used for validation of the model.

This furnace consists of a WS REKUMAT 150 recuperative Flame-FLOX burner and a thermally insulated but optically accessible combustion chamber (32x32x63 cm^3). Experiments were done using Dutch natural gas as fuel and at thermal input 9 kW (fuel mass flow rate based) at three values of equivalence ratio, namely 0.7, 0.8, 0.9. The ignition and flame structure in the flameless regime have been studied by the mean and time resolved OH* chemiluminescence images. Detailed measurements of velocity have been performed with forward scatter Laser Doppler Anemometry (LDA). The forward scatter configuration significantly increases the signal strength and the effects of seeding particles depositing on the optical window become tolerable. Gas temperatures were measured using Coherent anti-Stokes Raman Spectroscopy (CARS) and wall temperatures using thermocouples.

The chemiluminescence measurements show three types of ignition behaviour, namely individual autoignition kernel, multiple autoignition kernels and ignition kernel cluster. The reaction zone (the zone with significant chemiluminescence), is a collection of these three autoignition structures which together are keeping the conversion in the furnace going. We call this situation presence of "sustained combustion". It is different from situations having flame stabilization via explicit mechanisms such as a pilot flame, a bluff body or swirl. The autoignition is depending on local conditions, namely the flow, the mixture composition and the temperature. The latter two are determined by the air dilution level and by the enthalpy deficit of the diluent. This is supported by a numerical study of counterflow flames showing that there exists a dilution range where autoignition can be achieved in a wide range of flow conditions (strain rate). This range provides the best condition to sustain a stable flameless combustion.

The burner nozzle configuration (central fuel jet surrounded by four air jets) is important to establish flameless combustion because together with the confinement it determines the way in which reactant jets are diluted by recirculated flue gas. The main reaction zone occurs in the upper half of the furnace. CARS temperature histograms show a high temperature tail, but in the chemiluminescence images stable flame front like structures are absent. The maximal mean temperature rise in the furnace relative to the reactants is less than 600 K. The instantaneous peak temperatures are lower than 1800 K, the mean of the highest 5% of the samples lower than 1700 K. NOx emissions in the exhaust gas are below 1 ppmv in all cases.

An extended FGM model called diluted air FGM (DAFGM) has been developed for describing flameless combustion in furnaces. It includes the effects of dilution on local conditions using a transport equation for a dilution variable. The reaction zones are represented by conditions retrieved from counterflow flames of undiluted fuel and diluted air including heat loss of the diluted air. These were computed using Chem1D. The control parameters of the FGM for the laminar case are mixture fraction, progress variable, dilution parameter and enthalpy loss (4D table) and for the turbulent case concern the mean values of these variables and the variance of mixture fraction and progress variable (6D table). Local mean radiative source terms are also stored in the table. Radiation is solved using the DOM. The radiative

properties of gases are modelled with a weighted-sum-of-grey-gas (WSGG) model accounting for the local mole ratio between CO_2 and H_2O. The models have been implemented in the open source CFD package OpenFOAM-2.3.1.

The DAFGM model first is applied to the case 'DJHC-I Re=4100' of the DJHC burner database using both RANS and LES approaches [1,2]. It is found that the predictions for this flame are not sensitive to the progress variable fluctuations, but that the surrounding air inlet velocity has effects on the predicted temperature profile at high axial locations. The turbulent flow field statistics and temperature predictions are in overall good agreement with experimental data, with LES performing somewhat better. Next the model is applied to the simulation of the new furnace, operated at equivalence ratio equal 0.8. It is found that in this case the RANS model predictions are very sensitive to fluctuations in progress variable (Figure 1,left, b-c). The final mean temperature rise in the reaction zone is close to the measured mean temperature rise (Figure 2, right). The DAFGM model is found to very well describe the conditions in flameless combustion both in the JHC flame and in the furnace [3].

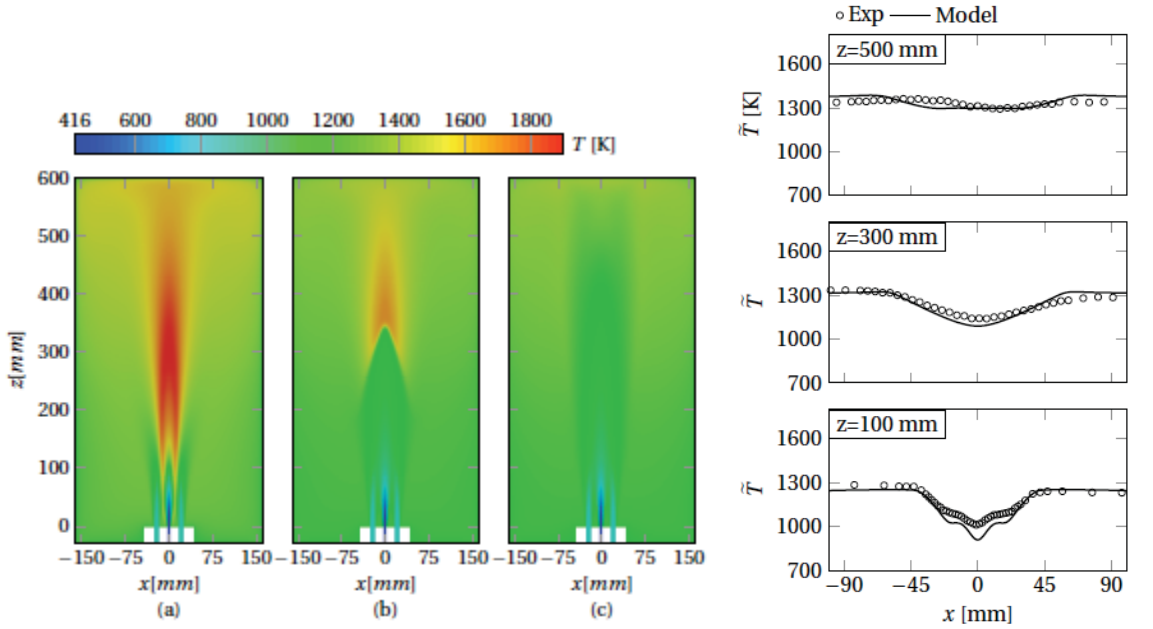

Figure 1: Left: Predicted temperature fields on the vertical mid-plane through two air nozzles: (a) excluding radiation and progress variable variance, (b) including radiation and excluding progress variable variance (c) including radiation and progress variable variance.
Right: Comparison of mean temperature predictions including radiation and progress variable variance with mean temperature from CARS measurements.

Acknowledgements
The first author received support from the China Scholar Council (CSC). The experimental setup was built with support from the Technology Foundation STW. The modelling was sponsored by the Netherlands Organization for Scientific Research (NWO) for the use of supercomputer facilities.

References
[1] E. Oldenhof et al., Combustion and Flame, 2010, 157 (6), 1167 -1178.
[2] E. Oldenhof et al., Combustion and Flame, 2011, 158 (8), 1553-1563
[3] X. Huang, Measurements and model development for flameless combustion in a lab-scale furnace, PhD Thesis, Delft University of Technology, to be published

Combustion regime investigations of turbulent flames by flame-resolved simulations

Eray Inanc[*,1] and Andreas. M. Kempf[1]

[1] Institute for Combustion and Gasdynamics, University Duisburg-Essen, Duisburg, Germany
[*] eray.inanc@uni-due.de

This work presents flame-resolved Large-Eddy Simulation (LES) of a turbulent non-premixed methane jet flame approaching its blow-off limit that is stabilized by hot pilot gas. The Sandia/Sydney Flame Series L by Dibble et al. (C&F 67:189-206) is reproduced. In this experiment, premixed and non-premixed regimes are simultaneously observed, hence the distinctive properties of these two regimes can be shown and analyzed.

The combustion is represented by a variant of the Flamelet Generated Manifold (FGM) method. Two separate manifolds that describe the individual properties of the premixed and the non-premixed regimes are created using one-dimensional flamelets computed by a detailed chemical mechanism. The first manifold uses the thermochemical data obtained from solving one-dimensional freely propagating flames (flamelets), while the latter uses the flamelet data from a counter-flow diffusion flame simulation setup. In the premixed-manifold, the composition-space is represented by local equivalence ratio and the progress-space is created by tracking the mass fraction of the Y_{CO2} and Y_{CO} species. Meanwhile, the non-premixed-manifold's composition-space is mapped considering Bilger's Mixture Fraction on a fixed strain rate, whereas the progress-space is filled by varying the strain-rate of the configuration by increasing mass flow rates of the fuel and/or oxidizer sides and again tracking the mass fractions for the same species as in the rival manifold. The results are then stored in two separate two-dimensional equidistant look-up tables.

The simulations are performed using the in-house LES/DNS solver PsiPhi (see, for example, Inanc et al. Comp&Fluids 140:435-449) in a pressure-based formulation. Favre-filtered governing equations for the mass, the momentum, the mixture fraction Z and the progress variable $Y_p=Y_{CO2}+Y_{CO}$ are solved with a low-storage explicit Runge-Kutta scheme. Convective fluxes of the momentum and the scalar are interpolated using central difference and total variation diminishing schemes, respectively. The computational domain of 160x56x56 mm^3 uses equidistantly spread 700 Million grid points on Cartesian coordinates, with a grid spacing of 90 um, which ensures at least five computation points to represent the thinnest flame fronts of around 0.5 mm. The turbulence is included by an approach developed by Nicoud et al. (Phy. Fluids 23:085106).

The simulated turbulent flame is decomposed into premixed and non-premixed zones based on a flame index, which is then used for deciding which one of the two manifolds is to be applied. The jumps of the applied density values due to the application of different manifolds are treated with smoothing the flame index field by applying a Gaussian-filter, whereas non-smoothed flame index field is used elsewhere. The Artificially Thickened Flame (ATF) method is employed to

resolve the flame front on the LES grid. An assumed top-hat PDF/FDF for Z and Y_p is used to consider the sub-grid part of the filtered scalar quantities.

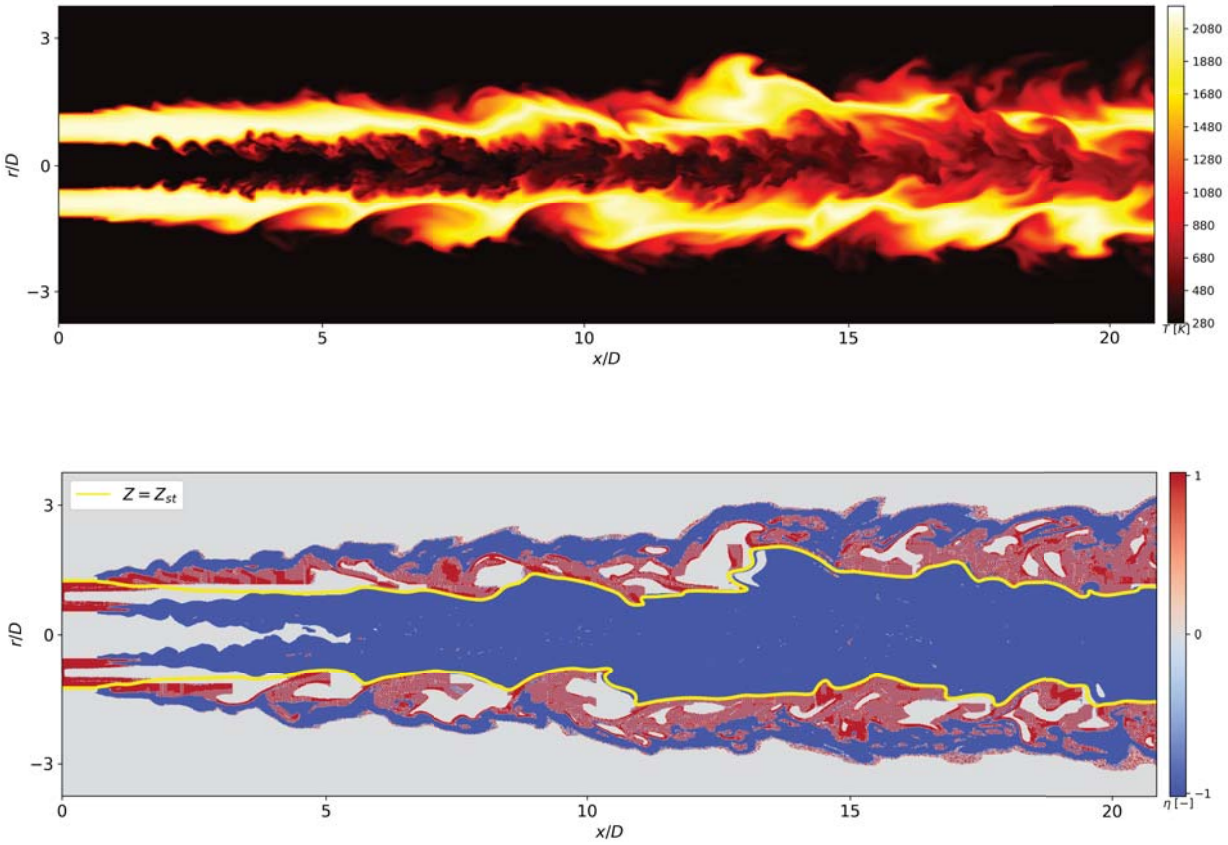

Figure 1: The top plot shows the instantaneous temperature field, the bottom plot shows the computed flame index, where the yellow line is the stoichiometric mixing line. The positive values indicate premixed zones, whereas zero and negative values show non-premixed behavior.

The initial findings show that the flame locally quenches towards the downstream locations (x/d=20), which can be observed from the top plot in Fig. 1. The flame index indicates that the lean side of the flame, where the pilot and the co-flow gases mix, behaves like a premixed flame, as shown in the bottom plot in Fig. 1. The further analysis is omitted for brevity, and will be included in the poster.

The authors gratefully acknowledge the financial support by the state North-Rhine-Westphalia, Germany, and the Center for Computational Sciences and Simulation (CCSS) for providing time on the HPC system magnitUDE (DFG grant INST 20876/209-1 FUGG) at the *Zentrum für Informations- und Mediendienste* (ZIM).

Quantifying kinetic uncertainty in turbulent combustion simulations using active subspaces

Weiqi Ji, Zhuyin Ren
Center for Combustion Energy, Tsinghua University, Beijing 100084, China
E-mail: zhuyinren@tsinghua.edu.cn **(**Zhuyin Ren**)**

Turbulent combustion simulation is usually associated with uncertainties from the turbulent combustion model, the chemical kinetic model, the boundary conditions, etc. To evaluate the performance of various turbulent combustion models on TNF target flames, it is essential to isolate the uncertainty resulted from the reaction kinetics. The uncertainty quantification in expensive turbulent combustion simulations usually adopts response surface techniques to accelerate Monte Carlo sampling. However, it is computationally intractable to build response surfaces for high-dimensional kinetic parameters.

We employ the *active subspaces* [1] approach to reduce the dimension of the parameter space, such that building a response surface on the resulting low-dimensional subspace requires many fewer runs of the expensive simulation. The active subspace can be identified by computing the "average gradient" of the simulation output over the uncertainty parameter space. Specifically, the active subspace can be computed via the eigendecomposition of following matrix $\boldsymbol{C}$.

$$\boldsymbol{C} = \int \nabla f(\mathbf{x}) \nabla f(\mathbf{x})^T \pi_x(\mathbf{x}) \mathrm{d}\mathbf{x} = \boldsymbol{W \Lambda W^T},$$

where $\mathbf{x}$ is the vector of the uncertain parameters, f is the function mapping the inputs to the simulation output, and $\pi_x(\mathbf{x})$ is the probability distribution of the uncertain parameters. The leading vectors can be chosen as the active directions, along which the simulation output may vary significantly with the inputs. Active directions in general correspond to linear combinations of the uncertainty parameters.

We demonstrate this approach in the transported PDF simulations of the Cabra H_2/N_2 jet flame [2], propagating the uncertainties of 21 kinetic parameters to the liftoff height H. The configuration of the simulation is identical to [3] and the OH contour plot is shown in . We identify a one-dimensional active subspace for the liftoff height using 84 runs of the simulations, from which a response surface with a one-dimensional input is built; the probability distribution of the liftoff height is then characterized by evaluating 50000 samples using the inexpensive response surface.

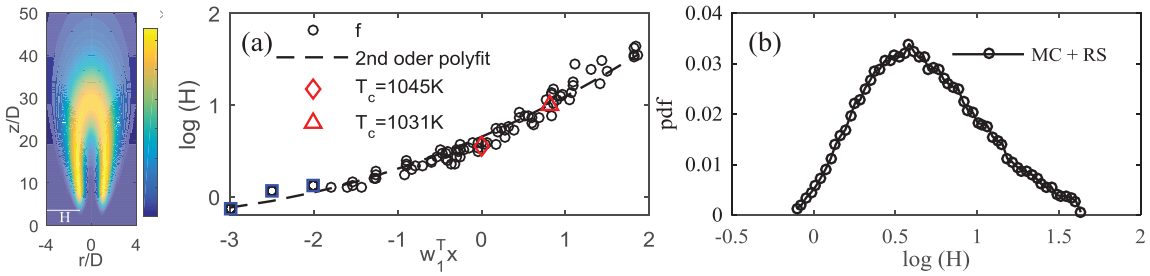

Fig. 1 The left side is the contour plot of OH concentration. (a) The summary plot of the lifted height H versus the projected variable of the 21-dimensional input parameters $\mathbf{x}$ onto the one-dimensional active direction $\mathbf{w}_1$. The red symbols corresponding to the equivalent

changes in the rate constants by changing the co-flow temperature. (b) The probability distribution function of the predicted lifted height *H*.

Figure 1a shows the summary plot of the predicted lifted height versus the projected variable of the input parameters in the active direction. All of the changes in the predicted lifted height can be explained by the changes within the one-dimensional active subspace. The uncertainty of the predicted lifted height is shown in Fig. 1b, and it reveals that the kinetic uncertainty alone is large enough to account for the discrepancies between the lifted height from measurements and simulations.

In addition, the active subspace provides a global sensitivity metric for determining the most influential reactions, i.e., large components of the active direction indicate high sensitivity. Figure 2 shows the components of the active subspace for the lifted height, together with the one for the ignition delay time (IDT) at the characteristic temperature of Cabra flame. The comparisons show that the sensitive reactions are generally the same between the auto-ignition case and the Cabra flame, and the difference in the value of the components reveals that the sensitivities to the HO_2-related reactions in the Cabra flame are promoted by the diffusion processes.

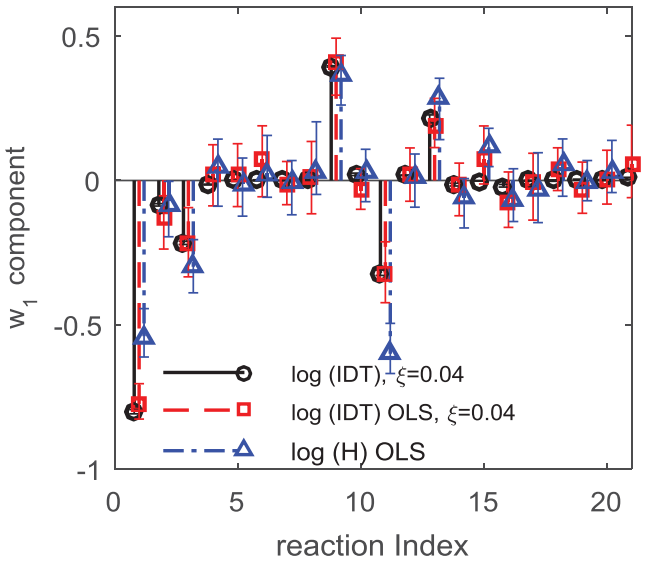

Fig. 2 The components of the active subspace. Both the circle and square symbols refer to the active subspace for the ignition delay time (IDT) but identified in different approaches.

References

[1] P.G. Constantine, E. Dow, Q. Wang, SIAM J. Sci. Comput, 36 (2014) A1500-A1524.
[2] R. Cabra, T. Myhrvold, J.Y. Chen, R.W. Dibble, A.N. Karpetis, R.S. Barlow, Proc. Combust. Inst., 29 (2002) 1881-1888.
[3] A. Masri, R. Cao, S. Pope, G. Goldin, Combust. Theor. Model., 8 (2004) 1-22.

LES of Cambridge Stratified Swirl Burner by using the Flamelet Generated Manifold Method

S. Karaca, D.M.J. Smeulders, L.P.H de Goey, J.A. van Oijen

Eindhoven University of Technology, s.karaca@tue.nl

Abstract

Controlling combustion and reducing the emissions of harmful gases such as CO and NO_x are challenging issues. Approximately two-thirds of the CO emissions come from transportation sources, therefore reduction of CO emissions in combustion engines has a significant importance. In this work, LES of the Cambridge stratified swirl burner (SwB3) is studied by using a low-Mach open-source OpenFOAM solver. Combustion is modeled by using the Flamelet Generated Manifold (FGM) method [1] which uses one-dimensional premixed flames computed with detailed chemistry and transport models to generate a flamelet database. The progress variable is defined as a combination of the mass fractions of CO_2, H_2O and O_2. To account for fuel stratification, flamelets are computed with changing equivalence ratio from 0.4 to 1.2. Chemical equilibrium assumption is used to extrapolate the FGM table in mixture fraction space towards the air stream. As an initial study, heat loss and turbulence-chemistry interaction are not included and CO is retrieved directly from the FGM table. As a further study the beta-pdf approach will be used to account for turbulence-chemistry interaction and a transport equation for CO will be solved.

The burner has a bluff-body in the center and two concentric pipes around that bluff-body with 34.8 mm and 23.6 mm diameter. A detailed description of the experimental geometry and injector geometry can be found in [2]. The computational domain has 110 mm diameter and 110 mm length with an extra 12 mm for the injector. The bulk velocity of the inner annulus, outer annulus and coflow are respectively U_i=8,3 m/s, U_o=18.7 and U_{co}=0.4 m/s. The LEMOS synthetic inflow turbulence generator is used to generate turbulent inflow with uniform velocity profile distribution. The swirl ratio is defined experimentally as U_t/U_o=0.79. Ambient pressure is defined as inflow boundary condition (b.c.) for inner and outer annulus and a wave-transmissive b.c. is used for pressure at the outflow and far field. Inflow temperature is set to 300 K. The equivalence ratio for inner and outer annulus are identical (0.75) for this case. Since the CFL number is restricted to 1.0, the physical time step is around $6x10^{-6}$ s. The computational domain has 1.7 million cells and the laminar flame thickness is resolved by 2-4 grid points.

Figure 1 shows mean velocity profiles at different axial locations. The numerical data match well with the experimental data. Figure 2 shows mean temperature and mean species profiles. The temperature difference between numerical and experimental data is around 200K close the burner, away from the injector numerical temperature field matches well with experiment. Close to the burner CO is over-predicted but further downstream the agreement with measurements is satisfactory. The overestimation of temperature and CO close to the burner can be attributed to heat loss to the bluff-body, which was neglected in this preliminary run (see Figure 3) but will be included in our next runs. The swirl and flow structures are visualized in Figure 4 by using the Lambda2 vortex criterion.

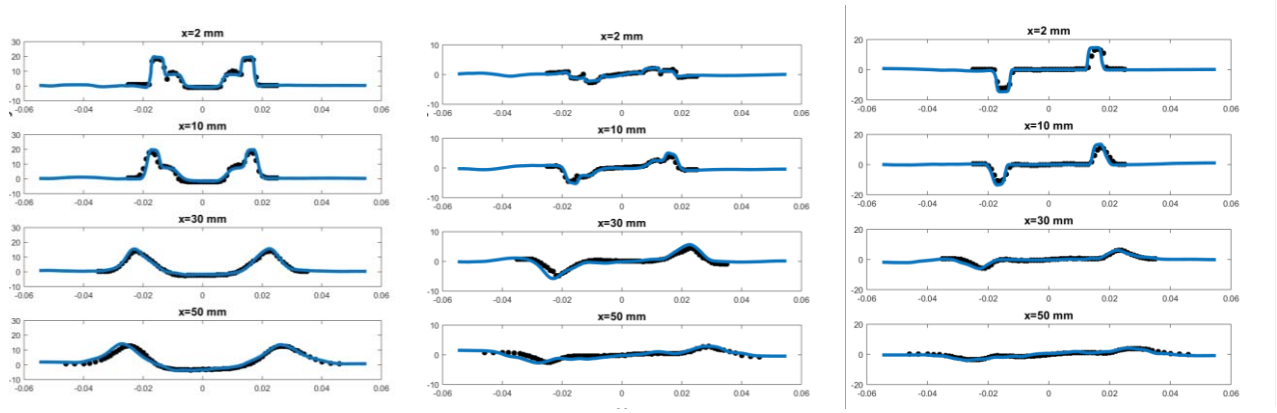

Figure 1 – Mean axial (left), radial (middle), and tangential (right) velocities at different axial locations

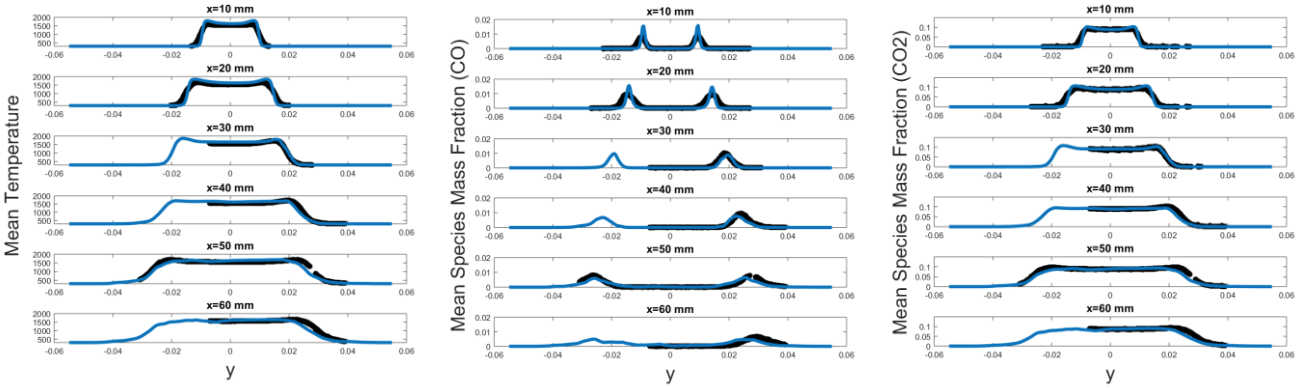

Figure 2 – Radial profiles of mean temperature, CO and CO_2 mass fraction at different axial locations

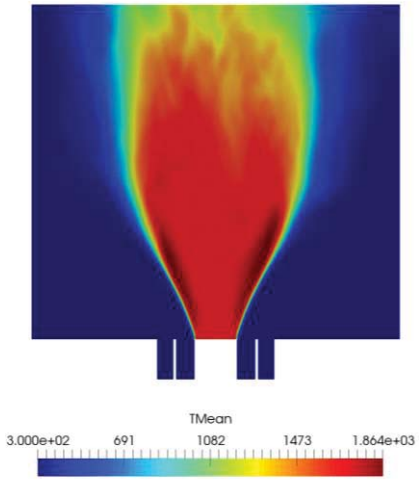

Figure 3 – Mean temperature field (YZ Slice)

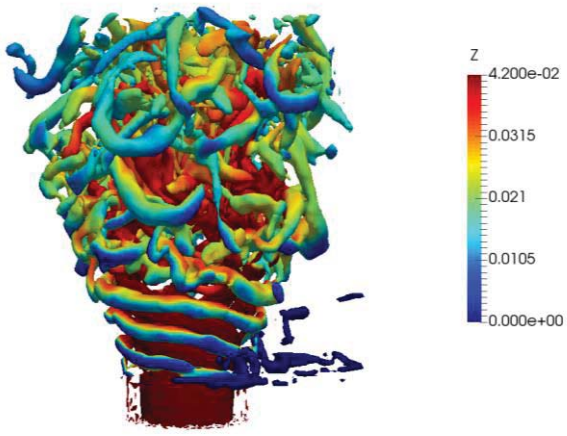

Figure 4 – Lambda2 criterion colored by mixture fraction (isovalue=10^6 $1/s^2$)

References

[1] van Oijen, J.A., et al., “State-of-the-art in premixed combustion modeling using flamelet generated manifolds”, *Prog. Energy Combust. Sci.* 57 (2016): 30-74.

[2] Sweeney, Mark S., et al. "The structure of turbulent stratified and premixed methane/air flames II: Swirling flows." *Combust. Flame* 159 (2012): 2912-2929.

MODELING FOR TURBULENT PILOTED PREMIXED JET FLAMES

N. Kim[1], J. Kim[2], Y. Kim[2*]
[1]KIER, [2]Hanyang University, Korea
ymkim@hanyang.ac.kr

The multi-environment PDF approach [1] has been applied to numerically investigate a series of the Sydney piloted premixed jet burner(PPJB)[2]. In the present multi-environment PDF model, one-point statistical properties of the joint scalar PDF are described by a deterministic Eulerian way. The joint composition PDF is expressed by the combination of weighted Dirac delta functions on composition and physical space. The important advantage of this model is that the mean chemical reaction term appears in closed form. The IEM mixing model is employed to represent the mixing process. In this PPJB burner [2], a central high-speed lean methane/air jet is stabilized by a pilot with a stoichiometric methane/air mixture and the burner is embedded in an outer vitiated coflow of lean hydrogen/air combustion products with the low velocity. This PPJB configuration was intentionally designed to resemble the combustion conditions relevant to partially-premixed gas turbine combustors without additional geometry complexities. The computations are made for three flames (PM1-100, PM1-150 and PM1-200). As shown in Figure 1, the present approach yields the reasonably good agreements for the mean temperature and CO mass fraction for all three cases even if there exist the noticeable deviations at the certain axial locations. Due to the much earlier local extinction, especially at x/D=15 for the higher jet velocity cases (PM1 150 and 200), the temperature levels in the inner hot flame zone are noticeably underestimated and the peak CO levels are underestimated. Fig. 2 shows OH conditional scatters in the central-jet mixture fraction space and CO conditional scatters in temperature space for three flames. The predicted environment-conditional statistics at the near-injector region clearly identify the dual premixed flame modes established by the stoichiometric pilot flame and the lean premixed central jet. The dual premixed flame modes are identified as the two near vertical transition of OH mass fraction in the mixture fraction space. One premixed flame mode is caused by the stoichiometric pilot flame propagation where the central-jet mixture fraction is close to zero. The other premixed flame structure is arising from the central lean stratified premixed flame propagation at the central-jet mixture fraction much larger than zero. The much higher injection velocity cases (PM1-150, PM1-200) yield the remarkably low peak OH level due to the local extinction. At further downstream location (x/D=45), it is observed that the peak OH levels are noticeably elevated for the higher injection velocity cases because of the reignition process. In terms of the measured conditional scatters and the environment-conditional values for the CO mass fraction in the temperature space, at the near-injector region (x/D=2.5), the present three-environment PDF approach well captures the dual flame modes at the temperature higher than 1500K. At this temperature range (T > 1550K), the upper branch is corresponding to the stoichiometric piloted flame mode while the lower branch represents the central-jet oriented lean premixed flame mode. It is also found that, by increasing the jet injection velocity, the peak CO location moves to the much higher temperature region. Moreover, the much higher injection velocity cases (PM1-150, 200) yield the much lower peak CO level due to the local extinction. At further downstream location (x/D=45), it is observed that the peak CO levels are slightly elevated for PM1-150 and PM1-200 owing to the reignition. Numerical results suggest that the present MEPDF approach has the capability to realistically predict the essential features of the highly stretched turbulent piloted stratified premixed flames with local extinction and reignition as well as the significant finite-rate chemistry effects.

References

[1] N. Kim, Y. Kim, Multi-environment probability density function approach for turbulent partially-premixed methane/air flame with inhomogeneous inlets, Combust. Flame 182 (2017), 190-205.
[2] M.J. Dunn, Finite-Rate Chemistry Effects in Turbulent Premixed Combustion. PhD thesis, The University of Sydney, 2008.

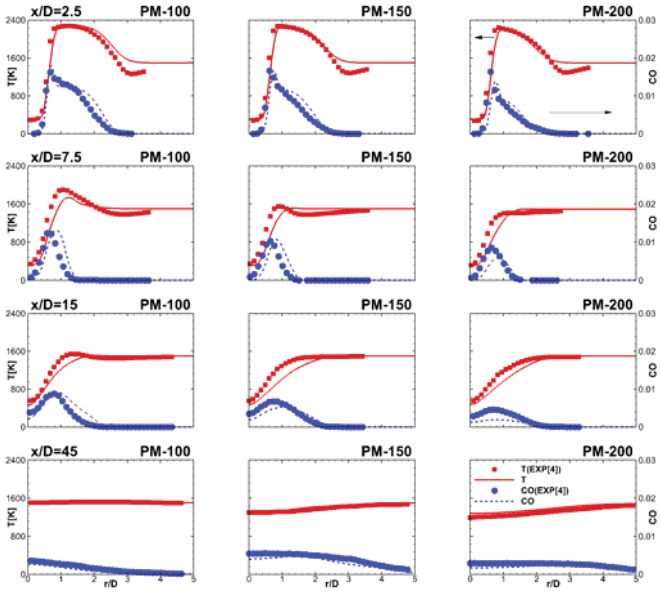

Fig. 1 Predicted and measured [2] unconditional means of temperature and CO mass fraction for three flames.

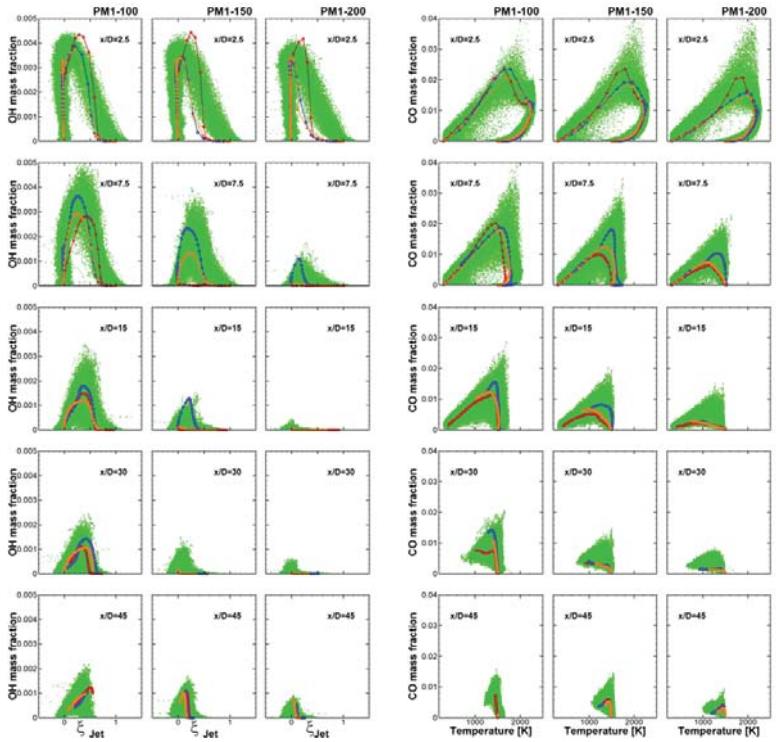

Fig. 2 OH conditional scatters in the central-jet mixture fraction space and CO conditional scatters in temperature space for three flames; fuel stream environment (red circle), pilot jet environment (blue circle), and air co-flow environment (yellow circle) are compared with experimental data [2] (green dots)**.**

Advanced laser diagnostics for an improved understanding of premixed flame-wall interactions

H. Kosaka [a)], F. Zentgraf [a)], A. Scholtissek [b)], C. Hasse [b)], A. Dreizler [*,a)]

a) *Institute of Reactive Flows and Diagnostics, TU Darmstadt, Darmstadt, Germany*
b) *Institute of Simulation of Reactive Thermo-Fluid Systems, TU Darmstadt, Germany*

* dreizler@rsm.tu-darmstadt.de

Flame quenching at cold walls and flame-wall interaction (FWI) play an important role in gas turbines and internal combustion engines. The interest in FWI is primarily related to heat losses, incomplete combustion (unburned hydrocarbons, carbon monoxide formation) and formation of wall deposits. An in-situ investigation of the phenomena during FWI in close-to-reality combustion systems is hindered by the limited access for optical diagnostic methods and small length scales in boundary layers at elevated pressures. To overcome these restrictions, generic FWI-experiments were developed in the past. Examples are devices to study head-on quenching (HOQ) [1] and side-wall quenching (SWQ) [2].

This study focusses on the characterization of thermochemical states and local heat release rates within atmospheric flames in a SWQ geometry, including laminar and turbulent flow conditions. The influence of different fuels is compared for stoichiometric methane and dimethyl ether (DME) flames.

A sketch of the SWQ burner [2] is shown in Fig. 1. The main flow passes through a Morel-type nozzle to provide a top-hat velocity profile at the exit (quadratic nozzle exit, 40×40 mm²). The Reynolds number of the premixed main flow is maintained at 5000. The main flow can be operated with an optional turbulence grid (TG) for generating turbulent flames and without TG for laminar conditions. An atmospheric V-flame is stabilized on a ceramic rod. One branch of the V-flame quenches at the wall which is made of stainless steel. The temperature of the wall is set to 330 K and controlled by internal water-cooling. Thermocouples are embedded in the wall to measure temperatures close to the wall surface.

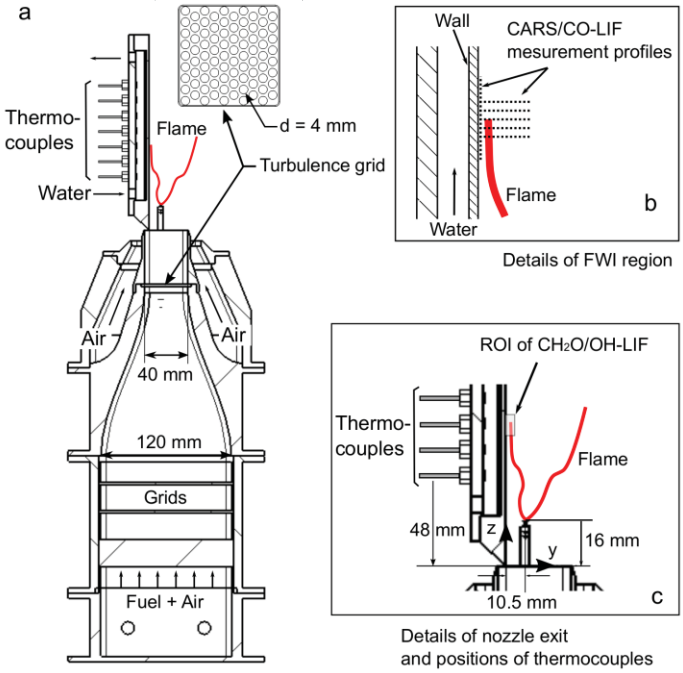

Fig. 1: a) Cross-section of the SWQ burner. b) Details of the FWI region. c) Details of the nozzle exit.

Thermochemical states are analysed using CO/T scatter plots. Gas phase temperatures are measured by Coherent anti-Stokes Raman spectroscopy (CARS) and CO-concentrations by two-photon laser induced fluorescence (LIF). For flame front tracking, planar OH-LIF is applied. All quantities are acquired simultaneously. The combined CARS, CO-LIF and planar OH-LIF setup was previously described in detail [3].

In Fig. 2, scatter plots are presented for a subset of two probe volume locations at the quenching height. The scatter plots are separated into CO formation and CO oxidation branches, based on the location of the probe volume relative to the flame front position derived from OH-LIF. To complement the experiment, the results from one-dimensional laminar flame calculations with and without heat losses are presented. Compared to flame calculations, the CO/T dependencies are influenced significantly by the presence of a wall. Very close to the wall (y = 0.1 mm), for methane/air flames and to a lesser extent for DME/air flames, the CO production branch is shifted towards lower temperatures. In contrast, the CO oxidation branch is shifted to lower temperatures in the entire near-wall region for both fuels. One-dimensional premixed flame calculations accounting for enthalpy losses indicate that heat losses to the wall are a likely cause rather than different chemical reaction pathways.

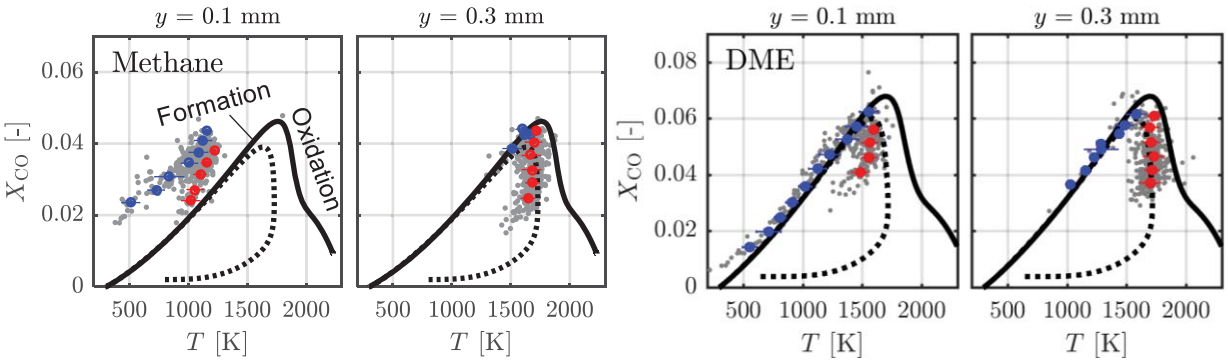

Fig. 2: Scatter plots of gas phase temperature and CO mole fractions at the quenching height. Conditional mean (blue: CO formation branch, red: CO oxidation branch) of experimental data are compared to the results obtained from flame calculation.

Additionally, the local heat release rate (HRR) distribution is estimated from the product of CH_2O and OH-PLIF signals. Figure 3 shows exemplary instantaneous CH_2O and OH-PLIF signals, and the corresponding relative HRR image from a turbulent stoichiometric DME-flame. The HRR-image is normalized to the maximum intensity in the unstretched flame region (rectangle in Fig. 3). Relative HRRs decrease when the flame approaches the wall. In the turbulent case, relative HRRs significantly fluctuate in the FWI-zone. These fluctuations will be identified in an ongoing statistical analysis.

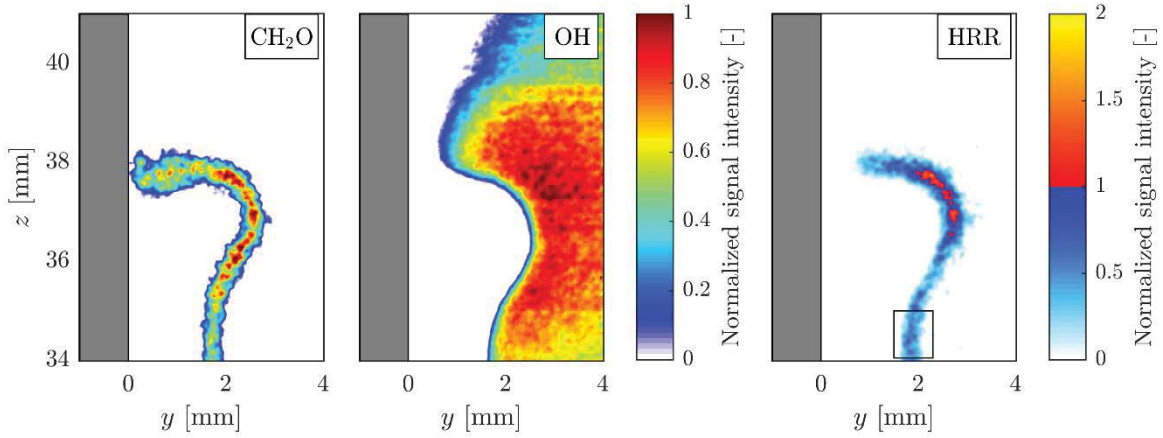

Fig. 3: Instantaneous relative CH_2O-, OH-PLIF images and corresponding relative HRR image during SWQ for a turbulent DME-air flame (ϕ = 1). The gray rectangle (y < 0 mm) marks the position of the wall.

[1] M. Mann, C. Jainski, M. Euler, B. Böhm, A. Dreizler, Combust. Flame, 161 (2014) 2371-2386
[2] C. Jainski, M. Rißmann, B. Böhm, J. Janicka, A. Dreizler, Combust. Flame 183 (2017) 271-282
[3] H. Kosaka, F. Zentgraf, A. Scholtissek, L. Bischoff, T. Häber, R. Suntz, B. Albert, C. Hasse and A. Dreizler, Int. J. Heat and Fluid Flow 70 (2018) 181-192

LARGE EDDY SIMULATION OF CAMBRIDGE TURBULENT STRATIFIED FLAME WITH PASR MODEL: CO PREDICTION

***Z. Li*[1,*], *P. Gruhlke*[2] *and A. Parente*[1,**]**

[1] ***Université Libre de Bruxelles, Aero-Thermo-Mechanics Department, Belgium***
[2] ***Universität Duisburg Essen, Institute for Combustion and Gas Dynamics, Germany***
[*] ***Zhiyi.Li@ulb.ac.be***
[**] ***Alessandro.Parente@ulb.ac.be***

1 Introduction

Stratification in lean pre-mixed combustion helps to increase the flame propagation speed and flame front wrinkling [1, 2]. Therefore, it is important to investigate the fundamental properties of stratified combustion. The Cambridge Stratified Swirl Burner [3, 4] provides a flame series that allows for the numerical investigation of stratified combustion at laboratory conditions. High fidelity scalar and vector measurement data are available for numerical validation.
Analysis of Cambridge flame in the literature [5, 6, 7, 8] has shown that most of the numerical strategies present fair predictions on the velocity and temperature fields, as well as the major species like CH_4 and O_2. However, larger discrepancies with the experimental data has been observed for the prediction on mean and RMS of CO. In comparison to the temperature or major species mass fractions, the CO prediction is more sensitive to the detailed combustion chemistry and the sub-grid scale flame wrinkling modelling approaches. As a result, in the current work, the Partially Stirred Reactor (PaSR) combustion model in combination with Large Eddy Simulation (LES) is used. The lean highly-swirled SwB3 case of Cambridge flame is chosen for validation.

2 Partially Stirred Reactor model

The Partially Stirred Reactor (PaSR) [9] separates each computational cell into two zones. Reaction happens only in a fraction of the cell, identified by the reacting fraction κ [10]. Thus, the mean source term can be expressed as:

$$\overline{\dot{\omega}}_k = \kappa \dot{\omega}_k^*(\widetilde{\boldsymbol{Y}}, \widetilde{T}). \tag{1}$$

In Equation 1, $\dot{\omega}_k^*(\widetilde{\boldsymbol{Y}}, \widetilde{T})$ represents the formation rate of species k based on the Favre-averaged mass fractions of species in the cell. The term κ is a coefficient which considers the non-perfect mixing, calculated as:

$$\kappa = \frac{\tau_c}{\tau_c + \tau_{mix}}, \tag{2}$$

where τ_c is the characteristic chemical time scale in each cell and τ_{mix} is the mixing time scale. In the present study, the chemical time scale of each species is estimated by $\tau_{c,k} = Y_k^*/(dY_k^*/dt)$, where Y_k^* and dY_k^*/dt are mass fraction of the k_{th} species and the corresponding formation rate in the reacting zone, respectively. The highest limiting value is chosen as the characteristic chemical time scale, considering only active species (the species characterized by an absolute rate of change (dY_k^*/dt) higher than a given threshold). The mixing time scale is represented with the geometrical mean of the sub-grid velocity stretch time ($\Delta/v^{'}$) and the Kolmogorov time scale ($(\nu/\epsilon_{sgs})^{1/2}$) [11].

The reactive zone is assumed to be a Perfectly Stirred Reactor (PSR) [12]. In this time-splitting approach, the reactive zone is modelled as a reactor:

$$\frac{dY_k}{dt} = \frac{\dot{\omega}_k}{\rho}. \tag{3}$$

The term $\dot{\omega}_k$ is the instantaneous formation rate of species k. The final integration of $\frac{dY_k}{dt}$ over the residence time τ in the reactor is Y_k^*. The term $\dot{\omega}_k^*(\widetilde{\boldsymbol{Y}}, \widetilde{T})$ in Equation 1 is thus estimated with:

$$\dot{\omega}_k^*(\widetilde{\boldsymbol{Y}}, \widetilde{T}) = (Y_k^* - \widetilde{Y}_k)/\tau. \tag{4}$$

In the present work, τ equals to CFD time step.

3 Numerical details

A 3D mesh containing around 6.8 million cells is used for LES simulation. The domain extends 112 mm further downstream after the jet exit and the radial direction expands 56 mm away from the centerline. The LEMOS [13] inflow generation method for velocity field is applied on the two pre-mixed streams and the `WaveTransmissive` [14] boundary condition is used for pressure outlet. LES sub-grid model of one Equation Eddy Viscosity (`oneEqnEddy`) is chosen as turbulence model [15]. A skeletal mechanism which contains 17 species and 58 reactions [16] (KEE58) is used for finite-rate chemistry approach.

4 Expected Results

A non-reacting case will be conducted first to check the boundary conditions used for velocity field. The simulation will be further extended to reacting case and the mean/RMS of temperature, major species mass fractions as well as the CO mass fraction profiles will be validated against the experimental measurements. The current chemical reaction approach with PaSR model can also be compared with the other choices like flamelet related approaches and Artificially Thickened Flame (ATF) model, to demonstrate the sensitivity of CO prediction regarding the combustion models selected.

Acknowledgments

This project has received funding from the European Union′s Horizon 2020 research and innovation program under the Marie Skłodowska-Curie grant agreement No. 643134. The research of the last author is sponsored by the European Research Council, Starting Grant No. 714605.

References

[1] B. Renou, E. Samson, A. Boukhalfa, Combust. Sci. Technol. 176 (11) (2004) 1867–1890.
[2] N. Pasquier, B. Lecordier, M. Trinité, A. Cessou, Proc. Combust. Inst. 31 (2007) 1567–1574.
[3] M. S. Sweeney, S. Hochgreb, M. J. Dunn, R. S. Barlow, Combust. Flame 159 (9) (2012) 2896 – 2911.
[4] M. S. Sweeney, S. Hochgreb, M. J. Dunn, R. S. Barlow, Combust. Flame 159 (9) (2012) 2912 – 2929.
[5] R. Mercier, T. Schmitt, D. Veynante, B. Fiorina, Proc. Combust. Inst. 35 (2) (2015) 1259–1267.
[6] S. Nambully, P. Domingo, V. Moureau, L. Vervisch, Combust. Flame 161 (7) (2014) 1775 – 1791.
[7] F. Proch, A. M. Kempf, Combust. Flame 161 (10) (2014) 2627 – 2646.
[8] T. Brauner, W. P. Jones, A. J. Marquis, Flow Turbul. Combust. 96 (4) (2016) 965–985.
[9] J. Chomiak, Combustion: a study in theory, fact and application, Abacus press/gorden and breach science publishers, 1990.
[10] F. P. Kärrholm, Numerical modelling of diesel spray injection, turbulence interaction and combustion, Phd thesis, Chalmers University of Technology, Chalmers, Sweden (2008).
[11] V. Sabelnikov, C. Fureby, Progress in Propulsion Physics 4 (2013) 539–568.
[12] C. Duwig, P. Iudiciani, Fuel 123 (2014) 256–273.
[13] N. Kornev, H. Kröger, E. Hasse, Commun. Numer. Meth. Engng 24 (2008) 875–877.
[14] T. J. Poinsot, S. K. Lele, J. Comput. Phys. 101 (1) (1993) 104–129.
[15] A. Yoshizawa, K. Horiuti, J. Phys. Soc. Jpn. 54 (1985) 2834–2839.
[16] R. W. Bilger, S. H. Stårner, R. J. KEE, Combust. Flame 80 (2) (1990) 135–149.

Coefficients Specification for a Conceptually Simplified Multiple Mapping Conditioning Model with Mixture Fraction like Reference Variable

Zisen Li[1*], Armin Wehrfritz[1], Bruno Savard[1] and Evatt R. Hawkes[1,2]
[1]School of Mechanical and Manufacturing Engineering, University of New South Wales, Sydney, NSW 2052, Australia
[2]School of Photovoltaic and Renewable Energy Engineering, University of New South Wales, Sydney, NSW 2052, Australia

Abstract

The multiple mapping conditioning (MMC) framework [1] for closure of the micro-mixing term in transported probability density function methods offers controllable locality of mixing without formal violation of the principle of independence of mixing [2]. Recently, a novel, conceptually simplified, MMC model with a mixture fraction-like reference variable (hereafter referred to as the SMMC model) was proposed [3, 4]. In the model, the reference variable, ξ, evolves by an Ornstein – Uhlenbeck (OU) process (eq. 1), and minor mixing is achieved by relaxation of scalars towards their means conditional on ξ (eq. 2).

$$d\xi^* = -\frac{C_\xi}{\tau}(\xi^* - \langle\xi\rangle)dt + b_0\sqrt{\frac{2C_\xi\langle\xi'^2\rangle}{\tau}}dW_\xi \quad (1)$$

$$d\phi^* = -\frac{C_{min}}{\tau}(\phi^* - \langle\phi\rangle)dt \quad (2)$$

There are three free coefficients to be determined for the SMMC model: the major mixing coefficient C_ξ (controlling drift in the OU process), the Wiener term coefficient b for ξ (controlling diffusion in the OU process), and the minor mixing coefficient, C_{min}. In the SMMC model, it is desired that ξ has the same mean and variance as mixture fraction, Z, and also that the implied scalar dissipation of mixture-fraction can be set to a user specified model, e.g. $\chi = C_\phi\langle Z'^2\rangle/\tau$. It is also desired that the user can control the localness of mixing, for example by specifying the correlation coefficient between ξ and Z, $r = \langle\xi'Z'\rangle/(\langle\xi'^2\rangle\langle Z'^2\rangle)^{1/2}$. In the original work [3], the coefficients of the SMMC model were specified to achieve these outcomes according to a homogeneous isotropic turbulence (HIT) reference case for which analytical expressions can be determined, and it was demonstrated numerically that this approach also works well in a jet flow for highly local models. However, it is unclear whether this result applies to other flows and whether it applies to less local models as well. In the current work, therefore, we compare the HIT settings to those determined in a homogeneous turbulence reference case with a mean scalar gradient (MSG), apply the models to a new flow where DNS is available, and assess the outcomes across a wider range of localness.

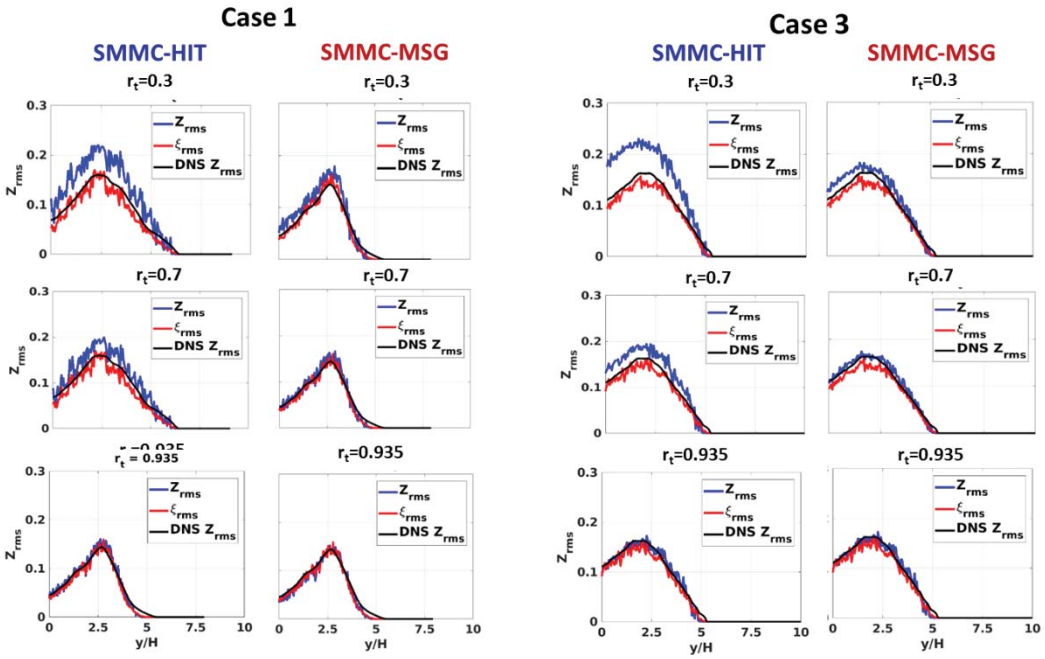

Fig. 1 Reference variable (red) and mixture fraction (blue) variance compared to DNS results (black) of Case 1 (left group) and Case 3 (right group) at 60 characteristic jet times. Results in each column in each case are obtained with SMMC-HIT and SMMC-MSG coefficient settings, respectively.

The SMMC model parametrised by the HIT and MSG cases is validated against DNS results. Three DNS datasets of a turbulent nonpremixed ethylene flame [5] with increasing extinction levels (Case 1, 2, 3) are used for comparison as well as to provide input data for the TPDF simulations. The TPDF code uses inputs from the

*Corresponding author. E-mail: zisen.li@student.unsw.edu.au

DNS data of the micro-mixing rate of mixture fraction, the turbulent diffusion coefficient of the mean mixture-fraction, and the mean flow velocities [6]. In models where the unconditional micro-mixing rate can be directly specified, e.g. IEM and MC, these inputs result in near-perfect agreement with the DNS for the mixture-fraction variance. In SMMC and in other MMC-like models, however, it is the unconditional mixing rates depend not only upon specified constants but on the correlations between real and reference scalars, which in turn depend on the flow history. The results of SMMC-MSG and SMMC-HIT cases are compared to DNS results. It is found that both sets of model coefficients yield good predictions for the mean mixture fraction and temperature profile for the default value [3, 4] of r_t, i.e. r_t =0.935. It is also found that SMMC-MSG yields improved predictions for mixture fraction variance. Figure 1 shows the mixture fraction variance (Z_{rms} in the figure) predicted by both models for Case 1 (lowest extinction) and Case 3 (highest extinction) with different r_t values. It shows that SMMC-MSG yields good predictions for Z_{rms} over a wide range of r_t values while SMMC-HIT only yields a good agreement when r_t approaches unity, i.e. when ξ and Z are highly correlated and leading to high level of localness in the SMMC mixing model. In conclusion, we have demonstrated that for highly local models, the HIT and MSG settings give very similar results in a new flow. The present results are more definitive than the previous ones in [3, 4] due to the availability of the DNS where the micro-mixing rate is known. Finally, setting the SMMC coefficients according to the MSG case allows the localness of the model to be varied without adversely affecting the prediction of mixture fraction variance, in contrast to the HIT settings which result in over-prediction of the variance for less local models. Future work is planned to conduct similar tests for other MMC-type models.

References

[1] A.Y. Klimenko, S.B. Pope, The modeling of turbulent reactive flows based on multiple mapping conditioning, Physics of Fluids 15 (2003) 1907-1925.

[2] S. Subramaniam, S.B. Pope, A mixing model for turbulent reactive flows based on Euclidean minimum spanning trees, Combustion and Flame 115 (1998) 487-514.

[3] A. Varna, M.J. Cleary, E.R. Hawkes, A multiple mapping conditioning mixing model with a mixture-fraction like reference variable. Part 1: Model derivation and ideal flow test cases, Combustion and Flame 181 (2017) 342-353.

[4] A. Varna, M.J. Cleary, E.R. Hawkes, A multiple mapping conditioning mixing model with a mixture-fraction like reference variable. Part 2: RANS implementation and validation against a turbulent jet flame, Combustion and Flame 181 (2017) 354-364.

[5] D.O. Lignell, J.H. Chen, H.A. Schmutz, Effects of Damköhler number on flame extinction and reignition in turbulent non-premixed flames using DNS, Combustion and Flame 158 (2011) 949-963.

[6] A. Krisman, J.C.K. Tang, E.R. Hawkes, D.O. Lignell, J.H. Chen, A DNS evaluation of mixing models for transported PDF modelling of turbulent nonpremixed flames, Combustion and Flame 161 (2014) 2085-2106.

Large-eddy simulation of Sandia Flame F using nonlinear structural subgrid-scale models and partially stirred reactor approach

Hao Lu[1], Wuzhong Chen, Chun Zou[2], Hong Yao

Huazhong University of Science and Technology, Wuhan 430074,China

E-mail: haolu@hust.edu.cn , zouchun@hust.edu.cn

METHODS

1.Subgrid-scale model

The SGS parameterization is the key to accurate LESs of turbulent flows. In this study, we adopt the Smagorinsky model[1] (SM) and the recently developed gradient-type structural models[2,3] (NLES).

1) Gradient-type structural models

$$\tau_{ij} = 2\bar{\rho}k_{sgs}\left(\frac{\tilde{G}_{ij}}{\tilde{G}_{mm}}\right) + \bar{\rho}\nu_{sgs}^{\mu}\nabla^2\tilde{S}_{ij}\,,\quad q_i = |q|\left(\frac{\tilde{G}_{\theta,i}}{|\tilde{G}_{\theta}|}\right)$$

where $\tilde{G}_{ij} = \frac{\tilde{\Delta}^2}{12}\frac{\partial\tilde{u}_i}{\partial x_m}\frac{\partial\tilde{u}_j}{\partial x_m}$ and $\tilde{G}_{\theta,i} = \frac{\tilde{\Delta}^2}{12}\frac{\partial\tilde{u}_i}{\partial x_m}\frac{\partial\tilde{\theta}}{\partial x_m}$ are the leading terms of the Taylor expansions of the exact SGS stress and flux. More, we solve the transport equation of the SGS kinetic energy to relax the local equilibrium hypothesis [2].

$$\frac{\partial k_{sgs}}{\partial t} + \tilde{u}_j\frac{\partial k_{sgs}}{\partial x_j} = -\frac{\tau_{ij}}{\bar{\rho}}\frac{\partial\tilde{u}_i}{\partial x_j} - C_c\frac{k_{sgs}^{3/2}}{\Delta} + \frac{\partial}{\partial x_j}\left[\left(\frac{\nu_{sgs}}{\sigma_k}+\nu\right)\frac{\partial k_{sgs}}{\partial x_j}\right]$$

2.Other settings

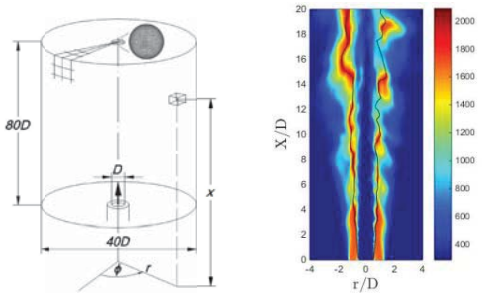

Figure 1: (L) Schematic representation of the simulation domain. (R) Snapshots of instantaneous temperature contours of Sandia Flame F. Black solid lines indicate isolines of the stoichiometric mixture fraction.

In this study, we adopt a PaSR approach[4] and the DRM19 reaction mechanism[5] to compute the reaction rate. A structured mesh to discretize the computational domain has been generated, and it is a non-uniform grid with 2119680 cells.

RESULTS

1.Central line measurements

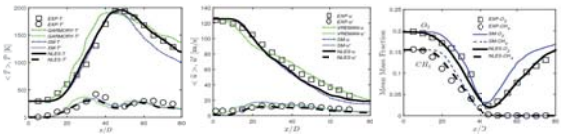

Figure 2: Time averaged and RMS measurements of temperature, velocity, Y_{O_2} and Y_{CH_4} along the axis.

2.Measurements in the radial direction

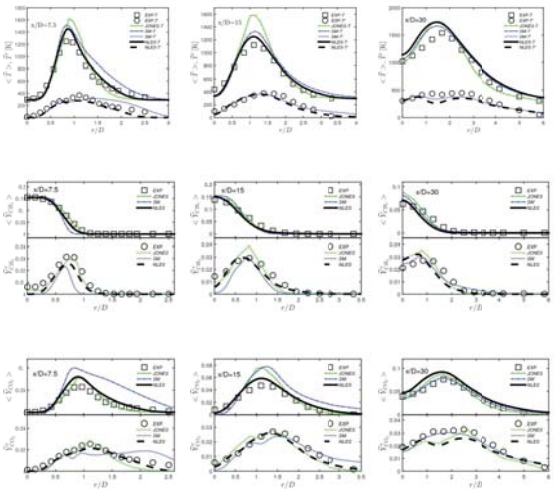

Figure 3: Mean and RMS measurements of temperature, Y_{CH_4} and Y_{CO_2} at different downstream positions.

Evidently, the NLES yields good agreement with experimental data (EXP[6]) and improvement over previous numerical results (GARMORY[7], VREMAN[8], JONES[9]) and the SM (with the PaSR combustion approach) results.

3. In mixture fraction space

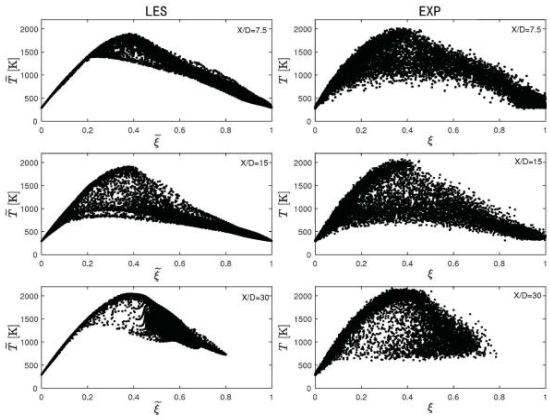

Figure 4: Scatter plots of instantaneous temperature at three positions.

At 15D, the scatter distribution of temperature near stoichiometric status is well predicted by using the NLES, indicating its ability of capturing and more extinction.

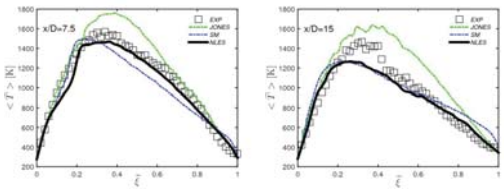

Figure 5: Conditional mean of resolved temperature at two positions.

It is clear that the NLES results show quite satisfactory predictions of temperature in the mixture fraction space.

4. Spectrum and SGS production

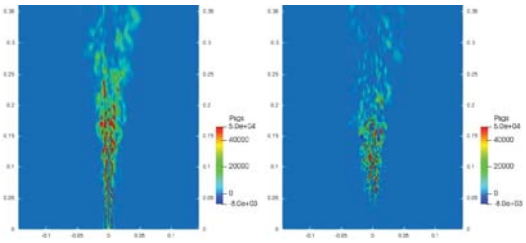

Figure 6: Filled contours of instantaneous SGS production, $P_{sgs} = -\tau_{ij}\tilde{S}_{ij}$, computed using (L) the SM and (R) the NLES.

It must be noted that the SM could not yield negative P_{sgs} but the nonlinear structural SGS stress model is able to deliver negative SGS productions, which represent reverse energy transfer from small to large scales, and are particularly important for the formation of large structures, such as Kelvin-Helmholtz vortices, in turbulent mixing layers.

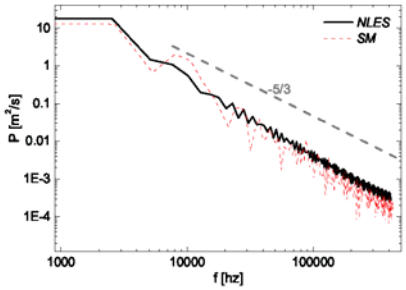

Figure 7: Power spectra of axial velocity sampled at the center axis position of $x/D = 15$.

The Kolmogorov -5/3 power law scaling in the inertial sub-range is better predicted by using the NLES, indicating its capability of accurately capturing flow structures in a wide range of scales.

CONCLUSIONS

1) The nonlinear LES framework is capable of accurately predicting the structure of the flame and capturing the local fire extinction events.
2) The nonlinear SGS models are accurate for capturing turbulent mixing, and the PaSR approach is suitable for simulating wide range reactions.

REFERENCES

[1] J. Smagorinsky, General circulation experiments with the primitive equations: I. the basic experiment, Mon. Weather Rev. 91 (3) (1963) 99–164.

[2] H. Lu, C. J. Rutland, L. M. Smith, A posteriori tests of one-equation LES modeling of rotating turbulence, Int. J. Mod. Phys. C 19 (2008) 1949–1964.

[3] H. Lu, F. Porté-Agel, A modulated gradient model for scalar transport in large-eddy simulation of the atmospheric boundary layer, Phys. Fluids 25 (2013) 015110.

[4] V. I. Golovitchev, N. Nordin, R. Jarnicki, J. Chomiak, 3-D diesel spray simulations using a new detailed chemistry turbulent combustion model, SAE Technical Paper (2000-01-1891).

[5] A. Kazakov, M. Frenklach, DRM19 reaction mechanism, http://www.me.berkeley.edu/drm/.

[6] R. S. Barlow, J. H. Frank, Effects of turbulence on species mass fractions in methane/air jet flames, Proc. Combust. Inst. (1998) 1087–1095

[7] A. Garmory, E. Mastorakos, Capturing localised extinction in Sandia Flame F with LES-CMC, Proc. Combust. Inst. 33 (2011) 1673–1680.

[8] A. Vreman, B. Albrecht, J.A. van Oijen, L.P.H. de Goey, R. Bastiaans, Premixed and non premixed generated manifolds in large-eddy simulation of Sandia flame D and F, Combustion and Flame 153 (2008) 394–416.

[9] W. P. Jones, V. N. Prasad, Large eddy simulation of the Sandia flame series (DCF) using the Eulerian stochastic field method, Combustion and Flame 157 (9) (2010) 1621–1636

Virtual chemistry for temperature and pollutant prediction in numerical simulations of turbulent flames

Giampaolo Maio[1]*, M. Cailler[1, 2] and B. Fiorina[1]

[1] *Laboratoire EM2C, CNRS, CentraleSupélec, Université Paris-Saclay, 3 rue Joliot Curie 91192 Gif-Sur-Yvette Cedex, France*

[2] *SAFRAN Tech, Rue des Jeunes Bois, Châteaufort - CS 80112, 78772 Magny-les-Hameaux, France*

1 Introduction

Flames stabilization and pollutant formation in laminar and turbulent configurations are affected by complex and multiple phenomena such as flame flow field interaction, heat exchanges and mixture stratification. Reliable numerical simulations must account for such complex phenomena at an affordable CPU cost. The computational cost of a flame simulation is strongly related to the employed chemistry model. Indeed the inclusion of detailed transported chemistry in numerical simulation of industrial chambers increases enormously the simulation cost. This is due to the high number of species to transport including intermediate species and to the numerical stiffness associated to the fastest species solution. Several reduced order chemistry models are currently employed to overcome this limitation such as mechanism reduction, chemistry tabulation and global mechanism approach. An alternative to above mentioned strategies has been recently introduced [1, 2], called *Virtual optimized chemistry*. The approach consists in : i) using a virtual main chemical mechanism coupled to the flow solver equations to predict temperature and heat release, ii) designing satellite sub-mechanisms dedicated to the description of flame quantities of interest (such as pollutant formation phenomena). The virtual mechanisms are trained over an ensemble of flame archetypes that are representative as close as possible of the final application of interest. In the present work the validity of the approach is broadened over two main routes:

- Include the effect of flame heat losses in the model. This step involve a LES (Large Eddy Simulation) validation using as test case the Preccinta burner, retained as TNF target flame for the CO modeling session.
- Validate the virtual chemistry approach in multi-modal flame regime conditions. Using as test case the TNF Inhomogeneous piloted jet burner configuration.

2 Applications

2.1 Non adiabatic virtual chemistry and LES of the Preccinsta combustion chamber

In this step burner-stabilized flamelets are introduced in the virtual chemistry learning database, to capture the influence of heat-losses on temperature, flame heat release and carbon monoxide formation. A strong sensitivity of carbon monoxide profiles to flame heat losses has been found in laminar flame profiles especially in the CO mass fraction peak. The proposed model has been validated in an LES context using as test case the Preccinsta turbulent combustion chamber [3]. The LES simulations have been conducted both in adiabatic conditions and including heat losses. Combustion chemistry is modeled using the non adiabatic virtual mechanism solving both the two-step main mechanism and the CO dedicated sub-mechanism. The inclusion of flame heat losses allows a better reproduction of temperature profiles in the outer recirculation zone and an improvement of the flame topology prediction, retrieving flame quenching phenomena over the outer branch of the flame. Heat losses impact on CO formation prediction (Fig.1): the CO formation is drastically reduced in the outer branch of the flame. This observations is enforced by a refining grid analysis.

2.2 Inhomogeneous jet piloted burner: Virtual chemistry simulations

Virtual chemistry is employed to simulate the TNF Sydney inhomogeneous piloted burner configuration [4, 5]. The simulated configuration is the *FJ200-5GP-Lr75-80*, characterized by a recession distance of the inner tube of 75mm and a bulk jet velocity of 80m/s. This burner is under investigation of the TNF research community

*Corresponding author. Email: giampaolo.maio@centralesupelec.fr

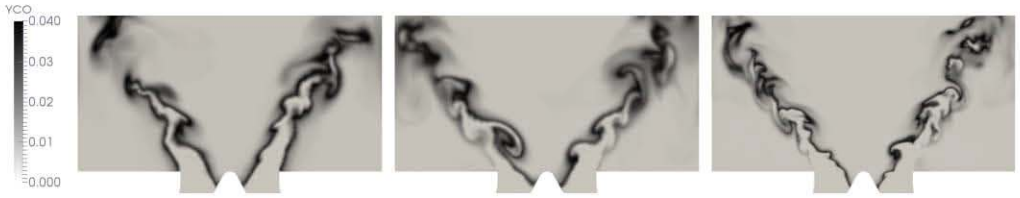

Figure 1: Instantaneous CO filtered mass fraction snapshot on the middle-plane of the combustion chamber. From left to right: adiabatic simulation, non adiabatic simulation and non adiabatic simulation on a finer grid.

since it represents a challenging flame configuration: it allows to stabilize multi-modal flame regime; here multi-modal flames stands for coexistence of premixed and non premixed flame structures. Another peculiarity of the analysed case is the occurrence of numerous phenomena of extinction in the flame region. The aim of the present simulations is to challenge virtual chemistry in inhomogeneous flame conditions and make a comparison with a tabulated chemistry solution, in the FPI approach, with a special attention to CO formation. Some preliminary result comparisons are made here at 5D downstream the burner exit plane (D is the main jet diameter) in Fig 2. They show an improvement of the CO levels using the virtual chemistry approach. The simulation results need to be still deeper investigated in order to isolate the impact of the turbulent combustion model. Furthermore the results on CO mean mass fraction are polluted by a non perfect temperature and mixing prediction. On that purpose the comparative study that will be carried out in the TNF inhomogeneous flame session will be of paramount importance.

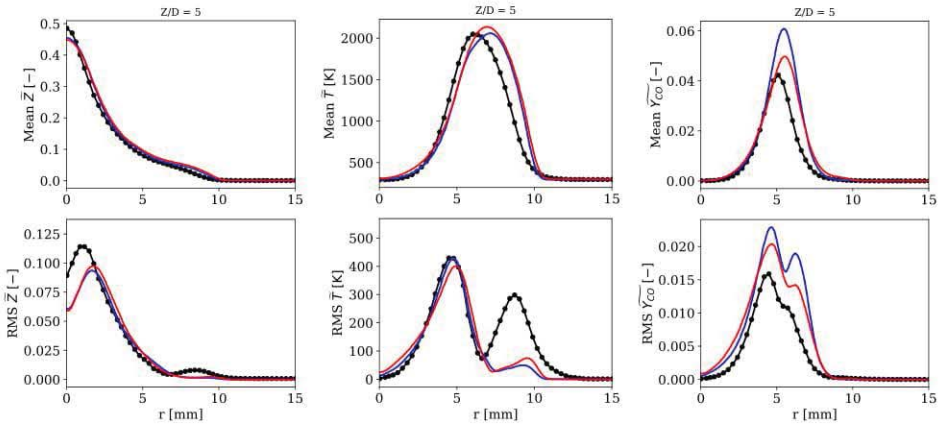

Figure 2: Mean and rms comparison between experimental data[4, 5] and simulation results at 5 diameters downstream the burner exit plane. From left to right: Mixture fraction, temperature and filtered CO mass fraction. Black dots: experimental data. Blue lines: tabulated FPI chemistry. Red lines: virtual chemistry.

References

[1] Mélody Cailler, Nasser Darabiha, Denis Veynante, and Benoît Fiorina. Building-up virtual optimized mechanism for flame modeling. *Proc. Combust. Inst.*, 2017.

[2] M. Cailler, N. Darabiha, and B. Fiorina. Virtual chemistry for pollutant emissions prediction. *Submitted to Combustion and Flame*, 2018.

[3] Weigand Meier, Peter Weigand, Xuru R Duan, and Robert Giezendanner-Thoben. Detailed characterization of the dynamics of thermoacoustic pulsations in a lean premixed swirl flame. *Combust. Flame*, 150(1):2–26, 2007.

[4] Shaun Meares and Assaad R Masri. A modified piloted burner for stabilizing turbulent flames of inhomogeneous mixtures. *Combustion and Flame*, 161(2):484–495, 2014.

[5] RS Barlow, S Meares, G Magnotti, H Cutcher, and AR Masri. Local extinction and near-field structure in piloted turbulent ch 4/air jet flames with inhomogeneous inlets. *Combustion and Flame*, 162(10):3516–3540, 2015.

Multiple Mapping Conditoning Modelling of a piloted partially-premixed Sandia DME flame series (D - G)

G. Neuber[1,*], J. Kirchmann[1], A. Kronenburg[1], O. T. Stein[1], S. Galindo-Lopez[2], M. J. Cleary[2], J. H. Frank[3], B. Coriton[3], R. S. Barlow[3], F. Fuest[3]

[1]Institut für Technische Verbrennung, Universität Stuttgart, Germany
[2]School of Aerospace, Mechanical and Mechatronic Engineering, The University of Sydney, Australia
[3]Combustion Research Facility, Sandia National Laboratories, Livermore, California 94551, USA
[*]Corresponding author: gregor.neuber@itv.uni-stuttgart.de

The Sandia dimethyl ether (DME) flames D - G constitute a target flame series of the International Workshop on Measurement and Computation of Turbulent Nonpremixed Flames (TNF) [1] and were experimentally investigated by Coriton et al. [2], Fuest et al. [3-5]. Due to the presence of an oxygen atom within the molecules' structure and the absence of a direct carbon-carbon bond, the emission of NO_x, CO and soot can notably reduced during the fuel conversion process and DME therefore is a promising "green" alternative compared to conventional diesel fuels.

We investigate the complete series of the turbulent, piloted dimethyl ether (DME)/air jet flames (DME flames D - G) with Reynolds numbers ranging from 29,300 to 73,250 with a sparse-Lagrangian multiple mapping conditioning (MMC) approach coupled to a large eddy simulation (LES) flow field solver. MMC is a probability density function (PDF) method and in the context of LES it models the sub-filter PDF of the composition, known as the filtered density function (FDF) [6]. To solve the FDF, a Lagrangian Monte-Carlo particle scheme is used. Thus, the FDF chemical reaction rate appears in closed form but the FDF mixing operator needs modelling. The MMC framework utilizes a mixing model which closes the conditional sub-filter scalar variance. Mixing between the Monte-Carlo particles is modelled by a generalized form of MMC combined with a sparse distribution of particles leading to significant computational savings compared to conventional mixing models.

The particles carry the composition scalar field, absolute enthalpy and particle mixture fraction and are transported according to stochastic differential equations with fractional steps for spatial transport, reactions and mixing [6]. We adopt the MMC version of Curl's mixing model to close the stochastic differential equations at the mixing operator level. Density coupling is based on schemes developed for the field of smoothed particle hydrodynamics [7].

Earlier attempts [8,9] to correctly predict the local extinction events for increasing Reynolds number cases failed due to an inconsistency of previously proposed mixing time scale models in the treatment of anisotropic sub-filter fields [10]. To remedy this inconsistency an anisotropic mixing time scale model is proposed by Vo et al. [10]. With this model much better results for the prediction of conditional variances of a reactive shear layer simulation are obtained. The current work shows first results of the application of the new mixing time scale model on a reactive jet flame with local extinction events.

The MMC-LES model has been implemented into the *mmcFoam* [11] code family which is compatible with the OpenFOAM-5.x open source C++ library. Our grid consists of 2 million LES cells and state-of-the-art convection schemes and standard BCs are used to solve for the transport equations of momentum, species, enthalpy and mixture fraction. The LES solves equations for spatially filtered quantities and a sigma-Model with a model constant of C = 1.5 is used for the sub-grid closure. The turbulent content of a pre-computed pipe flow serves as realistic inflow for the central jet. At all inlet boundaries the species composition was matched to that given in Fuest et al. [2].

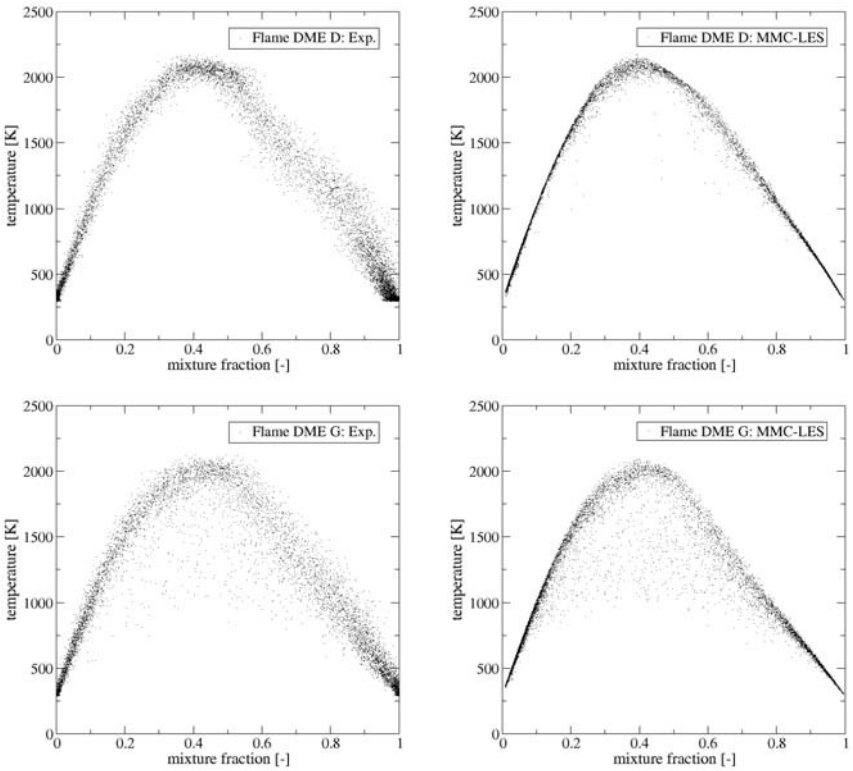

Figure 1: Conditional scatter data at axial location of z/D = 7.5 of the temperature for the Sandia DME D flame (top) and for the Sandia DME G flame (bottom). In all plots 10,000 instantaneous realisations are shown.

Experimental and numerical scatter data of the conditional temperature of flame DME D and G at an axial location of z/D = 7.5 are shown in Fig. 1. For the DME D flame far departures from the equilibrium composition is a rather rare event. In contrast the increased shear forces for the higher Reynolds number case has an strong impact regarding the conditional fluctuations in composition space. The MMC model correctly reproduces the more frequent local extinction events for flame DME G where deviations from the equilibrium are of similar magnitude compared to the experiment.

The predictive capabilities of MMC-LES are tested by modelling the whole series using a single set of mixing model parameters. A value of the MMC parameter f_m = 0.03, which controls the distance between mixing particles in the reference mixture fraction space, has once again been found to achieve a good match with the experimental data. Results shown on the TNF poster will include velocity, unconditional mixture fraction and temperature profiles and conditional temperature and species mole fractions for a selected variation of the Flame Reynolds numbers.

References

[1] International Workshop on Measurement and Computation of Turbulent Nonpremixed Flames (TNF). available at http://www.sandia.gov/TNF, 2016.

[2] B. Coriton, M. Zendehdel, S. Ukai, A. Kronenburg, O. T. Stein, S.-K. Im, M. Gamba, J. H. Frank, Proc. Combust. Inst. 35 (2015), 1251 - 1258.

[3] F. Fuest, R. Barlow, J.-Y. Chen, A. Dreizler, Combust. Flame 159 (2012) 2533 - 2562.

[4] F. Fuest, G. Magnotti, R. S. Barlow, J. A. Sutton, Proc. Combust. Inst. 35(2)(2015), 1235 - 1242.

[5] F. Fuest, R. S. Barlow, G. Magnotti, J. A. Sutton, Combust. Flame 188 (2018), 41 - 65.

[6] M. J. Cleary, A. Y. Klimenko, Phys. Fluids 23 (2011).

[7] J. J. Monaghan, Rep. Prog. Phys. 68(8)(2005), 1703.

[8] Y.Ge, M. J. Cleary, A. Y. Klimenko, Proc. Combust. Inst. 34 (2013), 1325 - 1332.

[9] G. Neuber, A. Kronenburg, O. T. Stein, M. J. Cleary, B. Coriton, J. H. Frank, (2016), 36th International Combustion Symposium, Seoul, Korea.

[10] S. Vo, O. T. Stein, A. Kronenburg, M. J. Cleary, Combust. Flame 179 (2017) 280-299.

[11] S. Galindo-Lopez, F. Salehi, M. J. Cleary, A. R. Masri, G. Neuber, O. T. Stein, A. Kronenburg, A. Varna, E. R.Hawkes, B. Sundaram, A. Y. Klimenko, Y. Ge, Computers and Fluids (2018) 1 - 18.

Challenges for Large Eddy Simulation of Partially Premixed Turbulent Combustion using Reduced-Order Manifold Flame Structure Models

Bruce A. Perry[1,*], Michael E. Mueller[1]

[1] *Department of Mechanical and Aerospace Engineering, Princeton University*
** baperry@princeton.edu*

Introduction: Many practical combustion systems involve inhomogeneous partial premixing of fuel and air, so combustion occurs outside of the asymptotic premixed and nonpremixed combustion modes. As reviewed by Masri [1], recent experimental and computational efforts have been moving beyond the traditional classification to understand partially premixed combustion. One area of need is to develop affordable models for partially premixed combustion that can be used in Large Eddy Simulations (LES). Reduced-order manifold models typically use the assumption of premixed or nonpremixed flame structures to reduce the dimensionality of the thermochemical state space by projecting onto a low-dimensional manifold, parameterized by a mixture fraction (Z) and/or progress variable (C). The Flamelet/Progress Variable (FPV) approach [2] for nonpremixed combustion and the Flamelet Generated Manifolds (FGM) approach [3] for premixed combustion, which both use 1D flame calculations as component problems to generate the low-dimensional manifold, have been successfully applied in the corresponding regimes but are not applicable to partially premixed combustion without modification.

The FPV approach can be extended to account for nonpremixed-like partially premixed combustion, where fuel and oxidizer may partially mix prior to the flame, but mixing between fuel and oxidizer remains the controlling factor in the flame. A second mixture fraction must be defined, which can be used to specify a variable boundary condition for 1D component flame calculations [4]. The Partially Premixed Flamelet Tabulation (2PFT) approach is similar [5], but the scalar dissipation rate is used as a parameterizing variable instead of a second mixture fraction. 2PFT can incorporate some multimodal combustion effects because the 1D component calculations, partially premixed counterflow flames between air and partially premixed fuel/air, include premixed flames for flammable fuel mixtures at low strain rates. Multi-modal combustion has also been modeled by determining the locally dominant combustion mode and switching between traditional nonpremixed or premixed models accordingly. The most rigorous approach is based on a flamelet-like coordinate transformation to a 2D space, with separate parameterizing variables related to premixed and nonpremixed combustion [6]. The Knudsen regime index is defined based on the balance between premixed and nonpremixed terms in the resulting equation and is used to identify which limiting model should be used. The major limitation of mode-switching is that it does not explicitly model intermediate combustion regimes.

The University of Sydney piloted jet burner with inhomogeneous inlets [7,8] has been used as a test case to validate reduced-order manifold flame structure models. The burner has a variable length mixing tube upstream of the nozzle where concentric fuel and air streams partially premix, and the intermediate Lr75 case features inhomogeneous partially premixed conditions that result in multi-modal combustion. No single approach has been able to fully predict the partially premixed flame structure for this case: Wu and Ihme [9] showed that neither premixed nor nonpremixed models can provide accurate predictions, Kleinheinz et al. [10] applied the Knudsen mode switching model but did not explicitly account for intermediate combustion regimes, and Perry et al. [4] found that a nonpremixed-based two mixture fraction model accurately predicts flame structure except in a small region where premixed combustion dominates. The objective of this work is to determine whether a combination of existing approaches can give accurate predictions for this configuration, even though all assume an inherently 1D flame structure. The two mixture fraction model of Perry et al. is extended to explicitly include premixed combustion using a similar methodology as 2PFT. Additional methods of incorporating premixed effects are considered, including the Knudsen regime indicator and an approach based on flammability limits.

Modeling Approach: The flame of interest has three main inlet streams: the central fuel stream, the annular air stream that surrounds and partially premixes with the fuel, and the air coflow. All the modeling approaches in this work build off the approach from [4], where two conserved-scalar mixture fractions (Z and Z^*) are defined and given boundary conditions such that Z corresponds to jet/coflow mixing and Z^* corresponds to fuel/air mixing. The fuel premixing fraction (F) is defined $F \equiv Z^*/Z$ and can be physically interpreted as the effective mixture originating from the nozzle. The reduced-order manifold is generated using solutions to the steady 1D flame equation in Z-space, which is solved for a range of fuel mass fraction boundary conditions at $Z = 1$ (corresponding to many values of F) and for many reference values of χ_Z, the scalar dissipation rate for Z. The dependence on χ_Z is then recast using the progress variable. Three approaches are considered for expanding this manifold generation method to include premixed combustion:

Nonpremixed+ Approach: Some of the 1D flame solutions with partially premixed boundary conditions plotted in Fig. 1 in the purple plane have increasingly vertical profiles near $Z = 1$. A premixed flame would be a vertical line, so the near vertical profiles, which occur at low $\chi_{Z,\mathrm{ref}}$, indicate that the 1D flames contain a premixed-like component. It is both mathematically and physically consistent to extend the nonpremixed-based model by explicitly including 1D premixed flames at the $Z = 1$ boundary of the state space. This forms the basis of the

"Nonpremixed+" approach, which is analogous to 2PFT, except the manifold is parameterized by the scalars *Z*, *F*, and *C*. The location in the cubic state space determines whether the nonpremixed (blue), nonpremixed-like (purple), or premixed (red) model is accessed. This approach implicitly assumes an order of mixing and reaction: first, nonreactive mixing between fuel and air in the jet, then either premixed flame propagation or reactive mixing with the coflow air.

Flammability-based Mode Switching: Phenomenologically, if the value of *F* indicates that the mixture of fuel and air in the central jet is flammable, premixed flame propagation should be expected. Therefore, this approach builds on the Nonpremixed+ approach by accessing a standard FGM premixed model if *F* is within the empirical flammability limits, taken to be $0.028 < F < 0.089$.

Knudsen Indicator Mode Switching: The Knudsen regime indicator [6] is used to switch between the Nonpremixed+ model and a standard FGM premixed model. Past approaches used this regime indicator with standard FPV models, but this work explicitly includes the nonpremixed-like flames in the intermediate region. The main purpose of the Knudsen switching is to be able to model premixed combustion of arbitrary mixtures, rather than limiting it to the $Z = 1$ plane as in the Nonpremixed+ model alone.

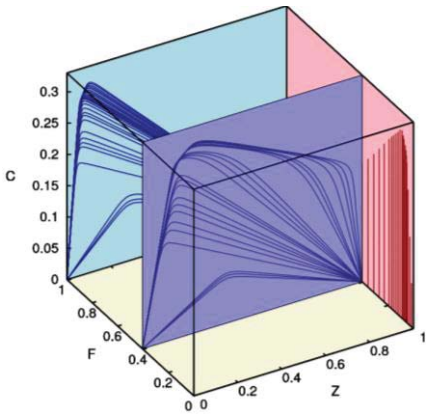

Fig. 1: Reduced-order state-space for the Nonpremixed+ approach. Each line within the blue and purple planes represents a 1D flame solution, with the $Z = 1$ boundary condition $Y_F = 1$ for the blue plane (recovering the FPV model) and $Y_F = 0.4$ for the purple plane. A total of 35 conditions ranging from $F = 0$ to $F = 1$ were considered. The red plane is equivalent to the FGM model, with vertical lines representing 1D premixed flames.

Results: Predictions for temperature and the formation of CO from LES using the three approaches are compared to experimental measurements from the burner with inhomogeneous inlets in Fig. 2. Results using the premixed FGM approach and the previous two mixture fraction FPV approach [4] are also plotted. The former is accurate only for $x/D \leq 5$ and the latter only for $x/D \geq 10$. This trend is consistent with experimental observations, which indicate that premixed combustion near the nozzle transitions to nonpremixed-like combustion downstream. This qualitative transition is reproduced by the mode switching models, and the Nonpremixed+ model in particular gives better predictions than either single mode model as a result. However, none of the approaches reproduce the transition at the correct location, instead predicting that premixed combustion persists too far downstream.

The mode-switching models used here fail to accurately capture the transition between modes because of the assumptions about the order of mixing and reaction in the Nonpremixed+ model. It is assumed that all mixing between the fuel and air in the jet occurs prior to nonpremixed combustion, which happens when the jet mixes with the coflow at constant *F* (in 1D along the *Z*-direction). Physically, nonpremixed-like behavior is also possible at $Z = 1$ (within the inhomogeneous jet, 1D nonpremixed flame in the *F*-direction), where the model presently assumes premixed combustion. This is a limitation of assuming combustion occurs in 1D in a specified direction within the reduced-order state space. Generating the manifold from solutions to a 2D equation, which is the subject of ongoing work, would bypass the issue.

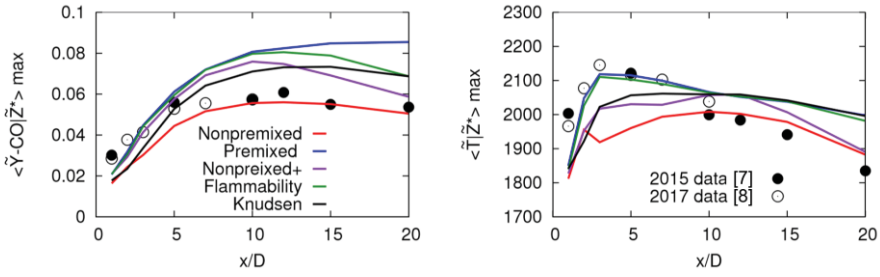

Figure 2: Peak conditional mean values of Y_{CO} (left) and Temperature (right) as a function of axial distance. The three multi-modal approaches, a purely premixed model, and the nonpremixed model from [4] are compared to experimental data**.**

References:

[1] A. R. Masri. *Proc. Combust. Inst. 35* (2015) 1115–1136.
[2] C. D. Pierce, P. Moin. *J. Fluid Mech.* 504 (2004) 73–97.
[3] J. A. Van Oijen, L. P. H. de Goey. *Combust. Sci. Tech.* 161 (2000) 113–137.
[4] B. A. Perry, M. E. Mueller, A. R. Masri. *Proc. Combust. Inst.* 36 (2017) 1767–1775.
[5] B. Franzelli, B. Fiorina, N. Darabiha. *Proc. Combust. Inst.* 34 (2013) 1659–1666.
[6] E. Knudsen, H. Pitsch. Combust. Flame 159 (2012) 242–264.
[7] R. S. Barlow, S. Meares, G. Magnotti, A. R. Masri. *Combust. Flame* 162 (2015) 3516–3540.
[8] H. Cutcher, R. S. Barlow, G. Magnotti, A. R. Masri. *Proc. Combust. Inst.* 36 (2017) 1737–1745.
[9] H. Wu and M. Ihme. *Fuel* 186 (2016) 853–863.
[10] K. Kleinheinz, T. Kubis, P. Trisjono, M. Bode, H. Pitsch. *Proc. Combust. Inst.* 36 (2017) 1747–1757.

The Conditional Dissipation Mapping Closure for all Regimes of Turbulent Premixed Combustion

Stephen B. Pope

s.b.pope@cornell.edu
Sibley School of Mechanical & Aerospace Engineering
Cornell University, Ithaca, New York 14853, USA

The Conditional Dissipation Mapping Closure (CDMC) is a new statistical approach that is applicable to all regimes of premixed turbulent combustion. In particular, CDMC realistically accounts for the coupling between reaction and diffusion in flamelet and non-flamelet regimes. Here we describe and apply CDMC to the simpler case of statistically homogeneous reaction-diffusion systems in one spatial dimension. With $c(x,t)$ being the reaction progress variable, the governing equation is

$$\frac{\partial c}{\partial t} = \Gamma \frac{\partial^2 c}{\partial x^2} + S(c[x,t]), \tag{1}$$

where Γ is the diffusivity and S is the chemical source term. While this is a much simpler case that premixed turbulent combustion, it retains the essence of the problem, i.e., the coupling between reaction and diffusion. Indeed, depending on the specification of the initial condition $c(x,0)$ and the chemical source term, there is a rich set of challenging problems.

The principal features of CDMC are as follows:

1. The closure is at the level of the PDF, $f(c)$, of the progress variable $c(x,t)$ and the conditional dissipation (or, equivalently, the conditional mean square gradient of c).

2. Terms in the resulting equations due to reaction are in closed form.

3. The unknown statistics involving derivatives of c are modeled using a new mapping closure. This involves a single physical parameter and no adjustable constants.

4. At time t, the mapping transforms a standardized Gaussian process $\theta(z)$ to a *surrogate* process $c_s(x,t)$ with the same PDF and conditional dissipation as $c(x,t)$. The only assumption in the approach is that the unknown statistics of $c(x,t)$ are the same as the known statistics of $c_s(x,t)$.

5. The mapping involves two transformations. First there is a straining transformation of the independent variable of the form $dx = \lambda dz$, where λ depends on the square of the gradient, θ_z^2, and a *straining function* $\beta(\eta,t)$, where η is a sample-space variable corresponding to θ. The transformed process is denoted by $\zeta(x[z],t) = \theta(z)$. By construction, this transformation maintains the standard Gaussian one-point PDF and creates the required conditional mean-square gradients of ζ.

6. Second, as in previous mapping closures (Kraichnan (1990), Pope (1991)) there is a *mapping function* $C(\eta,t)$ that transforms ζ to the surrogate process, i.e., $c_s(x,t) = C(\zeta[x,t],t)$.

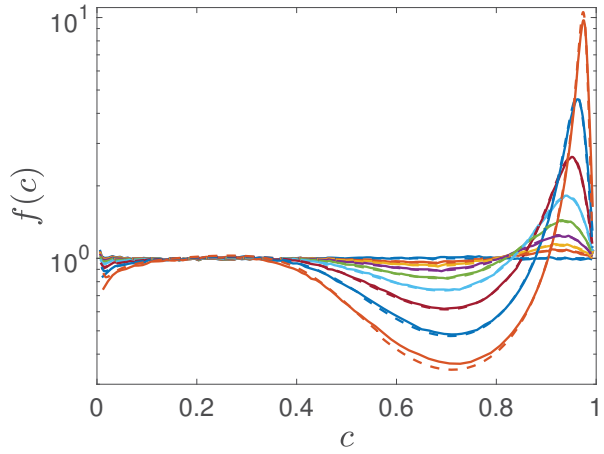

Figure 1: Evolution of the PDF of c for a test case: solid lines, DNS; dashed lines, CDMC.

7. The resulting model consists of two coupled PDEs for the mapping function $C(\eta, t)$ and the straining function $\beta(\eta, t)$. The PDF and conditional dissipation are readily obtained from these solutions.

8. Interestingly, the chemical source term appears only (and naturally) in the mapping equation as $\partial C/\partial t = S(C) + \ldots$. There is no direct effect of reaction on the straining $\beta(\eta, t)$.

9. The model guarantees realizability, boundedness, etc., since at each instant the statistics evolve exactly as those of a realizable process governed by Eq. (1)

10. At infinite Damkohler number, the model yields flamelet combustion with the correct structure: the equation for the mapping $C(\eta, t)$ becomes an exact mathematical analogy to the flame equation.

11. While a spectrum (or, equivalently, a two-point correlation) is needed to define the Gaussian process $\theta(z)$, the only related quantity appearing in the closure is the variance of second derivative of θ. This affects the initial rate of mixing.

Several cases, corresponding to different initial conditions and chemical source terms, have been studied. As an illustration, Fig. 1 shows the evolution of the PDF of c for a reactive case, starting from an initially flat PDF. The solutions obtained from CDMC (dashed lines) are compared to statistics obtained from direct numerical simulations (DNS), i.e., solutions to Eq. (1) (solid lines). As may be seen, there is good agreement.

References

Kraichnan, R. (1990). Models of intermittency in hydrodynamic turbulence. *Phys. Rev. Lett. 65*, 575.

Pope, S. B. (1991). Mapping closures for turbulent mixing and reaction. *Theor. Comput. Fluid Dyn. 2*, 255–270.

Novel Burner for Investigating Laminar Forced Premixed Flame-Wall Interaction

Jacob E. Rivera, Robert L. Gordon, Mohsen Talei
Department of Mechanical Engineering, The University of Melbourne, Parkville, Victoria, 3010, Australia
Corresponding author: jrivera@student.unimelb.edu.au

1. Introduction

Increasingly stringent regulatory standards, as well as a recent trend towards developing high power-density engines, has increased the potential impact of flame-wall interaction (FWI). The nature of the small length scales involved in FWI has presented significant challenges in the experimental study of this phenomenon [1]. These factors increase the challenges associated with modelling important pollutants, such as exhaust CO emissions ($[CO]_{exh}$). Hence, the objective of this work is to explore the impact of different parameters on $[CO]_{exh}$, in the context of transient flames undergoing heat loss due to FWI. To do this, a burner was designed to allow $[CO]_{exh}$ measurements, while being optically accessible to study flame dynamics, during FWI. Different flame behaviours can be induced by forcing the flame for a range of frequencies and amplitudes [2], flame chemiluminescence (CL) can then be used to measure quenching distance (δ_Q) [3]. This flame behaviour may be linked to $[CO]_{exh}$, which can be measured at ± 0.003 *ppm* uncertainty, using a vehicle certification-grade emissions bench. The effect of different wall cooling rates ($\dot{Q}_c$) can be explored to bring this study closer in relevance to practical engine systems, which use this parameter to control their combustor wall temperature (T_w) [4].

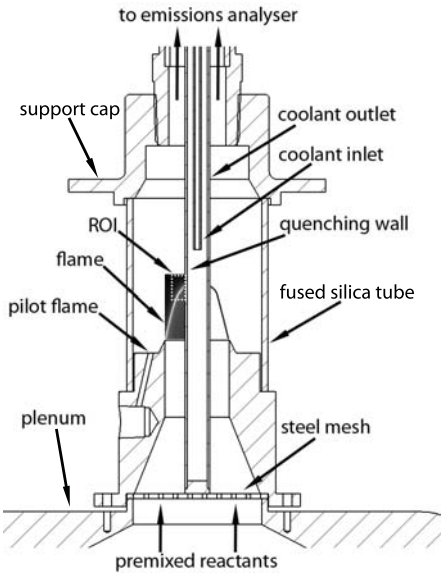

Figure 1: Annotated schematic cross section view of the burner test section.

2. Burner

The burner is a modified version of that used by Wiseman et al. [5], and features the same plenum and nozzle design, including the speaker that induces the forcing. Propane and air flow rates and equivalence ratios (ϕ) are controlled using two MKS thermal flow controllers. These premixed reactants then pass into the plenum, through some honeycomb and mesh flow straighteners, and then finally through the converging nozzle. The pilot flame ignites the mixture in the optical combustor section, and is extinguished once the main flame has stabilised.

The primary novelty of this burner is the addition of an internally water-cooled stainless steel tube, in line with the central axis of the nozzle (see Fig. 1). This quenching wall leads to three main flame shapes, and is largely controlled by $\dot{Q}_c$, ϕ and the inlet velocity (u) [6]. The flame configuration chosen for this study is shown in Fig. 2. This was chosen as its shape is similar to the canonical side-wall quenching (SWQ) configuration [7], when considering only the mid-plane of the burner. Though the focus of this study is on lean flames, the burner can accommodate a variety of ϕ, subject to flashback and blow-off limits.

3. Flame Imaging

The speaker is driven by an in-house built timing system, which is also used to trigger camera imaging. This timing system phase-locks the trigger signal to the forcing cycle at user-defined intervals. Hence, this system can be used to take multiple single-shot flame images (see Fig. 2a), at any point in the forcing cycle, for any forcing frequency. This allows a low-speed imaging system to capture the dynamics of higher-speed cyclic events, subject to signal and blur constraints on exposure time.

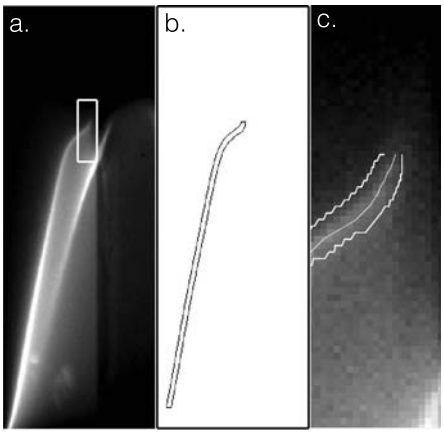

Figure 2: Example image of a flame raw image with the region of interest (ROI) highlighted (a), the flame edge dtected (b), and the flame edges overlaid on the flame within the ROI (c).

Due to the line-of-sight nature of flame CL, an Abel inversion needs to be conducted. This allows information from the focal plane to be estimated from the 2D projection given by the flame CL image. A linear translation variant (LTV) filter is used to further de-noise the image, while preserving the edges [8]. A Canny edge detector then extracts the two edges of the flame (see Fig. 2b) [9]. The flame edge seen in Fig. 2c can be used to measure the δ_Q under different forcing conditions. The frequency and amplitude response of δ_Q can then be correlated to the behaviour of the measured $[CO]_{exh}$. More details of this post-processing algorithm can be found in Rivera et al. [10].

4. Emissions Measurement

The emissions measurements are conducted using a water-cooled emissions probe situated $\approx 210\ mm$ downstream of the flame. The emissions bench uses a Non-Dispersive Infrared (NDIR) analyser to measure dry $[CO]_{exh}$ concentrations. Span gas concentrations of 100 ppm, 1000 ppm, 2% vol and 8% vol of CO-N_2 can be used to calibrate the analyser for different measurement ranges. Figure 3 shows $[CO]_{exh}$ measurements across ϕ. This shows the expected trend of increasing $[CO]_{exh}$ as ϕ is increased. This trend in the result agrees with simple non-adiabatic flame modelling across different equivalence ratios [6], as well as standard SI engine-out emissions profiles [11].

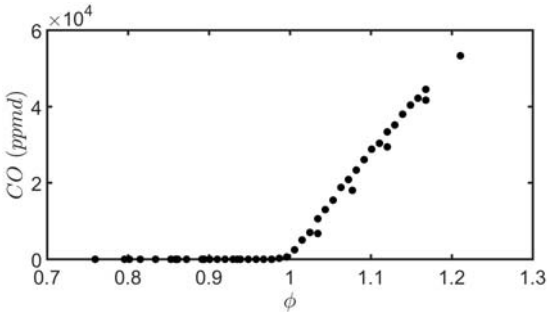

Figure 3: Exhaust CO measurements across ϕ.

References

[1] A. Dreizler, B. Böhm, Proc. Combust. Inst. 35 (1) (2015) 37–64.
[2] T. Schuller, D. Durox, S. M. Candel, Combust. Flame 135 (4) (2003) 525–537.
[3] M. Bellenoue, T. Kageyama, S. A. Labuda, J. Sotton, Exp.Therm. Fluid Sci. 27 (3) (2003) 323–331.
[4] A. H. Lefebvre, D. R. Ballal, Gas Turbine Combustion: Alternative Fuels and Emissions, CRC Press, Boca Raton, 3 edn., 2010.
[5] S. M. Wiseman, M. J. Brear, R. L. Gordon, I. Marusic, Combust. Flame 183 (2017) 1–14.
[6] J. E. Rivera, R. L. Gordon, M. Talei, M. J. Brear, Proc. 20th AFMC, Perth, Australia, 2016 .
[7] T. Poinsot, D. C. Haworth, G. Bruneaux, Combust. Flame 95 (1-2) (1993) 118–132.
[8] K. He, J. Sun, X. Tang, IEEE Trans. Pattern Anal. Mach. Intell. 35 (6) (2013) 1397–1409.
[9] J. Canny, IEEE Trans. Pattern Anal. Mach. Intell. 8 (6) (1986) 679–698.
[10] J. E. Rivera, R. L. Gordon, M. Talei, Proc. 11th ASPACC, Sydney, Australia, 2017 .
[11] J. B. Heywood, Internal Combustion Engine Fundamentals, McGraw-Hill, New York, 1988.

Experimental Analysis of Confined Premixed Recirculation-Stabilized Jet-Flames for Gas Turbine Applications

Michael Severin, Oliver Lammel, Wolfgang Meier

German Aerospace Center (DLR), Institute of Combustion Technology, Stuttgart, Germany

email: wolfgang.meier@dlr.de

1. Introduction

Most gas turbine combustors use swirl burners to stabilize the flame by vortex breakdown-induced recirculation of hot combustion products. An alternative concept is based on recirculation-stabilized jet-flames, closely related to MILD or FLOX® combustion. Such flames exhibit very low NO_x emissions, are less susceptible to thermo-acoustic instabilities and enable a stable combustion for a variety of fuels. Fig.1 shows a typical burner arrangement with 12 nozzles that has been used for high-pressure tests at DLR [1]. The high-momentum jets of (partially) premixed fuel and air issuing from the nozzles generate a recirculation zone in the central region of the combustion chamber and the mixing of burned gas and fresh load in the shear layers leads to a continuous ignition of the flame. One of the key questions concerns the flame stabilization mechanism, e.g., to what extent auto-ignition contributes to stabilizing the flame near the (lifted) flame root. To study the behavior in a simplified geometry and at laboratory conditions, a confined single-nozzle jet burner, equipped with an optical combustion chamber, has been set-up.

Fig.1: Photo of a gas turbine combustor based on jet-stabilized flames

2. Jet-stabilized single-nozzle burner and measurement techniques

The burner consists of a round nozzle (I.D. 10 mm) in a combustion chamber with rectangular cross section (40 x 50 mm^2). The nozzle is off-set from the center by 10 mm to resemble the nozzle placement of a multi-nozzle burner. Figure 2 presents a photo of the burner. Methane and air were perfectly premixed and preheated before entering the combustion chamber. Parameters such as equivalence ratio ϕ, preheat temperature T_i and jet exit velocity v were varied and a standard case was defined as ϕ=1, T_i=200°C, v=20 m/s [2].

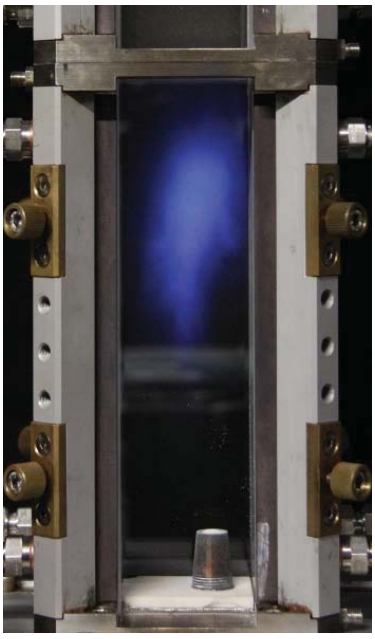

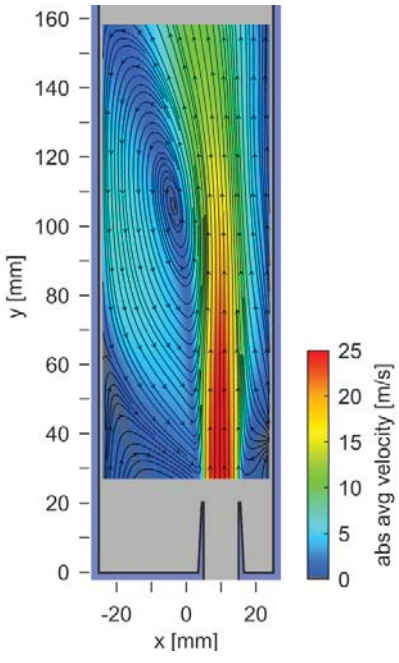

Fig.2: Photo of the burner (left) and mean flow field (right)

The flame shape was measured by OH chemiluminescence imaging and OH laser induced fluorescence, and the flow velocities were determined by stereoscopic particle image velocimentry (PIV). These

techniques were applied simultaneously at frame rates of 5 kHz. Thus, the temporal development and the interaction between the flow field and the flame could be revealed.

3. Results

The PIV measurements showed that the mean flow field was dominated by the high velocities of the jet and a pronounced recirculation zone on that side of the nozzle with the larger distance to the wall (see Fig.2). The flame was lifted and asymmetric as the photo in Fig.2 demonstrates. The time-resolved single-shot measurements revealed that the recirculation zone was composed of several smaller vortices in the shear layer between the inflow and the recirculation zone. The example displayed in Fig.3 shows that these vortices contributed strongly to the mixing of recirculated and fresh gas and thus promoted the stabilization of the flame. At axial locations between y=40 and 120 mm reacting flame sheets were often observed to be isolated, at least in 2D cuts. This can be explained by auto-ignition events, local flame extinction or cuts through connected three-dimensional structures with OH-free zones in the measurement plane. Time-series of instantaneous OH chemiluminescence images revealed that auto-ignition kernels frequently appeared near the flame root. Typically, they expanded, convected downstream and merged with the main flame body. It can thus be stated that auto-ignition contributed to flame stabilization under these conditions. Generally, the flame behaved very unsteady in the stabilization region with significant movements and jumps of the anchoring point.

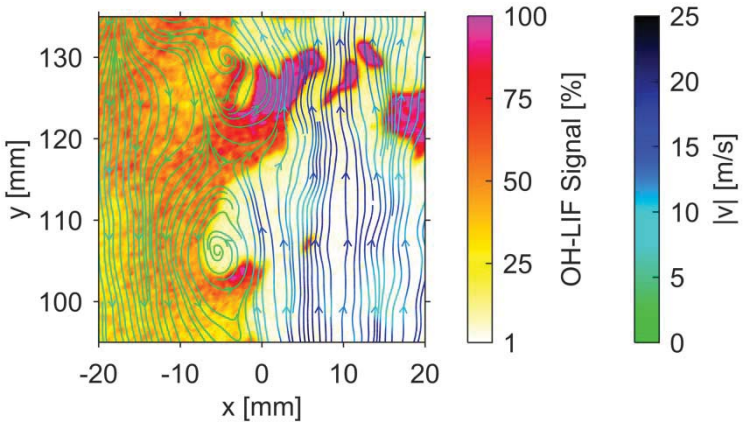

Fig.3: Single-shot of simultaneously recorded OH and velocity. High OH LIF signals are indicative of flame reactions.

4. References

[1] O. Lammel, H. Schütz, G. Schmitz, R. Lückerath, M. Stöhr, B. Noll, M. Aigner, M. Hase, W. Krebs, W., J. Eng. GT Power 132 (2010) 121503.

[2] M. Severin, O. Lammel, W. Meier, M. Aigner, Proc. 53rd AIAA/SAE/ASEE Joint Propulsion Conference, 10.-12.07.2017, Atlanta, USA. DOI: 10.2514/6.2017-4684.

WiPP Abstract for the 14th International Workshop on Measurement and Computation of Turbulent Flames

Modeling of a cyclonic burner under MILD combustion through FGM/IML approach. Effect of radiative heat transfer.

G. Sorrentino[1,], G. Ceriello[1], M. de Joannon[2], P. Sabia[2], R. Ragucci[2], J. van Oijen[3], A. Cavaliere[1], P. de Goey[3]*

1. DICMAPI-Università degli Studi di Napoli Federico II, P.le Tecchio 80, 80125, Naples, Italy
2. Istituto di Ricerche sulla Combustione-CNR, P.le Tecchio 80, 80125, Naples, Italy
3. Department of Mechanical Engineering, TU/e, Eindhoven, The Netherlands

**Corresponding author: Dr. Giancarlo Sorrentino*
Email address: g.sorrentino@unina.it

The development of MILD Combustion systems [1] in several practical applications is hampered by a lack of understanding into such regime and thus novel tools are required compared to conventional combustion systems.
In MILD combustion technologies, reactants are diluted with large amounts of burnt reaction products prior to ignition, which enables reactive structure stabilization under diluted conditions, thereby avoiding high-temperature regions that promote enhanced thermal NO_x formation.
In this background, computational fluid dynamics (CFD) for the prediction of the burner behavior and its optimization, appears essential for a successful introduction of such a concept in some industries.
A major issue in the modeling of diluted combustion is the pronounced sensitivity of the reactive structure to the reaction chemistry and therefore detailed kinetic schemes are necessary when a gas mixture is subjected to dilution by hot reaction products [2].
In order to include detailed chemistry in fluid-dynamics simulations, Flamelet Generated Manifold (FGM) was used with Igniting Mixing Layer as canonical configuration used for tabulation (IML) [3].
On the experimental side, the amount of detailed experimental data available for burners operating under MILD/Flameless conditions is relatively scarce, and in general, when reported, covers very few and narrow combustor operating conditions. Moreover, in conventional flameless configurations, such as JHC, the stabilization process is achieved by means of bluff-body or swirl flow, and the combustion typically occurs far from the walls. Thus, adiabatic conditions are often assumed in such models. However, heat loss effects play an influential role in furnace-like burners because of the confinement and longer residence time of internal EGR systems. Internal EGR is also the cause of the high content of the absorbing and emitting mixture of H_2O/CO_2 inside the combustion chamber, which poses further modeling challenges for MILD combustion.
Based on such considerations, we report a study of the characterization of MILD combustion in a novel cyclonic burner [4], reported in Fig. 1. Experiments were performed in a small-scale combustor and included detailed measurements of local mean temperatures and concentrations of gas species at the stack for several operating conditions. Such quantities are very important to characterize the reactive behavior of the MILD regime and to provide valuable information for the assessment of predictive models. Experimental measurements in terms of temperature and species profiles were compared with the detailed results of numerical computations in this configuration. This was done at ambient pressure for three mixture composition values.

Finally, the impact of heat loss at the walls was evaluated by reporting two cases for heat exchange inclusion: convection and convection with radiation modeling. The numerical results of this work, reported in Figure 2 for a stoichiometric case, demonstrated that FGM with IML is a promising tool for modeling the complex flame structures of a cyclonic burner working under MILD combustion regime, with room for improvements. The work pointed out the importance, for this type of burner under MILD conditions, of a proper modeling of the heat exchange. In particular, it was proved that the radiative properties concerning both the exhaust gases and walls, have a not negligible contribution to the stabilization of homogeneous MILD conditions.

References

[1] Cavaliere, A., de Joannon, M., Prog. Energy Combust. Sci. 2004, 30, 329-366.

[2] Lamouroux, J., Ihme, M., Fiorina, B., Gicquel, O., Comb.Flame 2014, 161(8), 2120-2136.

[3] Abtahizadeh, E., de Goey, P., van Oijen, J. Comb. Flame 2015, 162, 4358-4369.

[4] de Joannon, M., Sabia, P., Sorrentino, G., Bozza, P., Ragucci R., Proc. Comb. Inst. 2017, 36, 3361-3369.

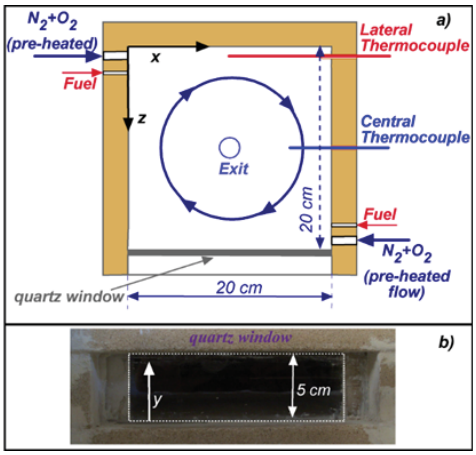

Fig. 1 *Sketch of the midplane section (a) and front view (b) of the cyclonic configuration*

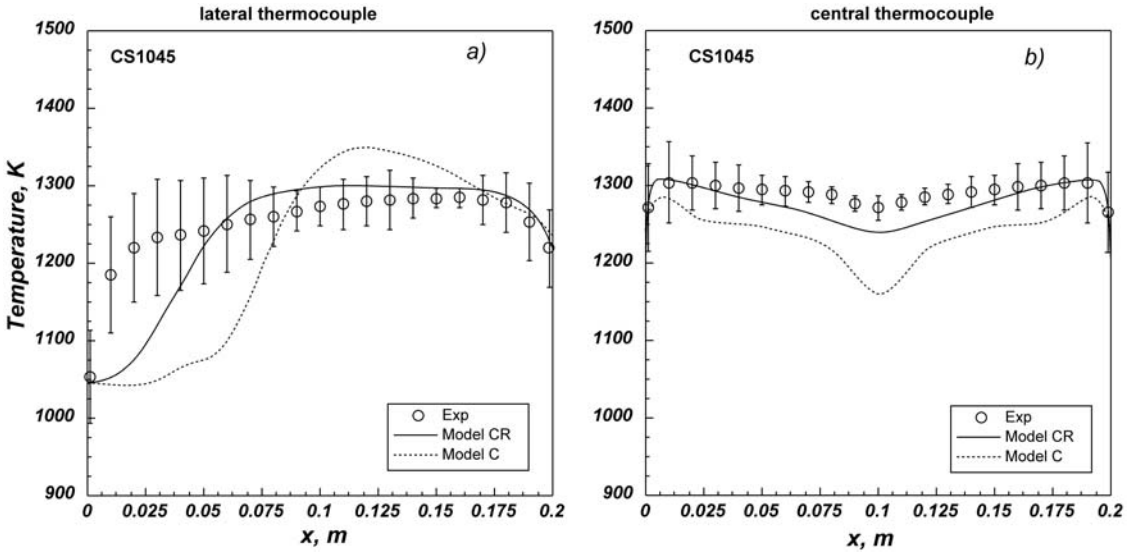

Fig. 2 *Axial profiles of the measured temperature with uncertainties (symbols with error bars) and predicted temperature at the midplane along the positions of the lateral (a) and central (b) thermocouples for the stoichiometric case for two heat transfer modeling approaches.*

14th International Workshop on Measurement & Computation of Turbulent Flames

Dublin, Ireland July 27-28 2018

Instantaneous 3D analysis of the Cambridge stratified swirled flame geometry using computed tomography

A. Unterberger[1]*, J. Menser[1], A Kempf[1] and K Mohri[1]

[1]University of Duisburg-Essen, Institute for Combustion and Gas Dynamics – Fluid Dynamics, Duisburg, Germany

*andreas.unterberger@uni-due.de

Abstract

We present the first instantaneous 3D reconstructions of the swirled (SwB3) Cambridge stratified flame by combing the flame chemiluminescence images with computed tomography. The burner was borrowed from the Hochgreb group at Cambridge University for testing. The experimental setup constituted 30 CCD cameras, Basler acA645-100gm with a ½" Sony ICX414 monochrome sensor and 659 by 494 square pixels of size 9.9 µm, that are fitted with Kowa C-mount lenses with a focal length of 12 mm. The cameras, which have a peak spectral response in the range of 400 - 680 nm, were placed in one horizontal plane around the burner, with a constant angular separation of 6° and a fixed distance to the burner, as shown in Figure 1. The optimum camera locations and settings of the algorithm were chosen based on our previous reconstructions of a swirl flame [1].

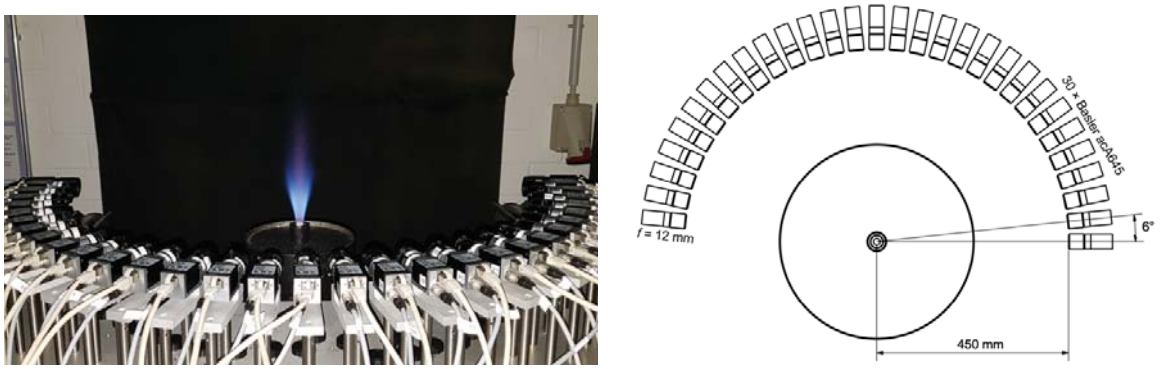

Figure 1: The 30-camera setup around the Cambridge stratified burner (left) and a schematic drawing of the setup from the top view (right).

The chemiluminescence intensities of CH*, C_2*, CO_2* and any possible thermally excited water can be captured by the cameras. We have obtained simultaneous images without any filters, and with different optical filters. To resolve finer flame structures, the camera exposure time t_{exp} must be reduced as much as possible, but this reduces the signal-to-noise ratio SNR, and hence a compromise between minimising motion blur and maintaining an adequate SNR was reached in every test. The feasible exposure times were in the range of $t_{\mathrm{exp}} = 100 - 700\ \mu s$, depending on the specific test case.

The reconstructions were performed directly in 3D, through volumetric discretisation of the field, using two of our in-house tomography algorithms: (I) the Computed Tomography of Chemiluminescence (CTC) that was originally provided by Floyd [2, 3], and that is based on the algebraic reconstruction technique (ART) [4], and (II) our recent Evolutionary Reconstruction Technique (EvoRec) that is based on a genetic algorithm. Our previous reconstructions of the non-swirl Cambridge stratified flame SwB1 compared well, qualitatively, to the direct numerical simulation (DNS) data of Proch et al. [5], as shown in Figure 2. The highly-resolved DNS data, 10 px / mm, was down-sampled and blurred to match the reconstruction domain

resolution and estimated image blurring based on the camera exposure time and the flame velocity from the DNS data. Examples of the reconstructed field for the swirled SwB3 flame are shown in Figure 3, for reconstructions that used flame images without any optical filters, obtained with two different exposure times. The sacrifice in the SNR for the shorter camera exposure time is reflected through the added noise in the reconstruction. The flame clearly spreads out more in the swirled SwB3 case compared to the non-swirled SwB1 case. We will discuss the flame geometry by presenting a series of reconstructions.

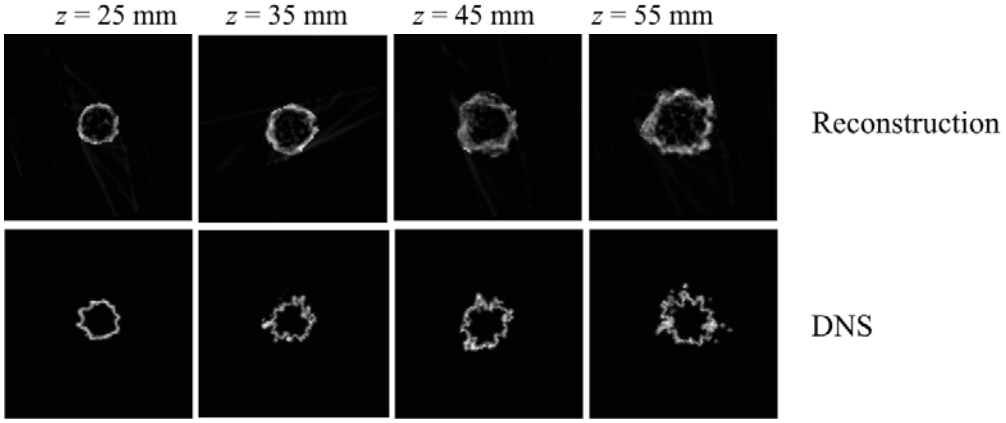

Figure 2: Horizontal slices from the previously reconstructed non-swirled Cambridge stratified flame SwB1 case using images obtained with $t_{\text{exp}} = 350\ \mu s$ (top row), and the corresponding slices from the DNS data (bottom row). The data presented is from randomly chosen instances in time.

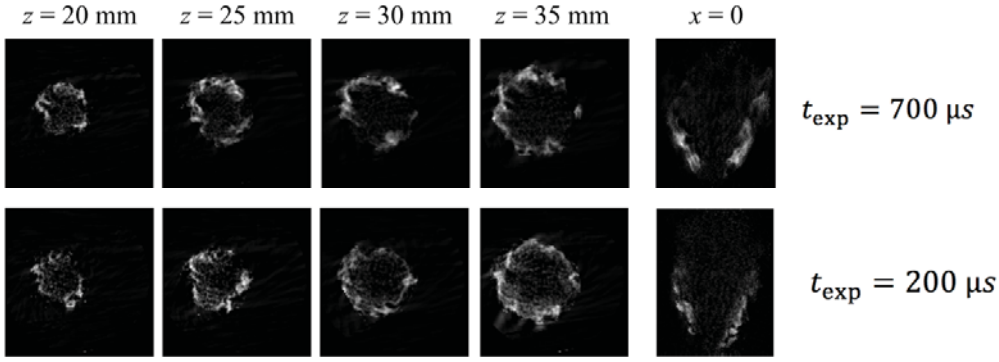

Figure 3: Horizontal slices at different heights above the burner, z, and the burner centre vertical slice as x = 0 from the reconstructed SwB3 flame, using flame images obtained with two different camera exposure times.

References

1. Mohri, K., et al., Appl. Opt, 2017. **56**(26): p. 7385-7395.
2. Floyd, J., et al., Combustion and Flame, 2011. **158**(2): p. 376-391.
3. Floyd, J. and A.M. Kempf, Proceedings of the Combustion Institute, 2011. **33**(1): p. 751-758.
4. Gordon, R., IEEE Transactions on Nuclear Science, 1974. **21**(3): p. 78 - 93.
5. Proch, F., et al., Combustion and Flame, 2017. **180**: p. 321-339.

Swirling flame dynamics investigated by burst mode laser PLIF/PIV and TDLAS

Guoqing Wang[a], Xunchen Liu[a], Yi Gao[a], Lei Li[a], Zhi X. Chen[b], Fei Qi[a]
[a]School of Mechanical Engineering, Shanghai Jiao Tong University, Shanghai, China
[b]Department of Engineering, University of Cambridge, Cambridge, UK
Email: lilei81@sjtu.edu.cn

A swirl-stabilized burner is constructed to investigate flame dynamics and thermoacoustic instability. As shown in Figure 1, it consists of a driver unit, a settling chamber, a contraction ended by a constant diameter duct, a horizontal end piece and an enclosed chamber. The rotation of the flow is induced by an axial swirler equipped with eight twisted airfoil vanes. A small bluff body is used to stabilize the flame during the unsteady motion of the flow. A loud speaker installed at the bottom of the setup provides acoustic excitation to the flame. Air and fuel (methane or the vapor of acetone) are premixed and enter the bottom of the burner through two tubes connected to the burner.

To investigate the response of the swirling flame to the acoustic excitation, both the unsteady flow field and the evolution of the flame surface are measured simultaneously. The measurement techniques mainly depend on a high-speed burst mode Nd:YAG laser (Spectral Energies, QuasiModo1000) with a repetition rate of up to 100 kHz and two intensified high-speed CMOS cameras. High speed PIV is used for the measurement of the unsteady flow field. PLIF for the distribution of CH_2O/acetone is used to capture the evolution of the flame front. Tunable diode laser absorption spectroscopy (TDLAS) is adopted for the measurement of flame temperature and concentrations of CO2/ H2O. Moreover, a hot wire is equipped in the downstream of the swirler used to measure the flow velocity variation due to the acoustic excitation.

Figure 2 shows the instantaneous flame patterns in a full cycle of acoustic modulations for equivalence ratio of 0.8. Phase conditioned flow field from PIV and CH* chemiluminescence images are given. The flame surface decreases from 0° to 180° and increases from 180° to 360°. This is mainly due to two effects, vortex roll-up from the rim of the bluff body, and the perturbations of the swirler number. The former induces the rolling up of the flame tip and the latter can cause the changes of the flame angle[1].

Figure 3 shows the flow field from planar PIV and the acetone PLIF. The fuel is vapor acetone with equivalence ratio ϕ = 0.8. As all of the acetone is consumed at the flame front and there is no PLIF signal in the downstream region, flame position can be approximately identified from acetone PLIF. From the PIV results it can be found that a distinct vortex is produced at the injector of the burner and rolled up with the flow. Meanwhile, in the center zone vortex break down is formed, and there is also a distinct vortex shedding in the inner zone. The flame is rolled up with the rolling up of the inner and outer vortex. Figure 4 shows the temperature fields measured using TDLAS in a period with 200Hz acoustic excitation. It can be found that the high and low temperature spots are produced with the rolling up of the flame tip and convected downstream.

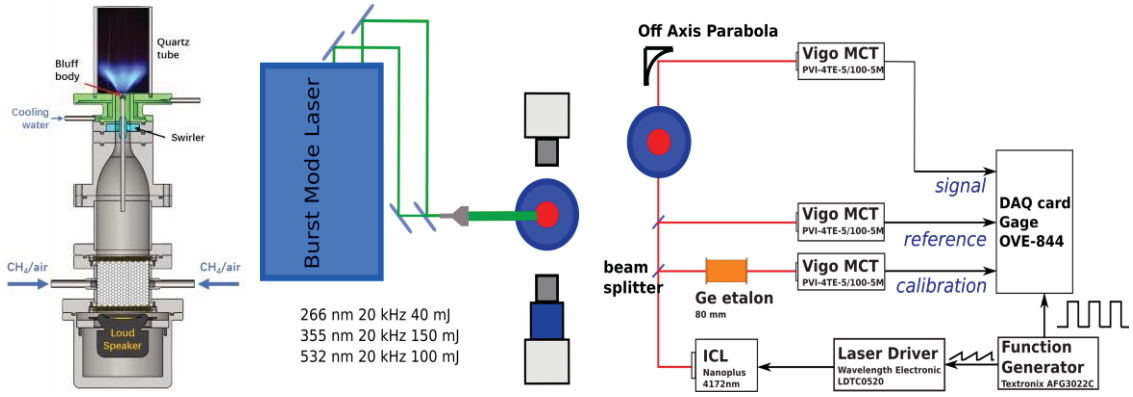

a. swirl burner b. PIV and PLIF system c. TDLAS

Figure 1. schematic of the swirler burner and burst mode laser diagnostic system

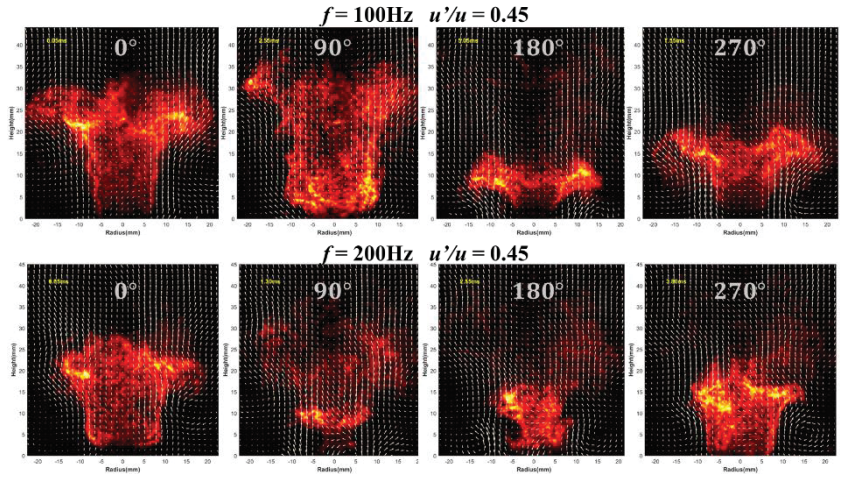

Figure 2. Flow field from PIV and CH* chemiluminescence images with 100-200 Hz acoustic excitation.

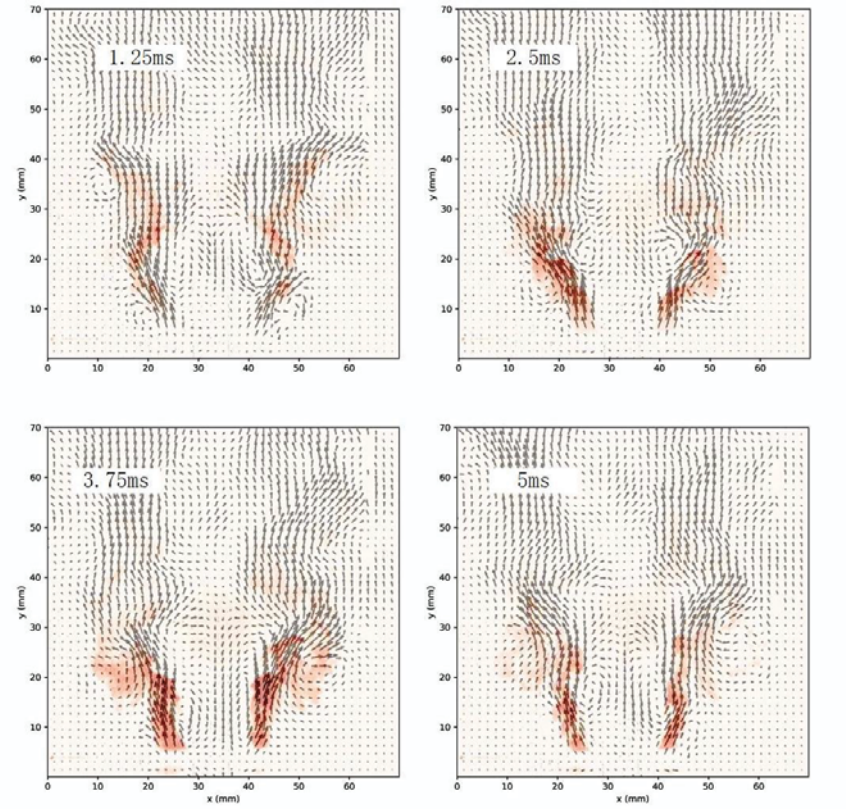

Figure 3. Flow field from PIV and Acetone PLIF of swirling flame with 200 Hz acoustic excitation.

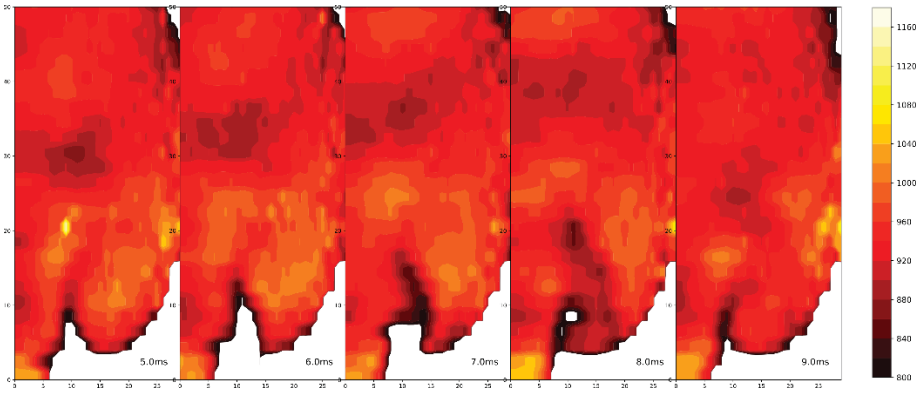

Figure 4. Temperature field of a period with 200 Hz acoustic excitation by TDLAS.

References:

1. P. Palies; D. Durox; T. Schuller; S. Candel, Combustion and Flame 157 (2010) 1698–1717

A Particle Mass-Based Implementation for Mixing Models with Differential Diffusion

Tianwei Yang [a,b], Hua Zhou [a], Zhuyin Ren [a,b]*

[a] *Center for Combustion Energy, Tsinghua University, China*

[b] *School of Aerospace Engineering, Tsinghua University, China*

**Corresponding Author Email: zhuyinren@tsinghua.edu.cn*

In modeling turbulent reactive flows based on one-point one-time transported PDF (TPDF) methods, while the nonlinear chemical reaction term is treated exactly, the molecular diffusion term is unclosed and is in general modelled by mixing models. Each mixing model specifies a specific mixing formulation describing the manner in which mixing occurs, coupled with the specification of the scalar mixing timescale. Different mixing formulations such as the interaction by exchange with the mean (IEM), the modified Curl's model (MC), and the Euclidean minimum spanning tree (EMST) model, binomial Langevin model etc. have been widely employed in TPDF simulations due to the relative simplicity of their implementation and the guarantee of realizability. The scalar mixing timescale τ_ϕ specifies the characteristic timescale of decay of scalar's variance $\widetilde{\phi''^2}$ and is defined as $\tau_\phi = \widetilde{\phi''^2}/\widetilde{\chi_\phi}$ where $\widetilde{\chi_\phi}$ is the scalar dissipation rate and $\widetilde{\phi''^2}$ is the scalar's variance.

Differential diffusion may be significant in turbulent flames. For turbulent premixed flames, reactive scalars feature their own characteristic lengthscales and timescales. It is desirable for mixing models to account for different mixing timescales for individual species. However, the extension of mixing models for different mixing timescale may result in realizability issue. In this work, a particle mass-based implementation for mixing models is proposed to account for differential diffusion in species mixing. This approach maintains realizability and requires no additional corrections. With the particle mass-based implementation, the IEM and the MC models have been augmented to account for different mixing timescales, denoted by IEM-DD and MC-DD respectively. The conservation of individual species mass and the desired exponential decay of variance are derived theoretically and validated numerically

For particle-based TPDF simulation, the n^{th} computational particle has the weight $w^{(n)}$ and the composition information consisting of the species mass fraction $Y_1^{(n)}, Y_2^{(n)}, \dots, Y_{N_s}^{(n)}$ and the specific sensible enthalpy $h_s^{(n)}$. Currently, the mixing model takes the per unit mass quantities as primitive variables during mixing. The particle weight remains constant during mixing, resulting in the violation of the realizability of species mass fraction conservation, i.e. $\sum_{\beta=1}^{N_s} Y_\beta \neq 1$ (N_s is the number of species), when different mixing timescales for individual species are applied. The key idea of the proposed particle mass-based implementation is to apply mass-based quantities as primitive variables, i.e. species mass $\{m_1^{(n)}, m_2^{(n)}, \dots, m_{N_s}^{(n)}\}$ and the sensible enthalpy $H_s^{(n)}$. The particle mass $m^{(n)} = \sum_{\beta=1}^{N_s} m_\beta^{(n)}$ corresponds to its weight $w^{(n)}$ but varies during mixing, and the species mass fraction is reconstructed after mixing, therefore the realizability is ensured automatically.

The IEM-DD model allowing for different mixing timescales has the following formulation,

$$\frac{\mathrm{d}m_\beta^{(n)}}{\mathrm{d}t} = -\frac{m_\beta^{(n)} - m^{(n)}\widetilde{Y_\beta}}{2\tau_\beta}\ ,\ \beta = 1, \dots, N_s,$$

$$\frac{\mathrm{d}H_s^{(n)}}{\mathrm{d}t} = -\frac{H_s^{(n)} - m^{(n)}\widetilde{h_s}}{2\tau_{h_s}}.$$

In the MC-DD model, the number of particle pairs selected during the mixing step Δt is $N_{pairs} = \frac{1.5\Delta t N_p}{\tau_{min}}$, where $\tau_{min} = \min_{\beta\in\{1,\dots,N_s+1\}} \tau_\beta$ ($N_s + 1$ represents the sensible enthalpy) is the minimal timescale among all the scalars. The particle pair (p, q) is selected with the probability proportional to the mass of this pair and has following composition after particle interaction,

$$m_\beta^{(n)} = \left(1 - \alpha\theta_\beta\right)m_{\beta,0}^{(n)} + \alpha\theta_\beta m_0^{(n)}\widetilde{Y_\beta}^{(p,q)}, \beta = 1, \dots, N_s,$$

$$H_s^{(n)} = \left(1 - \alpha\theta_{h_s}\right)H_{s,0}^{(n)} + \alpha\theta_{h_s} m_0^{(n)}\widetilde{h_s}^{(p,q)},$$

where $n = p, q$ and θ_β is the decay factor for scalar β which controls the degree of interaction of scalar β according to the desired mixing timescale τ_β,

$$\theta_\beta = \frac{3 - \sqrt{9 - 8\tau_{min}/\tau_\beta}}{2}, \beta = 1, \dots, N_s + 1.$$

The conservation of mean for these two models can be verified easily. And under the assumption that the change of $m^{(n)}$ is negligible, we can get the desired exponential decay of variance,

$$\frac{d\sigma_\beta^2}{dt} = -\frac{\sigma_\beta^2}{\tau_\beta}, \ \beta = 1, \dots, N_s + 1.$$

In order to validate the proposed models numerically, we apply the models to a closed inert mixing system. The system consists of 1000 computation particles and is used to represent the mixing process within a computational cell in TPDF calculation. The composition consists of 9 species, $H_2, O_2, H_2O, H, O, OH, HO_2, H_2O_2, N_2$, and the sensible enthalpy. The initial compositions of particles are set randomly and the initial mass $m^{(n)} = 1$ for all particles. Distinct mixing timescales are specified for each individual scalar as $\tau_\beta = \tau_{h_s} \times \sqrt{MW_\beta}/\sqrt{MW_{ave}}$, $\beta = 1, \dots, 9$ and τ_{h_s} is set to be 3×10^{-3} s, where MW_β is the molecular weight of the βth species and MW_{ave} is the average molecular weight of the system.

Figure 1 shows that the total mass of several species remain constant with IEM-DD and MC-DD models to demonstrate the conservation of mean. This also holds for the other species and the sensible enthalpy, but not shown for conciseness. Figure 2 shows the decay of H_2 and O_2 variance, predicted using the IEM-DD and MC-DD models respectively. The results from the original IEM and MC model, namely $\tau_\beta = \tau_{h_s}$ for every species, are also shown for comparison. As shown, when IEM-DD or MC-DD model is applied, $\sigma_{H_2}^2$ and $\sigma_{O_2}^2$ have different decaying rates, which are close to the desired exponential decay. Meanwhile, the original IEM and MC models predict the same decay rate of $\sigma_{H_2}^2$ and $\sigma_{O_2}^2$ as expected.

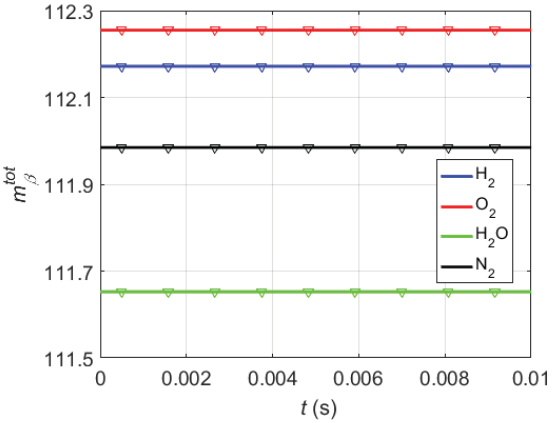

Fig. 1 Evolution of total masses of several species with IEM-DD (solid lines) / MC-DD (downward-pointing triangles).

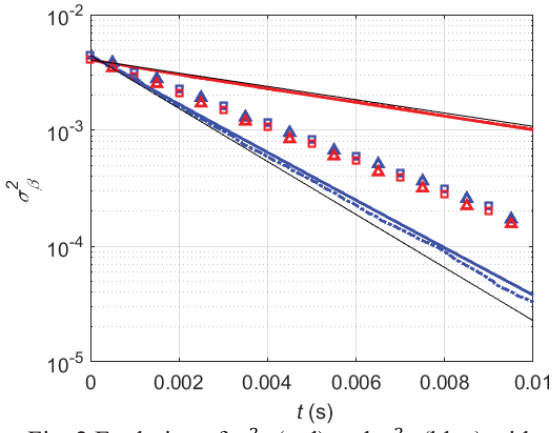

Fig. 2 Evolution of $\sigma_{O_2}^2$ (red) and $\sigma_{H_2}^2$ (blue) with IEM-DD (solid lines) and MC-DD (dashed lines) using different mixing timescales, and with original IEM (squares) and MC (upward-pointing triangles) using a single timescale. Thin black solid lines indicate the desired results of exponential decay

Acknowledgements
The work is supported by National Natural Science Foundation of China (51476087 and 91441202).

Turbulent Flame Structure and Dynamics in Swirling Reacting Flows—High-Speed Dual-Plane *Stereo*-PIV/OH-PLIF Measurements

Tongxun Yi(tongxun.yi@spectralenergies.com), Naibo Jiang, Christopher A. Fugger, Paul Hsu, Josef Felver & Sukesh Roy
Spectral Energies, LLC, Dayton, OH 45431

Ianko Chterev, Raghul M. Kumar, Danielle Stepien, Matthew *Sirignano, Benjamin L. Emerson & Timothy C. Lieuwen*
School of Aerospace Engineering, Georgia Institute of Technology, Atlanta, GA 31308

James R. Gord
Air Force Research Laboratory, Wright-Patterson Air Force Base, Dayton, OH 45433

Abstract

Turbulent swirling reacting flows, including the mean flow field, the large coherent structures (e.g. the precessing vortex core) and small-scale vortices, are highly three-dimensional. Recently we have conducted high-speed (10 kHz) dual-plane *stereo*-PIV/OH-PLIF measurements of a turbulent, swirling reacting jet. Preliminary analysis shows the advantages of fully resolving the nine-component velocity-gradient tensor and the three-component vorticity in gaining improved understanding of turbulent combustion.

1. Experimental Setup and Data Processing

High-speed (10 kHz) dual-plane *stereo*-PIV/OH-PLIF measurements are conducted on a turbulent premixed swirling reacting jet previously described in [1][2]. Figure 1 shows the optical setup. The beam separation, corresponding to the Taylor length scale, is 2.0 mm across the measurement section. The OH-PLIF plane bisects the two PIV planes. The flame front is inferred from regions with high magnitude in the OH-PLIF gradient.

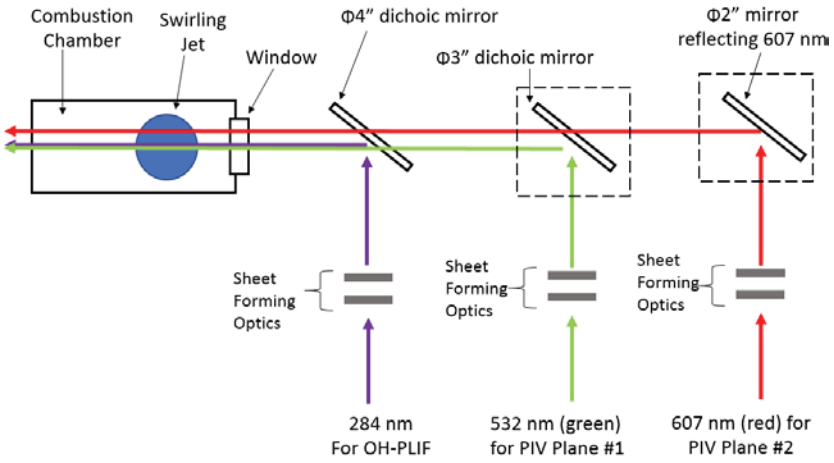

Fig. 1. The optical setup for high-speed (10 kHz) dual-plane *stereo*-PIV/OH-PLIF measurements of a turbulent swirling reacting jet. The 532-nm and 607-nm laser beams are generated from a burst-mode laser and an optical parametric oscillator.

2. Results

Figure 2(a) shows three consecutive snapshots of velocity, the out-of-plane vorticity ω_z and the OH-PLIF gradient on both PIV planes. The expected similarity in "large" flow structures on both PIV planes is clearly identifiable. Local flame quenching very likely occurs at locations with discontinuities in the OH-PLIF gradient. The enclosed, "tongue-shaped" flame front is associated with a vortex with a negative out-of-plane vorticity, large out-of-plane velocity gradients (i.e., $\partial u/\partial z$, $\partial w/\partial z$ and $\partial v/\partial z$), very likely corresponding to the precessing vortex core (PVC). The PVC is a large helical flow structure around the inner swirling shear layer and plays important roles in flame initiation, quenching, propagation and combustion instabilities [3–5]. Clearly, the large out-of-plane velocity gradient within the enclosed region cannot be captured with single-plane *stereo*-PIV/OH-PLIF measurements.

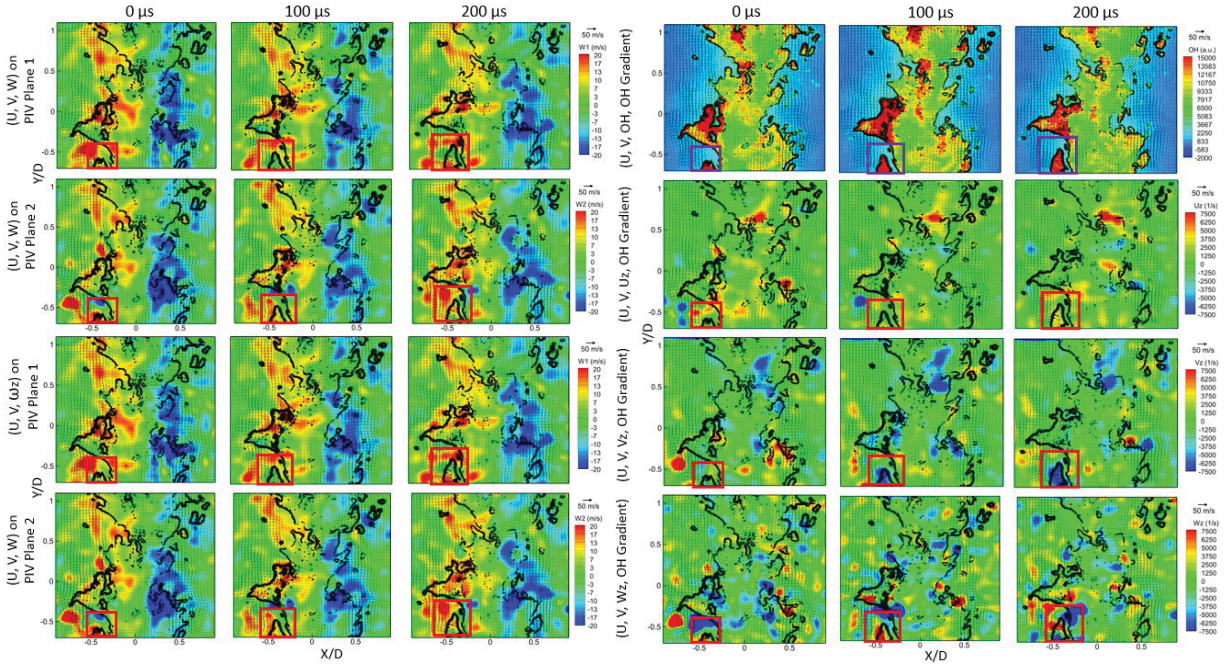

Fig. 2. High-speed dual-plane *stereo*-PIV/OH-PLIF measurements of turbulent swirling combustion. (a) Similarity of "large" flow structures on both PIV planes, and (b) a sequence of velocity, the in-plane velocity gradient $\partial u/\partial y$, the out-of-plane vorticity ω_z and the OH-PLIF gradient on both PIV planes. The planar velocity (*U*, *V*) is shown as vectors, with scalars in colors. The thick black line denotes the magnitude of the OH-PLIF gradient.

3. Conclusions

High-speed dual-plane *stereo*-PIV/OH-PLIF measurements, capable of spatially, temporally and fully resolving the nine-component velocity-gradient tensor, are conducted on a turbulent swirling reacting jet. Preliminary analysis shows the expected similarity of "large" and "medium" flow structures on both PIV planes and the advantages of gaining improved understanding of turbulent swirling combustion by fully resolving the nine-component velocity-gradient tensor and the three-component vorticity.

4. Acknowledgments

This work was funded, in part, by the Air Force Research Laboratory under Contract Nos. FA8650-15-D-2518 and by the Air Force Office of Scientific Research (AFOSR) (Dr. Enrique Parra, Program Officer, 15RQCOR202; and Dr. Chiping Li, Program Officer, 14RQ06COR).

References

1. T. Smith, B. Emerson, W. Proscia & T. Lieuwen 2018 Role of induced axial acoustics in transverse acoustic flame response. doi.org/10.1016/j.combustflame.2017.12.035, *Combust. Flame*
2. T. Yi et al., Complete determination of the velocity gradient tensor upstream of the flame front with high-speed Tomo-PIV/Dual-Plane-PIV/OH-PLIF Measurements. AIAA 2018-0153.
3. I. Boxx, M. Stohr, C. D. Carter & W. Meier 2010 Temporally resolved planar measurements of transient phenomena in a partially pre-mixed swirl flame in a gas turbine model combustor. *Combust. Flame* **157**, 1510–1525.
4. S. Roy, T. Yi, N. Jiang, G. H. Gunaratne, I. Chterev, B. Emerson, T. Lieuwen, A. W. Caswell, and J. R. Gord 2017 Dynamics of robust structures in turbulent swirling reacting flows. *J. Fluid Mech.* **816**, 554–585.
5. A. M. Steinberg, C. M. Arndt, and W. Meier 2013 Parametric study of vortex structures and their dynamics in swirl-stabilized combustion. *Combust. Flame* **34**(2), 3117–3125.
6. T. Yi & D. A. Santavicca 2012 Combustion instability and flame structure of turbulent swirl-stabilized liquid-fueled combustion. *J. Propul. Power* **28**(5), 1000–1014.

Characterization of anisotropic vortex tubes near flame fronts in high-Karlovitz-number turbulent premixed combustion

Jiaping You, Hao Zhou, Shiying Xiong, and Yue Yang*

State Key Laboratory of Turbulence and Complex Systems,
College of Engineering, Peking University, Beijing 100871, China
yyg@pku.edu.cn

The interaction between the premixed flame front and vortices plays a crucial role in practical combustion applications and modelling of turbulent premixed combustion. Since the density and viscosity vary significantly across the frame front, most of the existing Eulerian vortex-identification methods are not able to identify a continuous, complete vortical structure across the flame and characterize its evolution. Most of previous studies on the anisotropic vorticity are based on the statistical analysis [1,2]. It appears to be challenging to characterize and elucidate the effects of flame on global vortical structures and their evolution.

The vortex-surface field (VSF), whose isosurface is a vortex surface consisting of vortex lines, is developed to tackle the issue of the characterization of evolving vortical structures [3,4]. This method is rooted in the Helmholtz vorticity theorem, but it can describe the Lagrangian-like evolution of vortex surfaces in variable-density viscous flows with numerical regularization. Recently, the VSF method has been extended to visualize and quantify the flame-vortex interaction in a Taylor-Green reacting flow [5].

In the present study, we apply the VSF to investigate flame/vortex interactions in turbulent premixed combustion at moderate and high Karlovitz numbers (*Ka*). We consider a turbulent premixed flame propagating freely along the streamwise direction in statistically stationary homogeneous isotropic turbulence. The unburnt gas is a lean H_2/air mixture with the equivalence ratio 0.6 at the temperature T_u=300 K and atmospheric pressure. As listed in Table 1, we performed four direct numerical simulation (DNS) cases with the varied turbulent intensity *u'* scaled by the laminar flame speed S_L.

Table 1: Parameters for DNS of turbulent premixed combustion

Case	A	B	C	D
u'/S_L	2	5	10	20
Ka	2.9	11.6	32.9	93

The calculation of VSFs can be implemented as a postprocessing step based on a time series of velocity–vorticity fields in DNS. The two-time method [2] with a recently developed local optimization technique is applied to construct the VSF. Two different vortex-identification methods, the isosurfaces of the VSF and the conventional vorticity magnitude, are compared in Fig. 1. The VSF isosurface with attached vortex lines is displayed in Fig. 1(a). We observe that a tangle of twisted vortex tubes on the unburnt side are stretched along the streamwise direction near the flame front owing to the

thermal expansion, and the small-scale vortex tubes merge into bulky sheet-like vortical structures on the burnt side. In contrast, the isosurface of the vortcity magnitude in Fig. 1(b) suddenly disappears around the flame front owing to the rapid decay of vorticity across the flame front, so it is challenging to characterize how the flame influences continuous vortex dynamics using conventional Eulerian vortex visualization methods.

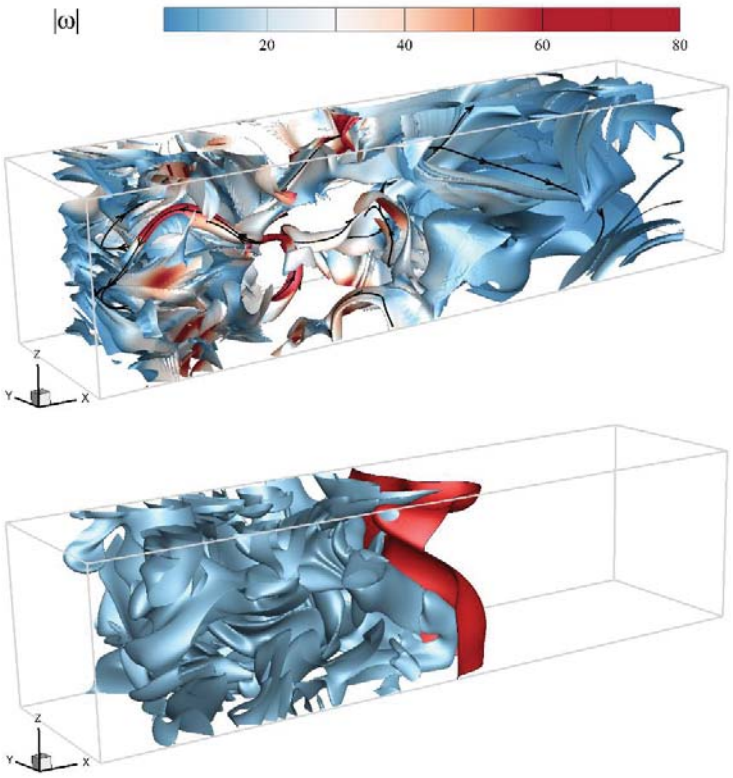

Fig. 1 Comparison of different vortex-identification methods for DNS case B of turbulent premixed combustion. (a) Isosurface of VSF colored by the vorticity magnitude with some black vortex lines integrated on the surfaces, (b) isosurface of the vorticity magnitude with the red flame front. (Note: This is a preliminary result, and we would replace this figure by the one at higher *Ka* in the final version.)

Furthermore, we find that the anisotropic vortex tubes near the flame front are highly correlated to the strong local anisotropy of the fluctuating velocity, which can affect the turbulence modelling. The local geometry of Reynolds stresses in the Lumley triangle indicates that the velocity field becomes increasingly anisotropic from the unburnt side to the burnt side and the vortex tubes are elongated in the streamwise direction.

References

[1] P. E. Hamlington, A. Y. Poludnenko, E. S. Oran, Phys. Fluids, 2011, 23:125111.
[2] B. Bobbitt, G. Blanquart, *Phys. Fluids*, 2016, 28:015101.
[3] Y. Yang and D. I. Pullin, *J. Fluid Mech.*, 661, 446–481, 2010.
[4] Y. Yang and D. I. Pullin, *J. Fluid Mech.*, 685, 146–164, 2011.
[5] H. Zhou *et al*., *Proc. Combust. Inst.*, 2018 (accepted for oral presentation)

On the alignment of strain rate eigenvectors in turbulent premixed counterflow flames

Bo Zhou, Jonathan H. Frank
Combustion Research Facility, Sandia National Laboratories, Livermore, CA 94551, USA
Email: bozhou@sandia.gov; jhfrank@sandia.gov

Scalar dissipation rate (N_c) plays a critical role in turbulent flame models [1]. The effects of strain rate on N_c are manifest in the transport equation of the scalar dissipation rate in which the turbulence-scalar interaction term depends on the scalar-normal strain rate $S_n=n_i s_{ij} n_j$, where $s_{ij}=0.5(u_{i,j}+u_{j,i})$ is the strain rate tensor and $\boldsymbol{n}$ is the scalar-normal unit vector [2]. The eigenvalues of s_{ij}, also known as the principal strain rates (PSRs), s_i, are defined such that $s_1 \geqslant s_2 \geqslant s_3$, where s_1 and s_3 are the most extensive and compressive strain rates, respectively, and s_2 is the intermediate strain rate. S_n can be written in terms of s_i as: $S_n=s_1\cos^2\theta_1+s_2\cos^2\theta_2+s_3\cos^2\theta_3$, where θ_i are the angles between the s_i-eigenvectors and scalar-normal. It is evident that S_n directly depends on the magnitudes of s_i and their alignments with the scalar-normal direction.

The present work studies the local s_i-$\boldsymbol{n}$ alignment in turbulent premixed counterflow flames using simultaneous TPIV and OH-LIF imaging for strain rate field quantification and flame front detection. The experimental setup is shown in Fig.1. The TPIV measurements provide access to the complete strain rate tensor and PSRs, which are not available from planar or stereoscopic PIV measurements. In jet turbulent flows, turbulence is driven by the mean shear layer due to velocity disparity of flows with ambience, and large bulk strain is typically absent. However, in the turbulent counterflow, existence of large bulk strain can be expected. It is unclear whether and to what extent bulk strain rates could influence the preferential s_i-$\boldsymbol{n}$ alignment, which need to be clarified for proper modeling of turbulent reacting flows in realistic environments.

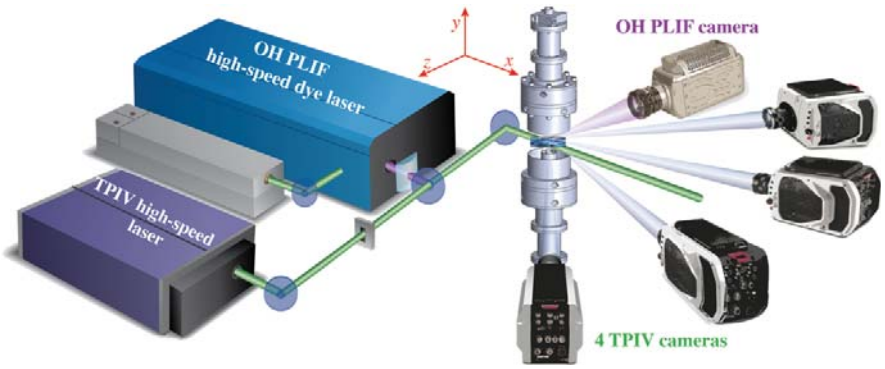

Fig.1 Experimental setup for simultaneous TPIV and OH LIF imaging.

Similar to the jet flames, measurements in the counterflow flames show that heat release enhanced the alignment of extensive strain, s_1, with the flame-normal, $\boldsymbol{n}$. However, the existence of compressive bulk strain in the counterflow introduced an additional inherent preferential alignment of compressive strain, s_3, with the flame front normal through their mutual alignment with the burner axis. As a result, a preferential s_3-$\boldsymbol{n}$ alignment was observed throughout the counterflow flame front despite the large heat release parameter in these flames. This result

represents a significant departure from turbulent jet flames or flames in idealized isotropic turbulence, which require substantially higher turbulence intensities to achieve such a strong s_3-$\boldsymbol{n}$ alignment. Such strike discrepancy in term of s_i-$\boldsymbol{n}$ alignment is manifested in Fig.2. Measurements further show that the effect of turbulence on the alignment was twofold: first, it counteracted the effect of heat release and promoted preferential s_3-$\boldsymbol{n}$ alignment slightly ahead of the flame front, similar to non-reacting turbulent flows. Second, increasing turbulence intensity reduced the geometry-reinforced preferential s_3-$\boldsymbol{n}$ alignment by increasing surface wrinkling. As a result of preferential alignments of s_3 parallel to $\boldsymbol{n}$ and s_1 orthogonal to $\boldsymbol{n}$, the mean flame-tangential strain rate, $\langle S_t \rangle$, was extensive and the mean flame-normal strain rate, $\langle S_n \rangle$, was dominantly compressive except for a small region near the flame front where $\langle S_n \rangle$ became slightly extensive due to strong dilatation. Further details of the results will be presented in the poster.

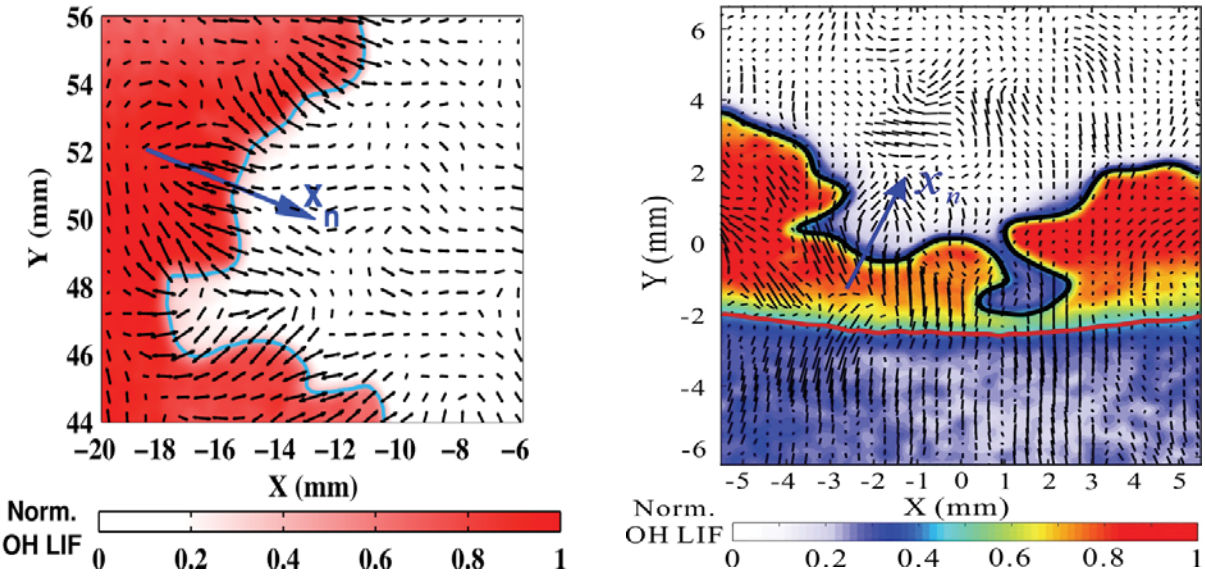

Figure2. Simultaneous OH-LIF image with (left) s1-eigenvectors in a Bunsen premixed turbulent flame and (right) s3-eigenvectors in a counterflow premixed turbulent flame. Eigenvectors are scaled to its magnitude, and 1 out of 9 eigenvectors are displayed for clarity. The arrows denote the direction of the flame front normal.

[1] Kolla H, Rogerson JW, Chakraborty N, Swaminathan N. Combust Sci Technol. 2009;181:518-35.

[2] Swaminathan N, Bray KNC. Combust Flame. 2005;143:549-65.

[3] Coriton B, Frank JH. Proc Combust Inst. 2017;36:1885-92.